Application of the Truncated Perturbed Chain-Polar Statistical Associating Fluid Theory (tPC-PSAFT) to Alcohol/Alkane mixtures at high pressures

Mishqah Hussain

BSc. (Eng.)

Submitted in fulfilment of the academic requirements for the degree of Master of Science in Engineering in the School of Engineering, University of KwaZulu-Natal

December 2020

Supervisors: Dr K. Moodley

ABSTRACT

Constitutive equations, such as equations of state (EoS) characterize mathematical relationships between state functions under set physical conditions and are imperative for the accurate design of chemical processes (Devilliers, 2011; Al-Malah, 2015). Most models, however, fail to accurately predict thermophysical properties of complex mixtures such as those exhibiting molecular association and hydrogen bonding. The Statistical Associating Fluid Theory (SAFT), based on thermodynamic perturbation theory, explicitly accounts for molecular association, hence, providing a more suitable prediction of thermophysical properties (Devilliers, 2011). This work investigates the performance of the truncated Perturbed Chain-Polar Statistical Associating Fluid Theory (tPC-PSAFT) model in accurately accounting for the effect of molecular association on compressed liquid density in liquid alkane-alcohol mixtures at elevated pressures. This was achieved by comparing the density predictions calculated by the tPC-PSAFT model to novel experimental density data.

Isothermal measurements were conducted utilizing an Anton Paar DMA HP densimeter with a supplier stated uncertainty ranging between 0.1 and 1 $kg.m^{-3}$. Measurements were conducted in the temperature and pressure ranges of 313.15 to 353.15 K and 0.1 to 20 MPa, respectively, over the entire composition range. Furthermore, a test system consisting of ethanol (1) + n-heptane (2) was used to confirm the reliability of the experimental setup and procedure. The density data obtained for the test system was compared to literature and demonstrate excellent correlation of the data, with a maximum relative difference of 0.0005, confirming the reliability of the procedure utilized in this study.

The density data of six novel binary systems namely, butan-1-ol/butan-2-ol/2-methylpropan-1-ol (1) + n-octane/n-decane (2) are presented in this work. The maximum expanded combined uncertainties for pressure, temperature, composition and density were 0.032 MPa, 0.02 K, 0.0002 mole fraction, and between 1.10 to 1.12 $kg.m^{-3}$, respectively.

Density data obtained experimentally for all six binary systems comply with the general trend regarding temperature and pressure in that the density of the liquid mixtures decreased with an increase in temperature and increase with an increase in pressure. Furthermore, derived thermodynamic properties namely, the excess molar volume, thermal expansivity and isothermal compressibility were computed for each of the binary systems. Large positive

deviations from ideality were noted for the excess volumes for all systems. This is attributed to the different shapes and sizes of the molecules as well as the attractive mixture interactions when compared to those of the individual pure components. In addition, the thermal expansivity and isothermal compressibility demonstrate highly non-linear behaviour which is indicative of systems comprising complex mixtures.

The experimental data were compared to correlations/predictions resulting from five models namely, the Modified Toscani-Szwarc (MTS) equation of state (EoS), the Benedict-Webb-Rubin-Starling (BWRS) EoS, Peng-Robinson (PR) EoS, Perturbed Chain-Statistical Associating Fluid Theory (PC-SAFT) model and the truncated Perturbed Chain-Polar Statistical Associating Fluid Theory (tPC-PSAFT) model. Both the MTS and BWRS EoS demonstrated excellent correlation of the data for all six of the binary systems attributed to the empirical nature of the model and the significant number of fitting parameters employed. The maximum root mean square deviation (RMSD) was found in the butan-2-ol (1) + n-octane (2) binary system at RMSD = 4.72×10^{-4}. In addition, improvements in model performance were noted for the BWRS EoS at higher temperatures and pressures. The PR EoS demonstrated poor correlation of the density data of the mixtures (exceeding RMSD = 0.024), attributed to the poor prediction of the pure component data by the model and the use of a single binary interaction fitting parameter in the cases of the mixtures.

Density predictions from the PC-SAFT model demonstrated significant deviation from experimental data (exceeding RMSD = 0.011) in that the PC-SAFT model underpredicts densities for the binary systems. Furthermore, a progressive deterioration in the model's performance was noted as the respective alcohol concentration increases. Accurate prediction of the density was however noted for the 2-methylpropan-1-ol binary systems in the alcohol dilute region. In addition, some improvement in model performance was observed at higher pressures and temperatures for the butan-2-ol and 2-methylpropan-1-ol binary systems.

The tPC-PSAFT model demonstrated improvement in accurately predicting the density data, for all six systems, when compared to those obtained via the PC-SAFT model, with an improvement in excess of 72% in some cases. In addition, the model performs well in the alcohol dilute region and at high pressures and temperatures. However, a progressive deterioration in the model's performance is noted as the concentration of the alcohol in solution is increased. This was unexpected as both the PC-SAFT and tPC-PSAFT models explicitly account for molecular association and were theorized to perform well in predicting the alcohol

mixture behaviour. The model's poor performance can be attributed to the lack of high precision pure component parameters currently available in the literature that do not effectively characterize the density of the systems under high pressure. All five models exhibit similar trends to that of the experimental data despite their individual merits and shortcomings.

DECLARATION: Statement of Authorship

The work presented in this dissertation was carried out in the Thermodynamic Research Unit in the School of Engineering at the University of KwaZulu-Natal, Durban, from January 2019 to December 2020 under the supervision of Doctor K. Moodley.

This dissertation is submitted as the full requirement for the degree M.Sc. (Eng.) in Chemical Engineering.

I, Mishqah Hussain, therefore declare that:

(i) The research reported in this dissertation, except where otherwise indicated, is my original work.

(ii) This dissertation has not been submitted for any degree or examination at any other university.

(iii) This dissertation does not contain other persons' data, pictures, graphs or other information, unless specifically acknowledged as being sourced from other persons.

(iv) This dissertation does not contain other persons' writing, unless specifically acknowledged as being sourced from other researchers. Where other written sources have been quoted, then:

a) Their words have been re-written, but the general information attributed to them has been referenced;

b) Where their exact words have been used, their writing has been placed inside quotation marks, and referenced.

(v) This dissertation does not contain text, graphics or tables copied and pasted from the Internet, unless specifically acknowledged, and the source being detailed in the dissertation and in the References sections.

(vi) As this thesis is submitted in the journal manuscript format, under Rule DR9 c) and d) of the University of KwaZulu-Natal, only manuscript versions of published or unpublished work are presented.

_____

Mishqah Hussain

As the candidate’s supervisor, I, Dr. K. Moodley, approved this dissertation for submission.

_____

Doctor K. Moodley

DECLARATION TWO: Contribution to publications

Details of contribution to publications and manuscripts

1. Hussain, M. and Moodley, K., 2020. P–ρ–T Data and Modeling for Butan-1-ol+ n-Octane or n-Decane between 313.15–353.15 K and 0.1–20 MPa. Journal of Chemical & Engineering Data, 65(4), pp.1636-1654. (Hussain and Moodley, 2020a)
   Contribution: I conceptualized the study, developed the experimental methodology, validated the procedure, measured modelled and analysed the data, prepared the manuscript with support from Dr K Moodley.

2. Hussain, M. and Moodley, K., 2020. Experimental P–ρ–T Data and Modeling for Butan-2-ol+ n-Octane or n-Decane in the Ranges of 313.15–353.15 K and 0.1–20 MPa. Journal of Chemical & Engineering Data, 65(8), pp.3848-3865. (Hussain and Moodley, 2020b)
   Contribution: I conceptualized the study, developed the experimental methodology, validated the procedure, measured modelled and analysed the data, prepared the manuscript with support from Dr K Moodley.

3. Hussain, M. and Moodley, K., 2021. P-ρ-T data and modelling for (2-methylpropan-1-ol+ n-octane or n-decane) between 313.15 K–353.15 K and 0.1–20 MPa. The Journal of Chemical Thermodynamics, 152, p.106279. (Hussain and Moodley, 2021)
   Contribution: I conceptualized the study, developed the experimental methodology, validated the procedure, measured modelled and analysed the data, prepared the manuscript with support from Dr K Moodley.

ACKNOWLEDGEMENTS

I would like to express my gratitude to the following individuals:

- My supervisor Dr. K. Moodley for his continuous guidance, assistance, enthusiasm, support and problem-solving techniques through the duration of this project.
- The University of KwaZulu-Natal's J.W. Nelson fund for their financial contributions toward the research.
- The chemical technicians for their assistance throughout the project.
- Finally, the authors parents and sibling for their support, love and motivation for the duration of this project.

TABLE OF CONTENTS

LIST OF FIGURES

LIST OF TABLES

NOMENCLATURE

Symbol	Definition	Units
a	Molar Helmholtz energy	$J.mol^{-1}$
$a, b, c, d, e, f/c_1, c_2, c_3, c_4, c_5$	Parameters for MTS EOS	Individual units defined in text
a	Fitting parameter in BWRS EOS	-
A	Fitting parameter in Tait	m^3
A_0	Fitting parameter in BWRS EOS	$m^3.kg^{-1}$
b	Fitting parameter in BWRS EOS	-
B	Fitting parameter in Tait	kPa
B_0	BWRS EOS	$J.m^3.kg^{-1}\ mol^{-1}$
c	Fitting parameter in BWRS EOS	-
C_0	Fitting parameter in BWRS EOS	$m^3.kg^{-1}.T^2$
D_0	Fitting parameter in BWRS EOS	$m^3.kg^{-1}.T^3$
E_0	Fitting parameter in BWRS EOS	$m^3.kg^{-1}.T^4$
m	segment number in SAFT-based equations	-
m	Mass	kg
M	Molar Mass	$kg.kmol^{-1}$
n	Moles	mol
P	Pressure	MPa
R	Universal gas constant	$J.mol^{-1}.K^{-1}$
T	Temperature	K
V	Volume	m^3
V^E	Excess Molar Volume	m^3/mol

v^{∞}	temperature-independent segment volume, in SAFT-based equations	m^3/mol
x_i	Mole fraction	-
Greek symbols		
α_P	Thermal Expansivity	K^{-1}
Δ	change in	
Δ^{AB},	strength of interaction between two sites A and B	$Å^3$
ε/k	dispersion energy of interaction between segments in SAFT-based equations	K
ε^{AB}/k	association energy of interaction between sites A and B	K
γ	Fitting parameters for BWRS	-
κ_T	Compressibility	kPa^{-1}
κ^{AB}	the effective association volume	-
ω	Acentric factor	-
σ	temperature independent segment diameter	Å
Π	Parameter in Tait equation	kPa
ρ	Density	$kg.m^{-3}$
Superscripts		
assoc	Association contribution	
calc	Calculated value	
chain	Chain contribution	
disp	Dispersive contribution	

exp	Experimental value	
hs	Hard sphere contribution	
ind	Induced dipole contribution	
polar	Polar contribution	
res	Residual contribution	
Subscripts		
1	Component 1	
2	Component 2	
i	Component *i*	

Note: The intermediate parameters and properties used in the equations of state and models are numerous and hence defined within Chapter 3: Thermodynamic Background with the equations.

CHAPTER ONE

Introduction

Thermophysical properties are utilized in various engineering applications and enable the design and optimization of chemical processes (Zúñiga-Moreno *et al.*, 2007). The accurate description of these properties by experiment, over various temperature and pressure ranges, is necessary for the development of equations of state and predictive models which provide insight into the behaviour of chemical systems and hence chemical processes (Yang et al., 2018). An essential thermophysical property is the liquid mass density, or the ratio of the mass of the liquid (m), to the volume (V) the liquid occupies. Density data is utilized extensively in various flow calculations for the precise design of pipelines and in most other unit operation design commonly employed in industry (Moodley et al., 2018). High-pressure liquid density data is also employed extensively in the field of petroleum engineering where the prediction of high-pressure liquid density is essential to classify the quality and composition of oils present in ultra-deep reservoirs for recovery, and also finds uses in aeronautics, car engine design, and the design of submarines (Wu, 2010). Chemical processes operating under extreme conditions of pressure such as approaching the supercritical region are becoming more common in industry (Economou, 2002).

Experimental data describing high-pressure liquid density can be used directly to achieve the accurate design goals. This can however be difficult to obtain, for instance, when multicomponent systems are considered. A more practical approach is to develop quantitative mathematical models that can describe high-quality high-pressure liquid density over wide temperature and pressure ranges, in order to gain further understanding regarding the behaviours exhibited by systems at high pressures (Hellström et al., 2017).

Equations of state are extensively employed in chemical thermodynamic research to demonstrate the relationship between state functions, such as pressure (P) and temperature (T), in a fluid system (Al-Malah, 2015). The virial equation of state (Onnes, 1901) was the first attempt to predict the phase behaviour of systems constituting supercritical components but was, unsuccessful at elevated pressures (Valderrama, 2003).

Since the development of the van der Waals cubic equation of state (EoS) (Van der Waals, 1873), various complex equations of state have been proposed in the literature, that can accurately predict and represent *PVT* properties and phase equilibria for many systems.

Redlich and Kwong (1948) proposed modifications to the original attractive term present in the van der Waals equation of state. While retaining the original hard-sphere term present within the van der Waals equation, the Redlich-Kwong equation of state introduces an attractive term that depends on temperature (Wei and Sadus, 2000). Several studies, (Zudkevitch and Kaufmann, nd; Carnahan and Starling, 1972; Mulholland, 1973), demonstrate the improvement of the Redlich-Kwong equation when compared to the original van der Waals equation. A study conducted by Spear et al. (1969) highlights the suitability of this equation for the computation of critical properties in binary mixtures. The mixtures constituted paraffin-paraffin mixtures, hydrocarbon mixtures containing non-paraffin hydrocarbons, hydrocarbon-non-hydrocarbon systems and non-hydrocarbon mixtures. Furthermore, a maximum error of 30 % was noted for hydrocarbon-non-hydrocarbon system when the interaction parameter was omitted while an error of 23 % was noted for the paraffin-paraffin system when employing the optimum interaction parameter. In addition, Chueh and Prausnitz (1967) showed how the Redlich-Kwong equation of state can be applied to predict properties in both the vapour and liquid phase for hydrocarbon-hydrocarbon and hydrocarbon-non-hydrocarbon mixtures with a maximum deviation of 2.8 % being noted. Studies conducted by Deiters and Schneider (1976) as well as Baker and Luks (1980) both demonstrated the applicability of the Redlich-Kwong equation to predict the phase equilibria of binary systems, consisting of hydrocarbon-non-hydrocarbon systems, at high pressures. Furthermore, both studies demonstrate the applicability of the Redlich-Kwong equation to the critical properties of these systems. Soave (1972) presented a modification of the original Redlich-Kwong equation through the introduction of a generalized attractive term, dependent on temperature. This modification enabled the model to describe phase behaviour of mixtures, close to the critical region. In addition, Soave's modification demonstrated improved accuracy in the computation of critical properties for mixtures constituting hydrocarbon/non-hydrocarbon-hydrocarbon/non-hydrocarbon components (Elliott and Daubert, 1987). Maximum deviations of 8.92 %, 37.62 %, 44.92 % were reported for the critical temperature, critical pressure, and critical volume, respectively.

Peng and Robinson (1976) presented another modification of the original van der Waals equation of state (PR-EOS) that redefined the temperature-dependent attractive term and the critical compressibility factor, overestimated by the Redlich-Kwong equation. This equation showed improvements in the values calculated for both the liquid volumes and critical compressibility factor (Wei and Sadus, 2000). During the development of the model, Peng and Robinson (1976), illustrated the applicability of PR-EOS to effectively predict several properties such as the vapour pressure, equilibrium ratios as well as multicomponent system behaviours. The mixtures consisted of hydrocarbon and non-hydrocarbon components with temperature and pressure ranges of -394-633 K and 1.3 MPa-27.6 MPa, respectively. The Soave-Redlich-Kwong and Peng-Robinson equations of state are often used in industry as they can suitably predict relations between state functions.

The phase behaviour and thermophysical properties of liquid mixtures are generally significantly affected by molecular association especially in oxygenated hydrocarbon systems. This may include self-association or cross-association. Molecules with association potential include most oxygenated components such as alcohols, ketones and aldehydes. Although cubic equations of state generally form the basis of predictive models for phase and thermophysical properties of high-pressure systems, prediction results are often poor in hydrogen bonding/associating systems at high pressures (de Villiers, 2011; Sadus, 1992; Peng *et al.*, 1994; Tumakaka, Gross and Sadowski, 2005; Vargas *et al.*, 2009). An alternative predictive method is the application of Statistical Associating Fluid Theory (SAFT) (Chapman et al., 1989), an extension of Wertheim's theory (1984a, 1984b, 1986a, 1986b), which employs statistical mechanical methods to characterize mixture behaviours by accounting for the hard-sphere repulsive forces, association, dispersion forces and chain formation, applicable to molecules that are non-spherical.

To date, several variations of the SAFT models exist that account for hard-chain contributions. However, one of the most widely applied is the perturbed chain SAFT (PC-SAFT) equation, proposed by Gross and Sadowski (2001, 2002). The PC-SAFT model and extensions such as the perturbed chain polar SAFT model (PC-PSAFT) can be employed to characterize systems consisting of dipolar, dipolar + induced polar, quadrupolar, polarizable dipoles and dipole + polarizable compounds (Kontogeorgis and Folas, 2010). Hence, the PC-SAFT equation of state is

extremely useful for the prediction of thermodynamic properties of polar-associating systems such as those comprised of alcohol constituents as they exhibit polar-association.

The truncated Perturbed Chain-Polar Statistical Associating Fluid Theory (tPC–PSAFT) (Karakatsani *et al.*, 2006; Karakatsani *et al.*, 2006) model is a simplified version of the perturbation expansion for polar interactions (Karakatsani et al., 2005). The advantage of the tPC–PSAFT model is that it has been shown to improve on the performance of the original PC-SAFT for associating mixtures, while having a simpler computational requirement than the original PC-PSAFT model (Karakatsani et al., 2005) . The tPC–PSAFT model has been employed to correlate the vapour-liquid equilibrium of methanol and n-alkane systems (Karakatsani and Economou, 2007), and can also predict liquid-liquid equilibrium, heat capacities and azeotropic compositions for a variety of polar-associating mixtures (Kontogeorgis and Folas, 2009). Studies conducted at high pressures (Song et al., 2014; Zhang et al., 2015), have employed the tPC-PSAFT model for the prediction of densities however, rigorous investigation into the performance for polar-associating systems has not been conducted to this regard.

The aim of this work was to determine the effectiveness of the tPC-PSAFT model to predict the density of mixtures containing associating species at pressures of 0.1-20 MPa and 313 to 353 K. The systems selected were based on a few factors including new interest on the effectiveness of C4 alcohols as drop-in biofuels for blends with conventional transport fuels such as n-alkanes in the C8-C10 range (Trindade and dos Santos, 2017). n-Alkanes were selected as representative components for petroleum derived fuels, while butan-1-ol, butan-2-ol, 2-methylpropan-1-ol were chosen as representative biofuels. Further, a study conducted by Chen and Zhao (2015) supports the use of middle carbon alcohols in enhanced oil recovery methods as they enhance the sweep and displacement efficiencies. In addition, several studies (Anderson and Prausnitz, 1986; Hammerschmidt, 1939; Kapateh et al., 2016; Masoudi and Tohidi, 2005; Munck et al., 1986; Nihous et al., 2010, 2009) have reported the effectiveness of employing alcohols to inhibit the formation of gas hydrates. Alcohols are also used as a gasoline additive as they improve the octane rating of the fuel (Brownstein, 2015). These application all require the mixture characterization at elevated pressures.

Since the relevant data for these systems did not previously exist in the literature, an objective of this work was to measure the densities for the novel systems of butan-1-ol/butan-2-ol/2-

methylpropan-1-ol + n-octane/n-decane utilizing an Anton Paar DMA HP densimeter connected to a pressurizing circuit that incorporated a Teledyne ISCO 100 DM high-pressure pump and a WIKA P-10 pressure transducer. The temperature and pressure ranges were 313-353 K and 1-20 MPa, respectively. The derived properties of thermal expansivity and isothermal compressibility of the mixtures have also been determined at these conditions. The experimental data was then regressed by various models, as well as compared to predictions by the tPC-PSAFT model for the wide pressure range of application considered in this work. Comparisons to additional correlations and models were also performed to assess the relative effectiveness of the model's capability.

In Chapter 2 of this work, a brief review of the literature of similar alcohol + alkane density measurements available in the literature is presented. Chapter 3 provides a thermodynamic background of the principles governing the behaviour of high-pressure density, and the models available in the literature to describe this behaviour. In Chapter 4, an equipment review for high pressure density measurements is presented, while the procedure and equipment description used in this work is described in Chapter 5. The experimental data measured are presented in a series of 3 data publications in Chapter 6-8. In Chapter 9, culminating results are presented, with a culminating discussion in Chapter 10. Because portions of this thesis are presented in manuscript format, a degree of repetition exists among chapter which could not be avoided to allow these sections to stand alone.

CHAPTER TWO

Literature review

An objective of this study was to assess the effects of temperature, pressure and composition on the density of alcohol + alkane mixtures, from both an experimental and thermodynamic model perspective. The densities of alcohol + alkane mixtures are well-studied in the literature at atmospheric pressure and ambient temperatures, but fewer studies are available at elevated temperatures and pressures. A survey of the literature was conducted to establish deficits in the literature, which were then addressed to an extent with an experimental study in this work.

2.1. Similar systems reported in the literature

Systems constituting alcohol-alkane mixtures have been extensively studied and are available in literature. These literature studies are summarized in Table 2.1. It is clear that measurements above atmospheric pressure for alcohol + alkane systems is limited in the literature.

Table 2.1. Similar alcohol-alkane systems measured in literature.

Component 1	Component 2	Temperature Range (K)	Pressure Range (MPa)	Device	Uncertainty	Reference
ethanol	n-heptane	293 - 318	10 - 90	Vibrating tube densimeter	$\pm 5x10^{-2}\,\frac{\mathrm{kg}}{\mathrm{m^3}}$	(Dzida and Marczak, 2005)
benzene, cyclohexane, ethanol	n-alkanes and alkanols	298.15	0.1	Paar digital precision density meter, Model DMA O2C	1.58430 -1.58451 $\frac{\mathrm{g}}{\mathrm{mL}}$,	(Edward et al., 1979)
1-alkanol	n-heptane	298	0.1	Anton Paar DMA-602 densimeter	$\pm 4x10^{-7}\,\frac{\mathrm{g}}{\mathrm{cm^3}}$	(El-Hefnawy et al., 2005)
ethanol	n-alkanes	288.15 – 323.15	0.1		< 10 %	(Gayol et al., 2007)
benzene	ethanol, n-heptane	298	0.1	Vibrating tube densimeter	$\pm 5x10^{-6}\,\frac{\mathrm{g}}{\mathrm{cm^3}}$	(Kouris and Panaylotou, 1989)
alkanols	n-heptane	298.15	0.1	Tilting dilution dilatometer	$\pm 0.0014\,\frac{\mathrm{cm^3}}{\mathrm{mol}}$	(Kumaran and Benson, 1983)
n-heptane, ethanol, methylcyclo-pentane	n-heptane, ethanol, methylcyclo-pentane	298.2 – 348.2	0.1 – 196.2	-	± 2 %	(Ozawa et al., 1980)

ethanol, 2, 2,s-trimethyl-pentane	n-heptane, 2-propanone	288.15 – 308.15	0.1-34	Vibrating tube densimeter	$\pm 1x10^{-4}\ \frac{g}{cm^3}$	(Papaioannou et al., 1991)
ethanol, propan-2-ol	n-hexane, n-heptane, butan-2-one, cyclohexane, ethylacetate	293.15-303.15	0.1	Vibrating tube densimeter	$\pm 2x10^{-4}\ \frac{g}{cm^3}$	(Pereiro and Rodríguez, 2007)
methanol, ethanol, propan-1-ol, butan-1-ol	n-heptane	298.15	0.1	Oscillator type densimeter and micrometer-syringe dilatometer	$\pm 2x10^{-5}\ \frac{g}{cm^3}$	(Treszczanowicz and Benson, 1977)
diisopropyl ether, ethanol	butan-1-ol, diethyl ketone, n-heptane	278.15-323.15	0.1-60	Vibrating tube densimeter	$\pm 5x10^{-5}\ \frac{g}{cm^3}$	(Ulbig et al., 1997)
ethanol	n-heptane	293.15-333.15	0.1-65	Vibrating tube densimeter	$\pm 0.5\ \frac{kg}{m^3}$	(Watson et al., 2006)
ethanol propan-1-ol	heptane, propan-1-ol	313.15	0.1	Dilution dilatometer	$\pm 0.0001\ \frac{g}{cm^3}$	(zielkiewicz, 1993)
ethanol, propan-1-ol, butan-1-ol, pentan-1-ol	n-octane	293.15-323.15	0.1	Vibrating tube densimeter	$\pm 3x10^{-2}\ \frac{kg}{m^3}$	(Estrada-Baltazar et al., 2013)
methanol, ethanol	n-hexane, n-heptane, n-octane	303.15-318.15	0.1	Anton Paar DSA-48 density and sound analyzer	$\pm 9x10^{-3}\ \frac{cm^3}{mol}$	(Orge et al., 1999)
ethanol	n-octane	298.15	0.1	DMA 60/602 densimeter	$\pm 1x10^{-5}\ \frac{g}{cm^3}$	(Segade et al., 2003)

ethanol	n-decane, n-octane, n-hexane	273.15-298.15	0.1	Anton Paar SVM 3000 digital oscillation U-tube	$\pm 0.0005 \frac{\mathrm{g}}{\mathrm{cm}^3}$	(Feitosa et al., 2009)
ethanol	n-decane	303.2-323.2	0.1-10	Anton Paar DMA HPM vibrating tube densimeter	$\pm 0.1 \frac{k\mathrm{g}}{\mathrm{m}^3}$	(Kariznovi et al., 2013)
ethanol	n-decane, n-undecane	278.15-308.15	0.1	Anton Paar DSA48 vibrating tube densimeter	$\pm 1x10^{-4} \frac{\mathrm{g}}{\mathrm{cm}^3}$	(Peleteiro et al., 2005)
ethanol	decane	313-363	1-20	Anton Paar 60/512P vibrating tube densimeter	$\pm 0.2 \frac{k\mathrm{g}}{\mathrm{m}^3}$	(Zamora-López et al., 2012)
cyclohexylamine, n-heptane	butan-1-ol, n-heptane	283.15-323.15	0.1	Vibrating tube densimeter	$\pm 1x10^{-5} \frac{\mathrm{g}}{\mathrm{cm}^3}$	(Kijevčanin et al., 2009)
butan-1-ol	carbon tetrachloride, 2, 2, 4-trimethylpentane, hexane, heptane, octane, pentane	288.15-298.15	0.1	Dilatometer	$\pm 2x10^{-5} \frac{\mathrm{g}}{\mathrm{cm}^3}$	(Nath and Pandey, 1997)
propan-1-ol, butan-1-ol	n-heptane	298.15-308.15	0.1	bicapillary pycnometer	$\pm 0.0001 \frac{\mathrm{g}}{\mathrm{cm}^3}$	(Sastry and Valand, 1996)
hexan-1-ol, octan-1-ol, butan-1-ol	n-heptane	288.15-308.15	0.1	Vibrating tube densimeter	$\pm 5x10^{-5} \frac{\mathrm{g}}{\mathrm{cm}^3}$	(Vijande et al., 2006)

butan-1-ol	n-heptane	316.85-458.15	4.93	pycnometer	$\pm 0.99 \frac{\text{kg}}{\text{m}^3}$	(Westwood and Kabadi, 2003)
butan-1-ol	n-octane	288.15-308.15	0.1	Anton Paar DSA-48 densimeter and sound analyzer	$\pm 2x10^{-2} \frac{\text{cm}^3}{\text{mol}}$	(Cominges et al., 2002)
butan-1-ol, pentan-1-ol	n-octane, water, sodium dodecylsulfate	288.15-308.15		Vibrating flow densimeter	-	(Chemistry and June, 1984)
n-octane	butan-1-ol, hexan-1-ol, octan-1-ol	298.15	0.1	Anton Paar Model DMA 601602 densimeter	$\pm 0.007 \frac{\text{cm}^3}{\text{mol}}$	(Franjo et al., 1995)
n-octane	propan-1-ol, butan-1-ol, pentan-1-ol			Kyoto Electronics DA-210 densimeter	$\pm 0.001 \frac{\text{cm}^3}{\text{mol}}$	(Iglesias et al., 1993)
butan-1-ol	n-hexane, n-octane, n-decane	298.15	0.1	Anton Paar DSA-5000 U-tube densimeter	$\pm 2x10^{-3} \frac{\text{kg}}{\text{m}^3}$	(Dubey et al., 2008)
n-propanpl, n-butanol, n-pentanol, n-hexanol	n-octane, n-decane, n-dodecane	298.15		Batch dilatometer	$\pm 0.009 \frac{\text{cm}}{\text{mol}}$	(Kaur et al., 1991)
methyl-tert-butyl ether, butan-1-ol	n-decane	298.15		Anton Paar DSA-48 densimeter	$\pm 5x10^{-5} \frac{\text{g}}{\text{cm}^3}$	(Piñeiro *et al.*, 2003)
butan-1-ol, ethanol, hexan-1-ol	n-decane, n-hexadecane, n-hexane	298.15	0.1	Vibrating tube densimeter	-	(Roux et al., 1993)

butan-1-ol, 2-methylpropan-1-ol	n-heptane	298.15-363.15		Anton Paar DMA 60 densimeter	$0.00002\,\frac{\mathrm{g}}{\mathrm{cm}^3}$	(Berro and Pneloux, 1984)
propan-1-ol, butan-1-ol, 2-methylpropan-1-ol	n-heptane	298.15-343.15	0.1-250	-	$\pm 0.015\,\frac{\mathrm{cm}^3}{\mathrm{mol}}$	(Oswald et al., 1986)
butan-2-ol	n-octane, n-decane, n-dodecane	293.15-303.15	0.1	Anton Paar DSA-5000 vibrating tube densimeter	$\pm 2x10^{-6}\,\frac{\mathrm{g}}{\mathrm{cm}^3}$	(González et al., 2004)
butan-1-ol	n-heptane	283.15-323.15	0.1	Anton Paar DMA-5000 vibrating tube densimeter	$\pm 5x10^{-6}\,\frac{\mathrm{g}}{\mathrm{cm}^3}$	(Kijevčanin et al., 2009)
propan-2-ol, butan-2-ol, pentan-2-ol, pentan-3-ol, 2-methylbutan-2-ol	n-heptane			Vibrating tube densimeter	$\pm 2x10^{-5}\,\frac{\mathrm{g}}{\mathrm{cm}^3}$	(Tanaka and Toyama, 1996)
butan-2-ol	n-heptane	293.15-308.15	0.1	Anton Paar densimeter	$\pm 0.02\,\frac{k\mathrm{g}}{\mathrm{m}^3}$	(Wieczorek, 1984)
2-methylpropan-1-ol	n-octane, n-decane, n-hexane	298	0.1	pycnometer	$0.0002x10^3\,\frac{k\mathrm{g}}{\mathrm{m}^3}$	(Dubey and Sharma, 2007)
2-methylpropan-1-ol, butan-1-ol, butan-2-ol	n-octane	298.15-299.15	0.1	Dilution dilatometer	$\pm 0.002\,\frac{\mathrm{cm}^3}{\mathrm{mol}}$	(Chaudhari and Katti, 1985)

2.2.Polarity, intermolecular forces and their effect on mixture densities

2.2.1. Polar components

Bond polarity measures the distribution of electrons shared between two atoms that form a bond and is proportional to the electronegativity between these atoms (Brown et al., 2010). The dipole moment described in Figure 2.1 measures the distribution of charge in a molecule and, for polyatomic molecules, it is influenced by the individual bond polarities as well as the shape of the molecule. Furthermore, the term bond dipole quantifies the dipole moment existing only between the two atoms forming a bond. Both the bond dipole and dipole moment are vector quantities and hence require special attention when summed. For molecules comprising two or more atoms, the dipole moment is equivalent to the vector summation of all the bond dipoles present and if the given sum is zero the molecule is non-polar. Molecules that exhibit a non-zero dipole moment are called polar molecules.

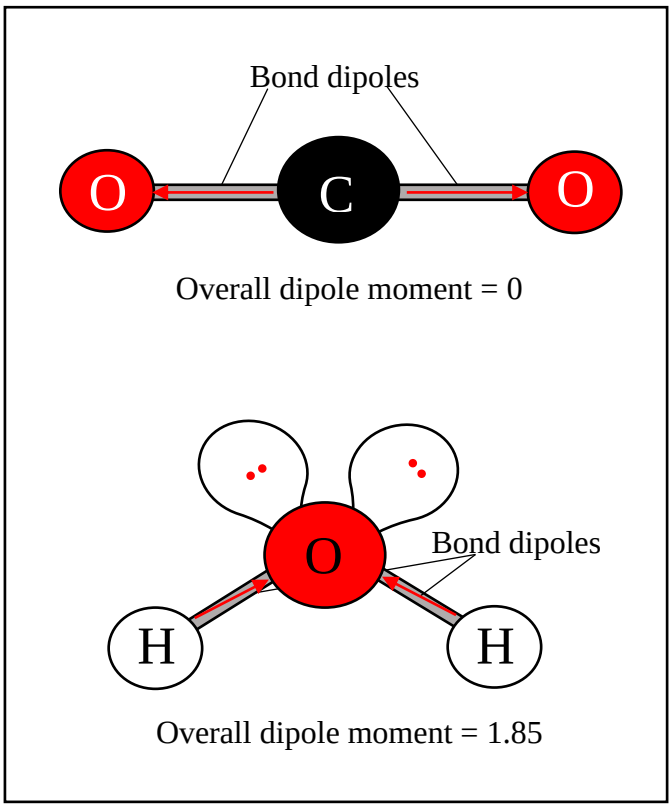

Figure 2.1. Non-polar and polar molecules. Redrawn from (Brown et al., 2010).

2.2.2. Intermolecular forces

Intramolecular forces hold atoms in molecules and polyatomic ions together. They constitute covalent bonds and influence the chemical behaviour, such as, the shape of molecules and the bond energy of molecular substances (Brown et al., 2010). Physical properties, however, are influenced by intermolecular forces that exist between molecules. Properties, such as, the boiling temperature of a liquid demonstrate the strength of the intermolecular force present. Liquids that exhibit stronger attractive forces will therefore boil at a higher temperature. For a non-ionic molecule, there are three common intermolecular forces that exist, namely, London dispersion, dipole-dipole and hydrogen-bonding forces. In solutions consisting of ionic substances, ion-dipole forces, a variation of attractive forces, is influential and hence considered. These forces involve attraction between positive and negative components or molecular regions and are considered electrostatic forces.

2.2.2.1. Dipole-dipole forces

When the positive and negative ends of neutral polar molecules are in close proximity to each other, they attract each other forming dipole-dipole forces (Brown et al., 2010) as shown in Figure 2.2. These forces are often weaker than ion-dipole forces and are usually only effective if polar molecules are near each other. A general trend observed for liquids, comprising molecules of similar size and mass, is that molecules exhibiting a greater attractive intermolecular force generally constitute molecules with a high polarity. Furthermore, the dipole-dipole attractive forces, for molecules exhibiting small volumes, are generally strong when present.

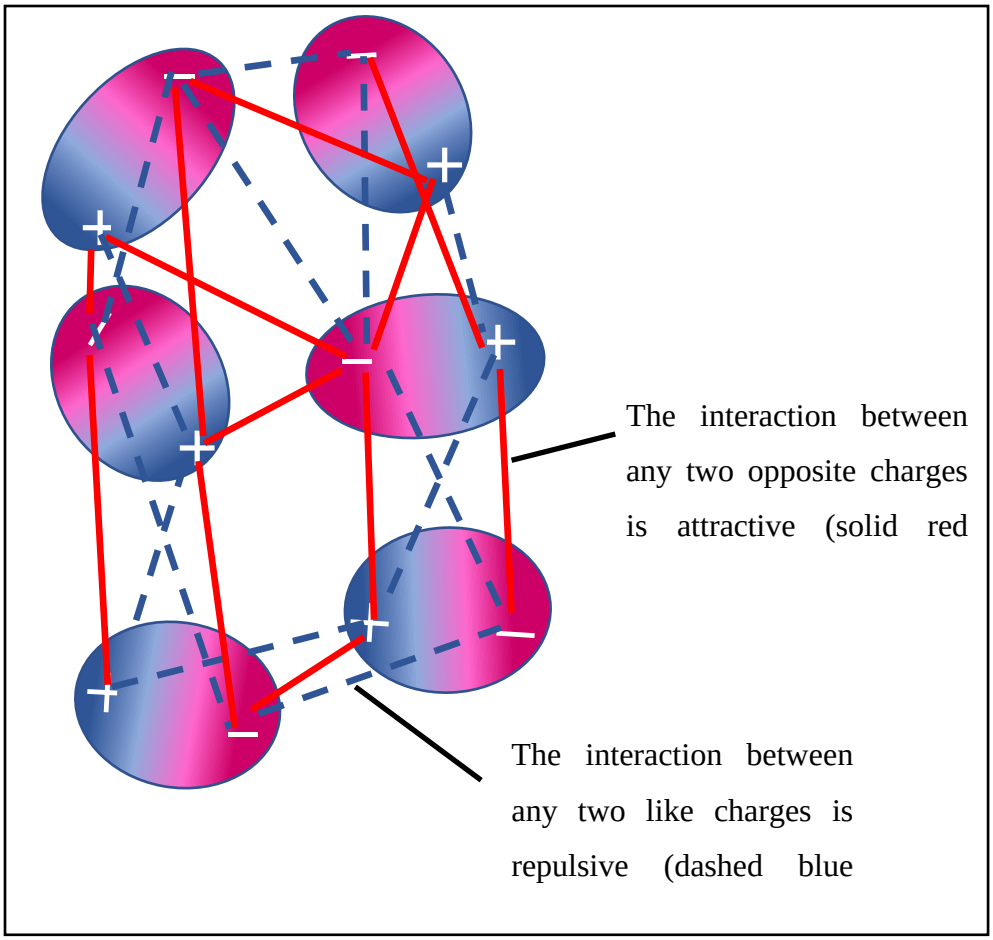

Figure 2.2. Dipole-Dipole Forces. Redrawn from (Brown et al., 2010).

2.2.2.2. Ion-dipole forces

The force of attraction that occurs among the partially charged end of a molecule, considered to be polar, and an ion is referred to as ion-dipole forces as shown in Figure 2.3. Polar molecules consist of dipoles with positive and negative ends (Brown et al., 2010). When positive ions interact with the negative end of the dipole, or vice-versa for negative ions, ion-dipole forces arise. The charge of the ion and the dipole moment both influence the strength of the attractive force. An increase in either of these two factors increases the strength of the attraction.

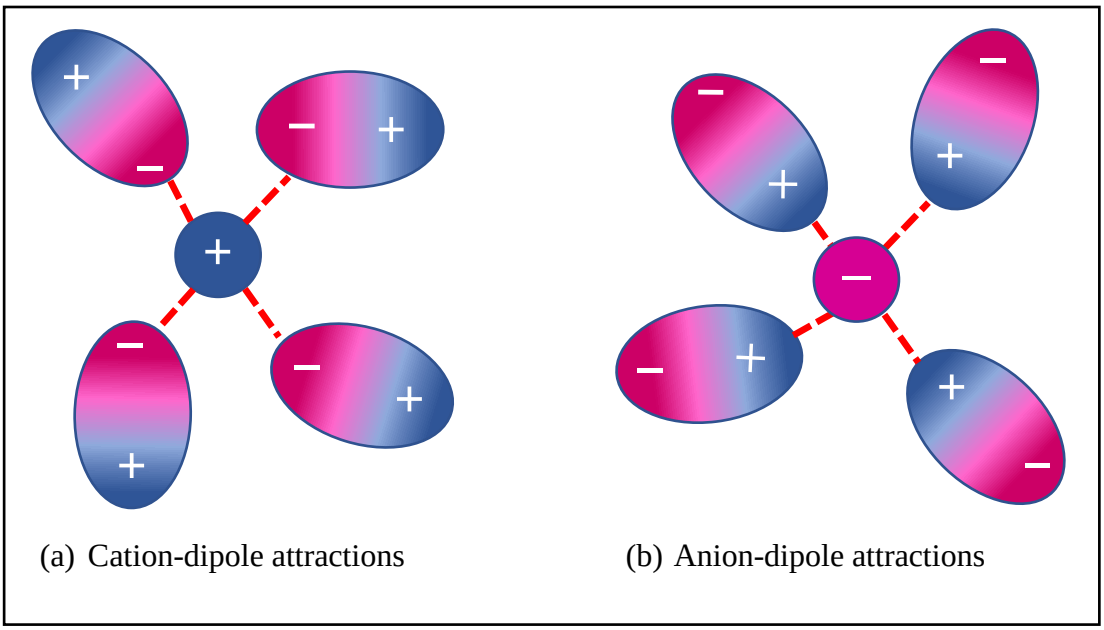

Figure 2.3. Ion-Dipole Forces. Redrawn from (Brown et al., 2010).

2.2.2.3. London dispersion forces

Dipole-dipole forces do not exist between non-polar atoms or molecules. However, since the liquefaction of non-polar gases is possible, it can be concluded that another type of attractive force occurs. London (1930) observed that the instantaneous distribution of electrons can differ from the average distribution thereby inducing an instantaneous dipole moment as shown in Figure 2.4. Since like forces repel, the electron movement in one atom/molecule affects the electron movements in the adjacent atoms/molecules. Hence, a momentary dipole induced on one atom/molecule can cause neighbouring atoms/molecules to exhibit a similar momentary dipole, thereby resulting in attraction between atoms/molecules. (Brown et al., 2010) The attractive force existing between these atoms/molecules is referred to as London dispersion forces and is apparent when atoms/molecules are near each other.

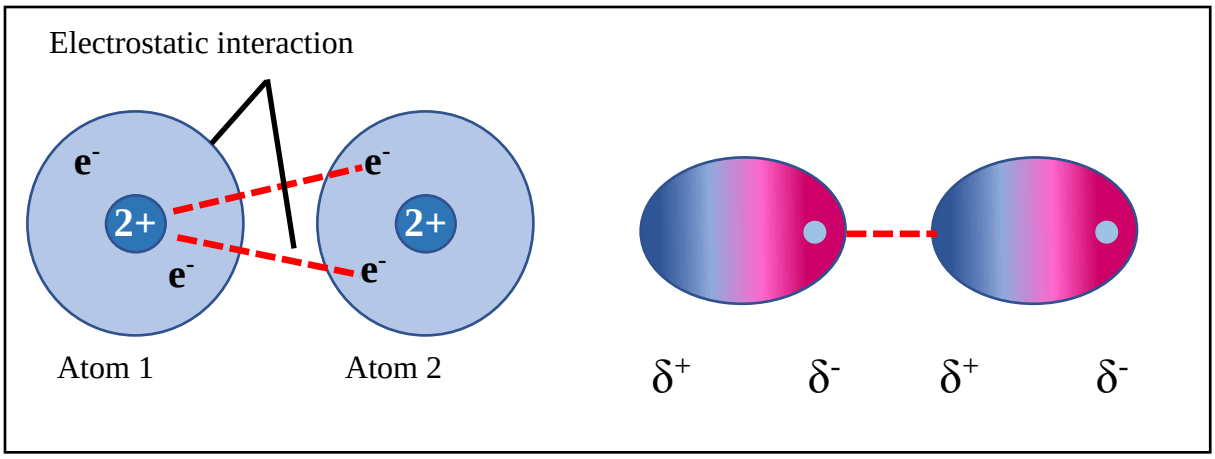

Figure 2.4. London Dispersion Forces. Redrawn from (Brown et al., 2010).

The instantaneous dipole induced on non-polar atoms/molecules is caused by a distortion of the electron dispersion which greatly affects the strength of the attractive interactions. Polarisability refers to the fluency of the distortion of the electron cloud and is greater when distortion of the electron dispersion is effortless. It is influenced by the molecular size and is greater for molecules that are larger in size as they comprise of more electrons that are widely spread away from the nucleus. Hence, as the molar mass of a species increases, the strength of the attractive interactions and thus, the London dispersion force, increases. The strength of this type of force is also influenced by molecular shape and tends to be lower for more compact and spherical molecules. Dispersion forces exist between polar and non-polar molecules, such as alcohols and alkanes, and, in polar molecules, they account for the majority of the attractive interactions that occur.

2.2.2.4. Hydrogen bonding

The intermolecular force of attraction occurring between a lone pair of electrons on an atom/ion considered to be electronegative and a hydrogen atom in a polar bond is called a hydrogen bond. (Brown et al., 2010). These bonds are a special type of dipole-dipole interaction and are significantly stronger than dipole-dipole or London dispersion attractions. They usually occur when hydrogen bonds to either fluorine, nitrogen or oxygen. The strength of this type of bond can be attributed to the absence of core electrons in the hydrogen atom thereby causing a concentration of charge, by the partially exposed proton in the hydrogen atoms nucleus. Hence, the positive

hydrogen atom is attracted to the electronegative atom/ion. The minute size of the hydrogen atom enables it to come into close proximity with the electronegative atom/ion thereby resulting in a powerful force of attraction. In alcohol systems such as C4 alcohols, hydrogen bonding can occur by self-association with other alcohol molecules as shown in Figure 2.5.

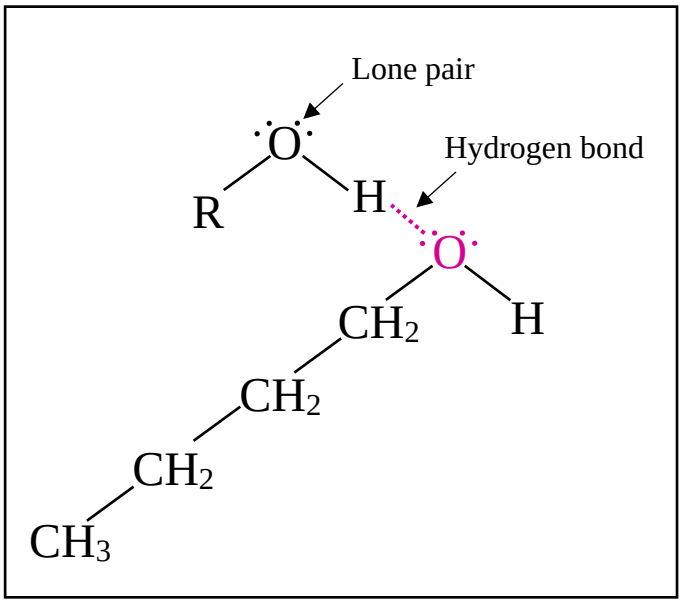

Figure 2.5. Hydrogen bond in butan-1-ol. Redrawn from (Brown et al., 2010).

CHAPTER THREE

Thermodynamic background

A brief description of the thermodynamic background for density as well as the models used in this work is described in this chapter.

3.1. Definition of density of a fluid

Mass density is the relation between the mass and volume of a substance. It can be calculated as follows (Smith et al., 2001):

$$\rho = \frac{m}{V} \tag{3.1}$$

Where, ρ is the density in kg.m^{-3}, m is the mass (kg) and V is the volume (m^3).

The molar density is similarly defined by replacing mass in equation (3.1) with number of moles (n):

$$\rho_n = \frac{n}{V} \tag{3.2}$$

Where, ρ_n is the density in kmol.m^{-3}, n is the moles (kmol) and V is the volume (m^3). The reciprocal of equation (3.2) is the molar volume V_m in m^3.kmol^{-1}.

It follows from equation (3.1) and (3.2) that:

$$\rho = \rho_n M = \frac{M}{V_m} \tag{3.3}$$

Where M is the molar mass in kg.kmol^{-1}

Density is used extensively in fluid mechanics for flow calculations and in thermodynamics for P-V-T relations, and hence, its precise characterization is of vital importance for the design and simulation of process units, pumps and pipelines. The density of a pure substance depends on the

temperature and pressure of the system, while composition is an additional influencing factor for mixtures. It is generally inversely proportional to temperature and directly proportional to pressure and is generally significantly non-linear at constant temperature and pressure for non-ideal mixtures. Several developments in the equipment utilized for accurate density measurements at both atmospheric and high pressures are available in the literature and will be discussed in Chapter 4.

3.2. Derived properties from ρ-P-T-x_i data

The influence of temperature, pressure and composition on the densities of mixtures can be very difficult to interpret and hence are usually characterized by exact thermodynamic relations.

3.2.1. Excess molar volumes

Densities of mixtures behave uniquely, especially in systems that are regarded as non-ideal, such as mixtures of non-polar and polar/hydrogen bonding liquids. This is because linear mixing of the constituent pure component densities does not usually occur in such mixtures, due to intermolecular forces between the non-polar and polar/hydrogen bonding liquids. This departure from ideality is quantified by an excess property i.e. the excess molar volume V_m^E.

The excess molar volume of a mixture is defined as the difference between the actual mixture volume and the volume the mixture would occupy as an ideal solution at the same temperature, pressure and composition. It is calculated by the following equation (interpreted from Smith et al., 2001):

$$V_m^E = \sum_{i=1}^{N} x_i M_i \left(\frac{1}{\rho} - \frac{1}{\rho_i}\right) \tag{3.4}$$

Where, N is the total number of components making up the mixture, M_i is the molecular mass of component i, x_i is the mole fraction of component i, ρ is the mixture density and ρ_i is the density of pure component i.

As mentioned, excess molar volumes are attributed to molecular interactions between the species constituting the mixture. For negative excess volumes the mixture volume is less than that of the ideal solution due to close or efficient packing of the molecules as well as attractive forces between the two chemical species while the opposite is true for mixture exhibiting positive excess volumes. The excess volume is often utilized to determine the effect of temperature and pressure on the properties of a system and thus helps give insight into the behaviour of the mixture.

3.2.2. Isobaric thermal expansivity

Isobaric thermal expansivity is defined as the differential change in volume with temperature at constant pressure and describes cross correlations between the enthalpy and volume of a system (Troncoso et al., 2011). It finds application in many engineering calculations such as pipeline and vessel design, riveting and the construction of bimetallic strips utilized in thermostats. The isobaric thermal expansivity usually exhibits an inversely proportional relationship to pressure except near the critical point. and a directly proportional relationship to temperature for systems at low pressures. However, the opposite is true for systems at elevated pressures. The isobaric thermal expansivity can be calculated utilizing the following formula (Troncoso et al., 2011):

$$\alpha_P = -\frac{1}{\rho}\left(\frac{\partial \rho}{\partial T}\right)_P \tag{3.5}$$

Where, α_P (K^{-1}) is the thermal expansivity at constant pressure, P, and ρ is the density of the mixture in $kg.m^{-3}$ and T is the temperature in kelvin.

3.2.3. Isothermal compressibility

Isothermal compressibility is defined as a differential change in volume with pressure at constant temperature and is the measure of fluctuations that occur in the volume of a component (Troncoso et al., 2011). In liquids, the isothermal compressibility displays a monotonic behaviour since it is related to volume fluctuations which are small except near the critical point or for systems at low

pressures. It is generally characterized as being inversely proportional to pressure and directly proportional to temperature, except near the critical point (Troncoso et al., 2011).

The isothermal compressibility can be calculated utilizing the following formula:

$$\kappa_T = \frac{1}{\rho}\left(\frac{\partial \rho}{\partial P}\right)_T \tag{3.6}$$

Where, κ_T (kPa^{-1}) is the compressibility at constant temperature, *T*.

3.3. Empirical models to represent density of pure components and mixtures

3.3.1. Tait equation

The Tait equation is commonly utilized for the correlation of liquid density data over large ranges of pressure. It was proposed in 1888 by Peter Guthrie Tait while conducting his study on the compressibility, at varying pressures, of sea and fresh water (Dymond and Malhotra, 1988). The success of the equation is due to its efficiency in representing high-pressure results for solids, liquids and dense gases (Dymond and Malhotra, 1988). The original equation formulated by Tait is given as follows:

$$\frac{V_0 - V}{PV_o} = \frac{A}{\Pi + P} \tag{3.7}$$

Where, V_o is the volume at atmospheric pressure and *A* and *Π* are model fitting parameters.

The above equation however, fits data to a hyperbola instead of a straight line which can be obtained through inversion as pointed out by Hayward (1967). Furthermore, Hayward (1967) suggests that by inverting equation (3.7) the linear pressure equation relating to the secant bulk modulus can be obtained, under constant temperature conditions.

$$\frac{PV_o}{V_0 - V} = \frac{\Pi}{A} + \frac{P}{A} \tag{3.8}$$

The equation presented in equation (3.8) has been successfully employed by Couchman and Reynolds (1976) as well as Stewart (1956) to correlate solid compressibility data for pressure ranging to a few gigapascals. In addition, for organic liquids, equation (3.8) provides satisfactory results up to 150-200 MPa (Dymond and Malhotra, 1988).

A modification to the Tait equation was proposed by Tammann (1895). The modification employs a coefficient of a differential nature that replaces the average compressibility and is given by:

$$\frac{\Delta V}{\Delta P} = \frac{A}{B + P} \tag{3.9}$$

Inversion of this equation gives the mixed-modulus equation that is of a linear nature.

Integration of (3.9) gives (3.10) as suggested by Tammann (1895).

$$V = V_o \left[1 - \frac{Aln(B + P)}{B}\right] \tag{3.10}$$

This was later re-arranged to give the well-known form of the equation, that is:

$$\frac{V_o - V}{V_o} = Clog\left(\frac{B + P}{B}\right) \tag{3.11}$$

Studies conducted by Cutler et al (1958)and Eduljee et al. (1951) on hydrocarbons found that while *C* does not depend on temperature, as the temperature is increased the value of *B* decreases. Furthermore, the value of parameter *C* was found to vary less at higher pressures greater than 150 MPa for a given series. Regarding mixtures, studies undertaken by Takagi and Teranishi (1982), Kashiwagi et al. (1980) and Takagi (1978) found that *C* varies relatively smoothly with composition. However, this is not true when hydrogen bonding is present. Kubota et al. (1980)and Moriyoshi and Uosaki (1984) observed that the composition dependence of *C* is similar to that of *B.*

In his comparative analysis conducted on various compressibility equations, Hayward (1967) concluded that equation (3.11) presents no favour over the linear secant bulk modulus equation. Furthermore, attention is drawn to the fact that equation (3.11) fails to correlate the experimental data of water as well as equation (3.8). Despite these limitations, the modified Tait equation has gained popularity and is utilized for the correlation of liquid density data under high-pressure conditions as demonstrated in the works of Taguchi *et al.* (2009), Sumara *et al.* (2013) and Aitbelale *et al.* (2019).

3.3.2. Benedict-Webb-Rubin-Starling (BWRS) equation of state

The Beattie-Bridgeman equation (Beattie and Bridgeman, 1928) presents a modification to the van der Waals equation of state (Van der Waals, 1873) and is able to accurately correlate *P-V-T* data over a large temperature range (Pedersen et al., 2018). In their original work, Beattie and Bridgeman (1928) developed the equation for the representation of thermodynamic properties of pure light hydrocarbons (Benedict et al., 1940). The equation is given by:

$$P = RT\rho + \left(B_o RT - A_o - \frac{Rc}{T^2}\right)\rho^2 + \left(-B_o bRT + A_o a - \frac{RB_o c}{T^2}\right)\rho^3 + \frac{RB_o bc\rho^4}{T^2} \quad (3.12)$$

Where, A_o, B_o, a, b and c are numerical constants that can be found by regressing *P-V-T* data.

However, in this form the Beattie-Bridgeman equation does not accurately correlate *P-V-T* properties, greater than the critical density, for liquids and gases, hence, hindering computation of the Helmholtz free energy above this point.

The Benedict-Webb-Rubin (BWR) equation (Benedict et al., 1940) was proposed as a modification to the Beattie-Bridgeman equation and can accurately predict fluid properties in the critical region as it accounts for the variation of the Helmholtz free energy (a), with density, at constant temperature. In the development of their equation the authors retain the assumption of continuity, as suggested by van der Waals, of both liquids and gases and hence propose the following fundamental equation to demonstrate the relationship between the residual Helmholtz free energy, density and temperature:

$$a^{res} = \left(B_o RT - A_o - \frac{C_o}{T^2}\right)\rho + \frac{(bRT-a)\rho^2}{2} + \frac{a\alpha\rho^5}{5} + \frac{c\rho^2}{T^2}\left[\frac{1-exp(-\gamma\rho^2)}{\gamma\rho^2} - \frac{exp(-\gamma\rho^2)}{2}\right] \quad (3.13)$$

By definition:

$$P = \rho^2 \left(\frac{\partial a}{\partial \rho}\right)_{T,x_i} \quad (3.14)$$

And with $$a = a^{ideal} + a^{res} \quad (3.15)$$

Equation (3.14) becomes:

$$P = RT\rho + \rho^2 \left(\frac{\partial a^{res}}{\partial \rho}\right)_{T,x} \quad (3.16)$$

From equation (3.16), the equation of state in the pressure explicit form, corresponding to the relation presented above in equation (3.12) is:

$$P = RT\rho + \left(B_o RT - A_o - \frac{C_o}{T^2}\right)\rho^2 + (bRT - a)\rho^3 + a\alpha\rho^6 + \frac{c\rho^3(1+\gamma\rho^2)\,exp(-\gamma\rho^2)}{T^2} \quad (3.17)$$

In equations (3.12) and (3.13) the model parameters A_o, B_o and C_o are considered to correspond to the parameters in the Beattie-Bridgeman equation and have similar roles and values. However, the remaining model parameters, a, b, c, α and γ are not considered to correspond to parameters present in the Beattie-Bridgeman equation.

Furthermore, in a later work Benedict et al. (1942) extend their equation to include mixtures of hydrocarbons and propose the following equation to calculate the Helmholtz free energy for mixtures:

$$a = a^{res} + \sum_i x_i[RTln\rho x_i + \lim_{\rho\to 0}(A_i - RTln\rho)] \quad (3.18)$$

Where,

$$a^{res} = \int_0^\rho \frac{P - RT\rho}{\rho^2}\delta\rho \quad (3.19)$$

And is calculated from mixture *P-V-T* data while the second part of the summation, in equation 3.13, can be computed from pure component properties evaluated at low pressures.

For mixtures of *i* components, Benedict et al. (1942) propose simplified equations that relate the 8 parameters, present in the equation of state, to the composition. They are:

$$A_o = \left[\sum_i x_i (A_{oi})^{1/2}\right]^2 \tag{3.20}$$

$$B_o = \sum_i x_i B_{oi} \tag{3.21}$$

$$B_o = \frac{\sum_{ij} x_i x_j \left[(B_{oi})^{1/3} + (B_{oj})^{1/3}\right]^3}{8} \tag{3.22}$$

$$C_o = \left[\sum_i x_i (C_{oi})^{1/2}\right]^2 \tag{3.23}$$

$$b = \left[\sum_i x_i (b_i)^{1/3}\right]^3 \tag{3.24}$$

$$a = \left[\sum_i x_i (a_i)^{1/3}\right]^3 \tag{3.25}$$

$$c = \left[\sum_i x_i (c_i)^{1/3}\right]^3 \tag{3.26}$$

$$\gamma = \left[\sum_i x_i (\gamma_i)^{1/2}\right]^2 \tag{3.27}$$

$$\alpha = \left[\sum_i x_i (\alpha_i)^{1/3}\right]^3 \tag{3.28}$$

Where, *i* refers to pure component parameters while the parameters without a subscript refers to mixture properties. Equation (3.21) and (3.22) refer to the linear and Lorentz combinations of B_o.

Comparisons utilizing both the Lorentz and linear forms of the equation of state were conducted for *P-V-T* as well as vapour-liquid equilibrium (VLE) data. Regarding the *P-V-T* data for hydrocarbon mixtures, it was concluded that pressure calculated using the Lorentz form of the equation of state provides results that are in better agreement with experimental data compared to the linear form. The average deviation for the Lorentz form is less than 0.5 % while for the linear

form a deviation of greater than 2 percent was reported. For VLE data, the linear form is preferred over the Lorentz form as its predictions are in better agreement with experimental data.

The most popular modification to the BWR equation of state was suggested by Starling. Starling (1973) introduced three more parameters to the original eight parameter equation that corrects for the temperature dependence of parameters C_o and a. The resulting modification is presented below.

$$P = RT\rho + \left(B_oRT - A_o - \frac{C_o}{T^2} + \frac{D_o}{T^3} - \frac{E_o}{T^4}\right)\rho^2 + (bRT - a - \frac{d}{T})\rho^3 + \alpha(a + \frac{d}{T})\rho^6 + \frac{c\rho^3(1+\gamma\rho^2)\,exp(-\gamma\rho^2)}{T^2} \quad (3.29)$$

Starling and Han (1972) proposed mixing rules to be employed in the above equation. These are as follows:

$$A_o = \frac{A_2 + B_2\omega}{\rho_c}RT_c \quad (3.30)$$

$$B_o = \frac{A_1 + B_1\omega}{\rho_c} \quad (3.31)$$

$$C_o = \frac{A_3 + B_3\omega}{\rho_c}{RT_c}^3 \quad (3.32)$$

$$D_o = \frac{A_9 + B_9\omega}{\rho_c}{RT_c}^4 \quad (3.33)$$

$$E_o = \frac{A_{11} + B_{11}\omega\, exp(-3.8\omega)}{\rho_c}{RT_c}^5 \quad (3.34)$$

$$a = \frac{A_6 + B_6\omega}{{\rho_c}^2}RT_c \quad (3.35)$$

$$b = \frac{A_5 + B_5\omega}{{\rho_c}^2} \quad (3.36)$$

$$c = \frac{A_8 + B_8\omega}{{\rho_c}^2}{RT_c}^3 \quad (3.37)$$

$$d = \frac{A_{10} + B_{10}\omega}{{\rho_c}^2}{RT_c}^2 \quad (3.38)$$

$$\alpha = \frac{A_7 + B_7\omega}{{\rho_c}^3} \quad (3.39)$$

$$\gamma = \frac{A_4 + B_4\omega}{{\rho_c}^2} \quad (3.40)$$

Where, ω is the acentric factor and the model parameters $A_{1,2,..,12}$ and $B_{1,2,...,12}$ can be computed utilizing multi-property least-squares regression.

Due to its applicability to both liquids and gases and the supporting mixing rules, the BWRS is commonly employed in the process simulation of pipelines constituting hydrocarbons with high densities (Atena and Muche, 2016). Furthermore, it is the most widely used model in Aspen Plus ® for the computation of density (Lielmezs et al., 1982).

3.3.3. Toscani-Szwarc equation of state and its modification

In 1993, Toscani and Szwarc developed a four-parameter empirical equation that enables the correlation of liquid specific volumes for pressures up to 300 MPa and in the temperature range, between the normal melting and boiling points. In their work, they have considered esters, alcohols, glycols, saturated hydrocarbons and alkyl halides and have successfully applied their empirical equation to 104 organic liquids. This equation, known as the original Toscani-Szwarc equation, is given below.

$$V = \frac{a + bp}{c - dT + P} \tag{3.41}$$

Where, *V*, *P* and *T* are the specific volume, pressure and temperature, respectively while *a*, *b*, *c*, and *d* are the empirical constants. Furthermore, the liquid specific volume at infinite pressure is denoted by parameter *b* while *d* relates to the liquid molecular dynamics.

Equation (3.41) can also be expressed in terms of pressure and yields the following result:

$$P = \frac{dVT}{V - b} - \frac{cV - a}{V - b} \tag{3.42}$$

In the above equation, pressure is “composed” by two factors, namely, the temperature dependent dynamic pressure stemming from molecular dynamics and the internal pressure arising from intermolecular forces which is not reliant on temperature (Toscani et al., 1993).

The internal pressure, $\left(\frac{\partial U}{\partial V}\right)_T$, is expressed in equation (3.43) and is identical to the expression formulated by Geissler (1918) (Toscani et al., 1993).

$$\left(\frac{\partial U}{\partial V}\right)_T = \frac{s}{(V-b)^n} \tag{3.43}$$

Where *n* is unity while *s* represents a linear function of the specific volume that increases and is zero at the point where both the pressure and temperature are also zero.

The pressure due to molecular dynamics, in equation (3.42), is expressed as follows:

$$\frac{dVT}{V-b} = dT + \frac{bdT}{V-b} \tag{3.44}$$

Unlike the van der Waals (Van der Waals, 1873) or the Tumlirz (Tumlirz, 1900) relations, the expression given in (3.42) can predict an increase in the thermal expansivity with increasing temperature. Furthermore, the original Toscani-Szwarc equation accounts for an increase in the isothermal compressibility as the temperature increases. However, certain limitations do exist, for instance, equation (3.41) does not yield reliable results for pressures that are lower than 100 MPa and for temperatures ranging between the normal boiling and critical points. In addition, two fundamental limitations exist.

Firstly, the term $(\frac{dp}{dT})_V$, referred to as the pressure coefficient, is only dependent on volume which is incorrect as in a highly pressurized liquid it should be a function of both volume and temperature. Secondly, equation (3.41) does not account for intersections that occur, at high pressures, between the isotherms representing the variation of thermal expansion against pressure. Hence, Toscani and Szwarc (Toscani and Szwarc, 2004) presented two modifications to their original equation to address these limitations.

The first modification aimed at improving the *P*-*V*-*T* data representation over a wider range (0 – 1177 MPa) by the addition of two pressure square-root terms and is given by equation (3.45).

$$V = \frac{a + bP + eP^{1/2}}{c - dT + P + fP^{1/2}} \tag{3.45}$$

The above equation was fitted to data presented by Bridgman (1913, 1931, 1932), Brostow et al. (1985), Dymond et al. (1979; 1982, 1988;1982) and Grindley and Lind Jr (1971) as the experimental pressure range exceeds 300 MPa. Equation (3.45) demonstrates an improvement in the results obtained for esters, alcohols, saturated hydrocarbons as well as alkyl halides. However, the opposite is true for glycols which was observed to be best represented by equation (3.41). In their work, Toscani and Szwarc concluded that although equation (3.45) does not consider the intersections of the thermal expansion curves, it provides a better correlation of *P*-*V*-*T* data over extensive pressure ranges.

The second modification proposed is not related to equation (3.44) and attempts to account for the intersections that occur between the isothermal thermal expansion and pressure curves in high pressure liquids as well as the isothermal nature of the pressure dependent heat capacity, C_p. The following relation applies:

$$\left(\frac{\partial C_P}{\partial P}\right)_T = -T\left(\frac{\partial^2 V}{\partial T^2}\right)_P = -VT\left[\alpha^2 + \left(\frac{\partial \alpha}{\partial T}\right)_P\right] \tag{3.46}$$

The term $\left(\frac{\partial \alpha}{\partial T}\right)_P$ is initially observed to be positive at low pressures however, as the pressure increases, a reversal in the sign is noted and relates to a minimum $C_{p.}$ This significant feature cannot be included in equation *F* as the value of $\left(\frac{\partial \alpha}{\partial T}\right)_P$ is always greater than zero as shown below.

$$\left(\frac{\partial \alpha}{\partial T}\right)_P = \frac{d^2}{(c - dT + P)^2} = \alpha^2 \tag{3.47}$$

However, the inclusion of a positive coefficient that is adjustable, ξ, in the following relation

$$V = \frac{a + bp}{c - dT(1 - \xi T) + P} \tag{3.48}$$

Gives a zero value for the $\left(\frac{\partial \alpha}{\partial T}\right)_P$, or α', term for a pressure determined according to

$$P_{inv}^{\alpha'} = \frac{d(1-2\xi T)^2}{2\xi} - [c - dT(1-\xi T)] \tag{3.49}$$

And is negative when $P > P_{inv}^{\alpha'}$. Similarly, equation (3.50) gives the pressure for which a sign reversal is noted for the term $\left(\frac{\partial C_p}{\partial p}\right)_T$, or C_p'.

$$P_{inv}^{C_p\prime} = \frac{d(1-2\xi T)^2}{\xi} - [c - dT(1-\xi T)] \tag{3.50}$$

Both $P_{inv}^{\alpha'}$ and $P_{inv}^{C_p\prime}$ are temperature dependent terms and thus intersections of the α curves occur in a pressure domain and not at a single point as demonstrated in a study conducted by Ter Minassian et al. (1988). The fitting of *P-V-T* data can be employed to determine the value of ξ for which an inversion of sign occurs and hence α can be computed via equation (3.51) and compared to experimental values.

$$\alpha = \frac{d(1-2\xi T)}{c - dT(1-\xi T) + P} \tag{3.51}$$

Alternatively, regarding equation (3.48), another independent parameter *e*, the product of ξd, can be considered. Hence,

$$V = \frac{a + bP}{c - dT + eT^2 + P} \tag{3.52}$$

A key observation of the above equation is that the trend followed by the gradient of the temperature derivative, the isochore, can be estimated when fitted to experimental data sets. Furthermore, in their study, Toscani and Szwarc (2004) concluded that equations (3.48) and (3.52) provides a more fitting physical rationality than their original equation, due to its ability to incorporate the points of intersection of the high-pressure thermal expansion curves. In addition, the decrease and inversion of the sign of the internal pressure, that occurs when pressure is increased under isothermal conditions is accounted for in both equations (3.48) and (3.52). Hence,

both these equations better predict the thermodynamic behaviour of high-pressure liquids regardless of their number of parameters.

The modified Toscani-Szwarc equation, employed in this work for the correlation of density data, was proposed by Zúñiga-Moreno et al. (2005). This equation has been successfully employed for the correlation of density data in studies conducted by Zúñiga-Moreno et al. (2005), Moodley et al. (2018), Zúñiga-Moreno et al. (2007), Quevedo-Nolasco et al. (2012). The equation is given below.

$$V = \frac{c_1 + c_2 P}{c_3 - \left(\frac{c_4}{T} + \frac{c_5}{T^{1/3}}\right) + P} \tag{3.53}$$

Or,

$$\rho = \frac{c_3 - \left(\frac{c_4}{T} + \frac{c_5}{T^{1/3}}\right) + P}{c_1 + c_2 P} \tag{3.54}$$

Where, c_1, c_2, c_3, c_4 and c_5 are parameters obtained via data regression.

3.4. Statistical associating fluid theory (SAFT)

Thermodynamic Perturbation Theory, derived by Wertheim in a series of four papers (Wertheim, 1986b, 1986a, 1984a, 1984b), characterizes the behaviour of fluids constituting highly directional attractive forces and a repulsive core, such as fluids that exhibit molecular association (Economou, 2002). Furthermore, it demonstrates the relationship between the residual Helmholtz free energy and the monomer density and forms the basis of the Statistical Associating Fluid Theory (SAFT) (de Villiers, 2011).

The Statistical Associating Fluid Theory, which employs statistical mechanics, was originally developed by Chapman and co-workers for the prediction of phase equilibria data (Chapman et al., 1989). In comparison to most van der Waals based equations of state that employ a simple hard-sphere reference fluid, SAFT utilizes a reference fluid that accounts for association between molecules as well as the shape of the molecule (de Villiers, 2011). Chen and Kreglewski (1977) proposed a modification to the dispersion term present in the SAFT equation by using experimental data obtained for Argon and fitting a perturbation expansion to the data. Huang and Radosz (1990)

employed this modified dispersion term in the original SAFT equation to give one of the most valuable modifications presented.

The SAFT equation of state is expressed as the residual Helmholtz free energy (a^{res}) and accounts for the following three contributions to the overall intermolecular potential: (i) association interactions between segments (a^{assoc}), such as hydrogen bonding, (ii) chain formation among segments (a^{chain}), such as Lennard-Jones segments, and (iii) interactions among segments (a^{seg}), for example, Lennard-Jones interactions. The residual Helmholtz free energy is thus expressed as follows:

$$a^{res} = a^{assoc} + a^{chain} + a^{seg} \tag{3.55}$$

In equation (3.55) a^{seg} is commonly expressed in terms of dispersion and hard-sphere repulsion terms and is given by:

$$a^{res} = a^{hs} + a^{chain} + a^{disp} + a^{assoc} \tag{3.56}$$

The hard-sphere repulsion term (a^{hs}), in the above equation, can be calculated by:

$$\frac{a^{hs}}{RT} = m\frac{4\eta - 3\eta^2}{(1-\eta)^2} \tag{3.57}$$

Where, m is the number of spherical segments per molecule and η, is the reduced density expressed as follows:

$$\eta = 0.74048\rho m v^o \tag{3.58}$$

Where the fluid hard-core close-packed volume, v^o , is given by equations (3.59), as proposed by Chapman et al. (1990), or equation (3.57), developed by Huang and Radosz (1990). It is calculated from the fluid soft-core volume which is independent of temperature.

$$v^o = \frac{v^\infty \left[1 + \frac{0.2977}{\frac{u^o}{kT}}\right]}{\left[1 + \frac{0.33163}{\frac{u^o}{kT}} + \frac{0.0010477 + \frac{0.025337(m-1)}{m}}{\left(\frac{u^o}{kT}\right)^2}\right]} \tag{3.59}$$

$$v^o = v^\infty [1 - C\ exp\left(-\frac{3u^o}{kT}\right)]^3 \tag{3.60}$$

Where, $\frac{u^o}{k}$ represents the dispersion energy for each segment and C = 0.12, unless the species of interest is hydrogen for which the value of C is 0.241. m, v^∞ and $\frac{u^o}{k}$ are the non-associating parameters for pure liquids.

The chain-term in equation (3.56) is calculated as follows:

$$\frac{a^{chain}}{RT} = (1-m)\ ln\frac{1-0.5\eta}{(1-\eta)^3} \tag{3.61}$$

While the association term is given by:

$$\frac{a^{assoc}}{RT} = \sum_{A=1}^{M}\left[ln\, X^A - \frac{X^A}{2}\right] + 0.5M \tag{3.62}$$

And,

$$X^A = (1 + \sum_{B=1}^{M} \rho X^B \Delta^{AB})^{-1} \tag{3.63}$$

Where, M is the number of association sites per molecule and X^A is the mole fraction of non-bonded molecules at site *A*. The association strength, Δ^{AB}, can be calculated by employing the

following two equations proposed by Chapman et al. (1989) and Huang and Radosz (1990), respectively.

$$\Delta^{AB} = \sqrt{2} v^{o} \frac{1 - 0.5\eta}{(1-\eta)^3} \left[\exp\left(\frac{\epsilon^{AB}}{kT}\right) - 1 \right] \kappa^{AB} \tag{3.64}$$

$$\Delta^{AB} = \sqrt{2} v^{\infty} \frac{1 - 0.5\eta}{(1-\eta)^3} \left[\exp\left(\frac{\epsilon^{AB}}{kT}\right) - 1 \right] \kappa^{AB} \tag{3.65}$$

The association energy is given by $\frac{\epsilon^{AB}}{k}$ while κ^{AB} is the association volume. These two parameters along with m, v^{∞} and $\frac{u^{o}}{k}$ are generally determined by fitting to vapour pressure and liquid density data for pure components.

The dispersion term in the residual Helmholtz free energy equation can be calculated utilizing equations proposed by Huang and Radosz (1991), based on square-well fluid molecular dynamics simulation data, or by Chapman et al. (1989) which was originally developed in the work of Cotterman et al. (1986). These are given by equations (3.66) and (3.68), respectively.

$$\frac{a^{disp}}{RT} = m \sum_{i=1}^{4} \sum_{j=1}^{9} D_{ij} \left(\frac{u}{kT}\right)^{i} \left(\frac{\eta}{0.74048}\right)^{j} \tag{3.66}$$

For,

$$\frac{u}{k} = \left(\frac{u^{o}}{k}\right)\left(1 + \frac{\mathrm{e}}{kT}\right) \tag{3.67}$$

And $\frac{\mathrm{e}}{k}$ = 10 K for most molecules, further details regarding this can be found in the paper presented by Huang and Radosz (1990).

$$\frac{a^{disp}}{RT} = m \frac{u^{o}}{kT} \left(a_1^{disp} + \frac{u^{o}}{kT} a_2^{disp}\right) \tag{3.68}$$

Where,

$$a_1^{disp} = -11.604\eta - 6.132\eta^2 - 2.871\eta^3 + 13.885\eta^4 \quad (3.69)$$

$$a_2^{disp} = -2.575\eta + 13.463\eta^2 - 29.992\eta^3 + 21.470\eta^4 \quad (3.70)$$

The SAFT equations can be extended to mixtures by applying the following mixing rules. These are given by equations (3.71) to (3.77).

$$m = \sum_i x_i m_i \quad (3.71)$$

$$v^o = \frac{\sum_i \sum_j x_i x_j m_i m_j v_{ij}^o}{\left(\sum_i x_i m_i\right)^2} \quad (3.72)$$

$$\frac{u^o}{k} v^o = \frac{\sum_i \sum_j x_i x_j m_i m_j \frac{u_{ij}^o}{k} v_{ij}^o}{\left(\sum_i x_i m_i\right)^2} \quad (3.73)$$

$$\frac{u}{k} = \frac{\sum_i \sum_j x_i x_j m_i m_j \frac{u_{ij}}{k} v_{ij}^o}{\sum_i \sum_j x_i x_j m_i m_j v_{ij}^o} \quad (3.74)$$

$$v_{ij}^o = \left[\frac{1}{2}\left((v_{ii}^o)^{\frac{1}{3}} + \left(v_{jj}^o\right)^{\frac{1}{3}}\right]^3 \quad (3.75)$$

$$\frac{u_{ij}^o}{k} = \left(\frac{u_{ii}^o}{k}\frac{u_{jj}^o}{k}\right)^{\frac{1}{2}}\left(1 - k_{ij}\right) \quad (3.76)$$

$$\frac{u_{ij}}{k} = \left(\frac{u_{ii}}{k}\frac{u_{jj}}{k}\right)^{\frac{1}{2}}\left(1 - k_{ij}\right) \quad (3.77)$$

Where, the subscripts *i* and *j* denote species *i* or *j* , k_{ij} is an adjustable binary parameter and x is the mole fraction. Equations (3.72) and (3.76) are employed by Chapman et al. (1990) while (3.74) and (3.77) are utilized by Huang and Radosz (1990). However, equations (3.71) and (3.75) are employed by both Chapman et al. (1990) and Huang and Radosz (1990). The chain and association contributions in mixtures are covered rigorously in the Thermodynamic Perturbation Theory, while mixtures constituting components regarded as hard-spheres can be modelled utilizing the equation developed by Mansoori and co-workers (1971).

Several improvements to the original SAFT equation exist which involve modifications ranging from simplifying the dispersion interaction term utilized, such as in the hard-sphere SAFT model (SAFT-HS) (1988) to utilizing Lennard-Jones or square-well reference fluids (Economou, 2002). SAFT equations have been successfully employed for several different species ranging from pure hydrocarbons, carboxylic acids, water and so on and have also been extended to mixtures comprising n-alkanes, alcohols, polymers, carbon dioxide, amphiphilic systems and so forth (Müller and Gubbins, 2001). Furthermore, SAFT equations have been employed to model extraction systems comprising of high-pressure gas, polynuclear aromatics extraction under supercritical conditions as well as polymer fractionation in gases that are supercritical and has also been successful in correlating systems exhibiting liquid-liquid and solid-liquid equilibria. Various studies, (Gregg et al., 1994; Hasch *et al.*, 1994; Xiong and Kiran, 1995; Albrecht *et al.*, 1996; Lee et al., 1996; Pan and Radosz, 1998; Kinzl *et al.*, 2000), demonstrate the suitability of SAFT to chain molecules as well as systems that exhibit molecular association and, in some cases, have shown excellent agreement with data obtained via molecular simulation.

3.5. Association schemes

Various association schemes have been developed within the SAFT framework and the appropriate selection of such schemes is imperative for the accurate estimation of parameters for the pure species of an associating compound. These schemes have been proposed by Huang and Radosz (1990) and have been employed in the formulation of the Cubic-Plus-Association (CPA) equation of state applicable to a range of associating categories. The physical nature and type of self-association exhibited influence the type of association scheme employed and hence the expression used for the monomer fraction (X^A). Association sites can be classified as either acceptor, donor or bipolar sites. Acceptor sites can form hydrogen bonds with either donor or bipolar sites while donor sites form hydrogen bonds between bipolar and acceptor sites. Bipolar association sites are able to form hydrogen bonds with any site. Table 3.1 further illustrates the association schemes for different species.

For acids, a 1A or one-site association scheme is used and assumes that bonding can occur between the site and a hydrogen atom, a lone electron pair or a similar type of site. Alcohols and amines are modelled using either the 2B (two-site) or 3B (three-site) association schemes. Regarding

alcohols, the 2B scheme groups both lone pairs on the oxygen atom as a single site while the second site is the hydrogen atom. However, in the 3B scheme, each lone pair on the oxygen atom is counted as a single site while the hydrogen atom is site 3. Furthermore, the fraction of hydrogen atoms that are non-bonding (X^C) and the fraction of lone electron pairs that are non-bonding are not equivalent due to the asymmetric nature of the association. The 3B association scheme can also be employed to model water and has two variations. The first type considers each hydrogen atom as a single site while the two lone pairs on the oxygen atom make up the third site or both hydrogen atoms can be grouped to form a single site and each lone pair on the oxygen atom are considered as a single site as is the case in the second type of 3B scheme for water. Lastly, the 4C association scheme, employed for glycols and water, contains two proton donor and acceptor sites. For water, the two lone pairs are considered a single site while, for glycols, both lone pairs are grouped as a single site.

Table 3.1. Association schemes proposed by Huang and Radosz (1990).

Species	Formula	Type	Site fraction
Alcohol	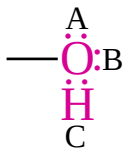	3B	$X^A = X^B$, $X^C = 2X^A\text{-}1$ $X_1 = X^A X^B X^C$
	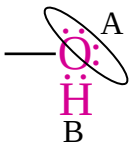	2B	$X^A = X^B$ $X_1 = X^A X^B$
Water	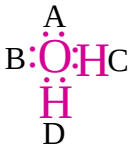	4C	$X^A = X^B = X^C = X^D$ $X_1 = X^A X^B X^C X^D$
	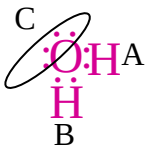	3B	$X^A = X^B$, $X^C = 2X^A\text{-}1$ $X_1 = X^A X^B X^C$
		3B	$X^A = X^B$, $X^C = 2X^A\text{-}1$ $X_1 = X^A X^B X^C$

Experimental liquid-liquid equilibrium (LLE) data, comprising systems of associating and inert compounds, has proven to be valuable in aiding the selection of an association scheme and is favoured over vapour-liquid equilibrium (VLE) data as it presents a more compelling test while eliminating the effects of cross-association. This approach has been applied to alcohols, water and glycols and has led to the conclusion that for water and glycols, the 4C association scheme is most suitable while the 2B scheme is useful and sufficient for modelling alcohols. Several studies, (Folas et al., 2006; Fouad et al., 2016; Kaarsholm et al., 2005; Kontogeorgis et al., 1999; von Solms et al., 2007) have reported similar results.

3.6. PC-SAFT

The perturbed-chain SAFT (PC-SAFT) equation, one of the leading SAFT theories, proposes a modification to the SAFT equation presented by Huang and Radosz (1990) (de Villiers, 2011). A significant improvement presented by Gross and Sadowski (2001), in the development of the PC-SAFT model, is the inclusion of the chain-length contribution in both the repulsive and dispersion interaction terms (Gross and Sadowski, 2001). The PC-SAFT equation utilizes a hard-chain reference fluid and is derived by employing the perturbation theory developed by Barker and Henderson (1967).

The phase behaviour and densities of mixtures constituting low molecular weight hydrocarbons and polymers, as well as polymers, straight-chain and branched alkanes, alkenes, cycloalkanes, gases, halogenated hydrocarbons, benzene derivatives, esters and ethers have been successfully correlated or predicted utilizing PC-SAFT (Burgess et al., 2012). Furthermore, the results from recent studies, (Liu et al., 2010; Yin et al., 2011), demonstrate the applicability of the PC-SAFT equation for the accurate prediction of the following pure component densities, namely, toluene, isooctane, n-pentane, n-decane, n-octane, cyclooctane, n-hexadecane, n-eicosane and n-octadecane. In their original work, Gross and Sadowski (2001), correlated the pure component data for 78 compounds as well as mixtures comprising of polymers, solvents and gases, all of which are non-associating and polar, and compared the results obtained from PC-SAFT to those obtained from SAFT, (Burgess et al., 2012).

A key observation was the improvement in the prediction of pure-component behaviour using the PC-SAFT model, attributed to accounting for non-spherical molecules in the dispersion interaction term (Gross and Sadowski, 2001). In addition, studies conducted by Ting et al. (2003) and Lasarte et al. (2008), among others, demonstrate the superiority of the PC-SAFT model over the SAFT, presented by Huang and Radosz (1990), and Peng-Robinson equations of state for the accurate prediction of densities and phase equilibria data. For systems consisting of non-associating, weakly polar molecules, the PC-SAFT model is defined as outlined below.

The modification to the square-well potential, proposed by Chen and Kreglewski (1977), is employed to calculate the pair potential, $u(r)$, for chain segments as follows:

$$u(r) = \begin{cases} \infty & r < (\sigma - s_1) \\ 3\epsilon & (\sigma - s_1) \leq r < \sigma \\ -\epsilon & \sigma \leq r < \lambda\sigma \\ 0 & r \geq \lambda\sigma \end{cases} \tag{3.78}$$

In the above equation, σ is the segment diameter, which is independent of temperature, r is the radial distance between two segments, ϵ is the potential well depth and λ is the width of the reduced well. A value of 0.12 is assumed for the ratio $\frac{s_1}{\sigma}$ (Chen and Kreglewski, 1977). Regarding the potential depth, unlike in the work of Chen and Kreglewski (1977), no further factors have been introduced for temperature correction. In formulating the PC-SAFT equation, Gross and Sadowski (2001), suggest that σ, ϵ and m, which is the number of segments in a chain, are the pure-component parameters that define systems comprising non-associating molecules. Despite the simplicity of this molecular model, a crucial factor relating to the behaviour of real molecules is accounted for. This is known as the soft repulsion and is included as a collision diameter of σ, and only exists between molecules when no temperature limit is present. The soft repulsion occurs at $r < \sigma$ in the pair potential step function.

Interactions between molecules are attributed to repulsive or attractive contributions to the pair potential. However, in order to compute the contribution of the repulsive term, a reference fluid in which attractive interactions are absent needs to be employed. Hence, regarding the reference system, any interactions attributed to the presence of attractive forces are treated as perturbations. The soft repulsion of molecules, in the perturbation theory formulated by Barker and Henderson

(1967), can accurately be described by utilizing a hard repulsion reference fluid with a segment diameter, $d(T)$, that is dependent on temperature and is given by equation (3.79). However, for the development of the PC-SAFT model, a hard-chain reference fluid is employed and $d(T)$ is defined as the chain segment effective collision diameter. Integration of the step function presented in equation (3.79) for the pair potential gives the hard segment diameter ($d_i(T)$), a temperature-dependent term. The final integrated result is presented in equation (3.80).

$$d(T) = \int_0^{\sigma} \left[1 - \exp\left(-\frac{u(r)}{kT}\right)\right] dr \tag{3.79}$$

$$d_i(T) = \sigma_i[1 - 0.12\exp(-\frac{3\epsilon_i}{kT})] \tag{3.80}$$

The final equation is influenced by effects due to the hard-chain contribution (*hc*), interactions due to attraction (*disp*) and ideal gas contributions (*id*). This can be expressed in terms of the compressibility factor (Z) according to the following relation:

$$Z = Z^{hc} + Z^{disp} + Z^{id} \tag{3.81}$$

Where,

$$Z = \frac{PV_m}{RT} \tag{3.82}$$

And *R* is the universal gas constant, *T* is the temperature, V_m is the molar volume, *P* is the pressure and Z^{id} is equal to 1.

The hard-chain contribution term, Z^{hc}, developed by Chapman et al. (1990) using Wertheim's formulation of thermodynamic perturbation theory, is defined by equation (3.83):

$$Z^{hc} = mZ^{hs} - \sum_i x_i(m_i - 1)\rho \frac{\partial ln g_{ii}^{hs}}{\partial \rho} \tag{3.83}$$

Where, ρ and g_{ii}^{hs} refer to the molecules total number density and distribution function for the radial pair, respectively. The subscript *i* and superscript *hs* refer to component *i* and properties associated with the hard-sphere system, respectively. Furthermore, by using equations presented by Boublik (1970) and Mansoori et al. (1971), equation (3.83) can be extended to mixtures of reference systems consisting of hard-spheres. The hard-sphere terms expressed in equation (3.83) are defined as:

$$Z^{hs} = \frac{\zeta_3}{(1-\zeta_3)} + \frac{3\zeta_1\zeta_2}{\zeta_o(1-\zeta_3)^2} + \frac{3\zeta_2^3 - \zeta_3\zeta_2^3}{\zeta_o(1-\zeta_3)^3} \tag{3.84}$$

$$g_{ij}^{hs} = \frac{1}{(1-\zeta_3)} + \left(\frac{d_i d_j}{d_i + d_j}\right)\frac{3\zeta_2}{(1-\zeta_3)} + \left(\frac{d_i d_j}{d_i + d_j}\right)^2 \frac{2\zeta_2^2}{(1-\zeta_3)^3} \tag{3.85}$$

Where,

$$\zeta_n = \frac{\pi}{6}\rho \sum_i x_i m_i d_i^n \qquad n \in \{0,1,2,3\} \tag{3.86}$$

Hence, perturbations can be computed by employing the second-order perturbation theory of Barker and Henderson (1967). Although the theory formulated by Barker and Henderson are applicable to molecules that are spherical in shape, it can also be applied to systems comprising chain molecules as individual chain segments considered are essentially spherical in shape. Expressed in terms of Helmholtz free energy, chain interactions due to attractive contributions is calculated as follows:

$$\frac{a^{disp}}{kTN} = \frac{A_1}{kTN} + \frac{A_2}{kTN} \tag{3.87}$$

For which,

$$\frac{A_1}{kTN} = -2\pi\rho m^2 \left(\frac{\epsilon}{kT}\right)\sigma^3 \int_1^\infty \tilde{u}(x) g^{hc}\left(m; x\frac{\sigma}{d}\right) x^2 dx \tag{3.88}$$

$$\frac{A_2}{kTN} = -\pi\rho m \left(1 + Z^{hc} + \rho\frac{\partial Z^{hc}}{\partial\rho}\right)^{-1} m^2 \left(\frac{\epsilon}{kT}\right)^2 \sigma^3 \frac{\partial}{\partial\rho}[\rho \int_1^\infty \tilde{u}(x)^2 g^{hc}\left(m; x\frac{\sigma}{d}\right) x^2 dx] \tag{3.89}$$

Where, $\tilde{u}(x) = \frac{u(x)}{\epsilon}$ is the reduced potential function, $x = \frac{r}{\sigma}$ and refers to the reduced radial distance around a segment and $g^{hc}\left(m; x\frac{\sigma}{d}\right)$, which includes the segment diameter $d(T)$, is the average segment-segment radial distribution function. In addition, the term consisting of the compressibility factors in equation (3.89) can be simplified by applying equation (3.83) and gives the following:

$$\left(1 + Z^{hc} + \rho\frac{\partial Z^{hc}}{\partial \rho}\right) = \left(1 + m\frac{8\eta - 2\eta^2}{(1-\eta)^4} + (1-m)\frac{20\eta - 27\eta^2 + 12n^3 - 2\eta^4}{[(1-\eta)(2-\eta)]^2}\right) \quad (3.90)$$

And η can be calculated utilizing equation (3.86) for which *n* is equal to 3.

The following substitutions are made, for the integrals presented in equations (3.88) and (3.89), to simplify the expressions:

$$I_1 = \int_1^\infty \tilde{u}(x) g^{hc}\left(m; x\frac{\sigma}{d}\right) x^2 dx \quad (3.90)$$

$$I_2 = \frac{\partial}{\partial \rho}[\rho \int_1^\infty \tilde{u}(x)^2 g^{hc}\left(m; x\frac{\sigma}{d}\right) x^2 dx] \quad (3.91)$$

Both these expressions depend on the segment number as well as density if a square-well chain reference fluid is employed. Additionally, if soft repulsion is present, they are temperature dependent.

In the formulation of the PC-SAFT equation however, the dependence on temperature for the term $g^{hc}\left(m; x\frac{\sigma}{d}\right)$ is limited and is therefore disregarded. Hence, equations (3.90) and (3.91) can be expressed as a power series regarding density and are given by:

$$I_1(\eta, m) = \sum_{i=0}^{6} a_i(m)\eta^i \quad (3.92)$$

$$I_2(\eta, m) = \sum_{i=0}^{6} b_i(m) n^i \tag{3.93}$$

The coefficients $a_i(m)$ and $b_i(m)$ can be calculated from equations (3.94) and (3.95) and are dependent on chain length. Both (3.94) and (3.95) use the sticky-point model employed by Cummings and Stell (1984, 1985) and consider bonding between the nearest-neighbour segments.

$$a_i(m) = a_{0,i} + \frac{m-1}{m} a_{1,i} + \frac{m-1}{m}\frac{m-2}{m} a_{2,i} \tag{3.94}$$

$$b_i(m) = b_{0,i} + \frac{m-1}{m} b_{1,i} + \frac{m-1}{m}\frac{m-2}{m} b_{2,i} \tag{3.95}$$

Where, $a_{0,i}$, $a_{1,i}$, $a_{2,i}$, $b_{0,i}$, $b_{1,i}$ and $b_{2,i}$ are the model constants and were fitted to pure-component data to a series of n-alkanes. In order to obtain the parameters of the pure-components, two important assumptions were made, namely, regarding equations (3.90) and (3.91), a Lennard-Jones perturbing potential is assumed and the equation presented by Chiew (1990) pertaining to the function describing the average radial distribution is employed. Furthermore, m, σ and $\frac{\epsilon}{k}$, the pure-species parameters, were calculated by fitting *P-V-T* and vapour pressure data of the n-alkanes. Thereafter, model constants were regressed by utilizing the pure-species parameters previously determined, as well as data for the liquid, gas and supercritical volumes and vapour pressures. The following objective function was minimized in the regression of the constants:

$$Min = \sum_{i=1}^{N^{exp}} \left(\frac{\Omega_i^{exp} - \Omega_i^{calc}}{\Omega_i^{exp}} \right)^2 \tag{3.96}$$

Where, N^{exp} is the total number of experimental data points and Ω is the volume (molar) or the vapour pressure. These universal model constants are presented in Table 3.2.

Table 3.2. Universal model constants employed in the PC-SAFT equation of state.

i	a_{i0}	a_{i1}	a_{2i}	b_{0i}	b_{1i}	b_{2i}
0	0.910563145	-0.30840169	-0.09061484	0.72409469	-0.57554981	0.09768831
1	0.636128145	0.18605312	0.45278428	2.23827919	0.69950955	-0.2557575
2	2.686134789	-2.50300473	0.59627007	-4.00258495	3.89256734	-9.15585615
3	-26.54736249	21.4197936	-1.72418291	-21.0035768	-17.2154717	20.642076
4	97.75920878	-65.2558853	-4.13021125	26.8556414	192.672265	-38.8044301
5	-159.5915409	83.3186805	13.7766319	206.551338	-161.826462	93.6267741
6	91.29777408	-33.7469229	-8.67284704	-355.602356	-165.207694	-29.6669056

In addition, the PC-SAFT equation can also be extended to mixtures by applying the one-fluid mixing rule, as developed by van der Waals, to the perturbation terms outlined in the model. This gives:

$$\frac{A_1}{kTN} = -2\pi\rho I_1(\eta, m) \sum_i \sum_j x_i x_j m_i m_j \left(\frac{\epsilon_{ij}}{kT}\right) \sigma_{ij}^3 \tag{3.97}$$

$$\frac{A_1}{kTN} = -2\pi\rho m \left(1 + Z^{hc} + \rho \frac{\partial Z^{hc}}{\partial \rho}\right)^{-1} I_2(\eta, m) \sum_i \sum_j x_i x_j m_i m_j \left(\frac{\epsilon_{ij}}{kT}\right)^2 \sigma_{ij}^3 \tag{3.98}$$

Where, Berthelot-Lorentz rules for combining parameters for unlike segment pairs are used to determine σ_{ij} and ϵ_{ij}.

$$\sigma_{ij} = \frac{1}{2}(\sigma_i + \sigma_j) \tag{3.99}$$

$$\epsilon_{ij} = \sqrt{\epsilon_i \epsilon_j}(1 - k_{ij}) \tag{3.100}$$

Where, k_{ij}, the parameter characterizing binary interactions for unlike chains, is included to adjust for segment-segment interactions. This parameter is usually unavailable and should be fit from

phase equilibrium data. Using conventional thermodynamic rules, other properties can be derived utilizing the Helmholtz free energy.

Gross and Sadowski (2002) further developed the PC-SAFT equation for systems comprising of molecules that exhibit association. The association term of Huang and Radosz (1990) is used (equation (3.62)).

In their work, they employ the association energy ($\epsilon^{A_iB_j}$) as well as the effective association volume ($\kappa^{A_iB_j}$), the pure-component parameters that characterize interactions of an associating nature.

The compressibility for the real fluid then becomes:

$$Z = Z^{hc} + Z^{disp} + Z^{id} + +Z^{assoc} \tag{3.101}$$

In order to obtain the parameters for cross-association in mixtures, the combining rules of Wolbach and Sandler (1998) were applied to give:

$$\epsilon^{A_iB_j} = \frac{1}{2}(\epsilon^{A_iB_i} + \epsilon^{A_jB_j}) \tag{3.102}$$

$$\kappa^{A_iB_j} = \sqrt{\kappa^{A_iB_i}\kappa^{A_jB_j}}\left(\frac{\sqrt{\sigma_{ii}\sigma_{jj}}}{1/2\left(\sigma_{ii}+\sigma_{jj}\right)}\right)^3 \tag{3.103}$$

Liquid density and vapour pressure data were simultaneously fitted to attain pure-component parameters of substances exhibiting molecular association. The effective association volume ($\kappa^{A_iB_j}$), association energy ($\epsilon^{A_iB_j}$), segment energy parameter ($\frac{\epsilon_i}{k}$), segment number (m_i) and segment diameter (σ_i), are the parameters that need to be employed for any component, *i*, exhibiting molecular association.

3.7. PC-PSAFT and tPC-PSAFT

Unlike non-polar fluids, whose properties largely depend on short-range interactions that are repulsive in nature, the properties of polar and associating fluids are influenced by electrostatic interactions such as, dipole-dipole, quadrupole-quadrupole, and so forth, that act on a longer-range (Karakatsani et al., 2005). Hence, the development of models that accurately predict the thermodynamic behaviour of these polar and associating fluids is imperative. Gubbins and Twu (1978) proposed one of the first polar fluid models, using thermodynamic perturbation theory as a basis, that accounted for strong intermolecular interactions. When compared to simulation results, their model demonstrated excellent agreement for polar and quadrupolar fluids. The perturbed anisotropic chain theory or PACT is an extension of the polar chain theory, developed by Gubbins and Twu (1978), and was formulated by Vimalchand et al. (1985). Despite its impressive predictive capabilities for modelling the phase behaviour of polar compounds and their respective mixtures, the PACT equation is overlooked, in various engineering applications, due to its high level of complexity.

The SAFT framework was first extended to polar fluids by Walsh et al. (1992) by combining Wertheim's perturbation theory with an expansion for both the multipolar and dispersion interactions. In this formulation, individual molecules were assumed to comprise of a repulsive core that was non-spherical with Lennard-Jones attractive interactions. Furthermore, molecules were assumed to have square-well attraction sites which would essentially lead to the formation of a hydrogen bond as well as non-axial multipole moments. However, despite the encouraging results documented, a more accurate theory for modelling associating fluids was essential. In their work, Xu et al. (1998) proposed a model for polar chain and associating fluids by combining SAFT and PACT however, this model lacked precision for systems comprising polar associating molecules such as alcohols. SAFT was extended to dipolar chains consisting of multiple dipolar sites, by Jog et al. (2001); Jog & Chapman (1999) and Sauer & Chapman (2003), with the assumption that dipolar chain fluids comprise of bonded dipolar and non-polar hard spheres. Furthermore, Jog et al. (2001); Jog & Chapman (1999) and Sauer & Chapman (2003) propose the use of two additional parameters namely, the fraction of dipolar segments per chain, an adjustable parameter, and the dipole moment of the functional group. This particular extension of the SAFT model demonstrates significant capability for handling real fluids.

In the formulation of polar SAFT models, i.e. polar SAFT (PSAFT) and PC-Polar SAFT (PC-PSAFT), Karakatsani et al. (2005) explicitly consider the dipole-dipole interactions which is treated as an additional perturbation in the conventional PC-SAFT model. The resulting equation is thus a sum of contributions due to chain formation, association, hard sphere, weak dispersion interactions and dipole-dipole interactions. The residual Helmholtz free energy can therefore be written as follows:

$$\frac{a^{res}}{RT} = \frac{a^{hs}}{RT} + \frac{a^{chain}}{RT} + \frac{a^{assoc}}{RT} + \frac{a^{disp}}{RT} + \frac{a^{dd}}{RT} \tag{3.104}$$

For the hard sphere contribution, the equation proposed by Carnahan and Starling (1969) can be employed and is given by equation (3.57). The chain and association contributions can be calculated using equations (3.61) and (3.62), respectively. The dispersion contribution for SAFT can be computed by equation (3.66) while for PC-SAFT the dispersion contribution is given by equation (3.87). The dipole-dipole contribution is formulated using the perturbation model proposed by Nezbeda and co-workers (1996; 2001) for dipolar fluids of a spherical nature. Hence, the following Padé approximant is obtained for the dipole-dipole contribution in both PSAFT and PC-PSAFT:

$$\frac{a^{dd}}{RT} = m\frac{a_2}{1-\frac{a_3}{a_2}} \tag{3.105}$$

Where,

$$a_2 = -\frac{4}{3}\left(\frac{u}{kT}\right)^2 \tilde{\mu}^4 \tilde{F}_2 \tag{3.106}$$

$$a_2 = \frac{10}{9}\left(\frac{u}{kT}\right)^3 \tilde{\mu}^6 \tilde{F}_3 \tag{3.107}$$

The reduced dipole moment, $\tilde{\mu}$, can be expressed as:

$$\tilde{\mu} = 85.12 \frac{\frac{\mu}{m}}{\sqrt{(\frac{u}{k})\sigma^3}} \tag{3.108}$$

Where, μ is the fluid dipole moment measured in debye (D).

The mean-spherical approximation can be applied to obtain expressions for $\tilde{F}_i$ in equations (3.106) and (3.107) and is given as follows:

$$\tilde{F}_2 = \frac{n}{K^3} \tag{3.109}$$

$$\tilde{F}_3 = \frac{n^2}{K^3} \tag{3.110}$$

Where *K* is expressed as $\frac{\sigma_d}{\sigma}$ and σ_d is a short-range cut-off that is introduced to account for dipolar interactions. A switch function is employed in the computation of the potential energy in the original development of the theory and warrants smooth transition between long-range dipolar interactions and short-range hydrogen bonding. This implies that the value of *K* is greater than 1 as the dipolar interaction range extends out of the polar species first coordination shell. In the development of the PSAFT and PC-PSAFT models, σ_d ,equivalently expressed as $v^{dd} = (\frac{\pi N_{AV}}{6\tau})\sigma_d{}^3$, is adjusted to ensure that the limits discussed are satisfied.

Finally, Karakatsani et al. (2005) propose the following mixing rules for dipolar interactions in both PSAFT and PC-PSAFT

$$\tilde{\mu} = \frac{\sum_i \sum_j x_i x_j m_i m_j \tilde{\mu}_{ij}}{\left(\sum_i x_i m_i\right)^2} \tag{3.111}$$

$$\tilde{\mu}_{ij} = \sqrt{\tilde{\mu}_i \tilde{\mu}_j} \tag{3.112}$$

$$K^3 = \frac{\sum_i x_i m_i (\frac{\sigma_d}{\sigma})_i^3}{\sum_i x_i m_i} \tag{3.113}$$

In PSAFT and PC-PSAFT there are six pure component parameters. The segment volume (v^{∞}), segment number (m) and segment energy ($\frac{\epsilon}{k}$) are the three non-associating, non-polar component parameters while the association volume (κ^{AB}) and association energy ($\frac{\varepsilon^{AB}}{k}$) make up the association parameters. Finally, the characteristic segment volume of dipole-dipole interactions (v^{dd}) is included for the dipolar term.

In their work on the development of the PSAFT and PC-PSAFT models, Karakatsani et al. (2005) apply the models to numerous polar and non-associating as well as associating fluids that include ketones, chloroform, ammonia, primary alcohols, water, ethylene glycol, acetic acid and hydrogen sulphide. Furthermore, experimental data for the saturated liquid density and vapour pressure are employed for parameter estimation. The critical constants, monomer fraction of associating fluids and second virial coefficient were also computed and demonstrates satisfactory agreement with experimental data. In addition, both models were utilized to predict phase-equilibria data for both binary and ternary mixtures that were polar in nature and demonstrates excellent correlation of the data.

By employing the model developed by (Larsen1 et al., 1977) as a basis, Karakatsani and Economou (2006) further extend the PC-SAFT model to include higher-order dipole-quadrupole and quadrupole-quadrupole interactions and account for dipole-induced dipole interactions. In the development of PC-PSAFT, Karakatsani and Economou (2006) consider both the second and third order perturbation terms presented by Larsen1 et al. (1977) while the truncated PC-PSAFT, or tPC-PSAFT, employs a simplified form of the abovementioned terms. To account for simplifications made regarding the polar term of the model, tPC-PSAFT includes one additional parameter for the pure component. Furthermore, PC-PSAFT and tPC-PSAFT assume that multipoles present in the segments are evenly distributed with an average quadrupole or dipole moment of ($\frac{Q}{m}$) or ($\frac{\mu}{m}$), respectively. The segmental approach employed is preferred over the average mole-fraction interactions as it provides a more fitting representation of mixtures comprised of large molecules.

The inclusion of interactions for the polar and induced polar contributions gives the following expression for the residual Helmholtz free energy:

$$\frac{a^{res}}{RT} = \frac{a^{hs}}{RT} + \frac{a^{chain}}{RT} + \frac{a^{assoc}}{RT} + \frac{a^{disp}}{RT} + \frac{a^{polar}}{RT} + \frac{a^{ind}}{RT} \tag{3.114}$$

The following Padé approximant can be utilized to compute the dipole-dipole, dipole-quadrupole and quadrupole-quadrupole contributions:

$$\frac{a^{polar}}{RT} = m\frac{a_2^{polar}}{1 - \frac{a_3^{polar}}{a_2^{polar}}} \tag{3.115}$$

Where, a_2^{polar} and a_3^{polar} refer to the second and third order perturbations terms, respectively. Rasaiah & Stell (1974) and Stell et al. (1974) established that three-body contributions profoundly affect the Helmholtz free energy hence the term a_3^{polar}, accounting for two and three-body contributions, cannot be ignored. The third-order perturbation term (a_3^{polar}) can be expressed as follows:

$$\frac{a_3^{polar}}{RT} = \frac{a_{3,2}^{polar}}{RT} + \frac{a_{3,3}^{polar}}{RT} \tag{3.116}$$

An expression similar to the one presented in equation (3.115) can be utilized to calculated induced polar contributions and is given below:

$$\frac{a^{ind}}{RT} = m\frac{a_2^{ind}}{1 - \frac{a_3^{ind}}{a_2^{ind}}} \tag{3.117}$$

Again, a_2^{ind} and a_3^{ind} refer to second and third order perturbation terms, respectively.

Regarding a_1^{polar} and a_1^{ind}, the first order polar and induced polar perturbation terms, respectively, Vega et al.. (1992) found that they have a zero value for molecules that are spherical in nature while for fluids comprised of hard sphero-cylinders or dumbbell shaped molecules, these terms

are non-zero and small. Hence, in the formulation of the PC-PSAFT and tPC-PSAFT models, these first order terms were assumed to be zero.

Expressions characterising the perturbation terms presented in equations (3.115) – (3.117) have been formulated by Larsen1 et al. (1977) for fluids comprising of spherical molecules and are extended to associating fluids of a non-spherical nature in the work of Karakatsani and Economou (2006). Hence, the following expressions apply:

$$\frac{a_2^{polar}}{RT} = -\frac{\rho^*}{\tilde{T}^2}\left[\frac{\tilde{\mu}^4}{6} I_6^{ref}(\rho^*) + \frac{\tilde{\mu}^2\tilde{Q}^2}{2} I_8^{ref}(\rho^*) + \frac{7\tilde{Q}^4}{10} I_{10}^{ref}(\rho^*)\right] \tag{3.118}$$

$$\frac{a_{3,2}^{polar}}{RT} = -\frac{\rho^*}{\tilde{T}^3}\left[\frac{2}{5}\tilde{\mu}^4\tilde{Q}^2 I_{11}^{ref}(\rho^*) + \frac{12}{35}\tilde{\mu}^2\tilde{Q}^4 I_{13}^{ref}(\rho^*) + \frac{36}{245}\tilde{Q}^6 I_{15}^{ref}(\rho^*)\right] \tag{3.119}$$

$$\frac{a_{3,3}^{polar}}{RT} = -\frac{(\rho^*)^2}{\tilde{T}^3}\left[\frac{\tilde{\mu}^6}{54} I_{TD}^{ref}(\rho^*) + \frac{\tilde{\mu}^4\tilde{Q}^2}{480} I_{DDQ}^{ref}(\rho^*) + \frac{\tilde{\mu}^2\tilde{Q}^4}{640}\tilde{Q}^6 I_{DQQ}^{ref}(\rho^*) + \frac{\tilde{Q}^6}{6400} I_{TQ}^{ref}(\rho^*)\right] \tag{3.120}$$

$$\frac{a_2^{ind}}{RT} = -\frac{\rho^*}{\tilde{T}}\tilde{\mu}^2\tilde{\alpha} I_6^{ref}(\rho^*) \tag{3.121}$$

$$\frac{a_3^{ind}}{RT} = \frac{a_{3,12}^{ind}}{RT} + \frac{a_{3,21}^{ind}}{RT} \simeq \frac{a_{3,12}^{ind}}{RT} = \frac{1}{6}\left(\frac{\rho^*}{\tilde{T}}\right)^2\tilde{\mu}^4\tilde{\alpha} I_{TD}^{ref}(\rho^*) \tag{3.122}$$

The superscript "*ref*"refers to the reference fluid employed. Larsen1 et al. (1977) employ a hard-sphere reference fluid while in the work of Karakatsani and Economou (2006), an associating hard-chain reference fluid is utilized. In equation (3.122), the term $\frac{a_{3,21}^{ind}}{RT}$ is small and hence, can be neglected. Furthermore, expressions for $\tilde{\mu}$, $\tilde{Q}$, $\tilde{\alpha}$ and ρ^* are given below.

$$\tilde{\mu} = 85.12\frac{\frac{\mu}{m}}{\sqrt{\left(\frac{u}{k}\right)\sigma^3}} \tag{3.123}$$

$$\tilde{Q} = 85.12\frac{\frac{Q}{m}}{\sqrt{\left(\frac{u}{k}\right)\sigma^5}} \tag{3.124}$$

$$\tilde{\alpha} = \frac{\alpha}{m\sigma^3} \tag{3.125}$$

$$\rho^* = \rho\sigma^3 \tag{3.126}$$

Where, α is a measure of the fluids polarizability in cubic Angstrome ($\mathring{A}^3$) and the quadrupole moment (Q) is measured in Debye Angstrome (D$\mathring{A}$).

In addition, the following expansions apply to integrals present in equations (3.118) – (3.122).

$$I_n^{ref}(\rho^*) \equiv 4\pi \int_0^\infty g^{ref}(\rho^*, y) y^{2-n} dy \tag{3.127}$$

Where, *n* is 6, 8, 10, 11, 13 or 15. $g^{ref}(\rho^*, y)$ is the hard sphere pair function and *y* is equal to $\frac{r}{\sigma}$.

$$I_{triple}^{ref}(\rho^*) \equiv \int_0^\infty g_{123}^{ref}(R, s, z) W_{triple}(R, s, z)\, \overrightarrow{ds}\overrightarrow{dz} \tag{3.128}$$

Where the subscript "*triple*" refers to triple dipoles (TD), dipole-dipole-quadrupole (DDQ), dipole-quadrupole-quadrupole (DQQ) or triple quadrupoles (TQ), *W* is the individual angularly averaged three body potentials, $g_{123}^{ref}(R, s, z)$ is the triple radial distribution function and $\vec{R}$, $\vec{s}$ and $\vec{z}$ are the reduced radii between bodies 1, 2 and 3, calculated by equations (3.129) – (3.131) provided below:

$$\vec{R} = \frac{\overrightarrow{r_{12}}}{\sigma} \tag{3.129}$$

$$\vec{s} = \frac{\overrightarrow{r_{13}}}{\sigma} \tag{3.130}$$

$$\vec{z} = \frac{\overrightarrow{r_{23}}}{\sigma} \tag{3.131}$$

Furthermore, the integrals presented in equations (3.127) and (3.128) were reduced to polynomials by Larsen1 et al. (1977) due to the smoothness of the functions. In the case of PC-PSAFT these polynomials are applied to hard-chain associating fluids.

$$I_n^{ref} = \sum_{i=0}^{5} J_{i,n}^{double} (\rho^*)^i \tag{3.132}$$

$$I_{triple}^{ref} = \sum_{i=0}^{3} J_{i,n}^{triple} (\rho^*)^i \tag{3.133}$$

Where, $J_{i,n}^{double}$ and $J_{i,n}^{triple}$ are the respective coefficients for equations (3.132) and (3.133).

In their work, Karakatsani and Economou (2006) develop a simpler model, applicable to polar fluids, that can be easily employed in engineering applications and based the development of their model on several arguments. Karakatsani and Economou (2006) argued that at short ranges, molecules experience strong repulsive intermolecular forces (excluding the effects of volume). For molecules that exhibit hydrogen bonding, attractive interactions that are strong in nature exist, however, these interactions are limited due to the limited range of angles that form between the atoms. Regarding long-range interactions, electrostatic interactions become more prominent beyond the first coordination shell and hence, outside the range of hydrogen-bonding interactions. This has been confirmed by Monte Carlo simulations. Lennard-Jones interactions are however considered an exception so long as their presence exists at any distance that inhibits the collapse of the system.

The use of realistic force fields has allowed the accessible volume to solute molecules to be quantified for aqueous mixtures using Monte Carlo simulations. Furthermore, when the Lennard-Jones diameter remained constant, results obtained demonstrated that the ratio is noticeably smaller for non-polar solutes when compared to polar molecules. Therefore, equating the hard-core diameter to the Lennard-Jones diameter is physically unlikely. Hence, Karakatsani and Economou (2006) argued that more emphasis should be placed on the range of polar interactions rather than their strength. Furthermore, they argued that a segment diameter, outside of which long-range electrostatic forces are dominant, should be specified. In their study, Karakatsani and Economou (2006) treat the effective polar interactions segment diameter (σ_p) as an adjustable parameter to describe the effective polar interactions.

For simplification purposes, in the development of tPC-PSAFT, the first terms in equations (3.132) and (3.133) are approximated as the zeroth-order coefficients and are calculated as follows:

$$J_{0,n}^{double} = \frac{4\pi}{n-3}, \qquad n \geq 4 \tag{3.134}$$

$$J_{0,n}^{triple} = \frac{5\pi^2}{3} \tag{3.135}$$

$$J_{0,n}^{triple} = \frac{424\pi^2}{25} \tag{3.136}$$

$$J_{0,n}^{triple} = 54\pi^2 \tag{3.137}$$

Where, equations (3.135), (3.136) and (3.137) are used for triple dipoles, dipole-dipole-quadrupole or dipole-quadrupole-quadrupole and triple quadrupoles, respectively. Hence,

$$\frac{a_2^{polar}}{RT} = -\left(\frac{1}{\tilde{T}}\right)^2 \frac{\eta}{K^3}\left[\frac{4}{3}\tilde{\mu}^4 + \frac{12}{5}\frac{\tilde{\mu}^2\tilde{Q}^2}{K^2} + \frac{12}{5}\frac{\tilde{Q}^4}{K^4}\right] \tag{3.138}$$

$$\frac{a_{3,2}^{polar}}{RT} = -\left(\frac{1}{\tilde{T}}\right)^3 \frac{\eta}{K^8}\left[\frac{6}{5}\tilde{\mu}^4\tilde{Q}^2 + \frac{144}{175}\frac{\tilde{\mu}^2\tilde{Q}^4}{K^2} + \frac{72}{245}\frac{\tilde{Q}^6}{K^4}\right] \tag{3.139}$$

$$\frac{a_{3,3}^{polar}}{RT} = -\left(\frac{1}{\tilde{T}}\right)^3 \frac{\eta^2}{K^3}\left[\frac{10}{9}\tilde{\mu}^6 + \frac{159}{125}\frac{\tilde{\mu}^4\tilde{Q}^2}{K^2} + \frac{689}{1000}\frac{\tilde{\mu}^2\tilde{Q}^4}{K^4} + \frac{243}{800}\frac{\tilde{Q}^6}{K^6}\right] \tag{3.140}$$

Where, $K = \frac{\sigma_p}{\sigma}$ considers special range interactions as oppose to hard sphere interactions and is dimensionless. Furthermore, it is worth noting that Nezbeda and co-workers (1996; 2001) as well as Karakatsani et al. (2005) have successfully employed equations (3.138) and (3.140) for pure fluids and mixtures that are dipolar in nature (Karakatsani and Economou, 2006).

Simplified expressions for both two and three-body dipole-induced dipole terms were proposed by Karakatsani and Economou (2006) in a similar manner and are presented by equations (3.141) and (3.142).

$$\frac{a_2^{ind}}{RT} = -\frac{8}{\tilde{T}}\frac{\eta}{K^3}\tilde{\mu}^2\tilde{\alpha} \tag{3.141}$$

$$\frac{a_3^{ind}}{RT} = 10\left(\frac{1}{\tilde{T}}\right)^2 \frac{\eta^2}{K^3}\tilde{\mu}^4\tilde{\alpha} \tag{3.142}$$

Furthermore, mixing rules are required for the evaluation of polarizability as well as the reduced multipole moments as a function of the pure component corresponding parameters and composition. When considering two-body terms, the following rules apply:

$$\tilde{Q} = \frac{\sum_i \sum_j x_i x_j m_i m_j \sqrt{\tilde{Q}_i \tilde{Q}_j}}{\left(\sum_i x_i m_i\right)^2} \tag{3.143}$$

$$\tilde{a} = \frac{\sum_i \sum_j x_i x_j m_i m_j \sqrt{\tilde{a}_i \tilde{a}_j}}{\left(\sum_i x_i m_i\right)^2} \tag{3.144}$$

Equation (3.111) gives the expression for the mixing rule applicable to $\tilde{\mu}$. In the case of three-body terms, the mixing rules presented by equations (3.145) – (3.147) can be used.

$$\tilde{\mu} = \frac{\sum_i \sum_j \sum_k x_i x_j x_k m_i m_j m_k (\tilde{\mu}_i \tilde{\mu}_j \tilde{\mu}_k)^{\frac{1}{3}}}{\left(\sum_i x_i m_i\right)^3} \tag{3.145}$$

$$\tilde{Q} = \frac{\sum_i \sum_j \sum_k x_i x_j x_k m_i m_j m_k (\tilde{Q}_i \tilde{Q}_j \tilde{Q}_k)^{\frac{1}{3}}}{\left(\sum_i x_i m_i\right)^3} \tag{3.146}$$

$$\tilde{a} = \frac{\sum_i \sum_j \sum_k x_i x_j x_k m_i m_j m_k (\tilde{a}_i \tilde{a}_j a_k)^{\frac{1}{3}}}{\left(\sum_i x_i m_i\right)^3} \tag{3.147}$$

Lastly, equations (3.148) and (3.149) present additional mixing rules required to account for cross three-body dipole-dipole-quadrupole and dipole-quadrupole-quadrupole terms found in equation (3.140).

$$(\tilde{\mu}^2 \tilde{Q})^{\frac{1}{3}} = \frac{\sum_i \sum_j \sum_k x_i x_j x_k m_i m_j m_k (\tilde{\mu}_i \tilde{\mu}_j \tilde{Q}_k)^{\frac{1}{3}}}{\left(\sum_i x_i m_i\right)^3} \tag{3.148}$$

$$(\tilde{\mu} \tilde{Q}^2)^{\frac{1}{3}} = \frac{\sum_i \sum_j \sum_k x_i x_j x_k m_i m_j m_k (\tilde{\mu}_i \tilde{Q}_j \tilde{Q}_k)^{\frac{1}{3}}}{\left(\sum_i x_i m_i\right)^3} \tag{3.149}$$

In their original paper, Karakatsani and Economou (2006) apply their proposed modifications to real polar fluids, particularly to fluids that are quadrupolar in nature. Carbon dioxide and ethylene were two such fluids that were studied. Regarding carbon dioxide, tPC-PSAFT demonstrates superior accuracy when compared to PC-PSAFT. However, in the case of ethylene similar results were obtained for both models. Furthermore, when compared to the conventional equations of state, both PC-PSAFT and tPC-PSAFT demonstrate similar accuracy.

The ability of the proposed models to accurately predict the thermodynamic behavior at supercritical and compressed liquid conditions was also studied. In this regard, the fluids selected were carbon dioxide and nitrogen as they are extensively utilized for high-pressure applications. The results obtained from both PC-PSAFT and tPC-PSAFT demonstrate high accuracy.

The accuracy of the proposed models was also investigated using water. The four-site model was employed and assumes that there are two electron acceptor and two electron donor sites. In addition, interactions, namely, dipole-dipole, quadrupole-quadrupole, dipole-quadrupole and dipole-induced dipole, were considered. Results obtained for both models demonstrated excellent correlation of the experimental data.

Furthermore, Karakatsani et al. (2006) further investigated the model accuracy for 1-alcohols such as methanol and demonstrated excellent correlation of the experimental liquid density data up to 50MPa. The accuracy of tPC-PSAFT was further explored through the correlation of VLE, LLE and density data. Systems investigated included water-1-alcohol, water-aliphatic hydrocarbons and acetone-n-alkane mixtures. In addition, the ternary systems water-methanol-ethanol and water-methanol-n-hexane were employed for the prediction of multicomponent phase equilibria. In all cases, tPC-PSAFT demonstrates satisfactory correlation of the data. However, systems consisting of alcohol-alkane mixtures are not well studied in literature.

In a study conducted by Karakatsani et al. (2006), the tPC-PSAFT model was further extended to model the phase behaviour of imidazolium-based ionic liquids and carbon dioxide systems up to 100 MPa and between 313.15 and 353.15K. In order to accurately predict the phase behaviour of the ionic liquid + carbon dioxide binary systems, dipole, quadrupolar and Lewis acid-base type of association were explicitly accounted for between the ionic liquid, carbon dioxide and ionic liquid and carbon dioxide molecules, respectively. The tPC-PSAFT model was able to predict the phase behaviour of these systems however, for binary systems with the highest alkyl chain length and

lowest temperature, the tPC-PSAFT model demonstrated excellent correlation of the experimental data.

In the work of Diamantonis and Economou (2011), the PC-SAFT and tPC-PSAFT equations were used to model the behaviour of water + carbon dioxide in the temperature and pressure ranges of 298 – 533 K and 0 – 60 MPa, respectively. Both models were also utilized to predict the density of the binary system at 298.15 and 332.15 K with PC-SAFT (% AAD of 0.6 %) demonstrating a more accurate correlation of the data when compared to tPC-PSAFT (% AAD of 0.8 %).

Like all models, tPC-PSAFT also exhibits certain limitations. For instance, assuming both the double and triple integrals, equations (3.132) and (3.133), are temperature independent terms is only valid for molecules with hard repulsive interactions. Furthermore, when a mean-spherical approximation is applied to chain segments, the low-density limits replace their expressions. However, the introduction of an adjustable parameter into the model can overcome this shortfall to a certain extent.

3.8. Root Mean Square Deviation

The difference between a calculated value and the actual value, and thus the measure therefore is defined as the root mean square deviation (RMSD). It is an efficient way to measure the accuracy of a model fit as it aggregates the residuals. The RMSD used in this work for fitting to the empirical models is calculated as follows:

$$RMSD = \frac{\sum_{k}^{Q}((\frac{\rho_k^{exp} - \rho_k^{calc}}{\rho_k^{exp}})^2)^{1/2}}{L} \tag{3.150}$$

Where L is the total number of points in the data set, k is a specific data point, ρ_k^{exp} is the experimental density of point k and ρ_k^{calc} is the calculated density of data point k. Minimizing the function for the RMSD via regression enabled model parameters to be determined.

CHAPTER FOUR

Equipment Review

The accurate description of thermophysical properties is imperative for the design and optimization of various chemical processes (Zúñiga-Moreno *et al.*, 2007). Furthermore, they are essential in the development of equations of state as well as predictive models which enable the modeling of chemical systems and hence processes (Yang et al., 2018). The density of a system is one such property. The thermophysical property, density, is employed extensively in fluid mechanics for the design and simulation of various unit operations and in chemical thermodynamics to demonstrate P-V-T relationships of chemical systems. In addition, high-pressure density data finds use in the fields of petroleum engineering, aeronautics, mechanical engineering and is particularly useful in the modeling of chemical processes operating at or near supercritical regions (Economou, 2002; Wu, 2010). Hence, the measurement of high-pressure density is imperative to accurately model the behavior of chemical systems under selected physical conditions. Several precise experimental methods exist for the estimation of density at high-pressures however, only three of the most widely applied methods will be discussed in this chapter. Namely, the vibrating tube densimeter, the bellow volumometer and the floating-piston densimeter.

4.1. Vibrating Tube Densimeter

Vibrating tube densimeters are extensively employed in both the petroleum and process industries due to their speed, precision and ease of operation (Ashcroft et al., 1990). They consist of a glass tube, either straight or U-tube that is made from borosilicate, nested in a thermostated jacket with a general capacity of 0.7 cm^3 (Fitzgerald et al., 2000). The mechanical resonant frequency, of the tube containing the experimental sample, forms the basis of operation of a vibrating tube densimeter. The oscillation period corresponds to a certain frequency and is correlated to the sample density which is largely dependent on the temperature and pressure at which experiments are conducted. The tube containing the liquid sample is mechanically excited, by means of an electromechanical device, such that it vibrates at right angles to its plane. This motion is described by two parameters namely, the period and width of the frequency curve. The liquid sample exerts

a hydrodynamic force on the tube which affects both parameters. A two-fluid calibration method is employed to determine the instrument parameters with water and air/nitrogen being the two most commonly used fluids. Furthermore, the experimental density can be obtained, with use of an empirical relationship, by noting the period.

Several studies have been conducted by employing the vibrating tube densimeter, at atmospheric and high pressures, and some relevant studies are outlined in Table 4.1 along with their temperature and pressure ranges as well as their uncertainties.

Table 4.1. Literature sources employing the vibrating tube densimeter for experimental measurements.

System	Temperature range (K)	Pressure range (MPa)	Uncertainty	Literature
diisopropyl ether (1) + butan-1-ol (2)	278.15 – 323.15	0.1 - 60	$\pm 5x10^{-5}\,\frac{g}{cm^3}$,	(Ulbig et al., 1997)
ethanol (1) + n-heptane (2)	293.15 – 333.15	0.1 - 65	$\pm 0.5\,\frac{kg}{m^3}$	(Watson et al., 2006)
ethanol (1) + n-hexane/n-octane/n-decane (2)	273.15 – 298.15	0.1	$\pm 0.0005\,\frac{g}{cm^3}$	(Feitosa et al., 2009)
hexan-1-ol/octan-1-ol/butan-1-ol (1) + n-heptane (2)	288.15 – 308.15	0.1	$\pm 5x10^{-5}\,\frac{g}{cm^3}$	(Vijande et al., 2006)
dimethyl ether	293 - 373	1 - 70	0.057 %	(Yin et al., 2011)
diethyl adipate	293.15 – 403.15	0.1 - 140	$\pm 0.5\,\frac{kg}{m^3}$	(Comuñas et al., 2008)
propan-1-ol (1) + n-octane/n-nonane/n-decane (2)	313.15 – 363.15	1 - 20	$\pm 0.0032\,\frac{kg}{m^3}$	(Moodley et al., 2018)
propan-1-ol and propan-2-ol	313 - 363	0.5 - 25	$\pm 0.86\,\frac{kg}{m^3}$	(Zúñiga-Moreno and Galicia-Luna, 2002)

4.2. Bellow Volumometer

Bellow volumometers were initially proposed by Bridgman during research into P-V and P-V-T relationships for several liquids at high pressures (Bridgman, 1931, 1932. 1942). An extensive range of literature has been found to support their simple yet efficient operation as well as their accuracy, some of which are highlighted in Table 4.2. The working principle of the bellow volumometer is that the pressure applied to the system will cause a change in the length of the bellow. This implies that the change in the length of the bellows directly relates to the change of volume, under set pressure conditions, and can be measured by instruments such as a linear variable differential transformer (LVDT). Hence, this allows for the determination of the fluid density, as the bellow is loaded with a known mass of liquid (Wu et al., 2013c).

The bellow is initially loaded with a known mass of a liquid sample inside a pressure vessel. During the compression of the liquid samples, the bellows travel vertically along the stainless-steel tubes in which they are encased. A magnetic core is situated at the end of a stainless-steel rod attached to a plug at the lower end of the bellow. The compression process is facilitated by the contraction of the bellow via the use of a hydraulic liquid. This contraction enables the volume change, of the liquid sample, to be measured. The following equation can be employed for the determination of the sample density:

$$\rho = \frac{m}{V_0 - \Delta V} \tag{4.1}$$

Where, ρ is the sample density, m is the sample mass, V_0 is the initial volume and ΔV is the change in volume.

The bellow volumometers ability to operate at ultra-high pressure is one of its most attractive features. Furthermore, the accuracy of the device was evaluated in studies conducted by (Back et al., 1982; Easteal and Woolf, 1987a, 1987b, 1987c; Malhotra and Woolf, 1990) for various hydrocarbon compounds. Measurements were conducted at pressures up to 500 MPa, and demonstrate high accuracy, with uncertainties within 0.2 % reported. Employing the bellow volumometer does however, have its drawbacks. These include permanent strain to the bellow if it is stretched continuously and inaccurate density measurements due to the loss of mechanical properties at high temperature conditions (Wu et al., 2013c).

Table 4.2. Literature sources employing the volumometer for experimental measurements.

System	Temperature range (K)	Pressure range (MPa)	Uncertainty	Literature
acetonitrile (1) + water (2)	298	0.1 - 250	$\pm 0.1 \frac{\text{kg}}{\text{m}^3}$,	(Back et al., 1982)
ethanol	310 - 480	0.1 - 200	$\pm 0.001\rho$	(Takiguchi and Uematsu, 1996)
benzene (1) + hexafluorobenzene/hexa-deuterobenzene (2)	298-373	0.1-400	$\pm 0.4 \frac{\text{kg}}{\text{m}^3}$	(J. H. Dymond et al., 1982)
n-heptane, toluene and oct-1-ene	298-373	0.1-400	0.2 %	(Dymond et al., 1988)

4.3. Floating-piston Densimeter

Floating-piston densimeters operate in a similar manner to the bellow volumometer in that they employ information regarding the change in volume to determine the density of a fluid. Measurements are generally conducted by fixing either the temperature/volume of the system and changing the pressure and volume/temperature, some examples of studies are highlighted in Table 4.3. However, unlike the bellow volumometer, floating-piston densimeters employ an o-ring to help establish high-pressure conditions. Furthermore, the ring enables the separation of the sample and hydraulic fluids.

The liquid sample is loaded into the cylindrical vessel, through a port, and is thereafter compressed to the experimental pressure. Compression of the liquid is achieved through the displacement of the piston, located inside the cell, by means of the pressurized hydraulic fluid. Much like bellow volumometers, floating-piston densimeters also employ the use of a magnetic core, attached to a

rod, which is connected to the side of the piston that contains the hydraulic fluid. This is also the side on which the pressure of the system is observed. The change in volume, due to the movement of the piston, can then be recorded by means of a LVDT. Furthermore, by noting the mass of the liquid sample, the density of the fluid can be computed under the experimental conditions.

Through the inclusion of the sapphire window, the floating-piston densimeter could possibly be employed to determine both density and phase behaviour of chemical systems simultaneously. Special attention should be paid to the type of o-ring employed in the densimeter as they affect the success and accuracy of the experimental run. Furthermore, the operating conditions as well as the fluid sample properties should be accounted for when choosing a ring (Wu et al., 2013c).

Table 4.3. Studies conducting for the experimental determination of density by employing a floating piston densimeter.

System	Temperature range (K)	Pressure range (MPa)	Uncertainty	Literature
Methylcyclohexane, ethylcyclohexane, cis-1,2-dimethylcyclohexane, cis-1,4-dimethylcyclohexane and trans-1,4-dimethylcyclohexane	293 - 525	3 - 275	$\pm 0.75\rho$ %,	(Wu et al., 2013)
o-xylene, m-xylene, p-xylene and 2-methylnaphthalene	294.9-523.8	3.6-265	± 0.4 %	(Wu et al., 2013a)

CHAPTER FIVE

Materials and Experimental

This chapter details the equipment, experimental procedure undertaken, and materials used in this project, and discusses the apparatus components and uncertainties, calibration procedure for the high-pressure densimeter and auxiliaries, the preparation of the apparatus and the operational procedure.

5.1. Apparatus

The apparatus utilized in this work is detailed in Chapters 6-8 and is paraphrased below for the readers convenience.

"The following is a description of the experimental setup utilized during this work as shown in Figure 6.1. A 100 ml, gas-tight syringe is connected, via a smooth rubber tube, to a Teledyne ISCO 100 DM high pressure pump. A high-pressure needle valve, with an operating limit of 69 MPa, controls the liquid sample fed into the high-pressure pump from the syringe. A heating jacket surrounds the piston inside the pump ensuring that the sample remains at a constant measurement temperature. The outlet of the high-pressure pump feeds a pressurized liquid into an Anton Paar DMA HP densimeter. The DMA HP consists of a U-tube with a capacity of 2 cm^3 into which the pressurized liquid sample, exiting the high-pressure pump, is fed. Subsequently, the U-tube is oscillated electronically with a characteristic vibrational period that changes with the density of the fluid inserted into the tube. This change can be directly related to the unknown fluid density by calibration. The operating range for the high-pressure densimeter is 263 – 473 K and 0.1 – 70 MPa for temperature and pressure, respectively. An uncertainty of 0.1-1 $kg.m^{-3}$, with respect to density, has been stated by the supplier. The uncertainty is dependent on the method of calibration as well as the temperature and pressure range utilized when conducting the measurements. A device temperature uncertainty of 0.01 K is stated by Anton Paar for both the atmospheric and high-pressure densimeter cell. The expanded uncertainty in temperature was calculated to be 0.02 K, using a coverage factor of $k = 2$. Viscosity effects on the density readings are automatically accounted for by the device software. A WIKA P-10 pressure transducer, with a supplier stated

uncertainty of 0.0125 MPa, is connected to the outlet of the densimeter via a T-junction. The P-10 transducer was calibrated utilizing nitrogen gas as a reference fluid and a Mensor standard model CPC6000, with an uncertainty of 0.01%. An expanded combined uncertainty of 0.032 MPa (k = 2) was calculated for the high-pressure measurements. A second high-pressure needle valve controls the liquid flow in the exit line from the densimeter. A vacuum pump for cleaning and a waste collection vessel, is connected to the exit from this second valve" (Hussain and Moodley, 2020a).

5.2. Preparation of the Anton Paar Densimeter

5.2.1. Leak Detection

Inaccurate measurement of data can occur due to the presence of leaks in the experimental set-up as these cause fluctuations in the pressure and temperature making these variables difficult to control. Hence, it is essential to detect and eliminate all leaks before the commencement of all experimental runs, especially since the experimental work involved measurements at high pressures. This was done by filling the Teledyne ISCO 100 DM high pressure pump with air, maintaining the closed device loop under high pressure, in this case 10 bar, and ensuring that the high pressure was held without the pump displacing further. A small amount of a soapy water solution was also applied to each of the connected points in the system. Any leaks present in the system would be indicated by the formation of air bubbles when applying the soapy solution and an appreciable decrease in the held pressure or an increase in displacement of the pump. Entry and exit lines to the system were checked regularly to ensure that they were tightly fitted to reduce the possibility of leaks in the system and to ensure safe operation.

5.2.2. Cleaning of the Densimeter

Cleaning of the densimeter is imperative to ensure that samples are not contaminated during the experiments. Distilled, deionized water was charged into the high-pressure pump via the 100 ml gas tight syringe. The high-pressure pump was set to 10 bar. Once the liquid was pressurized, it passed through the densimeter to flush the unit and lines. This was repeated 3 times. Thereafter, a similar procedure was followed using atmospheric air. This ensured that any remaining liquid

water was flushed out of the densimeter. The unit was then placed under vacuum for 20 minutes. Before measurements, the device was flushed 3 times with 15 cm^3 samples of the mixture for the run to further ensure no contamination occurred.

5.3. Temperature, pressure and densimeter calibration

5.3.1. Temperature calibration/checks

Since access to the internal temperature device for the DMA-HP was not easily achievable, temperature calibration was conducted *in situ* by performing density measurements using n-heptane as the standard fluid. The n-heptane ρ-T data at atmospheric pressure was compared to REFPROP standard predictions to determine the contribution to the temperature uncertainty.

5.3.2. Pressure Calibration

A WIKA P-10 pressure transducer (0-25 MPa, 0.05% of range accuracy) was utilized for experimental pressure measurements. The transducer was calibrated utilizing nitrogen gas as the reference fluid and a Mensor standard model CPC6000, with a stated uncertainty of 0.01%. A pressure was first set on the CPC6000. Thereafter the pressure of the system was allowed to stabilize for a duration of 15 minutes before the transducer reading was recorded. Once again, increasing and decreasing runs were undertaken to verify the repeatability of the results obtained. The pressure calibration curve is provided in Appendix D.

5.3.3. Calibration of the Densimeter

Calibration of the densimeter is detailed in Chapters 6-8 and is paraphrased below for the readers convenience.

“Several methods of calibration were conducted in order to assess the effect of the calibration procedure used on the calculated densities. These including the two-fluid calibration procedure, as outlined in the DMA HP user manual, the procedure of Ihmels and Gmehling (2001) and the procedure of Outcalt and McLinden (2007). The differences between the calculated pure component densities of 2-methylpropan-1-ol by each calibration procedure was used to determine the uncertainty introduced by variation in the calibration procedure used. These differences were within the range of uncertainty reported for measurements of similar systems in the literature, and

the expected range quoted by the supplier. Ultimately the two-fluid calibration procedure was used as it replicated the pure component literature data well and was recommended by the device supplier.

The reference fluids utilized for calibration purposes included distilled, deionized water and pure nitrogen gas. The high-pressure pump was first cleaned thoroughly before the calibration process. Distilled water was injected into the ISCO pump utilizing a gas-tight syringe. The liquid was pressurized and then fed into the densimeter where it was heated to the desired temperature at a set pressure. Once the desired temperature had been reached, the frequency of water was recorded at the corresponding temperature and pressure. This procedure was repeated for a temperature and pressure range of 313.15 – 353.15 K and 0 – 20 MPa, respectively. A similar technique was followed using the pure nitrogen gas.

The DMA HP supplier provides an equation that allows for the vibrational period obtained to be converted to density utilizing the two-fluid calibration procedure with water and nitrogen as reference fluids. The equation is expressed as follows:

$$\rho_m(P,T,\tau) = \rho_{H_2O}(P,T) + \frac{\left(\tau_m^2(P,T)-\tau_{H_2O}^2(P,T)\right)\left(\rho_{H_2O}(P,T)-\rho_{N_2}(P,T)\right)}{\tau_{H_2O}^2(P,T)-\tau_{N_2}^2(P,T)} \qquad (5.1)$$

Where ρ, T, P, τ are the density in kg.m^{-3}, temperature in Kelvin, pressure in MPa and vibrational period in μs. The reference property for water or nitrogen, respectively, are denoted by the subscript's H_2O and N_2 while the subscript *m* refers to the measurement sample.

The correlations proposed by Wagner and Pruß (2002) and Span et al. (1998) were utilized to determine the reference densities of water and nitrogen, respectively" (Hussain and Moodley, 2020a).

5.4. Uncertainties

The uncertainties in temperature, pressure and composition were calculated using standard procedures involving error propagation, as detailed by NIST (ISO, 2008).

The standard combined uncertainties ($u_c(\theta)$) for the measured variables (θ) were determined as follows:

$$u_c(\theta) = \sqrt{\sum u_i(\theta)^2} \tag{5.2}$$

Where $u_i(\theta)$ is the standard uncertainty of variable (θ) from source *i*. Sources include uncertainty from calibration, repeatability, accuracy, device precision, stability, chemical purity etc.

The combined uncertainties for temperature and pressure were calculated from:

$$u_c(T) = \sqrt{u_{check}(T)^2 + u_{supp}(T)^2 + u_{stab}(T)^2} \tag{5.3}$$

$$u_c(P) = \sqrt{u_{calib}(P)^2 + u_{supp}(P)^2 + u_{stab}(P)^2 + u_{type\,B}(P)^2} \tag{5.4}$$

Where u_{check}, u_{calib}, u_{supp}, u_{stab}, $u_{type\,B}$ are the temperature check, pressure calibration, supplier reported precision and stability during experiments for each parameter, type B from historical measurements/literature respectively. The uncertainty from the in-house calibration (u_{calib}) for pressure, includes the uncertainty due to the accuracy and repeatability of the transducer.

The standard combined uncertainty for composition is calculated by:

$$u_c(x_i) = \sqrt{u_{bal}(x_i)^2 + u_{pur}(x_i)^2} \tag{5.5}$$

Where u_{bal} and u_{pur} are the standard uncertainties due to the mass balance used for sample preparations, and the uncertainty introduced by chemical impurity, respectively.

Expanded uncertainties were calculated with a coverage factor of *k* = 2, yielding 95% confidence intervals. The uncertainty in density was calculated using error propagation. An example

uncertainty breakdown for density, including the influencing parameters, is provided in the manuscript chapters. These were found to be system and component specific.

5.5. Start-up procedure

At the start of the experiment, both the high-pressure and atmospheric pressure Anton Paar Densimeters were switched on. The experimental temperature was then set on the atmospheric pressure cell, which is used as the input display for the DMA HP, and all connections were thoroughly checked. The display box for the pressure transducer as well as the high-pressure pump were switched on. The valve on the line entering the pump was opened and 30 milliliters of the sample solution was charged into the pump. This valve was then tightly closed to isolate the experimental setup used for measurement purposes. A pressure was then set on the high-pressure pump and the pump was allowed to compress to the desired pressure by feeding into high-pressure densimeter via a connector tube, up to the closed exit valve.

5.6. Shut down procedure

The valve on the line entering the ISCO 100 DM pump was checked to ensure it was in the closed position. Thereafter, the high-pressure pump was switched to flow mode and the exit needle valve was opened gradually. The liquid sample was then pumped out of the densimeter and the temperature of the densimeter was set to 25 ℃. The valve on the line entering the high-pressure pump was then opened and the clean-up procedure, mentioned above, was followed.

5.7. Isothermal operating procedure for density measurements

The experimental procedure followed is detailed in Chapters 6-8 and is paraphrased below for the readers convenience.

“Standard solution mixtures of approximately 80 ml, were prepared using a Mettler-Toledo mass balance (model AB204-S) with a precision of 0.0001g. Component 1 was added to a sealable vessel and the mass was recorded. A second component was then added to the vessel to achieve a desired mass ratio between the two components. The solution was then stirred to ensure proper

mixing of both components. This standard solution was then injected into the evacuated high-pressure pump, in increments of approximately 15 ml, via a gas-tight syringe. This allowed the high-pressure pump, densimeter and lines to be flushed preventing any contamination of the sample utilized for measurement purposes and was repeated three times. The remaining sample was then injected into the pump before both needle valves were closed, ensuring that the system was isolated. Isothermal conditions were achieved by setting the temperature of the heating jacket to the desired experimental temperature. This ensures that any temperature gradient that exists between the pump and the densimeter are negligible. If, however, any small temperature gradients do exist, it is assumed that they are accounted for, before thermal equilibrium is achieved, by the temperature controller built into the DMA HP. The experimental temperature and pressures were set using the densimeter and high-pressure pump, respectively. The pressure, temperature and vibrational period of the sample were then allowed to stabilize for 60-90 minutes before the readings were recorded. The same procedure was followed for the entire temperature and pressure range.

5.8. Materials

The materials utilized in this work is detailed in Chapters 6-8 and is paraphrased below for the reader's convenience.

"The chemicals utilized for the density measurements in this work, namely n-octane, n-decane, n-heptane, butan-1-ol, butan-2-ol, 2-methylpropan-1-ol and ethanol were obtained from Sigma-Aldrich with a specified purity of greater than 99% by weight. The alcohols were dried by molecular sieve (3Å $K_nNa_{12-n}[(AlO_2)_{12}(SiO_2)_{12}]$) prior to use, and the water content was confirmed to be less than 0.0005 mass fraction by Karl-Fischer titration using an MKS 500 apparatus.

Purity checks were performed using an ATAGO RX-7000a refractometer, with a standard uncertainty of 0.0001, gas chromatography, with a capillary column consisting of the following dimensions: 30m x 0.25mm x 0.25µm film thickness – Zebron^{TM}7HG-G010-11, and an Anton Paar DMA 5000 densimeter for measurements at atmospheric pressure. The refractive indices and densities of the pure components were recorded at a temperature of 293.15 K and 298.15 K.

Distilled, deionized water and air was utilized for calibration of the DMA 5000 densimeter, while

Distilled, deionized water and pure nitrogen gas was used to calibrate the DMA HP apparatus used for the high-pressure density measurements. The results obtained from the purity checks as well as the supplier stated purities are presented in Tables 6.1 (Hussain and Moodley, 2020a).

5.9. Systems and conditions measured

In this work, six novel binary systems were measured. These systems as well as the approximate conditions considered for experiments are tabulated in Table 5.1. These conditions were selected as they cover a significant range to perform meaningful comparisons to model predictions and to assess model performances. Secondly the conditions considered are encountered in chemical processing of alkane-oxygenated hydrocarbon mixtures such as in the Fischer-Tropsch process (De Klerk, 2008). High-pressure density data is used extensively in the field of petroleum engineering to classify the quality and composition of the oils present, and can also be used in aeronautics, engine design and submarine design (Wu, 2010). Several studies focus on the benefits of using alcohols for enhanced oil recovery, quality biofuels as well as for the inhibition of gas hydrates. However, little information is available in the literature regarding the thermophysical properties such as density, excess volumes, thermal expansivity and compressibility's of alkane-oxygenated hydrocarbon mixtures at these conditions. In addition, equations of states and models generally provide poor predictions of the systems density hence, necessitating the need for experimental data at these elevated temperatures and pressures.

Table 5.1: Systems and measurement conditions for the experiments conducted in this work.

System	Temperature Range (K)	Pressure Range (MPa)	Composition Range (mole fraction)
butan-1-ol (1) + n-octane (2)	313 – 353	0.1 – 20	0 - 1
butan-1-ol (1) + n-decane (2)	313 – 353	0.1 – 20	0 - 1
butan-2-ol (1) + n-octane (2)	313 – 353	0.1 – 20	0 - 1
butan-2-ol (1) + n-decane (2)	313 – 353	0.1 – 20	0 - 1
2-methylpropan-1-ol (1) + n-octane (2)	313 – 353	0.1 – 20	0 - 1
2-methylpropan-1-ol (1) + n-decane (2)	313 – 353	0.1 – 20	0 - 1

CHAPTER 6

P−ρ−T Data and Modeling for Butan-1-ol + n-Octane or n-Decane between 313.15−353.15 K and 0.1−20 MPa

6.1.Abstract

Density measurements conducted for the binary systems of butan-1-ol (1) + n-octane (2) and butan-1-ol (1) + n-decane (2) at high pressures are presented in this work. These measurements were conducted utilizing an Anton Paar DMA HP densitometer and encompass the entire composition range, with a temperature and pressure range of T = (313.15−353.15 K) and P= (0.1−20) MPa, respectively. The modified Toscani−Szwarc equation of state was employed to successfully correlate the experimental density data. The measured data were observed to comply with general expected trends with regards to the relationship between density, temperature, and pressure. Derived thermodynamic properties, namely, excess molar volumes, thermal expansivity, and isothermal compressibility, are also presented. Deviations from ideality are attributed to differing molecule sizes and shapes as well as intermolecular interactions between components constituting the mixture.

6.2.Introduction

A biofuel is any fuel that is derived from plant or animal matter which is commonly referred to as biomass. Unlike fossil fuels such as petroleum, biofuel is seen as a source of renewable energy as its feedstocks can be replenished (Chen et al., 2014). It also has the potential to be a more cost-effective and environmentally safe alternative to fossil fuels. Liquid biofuels, such as alcohols, have been receiving greater interest for their applications in the transportation industry. In the United States of America, biofuel in the form of ethanol, is produced from maize and is blended into gasoline to produce a fuel containing 0.10−0.85 ethanol by mass fraction (Trindade and dos Santos, 2017). While in Brazil, ethanol is produced from sugarcane and is utilized to produce a fuel consisting of 0.85 ethanol by mass fraction (Harvey and Meylemans, 2011). Other commonly used biofuels include methane gas, methanol, and butan-1-ol (Rajesh Kumar and Saravanan, 2016).

In comparison to other commonly utilized alcohol fuels such as ethanol and methanol, butan-1-ol demonstrates a number of advantages. These include amongst others, the net heat of combustion

for butan-1-ol which is approximately 0.83 of that of gasoline compared to 0.65 and 0.48 for ethanol and methanol, respectively (Harvey and Meylemans, 2011). Lower weight alcohols such as methanol, ethanol, and propan-1-ol tend to be rather hygroscopic as compared to butan-1-ol. Based on its relatively high boiling and flash point, butan-1-ol is generally safer to work with compared to lower chain length alcohols (Rajesh Kumar and Saravanan, 2016). It is also less corrosive when compared to ethanol and can be transported via existing pipelines. Unlike lower weight alcohols, butan-1-ol is not fully miscible with water forming a heterogenous azeotrope at 365 K (101 kPa) and is also less hydrophilic (Moss et al., 2008). This makes low energy purification of butan-1-ol from bioreaction possible, by extraction. In respect to fuel performance, butan-1-ol has a research octane number of 96 which compares favorably with gasoline (Moss et al., 2008). Butan-1-ol also requires a lower air/fuel ratio compared to conventional gasoline which improves fuel conversion efficiency. Several studies (Harvey and Meylemans, 2011; Moss et al., 2008; Rajesh Kumar and Saravanan, 2016; Zúñiga-Moreno and Galicia-Luna, 2002) have highlighted the suitability of blending butan-1-ol biofuel with conventional petroleum to reduce the dependency on fossil fuels as transport fuels. However, little information is available in the literature regarding the physical properties such as density, thermal expansivity, and compressibility of mixtures of petroleum derived fuels with butan-1-ol (Estrada-Baltazar et al., 2013), especially at elevated temperatures and pressures. This information is extremely useful as it is essential for process design as well as unit design such as combustion engines where fuel pressures exceed 10 MPa (IMechE, 2012).

To address this, in this study, n-octane and n-decane are used as representative petroleum-derived fuels and are blended in different proportions with butan-1-ol to produce representative petroleum + biofuel mixtures. High-pressure measurements are then conducted for these mixtures in the temperature range of T = (313.15−353.15 K) and pressure range of P = (0.1−20 MPa). The data is modeled using empirical correlations and compared to correlations and predictions by various equations of state.

6.3. Theory

An excess thermodynamic property can be defined as the difference between the real value and the hypothetical value the property would have in an ideal solution at the same temperature, pressure, and composition. The experimental excess molar volume (V^E) can be calculated using the following equation:

$$V^E = \sum_{i=1}^{N} x_i M_i \left(\frac{1}{\rho} - \frac{1}{\rho_i}\right) \quad (6.1)$$

where, N is the total number of components making up the mixture, M_i is the molecular mass of component i, x_i is the mole fraction of component i, ρ is the mixture density, and ρ_i is the density of the pure component i.

Thermal expansivity is defined as the differential change in volume with temperature. The isobaric thermal expansivity can be calculated from density utilizing the following formula:

$$\alpha_P = -\frac{1}{\rho}\left(\frac{\partial \rho}{\partial T}\right)_P \quad (6.2)$$

where, α_P is the thermal expansivity at constant pressure (P), ρ is the density of the mixture in $kg \cdot m^{-3}$, and T is the temperature in kelvin.

Isothermal compressibility is defined as a differential change in volume with pressure. The isothermal compressibility can be calculated from density utilizing the following formula:

$$\kappa_T = \frac{1}{\rho}\left(\frac{\partial \rho}{\partial P}\right)_T \quad (6.3)$$

where, κ_T is the compressibility at constant temperature (T).

The modified Toscani−Szwarc equation of state (MTS EOS) (2004) with a further exponent modification by Quevedo-Nolasco *et al*. (2012) was employed to correlate the experimental density data presented in this work. The density is calculated as follows:

$$\rho^{calc} = \frac{c_3 - \frac{c_4}{T} - \frac{c_5}{T^{1/3}} + P}{c_1 + c_2 P} \tag{6.4}$$

where, ρ^{calc} is the density of the mixture in $kg \cdot m^{-3}$ calculated by the model, P is the pressure of the system in MPa, T is the experimental temperature in Kelvin, and c_1 to c_5 denotes the regressed model parameters.

The root-mean-square deviation (rmsd) is the difference between the calculated and actual values and is often utilized to quantify the quality of a model fit. It is given by:

$$RMSD = \frac{\sum_k^L ((\frac{\rho_k^{exp} - \rho_k^{calc}}{\rho_k^{exp}})^2)^{1/2}}{L} \tag{6.5}$$

where L is the total number of points in the data set, k is a specific data point, ρ_k^{exp} is the experimental density of point k, and ρ_k^{calc} is the calculated density of data point k. Minimizing the function for the rmsd via regression enabled model parameters to be determined.

With the MTS EOS characterized, the derivatives given by equations (6.2) and (6.3) can be evaluated to give the following equations:

$$\alpha_P = -\frac{\frac{c_4}{T^2} + \frac{c_5}{3T^{4/3}}}{c_3 - \frac{c_4}{T} - \frac{c_5}{T^{1/3}} + P} \tag{6.6}$$

$$\kappa_T = \frac{1}{c_3 - \frac{c_4}{T} - \frac{c_5}{T^{1/3}} + P} - \frac{c_2}{c_1 + c_2 P} \tag{6.7}$$

6.4. Experimental Section

6.4.1. Materials.

The chemicals utilized for the density measurements in this work, namely, n-octane, n-decane, and butan-1-ol, were obtained from Sigma-Aldrich with a specified purity of greater than 0.99 mass fraction. The butan-1-ol was dried by a molecular sieve (3 Å $K_nNa_{12-n}[(AlO_2)_{12}(SiO_2)_{12}]$) prior to use. The water content was confirmed to be less than 0.0005 mass fraction by Karl-Fischer titration using an MKS 500 apparatus.

Refractive index (RI) checks were performed using an ATAGO RX-7000a refractometer, with a standard uncertainty of 0.0001. Purity checks were performed by gas chromatography, using a Shimadzu GC2014 with a capillary column consisting of the following dimensions: 30 m × 0.25 mm × 0.25 μm film thickness - Zebron 7HG-G010-11. Density checks were performed using an Anton Paar DMA 5000 densitometer for measurements at atmospheric pressure. The refractive indices and densities of the pure components were recorded at a temperature of 293.15 or 298.15 and 313.15 K, respectively.

Distilled, deionized water and dry air were utilized for calibration of the DMA 5000 densitometer, while distilled, deionized water and pure nitrogen gas were used to calibrate the DMA HP apparatus used for the high-pressure density measurements. The results obtained from the RI, purity and density checks as well as the supplier stated purities are presented in Table 6.1.

Table 6.1. Chemical suppliers and purities.

Component	CAS No.	Supplier	Refractive index (RI) at 0.101 MPa.		Minimum stated mass fraction purity	GC peak relative area	Density at 313.15 K and 0.101 MPa /kg.m^{-3}.	
			Exp.[ǂ]	Lit. (Haynes, 2014)			Exp[*]	Lit.
n-heptane	142-82-5	Sigma-Aldrich	1.3852 (298.15 K)	1.3855 (298.15 K)	0.99	0.999	666.31	666.3 (Rahaman, Islam *et al*., 2011) 666.62 (Kijevčanin et al., 2009) 666.68 (Chorążewski, 2007)
n-octane	111-65-9	Sigma-Aldrich	1.3948 (298.15 K)	1.3944 (298.15 K)	0.99	0.999	686.25	686.22 (Lampreia and Nieto de Castro, 2011) 686.29 (Sanmamed et al., 2009) 686.36 (L. Lugo et al., 2001)
n-decane	124-18-5	Sigma-Aldrich	1.4092 (298.15 K)	1.4090 (298.15 K)	0.99	0.999	714.72	715.64 (Quevedo-Nolasco *et al.*, 2012) 714.40 (Banipal, *et al.* 1991) 714.79 (Troncoso et al., 2004)
ethanol[a]	64-17-5	Merck	1.3614 (293.15 K)	1.3611 (293.15 K)	0.99	0.999	772.13	772.53 (Langa et al., 2005) 772.1 (Zéberg-Mikkelsen et al., 2005b) 771.98 (Djojoputro and Ismadji, 2005)
butan-1-ol[a]	71-36-3	Sigma-Aldrich	1.3991 (293.15 K)	1.3988 (293.15 K)	0.99	0.999	794.17	794.16 (Gascón et al., 2003) 794.38 (Vallés et al., 2004) 794.14 (Coquelet et al., 2007)
nitrogen	7727-37-9	Afrox	-	-	0.99	-	-	-
air	132259-10-0	Afrox	-	-	0.78 nitrogen 0.21 oxygen 0.009 argon 0.0003 carbon dioxide Trace helium, neon, krypton, xenon	-	-	-
water	7732-18-5	-	1.3334 (293.15 K)	1.33336 (293.15 K)	-	0.9999	-	-

1. [ǂ] At sodium D-line = 589 nm. Expanded uncertainties $U_c(k=2)$ are $U_c(RI) = 0.0002$, $U_c(T) = 0.02K$, $U_c(P) = 0.002\ MPa$, [*] Expanded uncertainties $U_c(k=2)$ are $U_c(T) = 0.02K$, are $U_c(P) = 0.002\ MPa$ and $U_c(\rho) = 1.08\ kg.m^{-3}$
2. [a] Purified by molecular sieve

6.4.2. Apparatus

The following is a description of the experimental setup utilized during this work as shown in Figure 6.1 and described by Moodley *et al.* (2018). A 100 mL, gas-tight syringe is connected via a rubber tube to a Teledyne ISCO 100 DM high-pressure pump. A high-pressure needle valve, with an operating limit of 69 MPa, controls the liquid sample fed into the high-pressure pump from the syringe. A heating jacket surrounds the piston inside the pump ensuring that the sample remains at a constant temperature. The outlet of the high-pressure pump feeds a pressurized liquid into an Anton Paar DMA HP densitometer. The densitometer consists of a U-tube, with a capacity of 2 cm^3 and has a temperature and pressure range of 263−473 K and approximately 0.1−70 MPa, respectively. An uncertainty of 0.1−1 $kg \cdot m^{-3}$, with respect to density, has been stated by the supplier. The uncertainty is dependent on the method of calibration as well as the temperature and pressure range utilized when conducting the measurements. A device temperature uncertainty of 0.01 K is stated by Anton Paar for both the atmospheric and high-pressure densitometer cell. The expanded uncertainty in temperature was calculated to be 0.02 K, using a coverage factor of k = 2. Viscosity effects on the density readings are automatically accounted for by the device software. A WIKA P-10 pressure transducer, with a supplier stated uncertainty of 0.0125 MPa, is connected to the outlet of the densitometer via a T-junction. The P-10 transducer was calibrated utilizing nitrogen gas as a reference fluid and a Mensor standard model CPC6000, with a relative uncertainty of 0.0001. An expanded combined uncertainty of 0.032 MPa (k = 2) was calculated for the high-pressure measurements. A second high-pressure needle valve controls the liquid flow in the exit line from the densitometer. A vacuum pump for cleaning and a waste collection vessel are connected to the exit from this second valve.

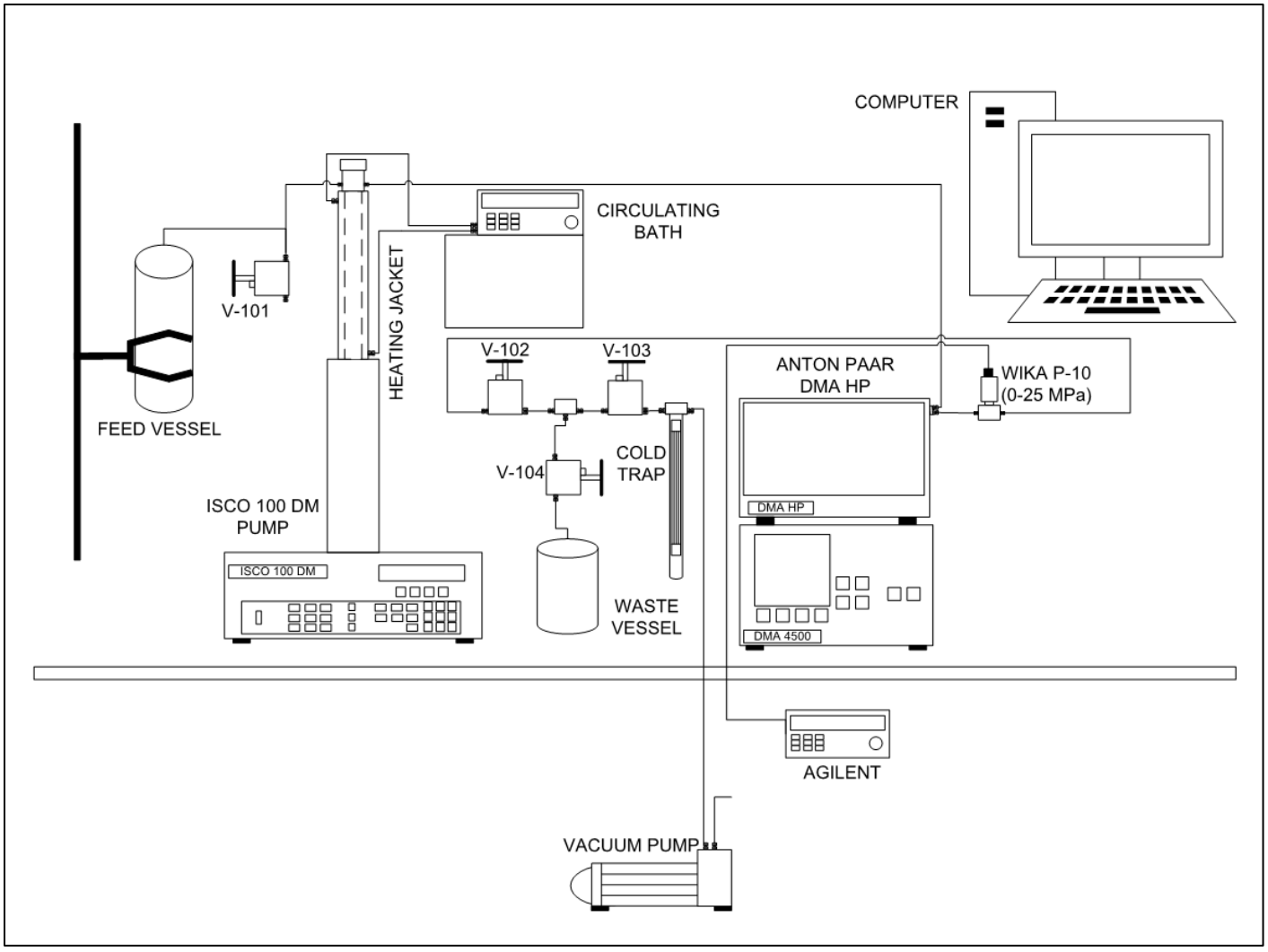

Figure 6.1. Schematic of the experimental apparatus used in this work (adapted from (Moodley *et al.*, 2018).

6.4.3. Measurements

6.4.3.1.Calibration of the DMA HP Densitometer

The two-fluid calibration procedure, a simple and accurate method, was utilized for the calibration of the DMA HP densitometer as described in the device manual. The reference fluids utilized for calibration purposes included distilled, deionized water and pure nitrogen gas. The high-pressure pump was first cleaned thoroughly before the calibration process. Distilled water was injected into the ISCO pump utilizing a gas-tight syringe. The liquid was pressurized and then fed into the densitometer where it was heated to the desired temperature at a set pressure. Once the desired

temperature had been reached, the frequency of water was recorded at the corresponding temperature and pressure. This procedure was repeated for a temperature and pressure range of 313.15−353.15 K and 0−20 MPa, respectively. A similar technique was followed using the pure nitrogen gas.

The DMA HP supplier provides an equation that allows for the vibrational period obtained to be converted to density utilizing the two-fluid calibration procedure with water and nitrogen as reference fluids. The equation is expressed as follows"

$$\rho_m(P,T,\tau) = \rho_{H_2O}(P,T) + \frac{\left(\tau_m^2(P,T) - \tau_{H_2O}^2(P,T)\right)\left(\rho_{H_2O}(P,T) - \rho_{N_2}(P,T)\right)}{\tau_{H_2O}^2(P,T) - \tau_{N_2}^2(P,T)} \quad (6.8)$$

where ρ, T, P, and τ are the density in $kg \cdot m^{-3}$, temperature in kelvin, pressure in MPa, and vibrational period in μs. The reference property for water or nitrogen, respectively, is denoted by the subscript's H_2O and N_2 while the subscript m refers to the measurement sample.

The correlations proposed by Wagner and Pruß (2002) and Span *et al.* (1998) was utilized to determine the reference densities of water and nitrogen, respectively.

6.4.3.2. Experimental Procedure

Standard solution mixtures of approximately 80 mL, were prepared using a Mettler-Toledo mass balance (model AB204-S) with a precision of 0.0001 g. Component 1 was added to a sealable vessel and the mass was recorded. A second component was then added to the vessel to achieve a desired mass ratio between the two components. The solution was then stirred to ensure proper mixing of both components. This standard solution was then injected into the evacuated high-pressure pump, in increments of approximately 15 mL, via a gas-tight syringe. This allowed the high-pressure pump, densitometer and lines to be flushed preventing any contamination of the sample utilized for measurement purposes and was repeated three times. The remaining sample was then injected into the pump before both the needle valves were closed, ensuring that the system was isolated. Isothermal conditions were achieved by setting the temperature of the heating jacket to the desired experimental temperature. This ensures that any temperature gradient that exists

between the pump and the densitometer are negligible. If, however, any small temperature gradients do exist, it is assumed that they are accounted for, before thermal equilibrium is achieved, by the temperature controller built into the DMA HP. The experimental temperature and pressures were set using the densitometer and high-pressure pump, respectively. The pressure, temperature, and vibrational period of the sample were then allowed to stabilize for 60−90 minutes before the readings were recorded. The same procedure was followed for the entire temperature and pressure range.

The method given by the Joint Committee for Guides in Metrology (JCGM) (2008) was employed to calculate the expanded combined uncertainty in density with a coverage factor of k = 2. These were found to be 1.08 and 1.1 kg·m^{-3} for pure components and mixtures, respectively, and include uncertainty introduced by impurities present in the chemicals. An example uncertainty breakdown is provided in Table 6.2. A second calibration model (different from eq 8) was used based on the procedures of Ihmels and Gmehling (2001) and Outcalt and McLinden (2007). The difference between the calibrated densities by both models was used as a contribution to the total uncertainty in density.

Table 6.2. Example of uncertainty breakdown for density*

Source	Uncertainty U	Contribution to $U_C(\rho)$/(kg·m^{-3})
Temperature $U(T)$, k =2	0.02 K	0.02
Pressure $U(P)$, k = 2	0.032 MPa	0.06
Period $U(\tau)$, k = 2 (repeatability)	0.003 μs	0.12
Mixture Composition x_i, k = 2	0.002 mol fraction	0.06
Uncertainty from Measurements $U_{meas}(\rho)$, k = 2		0.13
EOS of the calibration fluids $U_{EOS}(\rho)/\rho$, k = 2	0.05%	0.50
Calibration model (ρ), k = 2	0.94 kg·m^{-3}	0.94
Impurity x_i, k = 2	0.004 mol fraction	0.12
Combined expanded uncertainty in density $U_C(\rho)$, k = 2		1.10

* butan-1-ol (1) + n-decane (2) system at x_1= 0.4968 was used for this example

Table 6.3. Experimental Pure Component Densities for n-Heptane, n-Octane, n-Decane, Ethanol, and Butan-1-ol[a,b]

	T/K = 313.15		T/K = 323.15		T/K = 333.15		T/K= 343.15		T/K = 353.15	
Component	**P/MPa**	**ρ/ kg.m^{-3}**	**P/MPa**	**ρ/ kg.m^{-3}**	**P/MPa**	**ρ/ kg.m^{-3}**	**P/MPa**	**ρ/ kg.m^{-3}**	**P/MPa**	**ρ/ kg.m^{-3}**
n-heptane										
	0.1*	666.31	0.1	657.62	0.1	649.14	0.1	641.02	0.1	-
	1.09	667.01	1.20	659.38	1.19	650.67	1.24	642.71	1.23	633.56
	2.08	668.01	2.21	660.50	2.18	651.90	2.22	643.96	2.22	634.82
	3.11	669.30	3.21	661.61	3.18	653.09	3.23	645.22	3.22	636.34
	4.16	670.72	4.21	662.70	4.18	654.24	4.23	646.43	4.23	637.80
	5.23	671.78	5.22	663.82	5.18	655.46	5.24	647.68	5.23	639.15
	6.23	672.88	6.21	664.90	6.19	656.59	6.25	648.86	6.24	640.41
	7.24	673.94	7.21	665.98	7.18	657.76	7.25	650.23	7.25	641.65
	8.24	674.95	8.21	667.05	8.23	659.18	8.26	651.43	8.25	643.01
	9.25	675.95	9.26	668.15	9.24	660.07	9.26	652.55	9.26	644.28
	10.26	676.94	10.27	669.22	10.24	661.19	10.27	653.62	10.27	645.44
	11.26	677.92	11.27	670.32	11.25	662.26	11.28	654.78	11.27	646.64
	12.27	678.88	12.29	671.34	12.25	663.30	12.28	655.84	12.28	647.76
	13.27	679.79	13.29	672.34	13.26	664.29	13.29	656.95	13.28	648.93
	14.27	680.74	14.29	673.29	14.26	665.28	14.29	657.99	14.29	650.01
	15.28	681.64	15.30	674.00	15.27	666.31	15.29	659.03	15.29	651.11
	16.28	682.54	16.30	674.93	16.27	667.09	16.30	659.99	16.29	652.14
	17.29	683.42	17.30	675.81	17.28	668.01	17.30	660.98	17.30	653.20
	18.32	684.16	18.31	676.62	18.28	668.83	18.31	661.87	18.30	654.11
	19.30	684.94	19.31	677.38	19.28	669.60	19.31	662.75	19.31	655.00
	20.29	685.61	20.31	678.08	20.32	670.72	20.31	663.67	20.31	655.96
n-octane										
	0.1	686.25	0.1	677.93	0.1	669.55	0.1	661.09	0.1	652.28
	1.14	687.93	1.15	679.84	1.13	671.86	1.14	663.06	1.14	655.01
	2.14	689.22	2.15	680.83	2.13	672.95	2.14	664.23	2.14	655.91
	3.15	690.11	3.17	681.80	3.14	674.04	3.14	665.30	3.14	657.37
	4.16	690.96	4.18	682.75	4.15	675.01	4.16	666.37	4.16	658.67
	5.17	691.81	5.19	683.76	5.16	676.15	5.17	667.44	5.16	659.79
	6.18	692.75	6.20	684.75	6.17	677.09	6.18	668.51	6.18	660.97
	7.19	693.67	7.22	685.71	7.18	678.13	7.19	669.73	7.19	662.06
	8.20	694.55	8.23	686.67	8.19	679.60	8.20	670.77	8.20	663.27
	9.23	695.41	9.24	687.58	9.20	680.13	9.21	671.83	9.21	664.38
	10.23	696.29	10.25	688.49	10.21	681.14	10.22	672.73	10.22	665.33
	11.24	697.14	11.25	689.48	11.22	682.09	11.23	673.84	11.23	666.45
	12.25	697.99	12.27	690.28	12.23	683.03	12.24	674.73	12.24	667.45
	13.26	698.83	13.27	691.16	13.24	683.91	13.25	675.72	13.25	668.45

	14.27	699.73	14.26	692.05	14.25	684.81	14.26	676.69	14.26	669.39
	15.27	700.55	15.29	692.95	15.26	685.76	15.27	677.62	15.25	670.44
	16.28	701.40	16.30	693.83	16.27	686.55	16.27	678.47	16.27	671.44
	17.29	702.20	17.30	694.58	17.27	687.40	17.28	679.43	17.27	672.34
	18.30	702.88	18.30	695.35	18.28	688.22	18.28	680.26	18.29	673.14
	19.30	703.57	19.30	696.04	19.28	689.06	19.29	681.05	19.29	673.94
	20.31	704.17	20.29	696.70	20.28	689.70	20.29	681.76	20.29	674.81
n-decane										
	0.1	714.69	0.1	707.01	0.1	699.22	0.1	691.51	0.1	683.81
	1.13	715.64	1.12	708.27	1.13	700.88	1.13	693.49	1.12	685.90
	2.12	716.35	2.12	709.13	2.12	701.82	2.13	694.50	2.13	686.81
	3.13	717.13	3.13	710.01	3.13	702.75	3.14	695.47	3.14	688.00
	4.14	717.90	4.14	710.84	4.14	703.63	4.15	696.41	4.15	689.09
	5.15	718.67	5.15	711.74	5.15	704.59	5.16	697.23	5.16	690.11
	6.16	719.52	6.16	712.61	6.16	705.46	6.16	698.19	6.17	691.12
	7.17	720.34	7.17	713.47	7.17	706.37	7.18	699.25	7.18	692.10
	8.18	721.13	8.18	714.33	8.18	707.47	8.19	700.21	8.19	693.16
	9.19	721.91	9.19	715.17	9.18	708.16	9.20	701.13	9.20	694.14
	10.20	722.72	10.20	716.02	10.20	709.05	10.20	701.98	10.21	695.03
	11.21	723.51	11.21	716.92	11.21	709.91	11.22	702.97	11.22	696.02
	12.22	724.30	12.22	717.64	12.22	710.75	12.23	703.78	12.23	696.91
	13.23	725.06	13.23	718.46	13.22	711.56	13.23	704.69	13.24	697.83
	14.24	725.87	14.24	719.26	14.22	712.36	14.25	705.53	14.25	698.66
	15.24	726.63	15.25	720.03	15.24	713.23	15.25	706.36	15.26	699.58
	16.25	727.38	16.25	720.81	16.24	714.00	16.26	707.16	16.26	700.47
	17.26	728.12	17.25	721.53	17.25	714.72	17.27	707.99	17.27	701.28
	18.26	728.75	18.26	722.20	18.25	715.46	18.27	708.75	18.28	702.05
	19.26	729.40	19.27	722.84	19.26	716.13	19.27	709.43	19.28	702.78
	20.27	729.97	20.27	723.46	20.26	716.81	20.28	710.13	20.29	703.56
ethanol										
	0.1	772.13	0.1	763.15	0.1	754.23	0.1	744.72	0.1	-
	1.11	772.88	1.09	763.90	1.10	755.02	1.11	745.40	1.12	736.20
	2.11	773.68	2.09	764.87	2.11	756.14	2.12	746.57	2.13	737.33
	3.12	774.55	3.10	765.90	3.12	757.21	3.12	747.68	3.14	738.64
	4.12	775.35	4.10	766.88	4.12	758.24	4.13	748.76	4.14	739.86
	5.12	776.23	5.11	767.89	5.13	759.32	5.13	749.83	5.15	741.00
	6.13	777.20	6.12	768.90	6.13	760.32	6.14	750.94	6.15	742.12
	7.13	778.12	7.12	769.88	7.14	761.35	7.15	752.13	7.15	743.27
	8.14	778.93	8.13	770.85	8.14	762.55	8.15	753.19	8.17	744.46
	9.15	779.74	9.14	771.82	9.15	763.39	9.16	754.26	9.17	745.58
	10.15	780.68	10.14	772.78	10.15	764.41	10.16	755.26	10.18	746.59
	11.15	781.57	11.15	773.79	11.16	765.39	11.17	756.37	11.18	747.69
	12.16	782.42	12.16	774.66	12.16	766.36	12.17	757.36	12.18	748.72
	13.16	783.24	13.16	775.59	13.16	767.31	13.17	758.39	13.18	749.77
	14.16	784.08	14.17	776.53	14.16	768.26	14.18	759.21	14.19	750.76
	15.17	784.94	15.17	777.44	15.17	769.22	15.18	760.37	15.20	751.77

	16.17	785.79	16.18	778.29	16.17	770.09	16.18	761.31	16.20	752.78
	17.17	786.63	17.18	779.13	17.17	770.99	17.19	762.27	17.20	753.76
	18.17	787.40	18.18	779.92	18.17	771.87	18.19	763.18	18.20	754.68
	19.17	788.18	19.18	780.71	19.17	772.74	19.19	764.06	19.20	755.57
	20.19	788.89	20.18	781.48	20.19	773.51	20.19	764.88	20.23	756.46
butan-1-ol										
	0.1	794.17	0.1	786.26	0.1	778.11	0.1	769.7	0.1	761.04
	1.11	795.53	1.13	788.36	1.13	780.43	1.13	772.50	1.11	764.02
	2.12	796.23	2.12	789.22	2.13	781.31	2.12	773.44	2.12	764.89
	3.13	797.04	3.14	790.03	3.14	782.18	3.13	774.32	3.13	765.95
	4.14	797.72	4.14	790.82	4.15	783.02	4.14	775.24	4.14	766.94
	5.15	798.48	5.16	791.66	5.15	783.94	5.15	776.11	5.15	767.89
	6.16	799.32	6.16	792.47	6.16	784.76	6.16	777.00	6.16	768.83
	7.17	800.11	7.18	793.33	7.18	785.61	7.17	777.97	7.18	769.74
	8.18	800.87	8.19	794.12	8.19	786.62	8.19	778.88	8.19	770.75
	9.20	801.63	9.20	794.96	9.20	787.33	9.19	779.75	9.20	771.65
	10.20	802.46	10.21	795.77	10.21	788.17	10.20	780.55	10.21	772.52
	11.22	803.19	11.22	796.57	11.22	788.98	11.21	781.43	11.22	773.42
	12.23	803.95	12.23	797.32	12.23	789.79	12.22	782.30	12.23	774.30
	13.23	804.71	13.24	798.06	13.23	790.56	13.23	783.16	13.24	775.16
	14.24	805.50	14.24	798.85	14.25	791.35	14.24	783.98	14.25	775.99
	15.25	806.25	15.25	799.60	15.25	792.16	15.25	784.77	15.26	776.86
	16.26	806.96	16.26	800.36	16.26	792.89	16.25	785.55	16.26	777.68
	17.27	807.69	17.27	801.07	17.26	793.65	17.26	786.32	17.26	778.50
	18.27	808.36	18.28	801.77	18.27	794.37	18.26	787.07	18.28	779.24
	19.27	809.02	19.28	802.40	19.27	795.09	19.27	787.79	19.28	779.96
	20.28	809.65	20.28	803.02	20.28	795.73	20.27	788.42	20.29	780.74

[a]Expanded combined uncertainties (k = 2) U_c are $U_c(T) = 0.02$ K, $U_c(P) = 0.032$ MPa, $U_c(\rho) = 1.08$ kg·m^{-3}.
[b]At atmospheric pressures the expanded combined uncertainty in pressure is $U_c(P) = 0.002$ MPa. Densities were calculated using the calibration by equation (6.8).

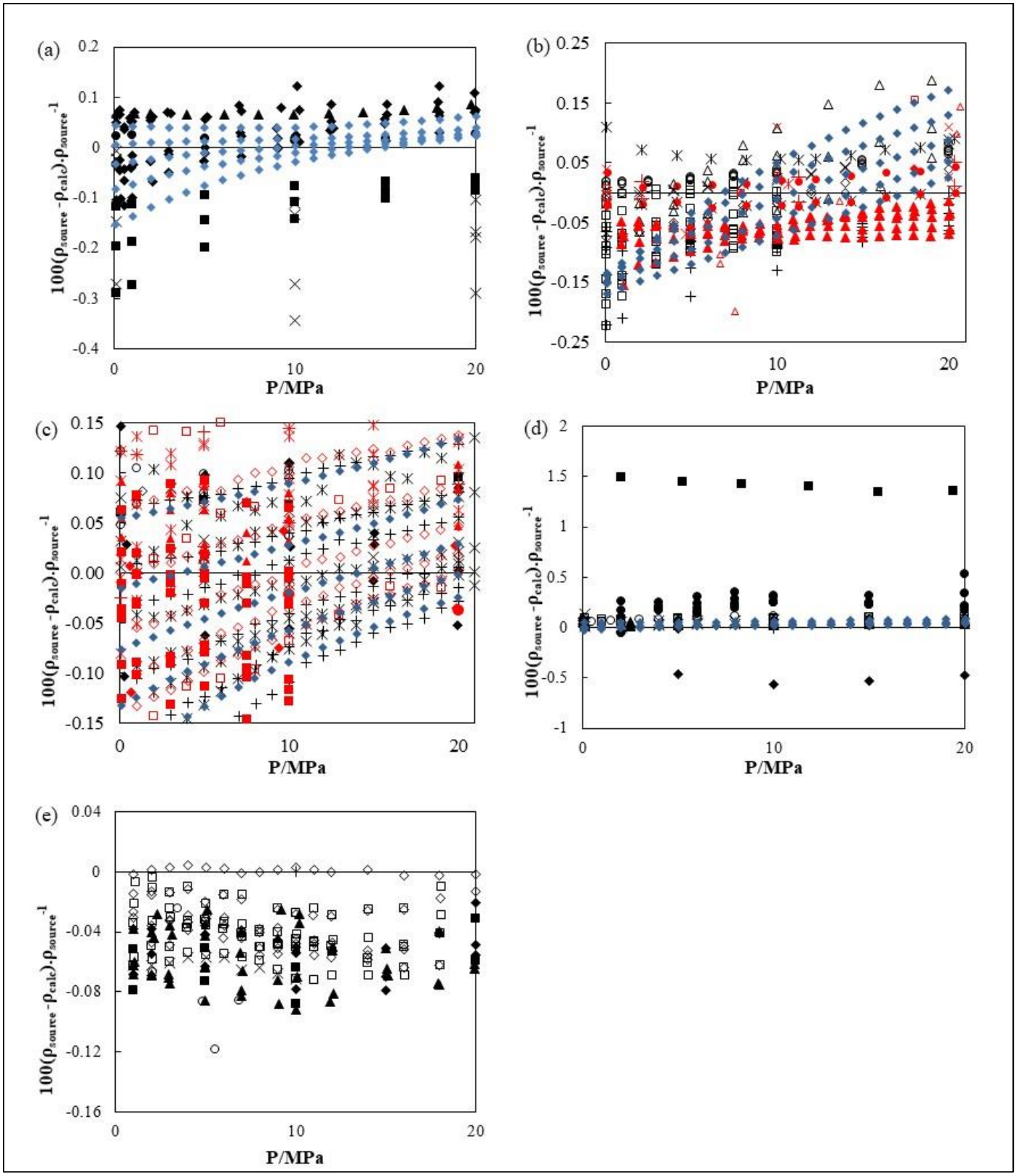
(a)
(b)
(c)
(d)
(e)
100(ρsource -ρcalc)·ρsource-1
P/MPa

Figure 6.2. (a-d) Comparison of the calculated pure component density (ρ_{calc}) at various temperatures as a function of pressure (P) using MTS EOS as correlated from the experimental data of this work, to data from literature and the REFPROP software package(ρ_{source}).

(a) n-heptane: ●-(Alaoui et al., 2013), ■-(Fandiño et al., 2005), ♦-(Iglesias-Silva et al., 2015), ▲-(Schilling, *et al.*, 2008), ×-(Toscani, *et al.*, 1989), ♦-REFPROP(Lemmon, *et al.*, 2010). (b) n-octane: □-(Banipal, *et al.*, 1991), ◊-(Lampreia and Nieto de Castro, 2011), ×-(Sanmamed et al., 2009), *- (Morávková, et al., 2008), +- (Abdussalam et al., 2016), ○- (L Lugo et al., 2001), ■-(Liu et al., 2010), +-(Morávková et al., 2006), ●- (Morávková et al., 2006), ×-(Kumagai, *et al.*, 2006), *-(Abdulagatov and Azizov, 2006), ♦-(Dymond, *et al.*, 1982), □-(Dix et al., 1991), ◊-(Kiran and Sen, 1992), Δ-(Goodwin et al., 2006), ○-(Boelhouwer, 1960), Δ - (Pimentel-rodas, *et al.*, 2017), ▲-(Moodley et al., 2018), ♦-REFPROP(Lemmon, *et al.*, 2010). (c) n-decane: +- (Zúñiga-Moreno, *et al.*, 2007),□-(Sage *et al.*, 1940), ◊-(Reamer et al., 1953), ○- (Segovia et al., 2009), ×- (Troncoso et al., 2004), *-(Quevedo-Nolasco *et al.*, 2012), ♦- (Audonnet and Pádua, 2004), ■-(Gayol et al., 2013), ■- (Banipal *et al.*, 1991), ♦-Gates et al.[48], ▲- (Valencia et al., 2009), ×- (Liu et al., 2010), ●- (Gehrig and Lentz, 1983), *- (Kang and Wang, 2018), +-(Regueira et al., 2016), □-(Pimentel-rodas *et al.*, 2017), ◊-(Moodley et al., 2018), ♦-REFPROP(Lemmon *et al.*, 2010). (d) ethanol: ●-(Gonalves et al., 2010)., ■-(Pöhler and Kiran, 1997) ♦-(Zéberg-Mikkelsen *et al.*, 2005), ▲-(Matkowska *et al.*, 2010), ×- (Sauermann et al., 1995), ◊- (Takiguchi and Uematsu, 1996), □-(Vega-Maza et al., 2013), ♦-REFPROP(Lemmon *et al.*, 2010). (e) Comparison of the calculated pure component density (ρ_{calc}) of butan-1-ol at various temperatures as a function of pressure (P) using MTS EOS as correlated from the experimental data of this work, to data from literature (ρ_{source}). □- (Zúñiga-Moreno *et al.*, 2007). (2006), ◊-(Zúñiga-Moreno *et al.*, 2007) , ○- (Wong and Hayduk, 1990), ×-(Kariznovi *et al.* , 2013), ♦-(Torín-Ollarves et al., 2012), ■-(Fang et al., 2017), ▲- (Iglesias-Silva et al., 2015).

Table 6.4. Experimental densities for ethanol (1) + n-heptane (2) at various temperatures and pressures.[a]

	x_1=0.1291		x_1=0.3756		x_1=0.4999		x_1=0.6253		x_1=0.7502		x_1=0.8748	
T/K	**P/MPa**	**ρ/ kg.m^{-3}**	**P/MPa**	**ρ/ kg.m^{-3}**	**P/MPa**	**ρ/ kg.m^{-3}**	**P/MPa**	**ρ/ kg.m^{-3}**	**P/MPa**	**ρ/ kg.m^{-3}**	**P/MPa**	**ρ/ kg.m^{-3}**
313.15	0.1*	670.18	0.1	683.24	0.1	692.22	0.1	704.25	0.1	720.04	0.1	741.15
313.15	1.11	670.92	1.12	684.01	1.12	692.91	1.16	705.04	1.11	720.83	1.08	741.94
313.15	2.12	671.94	2.11	684.99	2.12	693.94	2.17	706.00	2.12	721.77	2.09	742.84
313.15	3.13	673.24	3.11	686.23	3.13	695.19	3.18	707.16	3.13	722.88	3.09	743.89
313.15	4.13	674.66	4.12	687.57	4.13	696.47	4.18	708.39	4.13	724.03	4.10	744.92
313.15	5.14	675.74	5.12	688.63	5.14	697.52	5.19	709.41	5.14	725.03	5.10	745.90
313.15	6.15	676.87	6.13	689.72	6.14	698.60	6.20	710.50	6.15	726.11	6.11	746.96
313.15	7.15	677.95	7.13	690.80	7.15	699.65	7.21	711.53	7.15	727.13	7.12	747.96
313.15	8.15	678.99	8.14	691.78	8.15	700.64	8.22	712.51	8.16	728.09	8.12	748.89
313.15	9.16	680.01	9.15	692.77	9.16	701.61	9.22	713.47	9.16	729.03	9.13	749.80
313.15	10.17	681.04	10.15	693.81	10.17	702.66	10.22	714.48	10.17	730.04	10.13	750.81
313.15	11.18	682.04	11.16	694.77	11.17	703.64	11.23	715.45	11.17	731.00	11.14	751.77
313.15	12.18	683.03	12.16	695.74	12.18	704.52	12.23	716.40	12.18	731.95	12.15	752.71
313.15	13.18	683.97	13.16	696.65	13.18	705.49	13.24	717.32	13.19	732.86	13.15	753.61
313.15	14.19	684.94	14.17	697.62	14.18	706.45	14.25	718.26	14.19	733.79	14.15	754.53
313.15	15.19	685.88	15.17	698.52	15.19	707.40	15.25	719.18	15.20	734.71	15.16	755.45
313.15	16.20	686.82	16.17	699.45	16.19	708.26	16.25	720.10	16.20	735.63	16.16	756.37
313.15	17.19	687.72	17.18	700.35	17.19	709.19	17.25	720.99	17.20	736.53	17.16	757.27
313.15	18.20	688.51	18.18	701.12	18.19	709.92	18.26	721.78	18.20	737.33	18.16	758.09
313.15	19.21	689.32	19.18	701.92	19.20	710.73	19.26	722.60	19.21	738.15	19.17	758.92
313.15	20.21	690.03	20.18	702.62	20.19	711.44	20.27	723.32	20.21	738.89	20.16	759.68
323.15	0.1	661.28	0.1	674.15	0.1	683.12	0.1	695.09	0.1	710.88	0.1	732.00
323.15	1.13	663.03	1.13	675.79	1.13	684.73	1.18	696.56	1.11	712.19	1.10	733.10
323.15	2.12	664.17	2.11	676.91	2.12	685.78	2.18	697.66	2.11	713.28	2.09	734.17
323.15	3.12	665.31	3.12	678.03	3.13	686.95	3.19	698.78	3.12	714.39	3.09	735.27
323.15	4.13	666.43	4.14	679.13	4.13	688.01	4.20	699.86	4.13	715.46	4.10	736.34
323.15	5.14	667.58	5.13	680.25	5.13	689.12	5.20	700.97	5.14	716.57	5.11	737.43
323.15	6.14	668.69	6.14	681.35	6.14	690.23	6.21	702.06	6.14	717.65	6.11	738.52
323.15	7.15	669.80	7.15	682.43	7.15	691.29	7.22	703.14	7.15	718.73	7.12	739.58
323.15	8.15	670.90	8.15	683.51	8.15	692.34	8.22	704.20	8.15	719.79	8.12	740.63
323.15	9.16	672.04	9.16	684.62	9.15	693.46	9.23	705.29	9.16	720.87	9.13	741.70
323.15	10.16	673.14	10.16	685.70	10.16	694.57	10.23	706.36	10.17	721.92	10.14	742.75
323.15	11.17	674.27	11.16	686.80	11.16	695.63	11.24	707.46	11.17	723.02	11.14	743.83
323.15	12.17	675.32	12.17	687.82	12.17	696.66	12.24	708.46	12.18	724.00	12.14	744.80
323.15	13.17	676.34	13.17	688.83	13.18	697.68	13.25	709.46	13.18	725.01	13.15	745.80

323.15	14.19	677.33	14.18	689.81	14.18	698.65	14.26	710.44	14.19	726.00	14.16	746.80
323.15	15.18	678.10	15.18	690.59	15.18	699.41	15.26	711.27	15.19	726.86	15.16	747.72
323.15	16.19	679.06	16.18	691.53	16.19	700.39	16.26	712.20	16.19	727.79	16.16	748.64
323.15	17.19	679.97	17.18	692.43	17.19	701.29	17.27	713.10	17.20	728.69	17.16	749.55
323.15	18.20	680.82	18.19	693.26	18.19	702.14	18.27	713.95	18.17	729.54	18.16	750.40
323.15	19.19	681.63	19.19	694.06	19.20	702.90	19.27	714.76	19.20	730.36	19.17	751.24
323.15	20.20	682.36	20.19	694.80	20.20	703.63	20.28	715.52	20.20	731.14	20.17	752.05
333.15	0.1	652.57	0.1	665.23	0.1	674.16	0.1	686.08	0.1	701.84	0.1	722.94
333.15	1.13	654.10	1.11	666.67	1.13	675.59	1.20	687.43	1.13	703.06	1.10	724.01
333.15	2.11	655.36	2.11	667.91	2.12	676.81	2.19	688.68	2.12	704.31	2.09	725.21
333.15	3.12	656.58	3.12	669.12	3.12	678.01	3.19	689.88	3.12	705.54	3.09	726.38
333.15	4.13	657.76	4.13	670.27	4.13	679.15	4.20	690.98	4.13	706.58	4.09	727.50
333.15	5.13	659.01	5.13	671.47	5.14	680.36	5.20	692.21	5.14	707.76	5.10	728.68
333.15	6.14	660.18	6.14	672.62	6.14	681.48	6.21	693.30	6.14	708.88	6.11	729.77
333.15	7.15	661.38	7.14	673.76	7.15	682.65	7.22	694.46	7.15	710.02	7.11	730.90
333.15	8.15	662.82	8.15	675.11	8.15	684.03	8.22	695.86	8.15	711.37	8.12	732.21
333.15	9.16	663.76	9.15	676.11	9.16	684.95	9.23	696.77	9.16	712.24	9.13	733.13
333.15	10.16	664.91	10.16	677.24	10.15	686.07	10.24	697.87	10.16	713.39	10.13	734.24
333.15	11.17	666.01	11.16	678.37	11.17	687.14	11.25	698.94	11.17	714.37	11.14	735.30
333.15	12.17	667.09	12.17	679.39	12.17	688.20	12.25	699.99	12.18	715.47	12.14	736.36
333.15	13.18	668.12	13.17	680.40	13.18	689.21	13.25	701.06	13.18	716.48	13.14	737.37
333.15	14.18	669.15	14.18	681.41	14.18	690.22	14.26	702.04	14.18	717.47	14.15	738.39
333.15	15.19	670.21	15.16	682.45	15.19	691.26	15.26	703.05	15.19	718.59	15.15	739.44
333.15	16.19	671.03	16.18	683.22	16.19	692.10	16.27	703.92	16.19	719.46	16.16	740.33
333.15	17.19	672.00	17.19	684.22	17.19	693.05	17.27	704.90	17.19	720.43	17.15	741.30
333.15	18.19	672.86	18.19	685.01	18.20	693.91	18.27	705.74	18.20	721.32	18.16	742.23
333.15	19.16	673.68	19.19	685.71	19.20	694.74	19.28	706.56	19.20	722.19	19.16	743.13
333.15	20.20	674.82	20.19	686.99	20.20	695.81	20.28	707.60	20.21	723.07	20.17	744.06
343.15	0.1	644.20	0.1	656.46	0.1	665.32	0.1	677.07	0.1	692.65	0.1	713.59
343.15	1.13	645.84	1.12	658.04	1.13	666.83	1.20	678.45	1.13	693.90	1.09	714.60
343.15	2.12	647.13	2.11	659.31	2.12	668.09	2.19	679.77	2.11	695.15	2.08	715.86
343.15	3.13	648.41	3.12	660.56	3.12	669.34	3.20	680.97	3.12	696.38	3.09	717.07
343.15	4.13	649.66	4.13	661.77	4.13	670.55	4.20	682.17	4.13	697.57	4.10	718.24
343.15	5.14	650.94	5.13	663.02	5.13	671.78	5.21	683.39	5.14	698.77	5.10	719.43
343.15	6.14	652.17	6.14	664.22	6.14	672.98	6.21	684.55	6.15	699.96	6.11	720.61
343.15	7.15	653.56	7.14	665.58	7.15	674.32	7.22	685.86	7.15	701.29	7.11	721.92
343.15	8.16	654.79	8.15	666.79	8.16	675.51	8.22	687.11	8.15	702.46	8.12	723.08
343.15	9.16	655.95	9.16	667.93	9.16	676.65	9.23	688.24	9.16	703.60	9.12	724.22
343.15	10.17	657.06	10.16	669.01	10.16	677.73	10.24	689.27	10.17	704.69	10.13	725.30
343.15	11.17	658.26	11.16	670.20	11.17	678.92	11.24	690.50	11.17	705.87	11.13	726.50
343.15	12.18	659.37	12.17	671.28	12.17	679.99	12.24	691.57	12.18	706.95	12.14	727.57

343.15	13.18	660.52	13.17	672.40	13.18	681.11	13.25	692.65	13.18	708.06	13.14	728.69
343.15	14.19	661.59	14.18	673.43	14.18	682.13	14.25	693.65	14.18	709.04	14.15	729.63
343.15	15.19	662.68	15.19	674.52	15.18	683.22	15.26	694.81	15.17	710.19	15.15	730.81
343.15	16.20	663.68	16.18	675.51	16.19	684.21	16.26	695.82	16.19	711.19	16.15	731.82
343.15	17.20	664.71	17.19	676.53	17.18	685.20	17.27	696.81	17.20	712.22	17.15	732.86
343.15	18.20	665.65	18.19	677.45	18.19	686.14	18.27	697.78	18.20	713.17	18.16	733.83
343.15	19.20	666.58	19.19	678.37	19.19	687.06	19.28	698.69	19.21	714.10	19.16	734.77
343.15	20.21	667.53	20.20	679.30	20.20	688.00	20.28	699.58	20.21	715.02	20.16	735.69
353.15	1.13	636.44	1.13	648.45	1.12	657.27	1.13	668.90	1.09	684.34	1.09	705.17
353.15	2.12	637.75	2.12	649.72	2.13	658.53	2.12	670.15	2.08	685.59	2.08	706.39
353.15	3.12	639.29	3.12	651.23	3.14	660.02	3.12	671.63	3.09	687.04	3.09	707.78
353.15	4.13	640.78	4.13	652.67	4.14	661.45	4.13	673.03	4.09	688.43	4.09	709.14
353.15	5.14	642.16	5.14	654.01	5.15	662.77	5.14	674.34	5.10	689.72	5.10	710.38
353.15	6.15	643.46	6.14	655.28	6.15	664.03	6.18	675.59	6.11	690.96	6.10	711.63
353.15	7.15	644.75	7.15	656.54	7.15	665.28	7.16	676.84	7.11	692.20	7.11	712.89
353.15	8.16	646.14	8.16	657.89	8.17	666.62	8.17	678.17	8.12	693.53	8.12	714.17
353.15	9.16	647.44	9.16	659.16	9.17	667.89	9.17	679.43	9.13	694.77	9.12	715.44
353.15	10.17	648.64	10.17	660.33	10.18	669.04	10.17	680.57	10.13	695.90	10.13	716.51
353.15	11.18	649.89	11.17	661.55	11.18	670.25	11.18	681.78	11.13	697.11	11.13	717.74
353.15	12.18	651.05	12.18	662.68	12.18	671.38	12.19	682.90	12.14	698.23	12.14	718.85
353.15	13.19	652.26	13.18	663.86	13.18	672.55	13.19	684.07	13.14	699.39	13.14	720.00
353.15	14.19	653.38	14.19	664.96	14.19	673.64	14.20	685.16	14.15	700.48	14.14	721.09
353.15	15.19	654.53	15.19	666.08	15.20	674.75	15.20	686.27	15.15	701.59	15.16	722.19
353.15	16.20	655.61	16.20	667.14	16.20	675.81	16.20	687.33	16.16	702.66	16.15	723.27
353.15	17.20	656.70	17.20	668.21	17.20	676.88	17.21	688.40	17.16	703.73	17.16	724.34
353.15	18.21	657.67	18.17	669.16	18.20	677.83	18.21	689.36	18.16	704.70	18.16	725.32
353.15	19.21	658.61	19.20	670.09	19.20	678.76	19.21	690.30	19.17	705.65	19.16	726.29
353.15	20.21	659.62	20.21	671.07	20.23	679.74	20.21	691.28	20.17	706.63	20.15	727.27

[a]Expanded combined uncertainties (k = 2) U_c are $U_c(T) = 0.02$ K, $U_c(P) = 0.032$ MPa, and $U_c(xi) = 0.0002$, $U_c(\rho) = 1.10$ kg·m^{-3}.

[b]At atmospheric pressures the expanded combined uncertainty in pressure is $U_c(P) = 0.002$ MPa.

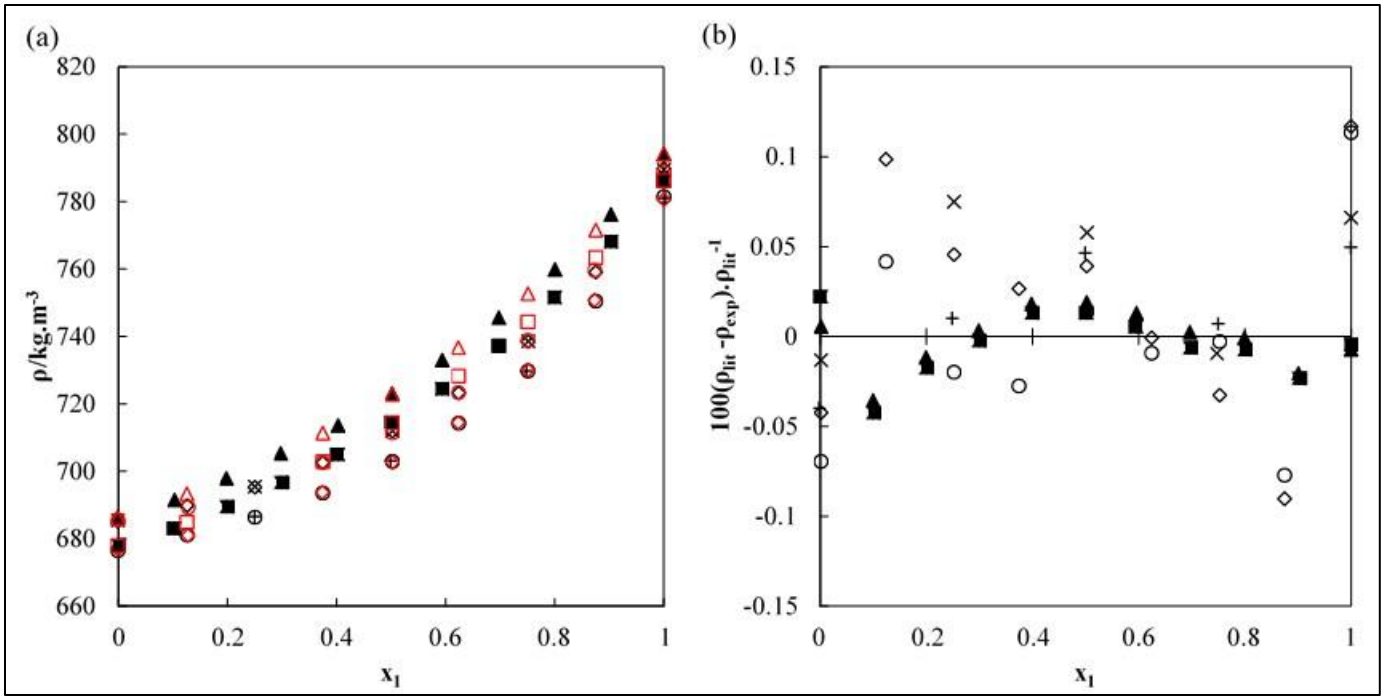

Figure 6.3. (a) Comparison of density data to literature.

Ethanol (1) + n-heptane (2) system: (○-This work 313.15 K and 10 MPa, ◊-This work 313.15 K and 20 MPa, ○-(Watson et al., 2006) 313.15 K and 10 MPa, ◊-(Watson et al., 2006) 313.15 K and 20 MPa, +-(Abdussalam et al., 2016) 313.15 K and 10 MPa, ×- (Abdussalam et al., 2016) 313.15 K and 20 MPa). Butan-1-ol (1) + n-octane: (Δ-This work 313.15 K and 0.1 MPa, □-This work 323.15 K and 0.1 MPa, ▲-(Estrada-Baltazar *et al.*, 2013) 313.15 K and 0.1 MPa, ■-(Estrada-Baltazar *et al.*, 2013) 323.15 K and 0.1 MPa). (b) Deviations between experimental density data and cited literature. Ethanol (1) + n-heptane (2) system: ○-(Watson et al., 2006) 313.15 K and 10 MPa, ◊-(Watson et al., 2006) 313.15 K and 20 MPa, +-(Abdussalam et al., 2016) 313.15 K and 10 MPa, ×-(Abdussalam et al., 2016) 313.15 K and 20 MPa). Butan-1-ol (1) + n-octane: ▲-(Estrada-Baltazar *et al.*, 2013) 313.15 K and 0.1 MPa, ■-(Estrada-Baltazar *et al.*, 2013) 323.15 K and 0.1 MPa).

6.5. Results and Discussion

Checks were conducted utilizing the refractometer, gas chromatograph for purity, and atmospheric pressure densitometer for the pure components used in this work. These results were compared to

the literature and are presented in Table 6.1. The measurements were found to be consistent with the literature with deviations within 0.0003 for RI and 0.07 $kg \cdot m^{-3}$ for density from at least one source. Purities were within the minimum stated supplier purities. Thereafter, pure component densities were measured to verify the setup and procedure followed in this experiment. These experimental densities, measured in the pressure and temperature ranges of 0.1−20 MPa and 313.15−353.15 K, are presented in Table 6.3. The results obtained for the pure component densities were compared to those measured in the literature and REFPROP as demonstrated in Figure 6.2 and Table 6.1. The percentage deviation between the correlated experimental density data by the MTS EOS (discussed in detail below) and those obtained from the literature and REFPROP are small (maximum relative difference within 0.002 excluding clear outliers) and hence demonstrates the similarity of the measurements from this work with pure component literature data. The MTS EOS correlation was used so that comparisons could be made at the exact temperatures and pressures measured in the literature. A maximum relative deviation of approximately 0.015 was observed for butan-1-ol. The literature source however does seem likely to be erroneous as the data does not conform with the several other reported sources.

A test system, consisting of ethanol (1) + n-heptane (2), was measured to evaluate the reliability of the setup and procedure used for the density measurements in this work, and the procedure used for the mixture preparation. Measurements were conducted under isothermal conditions at five different temperatures, namely, 313.15, 323.15, 333.15, 343.15, and 353.15 K, over the whole composition range and are presented in Table 6.4. These results were compared to the literature and demonstrate good correlation (maximum relative difference within 0.0012) as illustrated in Figure 6.3. Data for the butan-1-ol (1) + n-octane (2) system at 313.15 and 323.15 K and atmospheric pressure was also available in the literature and is compared to the data from this work shown in Figure 6.3. Again, a good correlation (maximum relative difference within 0.0005) is observed with deviations within the experimental uncertainties of the study here and the literature, which further confirms the procedures used here. In Figure 6.4, excess volumes for the test system of ethanol (1) + n-heptane (2) at elevated pressures are compared to the measurements performed in this work. It is clear that the general trend with temperature, pressure, and composition and the order of magnitude of values is replicated in this work.

Novel isothermal measurements were conducted for temperatures of T = (313.15, 323.15, 333.15, 343.15, and 353.15 K) and for pressures within P = (0.1−20 MPa), for the systems butan-1-ol (1) + n-octane (2) and butan-1-ol (1) + n-decane (2) over the entire composition range. The results obtained are presented in Tables 6.5 and 6.6. From these tables, it is observed that the experimental density decreases with increasing temperature and increases with increasing pressure, which is compliant with the general expected trends. These relationships are highly non-linear, and it is clear that linear approximations for density would be inaccurate.

The MTS EOS, with 5 regressed parameters, was employed to correlate the experimental data obtained. This model requires a separate correlation for each composition. In Figure 6.5a the binary system butan-1-ol (1) + n-decane (2) at 313.15 K is presented for selected compositions and demonstrates a successful correlation of the experimental data. The data is also compared to a correlation by the Peng and Robinson (1976), where the density data were regressed to the EOS to obtain the binary interaction parameters, k_{ij}, and a prediction by the PC-SAFT model (2001, 2002) using the 2B association scheme for butan-1-ol, assuming n-decane is non-associating. The 2B association scheme assumes that there are two association sites available on the butan-1-ol molecule (one for oxygen and one for hydrogen in the OH group). It is a simplification of the rigorous 3B scheme, where two oxygen sites and one hydrogen association site should strictly be used for the OH group but is recommended by Gross and Sadowski (2002). PC-SAFT parameters for butan-1-ol were taken from the reports by Gross and Sadowski (2002) while parameters for n-decane were taken from the work of Burgess *et al.* (2012), which is more applicable to predictions at high pressures. The pure component parameters are provided in Table 6.7 of the Supporting Information. The binary interaction parameters were unavailable for the Peng− Robinson model and were thus regressed from the density data. It must be noted that the k_{ij} obtained only applies to the density data and range measured here and should not be used in phase equilibrium calculations, as it would likely yield a poor result. Note that the Peng−Robinson EOS allows for simultaneous correlation of all compositions of a particular system with a single k_{ij} and hence its performance should not be compared directly to the performance of the multiparameter MTS EOS.

Similar results were obtained for the other 4 temperatures as well as for the butan-1-ol (1) + n-octane (2) system, with an example shown at 353.15 K, for selected compositions, in Figure 6.5b. It is clear that a poor representation of mixture density is obtained from the Peng− Robinson EOS

(especially for the pure butan-1-ol) while that of PC-SAFT is slightly better. Table 6.8 presents the regressed parameters obtained from the correlated Toscani−Szwarc EOS, using MATLAB software, for the pure components and binary systems. The rmsd between the density obtained experimentally and from the model fitting was generally within the experimental uncertainty in density.

The data correlated by the MTS EOS was utilized to calculate the molar excess volumes for both novel systems at selected temperatures and pressures, over the entire composition range. Figures 6.6 and 6.7 show the excess volumes for the binary butan-1-ol + n-octane/n-decane systems, respectively. A large positive excess volume is noted for both binary systems. This deviation from ideality can be attributed to attractive hydrogen bonding/Keesom interaction mixture interactions when compared to those of the pure components and the different shapes and sizes of the molecules interacting causing an increase in the volume occupied by the individual components. These behaviors are typical of alcohol + alkane systems (Bravo-Sánchez et al., 2013; Itsuki et al., 1987; Moodley et al., 2018; Wagner and Heintz, 1986) The maximum uncertainty for the calculated excess volumes were calculated to be 1.82×10^{-5} and 1.89×10^{-5} $m^3 \cdot kmol^{-1}$ for the butan-1-ol (1) + n-octane (2) and butan-1-ol (1) + n-decane (2) systems, respectively, using error propagation.

The regressed model parameters were also utilized to calculate both the thermal expansivity and isothermal compressibility. The calculated relative uncertainty for the thermal expansivity was 0.038 and 0.044 for the isothermal compressibility. The results obtained are shown in Figures 6.8−6.11, respectively, along with available data from the literature (pure components). The data from this work compare within experimental uncertainty with the literature for the majority of the components and conditions tested. From Figures 6.8 and 6.9, it is observed that the thermal expansivity increases with increasing temperatures and decreasing pressures for both binary systems. Figures 6.10 and 6.11 show that the isothermal compressibility increases with increasing temperature and decreasing pressure, for a specific composition for these mixtures. Again, it is clear that the thermal expansivity and the isothermal compressibility cannot be approximated by linear mixing of the two pure components.

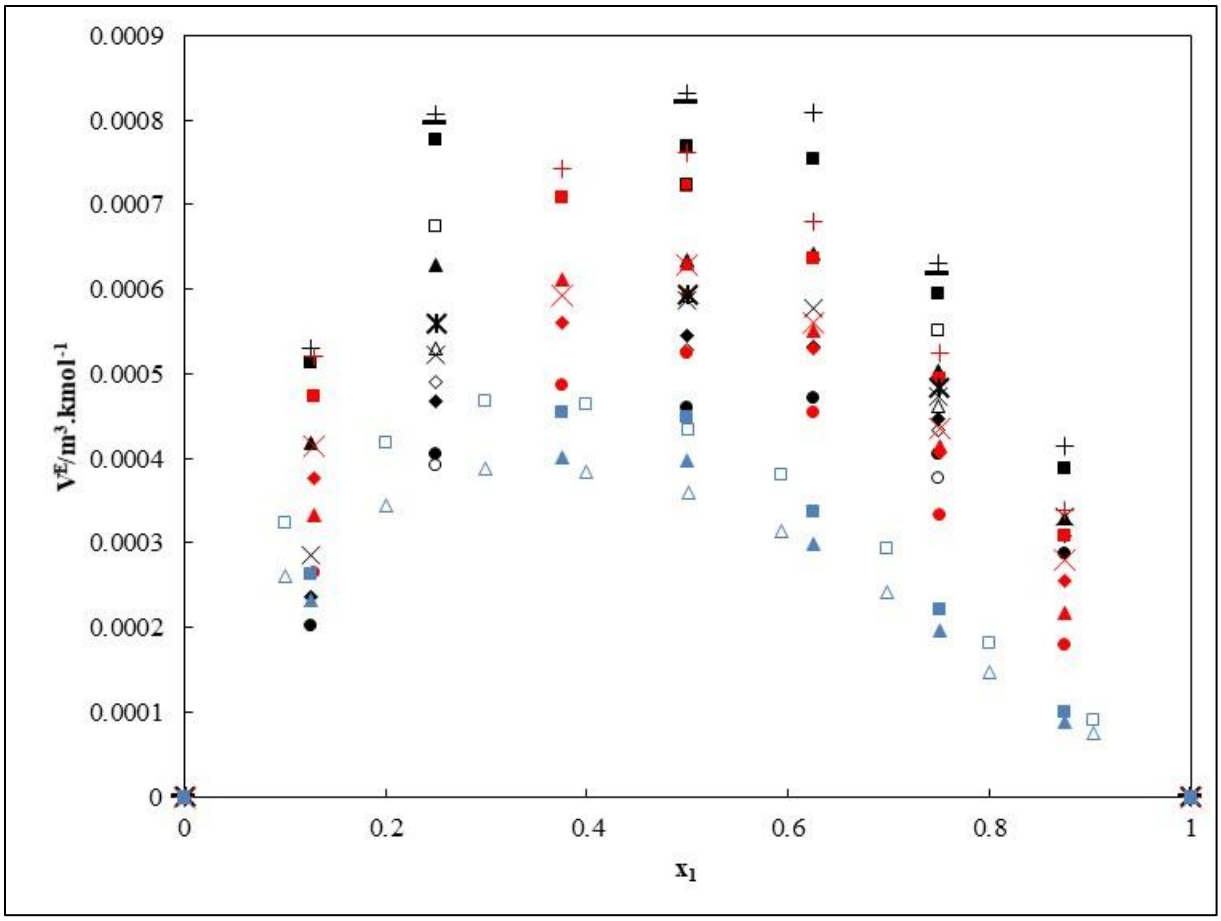

Figure 6.4. Excess volume (V^E) vs. x_1 at various temperatures and pressures.

For the ethanol (1) n-heptane (2) system: This work: (×- 313.15 K and 0.1 MPa, +- 333.15 K and 0.1 MPa, ♦- 313.15 K and 5 MPa, ■- 333.15 K and 5 MPa, ●- 313.15 K and 20 MPa, ▲- 333.15 K and 20 MPa). (Watson et al., 2006): (×- 313.15 K and 0.1 MPa, +- 333.15 K and 0.1 MPa, ♦- 313.15 K and 5 MPa, ■- 333.15 K and 5 MPa, ●- 313.15 K and 20 MPa, ▲- 333.15 K and 20 MPa). (Abdussalam et al., 2016): (*- 313.15 K and 0.1 MPa, ─- 333.15 K and 0.1 MPa, ◊- 313.15 K and 5 MPa, □- 333.15 K and 5 MPa, ○- 313.15 K and 20 MPa, Δ- 333.15 K and 20 MPa). For the for the butan-1-ol (1) n-octane (2) system: ▲-This work 313.15 K and 0.1 MPa, ■-This work 323.15 K and 0.1 MPa, Δ-(Estrada-Baltazar *et al.*, 2013) 313.15 K and 0.1 MPa, □-(Estrada-Baltazar *et al.*, 2013) 323.15 K and 0.1 MPa)

Table 6.5. Experimental densities for butan-1-ol (1) + n-octane (2) at various temperatures and pressures.[a]

T/K	P/MPa	ρ/ kg.m^{-3}	P/MPa	ρ/ kg.m^{-3}	P/MPa	ρ/ kg.m^{-3}	P/MPa	ρ/ kg.m^{-3}	P/MPa	ρ/ kg.m^{-3}	P/MPa	ρ/ kg.m^{-3}
	x_1=0.1259		x_1=0.3750		x_1=0.5002		x_1=0.6258		x_1=0.7503		x_1=0.8750	
313.15	0.100*	693.29	0.100	711.36	0.100	722.83	0.100	736.65	0.100	752.65	0.100	771.59
313.15	1.142	694.99	1.128	713.06	1.134	724.51	1.140	738.28	1.164	754.21	1.150	773.06
313.15	2.136	696.26	2.127	714.25	2.132	725.65	2.137	739.34	2.159	755.17	2.152	773.91
313.15	3.153	697.16	3.142	715.16	3.141	726.55	3.140	740.22	3.170	756.04	3.164	774.75
313.15	4.156	698.02	4.157	716.01	4.153	727.38	4.154	741.03	4.173	756.81	4.169	775.48
313.15	5.172	698.88	5.160	716.88	5.157	728.24	5.159	741.87	5.184	757.63	5.182	776.27
313.15	6.183	699.84	6.171	717.84	6.169	729.19	6.168	742.80	6.193	758.54	6.190	777.15
313.15	7.188	700.77	7.177	718.76	7.176	730.11	7.193	743.70	7.201	759.41	7.204	777.98
313.15	8.197	701.65	8.192	719.64	8.191	730.98	8.188	744.55	8.208	760.24	8.210	778.78
313.15	9.232	702.52	9.199	720.51	9.204	731.85	9.197	745.40	9.218	761.07	9.218	779.58
313.15	10.227	703.41	10.211	721.42	10.216	732.75	10.220	746.29	10.231	761.94	10.232	780.43
313.15	11.240	704.28	11.218	722.28	11.229	733.60	11.222	747.12	11.240	762.75	11.238	781.20
313.15	12.251	705.13	12.231	723.14	12.226	734.45	12.229	747.95	12.247	763.56	12.247	781.99
313.15	13.259	705.98	13.244	723.99	13.241	735.30	13.237	748.79	13.259	764.38	13.264	782.79
313.15	14.266	706.89	14.247	724.89	14.253	736.20	14.247	749.67	14.272	765.23	14.258	783.61
313.15	15.272	707.72	15.254	725.73	15.259	737.03	15.249	750.49	15.280	766.03	15.269	784.39
313.15	16.282	708.58	16.264	726.58	16.260	737.86	16.272	751.30	16.283	766.82	16.276	785.14
313.15	17.291	709.38	17.272	727.39	17.273	738.67	17.267	752.10	17.290	767.60	17.289	785.90
313.15	18.297	710.08	18.266	728.10	18.273	739.38	18.283	752.80	18.299	768.29	18.293	786.58
313.15	19.298	710.79	19.278	728.82	19.270	740.10	19.276	753.51	19.304	768.99	19.294	787.26
313.15	20.311	711.39	20.278	729.45	20.269	740.73	20.291	754.14	20.298	769.62	20.299	787.89
323.15	0.100	684.88	0.100	702.88	0.100	714.37	0.100	728.28	0.100	744.39	0.100	763.49
323.15	1.152	686.89	1.137	705.02	1.137	716.54	1.153	730.44	1.141	746.54	1.041	765.61
323.15	2.149	687.89	2.129	706.01	2.131	717.53	2.159	731.41	2.152	747.47	2.123	766.51
323.15	3.169	688.87	3.141	706.99	3.141	718.50	3.169	732.35	3.148	748.38	3.126	767.38
323.15	4.177	689.83	4.147	707.95	4.146	719.44	4.164	733.26	4.174	749.27	4.144	768.22
323.15	5.189	690.84	5.159	708.95	5.164	720.43	5.172	734.23	5.169	750.20	5.157	769.11
323.15	6.203	691.84	6.173	709.94	6.170	721.40	6.191	735.17	6.194	751.11	6.174	769.98
323.15	7.220	692.81	7.176	710.92	7.190	722.37	7.194	736.12	7.202	752.04	7.171	770.87
323.15	8.226	693.78	8.192	711.87	8.203	723.31	8.203	737.04	8.208	752.92	8.187	771.72
323.15	9.236	694.70	9.197	712.80	9.201	724.24	9.222	737.95	9.223	753.81	9.196	772.58
323.15	10.254	695.63	10.208	713.73	10.208	725.16	10.232	738.85	10.219	754.69	10.211	773.43
323.15	11.246	696.62	11.217	714.71	11.227	726.12	11.243	739.79	11.238	755.59	11.217	774.29
323.15	12.273	697.43	12.233	715.53	12.233	726.94	12.242	740.60	12.243	756.39	12.229	775.06
323.15	13.269	698.32	13.241	716.42	13.244	727.82	13.248	741.45	13.246	757.21	13.240	775.85

323.15	14.257	699.21	14.240	717.31	14.248	728.70	14.262	742.32	14.258	758.06	14.254	776.67
323.15	15.286	700.12	15.252	718.21	15.249	729.59	15.269	743.19	15.270	758.9	15.252	777.47
323.15	16.302	701.01	16.262	719.10	16.264	730.47	16.267	744.04	16.282	759.73	16.263	778.27
323.15	17.296	701.77	17.256	719.87	17.259	731.24	17.281	744.80	17.277	760.48	17.273	779.00
323.15	18.297	702.56	18.274	720.66	18.270	732.02	18.288	745.57	18.286	761.23	18.271	779.73
323.15	19.301	703.26	19.269	721.37	19.283	732.73	19.286	746.26	19.286	761.90	19.284	780.38
323.15	20.291	703.93	20.276	722.05	20.281	733.41	20.287	746.93	20.297	762.56	20.283	781.02
333.15	0.100	676.37	0.100	694.26	0.100	705.75	0.100	719.73	0.100	735.94	0.100	755.17
333.15	1.129	678.83	1.133	696.87	1.142	708.39	1.149	722.31	1.134	738.45	1.124	757.59
333.15	2.126	679.93	2.128	697.96	2.127	709.46	2.141	723.35	2.138	739.45	2.124	758.54
333.15	3.139	681.02	3.137	699.04	3.149	710.52	3.162	724.38	3.149	740.44	3.126	759.48
333.15	4.152	682.01	4.154	700.03	4.164	711.49	4.172	725.33	4.160	741.36	4.144	760.36
333.15	5.156	683.15	5.164	701.16	5.166	712.60	5.176	726.41	5.166	742.40	5.148	761.34
333.15	6.174	684.11	6.168	702.11	6.166	713.55	6.189	727.34	6.194	743.30	6.160	762.21
333.15	7.182	685.14	7.179	703.15	7.180	714.57	7.197	728.32	7.191	744.25	7.171	763.11
333.15	8.186	686.60	8.191	704.55	8.188	715.93	8.206	729.62	8.209	745.48	8.183	764.24
333.15	9.204	687.17	9.202	705.16	9.210	716.56	9.216	730.27	9.218	746.14	9.188	764.93
333.15	10.214	688.19	10.211	706.17	10.207	717.56	10.234	731.24	10.233	747.08	10.206	765.82
333.15	11.224	689.15	11.216	707.13	11.226	718.50	11.242	732.16	11.239	747.97	11.222	766.67
333.15	12.230	690.10	12.242	708.08	12.237	719.44	12.246	733.08	12.239	748.86	12.232	767.53
333.15	13.242	690.99	13.232	708.97	13.237	720.33	13.246	733.95	13.250	749.70	13.237	768.34
333.15	14.248	691.89	14.254	709.88	14.252	721.23	14.257	734.83	14.257	750.56	14.252	769.16
333.15	15.263	692.85	15.247	710.83	15.258	722.17	15.272	735.75	15.268	751.45	15.254	770.02
333.15	16.269	693.66	16.260	711.64	16.260	722.98	16.277	736.55	16.281	752.23	16.264	770.78
333.15	17.274	694.51	17.271	712.50	17.273	723.83	17.293	737.38	17.283	753.05	17.262	771.57
333.15	18.276	695.35	18.267	713.34	18.274	724.66	18.288	738.19	18.288	753.83	18.268	772.32
333.15	19.279	696.19	19.284	714.18	19.278	725.49	19.301	739.01	19.302	754.62	19.267	773.08
333.15	20.281	696.85	20.269	714.85	20.281	726.17	20.304	739.67	20.304	755.29	20.281	773.74
343.15	0.100	667.79	0.100	685.54	0.100	697.01	0.100	711.03	0.100	727.31	0.100	746.64
343.15	1.138	670.01	1.144	688.09	1.129	699.68	1.158	713.73	1.138	730.03	1.138	749.39
343.15	2.138	671.18	2.144	689.26	2.137	700.82	2.152	714.83	2.130	731.10	2.130	750.39
343.15	3.143	672.27	3.139	690.33	3.141	701.88	3.168	715.87	3.142	732.09	3.143	751.34
343.15	4.159	673.35	4.150	691.41	4.154	702.94	4.180	716.91	4.151	733.10	4.148	752.31
343.15	5.168	674.41	5.164	692.48	5.157	703.99	5.176	717.93	5.163	734.08	5.163	753.23
343.15	6.182	675.50	6.166	693.55	6.167	705.05	6.199	718.96	6.171	735.07	6.173	754.19
343.15	7.188	676.72	7.183	694.76	7.178	706.24	7.214	720.11	7.184	736.18	7.183	755.23
343.15	8.198	677.77	8.198	695.81	8.199	707.28	8.218	721.12	8.188	737.17	8.187	756.19
343.15	9.214	678.84	9.200	696.86	9.200	708.32	9.230	722.13	9.200	738.14	9.204	757.11
343.15	10.222	679.75	10.207	697.78	10.221	709.23	10.241	723.03	10.209	739.01	10.210	757.95
343.15	11.234	680.86	11.221	698.88	11.223	710.31	11.253	724.07	11.224	740.01	11.220	758.89
343.15	12.236	681.78	12.232	699.80	12.238	711.24	12.253	724.99	12.231	740.92	12.231	759.79

343.15	13.252	682.78	13.240	700.80	13.241	712.23	13.263	725.96	13.242	741.86	13.237	760.70
343.15	14.259	683.75	14.253	701.78	14.252	713.19	14.272	726.90	14.252	742.77	14.246	761.57
343.15	15.268	684.69	15.258	702.71	15.258	714.11	15.283	727.79	15.253	743.64	15.260	762.40
343.15	16.274	685.55	16.259	703.58	16.261	714.98	16.294	728.65	16.258	744.48	16.261	763.21
343.15	17.281	686.52	17.271	704.53	17.266	715.91	17.290	729.55	17.264	745.34	17.271	764.03
343.15	18.276	687.37	18.267	705.39	18.270	716.76	18.296	730.38	18.267	746.16	18.266	764.81
343.15	19.287	688.15	19.276	706.18	19.276	717.56	19.300	731.17	19.276	746.92	19.278	765.56
343.15	20.291	688.88	20.294	706.91	20.281	718.28	20.314	731.88	20.282	747.61	20.287	766.22
353.15	0.100	658.6	0.100	677.21	0.100	688.91	0.100	702.91	0.100	719.18	0.100	738.89
353.15	1.142	661.85	1.144	679.76	1.148	691.28	1.149	705.30	1.142	721.58	1.137	740.92
353.15	2.136	662.77	2.138	680.70	2.136	692.22	2.120	706.23	2.129	722.49	2.133	741.81
353.15	3.142	664.23	3.149	682.12	3.154	693.60	3.131	707.56	3.141	723.76	3.136	742.99
353.15	4.159	665.52	4.166	683.39	4.162	694.85	4.137	708.76	4.154	724.91	4.149	744.07
353.15	5.163	666.65	5.166	684.52	5.171	695.96	5.153	709.86	5.160	725.96	5.157	745.08
353.15	6.178	667.83	6.177	685.69	6.182	697.11	6.160	710.96	6.170	727.03	6.173	746.08
353.15	7.188	668.93	7.193	686.78	7.190	698.19	7.181	712.02	7.180	728.04	7.182	747.05
353.15	8.199	670.15	8.204	688.00	8.197	699.39	8.179	713.18	8.186	729.16	8.191	748.13
353.15	9.206	671.27	9.207	689.10	9.199	700.48	9.189	714.23	9.199	730.17	9.196	749.09
353.15	10.219	672.24	10.218	690.08	10.218	701.45	10.199	715.19	10.207	731.11	10.214	749.99
353.15	11.232	673.36	11.217	691.19	11.229	702.53	11.214	716.25	11.223	732.13	11.223	750.96
353.15	12.240	674.37	12.227	692.20	12.226	703.55	12.219	717.23	12.231	733.09	12.233	751.89
353.15	13.249	675.38	13.244	693.21	13.243	704.54	13.227	718.21	13.236	734.04	13.238	752.79
353.15	14.260	676.33	14.254	694.16	14.246	705.48	14.237	719.13	14.242	734.94	14.248	753.66
353.15	15.246	677.39	15.253	695.21	15.259	706.52	15.242	720.14	15.250	735.91	15.259	754.58
353.15	16.270	678.39	16.262	696.21	16.268	707.50	16.250	721.09	16.257	736.82	16.262	755.46
353.15	17.272	679.31	17.270	697.13	17.269	708.42	17.249	722.00	17.271	737.71	17.264	756.32
353.15	18.288	680.12	18.267	697.95	18.276	709.24	18.262	722.81	18.267	738.50	18.274	757.08
353.15	19.290	680.93	19.283	698.78	19.276	710.05	19.274	723.60	19.279	739.28	19.280	757.83
353.15	20.286	681.82	20.277	699.66	20.288	710.93	20.266	724.47	20.283	740.12	20.283	758.65

[a] Expanded combined uncertainties ($k = 2$) U_c are $U_c(T) = 0.02\ K$, $U_c(P) = 0.032\ MPa$, $U_c(x_i) = 0.0002$, $U_c(\rho) = 1.10\ kg.m^{-3}$

[*]At atmospheric pressures the expanded combined uncertainty in pressure is $U_c(P) = 0.002\ MPa$

Table 6.6. Experimental densities for butan-1-ol (1) + n-decane (2) at various temperatures and pressures.[a]

T/K	P/MPa	ρ/ kg.m^{-3}	P/MPa	ρ/ kg.m^{-3}	P/MPa	ρ/ kg.m^{-3}	P/MPa	ρ/ kg.m^{-3}	P/MPa	ρ/ kg.m^{-3}	P/MPa	ρ/ kg.m^{-3}
	x_1=0.1269		x_1=0.3746		x_1=0.4968		x_1=0.6234		x_1=0.7440		x_1=0.8731	
313.15	0.100*	718.64	0.100	729.78	0.100	737.13	0.100	746.93	0.100	758.79	0.100	774.18
313.15	1.133	719.63	1.146	730.90	1.139	738.29	1.106	748.16	1.101	760.02	1.104	775.49
313.15	2.127	720.37	2.139	731.68	2.163	739.07	2.111	748.94	2.103	760.78	2.101	776.23
313.15	3.144	721.19	3.149	732.54	3.153	739.94	3.121	749.81	3.110	761.63	3.121	777.07
313.15	4.153	721.99	4.169	733.36	4.159	740.77	4.132	750.61	4.123	762.40	4.126	777.80
313.15	5.159	722.78	5.170	734.20	5.171	741.60	5.138	751.44	5.143	763.21	5.134	778.60
313.15	6.173	723.66	6.179	735.11	6.181	742.52	6.148	752.36	6.150	764.10	6.140	779.47
313.15	7.183	724.51	7.187	735.99	7.188	743.41	7.156	753.23	7.146	764.96	7.148	780.30
313.15	8.193	725.34	8.204	736.84	8.203	744.26	8.173	754.07	8.163	765.78	8.173	781.10
313.15	9.199	726.14	9.221	737.67	9.214	745.10	9.183	754.90	9.176	766.59	9.167	781.90
313.15	10.214	726.98	10.223	738.54	10.224	745.98	10.191	755.78	10.187	767.45	10.182	782.75
313.15	11.223	727.79	11.227	739.38	11.231	746.81	11.199	756.61	11.203	768.25	11.204	783.52
313.15	12.231	728.60	12.241	740.21	12.243	747.65	12.206	757.43	12.199	769.06	12.208	784.31
313.15	13.237	729.39	13.250	741.03	13.254	748.48	13.224	758.25	13.208	769.86	13.224	785.11
313.15	14.252	730.22	14.258	741.88	14.259	749.33	14.230	759.11	14.230	770.70	14.228	785.92
313.15	15.252	731.00	15.268	742.69	15.274	750.15	15.236	759.92	15.230	771.49	15.231	786.70
313.15	16.257	731.78	16.273	743.49	16.268	750.95	16.237	760.70	16.243	772.26	16.241	787.45
313.15	17.268	732.53	17.282	744.26	17.280	751.73	17.250	761.48	17.238	773.02	17.243	788.20
313.15	18.268	733.19	18.283	744.95	18.276	752.42	18.262	762.17	18.249	773.71	18.246	788.88
313.15	19.277	733.86	19.280	745.65	19.288	753.13	19.261	762.87	19.253	774.40	19.250	789.56
313.15	20.288	734.45	20.291	746.27	20.296	753.76	20.269	763.51	20.249	775.03	20.259	790.20
323.15	0.100	710.67	0.100	721.54	0.100	728.80	0.100	738.63	0.100	750.58	0.100	766.07
323.15	1.118	712.06	1.140	723.11	1.132	730.45	1.104	740.39	1.099	752.42	1.110	768.04
323.15	2.127	712.96	2.146	724.05	2.142	731.40	2.113	741.34	2.113	753.34	2.106	768.93
323.15	3.134	713.86	3.137	724.99	3.151	732.35	3.121	742.27	3.124	754.24	3.106	769.81
323.15	4.139	714.73	4.163	725.90	4.168	733.26	4.133	743.17	4.131	755.11	4.128	770.65
323.15	5.149	715.66	5.169	726.86	5.173	734.23	5.140	744.12	5.139	756.03	5.144	771.54
323.15	6.164	716.57	6.181	727.80	6.177	735.17	6.146	745.05	6.147	756.92	6.150	772.40
323.15	7.176	717.47	7.190	728.73	7.192	736.11	7.158	745.98	7.146	757.84	7.160	773.30
323.15	8.179	718.35	8.201	729.65	8.200	737.03	8.169	746.88	8.167	758.71	8.169	774.14
323.15	9.191	719.23	9.210	730.56	9.206	737.95	9.182	747.80	9.180	759.60	9.171	775.01
323.15	10.212	720.10	10.218	731.47	10.222	738.86	10.191	748.70	10.188	760.48	10.194	775.87
323.15	11.223	721.02	11.230	732.41	11.229	739.80	11.200	749.62	11.203	761.37	11.201	776.72
323.15	12.217	721.78	12.239	733.20	12.238	740.60	12.212	750.42	12.212	762.15	12.198	777.50
323.15	13.230	722.62	13.253	734.07	13.253	741.47	13.219	751.27	13.221	762.98	13.210	778.29

323.15	14.239	723.45	14.258	734.92	14.263	742.33	14.230	752.13	14.220	763.81	14.222	779.11
323.15	15.251	724.25	15.262	735.75	15.261	743.16	15.242	752.95	15.234	764.62	15.228	779.90
323.15	16.261	725.05	16.274	736.58	16.266	744.00	16.253	753.78	16.238	765.42	16.242	780.69
323.15	17.264	725.79	17.267	737.35	17.281	744.77	17.249	754.55	17.242	766.18	17.239	781.43
323.15	18.270	726.49	18.282	738.09	18.281	745.52	18.258	755.29	18.254	766.91	18.246	782.15
323.15	19.271	727.16	19.290	738.78	19.288	746.21	19.257	755.98	19.247	767.58	19.247	782.81
323.15	20.279	727.80	20.290	739.45	20.291	746.89	20.273	756.65	20.248	768.24	20.256	783.45
333.15	0.100	702.49	0.100	712.94	0.100	720.01	0.100	729.91	0.100	742.04	0.100	757.640
333.15	1.118	704.31	1.142	714.91	1.151	722.12	1.122	732.07	1.099	744.22	1.106	759.90
333.15	2.123	705.28	2.158	715.92	2.140	723.13	2.112	733.06	2.110	745.19	2.102	760.84
333.15	3.140	706.24	3.174	716.91	3.147	724.13	3.120	734.05	3.119	746.14	3.113	761.76
333.15	4.146	707.16	4.168	717.86	4.162	725.09	4.130	734.99	4.131	747.06	4.118	762.65
333.15	5.159	708.15	5.187	718.89	5.169	726.12	5.137	736.01	5.142	748.04	5.128	763.61
333.15	6.157	709.05	6.186	719.82	6.179	727.06	6.153	736.94	6.152	748.94	6.144	764.48
333.15	7.172	710.00	7.211	720.79	7.193	728.03	7.157	737.90	7.161	749.87	7.154	765.38
333.15	8.189	711.12	8.222	721.94	8.198	729.18	8.171	739.03	8.170	750.97	8.162	766.45
333.15	9.192	711.84	9.230	722.70	9.209	729.95	9.177	739.80	9.171	751.72	9.183	767.19
333.15	10.200	712.76	10.239	723.66	10.226	730.91	10.191	740.74	10.188	752.64	10.190	768.08
333.15	11.222	713.65	11.254	724.57	11.231	731.82	11.197	741.64	11.201	753.52	11.188	768.93
333.15	12.220	714.52	12.256	725.47	12.242	732.73	12.213	742.54	12.208	754.39	12.213	769.78
333.15	13.239	715.35	13.266	726.33	13.254	733.59	13.220	743.40	13.211	755.22	13.218	770.59
333.15	14.237	716.18	14.273	727.19	14.263	734.46	14.233	744.26	14.221	756.06	14.222	771.41
333.15	15.251	717.07	15.292	728.11	15.257	735.38	15.239	745.16	15.227	756.94	15.232	772.27
333.15	16.254	717.87	16.289	728.93	16.271	736.21	16.237	745.98	16.236	757.74	16.232	773.04
333.15	17.261	718.62	17.298	729.72	17.282	737.00	17.250	746.77	17.236	758.52	17.230	773.82
333.15	18.271	719.38	18.302	730.51	18.279	737.80	18.250	747.56	18.240	759.29	18.248	774.57
333.15	19.274	720.08	19.311	731.24	19.293	738.55	19.261	748.31	19.247	760.03	19.246	775.31
333.15	20.274	720.79	20.313	731.98	20.290	739.28	20.256	749.03	20.262	760.73	20.247	775.99
343.15	0.100	694.23	0.100	703.91	0.100	710.96	0.100	720.87	0.100	733.87	0.100	748.91
343.15	1.119	696.44	1.166	706.45	1.134	713.50	1.100	723.47	1.093	735.83	1.103	751.63
343.15	2.119	697.48	2.149	707.51	2.141	714.56	2.111	724.52	2.104	736.85	2.098	752.62
343.15	3.137	698.47	3.160	708.53	3.147	715.59	3.119	725.53	3.107	737.83	3.114	753.57
343.15	4.136	699.45	4.182	709.54	4.163	716.60	4.132	726.53	4.121	738.80	4.120	754.52
343.15	5.153	700.30	5.189	710.44	5.169	717.51	5.143	727.44	5.128	739.70	5.129	755.41
343.15	6.161	701.28	6.203	711.45	6.177	718.52	6.154	728.44	6.138	740.67	6.154	756.35
343.15	7.171	702.37	7.206	712.55	7.186	719.62	7.163	729.53	7.148	741.73	7.156	757.38
343.15	8.180	703.35	8.221	713.57	8.203	720.64	8.166	730.54	8.157	742.71	8.164	758.34
343.15	9.192	704.30	9.228	714.54	9.212	721.61	9.180	731.50	9.167	743.65	9.172	759.25
343.15	10.198	705.18	10.239	715.44	10.221	722.52	10.192	732.39	10.182	744.52	10.179	760.10
343.15	11.208	706.19	11.253	716.47	11.233	723.55	11.203	733.40	11.186	745.49	11.204	761.03
343.15	12.221	707.04	12.263	717.36	12.242	724.45	12.214	734.30	12.198	746.38	12.210	761.92

343.15	13.229	707.97	13.257	718.32	13.248	725.41	13.219	735.25	13.211	747.31	13.207	762.82
343.15	14.240	708.83	14.270	719.21	14.259	726.31	14.232	736.14	14.224	748.18	14.219	763.68
343.15	15.242	709.69	15.276	720.09	15.258	727.19	15.237	737.02	15.230	749.03	15.222	764.51
343.15	16.250	710.51	16.282	720.94	16.268	728.05	16.241	737.87	16.241	749.87	16.239	765.32
343.15	17.261	711.36	17.292	721.81	17.266	728.92	17.249	738.73	17.239	750.70	17.236	766.13
343.15	18.263	712.15	18.290	722.63	18.276	729.75	18.259	739.54	18.250	751.50	18.240	766.91
343.15	19.270	712.86	19.303	723.38	19.289	730.50	19.263	740.30	19.256	752.24	19.254	767.65
343.15	20.269	713.58	20.314	724.11	20.294	731.24	20.273	741.02	20.260	752.94	20.262	768.33
353.15	0.100	686.07	0.100	694.83	0.100	701.43	0.100	711.349	0.100	724.04	0.100	739.99
353.15	1.134	688.19	1.161	697.39	1.142	704.20	1.113	714.20	1.104	726.81	1.110	742.75
353.15	2.128	689.12	2.151	698.34	2.152	705.16	2.110	715.15	2.106	727.74	2.100	743.65
353.15	3.136	690.33	3.157	699.56	3.154	706.37	3.116	716.34	3.118	728.90	3.107	744.78
353.15	4.148	691.43	4.174	700.67	4.173	707.49	4.134	717.44	4.127	729.97	4.123	745.82
353.15	5.164	692.47	5.181	701.73	5.171	708.55	5.138	718.49	5.143	730.99	5.127	746.81
353.15	6.166	693.50	6.204	702.78	6.192	709.60	6.148	719.52	6.147	732.00	6.136	747.80
353.15	7.181	694.50	7.203	703.80	7.196	710.61	7.157	720.53	7.163	732.98	7.152	748.75
353.15	8.176	695.58	8.207	704.90	8.207	711.72	8.170	721.62	8.167	734.05	8.159	749.80
353.15	9.198	696.59	9.227	705.92	9.221	712.73	9.182	722.62	9.182	735.03	9.169	750.75
353.15	10.214	697.50	10.228	706.85	10.221	713.67	10.194	723.56	10.186	735.94	10.184	751.65
353.15	11.210	698.51	11.242	707.88	11.240	714.69	11.213	724.56	11.201	736.93	11.190	752.60
353.15	12.229	699.42	12.248	708.82	12.254	715.64	12.210	725.50	12.211	737.85	12.198	753.51
353.15	13.229	700.36	13.257	709.77	13.254	716.60	13.219	726.45	13.224	738.77	13.209	754.41
353.15	14.236	701.22	14.269	710.66	14.269	717.49	14.234	727.34	14.230	739.64	14.216	755.27
353.15	15.247	702.15	15.280	711.61	15.272	718.44	15.242	728.28	15.226	740.57	15.220	756.17
353.15	16.248	703.06	16.281	712.54	16.279	719.37	16.244	729.19	16.241	741.46	16.233	757.03
353.15	17.262	703.90	17.288	713.40	17.282	720.24	17.248	730.06	17.247	742.31	17.244	757.88
353.15	18.258	704.69	18.296	714.22	18.286	721.06	18.258	730.87	18.250	743.11	18.244	758.66
353.15	19.263	705.44	19.298	714.99	19.298	721.84	19.264	731.65	19.253	743.86	19.246	759.40
353.15	20.269	706.24	20.309	715.82	20.297	722.67	20.258	732.47	20.261	744.68	20.261	760.20

[a] Expanded combined uncertainties ($k = 2$) U_c are $U_c(T) = 0.02\ K$, $U_c(P) = 0.032\ MPa$, $U_c(x_i) = 0.0002$, $U_c(\rho) = 1.10\ kg.m^{-3}$

[*]At atmospheric pressures the expanded combined uncertainty in pressure is $U_c(P) = 0.002\ MPa$

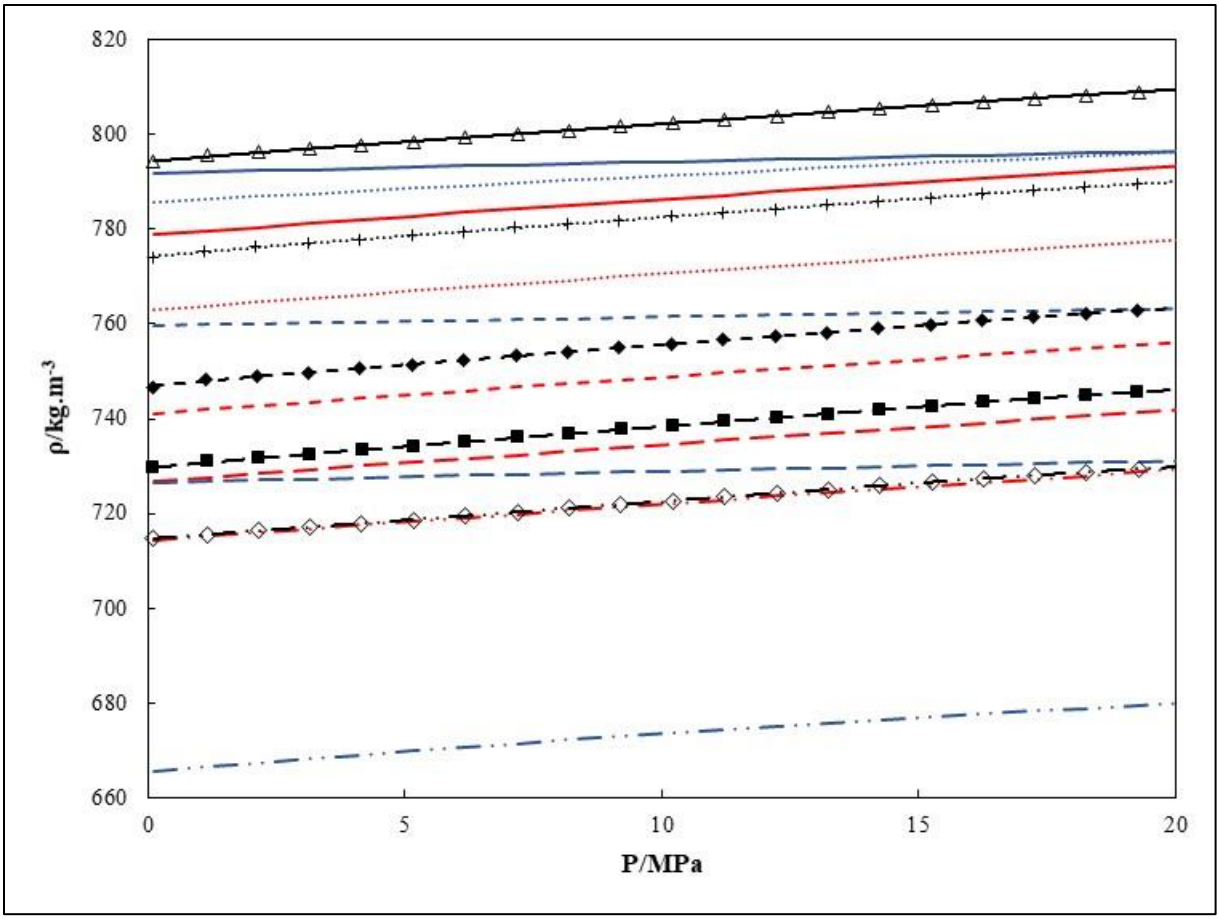

Figure 6.5a. Experimental and model calculated mixture density data (ρ) for the butan-1-ol (1) + n-decane (2) system as a function of pressure (P) at 313.15 K and various compositions. (exp, model) x_1: (◊, —·—)- x_1 = 0, (♦, − − −)- x_1 = 0.6234, (+, ····)- x_1 = 0.8734, (Δ, —)- x_1 = 1. Black lines-Modified Toscani-Szwarc EOS (Zúñiga-Moreno and Galicia-Luna, 2002), Blue lines-Peng-Robinson (Peng and Robinson, 1976) correlation (k_{ij} = -1.61), Red lines-PC-SAFT prediction (Gross and Sadowski, 2002, 2001).

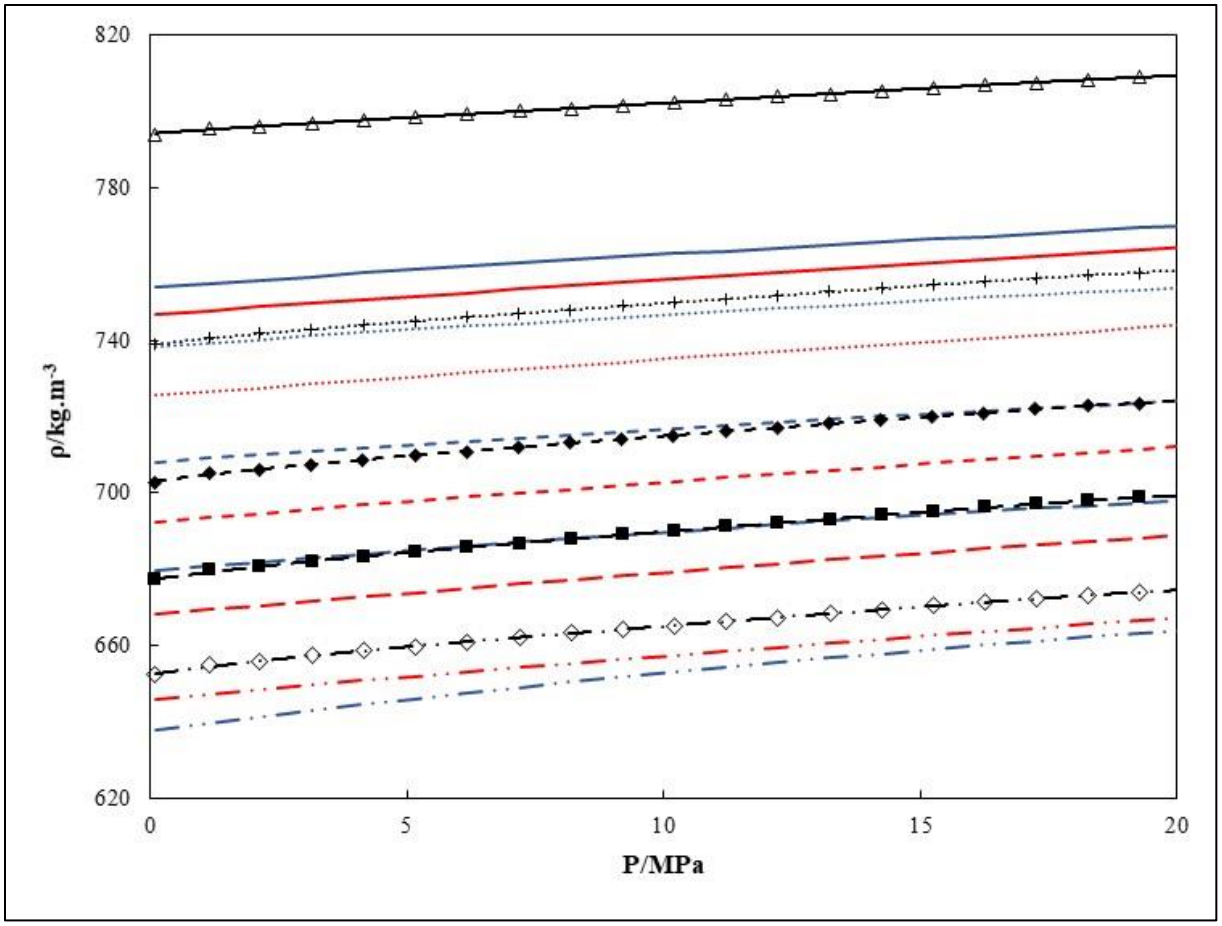

Figure 6.5b. Experimental and model calculated mixture density data (ρ) for the butan-1-ol (1) + n-octane (2) system as a function of pressure (P) at 353.15 K and various compositions. (exp, model) x_1: (◊, —·—)- x_1 = 0, (■, — — —)- x_1 = 0.3750, (♦, – – –), x_1 = 0.6258, (+, ····), x_1 = 0.8750, (Δ, —)- x_1 = 1. Black lines-Modified Toscani-Szwarc EOS(Zúñiga-Moreno and Galicia-Luna, 2002)**, Blue lines-Peng-Robinson** (Peng and Robinson, 1976) **correlation (k_{ij} = -0.23), Red lines-PC-SAFT prediction**(Gross and Sadowski, 2002, 2001)**.**

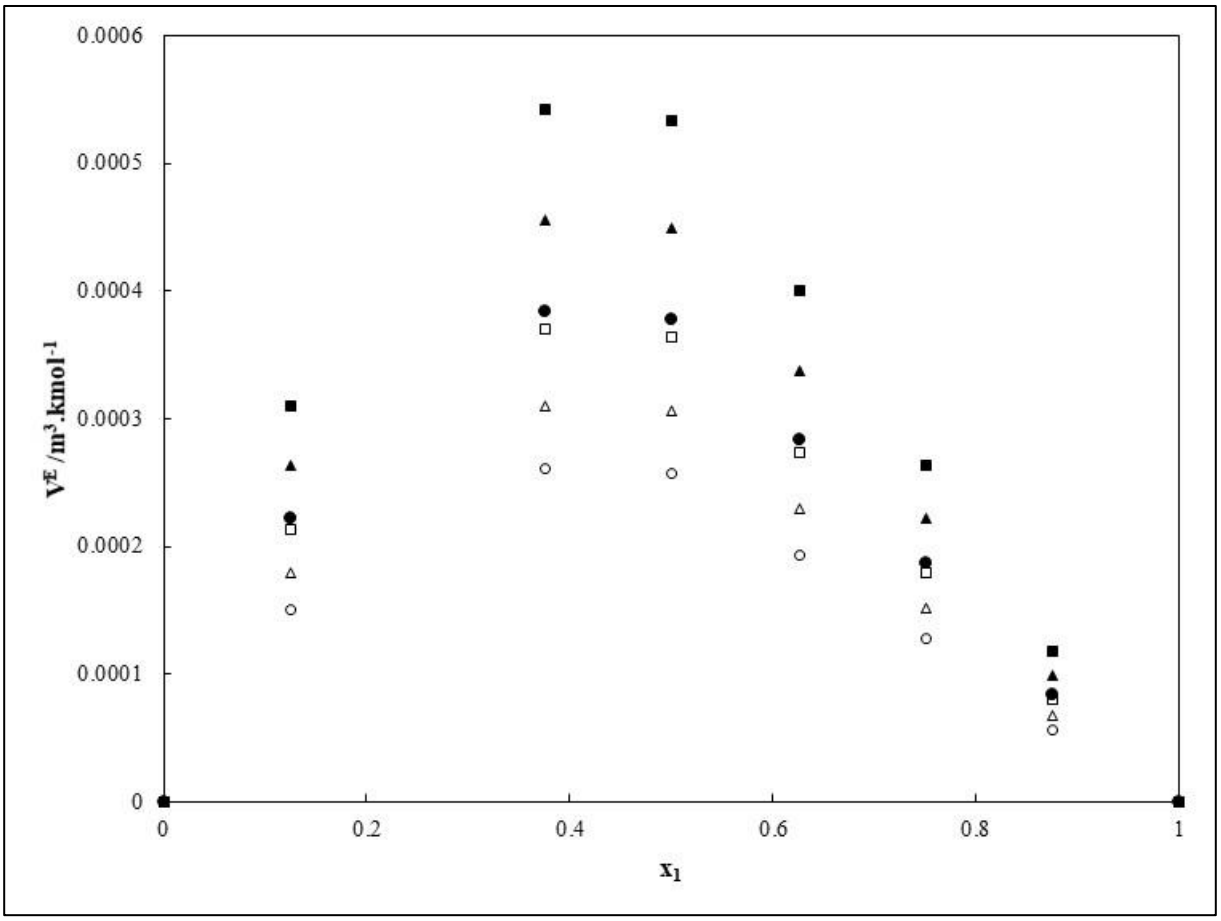

Figure 6.6. Calculated excess volume (V^E) for the butan-1-ol (1) + n-octane (2) system at selected temperatures and pressures. (symbol-T, P): (■- 353.15 K, 1 MPa), (□- 353.15 K, 20 MPa), (▲- 333.15 K, 1MPa), (∆- 333.15 K, 20- MPa), (●- 313.15 K, 1 MPa), (○- 313.15 K, 20 MPa).

Table 6.7. Pure component parameters used for Peng-Robinson Equation and PC-SAFT model.

Component	**T_c/K** (Poling et al., 2001)	**P_c/kPa** (Poling et al., 2001)	**Ω** (Poling et al., 2001)	**m**	**σ/Å**	**$\frac{\epsilon}{k}$/K**	**κ^{AB}**	**$\frac{\epsilon^{AB}}{k}$ /k**
butan-1-ol	536.05	4179	0.574	3.4400 Gross and Sadowski (2002)	3.3130 Gross and Sadowski (2002)	224.20 Gross and Sadowski (2002)	0.0104 Gross and Sadowski (2002)	2067.63 Gross and Sadowski (2002)
n-octane	568.7	2490	0.399	5.0291 (Burgess et al., 2012)	3.5167 (Burgess et al., 2012)	229.30 (Burgess et al., 2012)	-	-
n-decane	617.7	2110	0.490	6.9000 (Burgess et al., 2012)	3.3665 (Burgess et al., 2012)	226.86 (Burgess et al., 2012)	-	-

T_c and P_c are the critical temperature and pressure, ω is the acentric factor. m is the number of segments per chain, σ is the segment diameter, $\frac{\epsilon}{k}$ is the depth of pair potential over the Boltzman constant, κ^{AB} is the effective association volume, $\frac{\epsilon^{AB}}{k}$ is the association energy, in the PC-SAFT model.

Table 6.8. Regressed parameters for the Modified Toscani-Szwarc (MTS) equation of state.

x_1	c_1/MPa.m^3.kg^{-1}	c_2/m^3.kg^{-1}	c_3 /MPa	c_4 /K.MPa	c_5 /K$^{1/3}$.MPa	RMSD[a]
n-heptane						
1	0.1512	1.248E-03	-242.896	35264.725	-3098.438	2.635E-04
n-octane (1)						
1	0.1684	1.218E-03	-234.093	34305.804	-3119.462	2.75E-04
n-decane (1)						
1	0.1827	1.178E-03	-236.870	38103.225	-3321.140	1.053E-04
ethanol (1)						
1	0.1646	1.085E-03	-418.554	65121.216	-5116.954	1.814E-04
butan-1-ol (1)						
1	0.2181	1.033E-03	-559.630	92612.617	-6985.099	4.392E-04
ethanol (1) + n-heptane (2)						
0.1291	0.1508	1.233E-03	-269.780	39288.220	-3370.220	2.494E-04
0.3760	0.1577	1.206E-03	-307.399	44945.080	-3793.754	2.158E-04
0.4999	0.1595	1.190E-03	-324.923	47951.876	-3995.959	1.871E-04
0.6253	0.1594	1.171E-03	-325.938	48230.357	-4021.090	1.341E-04
0.7502	0.1583	1.149E-03	-343.642	51459.622	-4223.321	1.054E-04
0.8748	0.1570	1.120E-03	-369.296	56178.561	-4515.760	9.671E-05
butan-1-ol (1) + n-octane (2)						
0.1259	0.1686	1.203E-03	-250.789	37131.510	-3302.901	2.52E-04
0.3750	0.1700	1.171E-03	-288.011	43716.440	-3725.965	1.97E-04
0.5002	0.1730	1.152E-03	-311.270	47928.726	-4003.017	1.67E-04
0.6258	0.1777	1.130E-03	-331.365	51820.865	-4263.493	1.43E-04
0.7503	0.1849	1.105E-03	-376.608	60044.765	-4805.418	1.06E-04
0.8750	0.1959	1.075E-03	-433.653	70462.080	-5499.831	1.00E-04
butan-1-ol (1) + n-decane (2)						
0.1269	0.1925	1.153E-03	-388.612	61984.435	-4922.558	1.09E-04
0.3746	0.2084	1.110E-03	-602.880	95910.752	-7206.697	1.19E-04
0.4968	0.2137	1.091E-03	-676.013	107718.561	-7995.989	1.20E-04
0.6234	0.2146	1.079E-03	-674.567	107920.968	-8009.695	1.15E-04
0.7440	0.2132	1.070E-03	-616.032	99317.714	-7435.988	1.08E-04
0.8731	0.2145	1.053E-03	-593.917	96597.023	-7255.713	1.10E-04

$$RMSD = \frac{\sum_k^L ((\frac{\rho_k^{exp} - \rho_k^{calc}}{\rho_k^{exp}})^2)^{1/2}}{L}$$

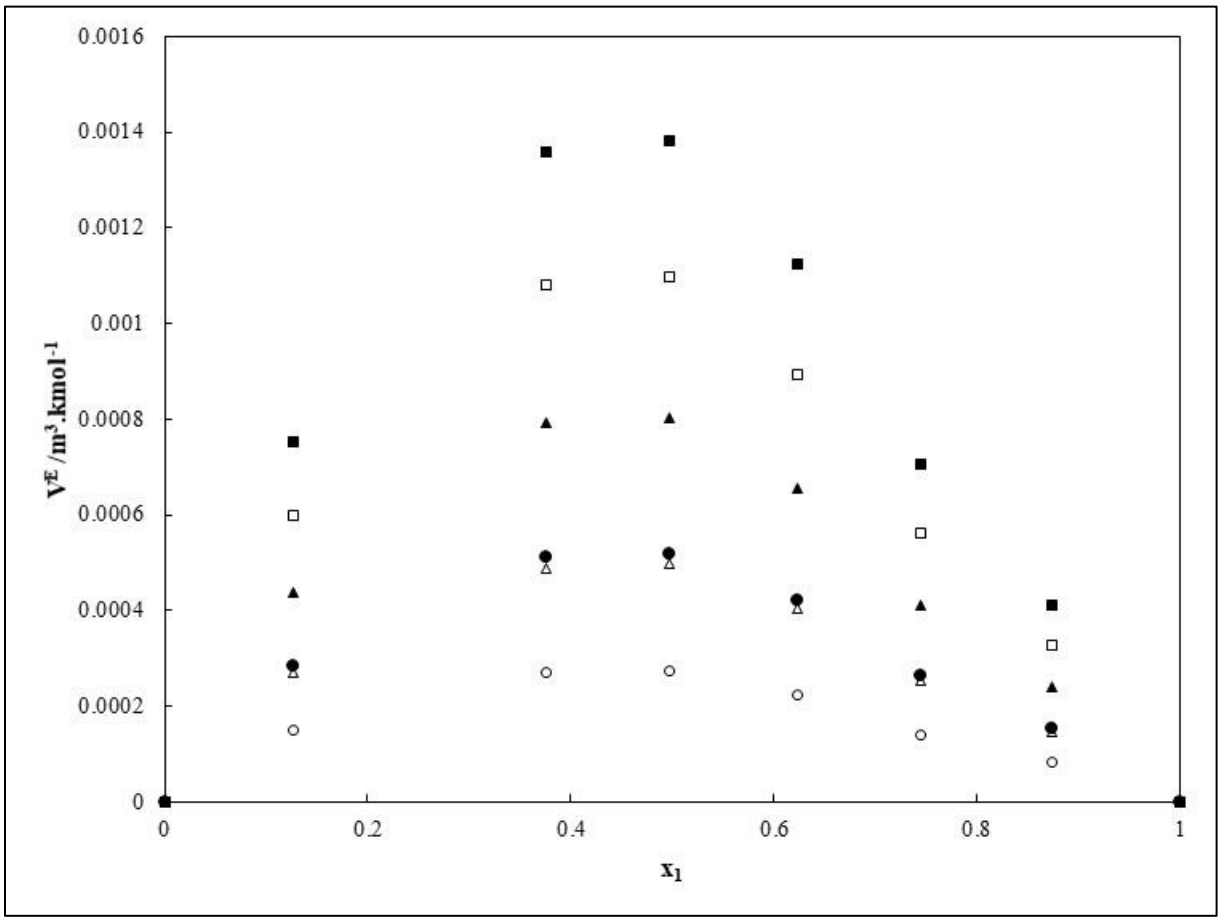

Figure 6.7. Calculated excess volume (V^E) for the butan-1-ol (1) + n-decane (2) system at selected temperatures and pressures. (symbol-T, P): (■- 353.15 K, 1 MPa), (□- 353.15 K, 20 MPa), (▲- 333.15 K, 1MPa), (Δ- 333.15 K, 20- MPa), (●- 313.15 K, 1 MPa), (○- 313.15 K, 20 MPa).

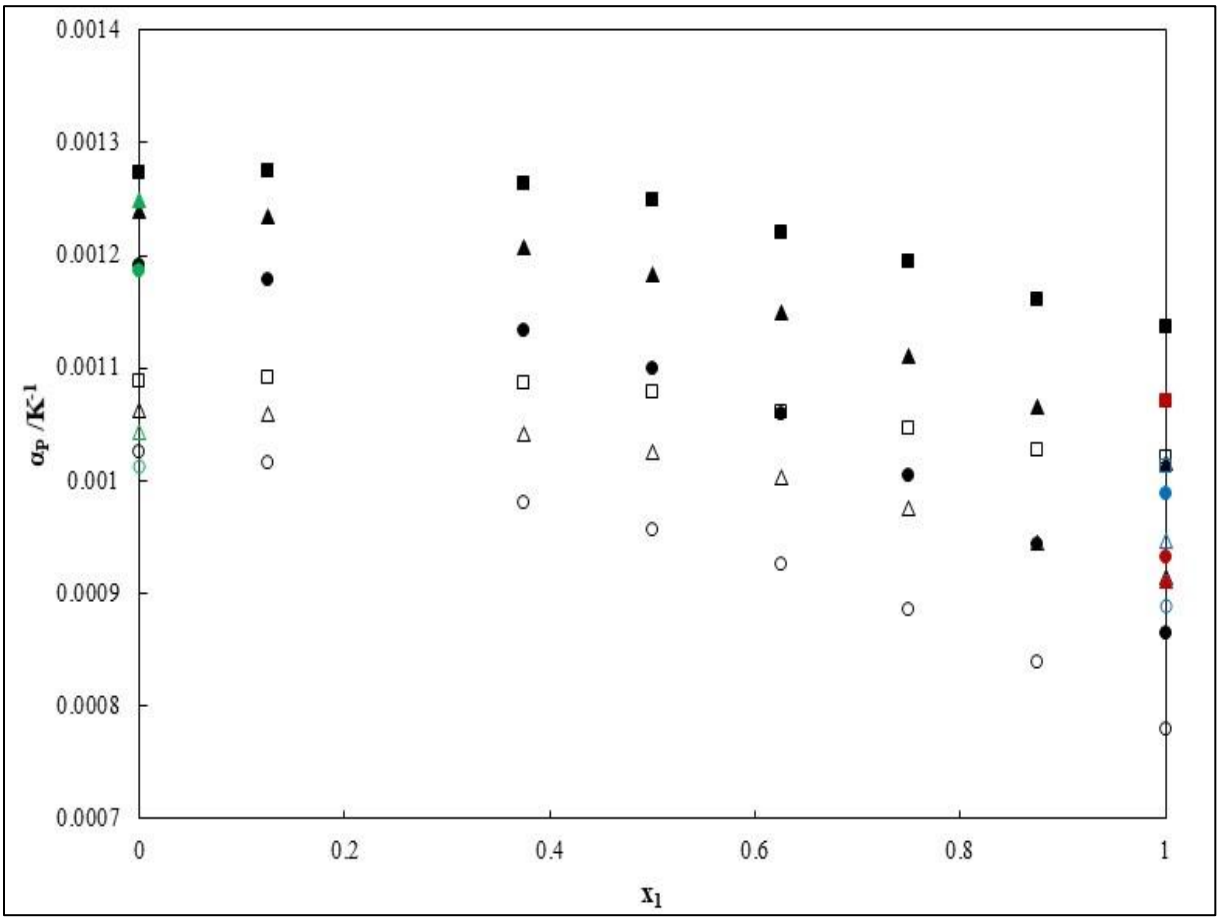

Figure 6.8. Calculated thermal expansivity (α_P) vs. x_1 for the butan-1-ol (1) + n-octane (2) system at selected temperatures and pressures. (symbol-T, P): (■- 353.15 K, 1 MPa), (□- 353.15 K, 20 MPa), (▲- 333.15 K, 1MPa), (Δ- 333.15 K, 20- MPa), (●- 313.15 K, 1 MPa), (○- 313.15 K, 20 MPa). Black markers are this work, red markers are the data of (Alaoui et al., 2011), blue markers are the data of (Safarov et al., 2015), green markers are the data of (Lugo, *et al.*, 2001)

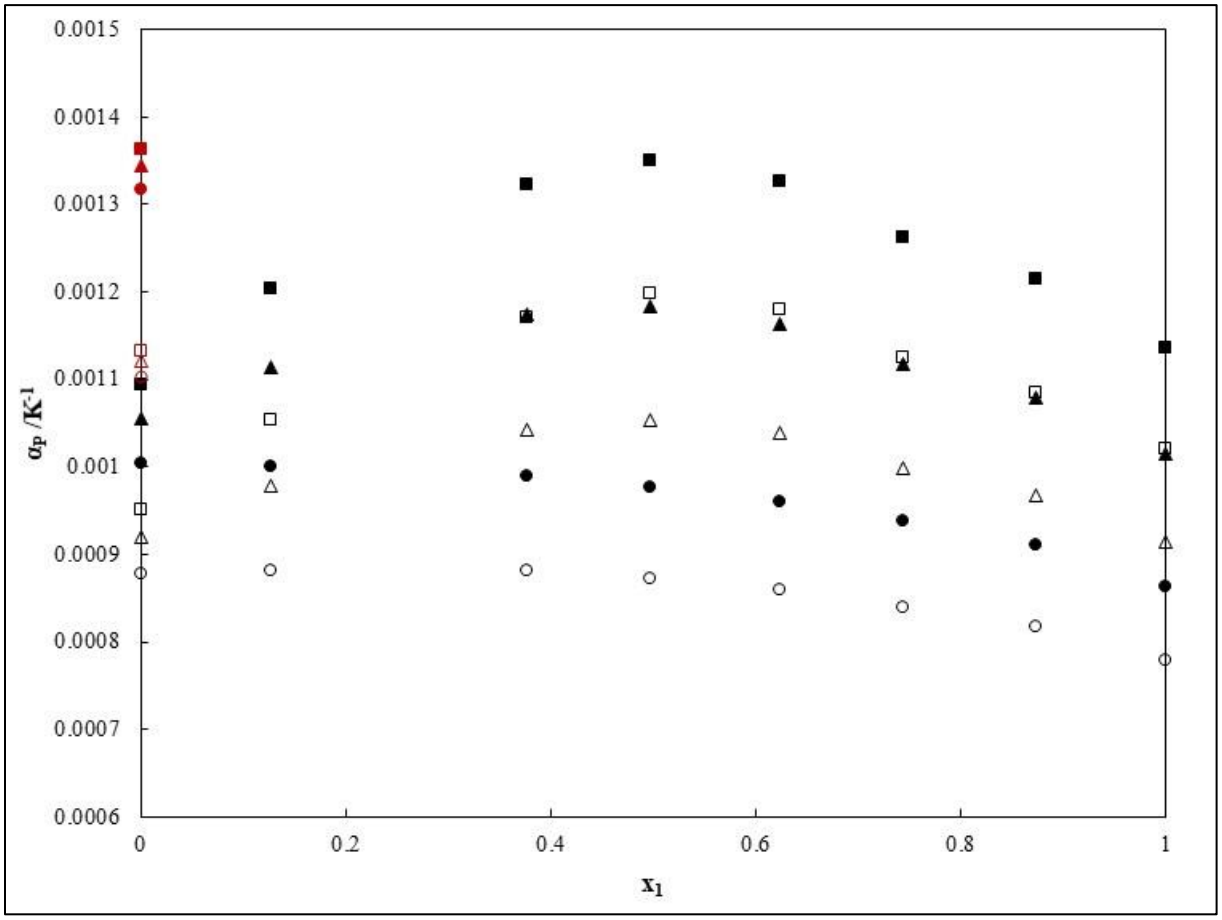

Figure 6.9. Calculated thermal expansivity (α_P) vs. x_1 for the butan-1-ol (1) + n-decane (2) system at selected temperatures and pressures. (symbol-T, P): (■- 353.15 K, 1 MPa), (□- 353.15 K, 20 MPa), (▲- 333.15 K, 1MPa), (∆- 333.15 K, 20- MPa), (●- 313.15 K, 1 MPa), (○- 313.15 K, 20 MPa). Black markers are this work, red markers are the data of (Quevedo-Nolasco *et al.*, 2012)

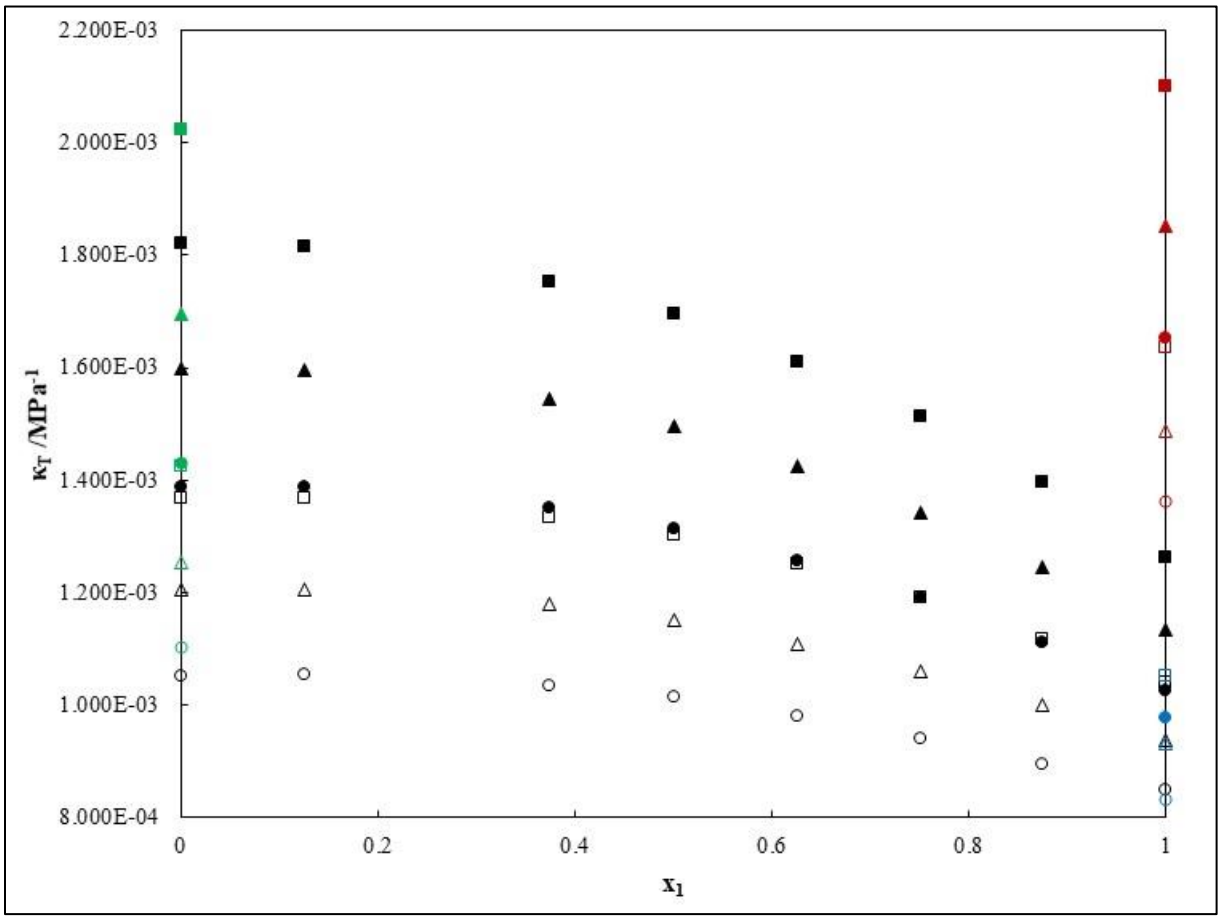

Figure 6.10. Calculated compressibility (κ_T) vs. x_1 for the butan-1-ol (1) + n-octane (2) system at selected temperatures and pressures. (symbol-T, P): (■- 353.15 K, 1 MPa), (□- 353.15 K, 20 MPa), (▲- 333.15 K, 1MPa), (Δ- 333.15 K, 20- MPa), (●- 313.15 K, 1 MPa), (○- 313.15 K, 20 MPa). Black markers are this work, red markers are the data of (Alaoui et al., 2011), blue markers are the data of (Safarov et al., 2015), green markers are the data of (Lugo *et al.*, 2001)

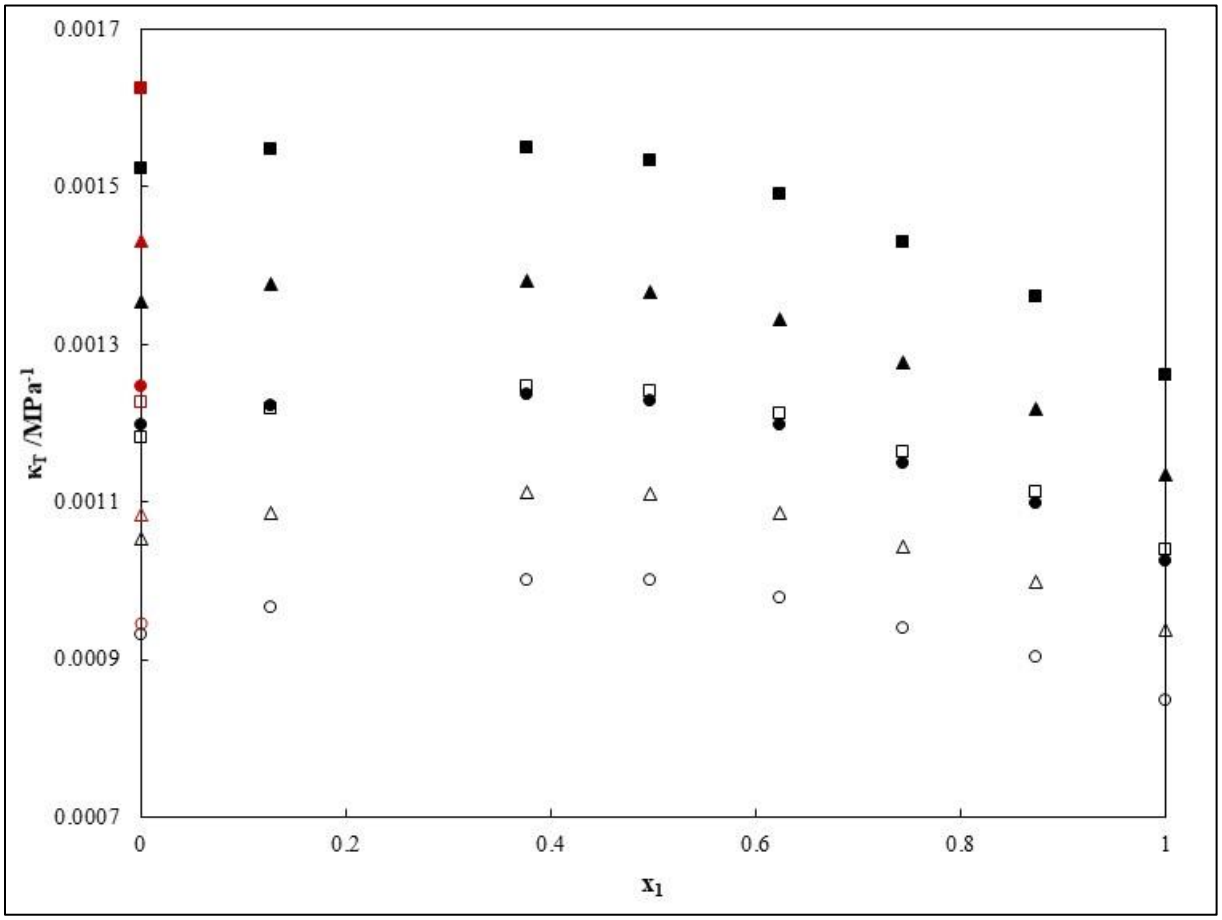

Figure 6.11. Calculated compressibility (κ_T) vs. x_1 for the butan-1-ol (1) + n-decane (2) system at selected temperatures and pressures. (symbol-T, P): (■- 353.15 K, 1 MPa), (□- 353.15 K, 20 MPa), (▲- 333.15 K, 1MPa), (Δ- 333.15 K, 20- MPa), (●- 313.15 K, 1 MPa), (○- 313.15 K, 20 MPa). Black markers are this work, red markers are the data of (Quevedo-Nolasco *et al.*, 2012)

6.6. Conclusions

Densities for the novel binary systems butan-1-ol (1) + n-octane (2) and butan-1-ol (1) + n-decane (2) were measured in this work in the temperature and pressure ranges of T = (313.15, 323.15, 333.15, 343.15, and 353.15 K) and P = (0.1−20 MPa). Experimental densities for the pure components were compared to those in the literature to test the reliability of the experimental setup and procedure. The measured pure component densities are in good agreement to those obtained from the literature. The MTS EOS was employed and successfully correlated the experimental density data; however, the model requires that each composition be regressed separately for a system. Poor predictions were obtained by the Peng−Robinson and PCSAFT equations of state; however, simultaneous correlation/prediction of all compositions from a single parameter set was conducted by these models. Excess volumes, thermal expansivity, and isothermal compressibility were also calculated utilizing the regressed data. The mixtures demonstrated significant positive excess volumes attributed to dissimilar molecule sizes and shapes as well as attractive mixture interactions when compared to pure components. The derived thermal expansivity and isothermal compressibility confirmed non-ideal mixing.

CHAPTER SEVEN

Experimental P−ρ−T Data and Modelling for Butan-2-ol + n-Octane or n-Decane in the Ranges of 313.15−353.15 K and 0.1−20 MPa

7.1. Abstract

Experimental density data at high pressures for two novel binary systems, butan-2-ol (1) + n-octane (2) and butan-2-ol (1) + n-decane (2), are presented in this work. Measurements were conducted in the temperature and pressure ranges of 313.15− 353.15 K and 0.1−20 MPa, respectively, and include the entire mixture composition range. The experimental data were successfully correlated utilizing the modified Toscani−Szwarc equation of state and comply with generally expected trends with regard to temperature and pressure. The data were also modeled by the Peng−Robinson equation of state and predicted by the perturbed chain statistical associating fluid theory (PC-SAFT) model; however, a poor representation of the data was observed for the mixtures. Excess molar volumes, thermal expansivity, and isothermal compressibility were calculated using the regressed model parameters and are also presented. Significant deviations from ideality regarding the calculated excess volume is mainly attributed to different molecule shapes and sizes, intermolecular mixture interactions, free volume changes, and interstitial accommodation.

7.2. Introduction

Enhanced oil recovery (EOR) methods, utilized for the recovery of heavy oils from existing reservoirs, have been gaining popularity in recent years due to the depletion of oil reserves (Pei et al., 2014). The various methods of EOR, which comprise thermal or chemical recovery including gas or liquid injection, and methods that focus on reducing the viscosity and surface tension of the oil, have the potential to recover up to 69.3% of the original oil in place (OOIP) (Lake, 1989).

The EOR method employed depends largely on the properties of the fluid present within the reservoir as well as on the geology of the reservoir. Gas injection is usually employed in light low-viscous oil reservoirs and generally involves injection of miscible gasses such as CO_2, natural gas, or nitrogen into the reservoir. With this method, reservoir pressures are maintained (Gbadamosi et al., 2018; Lake, 1989). The primary target of thermal methods is heavy oils and tar sands (Thomas, 2008). Chemical methods, which focus primarily on the recovery of light oils such as C_4 to C_{13}

hydrocarbons (Odden *et al.*, 1998), aim to improve the mobility ratio and reduce the interfacial tension within the reservoir. This method encompasses miscible flooding, chemical flooding, and other methods such as microbial EOR and has been employed successfully in Canada and Mexico for example (Thomas, 2008).

Recent studies1, (Salter, 1977, 1978; Dahami *et al.*, 1988; Odden *et al.*, 1998; Chen and Zhao, 2015, 2017; Fortenberry *et al.*, 2015; Yang *et al.*, 2019; Janssen *et al.*, 2020) have focused on utilizing C_4−C_6 alcohols as a surfactant/cosolvent in EOR including chemical flooding as they have been shown to improve the recovery of the OOIP by up to 11% (Chen and Zhao, 2017). Increased recovery is attributed to the enhanced sweep efficiency and displacement efficiency. The addition of alcohols improves the viscosity of the oil and the foaming properties and aids in the entrapment of oil droplets that have been emulsified, which collectively contribute to enhancing the sweep efficiency. Furthermore, the addition of alcohols to surfactant solutions enhances their emulsifying properties, thereby improving the displacement efficiency (Chen and Zhao, 2017).

Within the reservoir, the resultant alcohol-light oil mixtures can be exposed to high temperatures and pressures. Thermophysical properties, such as density, at these conditions are very limited in the literature, and equations of state generally perform poorly with respect to density predictions. Density, compressibility, and thermal expansivity for these systems have not been studied extensively in the literature. At atmospheric pressure, studies by Chaudhari and Katti (1985) and González *et al.* (2004) for butan-2-ol + n-octane and by González *et al.* (2004) for butan-2-ol + n-decane are available in the literature. To address the shortage of this data, n-octane and n-decane are considered as representative components for light oils, and density measurements of mixtures of these “light oils” with butan-2-ol were performed in this work.

The data were measured in the range of 313.15−353.15 K, from 0.1 to 20 MPa for the entire mixture composition range. The data were modeled using the modified Toscani−Szwarc (MTS) equation (2004), with a further minor modification by Quevedo-Nolasco *et al.* (2012), and derived properties of thermal expansivity and compressibility were calculated. The experimental data were also compared to correlations by the Peng and Robinson equation of state (EOS) (Peng and Robinson, 1976) and predictions by the perturbed chain statistical associating fluid theory (PC-SAFT) model (Gross and Sadowski, 2002, 2001).

7.3. Theory

The experimental density measured in this work was correlated utilizing the empirical modified Toscani−Szwarc equation of state, proposed by Quevedo-Nolasco *et al.* (2012)

$$\rho^{calc} = \frac{c_3 - \frac{c_4}{T} - \frac{c_5}{T^{1/3}} + P}{c_1 + c_2 P} \tag{7.1}$$

where ρ^{calc} is the density of the mixture in $kg \cdot m^{-3}$ calculated by the model, P is the pressure of the system in MPa, T is the experimental temperature in kelvin (K), and c_1 to c_5 denote the regressed model parameters.

Excess molar volumes (VE) represent positive or negative deviations from ideality and are attributed to several factors that include molecular size, shape, dispersion energy, molecular multipole moments, molecular polarizability as well as correlation of molecular orientation, effects of conformational equilibria, induction effects, and association equilibria (Wilhelm and Grolier, 2014). It can be calculated as follows:

$$V^E = \sum_{i=1}^{N} x_i M_i \left(\frac{1}{\rho} - \frac{1}{\rho_i}\right) \tag{7.2}$$

where N is the number of components comprising the system, M_i is the molar mass of component i, x_i is the mole fraction of component i, ρ is the density of the mixture, and ρ_i is the density of the pure component i.

The differential change in volume, at a constant pressure, with temperature is referred to as the isobaric thermal expansivity (α_P) and is calculated using density by the following equation:

$$\alpha_P = -\frac{1}{\rho} \left(\frac{\partial \rho}{\partial T}\right)_P \tag{7.3}$$

where α_P is the thermal expansivity at constant pressure (P), ρ is the density of the mixture in $kg \cdot m^{-3}$, and T is the temperature in kelvin.

A measure of relative volume change of a chemical species with pressure is defined as isothermal compressibility. It can be calculated using density by the following equation:

$$\kappa_T = \frac{1}{\rho} \left(\frac{\partial \rho}{\partial P}\right)_T \tag{7.4}$$

where κ_T is the compressibility at constant temperature (T).

The derivatives given by equation (7.3) and equation (7.4) can be evaluated from the modified Toscani−Swzarc equation of state:

$$\alpha_P = -\frac{\frac{c_4}{T^2} + \frac{c_5}{3T^{4/3}}}{c_3 - \frac{c_4}{T} - \frac{c_5}{T^{1/3}} + P} \tag{7.5}$$

$$\kappa_T = \frac{1}{c_3 - \frac{c_4}{T} - \frac{c_5}{T^{1/3}} + P} - \frac{c_2}{c_1 + c_2 P} \tag{7.6}$$

Equation (7.5) and equation (7.6) were employed for computing α_P and κ_T, respectively.

For an alternate modeling approach that simultaneously represented P−V−T−x_i, the Peng−Robinson equation of state (1976) was used:

$$P = \frac{RT}{V - b} - \frac{a}{V^2 + 2bV - b^2} \tag{7.7}$$

where P is the pressure, R is the universal gas constant, T is the temperature, and V is the molar volume.

The parameters a and b are usually calculated from correlations. For a component i

$$a_i = \frac{0.457235R^2{T_{c,i}}^2}{P_{c,i}}\, x\, a_i(T_{r,i}) \tag{7.8}$$

$$b_i = \frac{0.077796RT_{c,i}}{P_{c,i}} \tag{7.9}$$

$$a_i\left(T_{r,i}\right) = (1 + (0.37464 + 1.54226\omega_i - 0.26992\omega_i^2)(1 - T_{r,i}^{0.5})^2 \tag{7.10}$$

where ω_i is the acentric factor and $T_{r,i}$ is the reduced temperature, of component i. $T_{c,i}$ and $P_{c,i}$ are the critical temperature and pressure, respectively, of component i.

For mixtures of components i and j, a and b values are determined using classical mixing rules.

$$a = \sum_{i=1}^{N}\sum_{i=1}^{N} x_i x_j a_{ij} \tag{7.11}$$

$$b = \sum_{i=1}^{N}\sum_{i=1}^{N} x_i x_j b_{ij} \tag{7.12}$$

The combining rules for a_{ij} and b_{ij} are given by:

$$a_{ij} = \left(a_i a_j\right)^{0.5}(1 - k_{ij}) \tag{7.13}$$

And

$$b_{ij} = \frac{(b_i + b_j)}{2} \tag{7.14}$$

For binary mixtures, k_{ij} must be determined by regression of experimental mixture data.

The root-mean-square deviation (RMSD) is a useful measure of the model fitting quality and aggregates the residuals. It is calculated by

$$RMSD = \frac{\sum_k^L ((\frac{\rho_k^{exp} - \rho_k^{calc}}{\rho_k^{exp}})^2)^{1/2}}{L} \tag{7.15}$$

where L is the total number of points in the data set, k is a specific data point, ρ_k^{exp} is the experimental density of point k, and ρ_k^{calc} is the calculated density of data point k. Minimizing the function for the RMSD via regression enabled model parameters to be determined.

7.4. Experimental Section

7.4.1. Materials.

The chemicals utilized for the experiments, namely, n-octane, n-decane, and butan-2-ol, were procured from Sigma-Aldrich. All chemicals had a supplier-stated purity, by weight, of greater than 99% and were degassed prior to use using a Vigreux-type column. Karl Fischer titration was performed, utilizing an MKS-500 apparatus to determine the water content of the butan-2-ol, which was confirmed to be less than 0.0005 by mass. The titration was performed after a molecular sieve (3 Å $K_nNa_{12-n}[(AlO_2)_{12}(SiO_2)_{12}]$) was used to dry the butan-2-ol for 48 h.

Refractive index (RI) and density measurements, as well as purity checks by gas chromatography (GC) with a thermal conductivity detector, were conducted. A standard uncertainty of 0.0001 was determined for the ATAGO RX-7000a refractometer utilized in this work. An Anton Paar DMA 5000 device was utilized for density measurements of the pure components and mixtures at

ambient pressures, while a Shimadzu GC2014, with a capillary column with the dimensions 30 m × 0.25 mm × 0.25 μm film thickness- Zebron7HG-G010-11, was used to obtain GC relative peak areas.

Calibration of the DMA 5000 densitometer was conducted utilizing air and distilled, deionized water as the reference fluids. The estimated standard combined uncertainty in density using the DMA 5000 is $u_c(\rho) = 0.04$ kg·m^{-3}. The DMA HP apparatus was used to obtain the high-pressure density data presented in this work, by connecting the device to the DMA 5000, which is used as a display for the measured variables. The DMA HP was calibrated using distilled, deionized water and pure nitrogen gas. Table 7.1 presents the results obtained from the purity checks performed and shows comparisons to the literature.

7.4.2. Apparatus.

The apparatus has been reported in detail in previous works (Hussain and Moodley, 2020a; Moodley et al., 2018). Figure 7.1 shows the experimental setup used in this work. A tube is used to connect a gas-tight syringe to the high-pressure Teledyne ISCO 100 DM pump. The liquid sample, introduced into the high-pressure pump via the syringe, is controlled by a high-pressure needle valve that has an operating limit of 69 MPa. The heating jacket, surrounding the piston of the pump, ensures negligible temperature gradients, thus allowing isothermal conditions to be assumed. The pressurized liquid exiting the pump is then fed into the DMA HP densitometer that comprises a 2 cm^3 U-tube. The DMA HP uses the oscillating U-tube principle for density measurement of fluids within the U-tube. The U-tube is electronically excited to oscillate with a characteristic vibrational period. This characteristic vibrational period changes with the density of the fluid inserted into the tube. Measurement of the change in this vibrational period oscillation can be directly related to the unknown fluid density using standard calibrations.

The pressure and temperature ranges for the densitometer are 0.1−70 MPa and 263−473 K, respectively. The supplier stated uncertainty regarding density is influenced by the experimental pressure and temperature range as well as the calibration procedure employed and was stated to range from 0.1 to 1 kg·m^{-3}. An uncertainty of 0.01 K, regarding temperature, was stated for the densitometer using the internal sensor. This sensor was not calibrated independently in this study,

but a series of pure component measurements were performed in a recent work (Hussain and Moodley, 2020a) using the same device, which confirmed the precision of the temperature measurements.

A T-junction is used to connect a WIKA P-10 (0−25 MPa) pressure transducer to the line exiting the densitometer. A Mensor standard model CPC6000 was utilized to calibrate the pressure transducer with nitrogen gas as the reference fluid. An uncertainty of 0.0125 MPa and 0.0001 fraction of range (0−25 MPa) were stated for the P-10 transducer and CPC6000, respectively, while the calculated expanded uncertainty (k = 2) for pressure was 0.03 MPa. The liquid flow, in the line exiting the densitometer, is controlled by a second high-pressure needle valve. The exit from this valve leads to a vessel, used for the collection of waste, and a vacuum pump utilized for cleaning and evacuating.

Table 7.1. Chemical suppliers and purities.

Component	CAS No.	Supplier	Refractive index (RI) at 0.101 MPa.		Minimum stated mass fraction purity	GC peak relative area	Density at 313.15 K and 0.101 MPa /kg·m^{-3}.	
			Exp.[ǂ]	Lit. (Haynes, 2014)			Exp[*]	Lit.
n-octane	111-65-9	Sigma-Aldrich	1.3948 (298.15 K)	1.3944 (298.15 K)	0.99	0.99	686.25	686.22 (Lampreia *et al.*, 2011) 686.29 (Sanmamed et al., 2009) 686.36 (L. Lugo et al., 2001)
n-decane	124-18-5	Sigma-Aldrich	1.4092 (298.15 K)	1.4090 (298.15 K)	0.99	0.99	714.72	715.64 (Quevedo-Nolasco *et al.* 2012) 714.40 (Banipal *et al.*1991) 714.79 (Troncoso et al., 2004)
butan-2-ol[#]	78-92-2	Sigma-Aldrich	1.3982 (293.15 K)	1.3978 (293.15 K)	0.99	0.99	789.72	789.65 (Bravo-Sánchez et al., 2010) 790.11 (Awwad et al., 2008) 790.06 (Langa et al., 2006)
nitrogen	7727-37-9	Afrox	-	-	0.99	-	-	-
air	132259-10-0	Afrox	-	-	0.78 nitrogen 0.21 oxygen 0.009 argon 0.0003 carbon dioxide Trace helium, neon, krypton, xenon	-	-	-
water	7732-18-5	-	1.3334 (293.15 K)	1.33336 (293.15 K)	-	0.99	-	-

1.[ǂ] At sodium D-line = 589 nm. Expanded uncertainties $U_c(k=2)$ are $U_c(RI) = 0.0002$, $U_c(T) = 0.02K$, $U_c(P) = 0.002\ MPa$, [*]Expanded uncertainties $U_c(k=2)$ are $U_c(T) = 0.02K$, are $U_c(P) = 0.002\ MPa$ and $U_c(\rho) = 0.08\ kg \cdot m^{-3}$

2. [#]Purified by molecular sieve

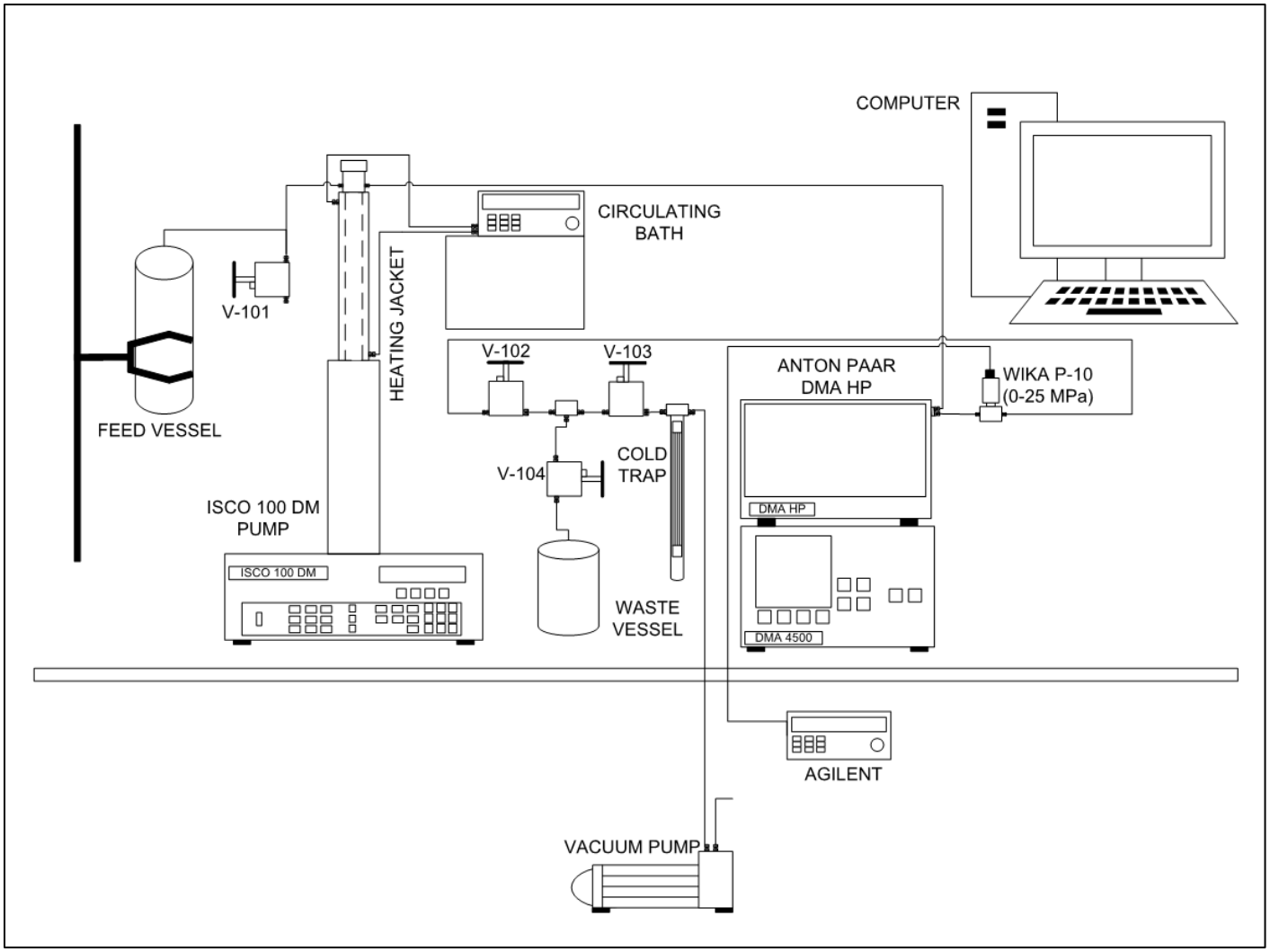

Figure 7.1. Layout of the apparatus used in this work (adapted from Moodley *et al.*, 2018, Hussain and Moodley, 2020).

7.4.3. Measurements.

7.4.3.1. Calibration of the Densitometer.

The calibration procedure outlined in the Anton Paar DMA HP manual is the two-fluid calibration method. To conduct this, distilled, deionized water and pure nitrogen gas were utilized as the reference fluids. Prior to calibration, the ISCO high-pressure pump was cleaned thoroughly. A gas-tight syringe was then used to inject the deionized water into the pump where the liquid was then

pressurized. The pressurized liquid was then fed into the DMA HP densitometer where it was heated to the desired experimental temperature. Thereafter the vibrational period of the U-tube filled with water was recorded once the desired temperature had been achieved. The calibration procedure was conducted for temperature and pressure ranges of 313.15−353.15 K and approximately 0.5−20 MPa, respectively. Calibration, with nitrogen gas as a reference fluid as well as at vacuum, was then undertaken utilizing a similar procedure. This allowed for three different calibration equations to be developed, which include the conventional two-fluid calibration procedure, as well as the procedures of Ihmels and Gmehling (2001) and Outcalt and McLinden (2007). Differences in the derived experimental densities, for the pure components, from each calibration procedure were included in the uncertainty calculation for density. These were found to be within experimental density uncertainties reported in the literature for similar components and conditions and within the expected range reported by Anton Paar in the device manual.

The densities presented in this work were calculated using the two-fluid calibration procedure, as was recommended by the device supplier. The following relationship was provided by the supplier and allows the user to convert the vibrational period to density using nitrogen and water as calibration fluids.

The relationship is given by:

$$\rho_m(P,T,\tau) = \rho_{H_2O}(P,T) + \frac{\left(\tau_m^2(P,T)-\tau_{H_2O}^2(P,T)\right)\left(\rho_{H_2O}(P,T)-\rho_{N_2}(P,T)\right)}{\tau_{H_2O}^2(P,T)-\tau_{N_2}^2(P,T)} \tag{7.16}$$

where T is the temperature in kelvin (K), τ is the vibrational period in μs, P is the system pressure measured in MPa, and ρ is the density in $kg \cdot m^{-3}$. The measurement sample is denoted by the subscript m, while the subscripts N_2 and H_2O denote the component reference property for nitrogen and water, respectively.

Reference densities for water and nitrogen were computed using correlations proposed by Wagner and Pruß (2002) and Span *et al.* (1998), respectively.

7.4.3.2. Experimental Procedure.

Again, the experimental procedure has been described in detail in previous works (Hussain and Moodley, 2020a; Moodley et al., 2018). A Mettler-Toledo mass balance, model AB204-S, with a stated precision of 0.0001 g, was utilized to prepare 80 mL standard solutions in a sealable vessel. The first component was added to the vessel, and thereafter the mass of the solution was recorded. The mass of component 2 was then computed to achieve the desired mass ratio, between components 1 and 2, which was then added to the vessel. The resultant solution was then stirred thoroughly to ensure that negligible concentration gradients were present. A gas-tight syringe was then utilized to inject the solution, in 15 mL increments, into the high-pressure pump, which was emptied, cleaned, flushed, and evacuated beforehand. This helped prevent contamination of the sample and was conducted three times to ensure that the composition within the piston, lines, and densitometer was uniform. Thereafter, the liquid sample was fed into the high-pressure pump, and the system was isolated by closing the two high-pressure needle valves. Isothermal conditions were attained by ensuring that minimal temperature gradients existed between the densitometer and the ISCO pump. To achieve this, the temperature of the heating jacket surrounding the piston of the pump was set to the experimental temperature. The high-pressure densitometer, DMA HP, comprises a built-in temperature controller that ensures that any temperature gradients that do exist are eliminated prior to thermal equilibrium. The DMA HP and the ISCO high-pressure pump were utilized to set the experimental temperatures and pressures, respectively. A period of 60−90 minute was allowed for thermal and mechanical equilibrium, before the vibrational period, temperature, and pressure were noted in triplicate. An excellent stability of all measured parameters was observed after equilibrium was established for a 30-minute waiting time. The procedure outlined above was adopted for the entire pressure and temperature range considered.

Computation of the expanded combined uncertainty in density with a coverage factor of k = 2 was undertaken employing the method outlined by the Joint Committee for Guides in Metrology (JCGM) (2008), and the values were found to be 1.09 and 1.11 $kg \cdot m^{-3}$ for the pure component and mixtures, respectively. A breakdown of the parameters considered for the uncertainty calculation is presented in Table 7.2 and includes the uncertainty due to chemical impurity as well as the uncertainty introduced by differences in the selected density calibration method used.

Table 7.2. Example of uncertainty breakdown for density*

Source	Uncertainty (*U*)	Contribution to $U_C(\rho)$/(kg·m^{-3})
Temperature $U(T)$, k =2	0.02 K	0.02
Pressure $U(P)$, k = 2	0.03 MPa	0.06
Period $U(\tau)$, k = 2 (repeatability)	0.002 μs	0.11
Mixture Composition x_i, k = 2	0.002 mol fraction	0.06
Uncertainty from Measurements $U_{meas}(\rho)$, k = 2		0.13
EOS of the calibration fluids $U_{EOS}(\rho)/\rho$, k = 2	0.05%	0.50
Calibration model (ρ), k = 2	0.95 kg·m^{-3}	0.95
Impurity x_i, k = 2	0.005 mol fraction	0.13
Combined expanded uncertainty in density $U_C(\rho)$, k = 2		1.11

* butan-2-ol (1) + n-decane (2) system at x_1= 0.5005 was used for this example
U_C is the combined expanded uncertainty in density (ρ)

7.5.Results and Discussion

The results obtained for the purity checks are presented in Table 7.1 and were found to be consistent with the literature. The experimental setup and procedure were verified by measuring the density of pure butan-2-ol in the temperature and pressure ranges of 313.15−353.15 K and 0.1−20 MPa, respectively. These results are presented in Table 7.3 and were compared to the literature as illustrated in Figure 7.2. A maximum relative deviation, between experimental and literature values, (Awwad et al., 2008; Behroozi and Zarei, 2011; Bravo-Sánchez et al., 2013, 2010; Dakkach et al., 2015; Faranda et al., 2004; González et al., 2014; Langa et al., 2006; Outcalt et al., 2010; Radzhabova et al., 2014; Živković et al., 2013; Zúñiga-Moreno et al., 2007a) of 0.0013 was noted. This demonstrates good correlation between the density measurements conducted in this work and those in the literature. Note that numerous literature sources are available at atmospheric pressure; however, those with the lowest reported uncertainties were selected for comparison.

Density measurements for both binary systems were conducted at atmospheric pressure (0.1 MPa) and a temperature range of 313.15−353.15 K over the entire mixture composition range and are presented in Tables 7.4 and 7.5. These results were compared to the literature (Chaudhari and Katti, 1985; González *et al.*, 2004), as illustrated in Figure 7.3, and comply with the general trends regarding the relationship between density, composition, and temperature that are observed in the literature data. It can be seen that the nonlinear density profile with composition for these mixtures,

which indicates nonideal mixing, is replicated at the higher temperatures considered in this work, similar to the literature at lower pressures. Data at the exact temperatures considered in this work was not available in the literature. The excess molar volumes were also calculated and are presented in Figure 7.4 with comparison to the literature data. It can be seen that the positive excess volume behavior is replicated, and the general trend of increasing excess volume with temperature is replicated in this work. Both systems exhibit positive excess volumes, which is expected of systems comprising components with differing molecular shapes and sizes, with one associating component. The behavior is attributed to the declustering of self-associated alcohol multimer series by the nonpolar alkane and the interaction between homomorphs of the alcohols with the alkanes. The addition of the nonpolar solvent is expected to decluster the alcohol complexes, which would contribute to an expansion in the volume upon mixing as the alcohol molecules occupy more space as monomers than as multimers. Negative contributions can occur from changes in the free volume in the real mixture or from limitations on the rotational motion when the n-alkane molecules are arranged interstitially within portions of the branched multimer structure. The interaction energy between the alcohol homomorphs and the alkane, which includes dipole−induced dipole (Debye) interactions, is expected to contribute to a positive excess volume (Rao and Naidu, 1974; Treszczanowicz and Benson, 1978).

The asymmetry of the V^E data for the butan-2-ol (1) + n-octane (2) system shown in Figure 7.4a with maxima at $x1 \approx 0.4$ is attributed to the increased capability of interstitial accommodation of the smaller n-octane molecule in comparison to the n-decane system, shown in Figure 7.4b (Treszczanowicz *et al.*, 1981). This contributes to a decrease in the excess volume in the alcohol-rich region, resulting in the appearance of a maximum in the n-octane-rich region for the butan-2-ol (1) + n-octane (2) system (Sastry, 1997). Since the interstitial accommodation is less pronounced in the butan-2-ol (1) + n-decane (2) system, a less pronounced decrease in the excess volume occurs in the alcohol-rich region, so there is no appearance of an asymmetrical maximum in the n-decane-rich region.

Isothermal measurements were conducted for novel binary systems butan-2-ol (1) + n-octane (2) and butan-2-ol (1) + n-decane (2) within the temperature and pressure ranges of 313.15−353.15 K and 0.1−20 MPa, respectively. Measurements were conducted over the entire mixture composition range and are presented in Tables 7.4 and 7.5. The data presented in this work is highly nonlinear

and complies with the expected trends of density with temperature and pressure. As demonstrated in Tables 7.4 and 7.5, the experimental densities increase with an increase in pressure and decrease with an increase in temperature.

The experimental data presented was correlated utilizing the five-parameter modified Toscani−Szwarc (MTS) equation of state. MATLAB was utilized to perform regression analysis of the experimental data and obtain these five parameters. These results as well as the associated RMSD are presented in Table 7.6. As illustrated in Figures 7.5 and 7.6, the modified Toscani−Szwarc equation demonstrates excellent agreement with experimental data with a maximum RMSD of 3.24×10^{-3}.

Predictions were also performed utilizing the PC-SAFT (Gross and Sadowski, 2002, 2001) model with the original mixing rules without a regressed binary interaction parameter along with correlations by the Peng−Robinson (1976) equation of state with the original mixing rules of Peng−Robinson (1976) with a regressed binary interaction parameter. These results were compared to the experimental data using RMSDs and are presented graphically in Figures 7.5 and 7.6.

For the PC-SAFT prediction, parameters presented by Burgess *et al.* (2012) were used for n-octane and n-decane, which were assumed to be non-associating, while a 2B association scheme was utilized for butan-2-ol for which parameters were obtained from the work of Zarei and Feyzi (2013). The 2B association scheme treats the oxygen and hydrogen atoms of the hydroxyl group on the alcohol as two individual association sites and is recommended by Gross and Sadowski (2002). The parameters used for these calculations are presented in Table 7.7.

Gross and Sadowski (2001, 2002) state that many engineers in the industry rely on the purely predictive capabilities of equations of state, as they do not have access to binary interaction parameters. Hence, binary interaction parameters for the PCSAFT model were not considered as the purely predictive capability of the PC-SAFT model for the systems presented here at high pressures was examined in this study.

The purely predictive capability of the Peng−Robinson model was found to be poor for the mixtures considered here. This is attributed to the model being designed to employ an interaction parameter for binary mixtures and hence would offer limited precision when the parameter is

omitted. These were not available in the literature and were thus regressed from the density data using the standard fitting procedure for liquid densities given by Walas (2013) involving a single real (liquid) root for the compressibility factor in the cubic equation of state. This is due to the system forming one homogenous phase at the temperature and pressure range considered in this work.

It must be noted that the k_{ij} obtained only applies to the density data and range measured here and should not be used in phase equilibrium calculations, as it would likely yield a poor result. The comparisons are presented in Figure 7.5 for the butan-2-ol + n-octane system at 313.15 K, and it can be seen that mostly qualitative representations can be made for the mixtures considered by both the PC-SAFT prediction (RMSD = 0.010) and the Peng−Robinson correlation (RMSD = 0.012). Figure 7.5 also includes the performances of the models for the prediction/correlation of the pure butan-2-ol behavior where the PC-SAFT prediction yielded an RMSD = 0.016 and the Peng−Robinson correlation yielded an RMSD = 0.024 for pure butan-2-ol. Similar results were obtained at other temperatures for this system, and for the binary system of butan-2-ol (1) + n-decane (2). Example calculations by the PC-SAFT prediction (RMSD = 0.011) and the Peng−Robinson correlation (RMSD = 0.019) are shown for this system at 353.15 K in Figure 7.6. The calculated k_{ij} values for the Peng−Robinson correlation are given in the respective figure captions. Note that since no binary interaction parameter was regressed for the PC-SAFT model, and the Peng−Robinson EOS allows for simultaneous correlation of all compositions of a particular system with a single k_{ij}, these model performances should not be compared directly to the performance of the multiparameter MTS EOS.

Excess molar volumes, for both novel systems, were calculated utilizing the regressed data. The pure n-octane and n-decane densities were estimated from model parameters presented in a recent previous work (Hussain and Moodley, 2020a). These parameters are also presented in Table 7.6. As illustrated in Figures 7.7 and 7.8, a significant positive excess volume is observed for both systems. This behavior is generally expected of alcohol + alkane systems (Bravo-Sánchez et al., 2013; Itsuki et al., 1987; Moodley and Dorsamy, 2018; Wagner and Heintz, 1986) of these chain lengths as stated above and again is attributed to the declustering of self-associated alcohol multimer series by the nonpolar alkane, and the dipole-induced dipole (Debye) interaction between homomorphs of the alcohols and the alkanes on the addition of the nonpolar solvent is expected to

decluster the alcohol complexes, contributing to an expansion in the volume upon mixing as the alcohol molecules occupy more space as monomers than as multimers. The interaction energy between the alcohol homomorphs and the alkane, which includes dipole−induced dipole interactions, is expected to contribute to a positive excess volume (Rao and Naidu, 1974; Treszczanowicz and Benson, 1978). The negative V^E effects of free volume changes and interstitial rearrangement are smaller than the positive contributions. The calculated excess volumes from the pseudo-experimental data via the MTS EOS predictions were compared to those calculated by the PC-SAFT and Peng−Robinson equations of state. An example of this comparison is provided in Figure 7.9. It can be seen that a poor representation of V^E is provided by the Peng−Robinson equations of state, while the PC-SAFT model does provide a degree of qualitative prediction.

Error propagation was employed to compute the standard uncertainties in the calculated excess molar volume for the binary systems. These were found to be 1.77×10^{-5} and 1.74×10^{-5} $m^3 \cdot kmol^{-1}$ for butan-2-ol (1) + n-octane (2) and butan-2-ol (1) + n-decane (2), respectively.

Figures 7.10−7.13 illustrate the thermal expansivity and isothermal compressibility also calculated utilizing the MTS parameters. From these figures, the nonlinear behavior of both of these derived thermodynamic properties is demonstrated. It is observed, for both systems, that the thermal expansivity decreases with an increase in pressure and increases with temperature. This is illustrated in Figures 7.10 and 7.11. Similarly, the isothermal compressibility is higher at higher temperatures and lower pressures as demonstrated in Figures 7.12 and 7.13. The relative uncertainties for thermal expansivity and isothermal compressibility were calculated to be 0.035 and 0.038, respectively. In Figures 7.11 and 7.12, the thermal expansivity and isothermal compressibility for pure butan-2-ol are also compared to the literature (Dakkach et al., 2015) with reasonable correlation within the estimated uncertainties.

Table 7.3. Experimental pure component densities for butan-2-ol. ǂ

P/MPa	ρ/ kg·m^{-3}	P/MPa	ρ/ kg·m^{-3}	P/MPa	ρ/ kg·m^{-3}	P/MPa	ρ/ kg·m^{-3}	P/MPa	ρ/ kg·m^{-3}
T/K = 313.15		T/K = 323.15		T/K = 333.15		T/K= 343.15		T/K = 353.15	
0.1*	789.72	0.1	780.50	0.1	771.1	0.1	760.92	0.1	750.72
1.14	790.2	1.15	781.6	1.13	772.1	1.14	762.5	1.14	752.4
2.14	791.0	2.15	782.5	2.13	773.0	2.14	763.5	2.14	753.3
3.15	791.8	3.17	783.3	3.14	774.0	3.14	764.5	3.14	754.5
4.16	792.6	4.18	784.2	4.15	774.9	4.16	765.5	4.16	755.7
5.17	793.5	5.19	785.1	5.16	775.9	5.17	766.5	5.16	756.7
6.18	794.3	6.2	786.0	6.17	776.8	6.18	767.5	6.18	757.8
7.19	795.2	7.22	786.9	7.18	777.8	7.19	768.6	7.19	758.9
8.20	796.0	8.23	787.8	8.19	778.8	8.2	769.6	8.2	760.0
9.23	796.8	9.24	788.6	9.2	779.6	9.21	770.6	9.21	761.0
10.23	797.6	10.25	789.5	10.21	780.5	10.22	771.4	10.22	761.9
11.24	798.4	11.25	790.4	11.22	781.4	11.23	772.4	11.23	763.0
12.25	799.2	12.27	791.1	12.23	782.3	12.24	773.3	12.24	763.9
13.26	800.0	13.27	791.9	13.24	783.1	13.25	774.2	13.25	764.9
14.27	800.8	14.26	792.6	14.25	784.0	14.26	775.1	14.26	765.8
15.27	801.6	15.29	793.5	15.26	784.9	15.27	776.0	15.25	766.8
16.28	802.4	16.3	794.3	16.27	785.7	16.27	776.9	16.27	767.7
17.29	803.1	17.3	795.1	17.27	786.5	17.28	777.7	17.27	768.6
18.30	803.8	18.3	795.8	18.28	787.3	18.28	778.6	18.29	769.4
19.30	804.5	19.3	796.5	19.28	788.1	19.29	779.3	19.29	770.2
20.31	805.2	20.29	797.1	20.28	788.8	20.29	780.1	20.29	771.1

ǂ Densities above atmospheric measured by DMA HP apparatus, and the expanded combined uncertainties (k = 2) U_c are $U_c(T) = 0.02\ K$, $U_c(P) = 0.03\ MPa$, $U_c(\rho) = 1.09\ kg \cdot m^{-3}$

*At atmospheric pressures the DMA 5000 apparatus was used, and the expanded combined uncertainties (k = 2) U_c are $U_c(T) = 0.02\ K$, $U_c(P) = 0.002\ MPa$, $U_c(\rho) = 0.08\ kg \cdot m^{-3}$,

where T is the temperature in K, P is the pressure in MPa and ρ is the density in $kg \cdot m^{-3}$

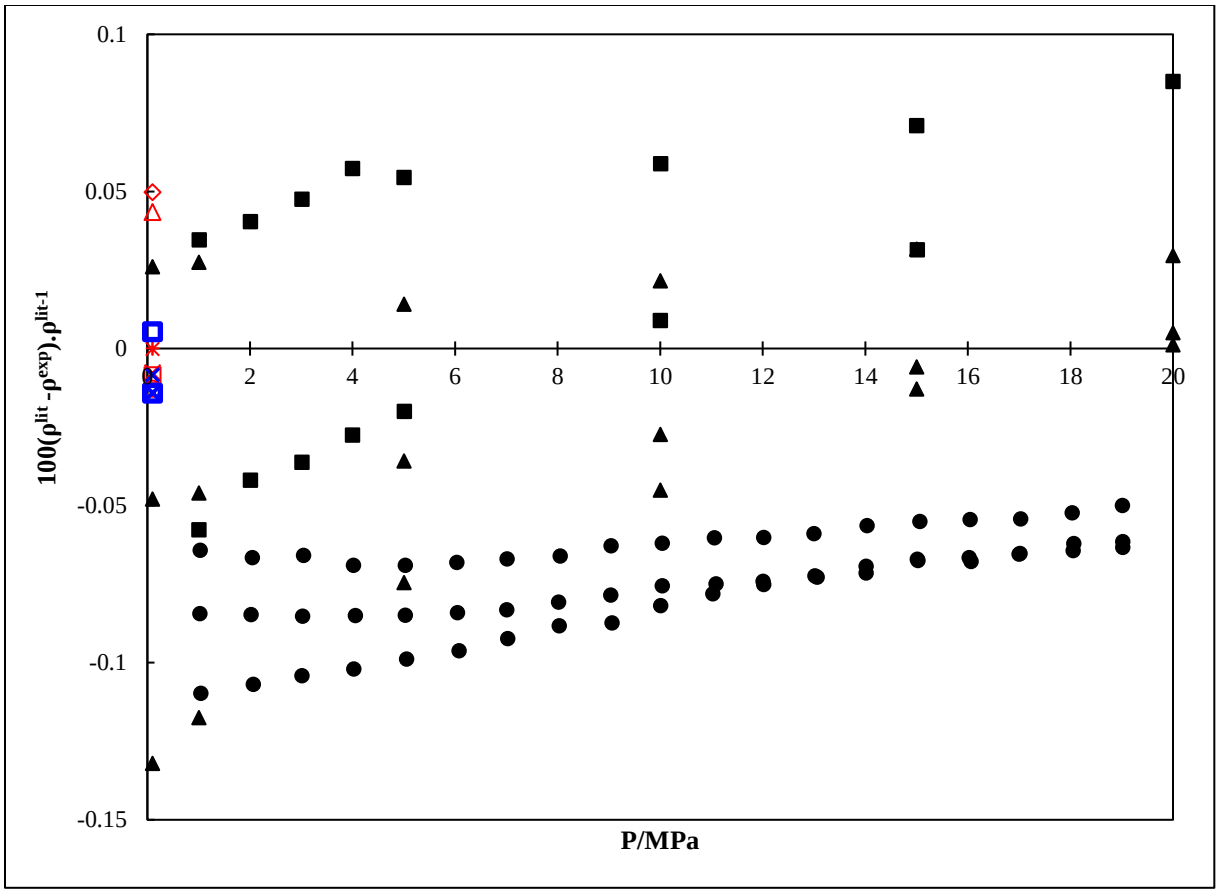

Figure 7.2. Comparison of experimental butan-2-ol density data (ρ_{exp}) at various temperatures as a function of pressure to literature (ρ_{lit}). ●- (Zúñiga-Moreno et al., 2007a), ▲- (Dakkach et al., 2015), ■- (Outcalt et al., 2010), □- (Bravo-Sánchez et al., 2010), ◊- (Awwad et al., 2008), △- (Langa et al., 2006), ×- (Radzhabova et al., 2014), *- (Živković et al., 2013), ○- (González et al., 2014), + - (Behroozi and Zarei, 2011), □- (Bravo-Sánchez et al., 2013), ×- (Faranda et al., 2004).

Table 7.4. Experimental densities for butan-2-ol (1) + n-octane (2) at various temperatures and pressures.‡

T/K	P/MPa	ρ/ kg·m^{-3}	P/MPa	ρ/ kg·m^{-3}	P/MPa	ρ/ kg·m^{-3}	P/MPa	ρ/ kg·m^{-3}	P/MPa	ρ/ kg·m^{-3}	P/MPa	ρ/ kg·m^{-3}
	x_1=0.1262		x_1=0.3742		x_1=0.5002		x_1=0.6257		x_1=0.7501		x_1=0.8747	
313.15	0.1	691.89	0.1	708.54	0.1	719.75	0.1	733.01	0.1	748.64	0.1	767.09
313.15	1.08	693.7	1.08	710.2	1.08	721.3	1.07	734.5	1.08	750.0	1.07	768.2
313.15	2.09	695.1	2.08	711.5	2.09	722.6	2.09	735.7	2.09	751.1	2.07	769.1
313.15	3.09	696.0	3.09	712.5	3.09	723.6	3.09	736.7	3.1	752.0	3.15	770.0
313.15	4.11	696.9	4.11	713.5	4.11	724.5	4.1	737.6	4.12	752.9	4.15	770.9
313.15	5.11	697.9	5.12	714.4	5.12	725.5	5.11	738.6	5.12	753.8	5.16	771.8
313.15	6.12	698.9	6.13	715.5	6.13	726.5	6.12	739.6	6.14	754.8	6.17	772.7
313.15	7.14	699.8	7.14	716.5	7.14	727.5	7.13	740.6	7.15	755.8	7.18	773.6
313.15	8.15	700.8	8.15	717.5	8.15	728.5	8.14	741.5	8.16	756.7	8.19	774.5
313.15	9.16	701.7	9.16	718.4	9.16	729.4	9.15	742.4	9.17	757.6	9.2	775.3
313.15	10.17	702.6	10.17	719.4	10.17	730.4	10.16	743.4	10.18	758.5	10.21	776.2
313.15	11.18	703.5	11.17	720.3	11.18	731.4	11.18	744.3	11.19	759.4	11.22	777.1
313.15	12.18	704.4	12.18	721.3	12.19	732.3	12.18	745.2	12.2	760.3	12.23	777.9
313.15	13.20	705.3	13.19	722.2	13.19	733.2	13.19	746.1	13.2	761.1	13.24	778.8
313.15	14.21	706.2	14.2	723.2	14.2	734.2	14.2	747.0	14.21	762.0	14.25	779.6
313.15	15.21	707.1	15.21	724.1	15.21	735.1	15.21	747.9	15.22	762.9	15.25	780.5
313.15	16.22	708.0	16.22	725.0	16.22	736.0	16.21	748.8	16.23	763.8	16.26	781.3
313.15	17.22	708.8	17.22	725.8	17.22	736.8	17.22	749.7	17.23	764.6	17.27	782.1
313.15	18.22	709.5	18.22	726.6	18.23	737.6	18.22	750.4	18.23	765.3	18.27	782.8
313.15	19.23	710.3	19.23	727.4	19.22	738.4	19.23	751.2	19.24	766.1	19.27	783.5
313.15	20.24	710.9	20.23	728.0	20.24	739.0	20.23	751.8	20.24	766.7	20.28	784.2
323.15	0.1	683.45	0.1	699.62	0.1	710.64	0.1	723.84	0.1	739.43	0.1	757.75
323.15	1.12	685.3	1.09	701.4	1.07	712.4	1.07	725.6	1.1	741.2	1.07	759.5
323.15	2.12	686.3	2.08	702.5	2.09	713.5	2.06	726.7	2.09	742.2	2.07	760.4
323.15	3.12	687.4	3.09	703.5	3.1	714.5	3.07	727.7	3.1	743.2	3.08	761.3
323.15	4.13	688.4	4.11	704.6	4.11	715.6	4.08	728.7	4.11	744.2	4.09	762.3
323.15	5.14	689.4	5.11	705.7	5.11	716.7	5.09	729.8	5.12	745.2	5.1	763.2
323.15	6.15	690.5	6.13	706.7	6.13	717.7	6.1	730.8	6.14	746.2	6.11	764.2
323.15	7.16	691.5	7.14	707.8	7.14	718.8	7.11	731.8	7.15	747.2	7.12	765.1
323.15	8.17	692.5	8.15	708.8	8.15	719.8	8.12	732.8	8.16	748.1	8.13	766.1
323.15	9.18	693.4	9.16	709.8	9.16	720.8	9.13	733.8	9.17	749.1	9.14	767.0
323.15	10.19	694.4	10.16	710.8	10.17	721.8	10.14	734.8	10.18	750.0	10.16	767.9
323.15	11.20	695.4	11.17	711.9	11.18	722.8	11.15	735.8	11.19	751.0	11.16	768.8

323.15	12.20	696.3	12.18	712.7	12.19	723.7	12.16	736.7	12.2	751.8	12.17	769.6
323.15	13.21	697.2	13.19	713.7	13.19	724.6	13.17	737.6	13.2	752.7	13.18	770.5
323.15	14.22	698.1	14.2	714.6	14.21	725.6	14.18	738.5	14.21	753.6	14.19	771.3
323.15	15.23	699.1	15.21	715.6	15.2	726.5	15.18	739.4	15.22	754.5	15.19	772.2
323.15	16.24	700.0	16.21	716.5	16.22	727.5	16.19	740.4	16.22	755.4	16.2	773.1
323.15	17.24	700.8	17.22	717.4	17.22	728.3	17.19	741.2	17.23	756.2	17.21	773.8
323.15	18.25	701.6	18.23	718.2	18.23	729.1	18.2	742.0	18.24	757.0	18.22	774.6
323.15	19.25	702.3	19.23	719.0	19.23	729.9	19.21	742.7	19.24	757.7	19.22	775.3
323.15	20.26	703.0	20.23	719.7	20.24	730.6	20.21	743.5	20.24	758.4	20.22	776.0
333.15	0.1	674.96	0.1	690.55	0.1	701.41	0.1	714.53	0.1	730.06	0.1	748.21
333.15	1.12	676.9	1.08	692.3	1.08	703.2	1.06	716.4	1.1	731.9	1.07	750.0
333.15	2.12	678.0	2.1	693.5	2.09	704.4	2.06	717.5	2.1	732.9	2.07	751.0
333.15	3.13	679.1	3.1	694.7	3.09	705.5	3.07	718.6	3.11	734.0	3.08	752.1
333.15	4.15	680.2	4.12	695.8	4.1	706.6	4.08	719.7	4.12	735.0	4.1	753.0
333.15	5.15	681.3	5.12	697.0	5.11	707.8	5.09	720.8	5.13	736.1	5.1	754.1
333.15	6.16	682.3	6.13	698.0	6.13	708.8	6.1	721.8	6.13	737.1	6.11	755.1
333.15	7.17	683.4	7.15	699.1	7.13	709.9	7.12	722.9	7.15	738.2	7.12	756.1
333.15	8.18	684.9	8.15	700.6	8.15	711.4	8.13	724.3	8.16	739.5	8.14	757.3
333.15	9.20	685.5	9.16	701.3	9.15	712.1	9.14	725.0	9.17	740.2	9.15	758.0
333.15	10.20	686.6	10.17	702.3	10.17	713.2	10.14	726.1	10.18	741.2	10.15	759.0
333.15	11.21	687.6	11.18	703.4	11.18	714.2	11.15	727.1	11.19	742.2	11.17	759.9
333.15	12.22	688.5	12.2	704.4	12.18	715.2	12.16	728.0	12.2	743.2	12.17	760.8
333.15	13.22	689.5	13.2	705.3	13.19	716.1	13.17	729.0	13.21	744.1	13.18	761.7
333.15	14.23	690.4	14.21	706.3	14.2	717.1	14.18	729.9	14.21	745.0	14.19	762.6
333.15	15.24	691.4	15.22	707.3	15.2	718.1	15.19	730.9	15.22	746.0	15.2	763.6
333.15	16.24	692.2	16.22	708.2	16.21	719.0	16.19	731.8	16.23	746.8	16.2	764.4
333.15	17.26	693.1	17.23	709.1	17.22	719.9	17.2	732.7	17.23	747.7	17.21	765.2
333.15	18.26	694.0	18.24	710.0	18.22	720.8	18.2	733.6	18.24	748.5	18.21	766.1
333.15	19.26	694.9	19.24	710.9	19.23	721.7	19.21	734.5	19.24	749.4	19.22	766.9
333.15	20.27	695.5	20.25	711.7	20.24	722.4	20.21	735.2	20.25	750.1	20.22	767.6
343.15	0.1	665.46	0.1	680.43	0.1	691.15	0.1	704.21	0.1	719.65	0.1	738.13
343.15	1.11	667.6	1.1	682.6	1.09	693.4	1.07	706.5	1.1	722.0	1.08	740.3
343.15	2.12	668.8	2.09	683.8	2.09	694.6	2.06	707.7	2.1	723.2	2.07	741.4
343.15	3.13	669.9	3.1	685.0	3.09	695.7	3.07	708.8	3.1	724.3	3.08	742.4
343.15	4.14	671.0	4.11	686.1	4.11	696.9	4.08	709.9	4.11	725.4	4.1	743.5
343.15	5.15	672.1	5.12	687.3	5.11	698.0	5.09	711.1	5.12	726.5	5.1	744.5
343.15	6.16	673.3	6.13	688.4	6.13	699.2	6.1	712.2	6.13	727.6	6.11	745.6
343.15	7.17	674.5	7.15	689.7	7.14	700.4	7.11	713.4	7.15	728.8	7.12	746.7
343.15	8.18	675.6	8.15	690.8	8.15	701.5	8.12	714.5	8.16	729.8	8.13	747.7
343.15	9.19	676.7	9.16	691.9	9.15	702.6	9.13	715.6	9.17	730.9	9.14	748.8
343.15	10.20	677.6	10.17	692.9	10.16	703.6	10.14	716.6	10.18	731.8	10.15	749.7

343.15	11.21	678.8	11.18	694.1	11.18	704.8	11.15	717.7	11.19	732.9	11.17	750.8
343.15	12.22	679.7	12.19	695.0	12.19	705.8	12.16	718.7	12.2	733.9	12.17	751.7
343.15	13.23	680.8	13.2	696.1	13.19	706.8	13.17	719.7	13.2	734.9	13.18	752.7
343.15	14.24	681.8	14.21	697.1	14.2	707.8	14.17	720.7	14.21	735.9	14.19	753.6
343.15	15.25	682.7	15.21	698.1	15.2	708.8	15.19	721.7	15.22	736.8	15.19	754.5
343.15	16.26	683.6	16.22	699.1	16.21	709.8	16.19	722.6	16.23	737.7	16.2	755.4
343.15	17.26	684.6	17.23	700.1	17.22	710.8	17.19	723.6	17.23	738.7	17.21	756.3
343.15	18.27	685.5	18.24	701.0	18.22	711.7	18.2	724.5	18.23	739.6	18.22	757.2
343.15	19.27	686.3	19.24	701.9	19.23	712.5	19.21	725.3	19.24	740.4	19.22	758.0
343.15	20.28	687.1	20.25	702.6	20.24	713.3	20.21	726.1	20.25	741.2	20.23	758.7
353.15	0.1	656.08	0.1	670.39	0.1	680.99	0.1	693.97	0.1	709.57	0.1	727.72
353.15	1.07	658.9	1.1	673.1	1.08	683.7	1.07	696.7	1.09	712.2	1.08	730.2
353.15	2.08	659.9	2.09	674.1	2.09	684.7	2.06	697.7	2.09	713.2	2.09	731.2
353.15	3.09	661.3	3.1	675.6	3.1	686.2	3.07	699.1	3.1	714.5	3.09	732.5
353.15	4.11	662.7	4.11	676.9	4.11	687.5	4.08	700.4	4.11	715.8	4.1	733.7
353.15	5.11	663.8	5.12	678.1	5.11	688.7	5.09	701.6	5.12	716.9	5.11	734.8
353.15	6.12	665.0	6.13	679.4	6.13	689.9	6.1	702.8	6.13	718.1	6.12	736.0
353.15	7.13	666.2	7.14	680.5	7.14	691.0	7.11	703.9	7.14	719.2	7.13	737.1
353.15	8.14	667.4	8.15	681.8	8.14	692.3	8.12	705.1	8.15	720.4	8.15	738.2
353.15	9.15	668.5	9.16	682.9	9.16	693.4	9.14	706.3	9.16	721.5	9.16	739.3
353.15	10.16	669.5	10.17	684.0	10.17	694.5	10.14	707.3	10.17	722.5	10.16	740.3
353.15	11.17	670.7	11.18	685.1	11.18	695.6	11.15	708.4	11.19	723.6	11.17	741.3
353.15	12.18	671.7	12.19	686.2	12.19	696.7	12.16	709.5	12.19	724.6	12.17	742.3
353.15	13.19	672.8	13.2	687.3	13.2	697.8	13.17	710.5	13.2	725.7	13.18	743.3
353.15	14.20	673.7	14.21	688.3	14.2	698.8	14.17	711.5	14.21	726.6	14.19	744.3
353.15	15.20	674.8	15.21	689.4	15.21	699.8	15.18	712.6	15.22	727.7	15.2	745.3
353.15	16.21	675.8	16.22	690.4	16.22	700.9	16.19	713.6	16.21	728.7	16.2	746.3
353.15	17.22	676.8	17.22	691.4	17.22	701.9	17.2	714.6	17.23	729.6	17.21	747.2
353.15	18.22	677.6	18.23	692.3	18.23	702.7	18.2	715.5	18.23	730.5	18.22	748.1
353.15	19.23	678.5	19.24	693.1	19.23	703.6	19.2	716.3	19.23	731.3	19.22	748.9
353.15	20.23	679.4	20.24	694.1	20.24	704.5	20.21	717.2	20.24	732.2	20.22	749.8

[‡] Densities above atmospheric measured by DMA HP apparatus, and the expanded combined uncertainties ($k = 2$) U_c are $U_c(T) = 0.02\ K$, $U_c(P) = 0.03\ MPa$, $U_c(x_i) = 0.0002, U_c(\rho) = 1.11\ kg \cdot m^{-3}$

[*] At atmospheric pressures the DMA 5000 apparatus was used and the expanded combined uncertainties ($k = 2$) U_c are $U_c(P) = 0.002\ MPa$, $U_c(T) = 0.02\ K$, $U_c(x_i) = 0.0002$, $U_c(\rho) = 0.09\ kg \cdot m^{-3}$

where T is the temperature in K, P is the pressure in MPa and ρ is the density in $kg \cdot m^{-3}$

Table 7.5. Experimental densities for butan-2-ol (1) + n-decane (2) at various temperatures and pressures.[ǂ]

T/K	P/MPa	ρ/ kg·m^{-3}	P/MPa	ρ/ kg·m^{-3}	P/MPa	ρ/ kg·m^{-3}	P/MPa	ρ/ kg·m^{-3}	P/MPa	ρ/ kg·m^{-3}	P/MPa	ρ/ kg·m^{-3}
	x_1=0.1254		x_1=0.3754		x_1=0.5055		x_1=0.6240		x_1=0.7519		x_1=0.8740	
313.15	0.1*	717.47	0.1	727.08	0.1	733.98	0.1	742.24	0.1	754.44	0.1	769.73
313.15	1.14	718.8	1.13	728.7	1.12	735.8	1.13	744.1	1.13	756.1	1.15	771.0
313.15	2.13	719.6	2.13	729.6	2.13	736.7	2.14	745.0	2.13	757.0	2.15	771.8
313.15	3.14	720.4	3.14	730.5	3.14	737.7	3.15	745.9	3.14	757.9	3.15	772.7
313.15	4.15	721.3	4.15	731.4	4.15	738.6	4.16	746.9	4.15	758.8	4.16	773.5
313.15	5.16	722.1	5.15	732.3	5.16	739.5	5.18	747.8	5.16	759.7	5.17	774.4
313.15	6.17	723.0	6.16	733.2	6.17	740.5	6.18	748.8	6.17	760.7	6.19	775.3
313.15	7.18	723.8	7.18	734.2	7.18	741.4	7.19	749.7	7.18	761.6	7.19	776.2
313.15	8.19	724.7	8.19	735.1	8.19	742.3	8.2	750.7	8.19	762.5	8.21	777.1
313.15	9.20	725.5	9.19	735.9	9.2	743.2	9.21	751.6	9.2	763.4	9.22	777.9
313.15	10.21	726.4	10.21	736.8	10.2	744.2	10.22	752.5	10.21	764.3	10.22	778.8
313.15	11.22	727.2	11.22	737.7	11.22	745.1	11.23	753.4	11.22	765.2	11.23	779.7
313.15	12.23	728.0	12.22	738.6	12.23	746.0	12.24	754.3	12.23	766.1	12.24	780.5
313.15	13.24	728.8	13.23	739.4	13.24	746.8	13.25	755.2	13.24	767.0	13.25	781.3
313.15	14.25	729.7	14.24	740.3	14.24	747.7	14.26	756.1	14.25	767.9	14.26	782.2
313.15	15.25	730.5	15.25	741.2	15.25	748.6	15.27	757.0	15.25	768.7	15.27	783.0
313.15	16.26	731.3	16.26	742.0	16.25	749.4	16.27	757.8	16.25	769.6	16.27	783.8
313.15	17.27	732.0	17.26	742.8	17.26	750.3	17.27	758.7	17.26	770.4	17.28	784.6
313.15	18.27	732.7	18.27	743.5	18.27	751.0	18.28	759.4	18.27	771.1	18.28	785.3
313.15	19.28	733.4	19.27	744.3	19.27	751.8	19.29	760.2	19.27	771.8	19.29	786.0
313.15	20.28	734.0	20.27	744.9	20.28	752.4	20.29	760.9	20.28	772.5	20.29	786.7
323.15	0.1	709.54	0.1	718.48	0.1	725.10	0.1	733.25	0.1	745.23	0.1	760.50
323.15	1.13	711.1	1.12	720.4	1.12	727.3	1.13	735.3	1.13	747.2	1.14	762.2
323.15	2.12	712.0	2.13	721.4	2.12	728.3	2.14	736.3	2.12	748.2	2.14	763.1
323.15	3.13	712.9	3.14	722.4	3.13	729.3	3.15	737.3	3.13	749.2	3.15	764.0
323.15	4.14	713.8	4.15	723.3	4.14	730.2	4.16	738.3	4.14	750.2	4.17	765.0
323.15	5.15	714.7	5.16	724.3	5.15	731.2	5.17	739.3	5.15	751.2	5.18	765.9
323.15	6.16	715.7	6.17	725.3	6.16	732.2	6.18	740.3	6.16	752.2	6.18	766.9
323.15	7.17	716.6	7.18	726.3	7.17	733.2	7.2	741.3	7.17	753.1	7.19	767.8
323.15	8.18	717.5	8.19	727.2	8.18	734.2	8.2	742.3	8.18	754.1	8.2	768.7
323.15	9.19	718.4	9.2	728.2	9.19	735.2	9.22	743.3	9.2	755.0	9.21	769.6
323.15	10.20	719.2	10.21	729.1	10.2	736.1	10.23	744.2	10.2	756.0	10.23	770.5
323.15	11.21	720.2	11.22	730.1	11.21	737.1	11.24	745.2	11.22	757.0	11.24	771.5
323.15	12.22	720.9	12.23	730.9	12.22	737.9	12.24	746.1	12.23	757.8	12.25	772.3
323.15	13.23	721.8	13.24	731.8	13.23	738.9	13.25	747.0	13.23	758.7	13.25	773.1

323.15	14.24	722.6	14.24	732.7	14.24	739.8	14.26	747.9	14.24	759.6	14.26	774.0
323.15	15.24	723.4	15.25	733.5	15.24	740.6	15.27	748.8	15.25	760.4	15.27	774.8
323.15	16.26	724.3	16.25	734.4	16.25	741.5	16.27	749.7	16.25	761.4	16.27	775.7
323.15	17.26	725.0	17.26	735.2	17.26	742.3	17.28	750.5	17.26	762.2	17.28	776.5
323.15	18.26	725.7	18.27	735.9	18.26	743.1	18.28	751.3	18.26	762.9	18.29	777.2
323.15	19.27	726.4	19.27	736.7	19.26	743.8	19.29	752.0	19.27	763.7	19.29	777.9
323.15	20.27	727.1	20.28	737.4	20.27	744.6	20.29	752.8	20.27	764.4	20.3	778.6
333.15	0.1	701.19	0.1	709.64	0.1	715.91	0.1	723.70	0.1	735.80	0.1	751.29
333.15	1.13	703.2	1.11	711.9	1.12	718.4	1.13	726.2	1.12	738.0	1.12	752.9
333.15	2.12	704.2	2.12	712.9	2.12	719.4	2.14	727.2	2.12	739.0	2.11	753.9
333.15	3.13	705.2	3.15	714.0	3.12	720.5	3.15	728.3	3.13	740.1	3.13	755.0
333.15	4.14	706.1	4.14	715.0	4.13	721.5	4.16	729.3	4.14	741.1	4.13	755.9
333.15	5.15	707.1	5.15	716.0	5.14	722.6	5.17	730.4	5.15	742.2	5.14	756.9
333.15	6.16	708.0	6.17	717.0	6.15	723.6	6.19	731.4	6.16	743.2	6.15	757.9
333.15	7.17	709.0	7.18	718.0	7.16	724.6	7.2	732.4	7.17	744.2	7.16	758.9
333.15	8.18	710.1	8.19	719.2	8.17	725.8	8.21	733.6	8.18	745.3	8.18	760.0
333.15	9.19	710.9	9.2	719.9	9.18	726.6	9.22	734.5	9.19	746.2	9.19	760.8
333.15	10.20	711.8	10.21	720.9	10.19	727.6	10.22	735.5	10.19	747.2	10.2	761.8
333.15	11.22	712.7	11.21	721.9	11.2	728.6	11.23	736.4	11.2	748.1	11.21	762.7
333.15	12.23	713.6	12.23	722.8	12.21	729.5	12.25	737.4	12.22	749.1	12.21	763.6
333.15	13.23	714.4	13.24	723.7	13.22	730.4	13.25	738.3	13.22	750.0	13.22	764.5
333.15	14.24	715.3	14.24	724.6	14.23	731.3	14.26	739.3	14.23	750.9	14.23	765.3
333.15	15.25	716.2	15.25	725.5	15.24	732.3	15.27	740.2	15.24	751.8	15.23	766.3
333.15	16.25	717.0	16.25	726.4	16.24	733.2	16.27	741.1	16.24	752.7	16.25	767.1
333.15	17.26	717.7	17.26	727.2	17.25	734.0	17.27	741.9	17.25	753.5	17.25	767.9
333.15	18.26	718.5	18.27	728.0	18.25	734.9	18.28	742.8	18.26	754.4	18.25	768.7
333.15	19.27	719.2	19.27	728.8	19.26	735.7	19.3	743.6	19.27	755.2	19.26	769.5
333.15	20.27	719.9	20.28	729.6	20.26	736.4	20.3	744.4	20.27	756.0	20.26	770.3
343.15	0.1	693.04	0.1	700.56	0.1	706.53	0.1	714.01	0.1	725.91	0.1	741.34
343.15	1.13	695.3	1.13	703.1	1.11	709.2	1.14	716.7	1.12	728.4	1.11	743.4
343.15	2.12	696.4	2.12	704.2	2.1	710.3	2.14	717.8	2.13	729.5	2.11	744.5
343.15	3.13	697.4	3.13	705.3	3.12	711.4	3.15	718.9	3.14	730.6	3.12	745.5
343.15	4.14	698.3	4.14	706.3	4.13	712.5	4.16	720.0	4.14	731.7	4.13	746.6
343.15	5.15	699.2	5.15	707.3	5.14	713.4	5.17	721.0	5.15	732.7	5.14	747.6
343.15	6.16	700.2	6.16	708.3	6.15	714.5	6.18	722.1	6.15	733.8	6.15	748.6
343.15	7.17	701.3	7.17	709.5	7.16	715.7	7.19	723.2	7.17	734.9	7.17	749.7
343.15	8.18	702.3	8.18	710.5	8.17	716.7	8.2	724.3	8.18	735.9	8.17	750.7
343.15	9.19	703.3	9.19	711.5	9.17	717.8	9.21	725.3	9.19	737.0	9.19	751.7
343.15	10.20	704.2	10.2	712.5	10.19	718.7	10.22	726.3	10.2	737.9	10.2	752.6
343.15	11.21	705.2	11.21	713.5	11.2	719.8	11.23	727.4	11.24	739.0	11.2	753.7
343.15	12.22	706.0	12.22	714.4	12.2	720.7	12.24	728.3	12.23	739.9	12.21	754.6

343.15	13.23	707.0	13.23	715.4	13.22	721.7	13.25	729.3	13.24	740.9	13.22	755.6
343.15	14.24	707.9	14.23	716.3	14.24	722.7	14.26	730.3	14.24	741.9	14.23	756.5
343.15	15.24	708.7	15.24	717.3	15.23	723.6	15.27	731.3	15.25	742.8	15.24	757.4
343.15	16.25	709.6	16.25	718.1	16.24	724.5	16.27	732.2	16.26	743.7	16.24	758.3
343.15	17.26	710.4	17.25	719.0	17.25	725.4	17.28	733.1	17.27	744.6	17.25	759.2
343.15	18.26	711.2	18.26	719.9	18.25	726.3	18.29	734.0	18.27	745.5	18.26	760.0
343.15	19.27	711.9	19.27	720.7	19.25	727.1	19.29	734.8	19.28	746.3	19.26	760.8
343.15	20.27	712.7	20.27	721.4	20.26	727.9	20.29	735.6	20.28	747.1	20.26	761.6
353.15	0.1	684.78	0.1	691.28	0.1	696.78	0.1	703.87	0.1	715.70	0.1	731.08
353.15	1.13	687.1	1.12	693.9	1.11	699.5	1.11	706.6	1.12	718.3	1.11	733.3
353.15	2.12	688.0	2.12	694.9	2.11	700.5	2.12	707.7	2.14	719.3	2.12	734.3
353.15	3.13	689.2	3.13	696.2	3.12	701.8	3.13	709.0	3.13	720.6	3.13	735.6
353.15	4.14	690.3	4.14	697.3	4.13	703.0	4.14	710.1	4.14	721.8	4.14	736.7
353.15	5.15	691.4	5.15	698.4	5.14	704.1	5.17	711.3	5.15	722.9	5.15	737.8
353.15	6.16	692.5	6.16	699.5	6.15	705.2	6.18	712.4	6.16	724.0	6.16	738.9
353.15	7.17	693.5	7.17	700.6	7.17	706.3	7.19	713.5	7.17	725.1	7.17	740.0
353.15	8.18	694.6	8.18	701.7	8.17	707.5	8.2	714.7	8.18	726.3	8.18	741.1
353.15	9.19	695.6	9.19	702.8	9.18	708.6	9.21	715.8	9.19	727.3	9.19	742.2
353.15	10.20	696.5	10.2	703.8	10.19	709.6	10.22	716.8	10.21	728.3	10.2	743.2
353.15	11.21	697.5	11.21	704.8	11.2	710.6	11.23	717.9	11.22	729.4	11.21	744.2
353.15	12.22	698.5	12.22	705.8	12.21	711.6	12.24	718.9	12.22	730.4	12.22	745.2
353.15	13.23	699.4	13.23	706.8	13.22	712.6	13.25	719.9	13.23	731.4	13.23	746.2
353.15	14.23	700.3	14.24	707.7	14.23	713.6	14.26	720.9	14.24	732.4	14.23	747.1
353.15	15.25	701.2	15.25	708.7	15.24	714.6	15.27	721.9	15.24	733.4	15.24	748.1
353.15	16.25	702.2	16.25	709.7	16.25	715.6	16.27	722.9	16.25	734.4	16.25	749.0
353.15	17.26	703.0	17.25	710.6	17.25	716.5	17.28	723.8	17.25	735.3	17.25	750.0
353.15	18.27	703.8	18.26	711.4	18.25	717.4	18.29	724.7	18.26	736.2	18.26	750.8
353.15	19.27	704.6	19.27	712.3	19.26	718.2	19.28	725.5	19.27	737.0	19.27	751.6
353.15	20.28	705.4	20.27	713.1	20.27	719.1	20.29	726.4	20.27	737.9	20.26	752.5

[‡] Densities above atmospheric measured by DMA HP apparatus, and the expanded combined uncertainties ($k = 2$) U_c are $U_c(T) = 0.02\ K$, $U_c(P) = 0.03\ MPa$, $U_c(x_i) = 0.0002, U_c(\rho) = 1.11\ kg \cdot m^{-3}$

[*] At atmospheric pressures the DMA 5000 apparatus was used and the expanded combined uncertainties ($k = 2$) U_c are $U_c(P) = 0.002\ MPa$, $U_c(T) = 0.02\ K$, $U_c(x_i) = 0.0002$, $U_c(\rho) = 0.09\ kg \cdot m^{-3}$

where T is the temperature in K, P is the pressure in MPa and ρ is the density in $kg \cdot m^{-3}$

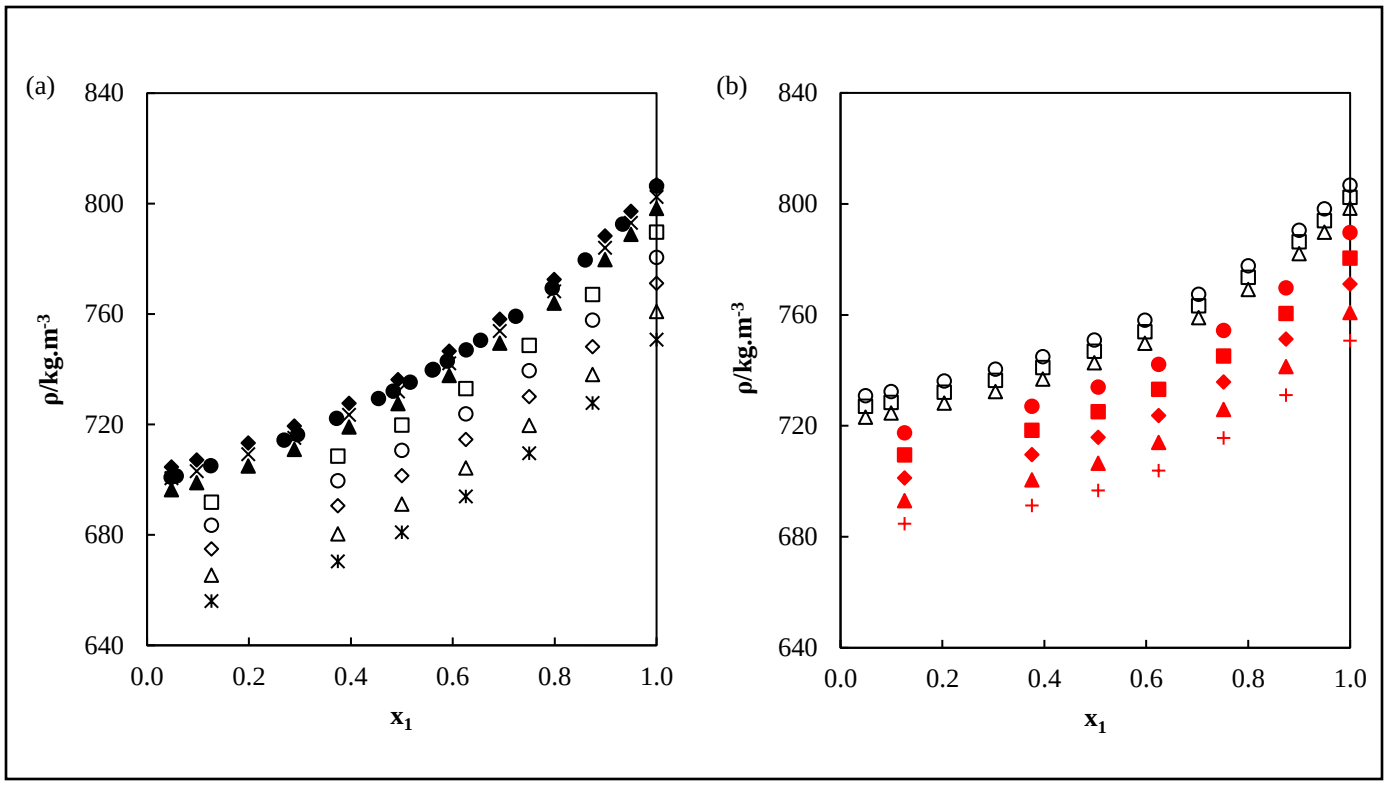

Figure 7.3. (a) Density data (ρ) for the butan-2-ol (1) + n-octane (2) system at 0.1 MPa. This work (□-313.15 K, ○-323.15 K, ◊-333.15 K, Δ-343.15 K, *-353.15 K). (Chaudhari and Katti, 1985), (●-298.14 K), (González *et al.*, 2004) (♦-293.15 K, ×-298.15 K, ▲-303.15 K). (b) butan-2-ol (1) + n-decane (2) system at 0.1 MPa. This work (●-313.15 K, ■-323.15 K, ♦-333.15 K, ▲-343.15 K, +-353.15 K). (González *et al.*, 2004) (○-293.15 K, □-298.15 K, Δ-303.15 K).

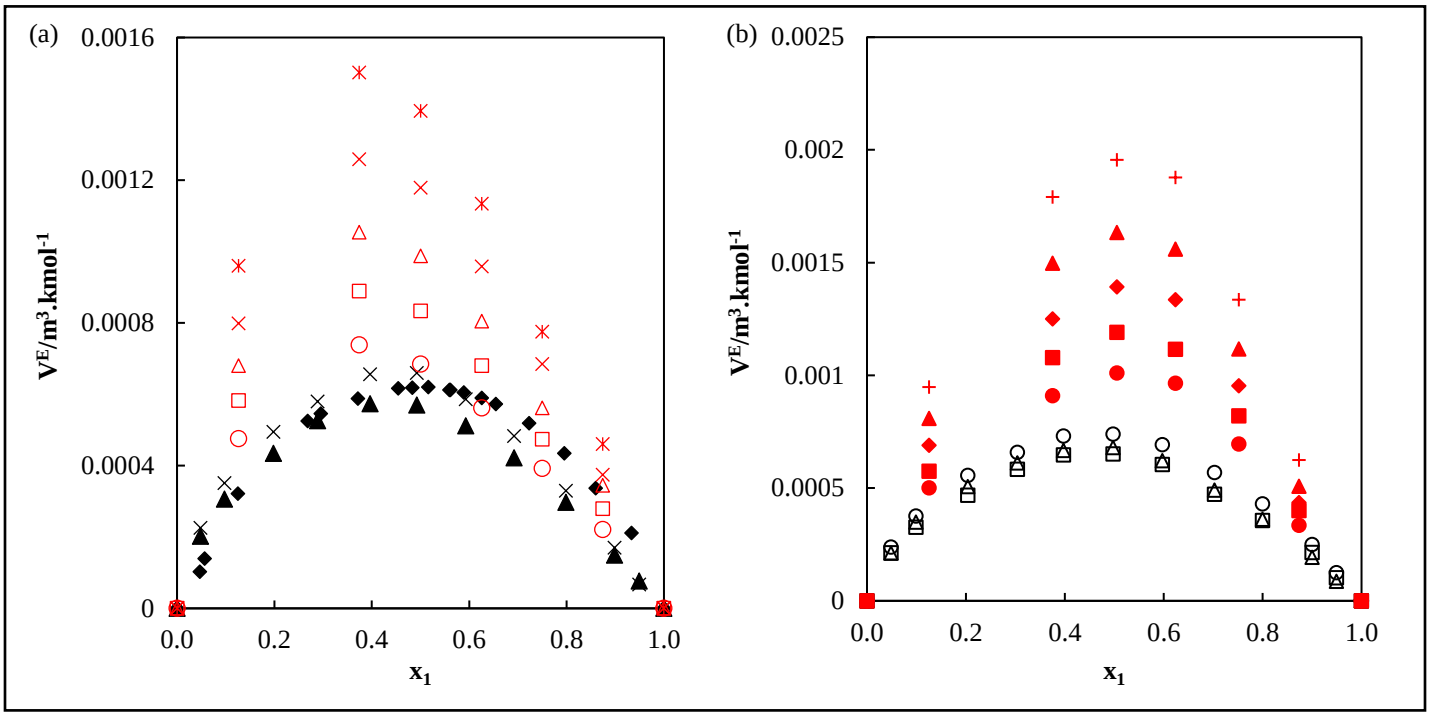

Figure 7.4. Excess volume (V^E) vs. x_1 at various temperatures and at 0.1 MPa. (a) butan-2-ol (1) + n-octane (2) system. This work (○-313.15 K, □-323.15 K, Δ-333.15 K, ×-343.15 K, *-353.15 K). (González *et al.*, 2004) (▲- 298.15 K, ×-303.15 K). (Chaudhari and Katti, 1985) (♦-298.14 K). (b) butan-2-ol (1) + n-decane (2) system. This work (●-313.15 K, ■-323.15 K, ♦-333.15 K, ▲-343.15 K, +-353.15 K). (González *et al.*, 2004) (□-293.15 K, Δ-298.15 K, ○-303.15 K).

Table 7.6. Regressed parameters for the Modified Toscani-Szwarc (*MTS*) equation of state.

x_1	c_1/MPa·m^3·kg^{-1}	c_2/m^3·kg^{-1}	c_3/MPa	c_4/K·MPa	c_5/K$^{1/3}$·MPa	*RMSD*[a]
n-octane (1)(Hussain, 2019)						
1	0.1684	1.218E-03	-234.093	34305.804	-3119.462	4.094E-04
n-decane (1)(Hussain, 2019)						
1	0.1827	1.178E-03	-236.870	38103.225	-3321.140	2.702E-04
butan-2-ol (1)						
1	0.1788	1.067E-03	-509.614	79446.688	-6141.756	1.606E-04
butan-2-ol (1) + n-octane (2)						
0.1262	0.1832	1.177E-03	-318.222	46557.484	-4032.607	4.72E-04
0.3742	0.1964	1.123E-03	-453.874	67343.402	-5488.869	4.26E-04
0.5002	0.1975	1.106E-03	-488.026	72934.118	-5862.132	4.09E-04
0.6257	0.1948	1.096E-03	-502.649	75786.344	-6027.431	3.94E-04
0.7501	0.1899	1.088E-03	-499.483	75968.205	-6005.375	3.57E-04
0.8747	0.1845	1.078E-03	-516.012	79496.630	-6189.225	3.14E-04
butan-2-ol (1) + n-decane (2)						
0.1254	0.1954	1.148E-03	-341.627	53814.816	-4439.448	3.37E-04
0.3754	0.2115	1.099E-03	-501.851	77771.083	-6139.300	4.14E-04
0.5055	0.2172	1.076E-03	-583.159	89999.867	-6995.527	4.53E-04
0.6240	0.2194	1.059E-03	-630.393	97022.077	-7491.649	4.39E-04
0.7519	0.2093	1.059E-03	-610.010	94097.068	-7256.039	3.87E-04
0.8740	0.1951	1.065E-03	-549.137	85138.239	-6595.231	2.74E-04

[a] $RMSD = \frac{(\sum_k^L (\frac{\rho_k^{exp} - \rho_k^{calc}}{\rho_k^{exp}})^2)^{1/2}}{L^{1/2}}$

c_i are fitting parameters for equation (7.1)

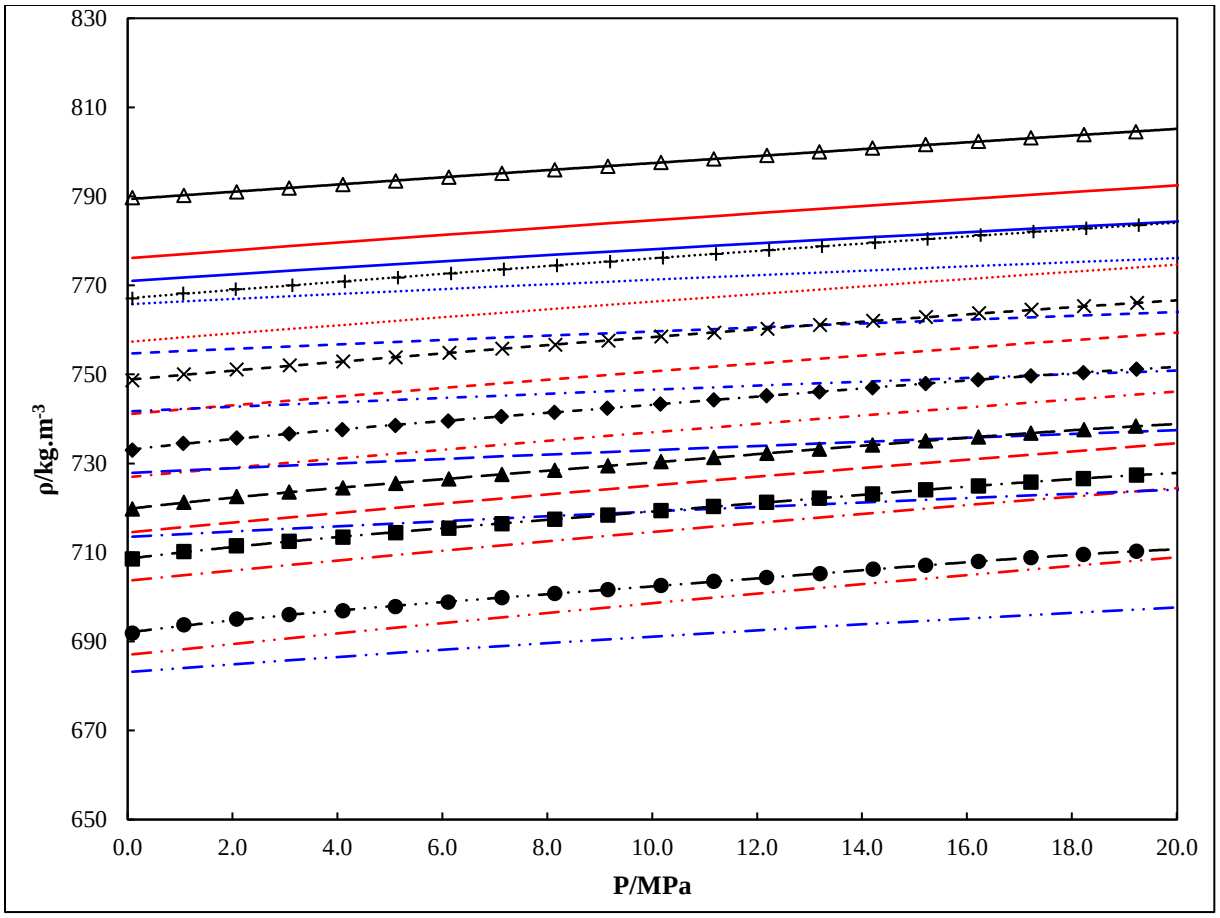

Figure 7.5. Experimental and model calculated mixture density data (ρ) for the butan-2-ol (1) + n-octane (2) system as a function of pressure (P) at 313.15 K and various compositions. (exp, model) x_1: (●, —··—)- x_1 = 0.1262, (■, —·—)- x_1 = 0.3742, (▲, -···-)- x_1 = 0.5002, (♦, -·-)- x_1 = 0.6257, (×, - - -)- x_1 = 0.7501, (+, ·····)- x_1 = 0.8747, (Δ, ─)- x_1 = 1. Black lines-Modified Toscani-Szwarc EOS (Zúñiga-Moreno and Galicia-Luna, 2002), Blue lines-Peng-Robinson (Peng and Robinson, 1976) correlation (k_{ij} = -0.534), Red lines-PC-SAFT prediction (Gross and Sadowski, 2002, 2001).

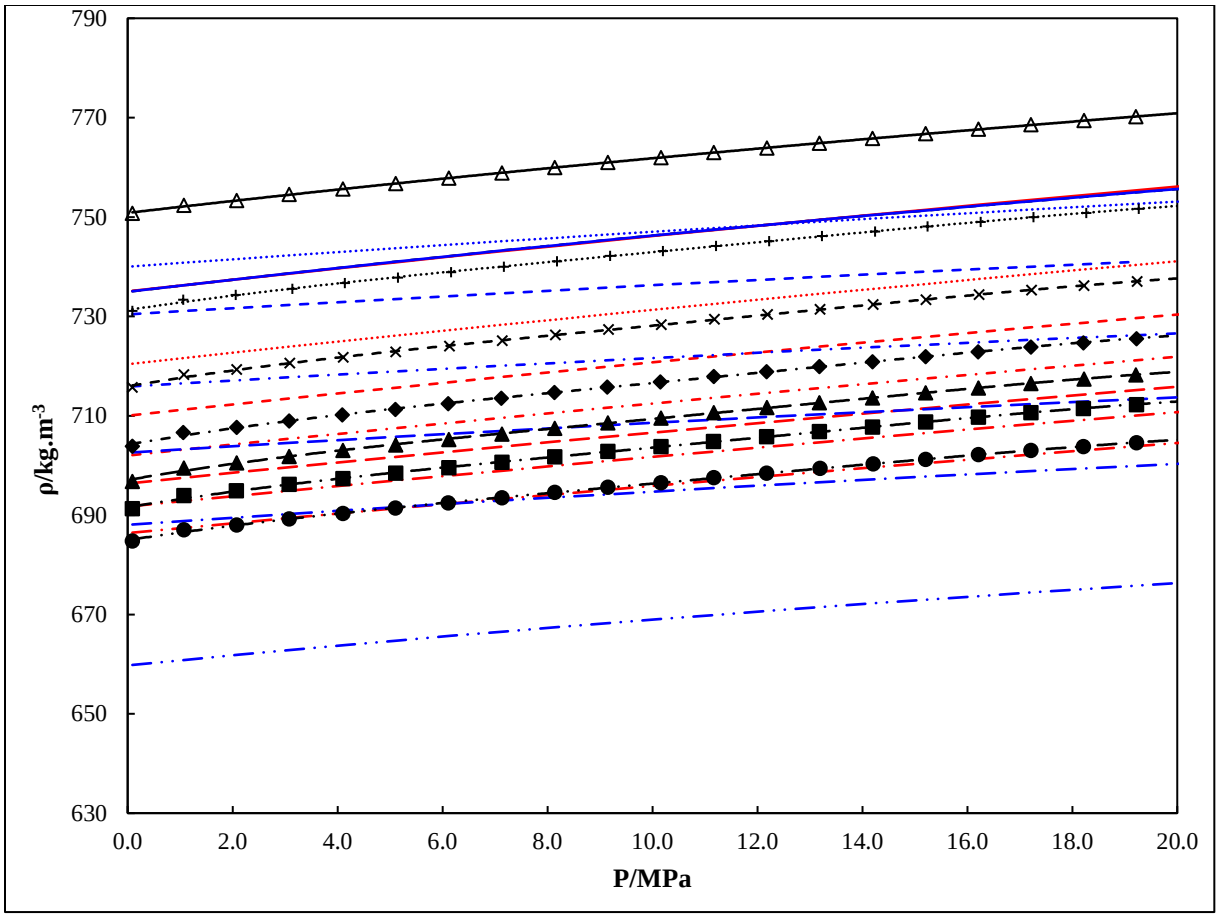

Figure 7.6. Experimental and model calculated mixture density data (ρ) for the butan-2-ol (1) + n-decane (2) system as a function of pressure (P) at 353.15 K and various compositions. (exp, model) x_1: (●, —··—)- x_1 = 0.1254, (■, —·—)- x_1 = 0.3754, (▲, -···-)- x_1 = 0.5055, (♦, -·-)- x_1 = 0.6240, (×, - - -)- x_1 = 0.7519, (+, ·····)- x_1 = 0.8740, (Δ, —)- x_1 = 1. Black lines-Modified Toscani-Szwarc EOS (Zúñiga-Moreno and Galicia-Luna, 2002), Blue lines-Peng-Robinson (Peng and Robinson, 1976) correlation (k_{ij} = -0.698), Red lines-PC-SAFT prediction (Gross and Sadowski, 2002, 2001).

Table 7.7. Pure component parameters used for Peng-Robinson Equation and PC-SAFT model.

Component	T_c/K (Poling et al., 2001)	P_c/kPa (Poling et al., 2001)	Ω (Poling et al., 2001)	m	σ/Å	$\frac{\epsilon}{k}$/K	κ^{AB}	$\frac{\epsilon^{AB}}{k}$ /k
butan-2-ol	536.05	4179	0.574	3.4400 (Zarei and Feyzi, 2013)	3.3130 (Zarei and Feyzi, 2013)	224.20 (Zarei and Feyzi, 2013)	0.0104 (Zarei and Feyzi, 2013)	2067.63 (Zarei and Feyzi, 2013)
n-octane	568.7	2490	0.399	5.0291 (Burgess et al., 2012)	3.5167 (Burgess et al., 2012)	229.30 (Burgess et al., 2012)	-	-
n-decane	617.7	2110	0.490	6.9000 (Burgess et al., 2012)	3.3665 (Burgess et al., 2012)	226.86 (Burgess et al., 2012)	-	-

T_c and P_c are the critical temperature and pressure, ω is the acentric factor. m is the number of segments per chain, σ is the segment diameter, $\frac{\epsilon}{k}$ is the depth of pair potential over the Boltzman constant, κ^{AB} is the effective association volume, $\frac{\epsilon^{AB}}{k}$ is the association energy, in the PC-SAFT model.

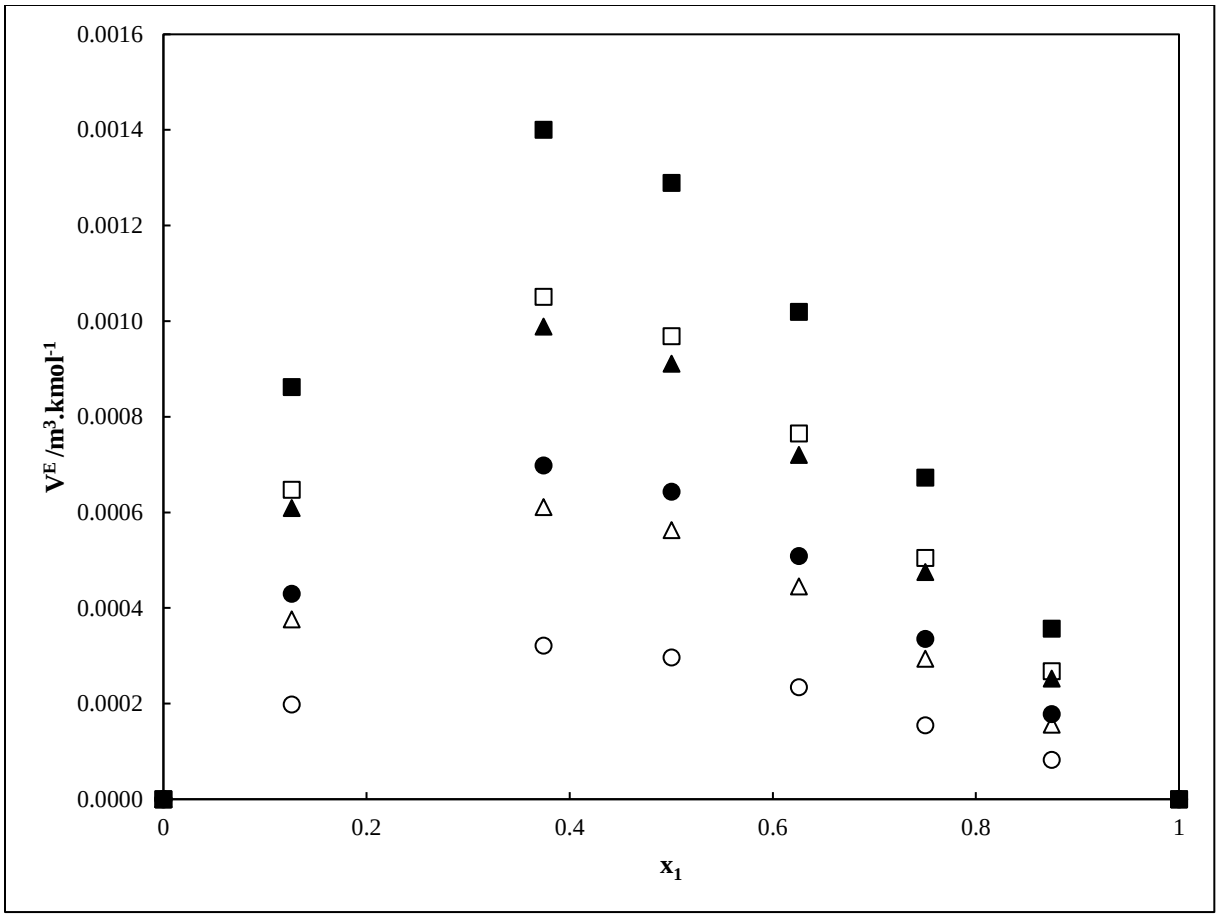

Figure 7.7. Calculated excess volume (V^E) for the butan-2-ol (1) + n-octane (2) system at selected temperatures and pressures. (symbol-T, P): (■- 353.15 K, 1 MPa), (□- 353.15 K, 20 MPa), (▲- 333.15 K, 1MPa), (∆- 333.15 K, 20 MPa), (●- 313.15 K, 1 MPa), (○- 313.15 K, 20 MPa).

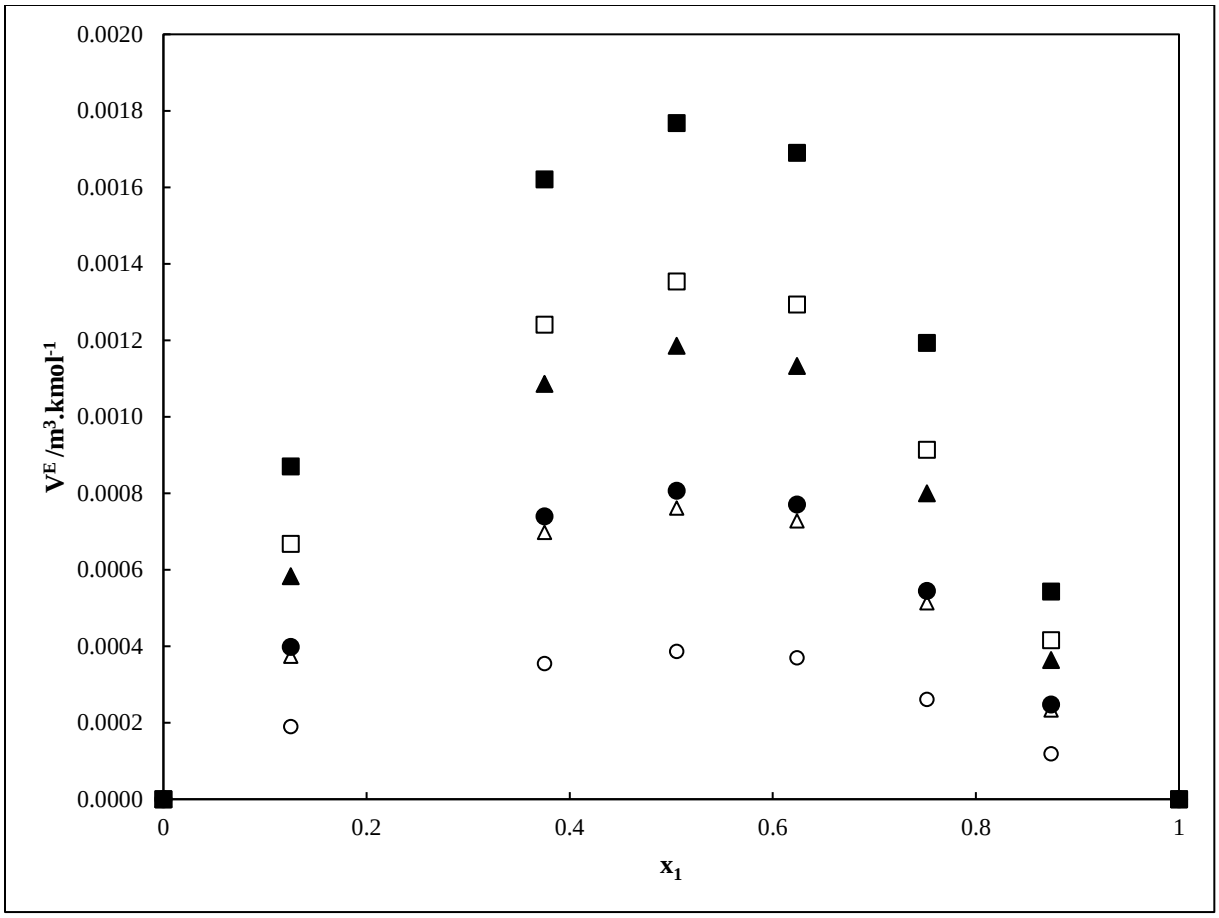

Figure 7.8. Calculated excess volume (V^E) for the butan-2-ol (1) + n-decane (2) system at selected temperatures and pressures. (symbol-T, P): (■- 353.15 K, 1 MPa), (□- 353.15 K, 20 MPa), (▲- 333.15 K, 1MPa), (Δ- 333.15 K, 20 MPa), (●- 313.15 K, 1 MPa), (○- 313.15 K, 20 MPa).

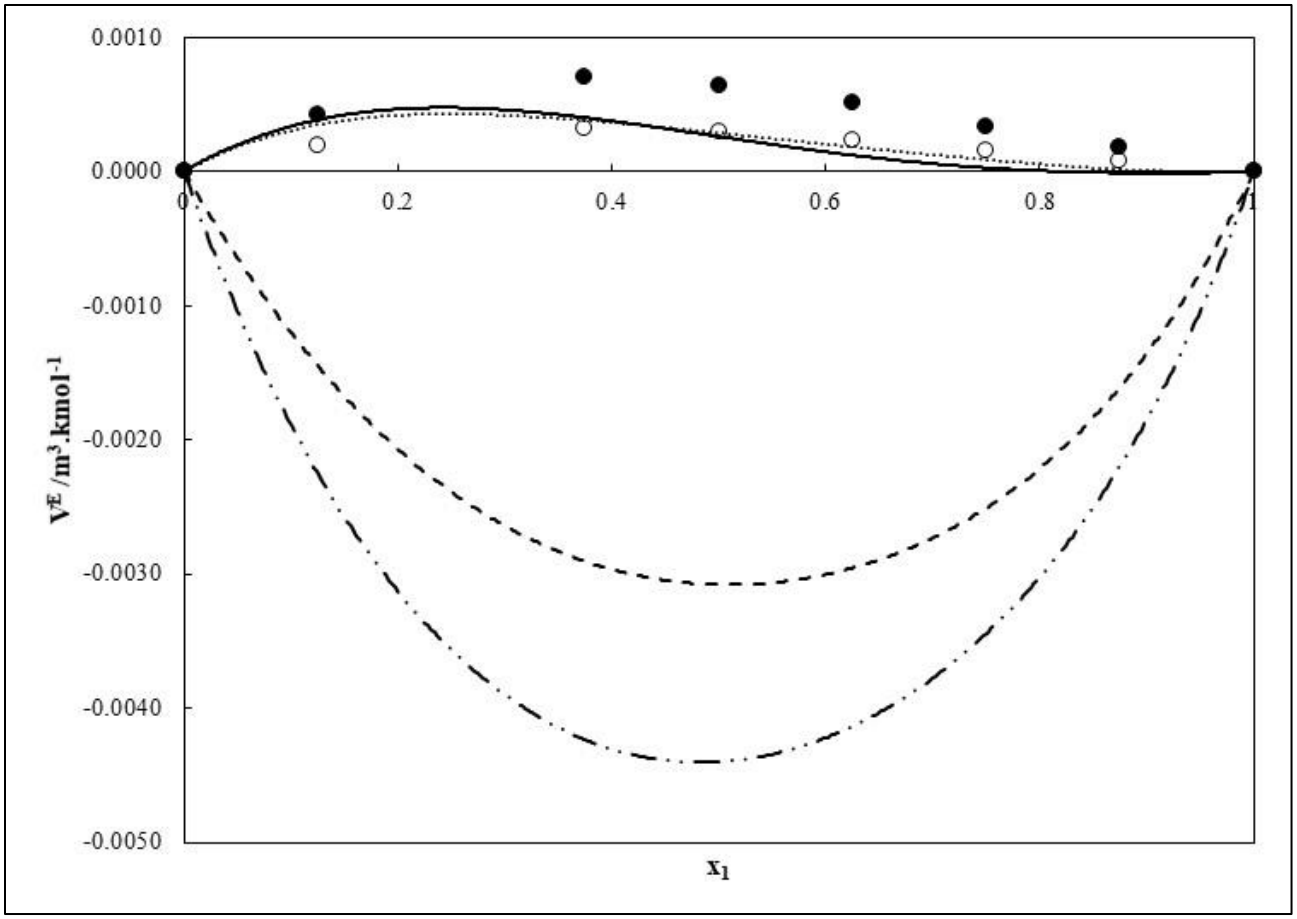

Figure 7.9. Comparison of calculated excess volume (V^E) for the butan-2-ol (1) + n-octane (2) system at selected temperatures and pressures to model predictions by the PC-SAFT and Peng-Robinson equations of state. (symbol (exp)/line (model)-T, P): (●- 313.15 K, 1 MPa), (○- 313.15 K, 20 MPa). (···-313.15 K, 1 MPa PC-SAFT), (—-313.15 K, 20 MPa PC-SAFT), (-···-·- -313.15 K, 1 MPa Peng-Robinson), (- - --313.15 K, 20 MPa Peng-Robinson).

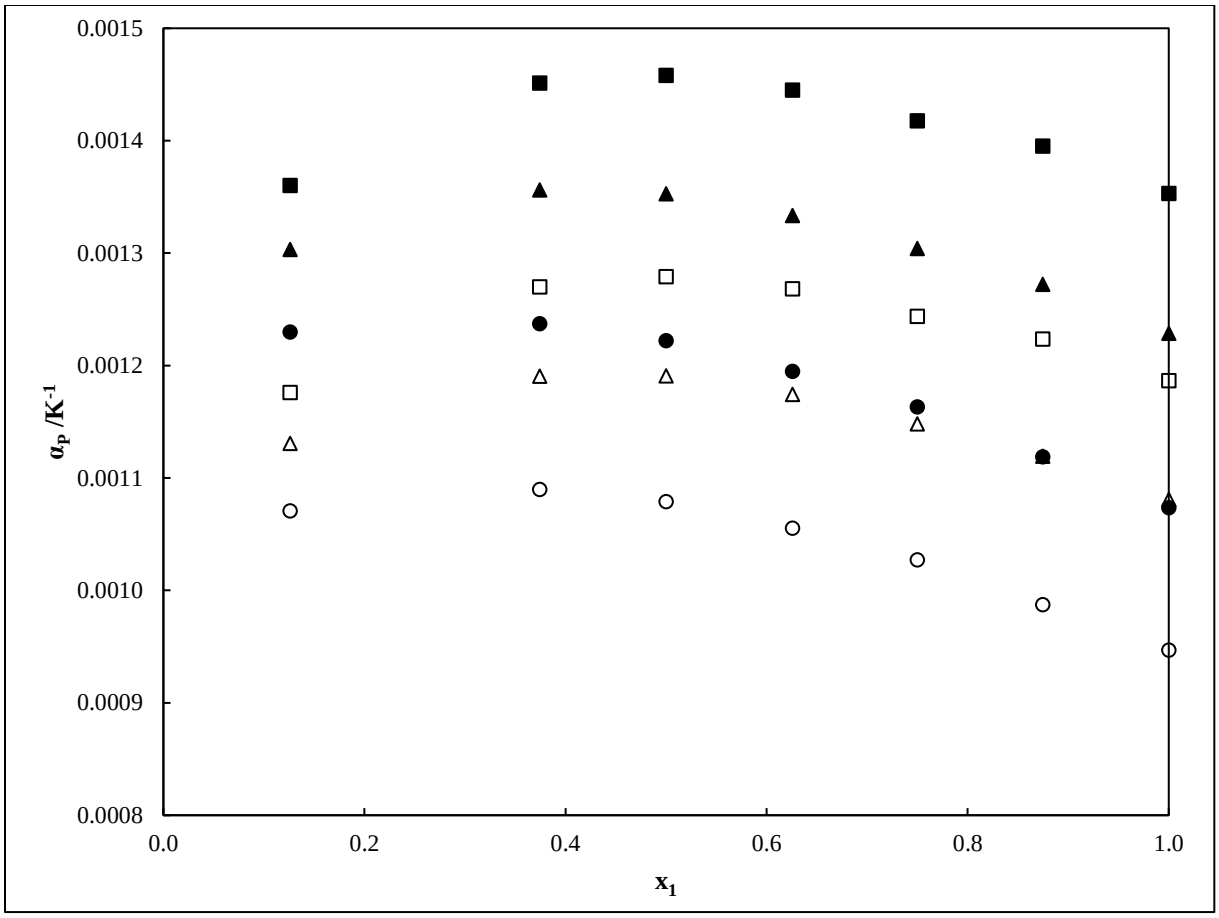

Figure 7.10. Calculated thermal expansivity (α_p) for the butan-2-ol (1) + n-octane (2) system at selected temperatures and pressures. (symbol-T, P): (■-353.15 K, 1 MPa), (□-353.15 K, 20 MPa), (▲-333.15 K, 1 MPa), (Δ -333.15 K, 20 MPa), (●-313.15 K, 1 MPa), (○-313.15 K, 20 MPa).

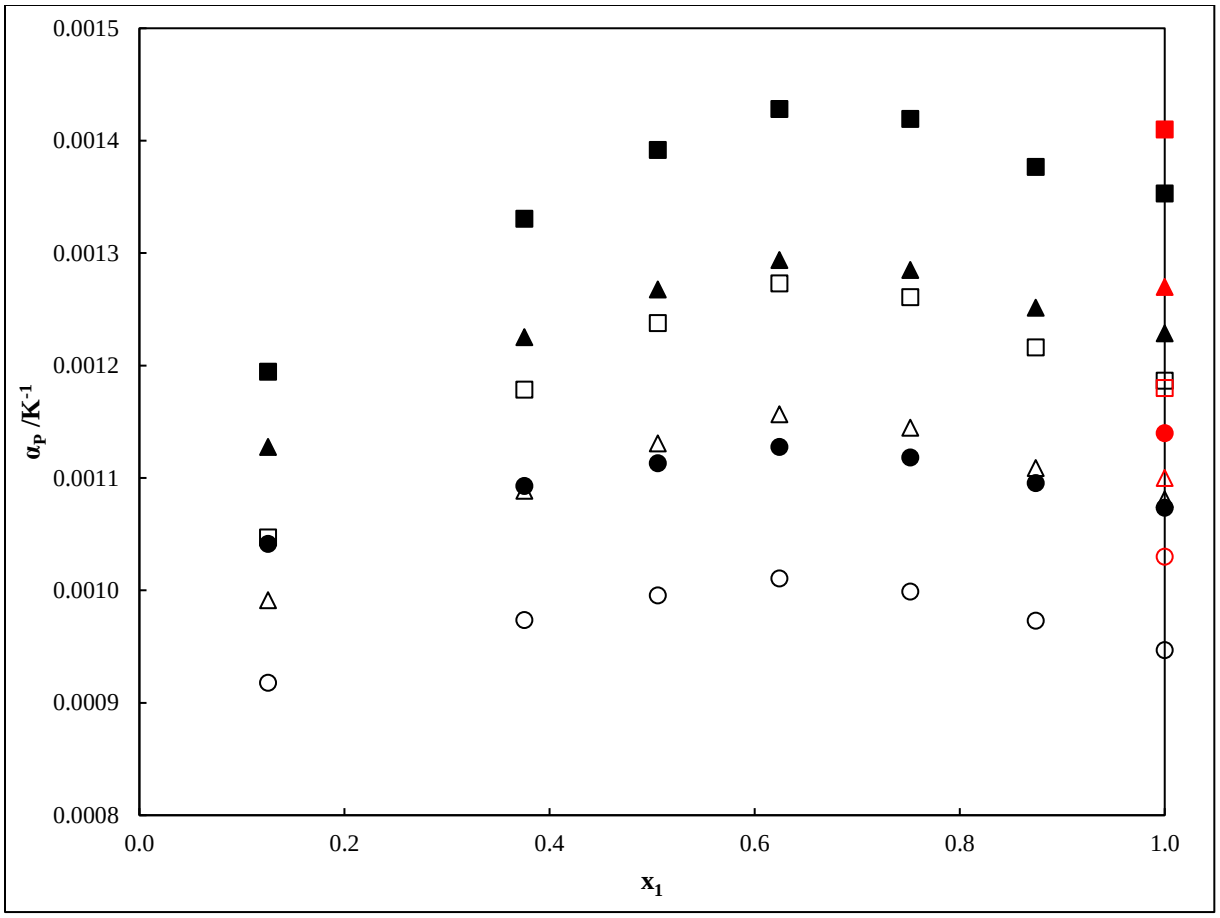

Figure 7.11. Calculated thermal expansivity (α_P) vs. x_1 for the butan-2-ol (1) + n-decane (2) system at selected temperatures and pressures. (symbol-T, P): (■- 353.15 K, 1 MPa), (□- 353.15 K, 20 MPa), (▲- 333.15 K, 1MPa), (Δ- 333.15 K, 20 MPa), (●- 313.15 K, 1 MPa), (○- 313.15 K, 20 MPa). Red symbols are data from the work of (Dakkach et al., 2015).

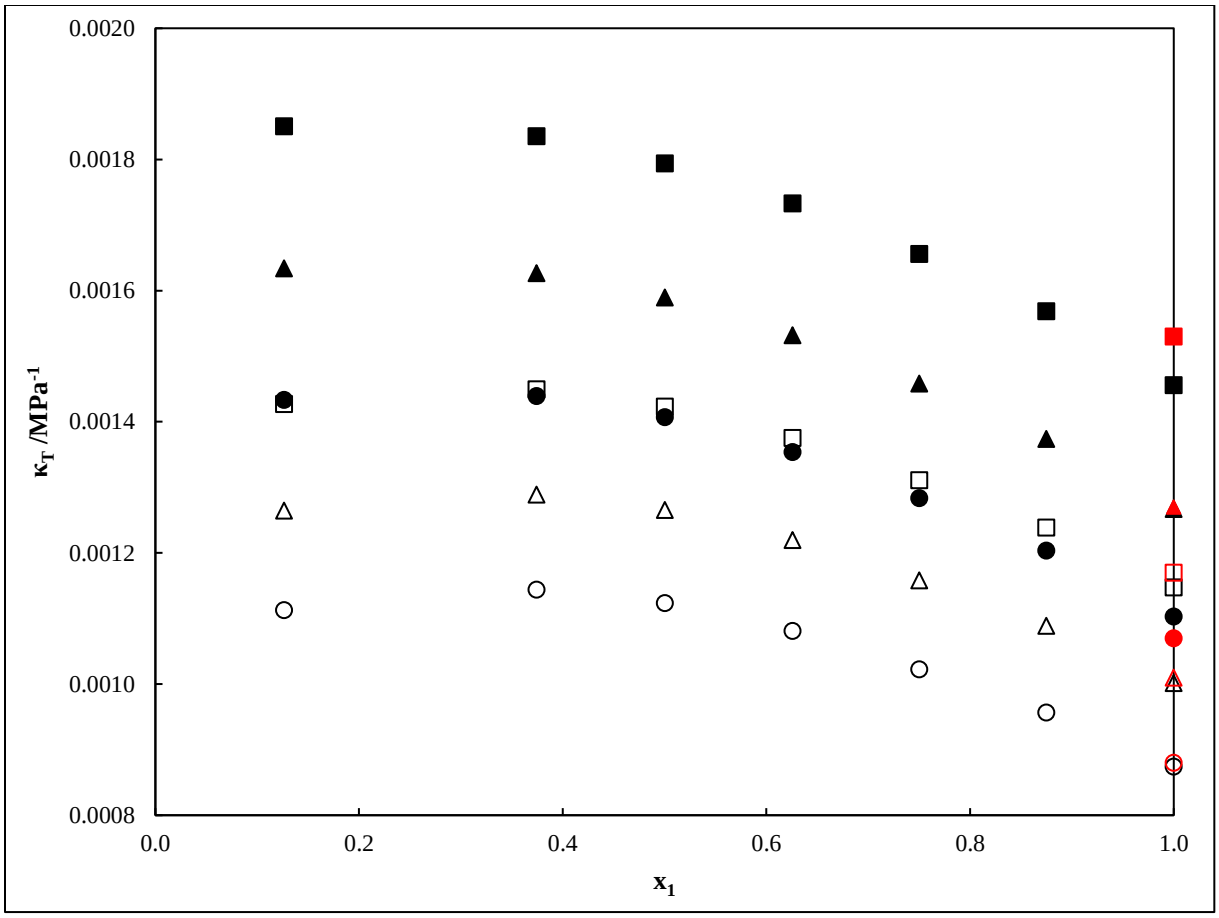

Figure 7.12. Calculated isothermal compressibility (κ_T) for the butan-2-ol (1) + n-octane (2) system at selected temperatures and pressures. (symbol-T, P): (■-353.15 K, 1 MPa), (□-353.15 K, 20 MPa), (▲-333.15 K, 1 MPa), (Δ -333.15 K, 20 MPa), (●-313.15 K, 1 MPa), (○-313.15 K, 20 MPa). Red symbols are data from the work of (Dakkach et al., 2015).

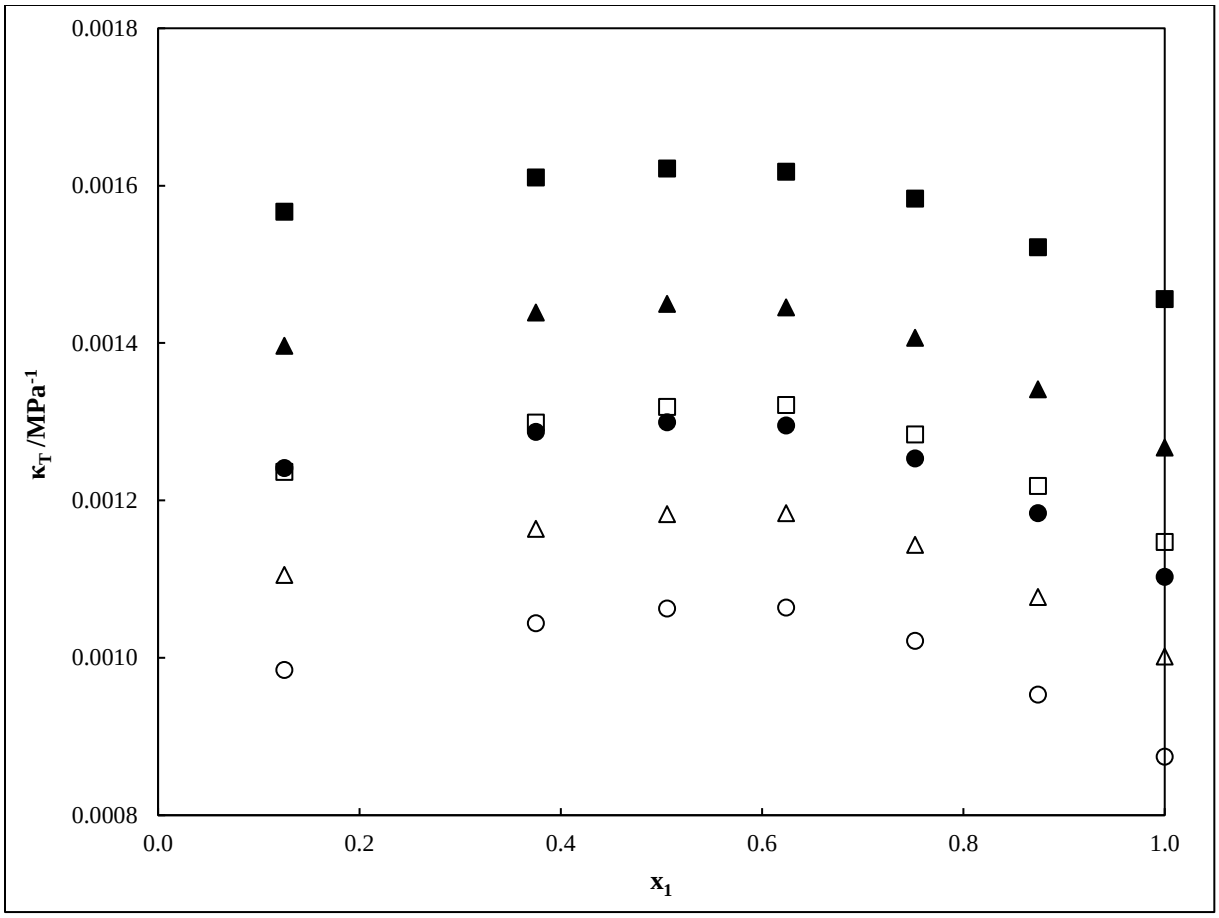

Figure 7.13. Calculated compressibility (κ_T) vs. x_1 for the butan-2-ol (1) + n-decane (2) system at selected temperatures and pressures. (symbol-T, P): (■- 353.15 K, 1 MPa), (□- 353.15 K, 20 MPa), (▲- 333.15 K, 1MPa), (Δ- 333.15 K, 20 MPa), (●- 313.15 K, 1 MPa), (○- 313.15 K, 20 MPa).

7.6. Conclusions

Experimental densities for the novel binary systems of butan-2-ol (1) + n-octane (2) and butan-2-ol (1) + n-decane (2) were measured in this work. Experiments were conducted in the temperature range of 313.15−353.15 K and a pressure range of 0.1−20 MPa. The equipment setup and experimental procedure were both verified by measuring the pure component densities of butan-2-ol as a function of temperature and pressure, which compared favorably with the literature. The mixture data was successfully correlated utilizing the modified five-parameter Toscani−Szwarc equation of state with RMSDs between 2.74×10^{-4} and 4.72×10^{-4}. Correlation by the Peng−Robinson equation of state (one binary interaction parameter) and prediction by the PC-

SAFT model were also conducted for selected cases but were unsatisfactory as they provided a poor representation of the data. RMSDs for the butan-2-ol + n-octane system at 313.15 K were 0.010 for the PC-SAFT prediction and 0.012 for the Peng−Robinson correlation and were 0.011 for the PC-SAFT prediction and 0.019 for the Peng−Robinson correlation for the system of butan-2-ol + n-decane at 353.15 K. Derived thermodynamic properties, namely, excess volume, thermal expansivity, and isothermal compressibility, were also presented in this work. Both binary systems demonstrated large positive excess molar volumes. This is expected for mixtures constituting dissimilar molecular shapes and sizes with one associating component. Furthermore, the nonideal mixing was further confirmed by the nonlinearity of thermal expansivity and isothermal compressibility of the mixtures.

CHAPTER EIGHT

P- ρ -T data and modelling for (2-methylpropan-1-ol + n-octane or n-decane) between 313.15 K–353.15 K and 0.1–20 MPa

8.1.Abstract

Isothermal measurements for 2-methylpropan-1-ol (1) + n-octane (2) and 2-methylpropan-1-ol (1) + n-decane (2) were conducted utilizing an Anton Paar DMA HP densimeter. Measurements include the entire mixture composition range and were conducted in the pressure range (0.1–20) MPa for 5 different temperatures between 313.15 and 353.15 K. The data were successfully correlated for each composition with the modified Toscani-Szwarc equation using 5 unique parameters. The data were also fit to the Peng-Robinson equation of state using a single binary interaction parameter, however quantitative results were poor. Mixture density predictions were also made by the PC-SAFT model, which also yielded mostly qualitative results. Three derived thermodynamic properties, namely excess molar volume, thermal expansivity and isothermal compressibility, were also computed using the regressed parameters.

8.2. Introduction

Alcohols are used extensively in various stages of gasoline production. In the extraction stage of crude, alcohols can be used as an inhibitor to prevent the formation of gas hydrates. Several studies (Hammerschmidt, 1939; Anderson and Prausnitz, 1986; Munck, Skjold-Jorgensen and Rasmussen, 1986; Masoudi and Tohidi, 2005; Nihous, Kinoshita and Masutani, 2009; Zhurko *et al.* 2010; Nihous *et al.*, 2010; Kapateh *et al.*, 2016; Wise *et al.*, 2016; Kondori, Zendehboudi and James, 2018; Teixeira *et al.*, 2018) have investigated the effects of alcohol inhibitors on hydrate formation. They are also used as a gasoline additive to improve octane number and can be blended directly into gasoline as a fuel -often from a renewable source such as a biofuel (Brownstein, 2015). Generally, isomerized alcohols have a higher-octane number than their non-isomers. For example, the research octane number RON of 2-methylpropan-1-ol (RON = 113) is higher than that of butan-1-ol (RON = 94). 2-methylpropan-1-ol is considered a second-generation bio-fuel as it can be produced from inedible biomass such as switch grass (Ezeji *et al*., 2014) which makes it advantageous over ethanol as a bio-fuel, as ethanol is conventionally produced from edible biomass on the large scale. It also has a higher energy density than ethanol and can be blended

with gasoline in larger proportions. The resulting blend has a lower vapour pressure than fuel blended with ethanol, or butan-1-ol, hence lighter components need not be removed in large quantities from the fuel by refiners, in order to meet air emission standards (Brownstein, 2015). The pressure-volume-temperature behaviour of gasoline + 2-methyl propan-1-ol fuel blends is not well studied in the literature (Chaudhari and Katti, 1985; Dubey and Sharma, 2007), especially at high pressures, however this information is essential to characterize vehicle engine performances for example, where pressures can exceed 15 MPa. These mixtures are also encountered, under pressure, during the blending, transport and storage process during production.

In order to advance the literature in this field, density measurements were conducted for the systems of 2-methylpropan-1-ol with n-octane/n-decane, where the alkanes were used as representative components for gasoline cuts. These measurements were conducted in the pressure and temperature ranges of 0.1–20 MPa and 313.15–353.15 K, respectively, over the entire mixture composition range. The modified Toscani-Szwarc (Quevedo-Nolasco *et al.*, 2012) equation of state was employed to correlate the density data obtained and the thermal expansivity, excess volume as well as the isothermal compressibility were calculated. In addition, comparisons between the experimental data and the correlated Peng- Robinson (Peng and Robinson, 1976) equation of state and predictions from the PCSAFT (Gross and Sadowski, 2002, 2001) model were made.

8.3.Theory

Quevedo-Nolasco et al. (2012) proposed the empirical modified Toscani-Szwarc equation (Toscani and Szwarc, 2004) of state for density correlation. This model was employed in this work and is given by:

$$\rho^{calc} = \frac{c_3 - \frac{c_4}{T} - \frac{c_5}{T^{1/3}} + P}{c_1 + c_2 P} \tag{8.1}$$

The ρ^{calc} is the density of the mixture in kg.m^{-3} calculated by the model, P is the pressure of the system in MPa, T is the experimental temperature in Kelvin, and c_1 to c_5 denotes the regressed model parameters.

Excess molar volume is the difference between the actual and ideal mixture volume at the same temperature, pressure and composition and is attributed to size, shape, dispersion energy, molecular multipole moments, molecular polarizability, correlation of molecular orientation, influence of conformational equilibria, induction effects and association equilibria (Wilhelm and Grolier, 2014). The excess molar volume of a mixture can be calculated using:

$$V^E = \sum_{i=1}^{N} x_i M_i \left(\frac{1}{\rho} - \frac{1}{\rho_i}\right) \tag{8.2}$$

where, N is the number of components comprising the system, M_i is the molar mass of component i, x_i is the mole fraction of component i, ρ is the density of the mixture and ρ_i is the density of pure component i.

The isobaric thermal expansivity finds application in many engineering calculations and can be used to determine the relationship between enthalpy and volume at constant pressure. It is defined by:

$$\alpha_P = -\frac{1}{\rho}\left(\frac{\partial \rho}{\partial T}\right)_P \tag{8.3}$$

where, α_P is the thermal expansivity at constant pressure, P, and ρ is the density of the mixture in kg:m^{-3} and T is the temperature in Kelvin.

A measure of the volume variation with pressure that occurs within a fluid at constant temperature is defined as the isothermal compressibility and can be calculated by:

$$\kappa_T = \frac{1}{\rho}\left(\frac{\partial \rho}{\partial P}\right)_T \tag{8.4}$$

where, κ_T is the compressibility at constant temperature, T.

The modified Toscani-Szwarc equation of state can be further employed to evaluate the partial derivatives expressed in equations (8.3) and (8.4) as follows:

$$\alpha_P = -\frac{\frac{c_4}{T^2} + \frac{c_5}{3T^{4/3}}}{c_3 - \frac{c_4}{T} - \frac{c_5}{T^{1/3}} + P} \tag{8.5}$$

$$\kappa_T = \frac{1}{c_3 - \frac{c_4}{T} - \frac{c_5}{T^{1/3}} + P} - \frac{c_2}{c_1 + c_2 P} \tag{8.6}$$

In this work, α_P and κ_T were computed by utilizing equations (8.5) and (8.6), respectively.

To fit parameters to the modified Toscani-Szwarc equation and the Peng-Robinson equation of state, the root mean square deviation (RMSD), which measures the difference between the calculated and actual values was calculated and minimized. It is given by:

$$RMSD = \frac{\sum_k^L \left(\left(\frac{\rho_k^{exp} - \rho_k^{calc}}{\rho_k^{exp}}\right)^2\right)^{1/2}}{L} \tag{8.7}$$

where L is the total number of points in the data set, k is a specific data point, ρ_k^{exp} is the experimental density of point k and ρ_k^{calc} is the calculated density of data point k.

8.4. Experimental

8.4.1. Materials

The chemicals utilized in this work were procured from Sigma- Aldrich and had a supplier stated purity of greater than 0.99 mass fraction. The chemicals were degassed prior to use using a Vigreux-type column. Since 2-methylpropan-1-ol is known to have some degree of hydrophilicity, it was dried by molecular sieve (3 Å K_n- $Na_{12-n}[(AlO_2)_{12}(SiO_2)_{12}]$) for 48 h and thereafter an MKS-500 device was used to conduct Karl-Fischer titration. The titration allowed for the moisture content of the alcohol to be determined which was confirmed to be less than 0.0005 mass fraction.

Purity checks were conducted utilizing a SHIMADZU GC2014 gas chromatograph (GC) for relative peak areas, and an ATAGO RX-7000a refractometer and Anton Paar DMA 5000 densimeter were used to determine the pure component refractive indices and densities respectively. A column with the following dimensions was employed for the GC: 30 m × 0.25 mm × 0.25 μm film thickness- ZebronTM7HG-G010-11 with a thermal conductivity detector and helium as the carrier gas. Regarding the refractometer, an expanded uncertainty (k = 2) of 0.0002 was determined. Results obtained from the purity checks were compared to literature and are presented in Table 8.1.

Two reference fluids, namely distilled, deionized water and air were employed for the calibration of the DMA 5000 densimeter which was used to conduct density measurements at atmospheric pressure. The estimated standard combined uncertainty in density using the DMA 5000 is $u_c(\rho)$ = 0.04 $kg.m^{-3}$. Unit specific damping coefficients were available for the DMA 5000, as recently certified by the supplier, which improves the precision of the apparatus. The high-pressure density data presented in this work was obtained utilizing a DMA HP device, connected to the DMA 5000 for display purposes and which was calibrated using pure nitrogen gas and distilled, deionized water. The DMA 5000 automatically compensates for fluid viscosities. The viscosity effects on the high-pressure measurements was accounted for in the reported uncertainties using the procedures of Segovia *et al*. (2009).

8.4.2. Apparatus

The experimental setup employed in this work was adapted from Moodley et al. (2018) and is illustrated in Figure 8.1. An air-tight syringe was connected to the Teledyne ISCO 100 DM high-pressure pump via a rubber tube. A high-pressure needle valve with an operating limit of 69 MPa controls the liquid sample entering the pump via the syringe. The piston of the pump is surrounded by a heating jacket that ensures any minor temperature gradients that exist are negligible hence leading to the assumption of isothermal conditions. The DMA HP consists of a U-tube with a capacity of 2 cm^3 into which the pressurized liquid sample, exiting the high-pressure pump, is fed. Subsequently, the U-tube is oscillated electronically with a characteristic vibrational period that changes with the density of the fluid inserted into the tube. This change can be directly related to the unknown fluid density by calibration. The operating range for the high-pressure densimeter is (263–473) K and (0.1–70) MPa for temperature and pressure, respectively. The range considered for both the experimental temperature and pressure directly influence the uncertainty for density, as stated by the supplier. The uncertainty is also dependent on the method of calibration employed. A range of (0.1–1) $kg{\cdot}m^{-3}$ was reported for the uncertainty in the density reading while a device uncertainty of 0.01 K was reported for temperature. The exit line from the densimeter is connected to a WIKA P-10 pressure transducer (0–25 MPa) via a T-junction. Pure species density measurements were executed in a recent work (Hussain and Moodley, 2020a) using the same device to confirm the precision of the temperature measurements. The P-10 transducer was calibrated using a Mensor standard model CPC6000 with the reference fluid being pure nitrogen gas. An expanded uncertainty of 0.03 MPa was computed for pressure (for the high-pressure measurements). This included the measurement transducer uncertainty (0.0125 MPa), the Mensor standard transducer (CPC6000) relative uncertainty (0.0001), and the maximum uncertainty obtained from the pressure calibration procedure. A second high-pressure needle valve controls the flow in the exit line of the densimeter. The line exiting this valve is fed to a vessel utilized for waste collection. A vacuum pump is also employed for cleaning purposes.

8.4.3. Measurements

8.4.3.1. Calibration of densimeters

Several methods of calibration were conducted in order to assess the effect of the calibration procedure used on the calculated densities. These including the two-fluid calibration procedure, as

outlined in the DMA HP user manual, the procedure of Ihmels and Gmehling (2001) and the procedure of Outcalt and McLinden (2007). The differences between the calculated pure component densities of 2-methylpropan-1-ol by each calibration procedure was used to determine the uncertainty introduced by variation in the calibration procedure used. These differences were within the range of uncertainty reported for measurements of similar systems in the literature, and the expected range quoted by the supplier. Ultimately the two-fluid calibration procedure was used as it replicated the pure component literature data well and was recommended by the device supplier.

For the two-fluid calibration procedure pure nitrogen gas and distilled, deionized water was used as the reference fluids. The Teledyne ISCO 100 DM high-pressure pump was cleaned thoroughly prior to calibration. This pump was utilized to pressurize the liquid water feed, fed via an air-tight syringe. Thereafter, the pressurized water was fed into the high-pressure densimeter where heating to the desired experimental temperature occurred. After achieving the experimental temperature, the vibrational period of oscillation of the tube filled with water was noted. Isothermal measurements were conducting for 5 different temperatures (313.15, 323.15, 333.15, 343.15, 353.15) K over the pressure range (0.1–20) MPa. A similar procedure was employed for the pure nitrogen gas.

Equation (8.8) below provides a relationship between the vibrational period and density and was used in this study to convert vibrational period to density.

$$\rho_m(P,T,\tau) = \rho_{H_2O}(P,T) + \frac{\left(\tau_m^2(P,T)-\tau_{H_2O}^2(P,T)\right)\left(\rho_{H_2O}(P,T)-\rho_{N_2}(P,T)\right)}{\tau_{H_2O}^2(P,T)-\tau_{N_2}^2(P,T)} \qquad (8.8)$$

where T is the temperature in Kelvin (K), s is the vibrational period in μs, P is the system pressure measured in MPa and ρ is the density in $kg \cdot m^{-3}$. The measurement sample is denoted by the subscript m while the subscript's N_2 and H_2O denotes the reference property for nitrogen and water, respectively.

Wagner and Pruß (2002) and Span et al. (1998) proposed precise density correlations for water and nitrogen, respectively. These correlations were utilized to calculate the reference densities for the calibration fluids.

8.4.3.2. Experimental procedure

The experimental procedure employed in this work has been described in previous work (Moodley *et al.*, 2018; Hussain and Moodley, 2020). Standard solutions of 80 cm^3 were prepared in a sealable vessel using a Mettler-Toledo mass balance with a precision of 0.0001 g. Component 1 was first added to the vessel and the solution mass was noted. Thereafter, the second component was added to the vessel to obtain a desired ratio between the two components and the mass was also recorded. The sealed solution was then stirred thoroughly to eliminate any concentration gradients that were present. The solution was then injected, via gas tight syringe, into the evacuated ISCO high-pressure pump, which had been cleaned and emptied prior to use, in increments of 15 cm^3. The 15 cm^3 increment injections were conducted 3 times and ensured a uniform composition in the piston, lines and densimeter. Furthermore, this also ensured contamination of the sample was prevented. The final sample was then loaded and both needle valves were closed to isolate the system. The heating jacket that surrounds the pumps piston was set to the experimental temperature to ensure temperature gradients between the high-pressure pump and DMA HP were negligible. This ensured isothermal conditions. The built-in temperature controller, present within the DMA HP, ensures that existing temperature gradients within the device are negligible before thermal equilibrium is confirmed. The experimental pressures and temperatures were set using the high-pressure pump and densimeter, respectively. The temperature, pressure and vibrational period were noted after (60–90) minutes and were taken three times. No significant variation in all three parameters was observed after equilibrium was established. This procedure was conducted for all temperatures and pressures.

The Joint Committee for Guides in Metrology (JCGM) (2008) method to estimate the expanded combined uncertainties in density was employed in this work. These were found to be 1.10 and 1.12 $kg \cdot m^{-3}$ for the pure 2-methylpropan-1-ol and the mixtures, respectively, with a coverage factor of k = 2. The variables considered to estimate this uncertainty are provided in Table 8.2.

Table 8.1. Chemical suppliers and purities.

Component	CAS No.	Supplier	Refractive index (RI) at 0.101 MPa.		Minimum stated mass fraction purity	GC peak relative area	Density at 313.15 K and 0.101 MPa /kg·m^{-3}.	
			Exp. ǂ	Lit. (Aminabhavi et al., 1993)			Exp*	Lit.
n-octane	111-65-9	Sigma-Aldrich	1.3949 (298.15 K)	1.3944 (298.15 K)	0.99	0.999	686.22	686.22 (Lampreia and Nieto de Castro, 2011) 686.29 (Sanmamed et al., 2009) 686.36 (L. Lugo et al., 2001)
n-decane	124-18-5	Sigma-Aldrich	1.4092 (298.15 K)	1.4090 (298.15 K)	0.99	0.999	714.74	715.64 (Quevedo-Nolasco et al., 2012) 714.40 (Banipal et al., 1991) 714.79 (Troncoso et al., 2004)
2-methylpropan-1-ol [a]	78-83-1	Sigma-Aldrich	1.3938 (298.15 K)	1.3938 (298.15 K)	0.99	0.999	786.32	786.30 (Cano-Gómez et al., 2017) 786.12 (Bravo-Sánchez et al., 2010) 786.04 (Kermanpour and Niakan, 2012)
nitrogen	7727-37-9	Afrox	-	-	0.99	-	-	-
air	132259-10-0	Afrox	-	-	0.78 nitrogen 0.21 oxygen 0.009 argon 0.0003 carbon dioxide Trace helium, neon, krypton, xenon	-	-	-
water	7732-18-5	-	1.3334 (293.15 K)	1.33336 (293.15 K)	-	0.999	-	-

1. ǂ At sodium D-line = 589 nm. Expanded uncertainties $U_c(k=2)$ are $U_c(RI) = 0.0002$, $U_c(T) = 0.02K$, $U_c(P) = 0.002\ MPa$, * Expanded uncertainties $U_c(k=2)$ are $U_c(T) = 0.02K$, are $U_c(P) = 0.002\ MPa$ and $U_c(\rho) = 0.08\ kg.m^{-3}$

2. [a] Purified by molecular sieve

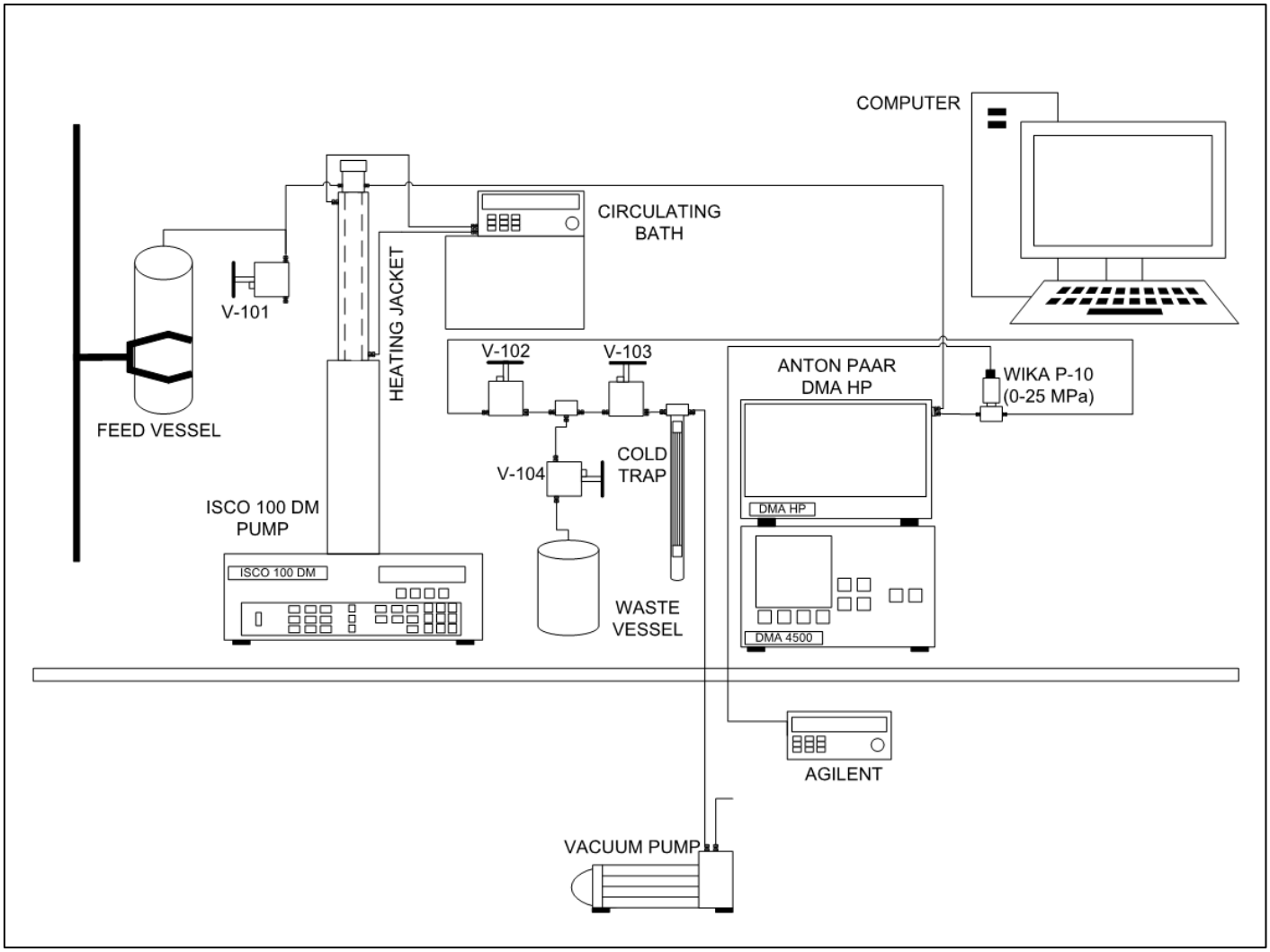

Figure 8.1. Layout of the apparatus used in this work (adapted from Moodley *et al.*, 2018; Hussain and Moodley, 2020).

Table 8.2. Example of breakdown of uncertainty for density*

Source	Uncertainty U	Contribution to $U_C(\rho)$/(kg·m^{-3})
Temperature $U(T)$, k =2	0.02 K	0.02
Pressure $U(P)$, k = 2	0.03 MPa	0.06
Period $U(\tau)$, k = 2 (repeatability and viscosity)	0.003 μs	0.13
Mixture Composition x_i, k = 2	0.002 mol fraction	0.06
Uncertainty from Measurements $U_{meas}(\rho)$, k = 2		0.13
EOS of the calibration fluids $U_{EOS}(\rho)/\rho$, k = 2	0.05%	0.50
Calibration model (ρ), k = 2	0.97 kg·m^{-3}	0.97
Impurity x_i, k = 2	0.005 mol fraction	0.13
Combined expanded uncertainty in density $U_C(\rho)$, k = 2		1.12

* 2-methylpropan-1-ol (1) + n-octane (2) system at x_1= 0.4996 was used for this example

U_C is the combined expanded uncertainty in density (ρ) and is calculated by $U_c(\rho)(k = 2) = (\sum(U(D)_i)^2)^{1/2}$

8.5.Results and discussion

Purity and physical property checks were conducted for 2-methylpropan-1-ol, n-octane and n-decane and the results are presented in Table 8.1. The results obtained from these checks were compared to literature and were found to be consistent within experimental uncertainty in most cases. Furthermore, the experimental setup and procedure were verified by conducting pure 2-methylpropan-1-ol measurements at 313.15 K to 353.15 K and (0.1–20) MPa, as well as for the binary systems {2-methylpropan-1-ol (1) + n-octane (2)} and {2-methylpropan-1-ol (1) + n-decane (2)} at 313.15 K to 353.15 K and at atmospheric pressure. These results are presented in Tables 8.3–8.5 and Figures 8.2–8.4. From Figure 8.2, a maximum relative deviation of 0.0018 exists between experimental and literature values (Cano-Gómez et al., 2017; Golubev et al., 1980a; Iglesias-Silva et al., 2015; Kermanpour and Niakan, 2012; Kubota et al., 1987; Majstorović et al., 2020), which is within the experimental uncertainties of the studies. In addition, the data measured in this work at atmospheric pressure is seen to follow the same trend with temperature as demonstrated by the literature (Chaudhari and Katti, 1985; Dubey and Sharma, 2007). This is illustrated in Figures 8.3 and 8.4. The nonlinear relationship of density with composition at constant temperature and pressure is replicated. The systems also replicated the positive excess

volume observed in the literature with magnitude increasing with temperature. In Figures 8.5 and 8.6, minor inconsistencies can be observed between the high-pressure data measured with the DMA HP and the atmospheric pressure data using the DMA 5000 for some compositions. This is attributed to the respective differences in uncertainty between the two devices.

Isothermal measurements were conducted for both binary systems, {2-methylpropan-1-ol (1) + n-octane (2)} and {2-methylpropan-1-ol (1) + n-decane (2)}, over the pressure range of (0.1–20) MPa for five different temperatures (313.15–353.15) K and include the entire mixture composition range. These results are presented in Tables 8.4 and 8.5. Results obtained in this work demonstrate compliance with the general expected trends that exist between density, pressure and temperature. Namely, as demonstrated in Table 8.4 and 8.5, density and pressure show a direct relationship thus an increase in pressure causes an increase in density however, an inverse relationship between temperature and density exists. For the mixtures, the variation of density with composition is non-linear.

The modified Toscani-Szwarc equation of state was employed for correlation of the experimental density data. The data were analysed using regression on MATLAB® to obtain the 5 parameters used in the model for 2-methylpropan-1-ol and both binary systems. Parameters for n-octane and n-decane have been presented in a previous recent study (Hussain and Moodley, 2020a) which were used in this work. These results, as well as the RMSD are presented in Table 8.6. As seen in Figures 8.5 and 8.6, the modified Toscani-Szwarc equation provides a good correlation of the experimental data with a maximum RMSD = 3.95×10^{-4}.

The Peng-Robinson equation of state (Peng and Robinson, 1976) and PC-SAFT (Gross and Sadowski, 2002, 2001) equation, two of the most commonly employed equations of state for high-pressure systems, were also employed for data prediction/correlation. The representation obtained from these equations were compared to experimental data and are illustrated in Figure 8.5 for the {2-methylpropan-1-ol (1) + n-octane (2)} system at 353.15 K, and Figure 8.6 for the {2-methylpropan-1-ol (1) + n-decane (2)} system at 333.15 K. Similar results were obtained at the remaining 4 temperatures in each system. The prediction of the pure 2-methylpropan-1-ol behaviour by the PC-SAFT and Peng- Robinson yielded RMSDs of 0.021 and 0.010, respectively.

The original mixing rules for both models were used. The binary interaction parameters for both models were initially excluded as this is not available in the literature, and sufficient phase

equilibrium data for the relevant systems and conditions were also not available to provide an accurate estimation. Gross and Sadowski (2001, 2002) have stated that this is a common practice of engineers in industry, where binary interaction parameters are seldom accessible. Parameters for the PC-SAFT (Gross and Sadowski, 2002, 2001) predictions were taken from the works of Zarei and Feyzi (2013)and Burgess et al. (2012) for 2-methylpropan-1-ol and n-octane/n-decane, respectively. These are provided in Table 8.7. A 2B association scheme was employed for the 2-methylpropan-1-ol where the hydrogen and oxygen atoms of the OH group are each treated as an association site, while the n-alkane components were assumed as non-associating. A qualitative prediction was obtained from the PC-SAFT (Gross and Sadowski, 2002, 2001) model with RMSDs of 0.011 and 0.011 for the {2-methylpropan-1- ol (1) + n-octane (2)} and {2-methylpropan-1-ol (1) + n-decane (2)} systems respectively.

For the Peng-Robinson equation of state the initial omission of the binary interaction parameter yielded very poor results, which was also due to the poor description of the pure component densities by the model. In an attempt to improve the correlation, binary interaction parameters (k_{ij}) were regressed using the standard fitting procedure for liquid densities given by Walas (2013). Note that the regressed k_{ij} values cannot be used to predicted phase equilibrium behaviour as only density data were used to regress them. Figures 8.5 and 8.6 illustrates the poor correlation of the density data by the Peng-Robinson (1976) equation of state with the binary interaction parameters considered with RMSDs of 0.006 and 0.020 for the {2-methylpropan-1-ol (1) + n-octane (2)} and {2- methylpropan-1-ol (1) + n-decane (2)} systems respectively. The Peng-Robinson and PC-SAFT model performances should not be compared to the performance of the empirical Toscani-Szwarc equation of state.

The regressed parameters, utilized in the modified Toscani- Szwarc equation, were also employed to calculate the excess molar volumes for both binary systems. Substantial deviations from ideality are illustrated in Figures 8.7 and 8.8 for both novel systems. The measured excess volumes are positive. This is likely due to the non-polar alkane breaking-down the alcohol multimer series that tend to self-associate, and the subsequent molecular interactions (e.g. dipole–induced dipole (debye)) between the alcohol homomorphs and the alkanes. This is an expected behaviour. The effect of interstitial arrangement of the n-alkane molecules with the alcohol branched multimer structure, which would cause negative contributions to the excess volume is not significant (Rao

and Naidu, 1974; Treszczanowicz and Benson, 1978). The standard uncertainties, in the excess molar volume, were estimated utilizing the error propagation method and were found to be $1.81x10^{-5}$ $m^3.kmol^{-1}$ for the {2-methylpropan-1-ol (1) + n-octane (2)} system and 1.88×10^{-5} $m^3.kmol^{-1}$ for the {2-methylpropan-1-ol (1) + n-decane (2)} system.

Furthermore, the thermal expansivity and isothermal compressibility derived thermodynamic properties were also computed utilizing the regressed MTS parameters and the results were found to be highly non-linear. Figures 8.9 and 8.10 illustrate a direct relationship between thermal expansivity and temperature, with an inverse response with pressure, while Figures 8.11 and 8.12 show a direct relationship between temperature and isothermal compressibility and an inverse one regarding pressure. Error propagation was employed for the estimation of relative uncertainties in thermal expansivity and isothermal compressibility, which were estimated as 0.041 and 0.044 respectively.

Table 8.3. Experimental pure component liquid densities for 2-methylpropan-1-ol.[ǂ]

Component	P/MPa	ρ/ kg·m^{-3}	P/MPa	ρ/ kg·m^{-3}	P/MPa	ρ/ kg·m^{-3}	P/MPa	ρ/ kg·m^{-3}	P/MPa	ρ/ kg·m^{-3}
	T/K = 313.15		T/K = 323.15		T/K = 333.15		T/K= 343.15		T/K = 353.15	
2-methylpropan-1-ol										
	0.1*	786.32	0.1	777.89	0.1	769.51	0.1	760.63	0.1	752.20
	1.11	788.3	1.10	780.0	1.11	771.8	1.07	762.6	1.09	753.8
	2.12	789.1	2.11	780.9	2.10	772.7	2.08	763.7	2.08	754.7
	3.13	790.0	3.12	781.8	3.11	773.7	3.09	764.7	3.09	755.9
	4.14	790.8	4.13	782.7	4.12	774.6	4.10	765.6	4.10	757.0
	5.15	791.6	5.14	783.6	5.13	775.6	5.11	766.6	5.11	758.0
	6.15	792.5	6.15	784.5	6.14	776.5	6.12	767.6	6.12	759.0
	7.17	793.3	7.15	785.4	7.15	777.4	7.14	768.7	7.13	760.1
	8.18	794.2	8.17	786.2	8.16	778.5	8.14	769.6	8.14	761.1
	9.19	795.0	9.18	787.1	9.17	779.3	9.15	770.6	9.15	762.1
	10.20	795.8	10.18	788.0	10.17	780.2	10.17	771.4	10.16	763.1
	11.21	796.7	11.20	788.9	11.19	781.1	11.17	772.4	11.17	764.1
	12.22	797.5	12.20	789.6	12.20	781.9	12.19	773.3	12.19	765.0
	13.22	798.3	13.21	790.5	13.21	782.8	13.19	774.2	13.19	765.9
	14.23	799.1	14.22	791.3	14.22	783.6	14.20	775.1	14.20	766.8
	15.24	799.9	15.22	792.1	15.22	784.5	15.21	776.0	15.21	767.8
	16.25	800.7	16.24	792.9	16.23	785.3	16.22	776.8	16.22	768.6
	17.25	801.4	17.24	793.7	17.23	786.1	17.22	777.6	17.22	769.5
	18.26	802.2	18.25	794.4	18.24	786.9	18.23	778.4	18.22	770.4
	19.26	802.9	19.26	795.1	19.25	787.6	19.23	779.2	19.23	771.1
	20.27	803.5	20.26	795.8	20.25	788.3	20.20	779.9	20.20	772.0

[ǂ] Densities above atmospheric measured by DMA HP apparatus and the expanded combined uncertainties ($k = 2$) U_c are $U_c(T) = 0.02\ K$, $U_c(P) = 0.03\ MPa$, , $U_c(\rho) = 1.10\ kg \cdot m^{-3}$

*At atmospheric pressures the DMA 5000 apparatus was used and the expanded combined uncertainties ($k = 2$) U_c are $U_c(T) = 0.02\ K$, $U_c(P) = 0.002\ MPa$, $U_c(\rho) = 0.08\ kg \cdot m^{-3}$ where T is the temperature in K, P is the pressure in MPa and ρ is the density in $kg \cdot m^{-3}$

Table 8.4. Experimental liquid densities for 2-methylpropan-1-ol (1) + n-octane (2) at various temperatures and pressures. ‡

T/K	P/MPa	ρ/ kg·m^{-3}	P/MPa	ρ/ kg·m^{-3}	P/MPa	ρ/ kg·m^{-3}	P/MPa	ρ/ kg·m^{-3}	P/MPa	ρ/ kg·m^{-3}	P/MPa	ρ/ kg·m^{-3}
	x_1=0.1267		x_1=0.3776		x_1=0.4996		x_1=0.6255		x_1=0.7499		x_1=0.8739	
313.15	0.1*	692.40	0.1	708.36	0.1	718.17	0.1	730.53	0.1	745.16	0.1	762.94
313.15	1.10	694.2	1.10	710.7	1.11	720.9	1.12	733.3	1.07	747.8	1.06	765.3
313.15	2.11	695.5	2.11	712.0	2.12	722.4	2.13	734.8	2.05	749.4	2.07	766.8
313.15	3.12	696.6	3.12	713.2	3.12	723.4	3.14	735.8	3.06	750.3	3.08	767.7
313.15	4.13	697.6	4.13	714.3	4.14	724.4	4.15	736.8	4.08	751.3	4.14	768.6
313.15	5.14	698.5	5.14	715.2	5.14	725.3	5.16	737.7	5.09	752.2	5.15	769.5
313.15	6.15	699.5	6.15	716.3	6.16	726.3	6.17	738.7	6.09	753.2	6.16	770.5
313.15	7.16	700.4	7.16	717.2	7.17	727.3	7.19	739.7	7.11	754.2	7.17	771.4
313.15	8.17	701.3	8.17	718.2	8.18	728.3	8.20	740.7	8.12	755.1	8.18	772.3
313.15	9.18	702.2	9.18	719.1	9.19	729.2	9.21	741.6	9.13	756.0	9.19	773.2
313.15	10.19	703.1	10.19	720.0	10.20	730.2	10.21	742.5	10.14	756.9	10.20	774.1
313.15	11.20	704.0	11.20	721.0	11.21	731.1	11.22	743.5	11.15	757.9	11.21	775.0
313.15	12.21	704.9	12.20	721.9	12.22	732.0	12.23	744.4	12.16	758.8	12.21	775.9
313.15	13.22	705.8	13.22	722.8	13.23	732.9	13.24	745.3	13.16	759.6	13.23	776.7
313.15	14.23	706.7	14.23	723.7	14.24	733.9	14.25	746.2	14.17	760.6	14.24	777.7
313.15	15.23	707.5	15.23	724.6	15.24	734.7	15.25	747.1	15.17	761.4	15.24	778.5
313.15	16.24	708.4	16.24	725.5	16.25	735.6	16.26	748.0	16.19	762.3	16.24	779.3
313.15	17.25	709.2	17.25	726.3	17.25	736.5	17.27	748.8	17.19	763.2	17.25	780.2
313.15	18.25	709.9	18.25	727.0	18.26	737.3	18.27	749.6	18.20	763.9	18.26	780.9
313.15	19.26	710.6	19.25	727.8	19.27	738.0	19.28	750.4	19.20	764.7	19.26	781.7
313.15	20.26	711.3	20.26	728.5	20.27	738.7	20.28	751.0	20.21	765.4	20.26	782.4
323.15	0.1	683.93	0.1	699.68	0.1	709.40	0.1	721.73	0.1	736.37	0.1	754.25
323.15	1.11	686.1	1.12	702.2	1.12	712.2	1.14	724.4	1.07	739.1	1.06	756.9
323.15	2.11	687.2	2.11	703.5	2.12	713.5	2.13	725.9	2.06	740.4	2.07	758.0
323.15	3.12	688.2	3.12	704.6	3.13	714.5	3.14	726.9	3.07	741.4	3.08	759.0
323.15	4.13	689.2	4.13	705.6	4.14	715.5	4.15	727.9	4.08	742.4	4.09	760.0
323.15	5.14	690.2	5.14	706.6	5.15	716.6	5.16	729.0	5.09	743.5	5.10	761.0
323.15	6.15	691.3	6.15	707.7	6.16	717.7	6.17	730.0	6.10	744.5	6.11	762.0
323.15	7.16	692.2	7.17	708.7	7.17	718.7	7.17	731.0	7.11	745.5	7.12	763.0
323.15	8.17	693.2	8.18	709.7	8.18	719.7	8.19	732.0	8.12	746.5	8.13	763.9
323.15	9.18	694.2	9.18	710.7	9.20	720.7	9.20	733.0	9.13	747.5	9.14	764.8
323.15	10.19	695.1	10.20	711.6	10.20	721.6	10.21	734.0	10.14	748.4	10.15	765.8
323.15	11.20	696.1	11.20	712.7	11.22	722.7	11.22	735.0	11.15	749.4	11.16	766.7
323.15	12.21	696.9	12.21	713.5	12.22	723.5	12.23	735.9	12.16	750.3	12.17	767.6
323.15	13.22	697.8	13.22	714.5	13.23	724.5	13.24	736.8	13.17	751.2	13.18	768.5
323.15	14.23	698.7	14.23	715.4	14.24	725.4	14.24	737.7	14.18	752.1	14.19	769.4
323.15	15.24	699.6	15.24	716.3	15.25	726.4	15.25	738.7	15.18	753.0	15.20	770.2
323.15	16.25	700.5	16.24	717.2	16.25	727.3	16.26	739.6	16.19	753.9	16.20	771.1
323.15	17.25	701.3	17.24	718.0	17.26	728.1	17.26	740.4	17.20	754.8	17.20	771.9
323.15	18.25	702.1	18.26	718.9	18.26	728.9	18.27	741.2	18.21	755.6	18.21	772.7

323.15	19.25	702.8	19.26	719.6	19.27	729.7	19.27	742.0	19.21	756.3	19.22	773.4
323.15	20.26	703.5	20.26	720.3	20.27	730.4	20.28	742.7	20.21	757.1	20.22	774.2
333.15	0.1	675.36	0.1	690.82	0.1	700.44	0.1	712.74	0.1	727.43	0.1	745.44
333.15	1.10	677.7	1.13	693.4	1.11	703.4	1.13	715.6	1.12	730.4	1.06	748.1
333.15	2.11	679.1	2.12	694.9	2.12	704.7	2.13	717.0	2.12	731.6	2.07	749.4
333.15	3.12	680.2	3.13	696.0	3.13	705.8	3.13	718.1	3.11	732.7	3.08	750.4
333.15	4.13	681.2	4.14	697.1	4.14	706.8	4.15	719.1	4.12	733.7	4.09	751.4
333.15	5.14	682.3	5.15	698.2	5.15	708.0	5.16	720.3	5.13	734.8	5.10	752.5
333.15	6.15	683.3	6.16	699.2	6.16	709.0	6.16	721.3	6.15	735.8	6.11	753.4
333.15	7.16	684.3	7.17	700.3	7.17	710.1	7.17	722.4	7.15	736.9	7.12	754.4
333.15	8.17	685.8	8.18	701.7	8.18	711.5	8.19	723.7	8.17	738.2	8.13	755.7
333.15	9.18	686.4	9.19	702.4	9.19	712.2	9.20	724.4	9.18	738.9	9.14	756.4
333.15	10.19	687.4	10.20	703.4	10.20	713.2	10.21	725.5	10.15	739.9	10.15	757.4
333.15	11.20	688.4	11.21	704.4	11.21	714.2	11.22	726.5	11.15	740.9	11.16	758.4
333.15	12.21	689.3	12.22	705.4	12.22	715.2	12.22	727.4	12.16	741.9	12.17	759.3
333.15	13.22	690.2	13.23	706.3	13.23	716.1	13.23	728.4	13.17	742.8	13.18	760.2
333.15	14.23	691.1	14.24	707.3	14.24	717.1	14.25	729.3	14.18	743.7	14.19	761.1
333.15	15.23	692.1	15.25	708.3	15.25	718.1	15.25	730.3	15.19	744.7	15.19	762.0
333.15	16.24	692.9	16.25	709.1	16.25	718.9	16.26	731.1	16.20	745.5	16.20	762.9
333.15	17.25	693.8	17.25	710.0	17.26	719.8	17.25	732.0	17.20	746.4	17.20	763.7
333.15	18.26	694.6	18.26	710.8	18.27	720.7	18.27	732.9	18.20	747.3	18.21	764.6
333.15	19.26	695.5	19.27	711.7	19.27	721.6	19.27	733.8	19.21	748.1	19.21	765.4
333.15	20.26	696.1	20.27	712.4	20.27	722.3	20.27	734.5	20.21	748.8	20.22	766.1
343.15	0.1	666.57	0.1	681.53	0.1	690.95	0.1	703.17	0.1	717.86	0.1	736.01
343.15	1.08	668.7	1.12	683.9	1.13	693.4	1.12	705.6	1.13	720.5	1.06	738.2
343.15	2.08	670.0	2.12	685.3	2.13	694.9	2.12	707.1	2.12	721.7	2.07	739.6
343.15	3.09	671.1	3.13	686.4	3.13	696.0	3.13	708.2	3.13	722.8	3.08	740.7
343.15	4.10	672.1	4.14	687.5	4.14	697.1	4.14	709.3	4.14	723.9	4.09	741.7
343.15	5.11	673.2	5.15	688.6	5.15	698.2	5.15	710.4	5.14	724.9	5.10	742.8
343.15	6.12	674.3	6.16	689.7	6.16	699.3	6.16	711.5	6.15	726.0	6.11	743.9
343.15	7.13	675.6	7.17	691.0	7.17	700.5	7.18	712.7	7.16	727.2	7.12	745.0
343.15	8.14	676.6	8.18	692.0	8.19	701.6	8.18	713.8	8.18	728.3	8.13	746.0
343.15	9.15	677.7	9.19	693.1	9.19	702.7	9.19	714.8	9.18	729.3	9.14	747.0
343.15	10.16	678.6	10.20	694.1	10.20	703.6	10.20	715.8	10.19	730.3	10.15	748.0
343.15	11.17	679.7	11.22	695.2	11.22	704.8	11.21	716.9	11.20	731.4	11.16	749.0
343.15	12.18	680.6	12.21	696.1	12.22	705.7	12.22	717.9	12.21	732.3	12.17	749.9
343.15	13.19	681.6	13.23	697.1	13.23	706.7	13.23	718.9	13.22	733.3	13.18	750.9
343.15	14.20	682.6	14.23	698.2	14.24	707.7	14.24	719.9	14.23	734.3	14.18	751.9
343.15	15.21	683.6	15.25	699.1	15.25	708.7	15.24	720.8	15.24	735.2	15.19	752.8
343.15	16.21	684.4	16.25	700.0	16.25	709.6	16.25	721.7	16.24	736.1	16.20	753.7
343.15	17.22	685.4	17.25	701.0	17.26	710.6	17.25	722.7	17.24	737.1	17.21	754.6
343.15	18.23	686.3	18.26	701.9	18.27	711.5	18.26	723.6	18.25	738.0	18.21	755.4
343.15	19.22	687.1	19.27	702.7	19.27	712.3	19.27	724.4	19.26	738.8	19.22	756.2
343.15	20.23	687.9	20.27	703.4	20.28	713.1	20.27	725.2	20.26	739.6	20.22	757.0
353.15	0.1	657.37	0.1	671.80	0.1	681.05	0.1	693.26	0.1	708.09	0.1	726.60

353.15	1.07	659.9	1.13	674.1	1.12	683.3	1.13	695.5	1.10	710.3	1.06	728.5
353.15	2.08	661.2	2.12	675.8	2.13	685.0	2.12	697.1	2.11	711.7	2.07	729.9
353.15	3.09	662.6	3.13	677.2	3.14	686.4	3.13	698.5	3.12	713.1	3.08	731.2
353.15	4.10	663.9	4.14	678.5	4.15	687.7	4.14	699.8	4.13	714.3	4.09	732.3
353.15	5.11	665.1	5.15	679.6	5.16	688.9	5.15	700.9	5.14	715.4	5.10	733.4
353.15	6.12	666.2	6.15	680.8	6.17	690.0	6.16	702.1	6.15	716.6	6.11	734.5
353.15	7.13	667.3	7.17	681.9	7.18	691.2	7.17	703.2	7.16	717.7	7.12	735.6
353.15	8.14	668.6	8.18	683.2	8.19	692.4	8.18	704.4	8.17	718.9	8.13	736.8
353.15	9.15	669.7	9.19	684.3	9.20	693.5	9.18	705.5	9.18	720.0	9.14	737.8
353.15	10.16	670.7	10.20	685.3	10.21	694.5	10.20	706.5	10.19	720.9	10.15	738.8
353.15	11.18	671.8	11.21	686.4	11.22	695.6	11.21	707.6	11.20	722.0	11.16	739.9
353.15	12.18	672.8	12.22	687.4	12.23	696.7	12.22	708.7	12.21	723.1	12.17	740.8
353.15	13.19	673.8	13.23	688.5	13.24	697.7	13.23	709.7	13.22	724.1	13.17	741.8
353.15	14.20	674.8	14.24	689.4	14.25	698.7	14.24	710.7	14.23	725.0	14.19	742.8
353.15	15.20	675.8	15.25	690.5	15.25	699.7	15.25	711.7	15.24	726.1	15.19	743.8
353.15	16.21	676.8	16.25	691.5	16.26	700.8	16.24	712.7	16.24	727.0	16.20	744.7
353.15	17.21	677.8	17.26	692.5	17.27	701.7	17.26	713.7	17.25	728.0	17.20	745.7
353.15	18.22	678.6	18.26	693.3	18.27	702.6	18.26	714.5	18.26	728.9	18.21	746.5
353.15	19.23	679.4	19.26	694.2	19.28	703.4	19.27	715.4	19.26	729.7	19.22	747.4
353.15	20.23	680.3	20.28	695.1	20.28	704.3	20.27	716.3	20.25	730.6	20.22	748.2

[‡] Densities above atmospheric measured by DMA HP apparatus, and the expanded combined uncertainties ($k = 2$) U_c are $U_c(T) = 0.02\ K$, $U_c(P) = 0.03\ MPa$, $U_c(x_i) = 0.0002, U_c(\rho) = 1.12\ kg \cdot m^{-3}$

[*] At atmospheric pressures the DMA 5000 apparatus was used and the expanded combined uncertainties ($k = 2$) U_c are $U_c(P) = 0.002\ MPa$, $U_c(T) = 0.02\ K$, $U_c(x_i) = 0.0002$, $U_c(\rho) = 0.09\ kg \cdot m^{-3}$ where T is the temperature in K, P is the pressure in MPa, x_1 is the mole fraction of 2-methylpropan-1-ol, and ρ is the density in $kg \cdot m^{-3}$

Table 8.5. Experimental liquid densities for 2-methylpropan-1-ol (1) + n-decane (2) at various temperatures and pressures. ǂ

T/K	P/MPa	ρ/ kg·m^{-3}	P/MPa	ρ/ kg·m^{-3}	P/MPa	ρ/ kg·m^{-3}	P/MPa	ρ/ kg·m^{-3}	P/MPa	ρ/ kg·m^{-3}	P/MPa	ρ/ kg·m^{-3}
	x_1=0.1276		x_1=0.3749		x_1=0.5015		x_1=0.6249		x_1=0.7502		x_1=0.8750	
313.15	0.1*	717.90	0.1	727.01	0.1	733.46	0.1	741.54	0.1	752.12	0.1	766.40
313.15	1.11	719.2	1.14	729.0	1.10	735.3	1.06	743.8	1.10	754.5	1.07	768.7
313.15	2.13	720.1	2.14	730.0	2.12	736.8	2.06	745.1	2.10	755.8	2.06	769.9
313.15	3.12	720.9	3.16	730.9	3.12	737.7	3.06	746.0	3.12	756.8	3.07	770.8
313.15	4.14	721.7	4.17	731.7	4.13	738.6	4.07	746.9	4.13	757.7	4.08	771.7
313.15	5.15	722.5	5.18	732.6	5.14	739.4	5.08	747.8	5.14	758.6	5.09	772.6
313.15	6.16	723.4	6.19	733.5	6.15	740.4	6.09	748.8	6.14	759.5	6.11	773.5
313.15	7.17	724.2	7.20	734.4	7.16	741.3	7.11	749.7	7.16	760.5	7.11	774.5
313.15	8.18	725.0	8.21	735.3	8.17	742.2	8.11	750.6	8.17	761.4	8.13	775.3
313.15	9.19	725.9	9.22	736.1	9.17	743.1	9.13	751.5	9.17	762.3	9.14	776.2
313.15	10.21	726.7	10.23	737.0	10.18	744.0	10.13	752.4	10.18	763.2	10.15	777.1
313.15	11.22	727.5	11.24	737.9	11.19	744.9	11.14	753.3	11.19	764.1	11.16	778.0
313.15	12.23	728.3	12.25	738.7	12.20	745.7	12.15	754.2	12.20	764.9	12.16	778.8
313.15	13.24	729.1	13.26	739.6	13.21	746.6	13.15	755.1	13.21	765.8	13.17	779.7
313.15	14.25	729.9	14.26	740.4	14.21	747.5	14.17	756.0	14.22	766.7	14.18	780.6
313.15	15.25	730.7	15.27	741.3	15.22	748.3	15.17	756.8	15.22	767.6	15.19	781.4
313.15	16.25	731.5	16.28	742.1	16.22	749.1	16.18	757.6	16.22	768.4	16.20	782.2
313.15	17.26	732.3	17.28	742.9	17.22	750.0	17.19	758.5	17.23	769.2	17.20	783.1
313.15	18.27	732.9	18.29	743.6	18.23	750.7	18.19	759.2	18.24	770.0	18.21	783.8
313.15	19.27	733.6	19.29	744.3	19.23	751.4	19.19	759.9	19.24	770.7	19.21	784.5
313.15	20.28	734.2	20.30	744.9	20.24	752.1	20.20	760.6	20.25	771.4	20.22	785.7
323.15	0.1	710.01	0.1	718.79	0.1	725.08	0.1	733.03	0.1	743.51	0.1	757.79
323.15	1.14	711.5	1.14	720.7	1.17	727.2	1.06	735.4	1.16	746.0	1.06	760.1
323.15	2.13	712.6	2.14	722.0	2.16	728.6	2.05	736.7	2.15	747.3	2.05	761.4
323.15	3.14	713.5	3.16	723.0	3.17	729.6	3.05	737.7	3.16	748.3	3.07	762.4
323.15	4.15	714.3	4.17	723.9	4.18	730.5	4.07	738.7	4.17	749.3	4.08	763.3
323.15	5.16	715.3	5.18	724.8	5.19	731.5	5.07	739.7	5.18	750.2	5.09	764.3
323.15	6.17	716.2	6.19	725.8	6.20	732.4	6.09	740.6	6.19	751.2	6.10	765.3
323.15	7.18	717.1	7.20	726.7	7.21	733.4	7.13	741.6	7.20	752.2	7.11	766.2
323.15	8.19	717.9	8.21	727.6	8.22	734.3	8.10	742.5	8.21	753.1	8.12	767.1
323.15	9.20	718.8	9.22	728.6	9.23	735.3	9.12	743.5	9.22	754.1	9.13	768.0
323.15	10.21	719.7	10.23	729.5	10.24	736.2	10.12	744.4	10.23	755.0	10.14	769.0
323.15	11.22	720.6	11.24	730.4	11.25	737.2	11.14	745.4	11.24	756.0	11.15	769.9
323.15	12.22	721.4	12.25	731.2	12.26	738.0	12.14	746.2	12.26	756.8	12.15	770.7
323.15	13.24	722.2	13.26	732.1	13.26	738.9	13.15	747.1	13.26	757.7	13.17	771.6
323.15	14.24	723.0	14.27	733.0	14.27	739.8	14.16	748.0	14.27	758.6	14.17	772.5
323.15	15.25	723.8	15.27	733.8	15.29	740.6	15.17	748.9	15.28	759.5	15.21	773.3
323.15	16.26	724.6	16.27	734.6	16.29	741.5	16.17	749.7	16.29	760.3	16.19	774.2
323.15	17.26	725.4	17.28	735.4	17.29	742.3	17.18	750.6	17.29	761.2	17.19	775.0
323.15	18.27	726.1	18.29	736.2	18.30	743.0	18.18	751.3	18.30	761.9	18.20	775.8

323.15	19.27	726.7	19.29	736.9	19.31	743.7	19.19	752.1	19.30	762.7	19.20	776.5
323.15	20.28	727.6	20.30	737.5	20.32	744.4	20.20	752.8	20.30	763.4	20.21	777.2
333.15	0.1	701.99	0.1	710.39	0.1	716.51	0.1	724.34	0.1	734.75	0.1	749.09
333.15	1.14	703.8	1.16	712.3	1.17	718.7	1.05	726.7	1.15	737.1	1.06	751.3
333.15	2.13	704.9	2.15	713.8	2.16	720.2	2.05	728.1	2.15	738.6	2.06	752.8
333.15	3.14	705.9	3.16	714.8	3.17	721.2	3.05	729.1	3.16	739.6	3.06	753.8
333.15	4.15	706.8	4.17	715.8	4.19	722.1	4.06	730.1	4.17	740.6	4.07	754.8
333.15	5.16	707.8	5.18	716.8	5.19	723.2	5.07	731.2	5.18	741.7	5.08	755.8
333.15	6.17	708.7	6.19	717.7	6.20	724.1	6.09	732.1	6.19	742.6	6.09	756.8
333.15	7.18	709.6	7.20	718.7	7.21	725.1	7.09	733.1	7.20	743.6	7.11	757.7
333.15	8.19	710.7	8.21	719.8	8.22	726.3	8.10	734.3	8.21	744.8	8.12	758.9
333.15	9.20	711.4	9.22	720.6	9.24	727.0	9.12	735.1	9.22	745.6	9.13	759.7
333.15	10.21	712.3	10.23	721.5	10.24	728.0	10.12	736.0	10.23	746.5	10.14	760.6
333.15	11.22	713.2	11.24	722.4	11.25	728.9	11.13	737.0	11.24	747.5	11.15	761.5
333.15	12.22	714.1	12.25	723.3	12.27	729.8	12.14	737.9	12.25	748.4	12.16	762.5
333.15	13.24	714.9	13.26	724.2	13.27	730.7	13.15	738.8	13.26	749.3	13.17	763.3
333.15	14.25	715.7	14.27	725.1	14.28	731.6	14.16	739.7	14.27	750.2	14.17	764.2
333.15	15.25	716.6	15.27	726.0	15.28	732.5	15.16	740.6	15.27	751.1	15.18	765.2
333.15	16.26	717.4	16.28	726.8	16.30	733.4	16.19	741.5	16.28	752.0	16.19	766.0
333.15	17.26	718.2	17.29	727.6	17.30	734.2	17.20	742.3	17.29	752.8	17.20	766.8
333.15	18.27	718.9	18.30	728.4	18.31	735.0	18.20	743.1	18.30	753.6	18.20	767.6
333.15	19.27	719.6	19.30	729.1	19.31	735.7	19.20	743.9	19.30	754.4	19.20	768.4
333.15	20.28	720.3	20.30	729.9	20.31	736.5	20.20	744.6	20.30	755.2	20.23	769.1
343.15	0.1	693.88	0.1	701.63	0.1	707.44	0.1	715.04	0.1	725.31	0.1	739.73
343.15	1.14	696.0	1.16	703.8	1.18	709.7	1.05	717.2	1.11	727.9	1.07	741.9
343.15	2.13	697.1	2.16	705.3	2.17	711.2	2.04	718.9	2.12	729.1	2.08	743.3
343.15	3.14	698.1	3.17	706.3	3.18	712.3	3.05	719.9	3.13	730.2	3.04	744.4
343.15	4.15	699.1	4.17	707.3	4.19	713.3	4.06	721.0	4.14	731.2	4.08	745.4
343.15	5.16	699.9	5.19	708.2	5.20	714.2	5.07	721.9	5.15	732.2	5.08	746.4
343.15	6.17	700.9	6.20	709.2	6.20	715.2	6.08	722.9	6.16	733.2	6.10	747.4
343.15	7.18	702.0	7.14	710.3	7.22	716.3	7.09	724.0	7.17	734.3	7.11	748.5
343.15	8.19	703.0	8.21	711.3	8.23	717.3	8.10	725.0	8.18	735.3	8.12	749.5
343.15	9.20	703.9	9.22	712.2	9.24	718.3	9.11	726.0	9.19	736.3	9.13	750.5
343.15	10.21	704.8	10.24	713.1	10.25	719.2	10.12	727.0	10.20	737.3	10.14	751.4
343.15	11.22	705.8	11.24	714.2	11.26	720.2	11.13	728.0	11.22	738.3	11.15	752.4
343.15	12.23	706.6	12.25	715.0	12.27	721.1	12.14	728.9	12.23	739.2	12.16	753.3
343.15	13.24	707.5	13.26	716.0	13.27	722.1	13.14	729.9	13.23	740.2	13.17	754.3
343.15	14.25	708.4	14.27	716.9	14.28	723.0	14.16	730.8	14.25	741.1	14.17	755.2
343.15	15.25	709.2	15.28	717.8	15.29	723.9	15.16	731.7	15.25	742.0	15.18	756.1
343.15	16.26	710.1	16.29	718.6	16.29	724.7	16.17	732.5	16.26	742.8	16.19	756.9
343.15	17.27	710.9	17.29	719.5	17.30	725.6	17.18	733.4	17.26	743.7	17.20	757.8
343.15	18.27	711.7	18.29	720.3	18.31	726.4	18.19	734.3	18.27	744.6	18.20	758.6
343.15	19.27	712.4	19.30	721.0	19.32	727.2	19.19	735.0	19.27	745.4	19.21	759.4
343.15	20.28	713.1	20.30	721.8	20.33	728.0	20.19	735.8	20.28	746.1	20.21	760.2
353.15	0.1	685.77	0.1	692.81	0.1	698.30	0.1	705.71	0.1	715.89	0.1	730.54

353.15	1.13	687.5	1.15	694.8	1.17	700.1	1.05	707.7	1.04	718.0	1.06	732.3
353.15	2.15	688.9	2.17	696.2	2.18	701.7	2.05	709.1	2.04	719.2	2.07	733.6
353.15	3.14	690.1	3.17	697.4	3.19	703.0	3.05	710.4	3.05	720.5	3.07	734.8
353.15	4.15	691.2	4.17	698.5	4.20	704.1	4.06	711.5	4.06	721.6	4.08	735.9
353.15	5.16	692.2	5.19	699.6	5.21	705.2	5.07	712.6	5.07	722.7	5.09	737.0
353.15	6.17	693.3	6.20	700.6	6.22	706.2	6.08	713.6	6.08	723.7	6.10	738.1
353.15	7.19	694.3	7.21	701.6	7.23	707.3	7.10	714.7	7.09	724.8	7.11	739.1
353.15	8.19	695.3	8.22	702.7	8.24	708.4	8.10	715.8	8.10	725.9	8.12	740.2
353.15	9.14	696.3	9.23	703.8	9.25	709.4	9.11	716.8	9.11	727.0	9.13	741.3
353.15	10.22	697.2	10.24	704.7	10.26	710.3	10.12	717.8	10.12	727.9	10.14	742.2
353.15	11.23	698.2	11.25	705.7	11.27	711.4	11.13	718.8	11.13	728.9	11.15	743.2
353.15	12.24	699.1	12.26	706.6	12.27	712.3	12.14	719.8	12.14	729.9	12.16	744.2
353.15	13.24	700.1	13.27	707.6	13.28	713.3	13.15	720.8	13.15	730.9	13.17	745.2
353.15	14.25	700.9	14.28	708.5	14.29	714.2	14.14	721.7	14.16	731.8	14.17	746.1
353.15	15.26	701.9	15.28	709.4	15.30	715.1	15.17	722.6	15.17	732.8	15.18	747.0
353.15	16.27	702.8	16.29	710.4	16.30	716.1	16.20	723.6	16.18	733.7	16.19	748.0
353.15	17.28	703.6	17.30	711.2	17.31	717.0	17.20	724.5	17.18	734.6	17.19	748.9
353.15	18.28	704.4	18.30	712.0	18.32	717.8	18.21	725.3	18.18	735.5	18.21	749.7
353.15	19.28	705.1	19.31	712.8	19.32	718.6	19.21	726.1	19.19	736.3	19.21	750.5
353.15	20.29	705.9	20.31	713.6	20.32	719.4	20.20	727.0	20.20	737.1	20.21	751.4
353.15												

[‡]Densities above atmospheric measured by DMA HP apparatus, and the expanded combined uncertainties (k = 2) U_c are $U_c(T) = 0.02\ K$, $U_c(P) = 0.03\ MPa$, $U_c(x_i) = 0.0002, U_c(\rho) = \ 1.12\ kg \cdot m^{-3}$

[*]At atmospheric pressures the DMA 5000 apparatus was used and the expanded combined uncertainties (k = 2) U_c are $U_c(P) = 0.002\ MPa$, $U_c(T) = 0.02\ K$, $U_c(x_i) = 0.0002$, $U_c(\rho) = \ 0.09\ kg \cdot m^{-3}$ where T is the temperature in K, P is the pressure in MPa, $x_1$is the mole fraction of 2-methylpropan-1-ol, and ρ is the density in $kg \cdot m^{-3}$

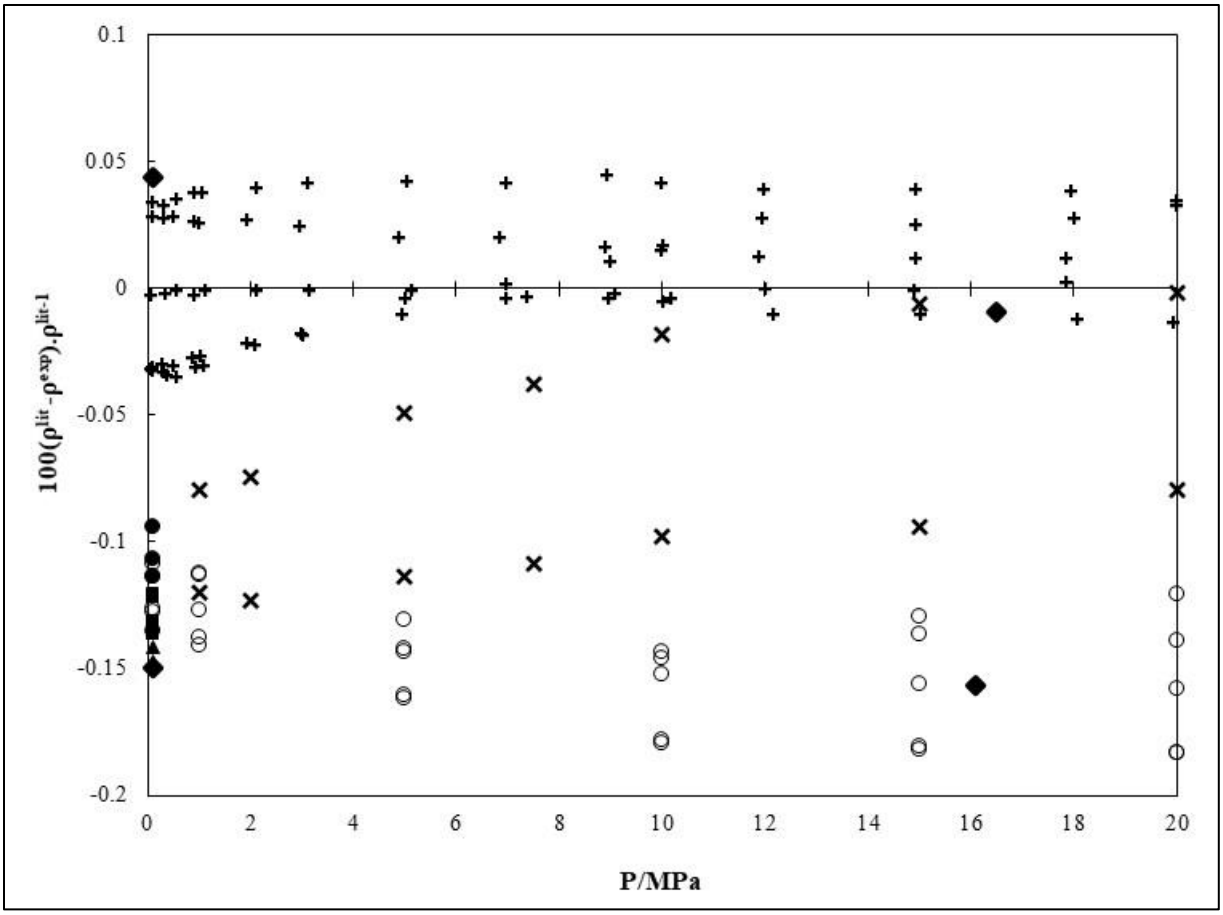

Figure 8.2. Comparison of experimental 2-methylpropan-1-ol density data (ρ_{exp}) at 0.1 MPa and various temperatures to literature (ρ_{lit}). ■-Bravo-Sánchez et al.(Iglesias-Silva et al., 2015), ●- Cano-Gómez et al.(Cano-Gómez et al., 2017), ▲- Kermanpour and Niakan(Kermanpour and Niakan, 2012), ♦- Kubota et al.(Kubota et al., 1987), ×-(Golubev *et al.*, 1980), +-(Iglesias-Silva et al., 2015), ○-(Majstorović et al., 2020).

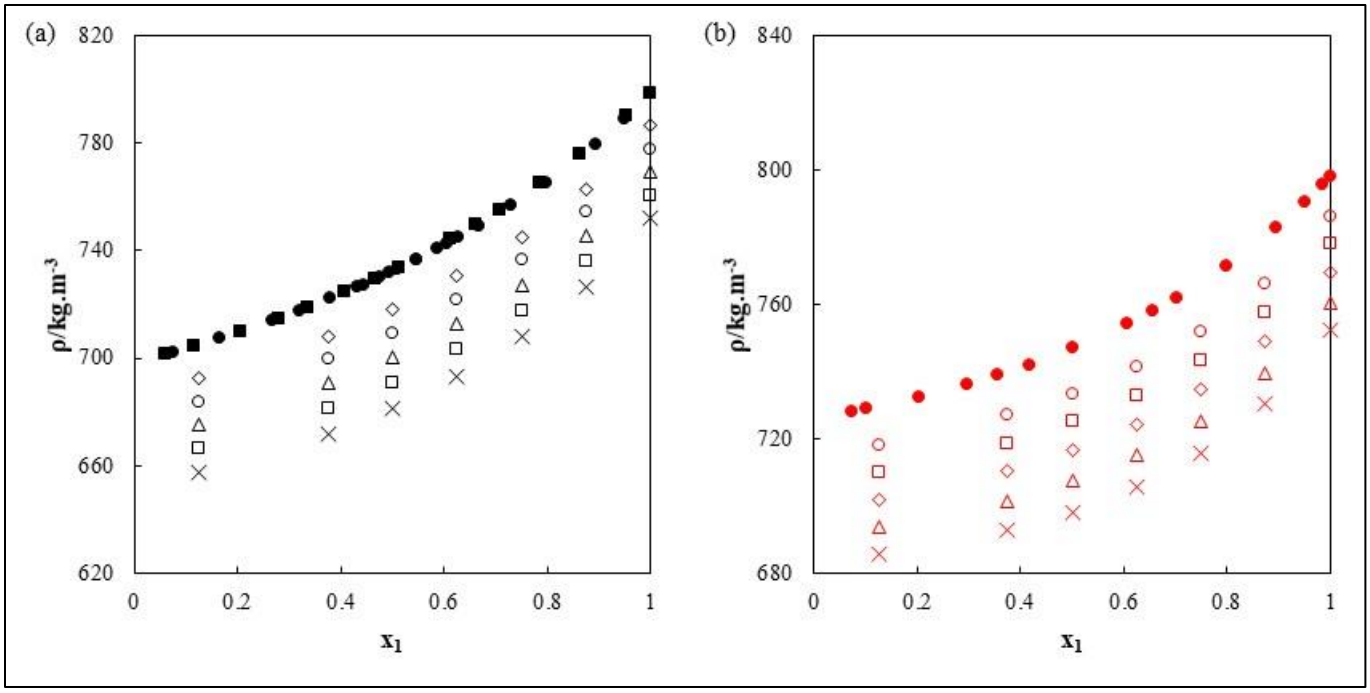

Figure 8.3. (a) Density data (ρ) for the 2-methylpropan-1-ol (1) + n-octane (2) system at 0.1 MPa. This work (◊-313.15 K, ○-323.15 K, Δ -333.15 K, □-343.15 K, ×-353.15 K). ●-(Chaudhari and Katti, 1985) at 298.14 K, ■-(Dubey and Sharma, 2007) at 298.15 K. (b) 2-methylpropan-1-ol (1) + n-decane (2) system at 0.1 MPa. This work (○-313.15 K, □-323.15 K, ◊-333.15 K, Δ -343.15 K, ×-353.15 K). ●-(Dubey and Sharma, 2007) at 298.15 K.

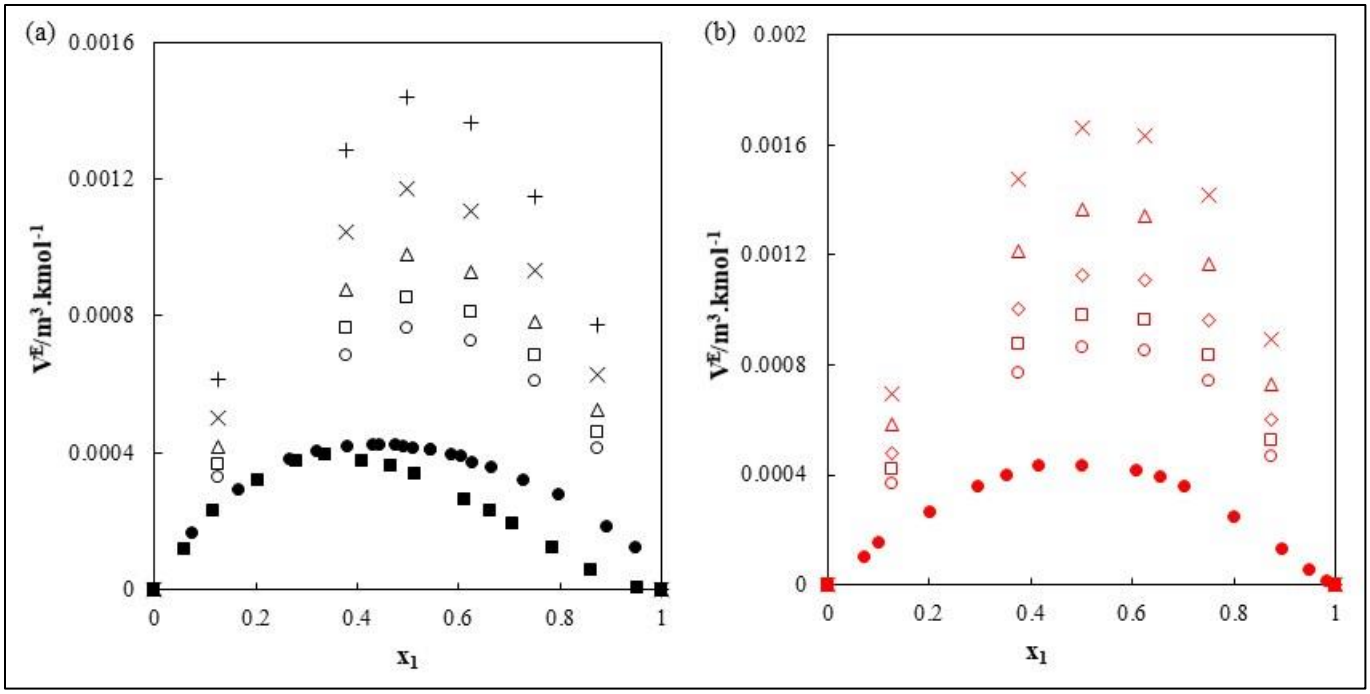

Figure 8.4. Excess volume (V^E) vs. x_1 at various temperatures and at 0.1 MPa. (a) 2-methylpropan-1-ol (1) + n-octane (2) system. This work (○-313.15 K, □-323.15 K, Δ-333.15 K, ×-343.15 K, +-353.15 K). ●- (Chaudhari and Katti, 1985) at 298.14 K, ■-(Dubey and Sharma, 2007) at 298.15 K. (b) 2-methylpropan-1-ol (1) + n-decane (2) system. This work (○-313.15 K, □-323.15 K, ◊-333.15 K, Δ-343.15 K, ×-353.15 K). ●-(Dubey and Sharma, 2007) at 298.15 K.

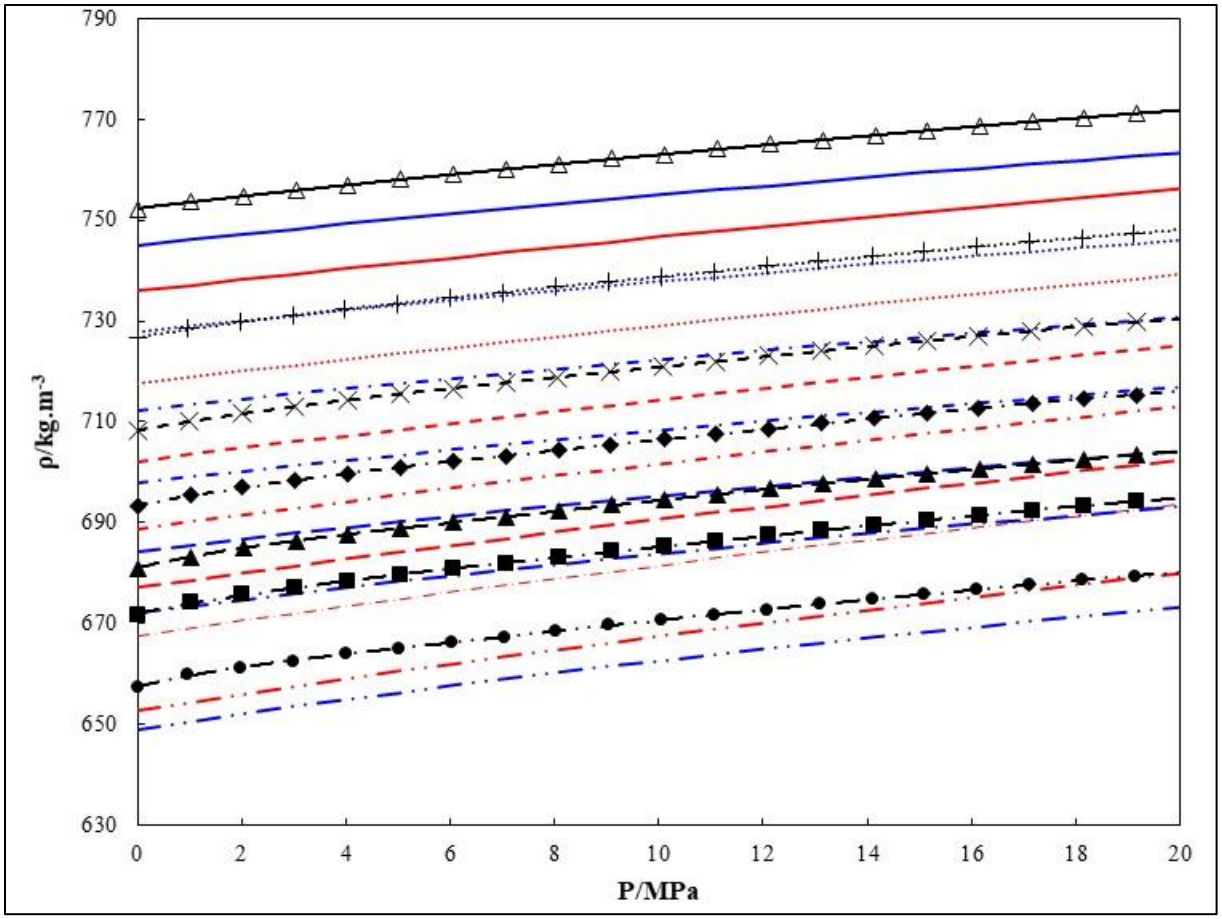

Figure 8.5. Experimental and model calculated mixture density data (ρ) for the 2-methylpropan-1-ol (1) + n-octane (2) system as a function of pressure (P) at 353.15 K and various compositions. (exp, model) x_1: (●, —·—)- x_1 = 0.1267, (■, —·—)- x_1 = 0.3776- (▲, -···-), x_1 = 0.4996- (♦, -·-), x_1 = 0.6255, (×, - - -)- x_1 = 0.7499- (+, ·····), x_1 = 0.8739, (Δ, —)- x_1 = 1. Black lines-Modified Toscani-Szwarc EOS (Zúñiga-Moreno and Galicia-Luna, 2002), Blue lines-Peng-Robinson (Peng and Robinson, 1976) correlation (k_{ij} = -0.146), Red lines-PC-SAFT prediction (Gross and Sadowski, 2002, 2001).

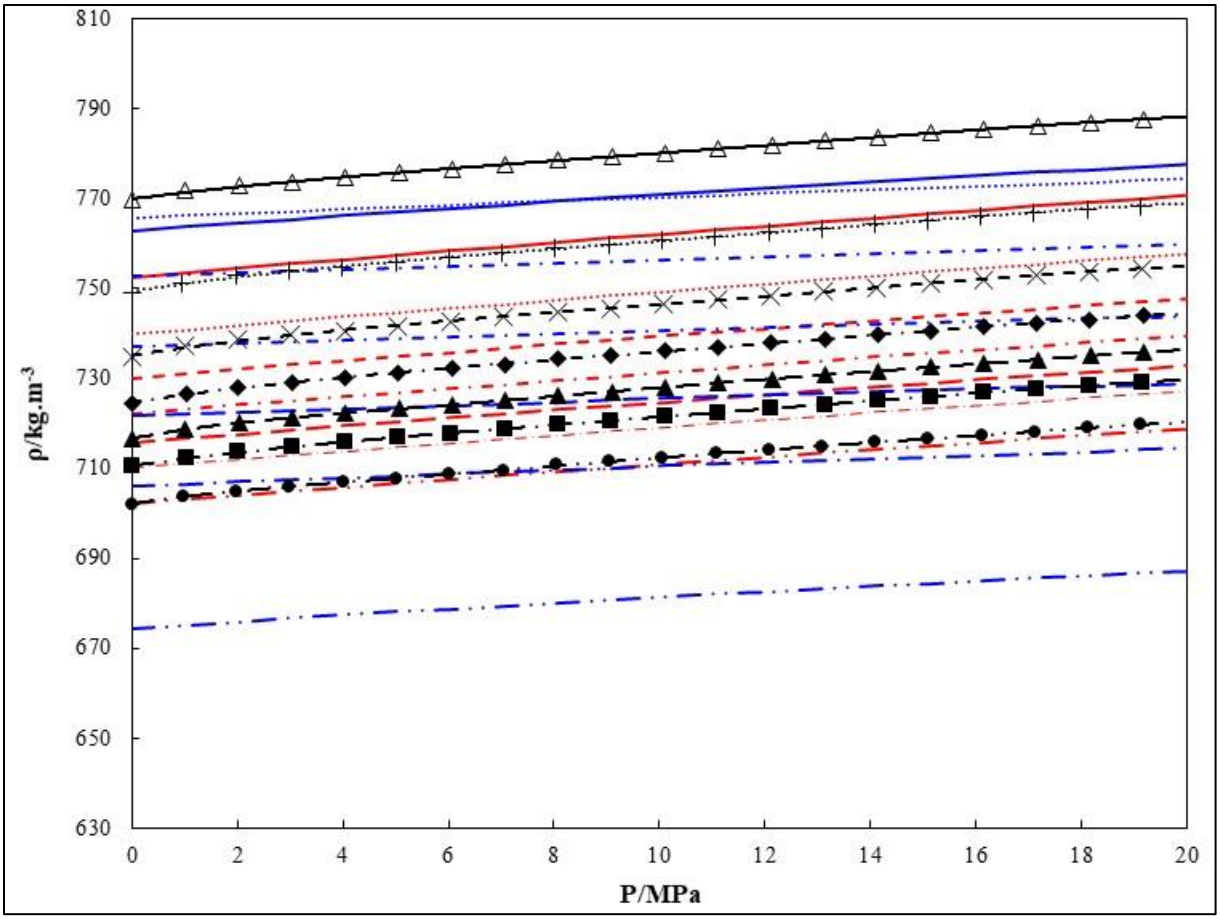

Figure 8.6. Experimental and model calculated mixture density data (ρ) for the 2-methylpropan-1-ol (1) + n-decane (2) system as a function of pressure (P) at 333.15 K and various compositions. (exp, model) x_1: (●, —··—)- x_1 = 0.1276, (■, —·—)- x_1 = 0.3749- (▲, -··-), x_1 = 0.5015- (♦, -·-), x_1 = 0.6249, (×, - - -)- x_1 = 0.7501- (+, ·····), x_1 = 0.8750, (Δ, —)- x_1 = 1. Black lines-Modified Toscani-Szwarc EOS (Zúñiga-Moreno and Galicia-Luna, 2002), Blue lines-Peng-Robinson (Peng and Robinson, 1976) correlation (k_{ij} = -0.957), Red lines-PC-SAFT prediction (Gross and Sadowski, 2002, 2001).

Table 8.6. Regressed parameters for the Modified Toscani-Szwarc (MTS) equation of state.

x_1	c_1/MPa.m^3.kg^{-1}	c_2/m^3.kg^{-1}	c_3 /MPa	c_4 /K.MPa	c_5 /K$^{1/3}$.MPa	*RMSD*[a]
n-octane (1)(Hussain and Moodley, 2020a)						
1	0.1684	1.218E-03	-234.093	34305.804	-3119.462	3.37E-04
n-decane (1)(Hussain and Moodley, 2020a)						
1	0.1827	1.178E-03	-236.870	38103.225	-3321.140	1.930E-04
2-methylpropan-1-ol (1)						
1	0.1876	1.056E-03	-407.246	64652.057	-5170.345	2.06E-04
2-methylpropan-1-ol (1) + n-octane (2)						
0.1267	0.1618	1.206E-03	-298.668	44293.447	-3750.576	3.44E-04
0.3776	0.1778	1.149E-03	-441.108	66365.128	-5291.641	3.91E-04
0.4996	0.1821	1.126E-03	-497.292	75180.303	-5897.628	3.95E-04
0.6255	0.1885	1.100E-03	-531.678	80846.146	-6301.010	3.90E-04
0.7499	0.1957	1.073E-03	-562.344	86224.208	-6681.165	3.71E-04
0.8739	0.1951	1.058E-03	-541.753	84061.912	-6514.672	3.19E-04
2-methylpropan-1-ol (1) + n-decane (2)						
0.1276	0.1727	1.175E-03	-300.308	47356.458	-3908.413	2.02E-04
0.3749	0.1961	1.121E-03	-465.584	72615.530	-5705.591	2.71E-04
0.5015	0.2065	1.092E-03	-549.106	85364.050	-6610.391	3.18E-04
0.6249	0.2133	1.068E-03	-612.202	95201.828	-7297.789	3.41E-04
0.7502	0.2221	1.042E-03	-625.973	97162.578	-7494.489	3.28E-04
0.8750	0.2149	1.036E-03	-594.858	92956.435	-7175.573	3.03E-04

[a] $RMSD = \frac{\left(\sum_k^L \left((\frac{\rho^{exp} - \rho^{calc}}{\rho^{exp}})^2 \right) \right)^{1/2}}{L^{1/2}}$

c_i are fitting parameters for equation (8.1)

Table 8.7. Pure component parameters used for Peng-Robinson Equation and PC-SAFT model[a]

Component	T_c/K (Poling et al., 2001)	P_c/kPa (Poling et al., 2001)	Ω (Poling et al., 2001)	m	σ/Å	$\frac{\epsilon}{k}$/K	κ^{AB}	$\frac{\epsilon^{AB}}{k}$ /k
2-methylpropan-1-ol	547.78	4300	0.59	2.02 (Zarei and Feyzi, 2013)	4.04 (Zarei and Feyzi, 2013)	287.17 (Zarei and Feyzi, 2013)	0.002503 (Zarei and Feyzi, 2013)	2754.71 (Zarei and Feyzi, 2013)
n-octane	568.7	2490	0.399	5.0291 (Burgess et al., 2012)	3.5167 (Burgess et al., 2012)	229.30 (Burgess et al., 2012)	-	-
n-decane	617.7	2110	0.490	6.9000 (Burgess et al., 2012)	3.3665 (Burgess et al., 2012)	226.86 (Burgess et al., 2012)	-	-

[a]T_c and P_c are the critical temperature and pressure, ω is the acentric factor. m is the number of segments per chain, σ is the segment diameter, $\frac{\epsilon}{k}$ is the depth of pair potential over the Boltzman constant, κ^{AB} is the effective association volume, $\frac{\epsilon^{AB}}{k}$ is the association energy, in the PC-SAFT model.

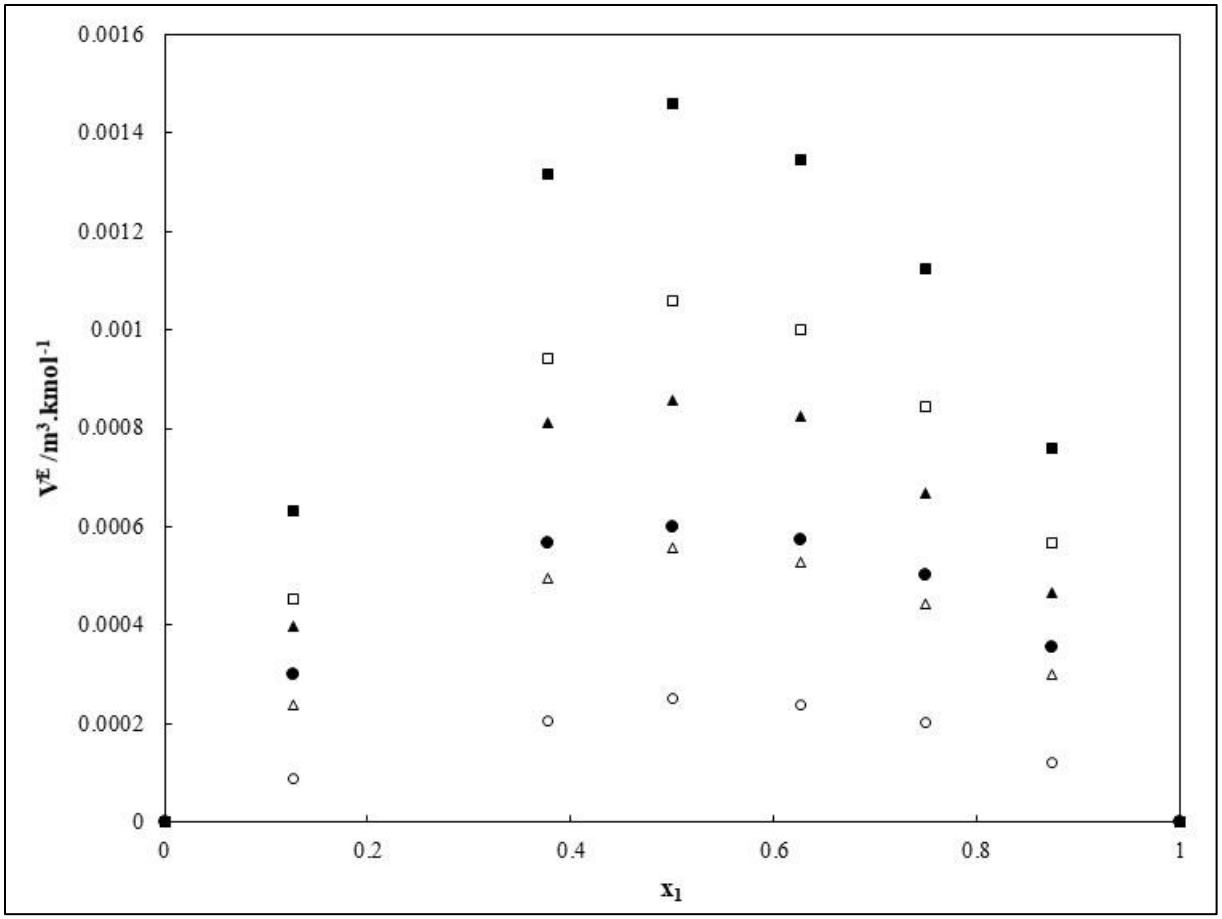

Figure 8.7. Calculated excess volume (V^E) for the 2-methylpropan-1-ol (1) + n-octane (2) system at selected temperatures and pressures. (symbol-T, P): (■- 353.15 K, 1 MPa), (□- 353.15 K, 20 MPa), (▲- 333.15 K, 1MPa), (∆- 333.15 K, 2- MPa), (●- 313.15 K, 1 MPa), (○- 313.15 K, 20 MPa).

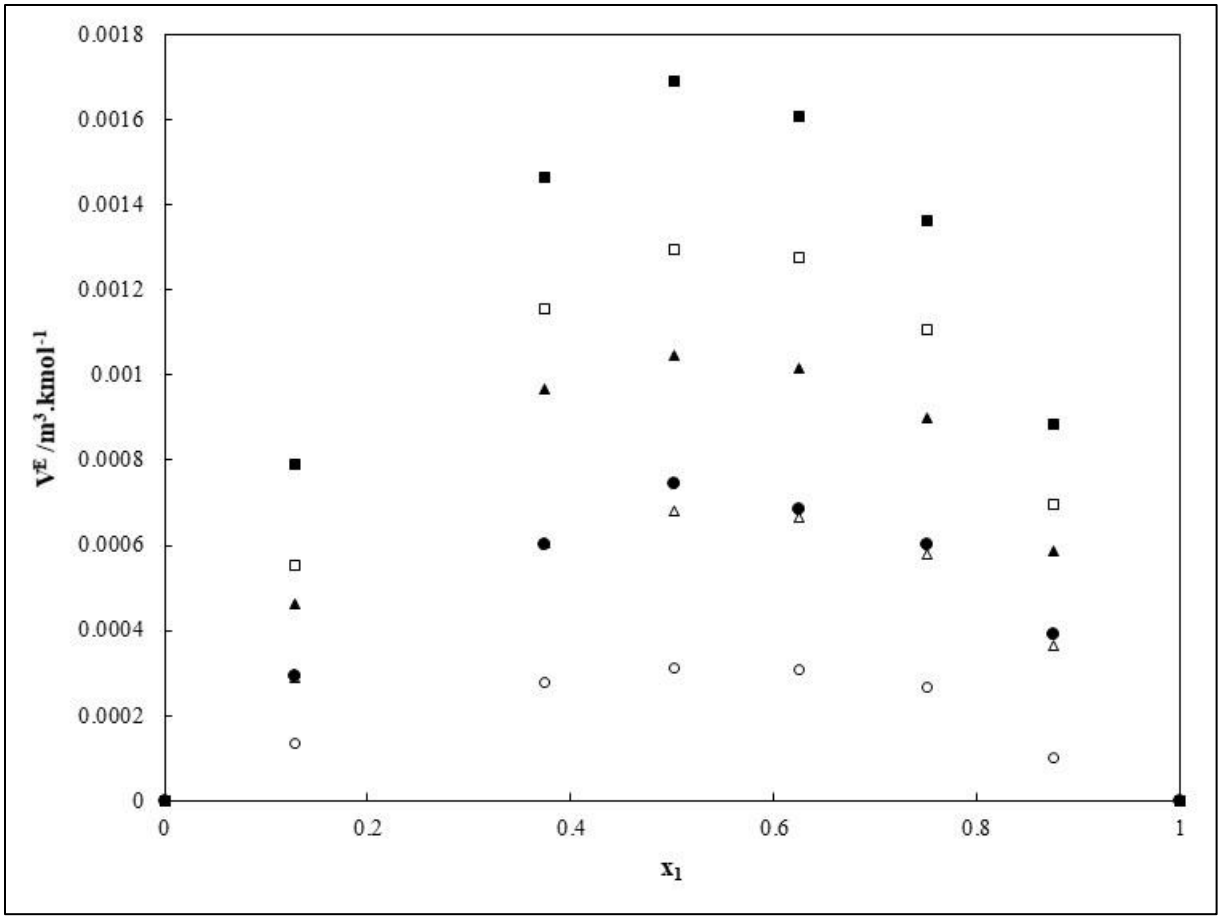

Figure 8.8. Calculated excess volume (V^E) for the 2-methylpropan-1-ol (1) + n-decane (2) system at selected temperatures and pressures. (symbol-T, P): (■- 353.15 K, 1 MPa), (□- 353.15 K, 20 MPa), (▲- 333.15 K, 1MPa), (Δ- 333.15 K, 2- MPa), (●- 313.15 K, 1 MPa), (○- 313.15 K, 20 MPa).

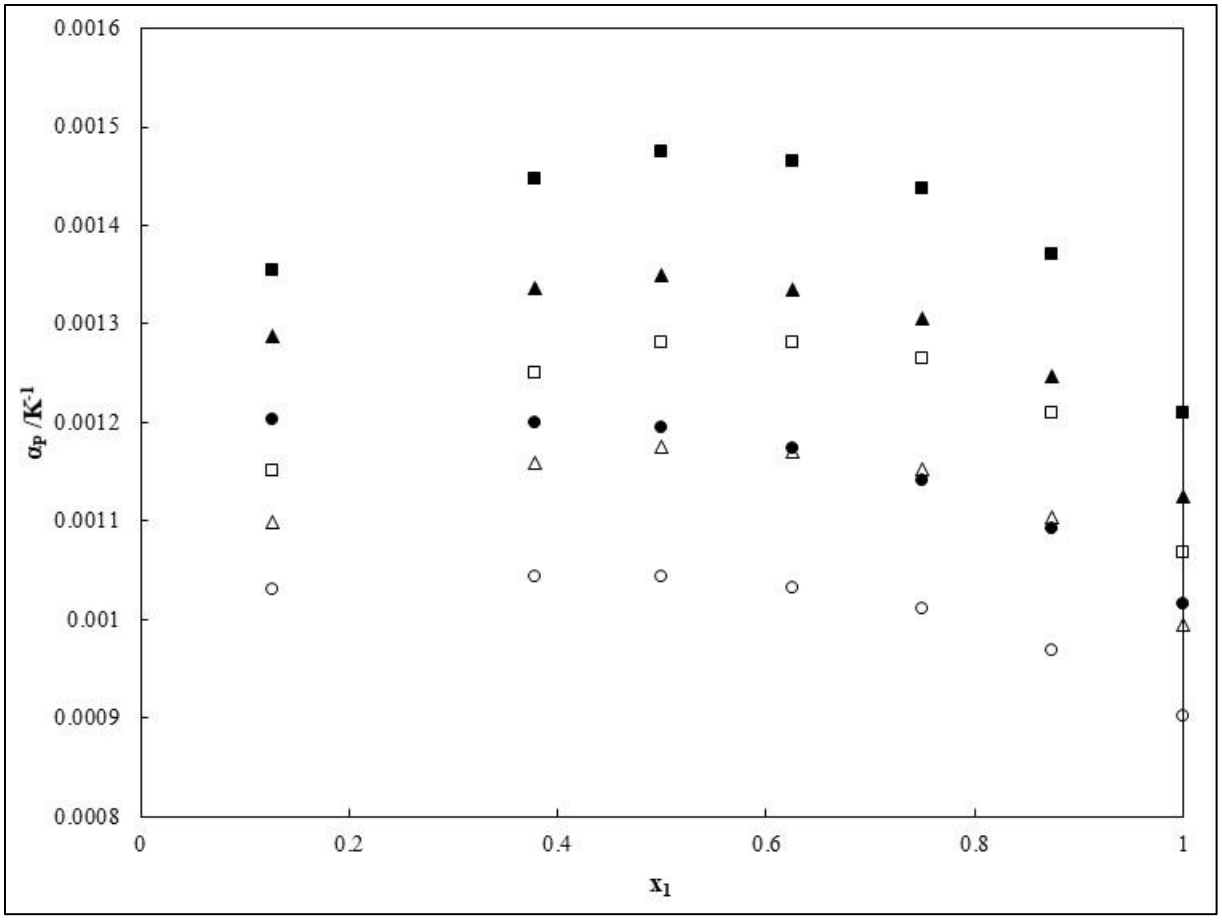

Figure 8.9. Calculated thermal expansivity (α_p) for the 2-methylpropan-1-ol (1) + n-octane (2) system at selected temperatures and pressures. (symbol-T, P): (■-353.15 K, 1 MPa), (□-353.15 K, 20 MPa), (▲-333.15 K, 1 MPa), (Δ -333.15 K, 20 MPa), (●-313.15 K, 1 MPa), (○-313.15 K, 20 MPa).

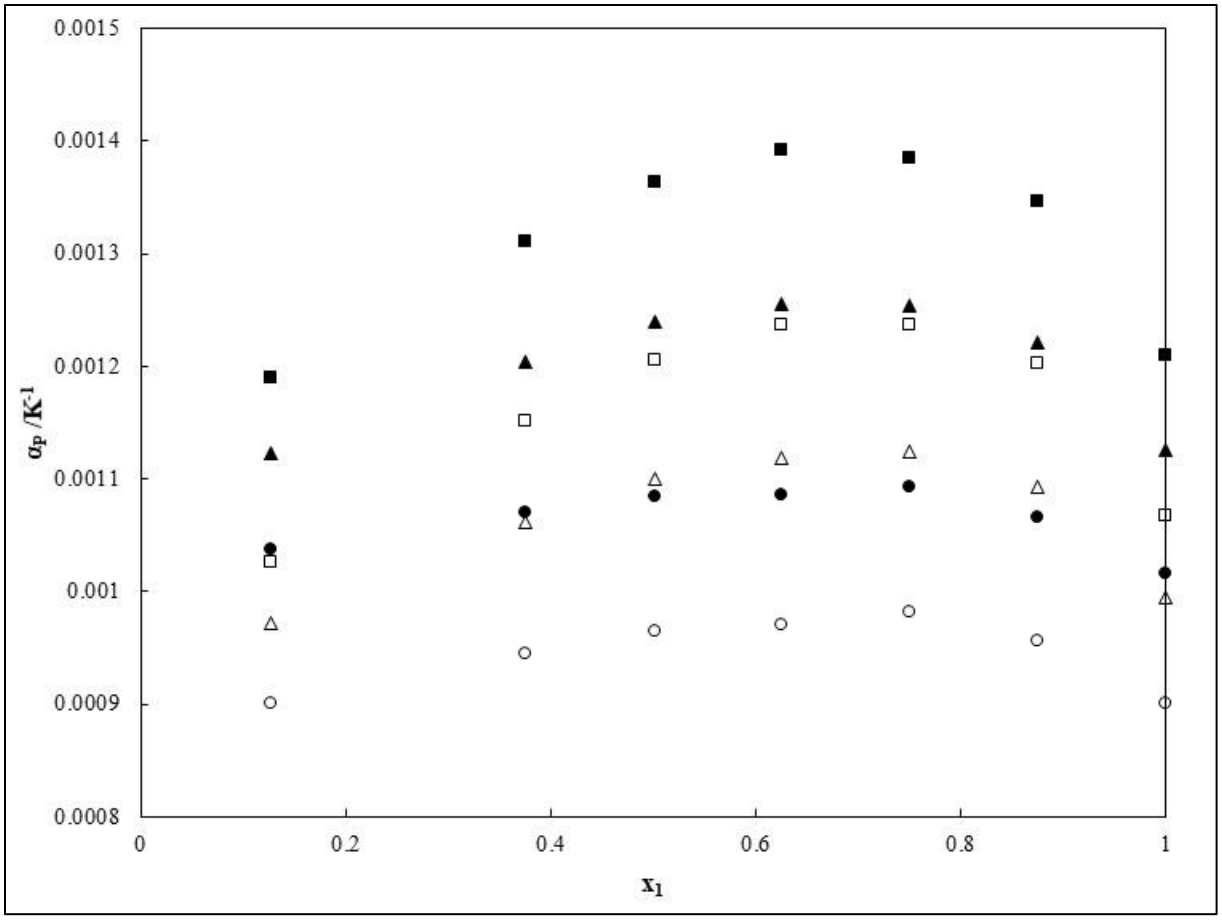

Figure 8.10. Calculated thermal expansivity (α_P) vs. x_1 for the 2-methylpropan-1-ol (1) + n-decane (2) system at selected temperatures and pressures. (symbol-T, P): (■- 353.15 K, 1 MPa), (□- 353.15 K, 20 MPa), (▲- 333.15 K, 1MPa), (∆- 333.15 K, 2- MPa), (●- 313.15 K, 1 MPa), (○- 313.15 K, 20 MPa).

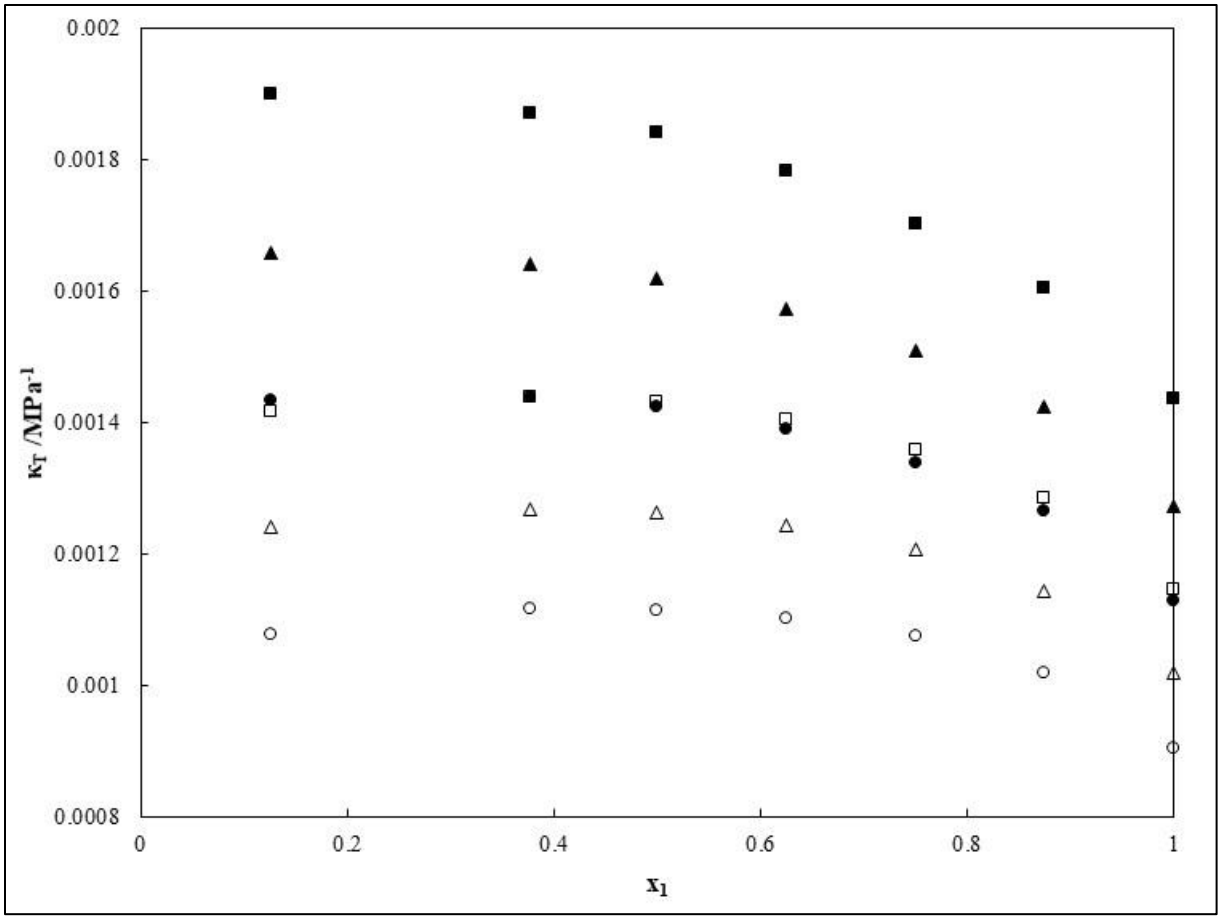

Figure 8.11. Calculated isothermal compressibility (κ_T) for the 2-methylpropan-1-ol (1) + n-octane (2) system at selected temperatures and pressures. (symbol-T, P): (■-353.15 K, 1 MPa), (□-353.15 K, 20 MPa), (▲-333.15 K, 1 MPa), (Δ -333.15 K, 20 MPa), (●-313.15 K, 1 MPa), (○-313.15 K, 20 MPa).

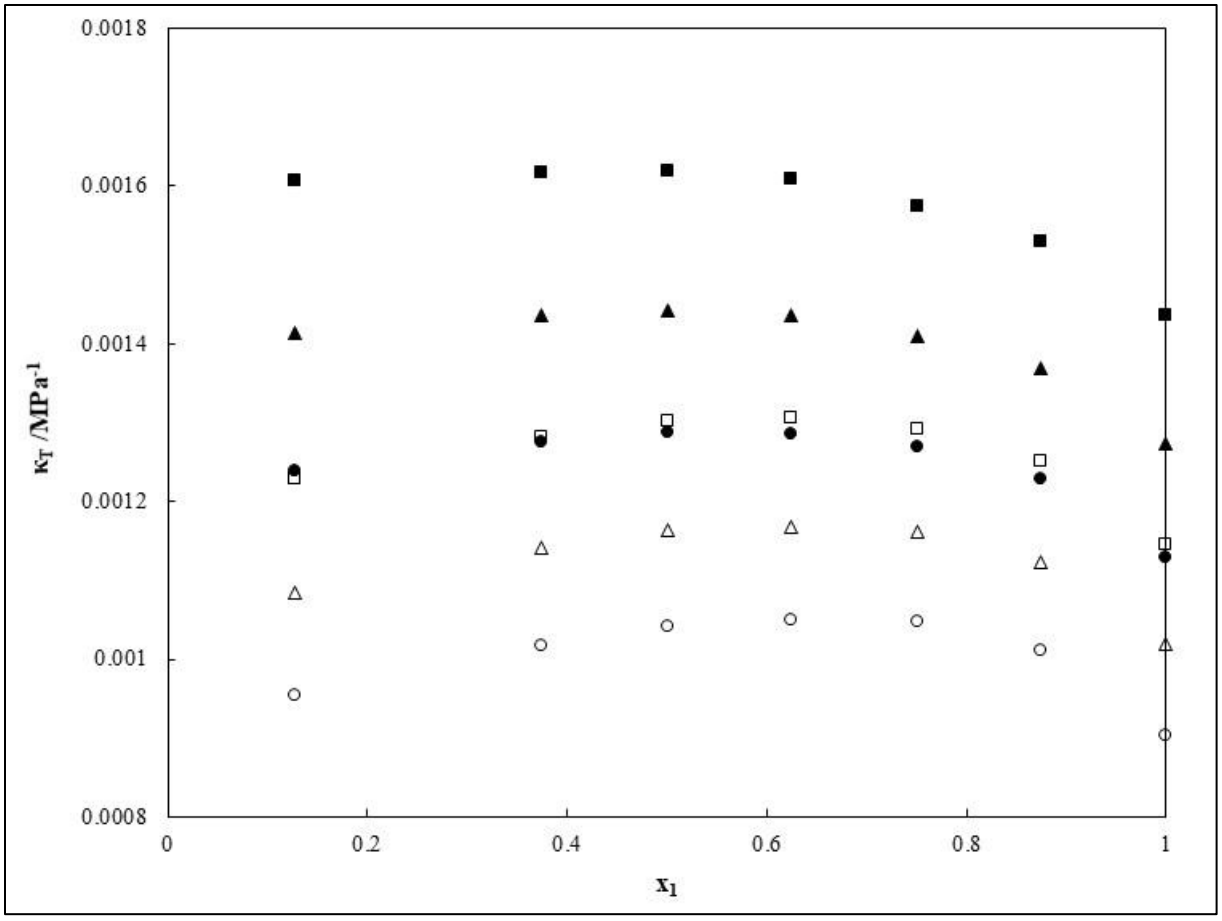

Figure 8.12. Calculated compressibility (κ_T) vs. x_1 for the 2-methylpropan-1-ol (1) + n-decane (2) system at selected temperatures and pressures. (symbol-T, P): (■- 353.15 K, 1 MPa), (□- 353.15 K, 20 MPa), (▲- 333.15 K, 1MPa), (Δ- 333.15 K, 2- MPa), (●- 313.15 K, 1 MPa), (○- 313.15 K, 20 MPa).

8.6. Conclusions

Novel isothermal measurements for the binary systems {2-methylpropan-1-ol (1) + n-octane (2)} and {2-methylpropan-1-ol (1) + n-decane (2)} are presented in this work. These measurements were conducted for 5 temperatures T = (313.15 to 353.15) K over the pressure range P = (0.1 to 20) MPa. An Anton Paar DMA HP densimeter was utilized to conduct the high-pressure experiments. The experimental procedure and setup were both verified by measuring pure component densities for 2-methylpropan-1-ol as well as conducting atmospheric pressure measurements for both binary systems, all of which demonstrate a satisfactory comparison with literature. The experimental data were regressed to obtain the 5 parameters required for the modified Toscani-Szwarc equation which provided a suitable correlation of the data with a

maximum RMSD = 3.95 x 10^{-4}. Furthermore, correlation by the Peng- Robinson (1976) equation of state, with a single binary interaction parameter, and prediction by the PC-SAFT (Gross and Sadowski, 2002, 2001) model were qualitative at best, when compared to the experimental data with RMSDs from the Peng-Robinson equation of state of 0.006 and 0.020, and from the PC-SAFT model of 0.011 and 0.011 for the n-octane and n-decane systems respectively. The excess molar volume, thermal expansivity and isothermal compressibility were also computed utilizing the regressed parameters. A large positive deviation is noted for the excess molar volumes of both systems. In addition, the highly non-linear behaviour demonstrated by both the thermal expansivity and isothermal compressibility further confirms the non-ideal mixing occurring in the systems.

CHAPTER NINE

Culminating results

9.1.Pure Components

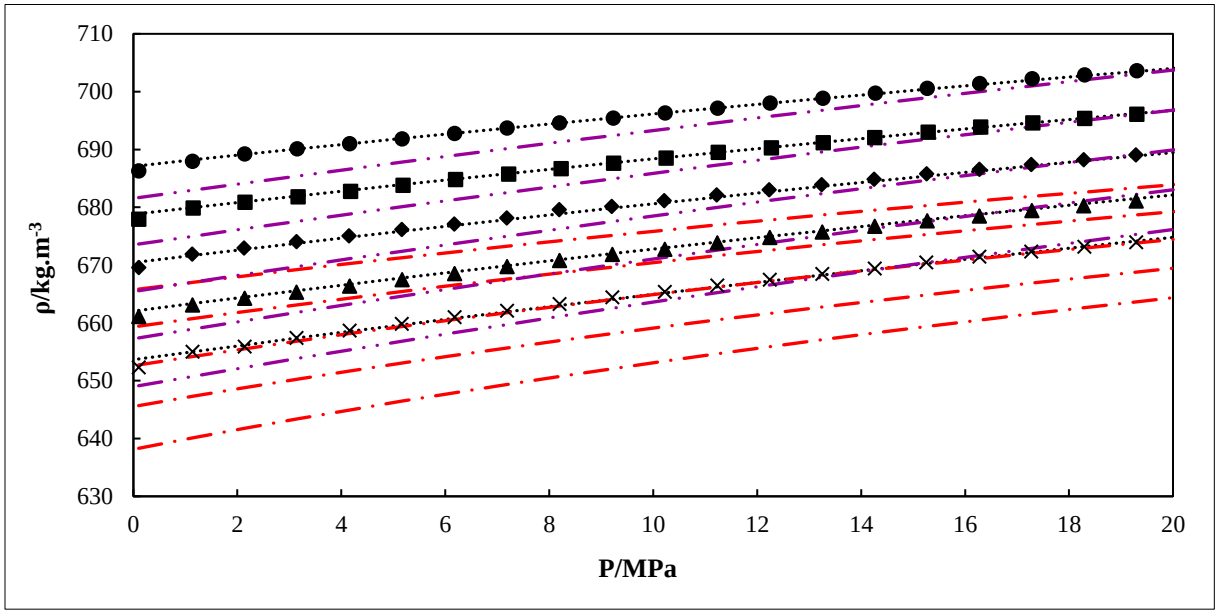

Figure 9.1. Experimental and model calculated density data (ρ) for n-octane as a function of pressure (P) and temperature (T). (Symbol-T): (●- 313.15 K), (■- 323.15 K), (♦- 333.15 K), (▲- 343.15 K), (×- 353.15 K). (Line-Model): (···· - MTS), (—·— - PR), (—··— - PC-SAFT).

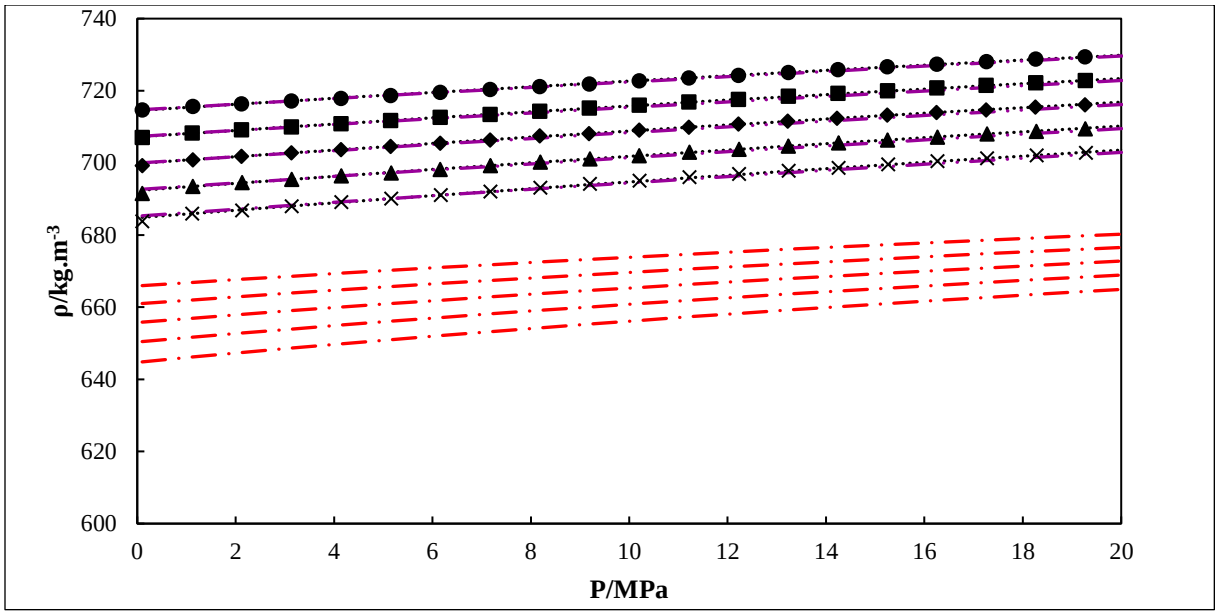

Figure 9.2. Experimental and model calculated density data (ρ) for n-decane as a function of pressure (P) and temperature (T). (Symbol-T): (●- 313.15 K), (■- 323.15 K), (♦- 333.15 K), (▲- 343.15 K), (×- 353.15 K). (Line-Model): (···· - MTS), (—·— - PR), (—··— - PC-SAFT).

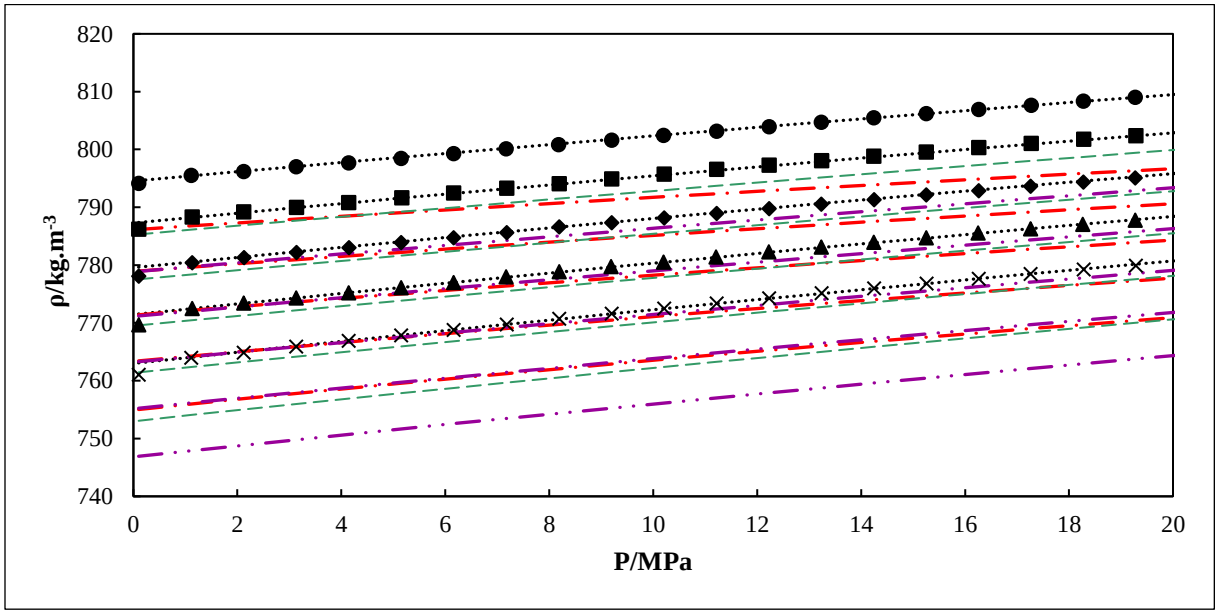

Figure 9.3. Experimental and model calculated density data (ρ) for butan-1-ol as a function of pressure (P) and temperature (T). (Symbol-T): (●- 313.15 K), (■- 323.15 K), (♦- 333.15 K), (▲- 343.15 K), (×- 353.15 K). (Line-Model): (···· - MTS), (—·— - PR), (—··— - PC-SAFT), (— — - tPC-PSAFT).

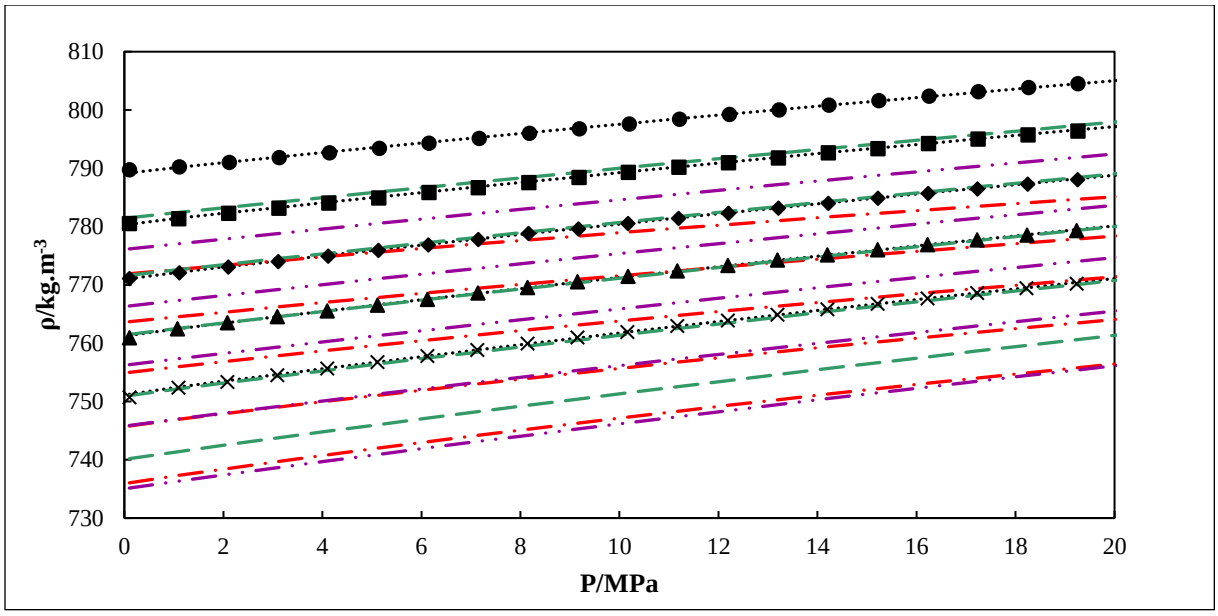

Figure 9.4. Experimental and model calculated density data (ρ) for butan-2-ol as a function of pressure (P) and temperature (T). (Symbol-T): (●- 313.15 K), (■- 323.15 K), (♦- 333.15 K), (▲- 343.15 K), (×- 353.15 K). (Line-Model): (···· - MTS), (—·— - PR), (—··— - PC-SAFT), (— — - tPC-PSAFT).

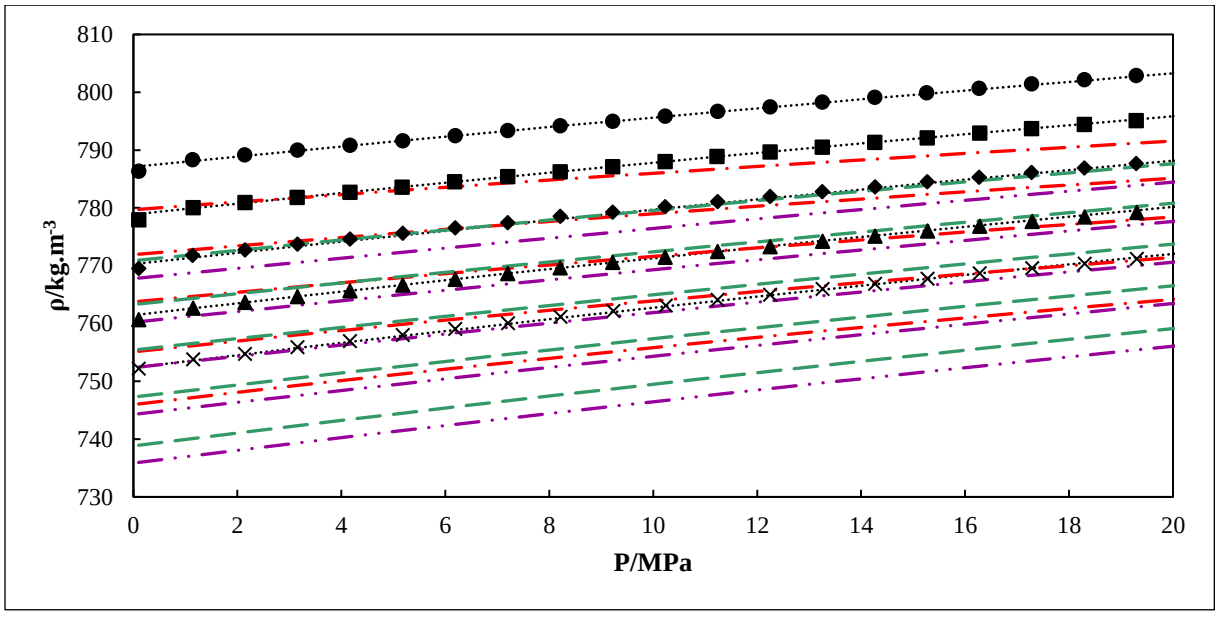

Figure 9.5. Experimental and model calculated density data (ρ) for 2-methylpropan-1-ol as a function of pressure (P) and temperature (T). (Symbol-T): (●- 313.15 K), (■- 323.15 K), (♦- 333.15 K), (▲- 343.15 K), (×- 353.15 K). (Line-Model): (···· - MTS), (—·— - PR), (—··— - PC-SAFT), (— — - tPC-PSAFT).

9.2. Binary Mixtures

9.2.1. Butan-1-ol (1) + n-octane (2)

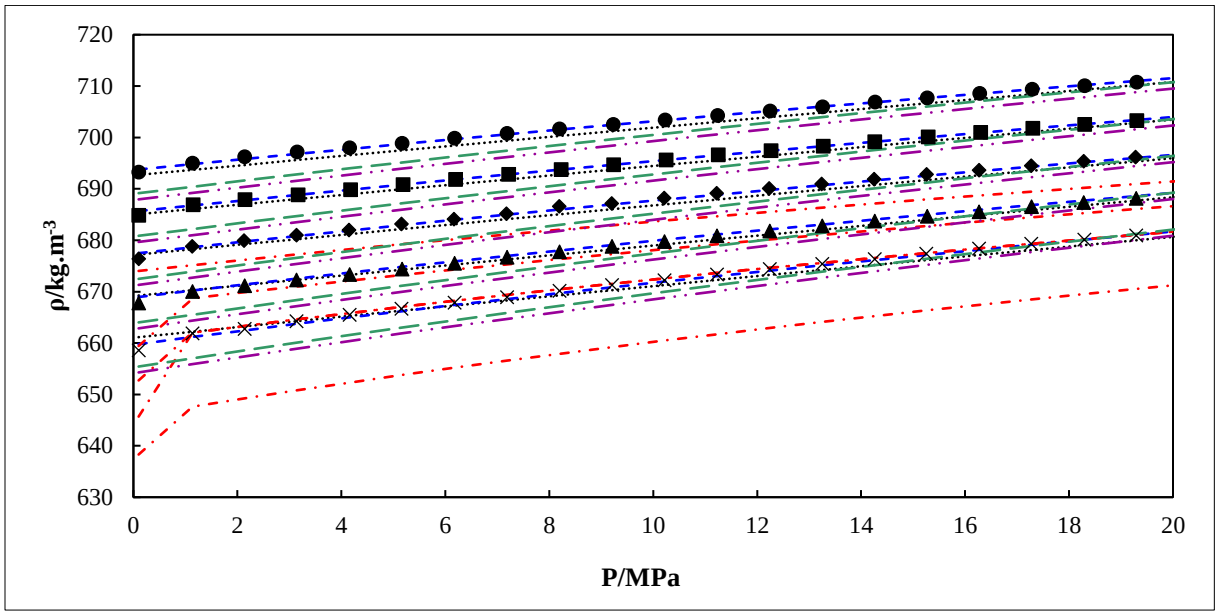

Figure 9.6. Experimental and model calculated density data (ρ) for the butan-1-ol (1) + n-octane (2) as a function of pressure (P) and temperature (T) at x_1 = 0.1259. (Symbol-T): (●- 313.15 K), (■- 323.15 K), (♦- 333.15 K), (▲- 343.15 K), (×- 353.15 K). (Line-Model): (···· - MTS), (- - - - BWRS), (—·— - PR), (—··— - PC-SAFT), (— — - tPC-PSAFT).

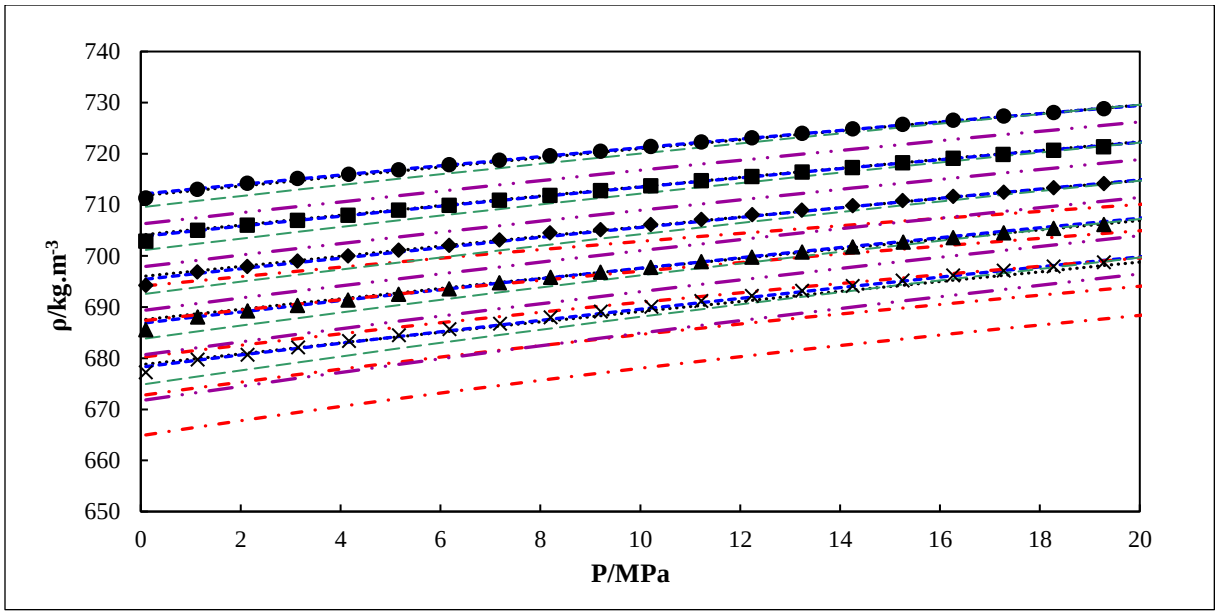

Figure 9.7. Experimental and model calculated density data (ρ) for the butan-1-ol (1) + n-octane (2) as a function of pressure (P) and temperature (T) at x_1 = 0.3750. (Symbol-T): (●- 313.15 K), (■- 323.15 K), (♦- 333.15 K), (▲- 343.15 K), (×- 353.15 K). (Line-Model): (···· - MTS), (- - - - BWRS), (—·— - PR), (—··— - PC-SAFT), (— — - tPC-PSAFT).

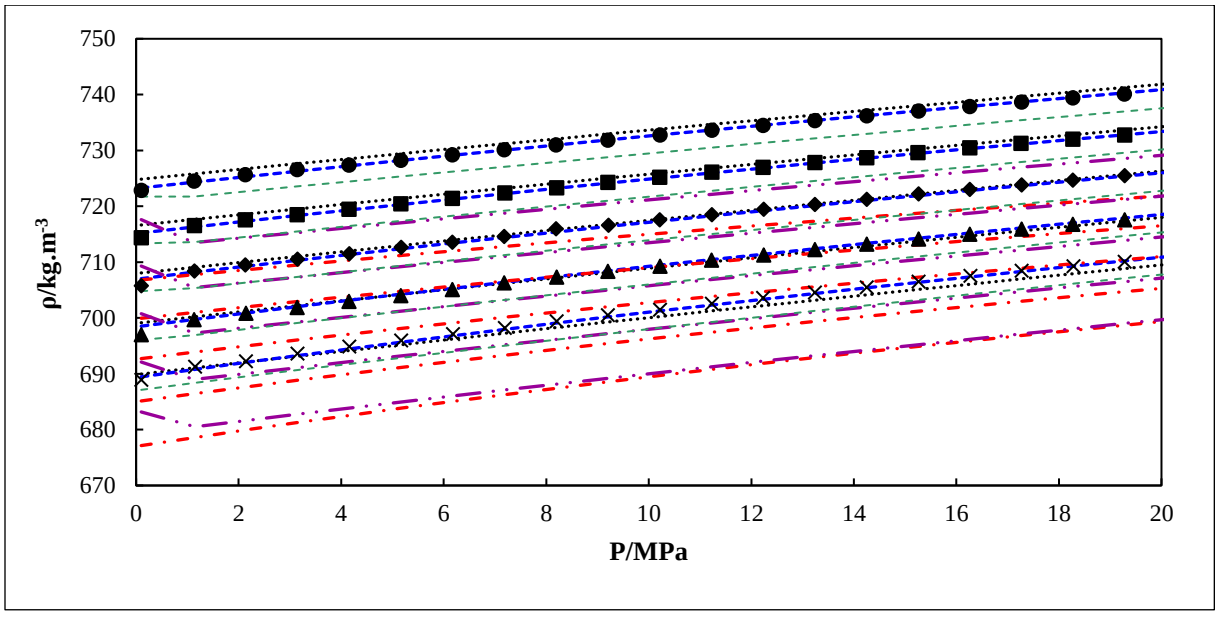

Figure 9.8. Experimental and model calculated density data (ρ) for the butan-1-ol (1) + n-octane (2) as a function of pressure (P) and temperature (T) at x_1 = 0.5002. (Symbol-T): (●- 313.15 K), (■- 323.15 K), (♦- 333.15 K), (▲- 343.15 K), (×- 353.15 K). (Line-Model): (···· - MTS), (- - - - BWRS), (—·— - PR), (—··— - PC-SAFT), (— — - tPC-PSAFT).

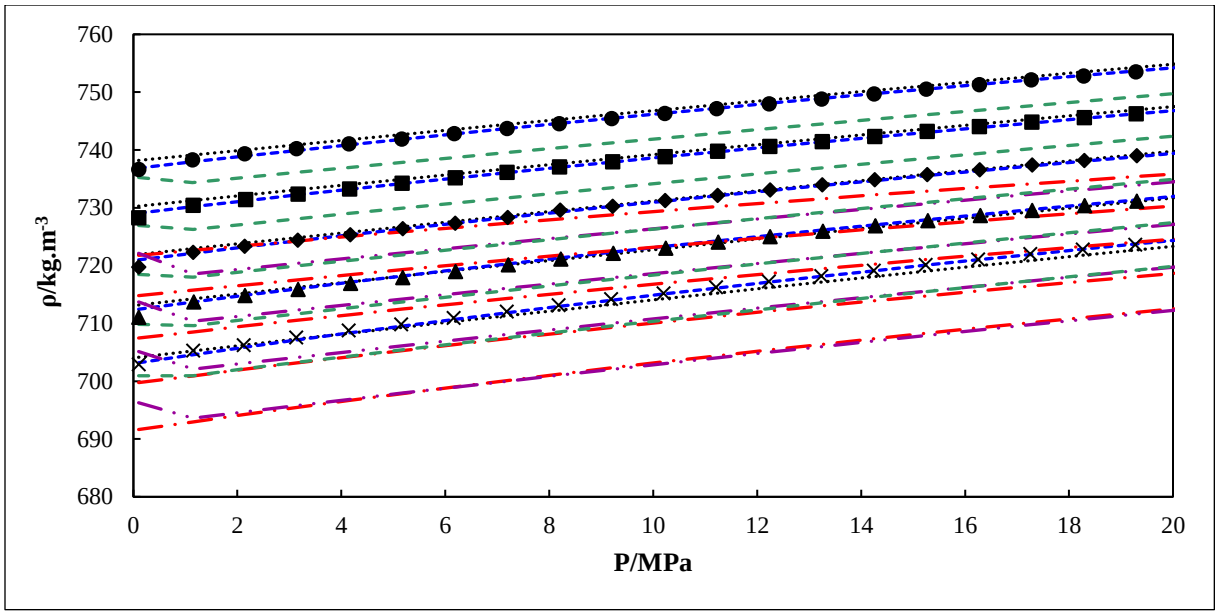

Figure 9.9. Experimental and model calculated density data (ρ) for the butan-1-ol (1) + n-octane (2) as a function of pressure (P) and temperature (T) at x_1 = 0.6258. (Symbol-T): (●- 313.15 K), (■- 323.15 K), (♦- 333.15 K), (▲- 343.15 K), (×- 353.15 K). (Line-Model): (···· - MTS), (- - - - BWRS), (—·— - PR), (—··— - PC-SAFT), (— — - tPC-PSAFT).

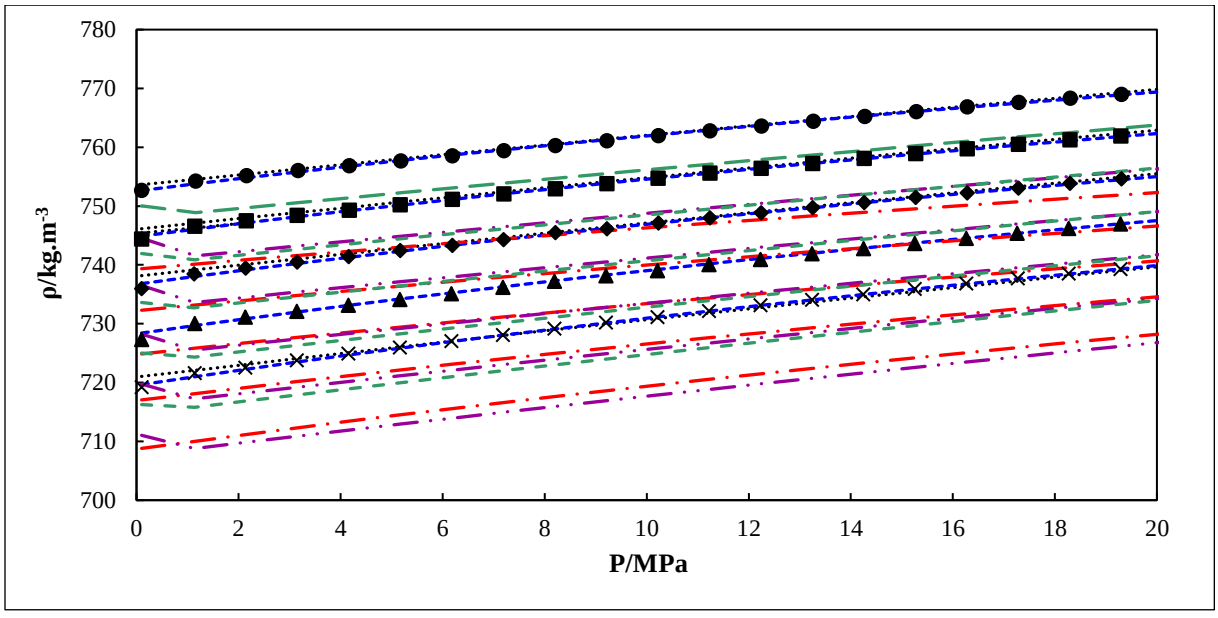

Figure 9.10. Experimental and model calculated density data (ρ) for the butan-1-ol (1) + n-octane (2) as a function of pressure (P) and temperature (T) at x_1 = 0.7503. (Symbol-T): (●- 313.15 K), (■- 323.15 K), (♦- 333.15 K), (▲- 343.15 K), (×- 353.15 K). (Line-Model): (···· - MTS), (- - - - BWRS), (—·— - PR), (—··— - PC-SAFT), (— — - tPC-PSAFT).

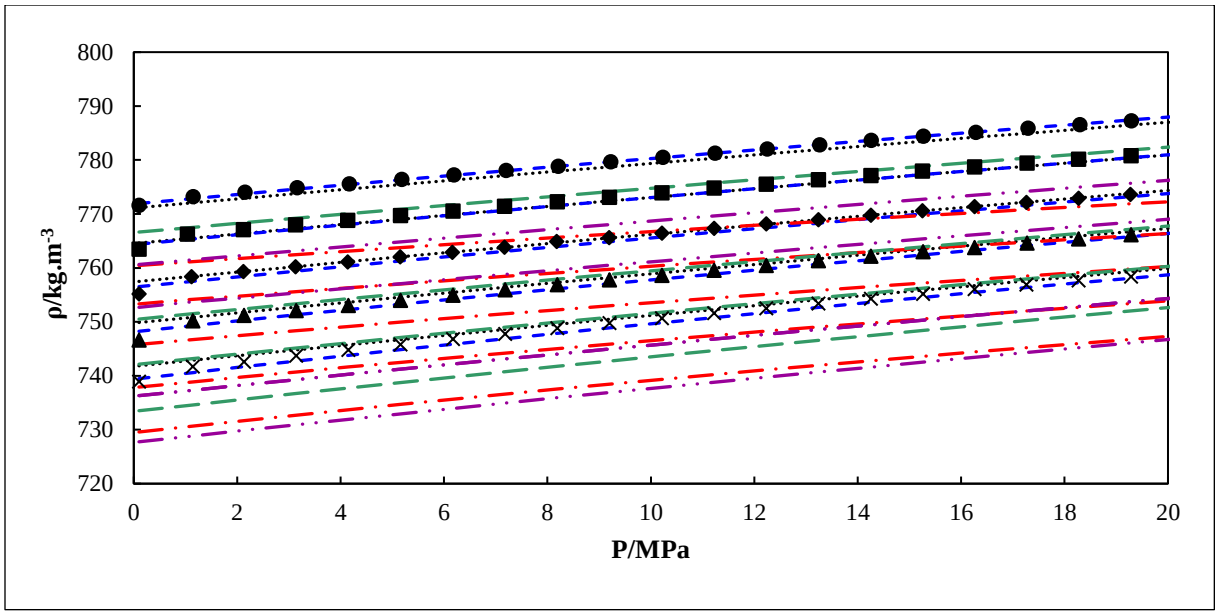

Figure 9.11. Experimental and model calculated density data (ρ) for the butan-1-ol (1) + n-octane (2) as a function of pressure (P) and temperature (T) at x_1 = 0.8750. (Symbol-T): (●- 313.15 K), (■- 323.15 K), (♦- 333.15 K), (▲- 343.15 K), (×- 353.15 K). (Line-Model): (···· - MTS), (- - - - BWRS), (—·— - PR), (—··— - PC-SAFT), (— — - tPC-PSAFT).

9.2.2. Butan-1-ol (1) + n-decane (2)

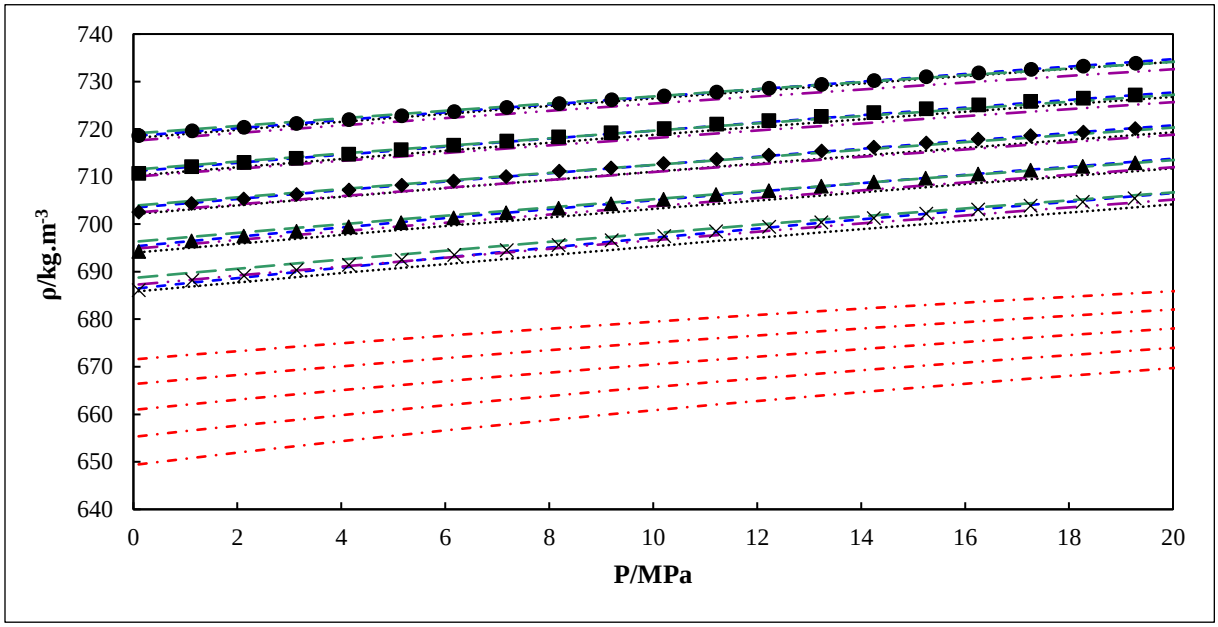

Figure 9.12. Experimental and model calculated density data (ρ) for the butan-1-ol (1) + n-decane (2) as a function of pressure (P) and temperature (T) at x_1 = 0.1269. (Symbol-T): (●- 313.15 K), (■- 323.15 K), (♦- 333.15 K), (▲- 343.15 K), (×- 353.15 K). (Line-Model): (···· - MTS), (- - - - BWRS), (—·— - PR), (—··— - PC-SAFT), (— — - tPC-PSAFT).

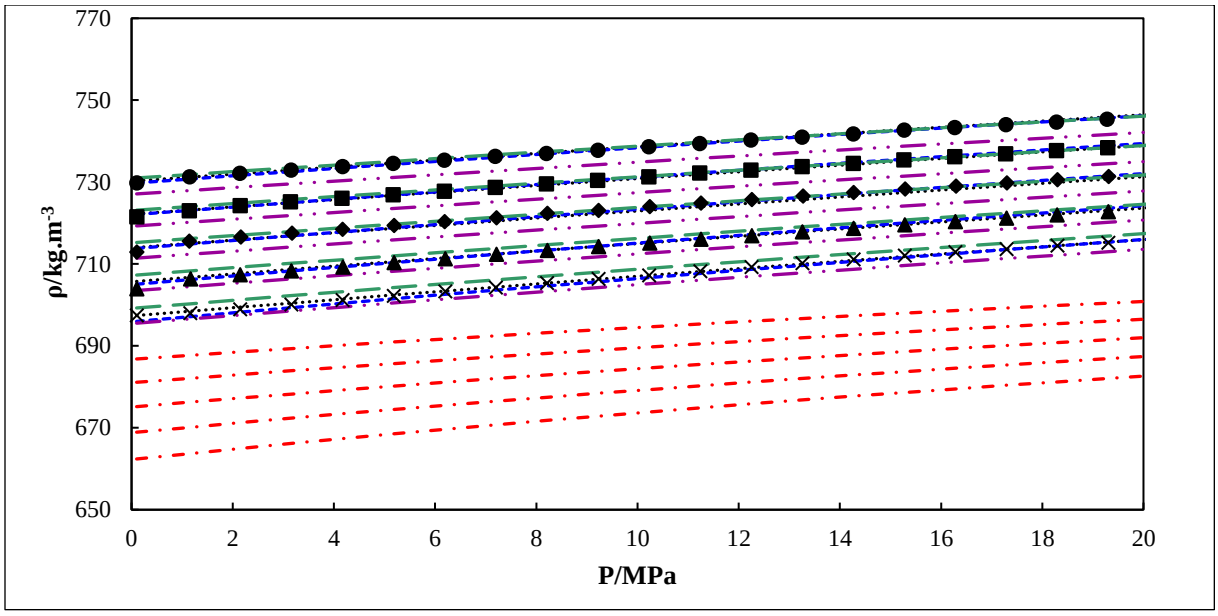

Figure 9.13. Experimental and model calculated density data (ρ) for the butan-1-ol (1) + n-decane (2) as a function of pressure (P) and temperature (T) at x_1 = 0.3746. (Symbol-T): (●- 313.15 K), (■- 323.15 K), (♦- 333.15 K), (▲- 343.15 K), (×- 353.15 K). (Line-Model): (···· - MTS), (- - - - BWRS), (—·— - PR), (—··— - PC-SAFT), (— — - tPC-PSAFT).

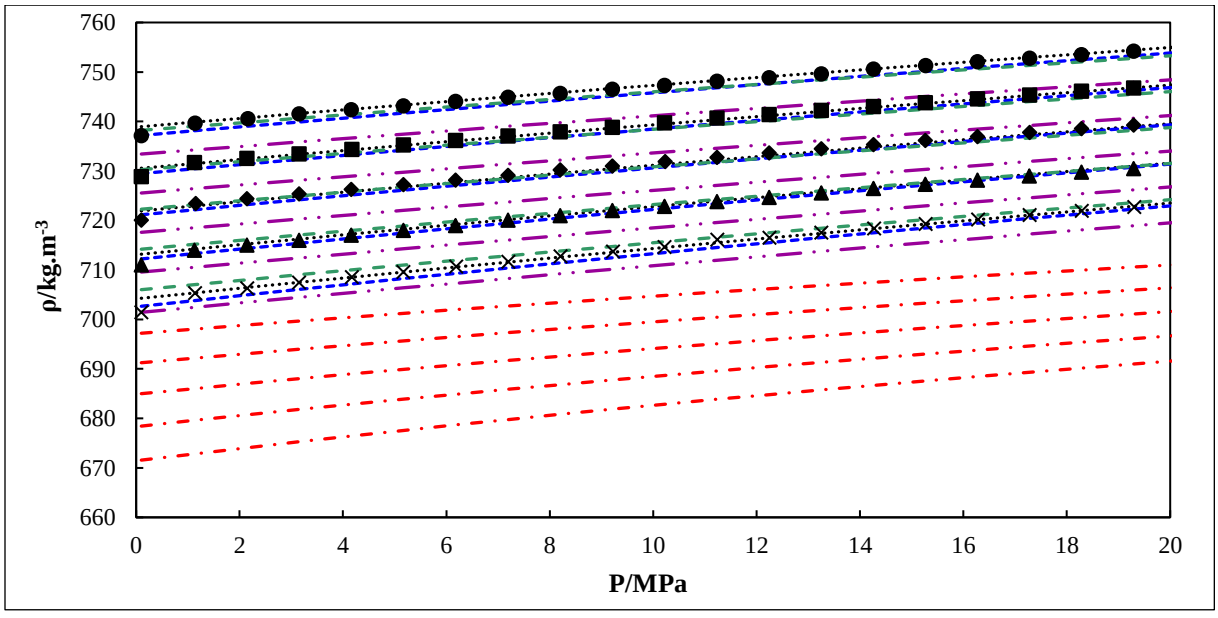

Figure 9.14. Experimental and model calculated density data (ρ) for the butan-1-ol (1) + n-decane (2) as a function of pressure (P) and temperature (T) at x_1 = 0.4968. (Symbol-T): (●- 313.15 K), (■- 323.15 K), (♦- 333.15 K), (▲- 343.15 K), (×- 353.15 K). (Line-Model): (···· - MTS), (- - - - BWRS), (—·— - PR), (—··— - PC-SAFT), (— — - tPC-PSAFT).

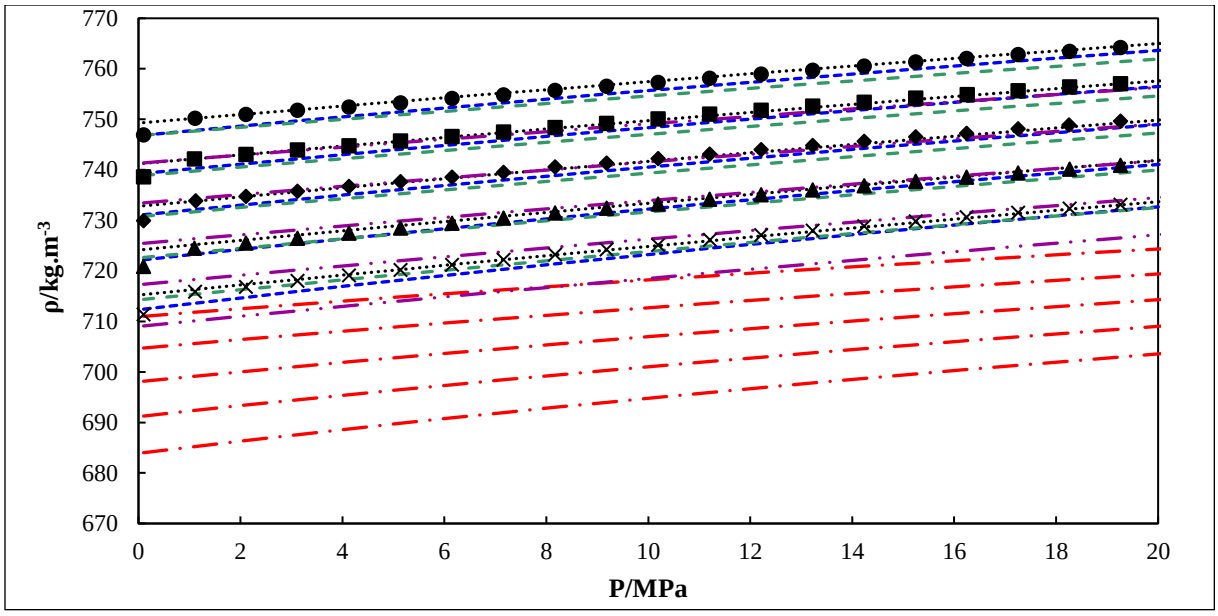

Figure 9.15. Experimental and model calculated density data (ρ) for the butan-1-ol (1) + n-decane (2) as a function of pressure (P) and temperature (T) at x_1 = 0.6234. (Symbol-T): (●- 313.15 K), (■- 323.15 K), (♦- 333.15 K), (▲- 343.15 K), (×- 353.15 K). (Line-Model): (···· - MTS), (- - - - BWRS), (—·— - PR), (—··— - PC-SAFT), (— — - tPC-PSAFT).

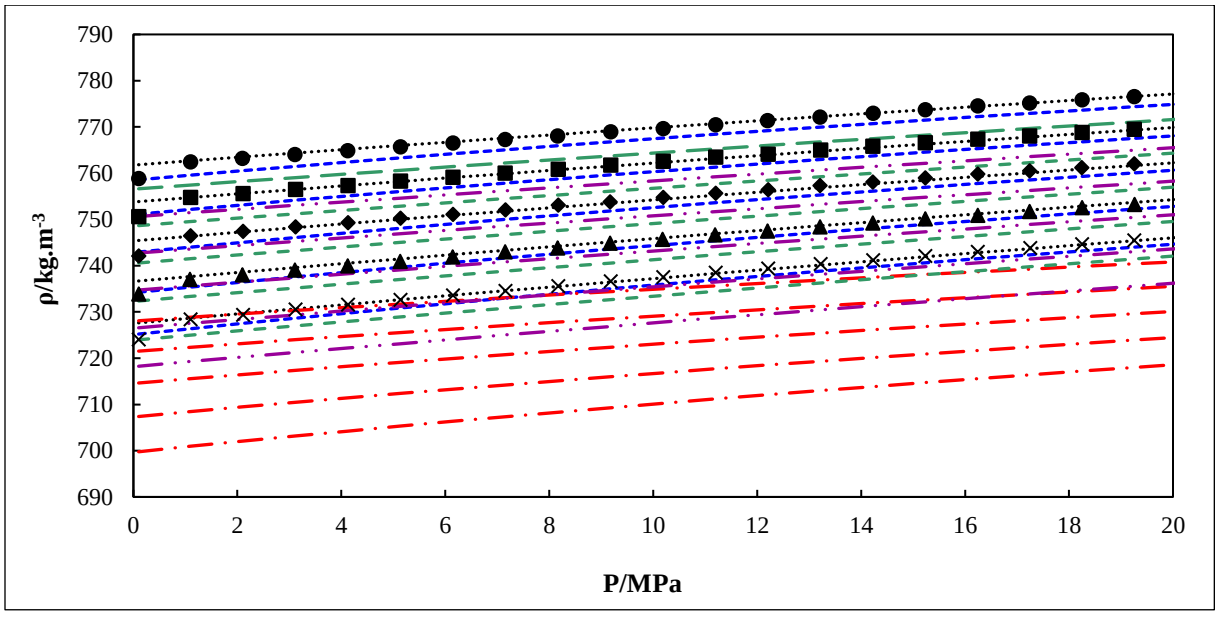

Figure 9.16. Experimental and model calculated density data (ρ) for the butan-1-ol (1) + n-decane (2) as a function of pressure (P) and temperature (T) at x_1 = 0.7440. (Symbol-T): (●- 313.15 K), (■- 323.15 K), (♦- 333.15 K), (▲- 343.15 K), (×- 353.15 K). (Line-Model): (···· - MTS), (- - - - BWRS), (—·— - PR), (—··— - PC-SAFT), (— — - tPC-PSAFT).

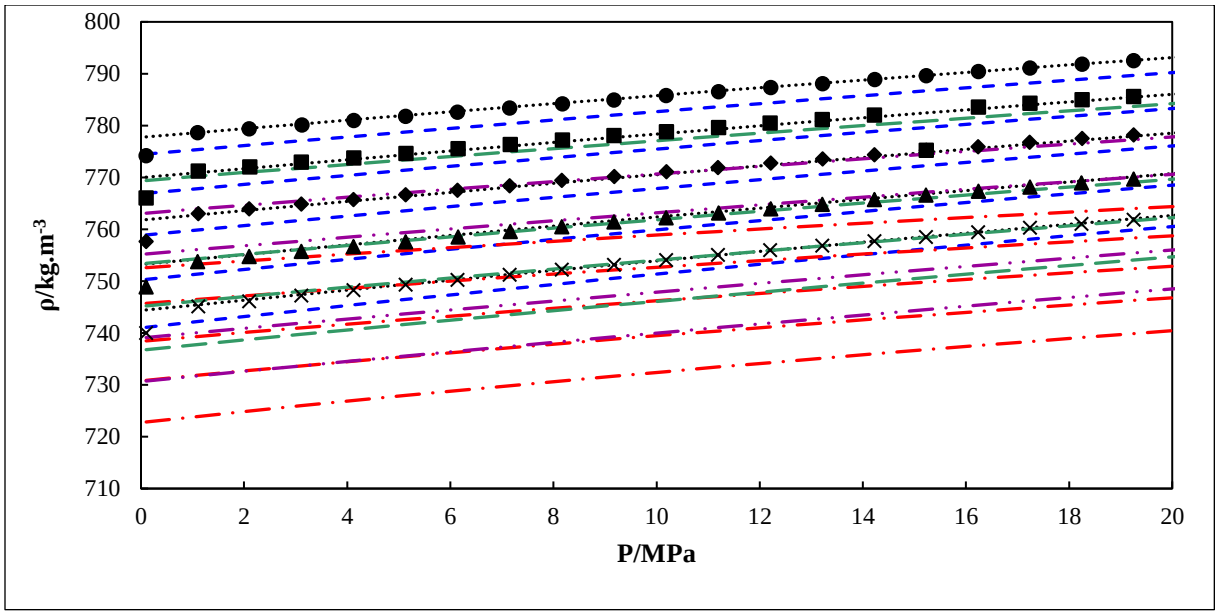

Figure 9.17. Experimental and model calculated density data (ρ) for the butan-1-ol (1) + n-decane (2) as a function of pressure (P) and temperature (T) at x_1 = 0.8731. (Symbol-T): (●- 313.15 K), (■- 323.15 K), (♦- 333.15 K), (▲- 343.15 K), (×- 353.15 K). (Line-Model): (···· - MTS), (- - - - BWRS), (—·— - PR), (—··— - PC-SAFT), (— — - tPC-PSAFT).

9.2.3. Butan-2-ol (1) + n-octane (2)

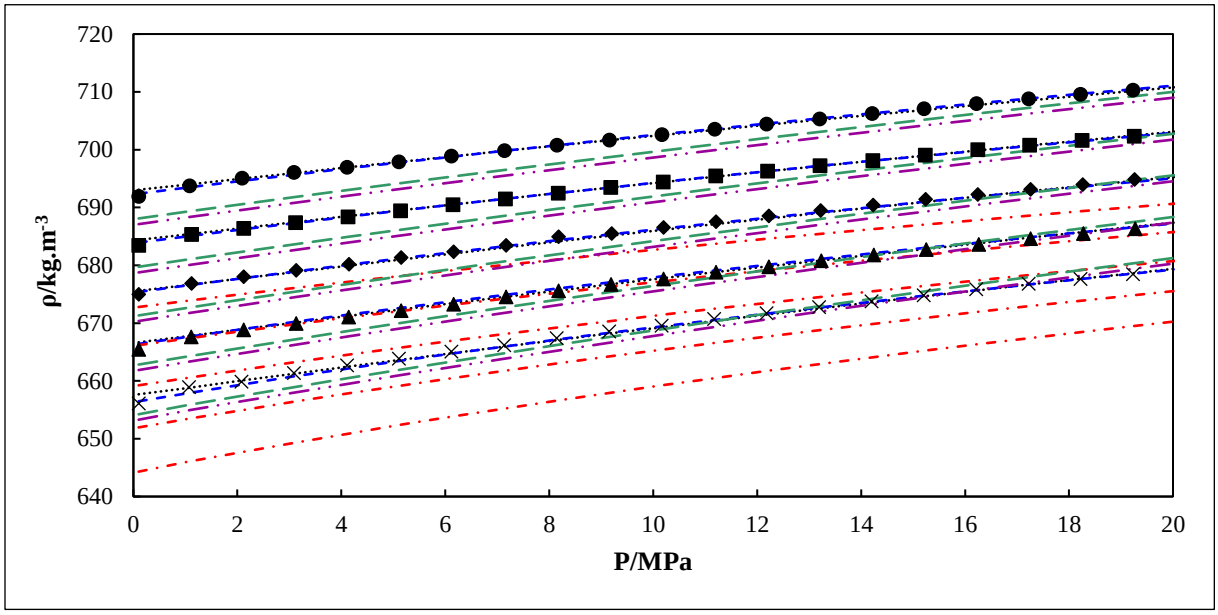

Figure 9.18. Experimental and model calculated density data (ρ) for the butan-2-ol (1) + n-octane (2) as a function of pressure (P) and temperature (T) at x_1 = 0.1262. (Symbol-T): (●- 313.15 K), (■- 323.15 K), (♦- 333.15 K), (▲- 343.15 K), (×- 353.15 K). (Line-Model): (···· - MTS), (- - - - BWRS), (—·— - PR), (—··— - PC-SAFT), (— — - tPC-PSAFT).

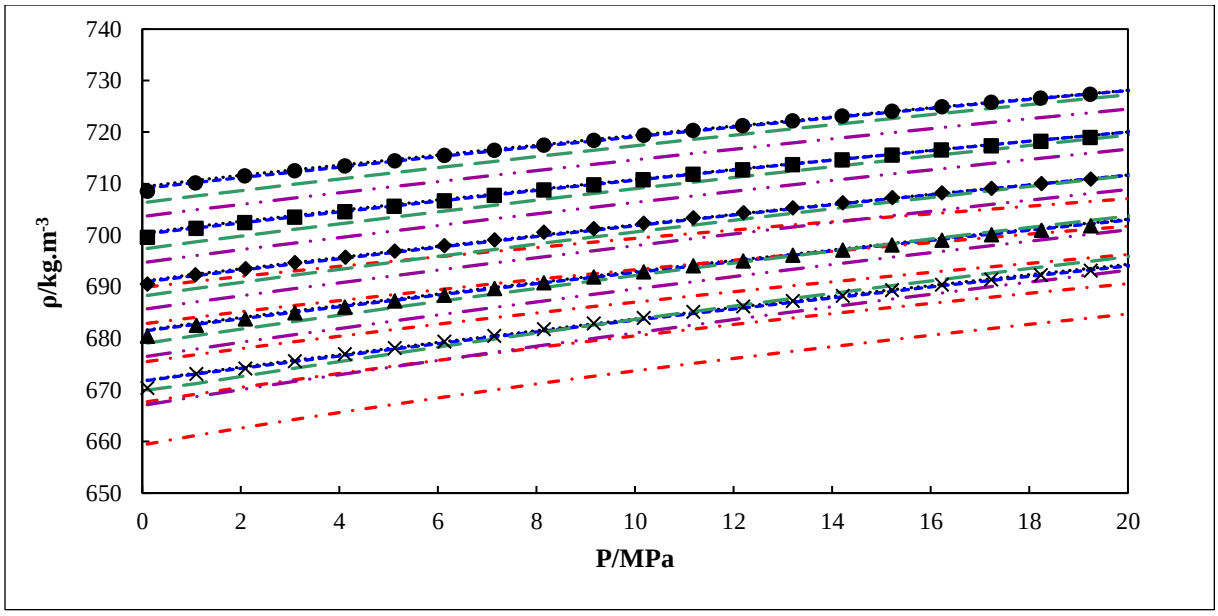

Figure 9.19. Experimental and model calculated density data (ρ) for the butan-2-ol (1) + n-octane (2) as a function of pressure (P) and temperature (T) at x_1 = 0.3742. (Symbol-T): (●- 313.15 K), (■- 323.15 K), (♦- 333.15 K), (▲- 343.15 K), (×- 353.15 K). (Line-Model): (···· - MTS), (- - - - BWRS), (—·— - PR), (—··— - PC-SAFT), (— — - tPC-PSAFT).

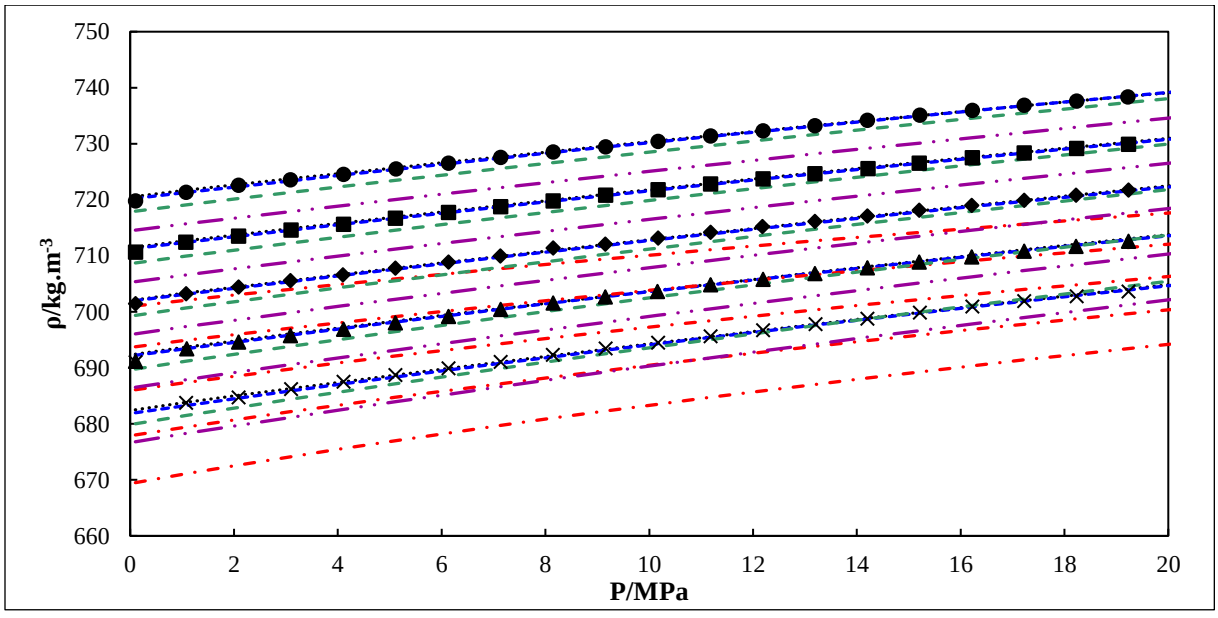

Figure 9.20. Experimental and model calculated density data (ρ) for the butan-2-ol (1) + n-octane (2) as a function of pressure (P) and temperature (T) at x_1 = 0.5002. (Symbol-T): (●- 313.15 K), (■- 323.15 K), (♦- 333.15 K), (▲- 343.15 K), (×- 353.15 K). (Line-Model): (···· - MTS), (- - - - BWRS), (—·— - PR), (—··— - PC-SAFT), (— — - tPC-PSAFT).

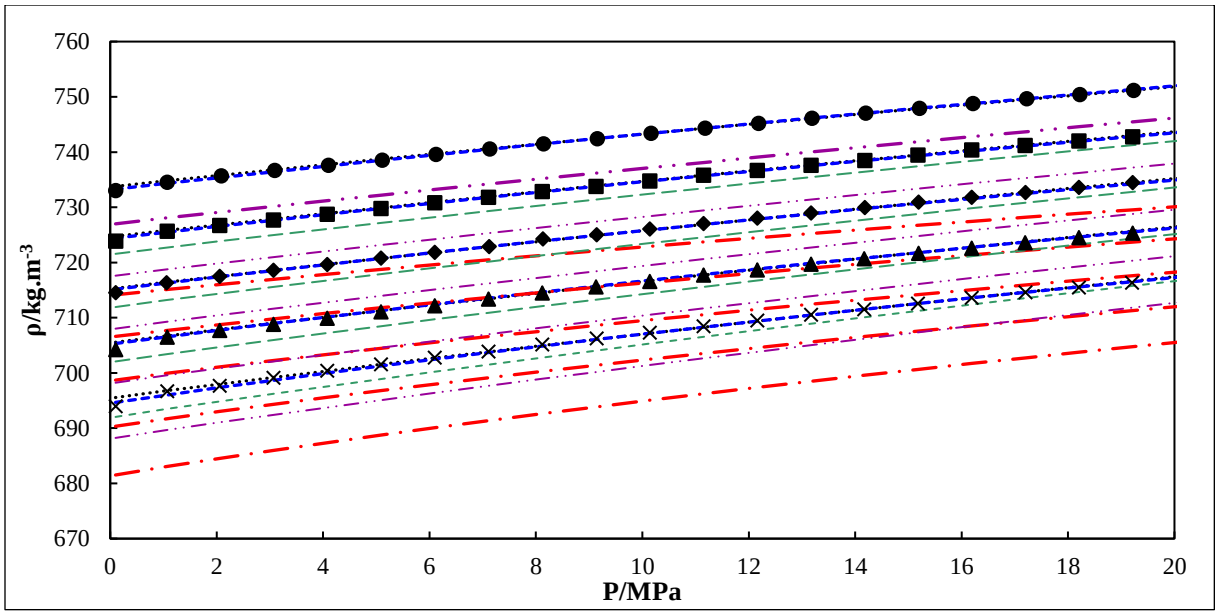

Figure 9.21. Experimental and model calculated density data (ρ) for the butan-2-ol (1) + n-octane (2) as a function of pressure (P) and temperature (T) at x_1 = 0.6257. (Symbol-T): (●- 313.15 K), (■- 323.15 K), (♦- 333.15 K), (▲- 343.15 K), (×- 353.15 K). (Line-Model): (···· - MTS), (- - - - BWRS), (—·— - PR), (—··— - PC-SAFT), (— — - tPC-PSAFT).

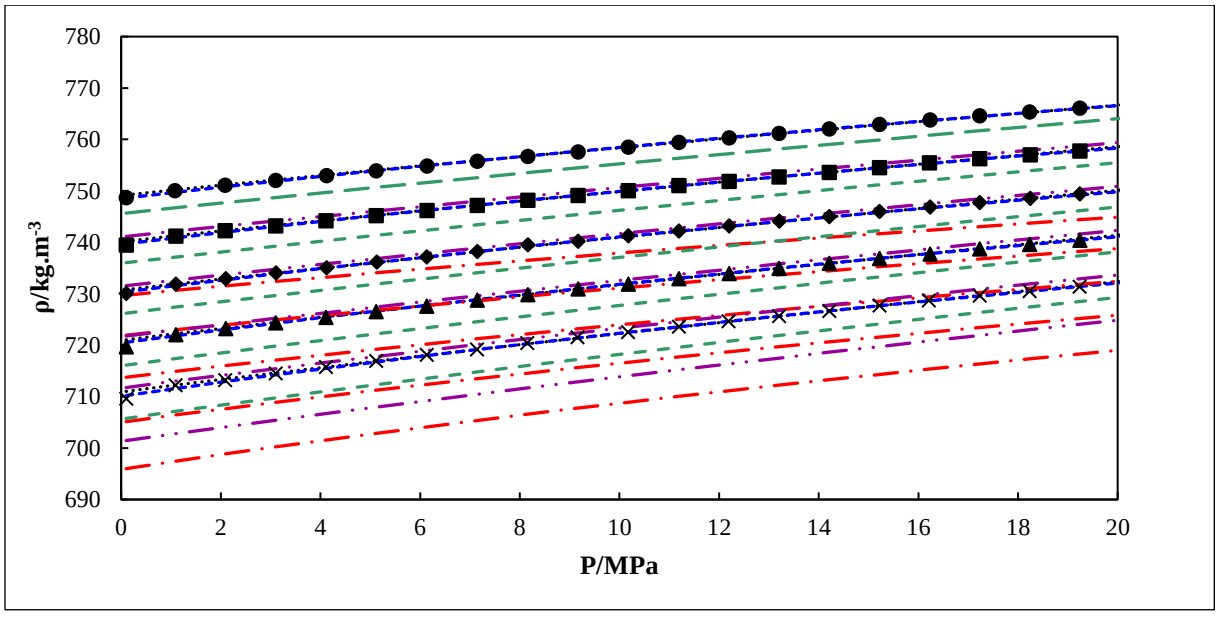

Figure 9.22. Experimental and model calculated density data (ρ) for the butan-2-ol (1) + n-octane (2) as a function of pressure (P) and temperature (T) at x_1 = 0.7501. (Symbol-T): (●- 313.15 K), (■- 323.15 K), (♦- 333.15 K), (▲- 343.15 K), (×- 353.15 K). (Line-Model): (···· - MTS), (- - - - BWRS), (—·— - PR), (—··— - PC-SAFT), (— — - tPC-PSAFT).

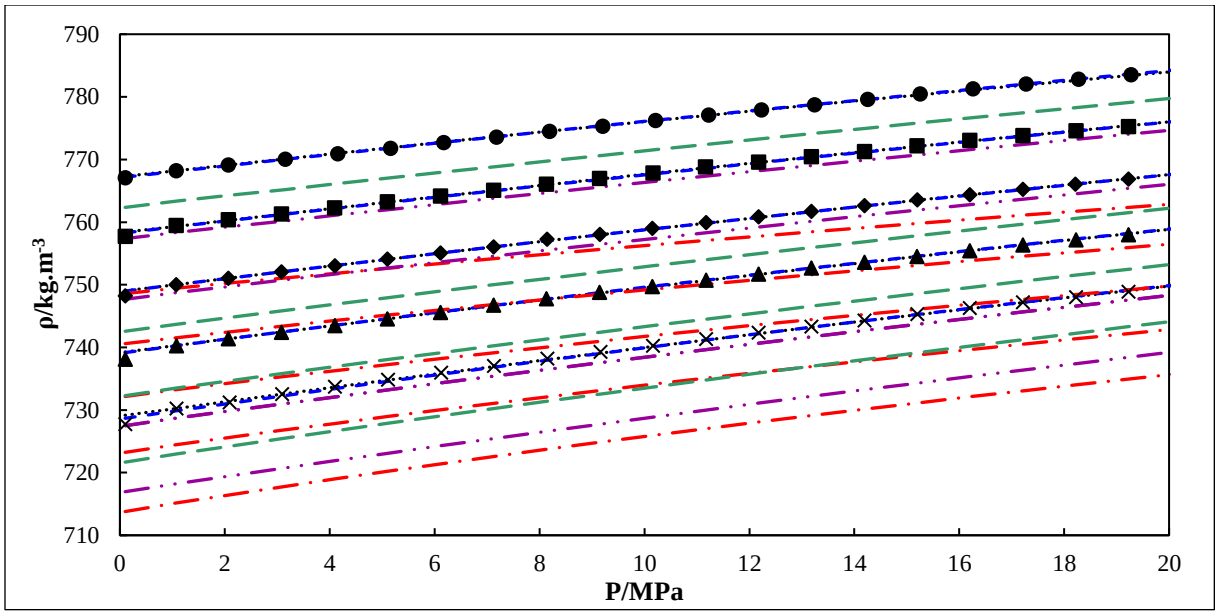

Figure 9.23. Experimental and model calculated density data (ρ) for the butan-2-ol (1) + n-octane (2) as a function of pressure (P) and temperature (T) at x_1 = 0.8747. (Symbol-T): (●- 313.15 K), (■- 323.15 K), (♦- 333.15 K), (▲- 343.15 K), (×- 353.15 K). (Line-Model): (···· - MTS), (- - - - BWRS), (—·— - PR), (—··— - PC-SAFT), (— — - tPC-PSAFT).

9.2.4. Butan-2-ol (1) + n-decane (2)

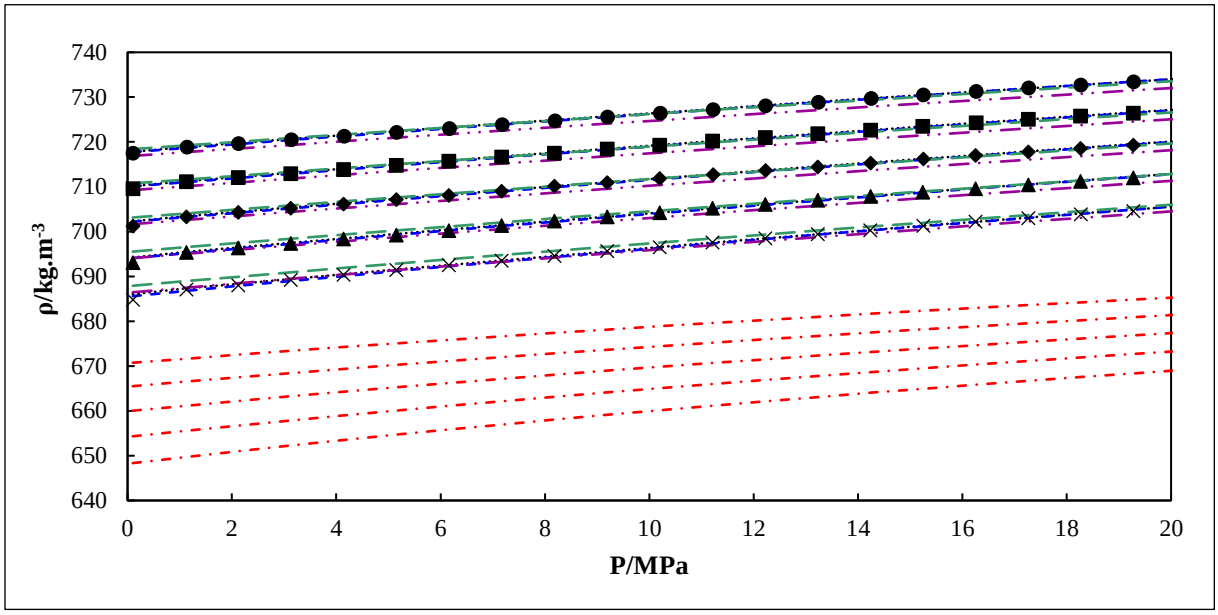

Figure 9.24. Experimental and model calculated density data (ρ) for the butan-2-ol (1) + n-decane (2) as a function of pressure (P) and temperature (T) at x_1 = 0.1254. (Symbol-T): (●- 313.15 K), (■- 323.15 K), (♦- 333.15 K), (▲- 343.15 K), (×- 353.15 K). (Line-Model): (···· - MTS), (- - - - BWRS), (—·— - PR), (—··— - PC-SAFT), (— — - tPC-PSAFT).

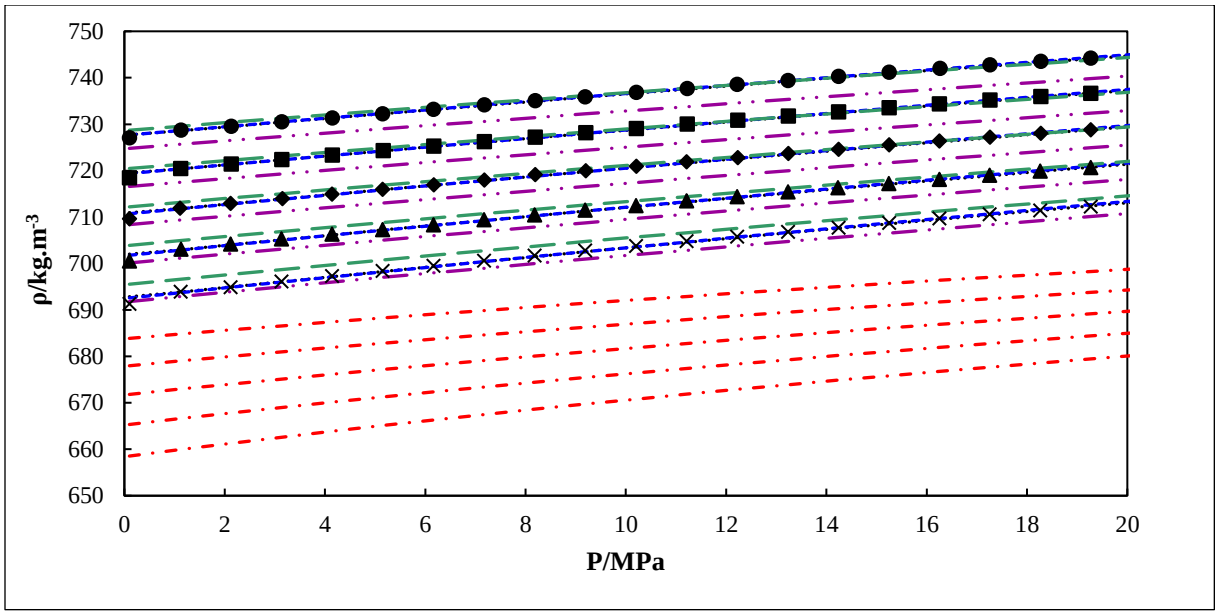

Figure 9.25. Experimental and model calculated density data (ρ) for the butan-2-ol (1) + n-decane (2) as a function of pressure (P) and temperature (T) at x_1 = 0.3754. (Symbol-T): (●- 313.15 K), (■- 323.15 K), (♦- 333.15 K), (▲- 343.15 K), (×- 353.15 K). (Line-Model): (···· - MTS), (- - - - BWRS), (—·— - PR), (—··— - PC-SAFT), (— — - tPC-PSAFT).

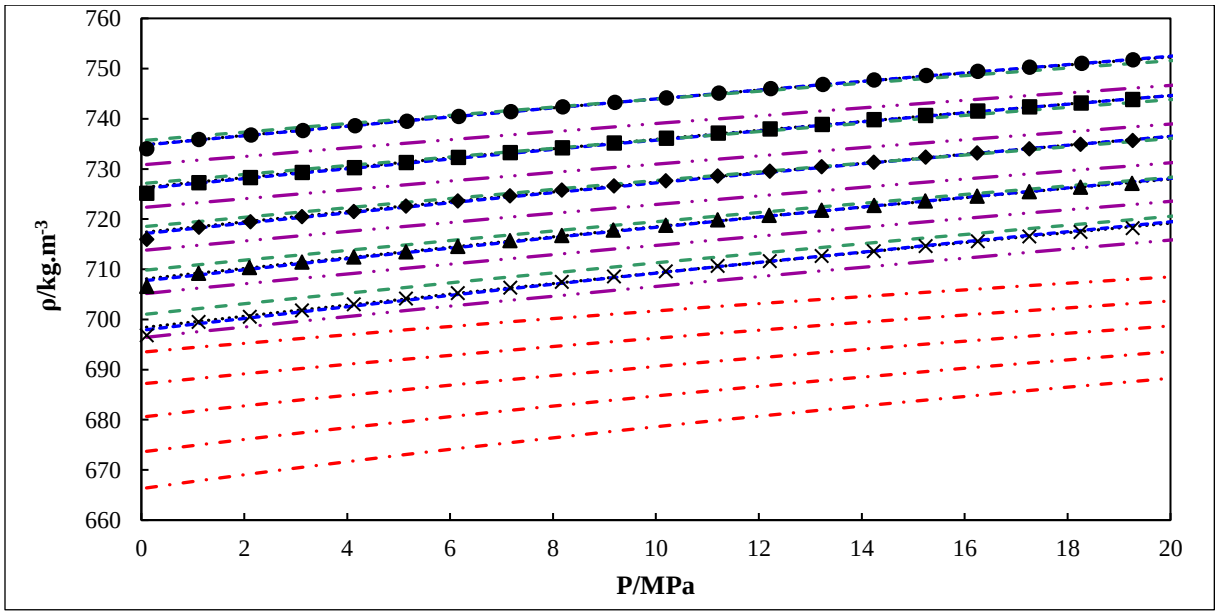

Figure 9.26. Experimental and model calculated density data (ρ) for the butan-2-ol (1) + n-decane (2) as a function of pressure (P) and temperature (T) at x_1 = 0.5055. (Symbol-T): (●- 313.15 K), (■- 323.15 K), (♦- 333.15 K), (▲- 343.15 K), (×- 353.15 K). (Line-Model): (···· - MTS), (- - - - BWRS), (—·— - PR), (—··— - PC-SAFT), (— — - tPC-PSAFT).

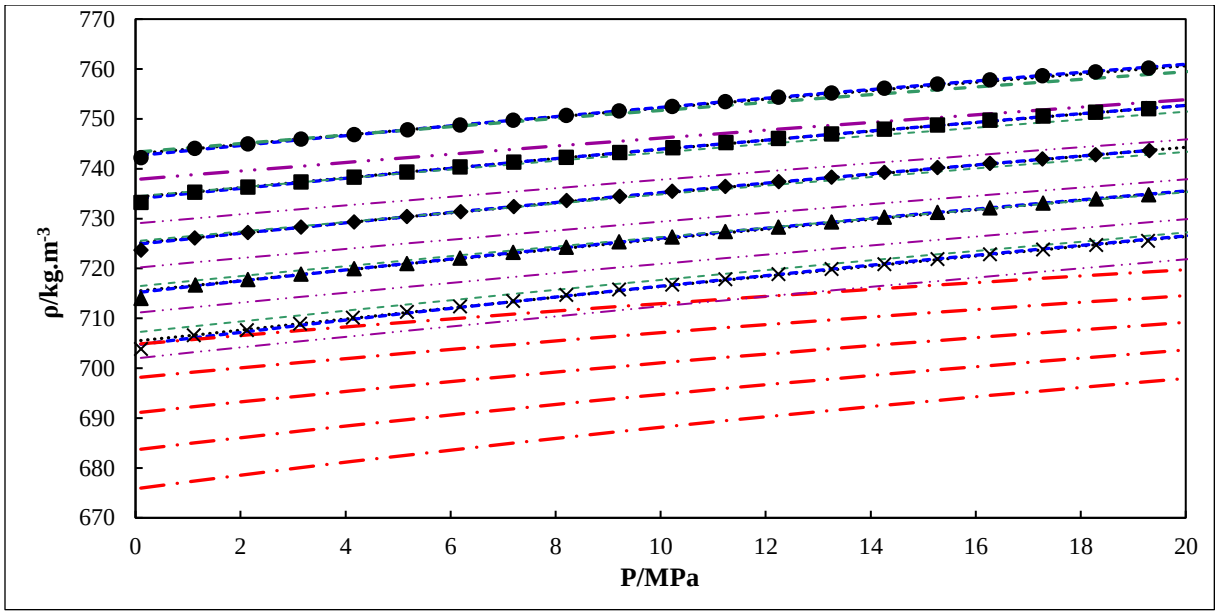

Figure 9.27. Experimental and model calculated density data (ρ) for the butan-2-ol (1) + n-decane (2) as a function of pressure (P) and temperature (T) at x_1 = 0.6240. (Symbol-T): (●- 313.15 K), (■- 323.15 K), (♦- 333.15 K), (▲- 343.15 K), (×- 353.15 K). (Line-Model): (···· - MTS), (- - - - BWRS), (—·— - PR), (—··— - PC-SAFT), (— — - tPC-PSAFT).

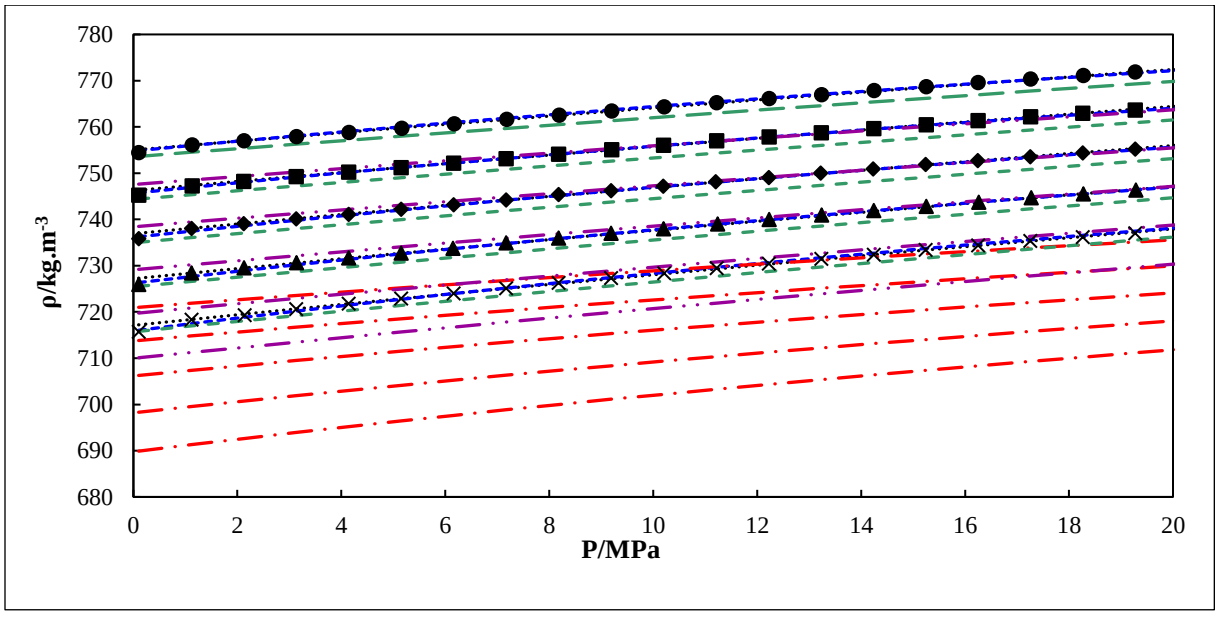

Figure 9.28. Experimental and model calculated density data (ρ) for the butan-2-ol (1) + n-decane (2) as a function of pressure (P) and temperature (T) at x_1 = 0.7519. (Symbol-T): (●- 313.15 K), (■- 323.15 K), (♦- 333.15 K), (▲- 343.15 K), (×- 353.15 K). (Line-Model): (···· - MTS), (- - - - BWRS), (—·— - PR), (—··— - PC-SAFT), (— — - tPC-PSAFT).

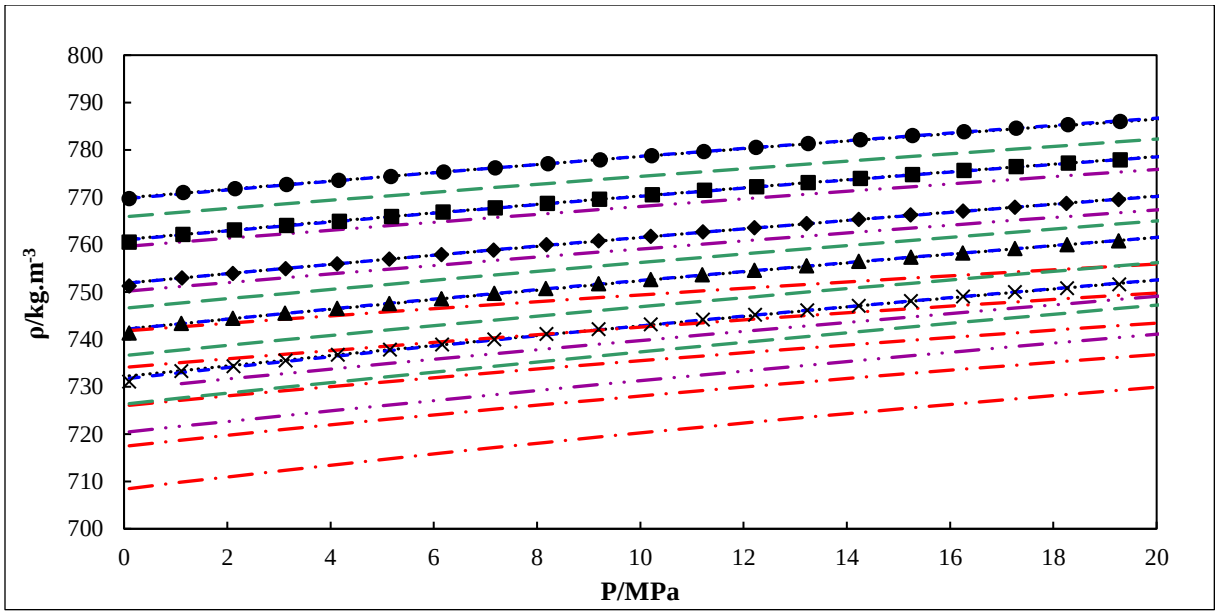

Figure 9.29. Experimental and model calculated density data (ρ) for the butan-2-ol (1) + n-decane (2) as a function of pressure (P) and temperature (T) at x_1 = 0.8740. (Symbol-T): (●- 313.15 K), (■- 323.15 K), (♦- 333.15 K), (▲- 343.15 K), (×- 353.15 K). (Line-Model): (···· - MTS), (- - - - BWRS), (—·— - PR), (—··— - PC-SAFT), (— — - tPC-PSAFT).

9.2.5. 2-methylpropan-1-ol (1) + n-octane (2)

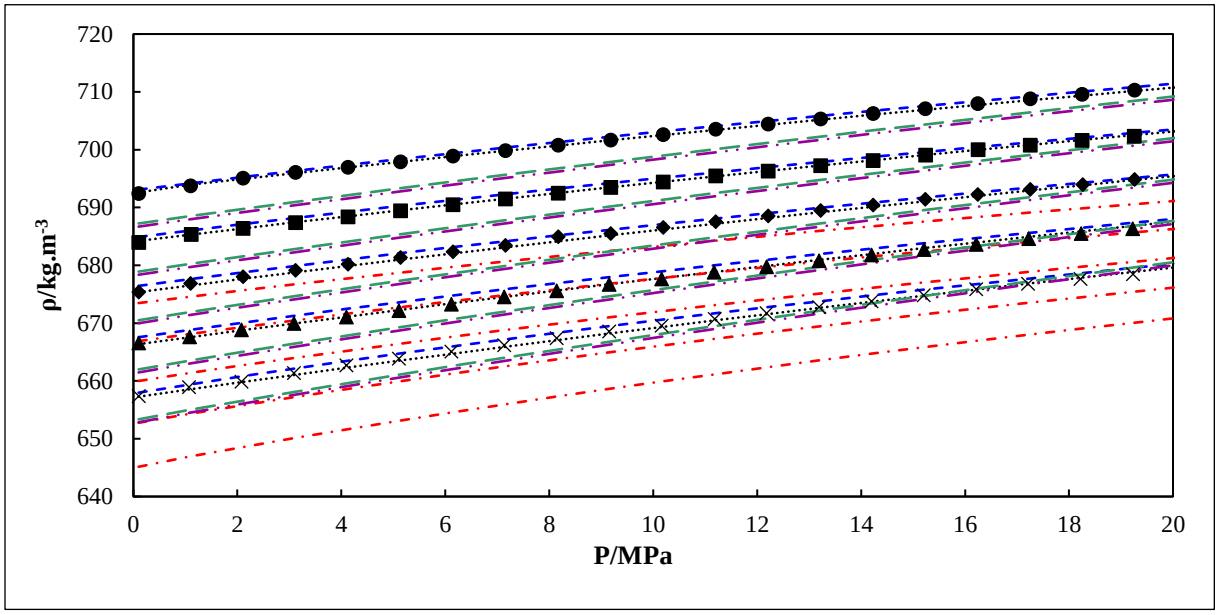

Figure 9.30. Experimental and model calculated density data (ρ) for the 2-methylpropan-1-ol (1) + n-octane (2) as a function of pressure (P) and temperature (T) at x_1 = 0.1267. (Symbol-T): (●- 313.15 K), (■- 323.15 K), (♦- 333.15 K), (▲- 343.15 K), (×- 353.15 K). (Line-Model): (···· - MTS), (- - - - BWRS), (—·— - PR), (—··— - PC-SAFT), (— — - tPC-PSAFT).

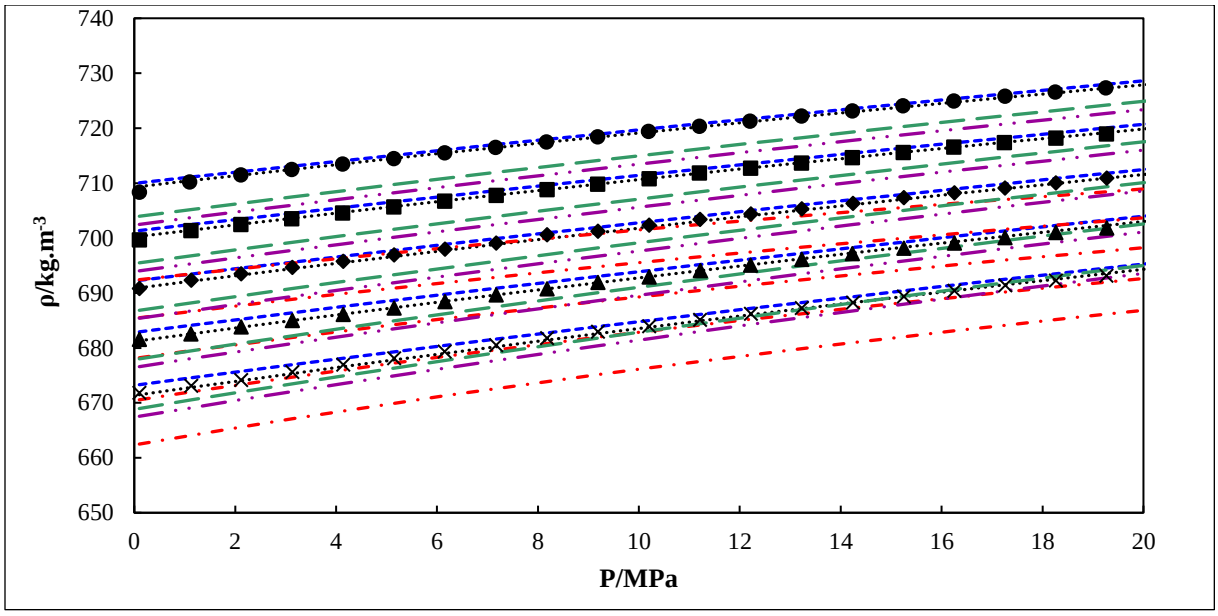

Figure 9.31. Experimental and model calculated density data (ρ) for the 2-methylpropan-1-ol (1) + n-octane (2) as a function of pressure (P) and temperature (T) at x_1 = 0.3776. (Symbol-T): (●- 313.15 K), (■- 323.15 K), (♦- 333.15 K), (▲- 343.15 K), (×- 353.15 K). (Line-Model): (···· - MTS), (- - - - BWRS), (—·— - PR), (—··— - PC-SAFT), (— — - tPC-PSAFT).

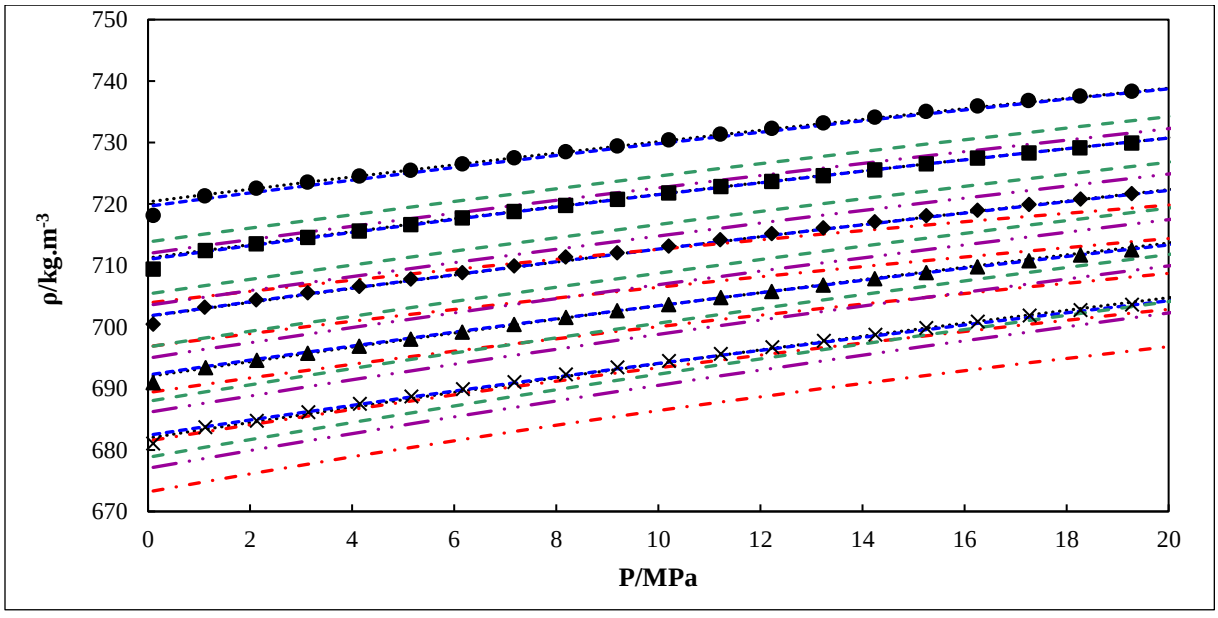

Figure 9.32. Experimental and model calculated density data (ρ) for the 2-methylpropan-1-ol (1) + n-octane (2) as a function of pressure (P) and temperature (T) at x_1 = 0.4996. (Symbol-T): (●- 313.15 K), (■- 323.15 K), (♦- 333.15 K), (▲- 343.15 K), (×- 353.15 K). (Line-Model): (···· - MTS), (- - - - BWRS), (—·— - PR), (—··— - PC-SAFT), (— — - tPC-PSAFT).

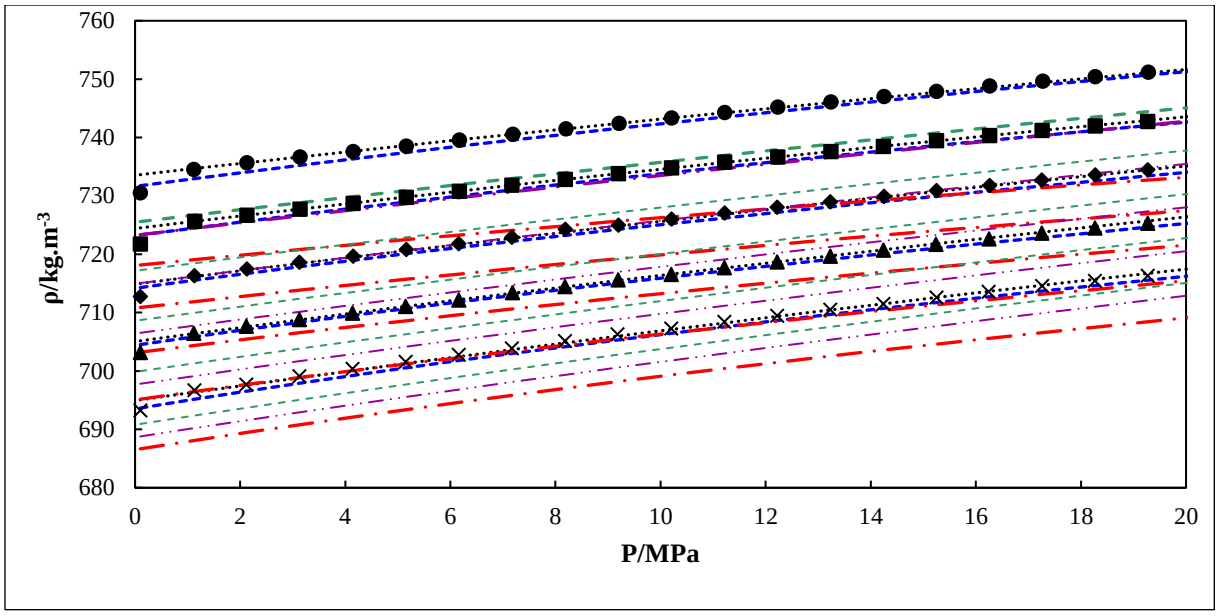

Figure 9.33. Experimental and model calculated density data (ρ) for the 2-methylpropan-1-ol (1) + n-octane (2) as a function of pressure (P) and temperature (T) at x_1 = 0.6255. (Symbol-T): (●- 313.15 K), (■- 323.15 K), (♦- 333.15 K), (▲- 343.15 K), (×- 353.15 K). (Line-Model): (···· - MTS), (- - - - BWRS), (—·— - PR), (—··— - PC-SAFT), (— — - tPC-PSAFT).

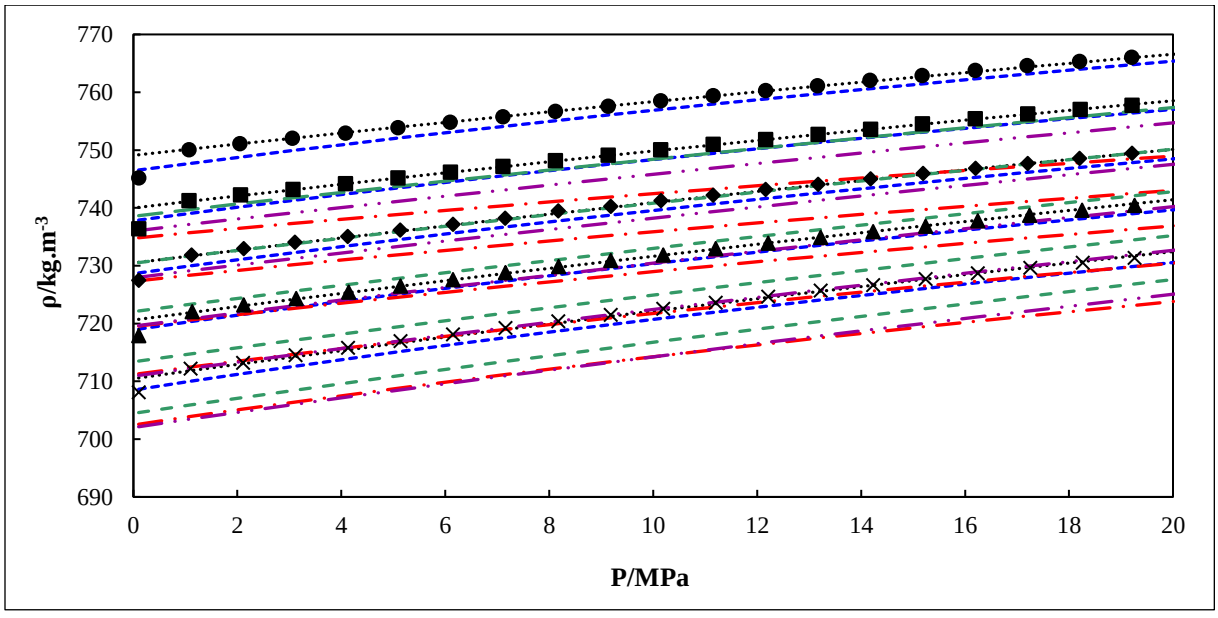

Figure 9.34. Experimental and model calculated density data (ρ) for the 2-methylpropan-1-ol (1) + n-octane (2) as a function of pressure (P) and temperature (T) at x_1 = 0.7499. (Symbol-T): (●- 313.15 K), (■- 323.15 K), (♦- 333.15 K), (▲- 343.15 K), (×- 353.15 K). (Line-Model): (···· - MTS), (- - - - BWRS), (—·— - PR), (—··— - PC-SAFT), (— — - tPC-PSAFT).

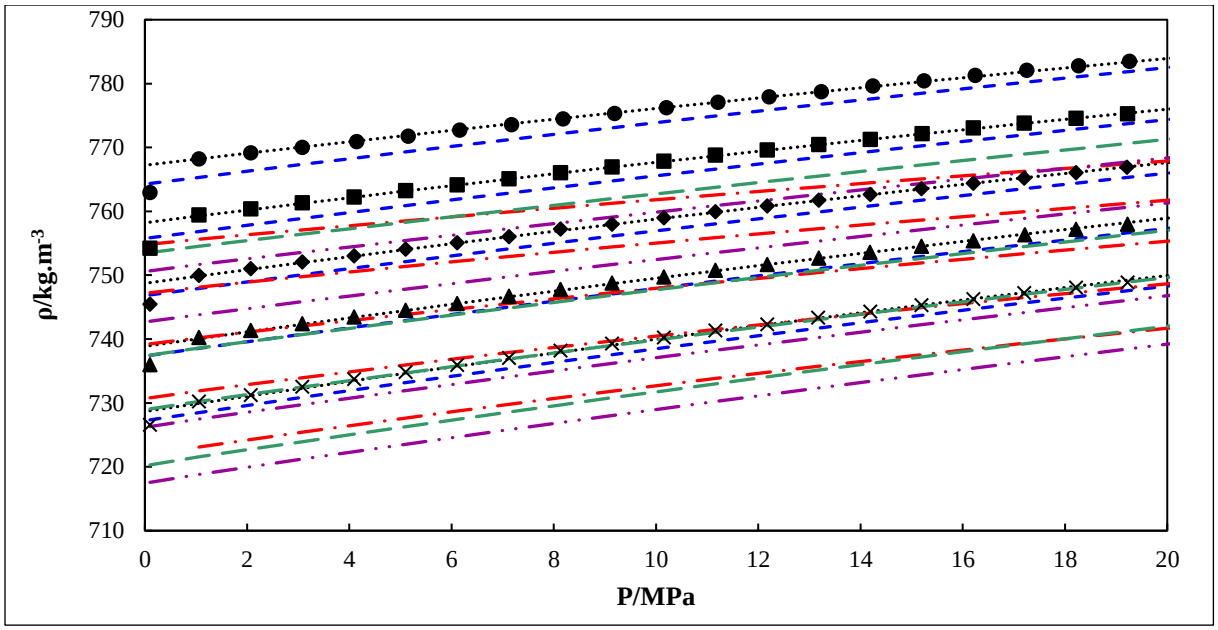

Figure 9.35. Experimental and model calculated density data (ρ) for the 2-methylpropan-1-ol (1) + n-octane (2) as a function of pressure (P) and temperature (T) at x_1 = 0.8739. (Symbol-T): (●- 313.15 K), (■- 323.15 K), (♦- 333.15 K), (▲- 343.15 K), (×- 353.15 K). (Line-Model): (···· - MTS), (- - - - BWRS), (—·— - PR), (—··— - PC-SAFT), (— — - tPC-PSAFT).

9.2.6. 2-methylpropan-1-ol (1) + n-decane (2)

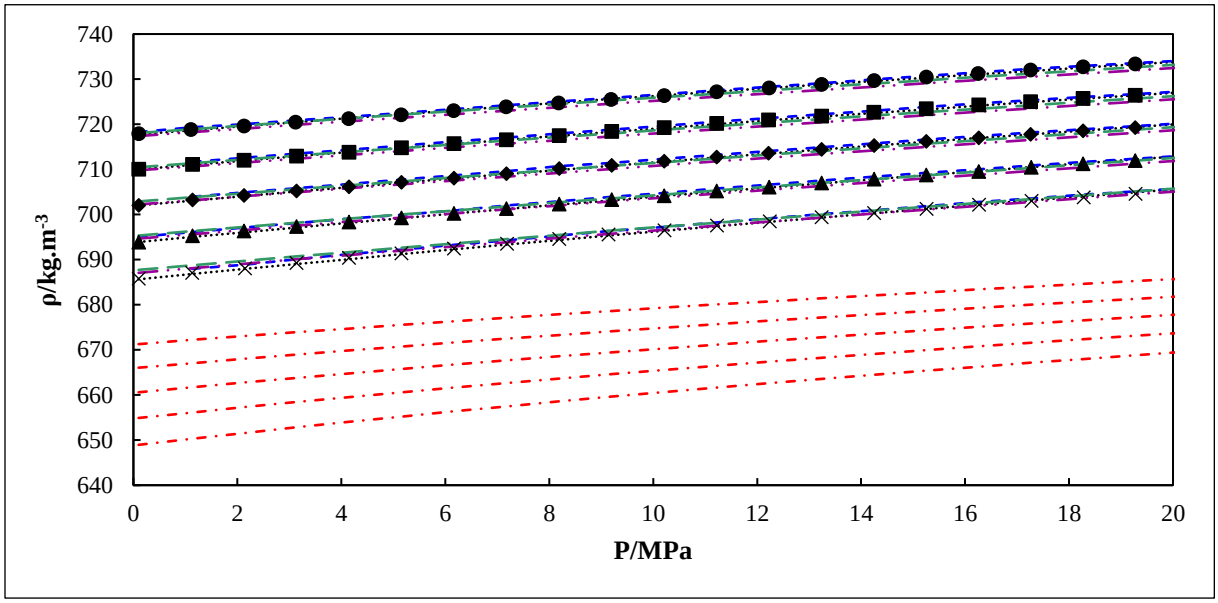

Figure 9.36. Experimental and model calculated density data (ρ) for the 2-methylpropan-1-ol (1) + n-decane (2) as a function of pressure (P) and temperature (T) at x_1 = 0.1276. (Symbol-T): (●- 313.15 K), (■- 323.15 K), (♦- 333.15 K), (▲- 343.15 K), (×- 353.15 K). (Line-Model): (···· - MTS), (- - - - BWRS), (—·— - PR), (—··— - PC-SAFT), (— — - tPC-PSAFT).

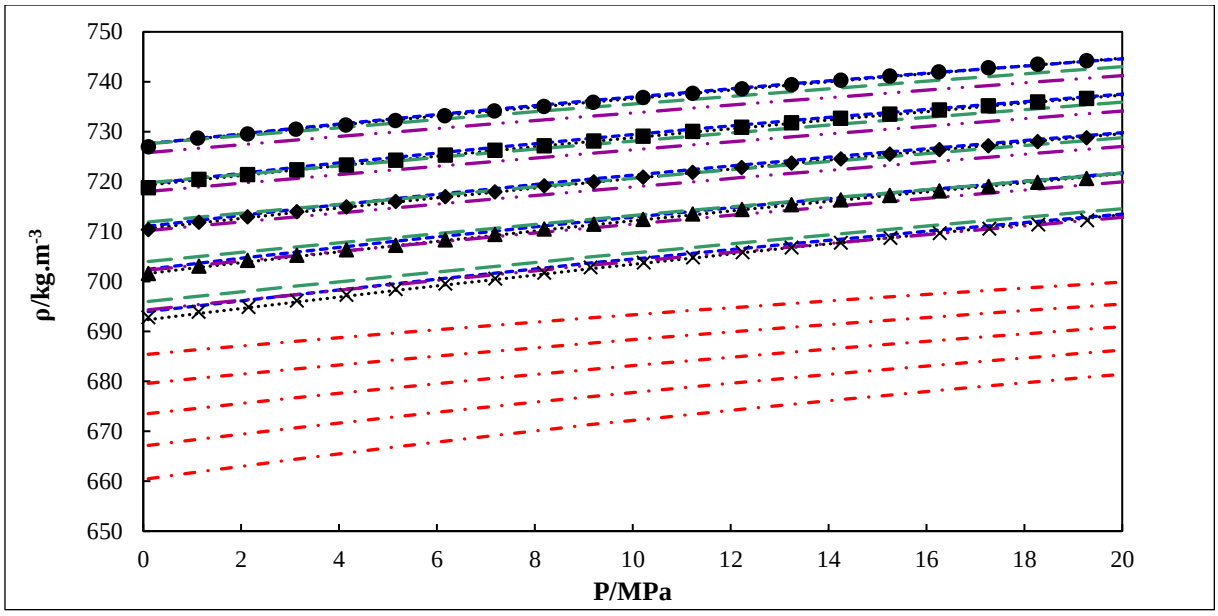

Figure 9.37. Experimental and model calculated density data (ρ) for the 2-methylpropan-1-ol (1) + n-decane (2) as a function of pressure (P) and temperature (T) at x_1 = 0.3749. (Symbol-T): (●- 313.15 K), (■- 323.15 K), (♦- 333.15 K), (▲- 343.15 K), (×- 353.15 K). (Line-Model): (···· - MTS), (- - - - BWRS), (—·— - PR), (—··— - PC-SAFT), (— — - tPC-PSAFT).

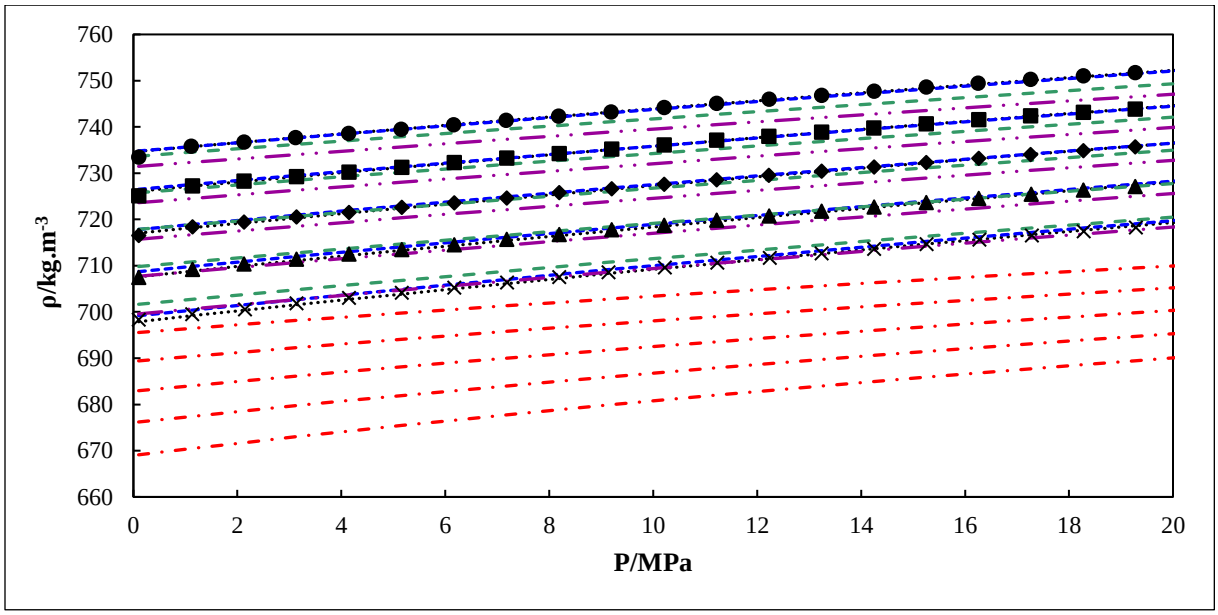

Figure 9.38. Experimental and model calculated density data (ρ) for the 2-methylpropan-1-ol (1) + n-decane (2) as a function of pressure (P) and temperature (T) at x_1 = 0.5015. (Symbol-T): (●- 313.15 K), (■- 323.15 K), (♦- 333.15 K), (▲- 343.15 K), (×- 353.15 K). (Line-Model): (···· - MTS), (- - - - BWRS), (—·— - PR), (—··— - PC-SAFT), (— — - tPC-PSAFT).

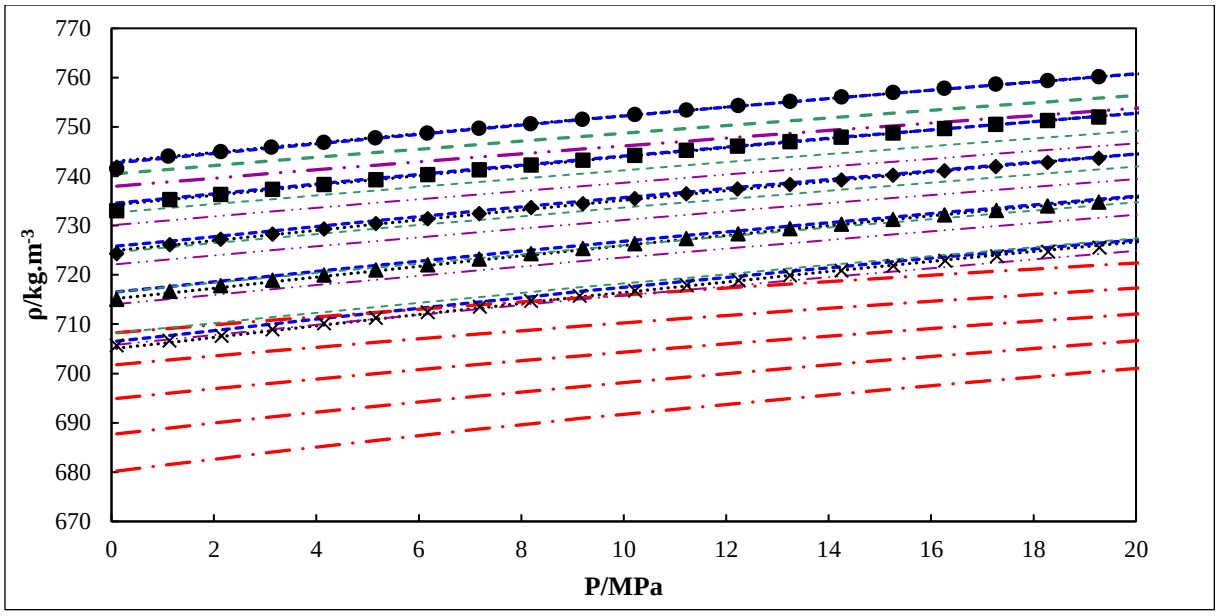

Figure 9.39. Experimental and model calculated density data (ρ) for the 2-methylpropan-1-ol (1) + n-decane (2) as a function of pressure (P) and temperature (T) at x_1 = 0.6249. (Symbol-T): (●- 313.15 K), (■- 323.15 K), (♦- 333.15 K), (▲- 343.15 K), (×- 353.15 K). (Line-Model): (···· - MTS), (- - - - BWRS), (—·— - PR), (—··— - PC-SAFT), (— — - tPC-PSAFT).

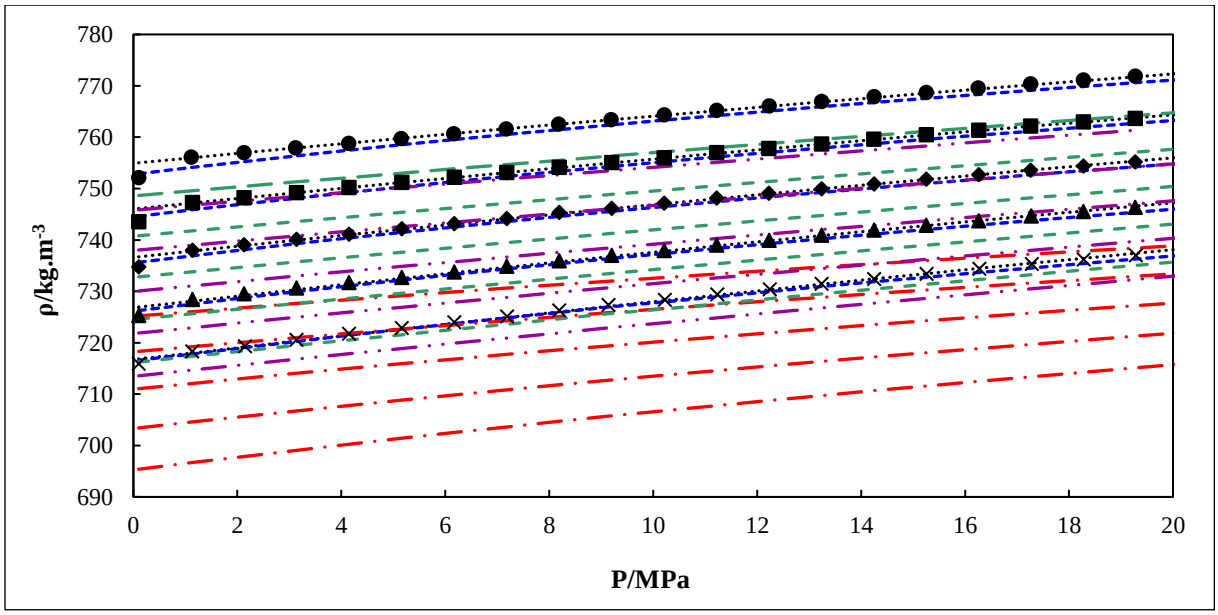

Figure 9.40. Experimental and model calculated density data (ρ) for the 2-methylpropan-1-ol (1) + n-decane (2) as a function of pressure (P) and temperature (T) at x_1 = 0.7502. (Symbol-T): (●- 313.15 K), (■- 323.15 K), (♦- 333.15 K), (▲- 343.15 K), (×- 353.15 K). (Line-Model): (···· - MTS), (- - - - BWRS), (—·— - PR), (—··— - PC-SAFT), (— — - tPC-PSAFT).

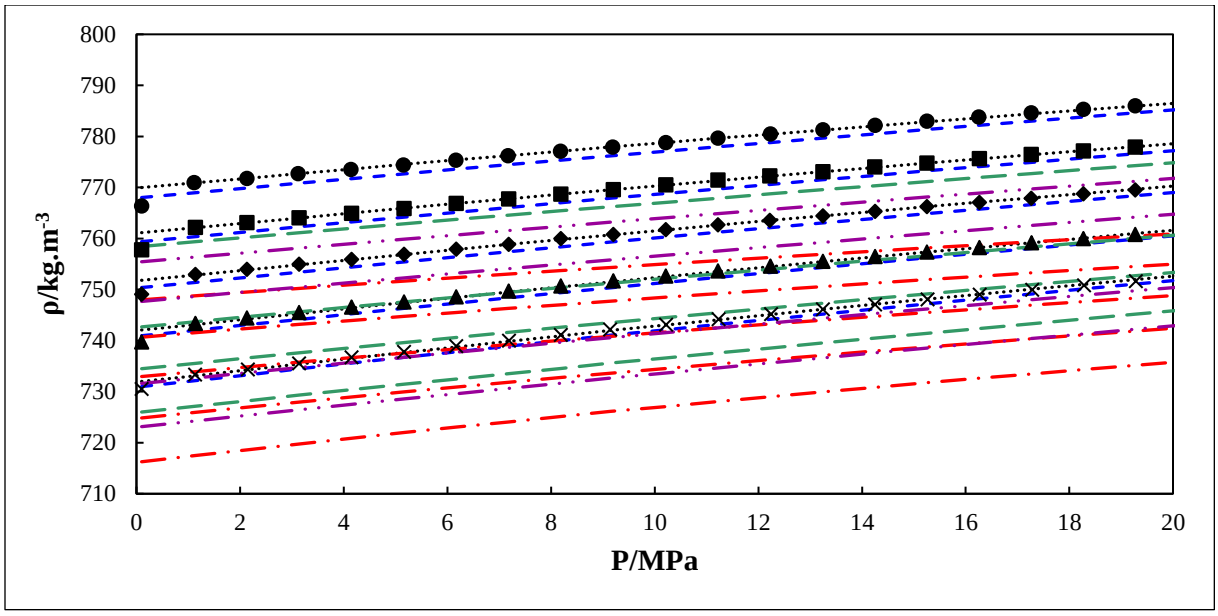

Figure 9.41. Experimental and model calculated density data (ρ) for the 2-methylpropan-1-ol (1) + n-decane (2) as a function of pressure (P) and temperature (T) at x_1 = 0.8750. (Symbol-T): (●- 313.15 K), (■- 323.15 K), (♦- 333.15 K), (▲- 343.15 K), (×- 353.15 K). (Line-Model): (···· - MTS), (- - - - BWRS), (—·— - PR), (—··— - PC-SAFT), (— — - tPC-PSAFT).

Table 9.1 Average RMSDs for system groups by each model employed.

Model	Average RMSDs for system					
	System					
	butan-1-ol (1) + n-octane (2)	butan-1-ol (1) + n-decane (2)	butan-2-ol (1) +n-octane (2)	butan-2-ol (1) + n-decane (2)	2-methylpropan-1-ol (1) + n-octane (2)	2-methylpropan-1-ol (1) + n-decane (2)
MTS	9.94E-04	4.37E-04	2.90E-04	2.13E-04	2.67E-04	1.95E-04
BWRS	1.13E-03	1.83E-03	3.12E-04	2.34E-04	2.45E-03	1.80E-03
PR	2.12E-02	5.73E-02	2.30E-02	5.91E-02	2.09E-02	5.84E-02
PC-SAFT	1.81E-02	1.90E-02	1.48E-02	1.48E-02	1.81E-02	1.61E-02
tPC-PSAFT	8.49E-03	1.09E-02	7.55E-03	6.70E-03	1.43E-02	1.22E-02

CHAPTER TEN

Culminating Discussion

10.1. Purity checks

Purity checks were conducted for all chemicals used via a refractometer, gas chromatographer and densimeter. A summary of the results obtained for the purity checks is presented in Tables 6.1, 7.1 and 8.1. The refractive index of the individual chemicals was analyzed at 293.15 or 298.15 K, using an ATAGO RX-7000a refractometer and thereafter compared to literature. It was noted that the refractive indices obtained experimentally were acceptably similar to their corresponding literature values generally within the experimental uncertainty of 0.0002. Thereafter, GC peak area checks were conducted using a Shimadzu GC2014. The pure components were injected into the GC using a 1 μL syringe yielding only single visible peaks at their respective retention times, with virtually no other detected impurities. The peak areas were compared to the percentage purities provided by the chemical suppliers. As shown in Tables 6.1, 7.1 and 8.1, the presence of very small amounts of impurities were noted, corresponding with the suppliers' declared proof. Lastly, the densities of the chemicals were analyzed by conducting atmospheric pressure density measurements at common temperatures using a DMA 5000 densimeter. These values were compared to literature and it was observed that experimental and literature values were similar within the experimental uncertainty of 0.08 $kg.m^{-3}$.

10.2. Calibration

Calibration of the pressure transducer and densimeter were conducted to ensure the accuracy and reproducibility of the equipment utilized for data measurement. After density and pressure calibration, temperature checks were conducted by an *in situ* method using high-purity n-heptane as a standard. The pressure calibration curve and scatter plot are presented in Figures D1 and D2, respectively. The maximum expanded combined uncertainty for pressure was $U_c(P) = 0.032$ MPa. The scatter plot presented in Figure D2 show randomness, which confirms that the pressure measurements did not exhibit any systematic error. The maximum expanded combined uncertainty in temperature measurements was estimated as $U_c(T) = 0.02$ K. The calibration procedure for the density measurements has been described in detail in the previous sections. The expanded

combined uncertainties in density were system dependent and are provided in the relevant result tables (Tables 6.5, 6.6, 7.4, 7.5, 8.4 and 8.5). These values ranged from 1.08 to 1.12 $kg.m^{-3}$.

10.3.Ethanol – n-heptane test system

High-pressure density measurements were conducted using a test system consisting of ethanol and n-heptane to evaluate the reliability of the experimental setup and the procedure used for measurements. Measurements were performed under isothermal conditions to gain familiarity with the measurement procedure as well as the operation of the densimeter. Isothermal measurements were conducted at 313.15, 323.15, 333.15, 343.15, and 353.15 K across the entire composition range and in the pressure range of 0.1 to 20 MPa. The results obtained were compared to literature and demonstrate good correlation within experimental uncertainty as presented in Figure 6.3. Maximum percentage relative deviations are approximately 0.30 %, which confirms the accuracy of the measurements presented in this work.

10.4.Temperature effects

The experimental data for all six binary systems comply with the generally accepted trends regarding density and temperature for liquid hydrocarbons. For each of the six systems, the density is observed to decrease with an increase in temperature, as observed in Figures 9.1 to 9.41. This is because the increased heat energy causes the liquid molecules to increase in velocity and thus occupy more space. Regarding excess volumes (example plots are shown in Figures 6.6, 6.7, 7.7, 7.8, 8.7 and 8.8 and calculated values are presented in Tables A1-A6), a large positive deviation from ideality is noted for all six systems which increases with temperature. This can be attributed to increases in mixture interactions when compared to those of the pure components, as well as the different shapes and sizes of the molecules interacting caused by the increase in the volume occupied by the individual components and is typical for alcohol/alkane systems. These behaviours were discussed in detail in the previous sections. In addition, the isothermal compressibility and thermal expansivity follow a similar trend for all six binary systems. From Figures 6.8-6.11, 7.10-7.13 and 8.9-8.12, it is noted that there is an increase with increasing temperature for both the thermal expansivity and isothermal compressibility.

10.5.Pressure effects

The experimental density data is compliant with the generally accepted trends regarding pressure and density, in that the density of the six systems increases with increasing pressure. This can largely be attributed to the fact that the molecules of the solution are compressed to a greater degree at higher pressures, and thus are closer together and occupying less volume. Derived thermodynamic properties namely, the excess molar volume, thermal expansivity and isothermal compressibility were calculated for all six systems. It was noted that all six systems demonstrate similar trends for the three calculated properties. The excess molar volume of the systems decrease as the pressure is increased as presented by Figures 6.6, 6.7, 7.7, 7.8, 8.7 and 8.8. Furthermore, regarding the thermal expansivity and isothermal compressibility, a decrease with increasing pressure is observed for both properties.

10.6. Modelling

The Modified Toscani-Szwarc (MTS) (Zúñiga-Moreno and Galicia-Luna, 2002), Benedict-Webb-Rubin-Starling (BWRS) (1973), Peng-Robinson (PR) (1976)equations of state and the Perturbed Chain-Statistical Associating Fluid Theory (PC-SAFT) (Gross and Sadowski, 2002) model were included in addition to the more sophisticated truncated Perturbed Chain-Polar Statistical Associating Fluid Theory (tPC-PSAFT) model (Karakatsani et al., 2006a). Note that the MTS and BWRS equations of state are composition specific empirical correlations; thus their performances were not compared directly with the cubic and SAFT-based equations of state. However, comparisons were made among the cubic and SAFT-based models.

In Chapter 9, Figures 9.1-9.41 present the model comparisons graphically for all binary components and six binary systems (butan-1-ol + n-octane/n-decane, butan-2-ol + n-octane/n-decane, 2-methylpropan-1-ol + n-octane/n-decane) in the temperature and pressure ranges 313.15 to 353.15 K and 0.1 to 20 MPa, respectively, and over the entire composition range. The RMSDs for the modelling of each system are summarized in Table 9.1.

The following key points are of particular interest for all five models with special attention paid to tPC-PSAFT:

1. The model's ability to accurately predict density for pure components and their respective mixtures. The RMSD is useful in this regard as low values of the RMSD generally indicate a more accurate model prediction. The relative trends exhibited by model and experimental data are also considered.
2. For models that perform poorly (high RMSD values), the trends exhibited are still considered. As a minimum, the model should demonstrate similar trends to the experimental data.
3. To highlight model deficiencies, especially when poor predictions for pure component properties are exhibited.

10.6.1. Pure component parameters used

The significant pure component parameters used in the PR-EOS, PC-SAFT and tPC-PSAFT predictions were obtained from numerous literature sources and are presented in Table 6.7, 7.7 and 8.7. As such, a certain degree of bias is introduced due to the differences in regression procedures as well as the quality of data employed by the various authors in determining these pure component parameters. Model performance for mixtures is greatly influenced by the rigor of the regression procedures employed to determine the pure component parameters. Hence, the likelihood of employing a regression procedure with the same degree of complexity by any two different authors is unlikely.

10.6.2. Non-polar components

The influence of repulsive and dispersive interactions (London force) can be isolated through the investigation of non-polar components. This allows for equations of states to be evaluated based on their ability to account for such interactions. The contribution due to association is zero in both the PC-SAFT and tPC-PSAFT models for non-polar components. Hence, the tPC-PSAFT model reduces to that of the PC-SAFT model and demonstrates superior predictions of pure alkane liquid density when compared to the Peng-Robinson EOS despite this generally being a commonly used EOS for alkane systems at high pressures.

10.6.2.1. n-Octane and n-decane

The density of pure n-octane and n-decane in the temperature and pressure ranges previously mentioned are shown in Figures 9.1 and 9.2 The figures demonstrate a good correlation of the experimental data and data trends using the MTS and BWRS equations of state within experimental uncertainty. The PC-SAFT model and PR EOS predictions demonstrate deviations from experimental data, especially at lower pressures. The PC-SAFT model under predicts the density of n-octane slightly (approximately 0.73 % relative deviation), at lower pressures but provides better predictions of the experimental data at higher pressures, greater than 10 MPa. An increase in model accuracy is also noted with an increase in the experimental temperature. The PR EOS, however, demonstrates a poor representation by grossly under predicting the density over the entire temperature and pressure range (excess of 3 % relative deviation) for n-octane. The density of n-decane is predicted reasonably well by the PC-SAFT model, mostly within experimental uncertainty (0.10 % relative deviation). The PR EOS demonstrates a considerable under-prediction of the n-decane density under all the experimental conditions considered in this work in excess of 6 % relative deviation. Similar trends to those followed by the experimental data, are depicted by the PR EOS despite the poor performance.

10.6.3. Polar components

When modelling components that exhibit hydrogen bonding, improved predictions are expected from the PC-SAFT and tPC-PSAFT models as they explicitly account for self-association and polar interactions or Keesom interactions that occur between the alcohol molecules. Significant improvement in the prediction of density data is observed over the PR EOS. This may be attributed to the inclusion of the association energy and effective association volume in both the PC-SAFT and tPC-PSAFT models and the polar and induction terms in the tPC-PSAFT model.

10.6.3.1. Butan-1-ol, butan-2-ol, and 2-methylpropan-1-ol

Figure 9.3 to 9.5 presents the experimental and predicted data for pure alcohols. Excellent correlation of the experimental data and data trends are noted for the MTS and BWRS EOS, within experimental uncertainty. The PC-SAFT model is the worst performing predictive model for butan-1-ol as it grossly under-predicts the system density across all temperatures and pressures

(exceeding 2 % relative deviation). The PR EOS generally demonstrates poor performance with regard to accurately predicting the density however, it demonstrates some improvement over the PC-SAFT model. This result is unexpected since the model should account for self-association and polar interactions occurring (Keesom interaction) in the alcohol, which the PR EOS does not do. For butan-2-ol, the PC-SAFT model prediction demonstrates some improvement over the PR EOS especially at lower temperatures. The model, however, displays significant deviation from the experimental data by under-predicting the respective densities (exceeding 2 % relative deviation). The tPC-PSAFT model demonstrates significant improvement over the PC-SAFT model (1.46 % relative deviation) and exhibits a similar trend to the experimental data. Furthermore, improved performance of the PR, PC-SAFT and tPC-PSAFT models is observed when compared to the respective model's performance for the butan-1-ol data. This may indicate that the pure component butan-1-ol model parameters used (obtained from reputable published sources) may need re-examination for the conditions considered here. Both the PC-SAFT and tPC-PSAFT models perform poorly for the 2-methylpropan-1-ol prediction (exceeding 2.4 % relative deviation) with the tPC-PSAFT model displaying some improvement over the PC-SAFT model. Furthermore, it should be noted that the PC-SAFT and tPC-PSAFT models perform the worst for the abovementioned alcohol. Again, this may be attributed to the quality of the pure component parameters used for the prediction or a deficiency of the models themselves in describing branched alcohols. In this case, the Peng-Robinson EOS demonstrates substantial improvement over the PC-SAFT and tPC-PSAFT models. All models, however, exhibit similar trends to those followed by the experimental data.

10.6.4. Modelling of binary mixtures

This study focuses not only on the correlation and prediction of thermodynamic properties for pure components but also for that of the binary mixtures. The binary mixtures investigated are those of non-polar/hydrogen bonding systems namely, alkane/alcohol systems. These systems account for repulsive, polar and dispersive interactions as well as self-association that exists between molecules of the alcohol components. The models' applicability to mixtures, using mixing rules, can be tested through the investigation of the thermodynamic properties of these binary mixtures. Once again, the ability of the model to reproduce the trends exhibited by the experimental density

data was investigated with pure component parameters being employed. A key point of observation is the model's ability to account for interactions that occur between dissimilar molecules. These interactions are governed by dispersive forces from the alkanes and hydrogen bonding and polar forces from the pure alcohol. Investigation of non-polar/hydrogen bonding systems allows for a model's ability to account for increasing levels of polar interactions (Keesom interactions) as well as hydrogen bonding to be tested.

To examine the models' capability to represent mixtures without the bias due to a superior pure component fit, excess volumes were initially predicted by each model and compared to the experimental data. Unfortunately, these results were inconclusive, as the excess volumes predicted by the models followed no observable trend. This is expected as the excess volume is highly sensitive to small variations in density and would require a superior model precision than those predicted for the pure component densities of the alcohols for example.

10.6.4.1. Butan-1-ol (1) + n-octane (2)/ n-decane (2)

The densities of the butan-1-ol (1) + n-octane (2)/ n-decane (2) systems are presented in Figures 9.6 to 9.17 along with model comparisons. These figures present the density data at five temperatures (313.15 – 353.15 K) in the pressure range 0.1 to 20 MPa, at various compositions. Model accuracy is demonstrated graphically by observing the trends of each model and by assessing their RMSD from the experimental data.

The MTS and BWRS EOS demonstrate an excellent correlation of the experimental density data under the investigated conditions within the experimental uncertainty (with RMSD of $2.540\ x\ 10^{-4}$ and $3.622\ x\ 10^{-4}$, respectively). However, regarding the BWRS EOS for the n-octane containing mixtures, a slight deviation from the experimental data was noted for compositions of $x_1 = 0.1259$, with a small overprediction (approximately 0.21 % relative deviation) at lower temperatures (313.15 – 343.15 K), of $x_1 = 0.7503$, with a slight under-prediction of density (approximately 0.16 % relative deviation) at lower pressures (0.1 – 5 MPa) and of $x_1 = 0.8750$, with an under-prediction of density (approximately 0.15 % relative deviation) especially noted at 353.15 K. For the n-decane containing systems, progressive deterioration in the model's ability to accurately predict the density is observed as the concentration of the butan-1-ol increases. At near

equimolar concentrations, a slight under-prediction of density (approximately 0.22 % relative deviation) is observed and increases as the composition approaches that of pure butan-1-ol. Furthermore, it is observed that the model is able to predict density data more accurately at higher temperatures, above 333.15 K, and pressures greater than 10 MPa.

Progressive deterioration in the performance of the PR EOS is observed in both butan-1-ol + alkane mixtures, with an increasing butan-1-ol composition, which is likely primarily due to the result of the poor pure butan-1-ol prediction by the model (RMSD = $1.25\,x\,10^{-2}$). Binary interaction parameters were calculated when fitting to the PR EOS, which are available in Chapters 6-8.

A significant improvement in the prediction of density data was expected by both PC-SAFT and tPC-PSAFT as these models explicitly account for polar and association interactions present in the system. However, upon review of the model predictions, it was observed that PC-SAFT grossly under-predicts the density over the entire composition range in both the butan-1-ol + n-octane/ n-decane systems under all temperature and pressure conditions (with RMSDs of $1.81\,x\,10^{-2}$ and $1.90\,x\,10^{-2}$, respectively). Despite the under-prediction of density by the tPC-PSAFT model, the model still demonstrates some improvement over the PC-SAFT model (RMSD = $1.09\,x\,10^{-2}$). Special attention is drawn to Figures 9.6, 9.7, 9.9, 9.12, 9.13 and 9.15. However, it is observed that as the concentration of the alcohol solution approaches one, $x_B = 1$, the tPC-PSAFT model under-predicts the density of the mixture, again compounded by the poor pure component representation of the butan-1-ol densities. The model performance is slightly improved at higher temperatures and pressures. All five models exhibit similar trends to those followed by the experimental data.

10.6.4.2. Butan-2-ol (1) + n-octane (2)/ n-decane (2)

Experimental and predicted density data for the system butan-2-ol (1) + n-octane (2)/ n-decane (2) are presented in Figures 9.18 to 9.29 along with model comparisons. Excellent correlation of the experimental data is demonstrated by both the MTS and BWRS EOS over the entire composition range (with RMSDs of $2.90\,x\,10^{-4}$ and $3.12\,x\,10^{-4}$, respectively). Furthermore, when comparing the BWRS predictions for the butan-1-ol mixtures to the prediction of the butan-2-ol + n-octane system, a significant improvement in the prediction of density data is observed. Poor

correlation is demonstrated by the Peng-Robinson EOS for these systems (RMSD = $5.91\ x\ 10^{-2}$) and is attributed to the model's poor performance in predicting the pure butan-2-ol behavior.

The PC-SAFT model under-predicts the data (RMSD = $1.48\ x\ 10^{-2}$) and progressively deteriorates with increasing concentration of butan-2-ol, again compounded by the poor pure component prediction. Furthermore, improvement in model predictions is observed for high temperature and pressure conditions. For the n-octane systems, the tPC-PSAFT model demonstrates some improvement over the PC-SAFT model (RMSD = $7.55\ x\ 10^{-3}$). However, as the concentration of the solution approaches that of pure butan-2-ol, the model performance deteriorates, coinciding with its poor performance in predicting the pure butan-2-ol density. In addition, it is observed that the model provides a more accurate prediction of the data at higher temperatures and pressures. For the n-decane systems, the tPC-PSAFT model performs fairly well (RMSD = $6.70\ x\ 10^{-3}$) in the alcohol dilute region and is observed to accurately predict the density data for lower temperatures, 313.15 to 333.15 K. At higher temperatures, 343.15 and 353.15 K, the model slightly deviates from experimental data (approximately 0.74 % relative deviation) in that it over-predicts the density of the binary mixture. For butan-2-ol concentrations above approximately 0.6, the model under-predicts the density slightly (by approximately 0.67 % relative deviation) and performs especially poorly in the alcohol rich region. Despite the shortcomings exhibited by some of the models, all five models exhibit similar trends to those followed by the experimental data.

10.6.4.5. 2-Methylpropan-1-ol (1) + n-octane (2)/ n-decane (2)

Experimental density data as well as the MTS, BWRS, PR, PC-SAFT and tPC-PSAFT model predictions are presented in Figures 9.30 to 9.41.

The MTS EOS demonstrates a good correlation of the experimental data across the entire composition range (RMSD = $2.67\ x\ 10^{-4}$) as well as in both the experimental temperature and pressure ranges. However, unlike in the case of butan-2-ol, the BWRS EOS demonstrates minor deviations from the experimental data (approximately 0.18 % relative deviation) in the alcohol rich region. The model performs fairly well in the alcohol dilute region at higher temperatures and pressures. Thereafter, as the alcohol concentration increases, $x_1 > 0.7$, the model under-predicts

the density of the mixture with smaller deviations from the experimental data (approximately 0.24 % relative deviation) noted at higher temperatures and pressures.

For the n-octane systems, the Peng-Robinson EOS poorly predicts the density across the entire composition range and is the model that demonstrates the most significant deviation from the experimental data (RMSD = $2.09\,x\,10^{-2}$). Furthermore, it is noted that the model accuracy improves slightly as the concentration of alcohol in the solution increases. This is expected as the PR-EOS density prediction of pure component 2-methylpropan-1-ol was superior to the other alcohols used in this investigation. Due to the poor pure n-decane prediction, the Peng-Robinson EOS does not correlate the density for the n-decane systems well, across the entire composition range (approximately 5.84 % relative deviation).

The PC-SAFT model accurately predicts the density of the binary system initially, in the 2-methylpropan-1-ol dilute region, at high temperatures, 343.15 and 353.15 K, and pressures, 10 MPa and higher (approximately 0.49 % relative deviation). However, a significant drop in the performance of the model is noted at equimolar concentration with a progressive worsening of the predicted density (approximately 1.81 % relative deviation) as the alcohol concentration approaches $x_1 = 1$.

An improvement in the predicted data is noted when comparing the tPC-PSAFT (approximately 1.43 % relative deviation) and PC-SAFT predictions. However, similarly to PC-SAFT, the tPC-PSAFT model accurately predicts density data at high temperatures, and pressures in the alcohol dilute regions; however, poor prediction of density is noted for the lower temperatures and pressures. As the concentration of the solution approaches that of pure 2-methylpropan-1-ol, $x_1 = 1$, a significant decline in the model's performance is noted. Again, the deficiency in both the PC-SAFT and tPC-PSAFT models' ability to accurately predict density data in the alcohol rich regions is unexpected as in their formulation, self-association and polar interactions (Keesom interaction) between the alcohol molecules should be explicitly accounted for. The predicted density data by all five models exhibit similar trends when compared to that of the experimental data regardless of their individual shortcomings.

10.6.5. Comparison of PC-SAFT prediction to tPC-SAFT prediction

The additional model parameters for the tPC-SAFT predictions were mostly taken from Karakatsani and co-workers (2005), or extrapolated from rules provided there. A reasonable improvement over the PC-SAFT model is observed when applying the tPC-SAFT model with an improvement in excess of 72% in some cases. The tPC-SAFT model provides a reasonable prediction for the systems containing butan-1-ol and butan-2-ol over PC-SAFT. This is attributed to the model's ability to reasonably account for the effects of hydrogen bonding in these systems, with the additional polar term, where bonding cooperativity has shown that secondary hydrogen bonds form easily in these mixtures (Gupta and Brinkley, 1998). Conversely, it has been reported that such effects are more complex in branched alcohols (Suhm, 2008) such as 2-methylpropan-1-ol, which cannot be easily accounted for by tPC-SAFT. The tPC-SAFT model is also able to represent induced dipole-induced dipole (Debye) interactions more easily due to the induction term. In the alcohol + alkane mixtures, the angle-dependent interactions cause asymmetrical molecular shapes that become anisotropic. Molecular ordering and packing cause the coordination numbers and degree of induced dipole-dipole to increase, which subsequently affects the polar force range (Karakatsani et al., 2005).

CHAPTER ELEVEN

Concluding Remarks

- An Anton Paar DMA HP densimeter and pressurizing network was used to measured high pressure densities in the temperature and pressure ranges 313.15 to 353.15 K and 0.1 to 20 MPa. The reliability of the experimental setup and procedure used for experimental purposes was confirmed by performing measurements of the ethanol-n-heptane test system. The results were compared to literature and demonstrate excellent correlation of the data, with a maximum percentage relative deviation of 0.12%, confirming the reliability of the procedures.

- Novel experimental density measurements were successfully conducted for six binary systems namely, butan-1-ol/butan-2-ol/2-methylpropan-1-ol (1) + n-octane/n-decane (2) utilizing an Anton Paar DMA HP densimeter in the temperature and pressure ranges 313.15 to 353.15 K and 0.1 to 20 MPa, respectively and over the entire composition range. The maximum expanded combined uncertainties for pressure, temperature and density were 0.032 MPa, 0.02 K and between 1.10 to 1.12 $kg.m^{-3}$, respectively.

- The experimental data for all six binary systems were found to comply with the generally accepted trends regarding density, pressure and temperature for liquid hydrocarbons in that the density of a solution decreases with increasing temperature and increases with increasing pressure. Excess volumes were found to be positive, and isothermal compressibility and thermal expansivity of the mixtures were non-linear, indicating complex mixture behaviour.

- The experimental data were compared to correlation by the MTS, BWRS, PR models, and prediction by the PC-SAFT and tPC-PSAFT models. The empirical MTS and BWRS equations of state demonstrated excellent correlation of the experimental data for all six binary systems with a maximum RMSDs of $2.90\,x\,10^{-4}$, for the MTS EoS and $3.622\,x\,10^{-4}$, for the BWRS EoS, for the butan-2-ol/butan-1-ol + n-octane systems, respectively. The BWRS EoS demonstrated significant improvement in density predictions for the butan-2-ol binary systems with general improvements in model prediction noted at higher temperatures and pressures. The Peng-Robinson EoS provided

a poor correlation of the density for all six binary systems especially in the alcohol rich regions. This was attributed to the use of a single fitting parameter, and the poor prediction of the pure component density behaviour using critical properties and standard mixing rules for model parameters.

- The PC-SAFT model under-predicts the density data for all six binary systems with a progressive worsening of the model's performance noted as the concentration of the respective alcohol increases. The model does however accurately predict data for the 2-methylpropan-1-ol binary systems in the alcohol dilute region. Improvement in the density predictions (about 78% better) is noted at higher temperatures and pressures for both the butan-2-ol and 2-methylpropan-1-ol binary systems, in comparison to lower temperatures.

- The tPC-PSAFT model demonstrates improved prediction of the density data when compared to those obtained by the PC-SAFT model in excess of 72% in some cases. Furthermore, improved accuracy is noted in the alcohol dilute regions and at high temperatures and pressures with progressive deterioration in model performance observed at high alcohol concentrations. This was not as expected as both the PC-SAFT and tPC-PSAFT models explicitly account for polar interactions (Keesom interaction) that occur between the alcohol molecules. This was attributed to poor pure component model parameters, that are usually acceptably applied to wide pressure and temperature ranges for phase equilibrium calculations, but do not characterize high pressure density behaviour well. Despite the shortcomings displayed by some of the models, all five models exhibited similar trends to that of the experimental data.

CHAPTER TWELVE

Recommendations

- The experimental operational range considered in this work was up to 20 MPa due to safety limitations of auxiliary equipment. The setup however is rated up to 65 MPa, and mixture data of alkane-alcohol systems are generally unavailable at these higher pressures. To fully characterize these mixtures, it's recommended that in future work, the safety limitations of the auxiliary equipment used in this work be improved to conduct these unique, high valued measurements.

- This study focused on the evaluation of the truncated Perturbed Chain-Polar Statistical Associating Fluid Theory (tPC-PSAFT) model in accounting for complex molecular interactions. This was achieved by comparing the density predictions obtained using the tPC-PSAFT model to the experimental density of six novel binary systems namely, butan-1-ol/butan-2-ol/2-methylpropan-1-ol (1) + n-octane/n-decane (2). The data measured here contributes to a databank that can be used to improve the model parameters used for the PC-SAFT and tPC-SAFT model. It is recommended that phase equilibria studies be conducted for the novel systems and conditions measured here. That data, along with the high-pressure density data measured here, can be used together to improve the PC-SAFT and tPC-SAFT model parameters for high pressures, and to determine accurate binary interaction parameters for these models, that could not be accurately determined in this work from density data alone.

- In future work, alcohol-water mixtures at the conditions measured here should be explored to further assess the rigour of the PC-SAFT and tPC-SAFT models in describing strongly associating systems at high pressures.

References

Abdulagatov, I.M., Azizov, N.D., 2006. (p,$ρ$,T,x) and viscosity measurements of {x1n-heptane + (1 - x1)n-octane} mixtures at high temperatures and high pressures. J. Chem. Thermodyn. 38, 1402–1415.

Abdussalam, A.A., Ivaniš, G.R., Radović, I.R., Kijevčanin, M.L., 2016. Densities and derived thermodynamic properties for the (n-heptane+n-octane), (n-heptane+ethanol) and (n-octane+ethanol) systems at high pressures. J. Chem. Thermodyn. 100, 89–99.

Aitbelale, R., Chhiti, Y., Ezzahrae, F., Alaoui, M., Eddine, A.S., Mun, N., Aguilar, F., 2019. High-Pressure Soybean Oil Biodiesel Density : Experimental Measurements , Correlation by Tait Equation , and Perturbed Chain. J. Chem. \& Eng. Data 3994--4004.

Al-Malah, K.I., 2015. RK-, SRK-, & SRK-PR-type equation of state for hydrocarbons, based on simple molecular properties. J. Appl. Chem. Sci. Int. 2, 65–74.

Alaoui, F., Montero, E., Bazile, J.P., Comuñas, M.J.P., Galliero, G., Boned, C., 2011. Liquid density of 1-butanol at pressures up to 140MPa and from 293.15K to 403.15K. Fluid Phase Equilib. 301, 131–136.

Alaoui, F.E.M., Montero, E.A., Qiu, G., Aguilar, F., Wu, J., 2013. Liquid density of biofuel mixtures: 1-Heptanol + heptane system at pressures up to 140 MPa and temperatures from 298.15 K to 393.15 K. J. Chem. Thermodyn. 65, 174–183.

Albrecht, K.L., Stein, F.P., Han, S.J., Gregg, Christopher J Radosz, M., 1996. Phase equilibria of saturated and unsaturated polyisoprene in sub-and supercritical ethane, ethylene, propane, propylene, and dimethyl ether. Fluid Phase Equilib. 117, 84--91.

Aminabhavi, T.M., Aralaguppi, M.I., Harogoppad, S.B., Balundgi, R.H., 1993. Densities, Viscosities, Refractive Indices, and Speeds of Sound for Methyl Acetoacetate + Aliphatic Alcohols (C1–C8). J. Chem. Eng. Data 38, 31–39.

Anderson, F.E., Prausnitz, J.M., 1986. Inhibition of gas hydrates by methanol. AIChE J. 32, 1321–1333.

Ashcroft, S.J., Booker, D.R., Turner, J.C.R., 1990. Density measurement by oscillating tube. Effects of viscosity, temperature, calibration and signal processing. J. Chem. Soc. Faraday Trans. 86, 145–149.

Atena, A., Muche, T., 2016. Modeling and Simulation of Real Gas Flow in a Pipeline. J. Appl. Math. Phys. 04, 1652–1681.

Audonnet, F., Pádua, A.A.., 2004. Viscosity and density of mixtures of methane and n-decane from 298 to 393 K and up to 75 MPa. Fluid Phase Equilib. 216, 235–244.

Awwad, A.M., Alsyouri, H.M., Abu-Daabes, M.A., Jbara, K.A., 2008. Densities and volumetric properties of (N-(2-hydroxyethyl)morpholine + ethanol, + 1-propanol, + 2-propanol, + 1-butanol, and + 2-butanol) at (293.15, 298.15, 303.15, 313.15, and 323.15) K. J. Chem. Thermodyn. 40, 592–598.

Back, P., Easteal, A., Hurle, R., Woolf, L., 1982. High-precision measurements with a bellows volumometer. J. Phys. E. 15, 360.

Baker, L.E., Luks, K.D., 1980. Critical Point and Saturation Pressure Calculations for Multipoint Systems (includes associated paper 8871). Soc. Pet. Eng. J. 20, 15–24.

Banipal, T.S., Garg, S.K., Ahluwalia, J.C., 1991. Heat capacities and densities of liquid n-octane, n-nonane, n-decane, and n-hexadecane at temperatures from 318.15 K to 373.15 K and at pressures up to 10 MPa. J. Chem. Thermodyn. 23, 923–931.

Barker, J.A., Henderson, D., 1967. Perturbation Theory and Equation of State for Fluids. II. A Successful Theory of Liquids. J. Chem. Phys. 47, 4714–4721.

Beattie, J.A., Bridgeman, O.., 1928. A new equation of state for fluids. Proc. Am. Acad. Arts Sci. 63, 229–308.

Behroozi, M., Zarei, H., 2011. Application of the ERAS model to volumetric properties of binary mixtures of banana oil with primary and secondary alcohols (C1–C4) at different temperatures. J. Chem. Thermodyn. 43, 696–704.

Benedict, M., Webb, G.B., Rubin, L.C., 1940. An empirical equation for thermodynamic properties of light hydrocarbons and their mixtures. I. Methane, ethane, propane and n-butane.

J. Chem. Phys. 8, 334–345.

Benedict, M., Webb, G.B., Rubin, L.C., 1942. An empirical equation for thermodynamic properties of light hydrocarbons and their mixtures: II. Mixtures of methane, ethane, propane, and n-butane. J. Chem. Phys. 10, 747–758.

Berro, C., Pneloux, A., 1984. Excess Gibbs Energies and Excess Volumes of I-Butanol-n -Heptane and 2-Methyl-I-propanol-n-Heptane Binary Systems 206–210.

Boelhouwer, J.W.M., 1960. PVT relations of five liquid n-alkanes. Physica 26, 1021–1028.

Boublík, T., 1970. Hard-Sphere Equation of State. J. Chem. Phys. 53, 471–472.

Bravo-Sánchez, M.G., Iglesias-Silva, G.A., Estrada-Baltazar, A., Hall, K.R., 2010. Densities and viscosities of binary mixtures of n -butanol with 2-butanol, isobutanol, and tert -butanol from (303.15 to 343.15) K. J. Chem. Eng. Data 55, 2310–2315.

Bravo-Sánchez, M.G., Iglesias-Silva, G.A., Estrada-Baltazar, A., Hall, K.R., 2013. Densities and Viscosities of Binary Mixtures of 2-Butanol + Isobutanol, 2-Butanol + tert -Butanol, and Isobutanol + tert -Butanol from (308.15 to 343.15) K. J. Chem. Eng. Data 58, 2538–2544.

Bridgman, P., 1913. Thermodynamic Properties of Twelve Liquids Between 20 and 80 and up to 12000 kgm. per sq. cm.

Bridgman, P., 1932. Volume-temperature-pressure relations for several non-volatile liquids. In: Proceedings of the American Academy of Arts and Sciences. pp. 1--27.

Bridgman, P.W., 1931. The volume of eighteen liquids as a function of pressure and temperature. In: Proceedings of the American Academy of Arts and Sciences. pp. 185--233.

Bridgman, P.W., 1942. Pressure-Volume Relations for Seventeen Elements to 100,000 Kg/Cm□. In: Proceedings of the American Academy of Arts and Sciences. pp. 425--440.

Brostow, W., Grindley, T., Macip, M.A., 1985. Volumetric properties of organic liquids as a function of temperature and pressure: experimental data and prediction of compressibility. Mater. Chem. Phys. 12, 37--97.

Brown, T., Lemay Jr, Eugene Bursten, B., Murphy, Catherine Langford, Steven Sagatys, D., 2010. Chemistry the central science: a broad perspective.

Brownstein, A.M., 2015. Isobutanol. In: Renewable Motor Fuels. Elsevier, pp. 47–56.

Burgess, W.A., Tapriyal, D., Morreale, B.D., Wu, Y., McHugh, M.A., Baled, H., Enick, R.M., 2012. Prediction of fluid density at extreme conditions using the perturbed-chain SAFT equation correlated to high temperature, high pressure density data. Fluid Phase Equilib. 319, 55–66.

Cano-Gómez, J.J., Iglesias-Silva, G.A., Rivas, P., Díaz-Ovalle, C.O., De Jesús Cerino-Córdova, F., 2017. Densities and Viscosities for Binary Liquid Mixtures of Biodiesel + 1-Butanol, + Isobutyl Alcohol, or + 2-Butanol from 293.15 to 333.15 K at 0.1 MPa. J. Chem. Eng. Data 62, 3391–3400.

Carnahan, N.F., Starling, K.E., 1969. Equation of state for nonattracting rigid spheres. J. Chem. Phys. 51, 635--636.

Carnahan, N.F., Starling, K.E., 1972. Intermolecular repulsions and the equation of state for fluids. AIChE J. 18, 1184–1189.

Chapman, W.G., Gubbins, K.E., Jackson, G., Radosd, M., 1990. Saftfirstpaper.pdf 1709–1721.

Chapman, W.G., Gubbins, K.E., Jackson, G., Radosz, M., 1989. SAFT: Equation-of-state solution model for associating fluids. Fluid Phase Equilib. 52, 31–38.

Chaudhari, S.K., Katti, S.S., 1985. Excess volumes of (an isomer of butanol + n-octane) at 298.15 K, measured with a continuous-dilution dilatometer. J. Chem. Thermodyn. 17, 101–104.

Chemistry, S., June, R., 1984. Thermodynamic Properties of Alcohols in a Micellar Phase . Binding Constants and Partial Molar Volumes of Pentanol in Sodium Rosario De Lisi , ~ Calogero Genova , ~ Rosaria Testa , 1 and Vincenzo Turco Liveri 1 13.

Chen, S.S., Kreglewski, A., 1977. Applications of the augmented van der Waals theory of fluids.: I. Pure fluids. Berichte der Bunsengesellschaft f{\"u}r Phys. Chemie 81, 1048--1052.

Chen, Z., Wu, Z., Liu, J., Lee, C., 2014. Combustion and emissions characteristics of high n-butanol/diesel ratio blend in a heavy-duty diesel engine and EGR impact. Energy Convers. Manag. 78, 787–795.

Chen, Z., Zhao, X., 2015. Enhancing Heavy-Oil Recovery by Using Middle Carbon Alcohol-

Enhanced Water fl ooding , Surfactant Flooding , and Foam Flooding.

Chen, Z., Zhao, X., 2017. Enhancing heavy-oil recovery by using middle carbon alcohol-enhanced hot polymer flooding. J. Pet. Sci. Eng. 149, 193–202.

Chiew, Y.C., 1990. Percus-Yevick integral-equation theory for athermal hard-sphere chains: Part I: Equations of state. Mol. Phys. 70, 129--143.

Chorążewski, M., 2007. Thermophysical and Acoustical Properties of the Binary Mixtures 1,2-Dibromoethane + Heptane within the Temperature Range from 293.15 K to 313.15 K. J. Chem. Eng. Data 52, 154–163.

Chueh, P.L., Prausnitz, J.M., 1967. Vapor-liquid equilibria at high pressures: Calculation of partial molar volumes in nonpolar liquid mixtures. AIChE J. 13, 1099–1107.

Cominges, B.E. De, Piñeiro, M.M., Mosteiro, L., Mascato, E., 2002. Temperature Dependence Of Thermophysical Properties Of Octane + 1-Butanol System. J. Therm. Anal. Calorim. 70, 217–227.

Comuñas, M.J.P., Bazile, J., Baylaucq, A., Boned, C., 2008. María J. P. Comuñas,* ,†,‡ Jean-Patrick Bazile, † Antoine Baylaucq, † and Christian Boned †. Engineering 986–994.

Coquelet, C., Valtz, A., Richon, D., de la Fuente, J.C., 2007. Volumetric properties of the boldine + alcohol mixtures at atmospheric pressure from 283.15 to 333.15 K. A new method for the determination of the density of pure boldine. Fluid Phase Equilib. 259, 33–38.

Cotterman, R., Schwarz, B., Prausnitz, J., 1986. Molecular thermodynamics for fluids at low and high densities. Part I: Pure fluids containing small or large molecules. AIChE J. 32, 1787--1798.

Couchman, P., Reynolds Jr, C., 1976. Tait equation for inorganic solids with applications to the pressure dependence of melting temperature. J. Appl. Phys. 47, 5201--5205.

Cummings, P., Stell, G., 1984. Statistical mechanical models of chemical reactions: Analytic solution of models of A+ B⇌ AB in the Percus-Yevick approximation. Mol. Phys. 51, 253--287.

Cummings, P.T., Stell, G., 1985. Statistical mechanical models of chemical reactions: II. Analytic

solution of the Percus-Yevick approximation for a model of homogeneous association. Mol. Phys. 55, 33--48.

Cutler, W.G., McMickle, R.H., Webb, W., Schiessler, R.., 1958. Study of the compressions of several high molecular weight hydrocarbons. J. Chem. Phys. 29, 727–740.

Dahami, M.A., Constant, W.D., Wolcott, J.M., 1988. Alcohol-assisted alkaline flooding for enhanced oil recovery. Fuel 67, 1242–1248.

Dakkach, M., Aguilar, F., Alaoui, F.E.M., Montero, E.A., 2015. Liquid density of oxygenated additives to biofuels: 2-Butanol at pressures up to 140 MPa and temperatures from (293.15 to 393.27) K. J. Chem. Thermodyn. 89, 278–285.

De Klerk, A., 2008. Fischer-Tropsch refining: Technology selection to match molecules. Green Chem. 10, 1249–1279.

De Villiers, A.J., 2011. Evaluation and improvement of the sPC-SAFT equation of state for complex mixtures. Stellenbosch University.

Deiters, U., Schneider, G.M., 1976. Fluid Mixtures At High Pressures. Computer Calculations of the Phase Equilibria and the Critical Phenomena in Fluid Binary Mixtures From the Redlich-Kwong Equation of State. Berichte der Bunsengesellschaft/Physical Chem. Chem. Phys. 80, 1316–1321.

Diamantonis, N.I., Economou, I.G., 2011. Evaluation of statistical associating fluid theory (SAFT) and perturbed chain-SAFT equations of state for the calculation of thermodynamic derivative properties of fluids related to carbon capture and sequestration. Energy and Fuels 25, 3334–3343.

Dix, M., Fareleira, J.M.N.A., Takaishi, Y., Wakeham, W.A., 1991. A vibrating-wire densimeter for measurements in fluids at high pressures. Int. J. Thermophys. 12, 357–370.

Djojoputro, H., Ismadji, S., 2005. Density and Viscosity of Binary Mixtures of Ethyl-2-methylbutyrate and Ethyl Hexanoate with Methanol, Ethanol, and 1-Propanol at (293.15, 303.15, and 313.15) K. J. Chem. Eng. Data 50, 1343–1347.

Dubey, G.P., Sharma, M., 2007. Thermophysical properties of binary mixtures of 2-methyl-1-

propanol with hexane, octane and decane at 298.15 K. J. Chem. Eng. Data 52, 449–453.

Dubey, G.P., Sharma, M., Dubey, N., 2008. Study of densities , viscosities , and speeds of sound of binary liquid mixtures of butan-1-ol with n -alkanes (C 6 , C 8 , and C 10) 40.

Dymond, J., Young, K., Isdale, J., 1979. p, ϱ, T behaviour for n-hexane+ n-hexadecane in the range 298 to 373 K and 0.1 to 500 MPa. J. Chem. Thermodyn. 11, 887--895.

Dymond, J.H., Glen, N., Robertson, J., Isdale, J.D., 1982. (p, ρ{variant}, T) for {(1-x)C6H6 + xC6D6} and {(1-x)C6H6 + xC6F6} in the range 298 to 373 K and 0.1 to 400 MPa. J. Chem. Thermodyn. 14, 1149–1158.

Dymond, J.H., Malhotra, R., 1988. The Tait equation: 100 years on. Int. J. Thermophys. 9, 941–951.

Dymond, J.H., Malhotra, R., Isdale, J.D., Glen, N.F., 1988. (p, ϱ, T) of n-heptane, toluene, and oct-1-ene in the range 298 to 373 K and 0.1 to 400 MPa and representation by the Tait equation. J. Chem. Thermodyn. 20, 603–614.

Dymond, J.H., Robertson, J., Isdale, J.D., 1982. (p, $ρ${variant}, T) of some pure n-alkanes and binary mixtures of n-alkanes in the range 298 to 373 K and 0.1 to 500 MPa. J. Chem. Thermodyn. 14, 51–59.

Dzida, M., Marczak, W., 2005. Thermodynamic and acoustic properties of binary mixtures of alcohols and alkanes. II. Density and heat capacity of (ethanol + n-heptane) under elevated pressures. J. Chem. Thermodyn. 37, 826–836.

Easteal, A., Woolf, L., 1987a. p, V, T and derived thermodynamic data for bromobenzene at temperatures from 278 to 323 K and pressures up to 280 MPa. Int. J. Thermophys. 8, 557--565.

Easteal, A., Woolf, L., 1987b. Volume ratios for n-pentane in the temperature range 278--338 K and at pressures up to 280 MPa. Int. J. Thermophys. 8, 231--238.

Easteal, A., Woolf, L., 1987c. Freezing pressures, p, V, T, and self-diffusion data at 298 and 313 K and pressures up to 300 MPa for 1, 3, 5-trimethylbenzene. Int. J. Thermophys. 8, 71--79.

Economou, I.G., 2002. Statistical associating fluid theory: A successful model for the calculation

of thermodynamic and phase equilibrium properties of complex fluid mixtures. Ind. Eng. Chem. Res. 41, 953–962.

Edward, J.T., Farrel, P.G., Shahidi, F., 1979. Effect of solvent (benzene, ethanol, cyclohexane) on the partial rnolah volumes of organic compounds. Can. Journa Chem. 57, 2887--2891.

El-Hefnawy, M., Sameshima, K., Matsushita, T., Tanaka, R., 2005. Apparent dipole moments of 1-alkanols in cyclohexane and n-heptane, and excess molar volumes of (1-alkanol + cyclohexane or n-heptane) at 298.15 K. J. Solution Chem. 34, 43–69.

Elliott, J.R., Daubert, T.E., 1987. Evaluation of an Equation of State Method for Calculating the Critical Properties of Mixtures. Ind. Eng. Chem. Res. 26, 1686–1691.

Estrada-Baltazar, A., Iglesias-Silva, G.A., Caballero-Cerón, C., 2013. Volumetric and Transport Properties of Binary Mixtures of n -Octane + Ethanol, + 1-Propanol, + 1-Butanol, and + 1-Pentanol from (293.15 to 323.15) K at Atmospheric Pressure. J. Chem. Eng. Data 58, 3351–3363.

Ezeji, T.C., Qureshi, N., Ujor, V., 2014. Isobutanol Production from Bioenergy Crops. In: Bioenergy Research: Advances and Applications. Elsevier, pp. 109–118.

Fandiño, O., Pensado, A.S., Lugo, L., Comuñas, M.J.P., Fernández, J., 2005. Compressed liquid densities of squalane and pentaerythritol tetra(2-ethylhexanoate). J. Chem. Eng. Data 50, 939–946.

Fang, D., Meng, X., Wu, J., 2017. Compressed Liquid Densities of Binary Mixtures of 1-Butanol and Diethylene Glycol Dimethyl Ether from (283 to 363) K at Pressures up to 100 MPa. J. Chem. Eng. Data 62, 2937–2943.

Faranda, S., Foca, G., Marchetti, A., Pályi, G., Tassi, L., Zucchi, C., 2004. Density measurements of the binary mixtures of 2-butanone and 2-butanol at temperatures from -10 to 80 °C. J. Mol. Liq. 111, 117–123.

Feitosa, F.X., Caetano, A.C.R., Cidade, T.B., Sant'Ana, H.B.D., 2009. Viscosity and Density of Binary Mixtures of Ethyl Alcohol with n-Alkanes (C6, C8, and C10). J. Chem. Eng. Data 54, 2957–2963.

Fitzgerald, D., Du, C., Asaph, S., 2000. Technical Assessment of the Anton Paar DMA5000 density meter. Assessment 44, 0–8.

Folas, G.K., Kontogeorgis, G.M., Michelsen, M.L., Stenby, E.H., 2006. Application of the cubic-plus-association (CPA) equation of state to complex mixtures with aromatic hydrocarbons. Ind. Eng. Chem. Res. 45, 1527–1538.

Fortenberry, R., Kim, D.H., Nizamidin, N., Adkins, S.S., Pinnawala Arachchilage, G.W.P., Koh, H., Weerasooriya, U., Pope, G.A., 2015. Use of cosolvents to improve alkaline/polymer flooding. SPE J. 20, 255–266.

Fouad, W.A., Wang, L., Haghmoradi, A., Asthagiri, D., Chapman, W.G., 2016. Understanding the Thermodynamics of Hydrogen Bonding in Alcohol-Containing Mixtures: Cross-Association. J. Phys. Chem. B 120, 3388–3402.

Franjo, C., Menaut, C.P., Jimenez, E., Legido, J.L., Andrades, M.I.P., 1995. Viscosities and Densities of Octane Octan-1-01 at 298.15 992–994.

Gascón, I., Giner, B., Martín, S., Cea, P., Artigas, H., 2003. Excess properties of the ternary system (hexane + 1,3-dioxolane + 1-butanol) at 298.15 and 313.15 K. Fluid Phase Equilib. 211, 61–73.

Gayol, A., Casás, L.M., Martini, R.E., Andreatta, A.E., Legido, J.L., 2013. Volumetric properties of (dialkyl carbonate + n-alkane) mixtures at high pressures: Experimental measurement and Nitta-Chao model prediction. J. Chem. Thermodyn. 58, 245–253.

Gayol, A., Iglesias, M., Goenaga, J.M., Concha, R.G., Resa, J.M., 2007. Temperature influence on solution properties of ethanol + n-alkane mixtures. J. Mol. Liq. 135, 105–114.

Gbadamosi, A.O., Kiwalabye, J., Junin, R., Augustine, A., 2018. A review of gas enhanced oil recovery schemes used in the North Sea. J. Pet. Explor. Prod. Technol. 8, 1373–1387.

Gehrig, M., Lentz, H., 1983. Values of p(Vm, T) for n-decane up to 300 MPa and 673 K. J. Chem. Thermodyn. 15, 1159–1167.

Golubev, I.F., Vasil'kovskaya, T.N., Zolin, V.S., 1980a. Experimental study of the density of aliphatic alcohols at various temperatures and pressures. J. Eng. Phys. 38, 399–401.

Golubev, I.F., Vasil'kovskaya, T.N., Zolin, V.S., 1980b. Experimental study of the density of aliphatic alcohols at various temperatures and pressures. J. Eng. Phys. 38, 399–401.

Gonalves, F.A.M.M., Trindade, A.R., Costa, C.S.M.F., Bernardo, J.C.S., Johnson, I., Fonseca, I.M.A., Ferreira, A.G.M., 2010. PVT, viscosity, and surface tension of ethanol: New measurements and literature data evaluation. J. Chem. Thermodyn. 42, 1039–1049.

González, B., Domínguez, A., Tojo, J., 2004. Dynamic viscosities of 2-butanol with alkanes (C8, C 10, and C12) at several temperatures. J. Chem. Thermodyn. 36, 267–275.

González, E.J., Calvar, N., Macedo, E.A., 2014. Osmotic coefficients and apparent molar volumes of 1-hexyl-3- methylimidazolium trifluoromethanesulfonate ionic liquid in alcohols. J. Chem. Thermodyn. 69, 93–100.

Goodwin, A.R.H., Donzier, E.P., Vancauwenberghe, O., Fitt, A.D., Ronaldson, K.A., Wakeham, W.A., De Lara, M.M., Marty, F., Mercier, B., 2006. A Vibrating edge supported plate, fabricated by the methods of micro electro mechanical system for the simultaneous measurement of density and viscosity: Results for methylbenzene and octane at temperatures between (323 and 423) K and pressures in the ran. J. Chem. Eng. Data 51, 190–208.

Gregg, C.J., Stein, F.P., Radosz, M., 1994. Phase behavior of telechelic polyisobutylene (PIB) in subcritical and supercritical fluids. 1. Inter-and Intra-association effects for blank, monohydroxy, and dihydroxy PIB (1K) in ethane, propane, dimethyl ether, carbon dioxide, and chlorodifluoromethane. Macromolecules 27, 4972--4980.

Grindley, T., Lind Jr, J.E., 1971. No TitlePVT properties of water and mercury. J. Chem. Phys. 54, 3983--3989.

Gross, J., Sadowski, G., 2001. Perturbed-Chain SAFT: An Equation of State Based on a Perturbation Theory for Chain Molecules. Ind. Eng. Chem. Res. 40, 1244–1260.

Gross, J., Sadowski, G., 2002. Application of the Perturbed-Chain SAFT Equation of State to Associating Systems. Ind. Eng. Chem. Res. 41, 5510–5515.

Gubbins, K.E., Twu, C., 1978. Thermodynamics of polyatomic fluid mixtures—I theory. Chem. Eng. Sci. 33, 863--878.

Gupta, R.B., Brinkley, R.L., 1998. Hydrogen-bond cooperativity in 1-alkanol+ n-alkane binary mixtures. AIChE J. 44, 207–213.

Hammerschmidt, E.G., 1939. Preventing and removing gas hydrate formations in Natural Gas pipelines. Oil Gas J. 68–72.

Harvey, B.G., Meylemans, H.A., 2011. The role of butanol in the development of sustainable fuel technologies. J. Chem. Technol. Biotechnol. 86, 2–9.

Hasch, B.M., Maurer, E.J., Ansanelli, L.F., McHugh, M.A., 1994. (Methanol+ ethene): phase behavior and modeling with the SAFT equation of state. J. Chem. Thermodyn. 26, 625--640.

Haynes, W.M., 2014. CRC Handbook of Chemistry and Physics, 95th Edition, 95th ed. N. ed. CRC Press, Hoboken.

Hayward, A.T.J., 1967. Compressibility equations for liquids: a comparative study. Br. J. Appl. Phys. 18, 965.

Huang, S.H., Radosz, M., 1990. Equation of state for small, large, polydisperse, and associating molecules. Ind. Eng. Chem. Res. 29, 2284–2294.

Huang, S.H., Radosz, M., 1991. Equation of State for Small, Large, Polydisperse, and Associating Molecules: Extension to Fluid Mixtures. Ind. Eng. Chem. Res. 30, 1994–2005.

Hussain, M., Moodley, K., 2020a. P –ρ– T Data and Modeling for Butan-1-ol + n -Octane or n -Decane between 313.15–353.15 K and 0.1–20 MPa. J. Chem. Eng. Data acs.jced.9b01042.

Hussain, M., Moodley, K., 2020b. Experimental P –ρ– T Data and Modeling for Butan-2-ol + n -Octane or n -Decane in the Ranges of 313.15–353.15 K and 0.1–20 MPa. J. Chem. Eng. Data 65, 3848–3865.

Hussain, M., Moodley, K., 2021. P-ρ-T data and modelling for (2-methylpropan-1-ol + n-octane or n-decane) between 313.15 K–353.15 K and 0.1–20 MPa. J. Chem. Thermodyn. 152, 106279.

Iglesias-Silva, G.A., Bravo-Sánchez, M., Estrada-Baltazar, A., Bouchot, C., Hall, K.R., 2015. P -ρ- T Data for 1-Butanol and Isobutyl Alcohol from (283.15 to 363.15) K at Pressures up to 66 MPa. J. Chem. Eng. Data 60, 1076–1090.

Iglesias, T., Legido, J., Roman{\i}, L., Peleteiro, J., Andrade, M.P., 1993. Dielectric permittivities, densities, and excess molar volumes of $\{$xCH3 (CH2) 6CH3+ (1-x)(CH3 (CH2) vOH$\}$(v= 2 to 4) at the temperature 298.15 K. J. Chem. Thermodyn. 25, 1325--1332.

Ihmels, E.C., Gmehling, J., 2001. Densities of Toluene, Carbon Dioxide, Carbonyl Sulfide, and Hydrogen Sulfide over a Wide Temperature and Pressure Range in the Sub- and Supercritical State. Ind. Eng. Chem. Res. 40, 4470–4477.

IMechE, 2012. Fuel Systems for IC Engines. Woodhead Publishing.

ISO, 2008. JCGM 100:2008. Int. Organ. Stand. Geneva ISBN 50, 134.

Itsuki, H., Terasawa, S., Shinohara, K., Ikezawa, H., 1987. Partial molar volumes at infinite dilution for CmH2m+2 as solute in CnH2n+2 as solvent for m, n = 6 to 16 at 298.15 K. J. Chem. Thermodyn. 19, 555–559.

Janssen, M.T.G., Pilus, R.M., Zitha, P.L.J., 2020. A Comparative Study of Gas Flooding and Foam-Assisted Chemical Flooding in Bentheimer Sandstones. Transp. Porous Media 131, 101–134.

Jog, P.K., Chapman, W., 1999. Application of Wertheim's thermodynamic perturbation theory to dipolar hard sphere chains. Mol. Phys. 97, 307--319.

Jog, P.K., Sauer, S.G., Blaesing, J., Chapman, W.G., 2001. Application of dipolar chain theory to the phase behavior of polar fluids and mixtures. Ind. \& Eng. Chem. Res. 40, 4641--4648.

Kaarsholm, M., Derawi, S.O., Michelsen, M.L., Kontogeorgis, G.M., 2005. Extension of the cubic-plus-association (CPA) equation of state to amines. Ind. Eng. Chem. Res. 44, 4406–4413.

Kamerlingh Onnes, H., 1901. Expression of the equation of state of gases and liquids by means of series. KNAB 4, 125--147.

Kang, K., Wang, X., 2018. Liquid densities for n-decane + p-xylene mixtures from 293.15 K to 363.15 K at pressures up to 60 MPa. Fluid Phase Equilib. 458, 142–152.

Kapateh, M.H., Chapoy, A., Burgass, R., Tohidi, B., 2016. Experimental Measurement and Modeling of the Solubility of Methane in Methanol and Ethanol. J. Chem. Eng. Data 61, 666–

673.

Karakatsani, E.K., Economou, I.G., 2006. Perturbed chain-statistical associating fluid theory extended to dipolar and quadrupolar molecular fluids. J. Phys. Chem. B 110, 9252–9261.

Karakatsani, E.K., Economou, I.G., 2007. Phase equilibrium calculations for multi-component polar fluid mixtures with tPC-PSAFT. Fluid Phase Equilib. 261, 265–271.

Karakatsani, E.K., Economou, I.G., Gross, J., Sadowski, G., Camacho-Camacho, L.E., Galicia-Luna, L.A., De Villiers, A.J., Fu, Y.H., Sandler, S.I., Gross, J., Sadowski, G., Karakatsani, E.K., Economou, I.G., Solms, N. Von, Kouskoumvekaki, I.A., Michelsen, M.L., Kontogeorgis, G.M., Passarello, J., Tobaly, P., Equilibria, F.P., 2006a. A Simplified SAFT Equation of State for Associating Compounds and Mixtures. Ind. Eng. Chem. Res. 41, 9252–9261.

Karakatsani, E.K., Economou, I.G., Kroon, M.C., Bermejo, M.D., Peters, C.J., Witkamp, G.J., Spyriouni, T., Economou, I.G., Kontogeorgis, G.M., Economou, I.G., Larsen1, B., Rasaiah, J.C., Stell, G., 2006b. Thermodynamic perturbation theory for multipolar and ionic liquids. Mol. Phys. 45, 6063–6074.

Karakatsani, E.K., Kontogeorgis, G.M., Economou, I.G., 2006c. Evaluation of the truncated perturbed chain-polar statistical associating fluid theory for complex mixture fluid phase equilibria. Ind. Eng. Chem. Res. 45, 6063–6074.

Karakatsani, E.K., Spyriouni, T., Economou, I.G., 2005. Extended statistical associating fluid theory (SAFT) equations of state for dipolar fluids. AIChE J. 51, 2328–2342.

Kariznovi, M., Nourozieh, H., Abedi, J., 2013. Solubility of carbon dioxide, methane, and ethane in 1-butanol and saturated liquid densities and viscosities. J. Chem. Thermodyn. 67, 227–233.

Kashiwagi, H., Fukunaga, T., Tanaka, Y., Kubota, H., Makita, T., 1980. Dielectric constant and density of cyclohexane-benzene mixtures under high pressure. Rev. Phys. Chem. Japan, 49, 70–84.

Kaur, H., Samra, N.S., Mahl, B.S., 1991. Excess Volumes of Binary Li uid Mixtures of n-Alkanols and Cycloalkanols with n- Ail kanes and the Theoretical Treatment Using the ERAS-Model 67, 241–257.

Kermanpour, F., Niakan, H.Z., 2012. Measurement and modeling the excess molar properties of binary mixtures of {[C 6mim][BF 4] + 3-amino-1-propanol} and {[C 6mim][BF 4] + isobutanol}: Application of Prigogine-Flory-Patterson theory. J. Chem. Thermodyn. 48, 129–139.

Kijevčanin, M.L., Radović, I.R., Šerbanović, S.P., Tasić, A.Ž., Djordjević, B.D., 2009. Experimental determination and modelling of densities and excess molar volumes of ternary system (1-butanol+cyclohexylamine+n-heptane) and corresponding binaries from 288.15 to 323.15K. Thermochim. Acta 496, 71–86.

Kinzl, M., Luft, G., Adidharma, H., Radosz, M., 2000. SAFT modeling of inert-gas effects on the cloud-point pressures in ethylene copolymerization systems: Poly (ethylene-co-vinyl acetate)+ vinyl acetate+ ethylene and poly (ethylene-co-hexene-1)+ hexene-1+ ethylene with carbon dioxide, nitrogen, or n-butane. Ind. \& Eng. Chem. Res. 39, 541--546.

Kiran, E., Sen, Y.L., 1992. High-pressure viscosity and density of n-alkanes. Int. J. Thermophys. 13, 411–442.

Kondori, J., Zendehboudi, S., James, L., 2018. Evaluation of Gas Hydrate Formation Temperature for Gas/Water/Salt/Alcohol Systems: Utilization of Extended UNIQUAC Model and PC-SAFT Equation of State. Ind. Eng. Chem. Res. 57, 13833–13855.

Kontogeorgis, G.M., Folas, G.K., 2009. Thermodynamic Models for Industrial Applications: From Classical and Advanced Mixing Rules to Association Theories, Thermodynamic Models for Industrial Applications: From Classical and Advanced Mixing Rules to Association Theories.

Kontogeorgis, G.M., Folas, G.K., 2010. Thermodynamic Models for Industrial Applications From Classical and Advanced Mixing Rules to Association Theories. United Kingdom.

Kontogeorgis, G.M., Yakoumis, I. V., Meijer, H., Hendriks, E., Moorwood, T., 1999. Multicomponent phase equilibrium calculations for water-methanol-alkane mixtures. Fluid Phase Equilib. 158–160, 201–209.

Kouris, S., Panaylotou, C., 1989. Dynamic Viscosity of Mixtures of Benzene, Ethanol, and n-Heptane at 298.15 K. J. Chem. Eng. Data 34, 200–203.

Kubota, H., Tanaka, Y., Makita, T., 1987. Volumetric behavior of pure alcohols and their water

mixtures under high pressure. Int. J. Thermophys. 8, 47–70.

Kubota, H., Tsuda, S., Murata, M., Yamamoto, T., Tanaka, Y., Makita, T., 1980. Specific volume and viscosity of methanol-water mixtures under high pressure. Rev. Phys. Chem. Japan 49, 59–69.

Kumagai, A., Tomida, D., Yokoyama, C., 2006. Measurements of the liquid viscosities of mixtures of n-butane, n-hexane, and n-octane with squalane to 30 MPa. Int. J. Thermophys. 27, 376–393.

Kumaran, M., Benson, G.C., 1983. Limiting partial molar volumes of ethanol, propan-1-ol, butan-1-ol, pentan-1-ol, and hexan-1-ol in n-heptane at 298.15 K. J. Chem. Thermodyn. 15, 245--248.

Lake, L.W., 1989. Enhanced Oil recovery.

Lampreia, I.M.S., Nieto de Castro, C.A., 2011. A new and reliable calibration method for vibrating tube densimeters over wide ranges of temperature and pressure. J. Chem. Thermodyn. 43, 537–545.

Langa, E., Mainar, A.M., Pardo, J.I., Urieta, J.S., 2005. Excess enthalpy, excess volume, and speed of sound deviation for the mixtures β-pinene + ethanol and β-pinene + 1-propanol at (283.15, 298.15, and 313.15) K. J. Chem. Eng. Data 50, 1255–1261.

Langa, E., Mainar, A.M., Pardo, J.I., Urieta, J.S., 2006. Excess Enthalpy, Density, and Speed of Sound for the Mixtures β-Pinene + 1-Butanol or 2-Butanol at (283.15, 298.15, and 313.15) K. J. Chem. Eng. Data 51, 392–397.

Larsen1, B., Rasaiah, J.C., Stell, G., 1977. Thermodynamic perturbation theory for multipolar and ionic liquids. Mol. Phys. 33, 987–1027.

Lasarte, J.M., Martín, L., Langa, E., Urieta, J.S., Mainar, A.M., 2008. Setup and validation of a PρT measuring device. Volumetric behavior of the mixture 1,8-cineole + ethanol. J. Chem. Eng. Data 53, 1393–1400.

Lee, S.-H., Hasch, B.M., McHugh, M.A., 1996. Calculating copolymer solution behavior with statistical associating fluid theory. Fluid Phase Equilib. 117, 61--68.

Lemmon, E.W., Huber, M.L., McLinden, M.O., 2010. NIST Standard Reference Database 23: Reference Fluid Thermodynamic and Transport Properties (REFPROP), Version 9.0. Phys. Chem. Prop. ….

Lielmezs, J., Lin, C. -J, Kwok, Y.C., Starling, K.E., McFee, D.G., Mueller, K.H., Lielmezs, J., Pedersen, K.S., Christensen, P.L., Shaikh, J.A., Mills, M.B., Wills, M.J., Bhirud, V.L., Zudkevitch, D., Kaufmann, T.G., Beret, S., Prausnitz, J.M., Atena, A., Muche, T., Kumar, K.H., Starling, K.E., Milano, P.D.I., Approach, O., Aspen Institution, Shah, K.K., Thodos, G., Starling, K.E., Powers, J.E., Republic, C., Benedict, M., Webb, G.B., Rubin, L.C., 1982. The calculation of density by the BWRS equation of state in process simulation contexts. J. Chem. Phys. 21, 4857990.

Liu, K., Wu, Y., McHugh, M.A., Baled, H., Enick, R.M., Morreale, B.D., 2010. Equation of state modeling of high-pressure, high-temperature hydrocarbon density data. J. Supercrit. Fluids 55, 701–711.

London, F., 1930. Zur theorie und systematik der molekularkr{\"a}fte. Zeitschrift f{\"u}r Phys. 63, 245--279.

Lugo, L., Comunas, M.J.P., López, E.R., Fernández, J., 2001. (p, Vm, T, x) measurements of dimethyl carbonate+octane binary mixtures. I. Experimental results, isothermal compressibilities, isobaric expansivities and internal pressures. Fluid Phase Equilib. 186, 235–255.

Lugo, L., Comuñas, M.J.P., López, E.R., Fernández, J., 2001. (p, Vm, T, x) measurements of dimethyl carbonate+octane binary mixtures. Fluid Phase Equilib. 186, 235–255.

Majstorović, D.M., Radović, I.R., Kijevčanin, M.L., Živković, E.M., 2020. Thermodynamic study of ester diethyl tartrate and its binary systems with iso-alcohols. Fluid Phase Equilib. 509, 112461.

Malhotra, R., Woolf, L., 1990. Thermodynamic properties of 2, 2, 4-trimethylpentane. Int. J. Thermophys. 11, 1059--1073.

Mansoori, G.A., Carnahan, N.F., Starling, K.E., Leland, T.W., 1971. Equilibrium thermodynamic properties of the mixture of hard spheres. J. Chem. Phys. 54, 1523–1526.

Masoudi, R., Tohidi, B., 2005. Estimating the hydrate stability zone in the presence of salts and/or organic inhibitors using water partial pressure. J. Pet. Sci. Eng. 46, 23–36.

Matkowska, D., Gołdon, A., Hofman, T., 2010. Densities, excess volumes, isobaric expansivities, and isothermal compressibilities of the 1-ethyl-3-methylimidazolium ethylsulfate + ethanol system at temperatures (283.15 to 343.15) K and pressures from (0.1 to 35) MPa. J. Chem. Eng. Data 55, 685–693.

Moodley, K., Adam, S., Naidoo, P., Naidu, S., Ramjugernath, D., 2018. P -ρ- T Data and Modeling for Propan-1-ol + n -Octane or n -Nonane or n -Decane from 313.15 K to 363.15 K and 1 MPa to 20 MPa. J. Chem. Eng. Data 63, 4136–4156.

Moodley, K., Dorsamy, C.-L., 2018. Isothermal Vapor–Liquid Equilibrium Measurements of Butan-2-one + 2-Methyl-propan-1-ol/Pentan-1-ol. J. Chem. Eng. Data 63, 4128–4135.

Morávková, L., Wagner, Z., Aim, K., Linek, J., 2006. (P, V m , T) Measurements of (octane + 1-chlorohexane) at temperatures from 298.15 K to 328.15 K and at pressures up to 40 MPa. J. Chem. Thermodyn. 38, 861–870.

Morávková, L., Wagner, Z., Linek, J., 2008. (p, Vm, T) measurements of (octane + benzene) at temperatures from (298.15 to 328.15) K and at pressures up to 40 MPa. J. Chem. Thermodyn. 40, 607–617.

Moriyoshi, T., Uosaki, Y., 1984. Compressive and dielectric properties of aqueous non-electrolyte mixtures. J. Soc. Mater. Sci. Jpn 33, 127–133.

Moss, J.T., Berkowitz, A.M., Oehlschlaeger, M.A., Biet, J., Warth, V., Glaude, P.A., Battin-Leclerc, F., 2008. An experimental and kinetic modeling study of the oxidation of the four isomers of butanol. J. Phys. Chem. A 112, 10843–10855.

Mulholland, J.D., 1973. An interpretive review. Moon 8, 548–556.

Müller, E.A., Gubbins, K.E., 2001. Molecular-Based Equations of State for Associating Fluids: A Review of SAFT and Related Approaches. Ind. Eng. Chem. Res. 40, 2193–2211.

Munck, J., Skjold-Jorgensen, S., Rasmussen, P., 1986. Computations of the Formation of Gas Hydrates. Soc. Pet. Eng. AIME, SPE 43.

Nath, J., Pandey, J.G., 1997. Binary mixtures of butanol + pentane, + hexane, + heptane, + octane, + 2,2,4-trimethylpentane, and + carbon tetrachloride. 1. Excess molar volumes at 288.15 K and 298.15 K and refractive indexes at 298.15 K. J. Chem. Eng. Data 42, 128–131.

Nezbeda, I., Pavlíček, J., 1996. Application of primitive models of association: A simple theoretical equation of state of water. Fluid Phase Equilib. 116, 530–536.

Nezbeda, I., Weingerl, U., 2001. A molecular-based theory for the thermodynamic properties of water. Mol. Phys. 99, 1595--1606.

Nihous, G.C., Kinoshita, C.K., Masutani, S.M., 2009. A determination of the activity of water in water-alcohol mixtures using mobile order thermodynamics. Chem. Eng. Sci. 64, 2767–2771.

Nihous, G.C., Kuroda, K., Lobos-González, J.R., Kurasaki, R.J., Masutani, S.M., 2010. An analysis of gas hydrate dissociation in the presence of thermodynamic inhibitors. Chem. Eng. Sci. 65, 1748–1761.

Odden, W., Patience, R.L., Van Graas, G.W., 1998. Application of light hydrocarbons (C4-C13) to oil/source rock correlations: A study of the light hydrocarbon compositions of source rocks and test fluids from offshore Mid-Norway. Org. Geochem. 28, 823–847.

Orge, B., Rodríguez, A., Canosa, J.M., Marino, G., Iglesias, M., Tojo, J., 1999. Variation of Densities, Refractive Indices, and Speeds of Sound with Temperature of Methanol or Ethanol with Hexane, Heptane, and Octane. J. Chem. Eng. Data 44, 1041–1047.

Oswald, G., Schmittecker, B., Wagner, D., Lichtenthaler, R., 1986. Excess enthalpies and excess volumes of alkanol+ n-heptane mixtures at high pressures. Fluid Phase Equilib. 27, 119–135.

Outcalt, S.L., Laesecke, A., Fortin, T.J., 2010. Density and speed of sound measurements of 1- and 2-butanol. J. Mol. Liq. 151, 50–59.

Outcalt, S.L., McLinden, M.O., 2007. Automated Densimeter for the Rapid Characterization of Industrial Fluids. Ind. Eng. Chem. Res. 46, 8264–8269.

Ozawa, S., Ooyatsu, N., Yamabe, M., Honmo, S., 1980. Volumes of Binary Liquid Mixtures At High Pressures. Glass.

Pan, C., Radosz, M., 1998. Copolymer SAFT modeling of phase behavior in hydrocarbon-chain

solutions: Alkane oligomers, polyethylene, poly (ethylene-co-olefin-1), polystyrene, and poly (ethylene-co-styrene). Ind. \& Eng. Chem. Res. 37, 3169--3179.

Papaioannou, D., Ziakas, D., Panayiotou, C., 1991. Volumetric properties of binary mixtures. 1. 2-Propanone+ 2, 2, 4-trimethylpentane and n-heptane+ ethanol mixtures. J. Chem. Eng. Data 36, 35--39.

Pedersen, K.S., Christensen, P.L., Shaikh, J.A., 2018. Equations of State. Phase Behav. Pet. Reserv. Fluids V, 97–118.

Pei, H., Zhang, G., Ge, J., Zhang, L., Ma, M., 2014. Effect of the Addition of Low Molecular Weight Alcohols on Heavy Oil Recovery during Alkaline Flooding. Ind. Eng. Chem. Res. 53, 1301–1307.

Peleteiro, J., Troncoso, J., González-Salgado, D., Valencia, J.L., Souto-Caride, M., Romani, L., 2005. Excess isobaric molar heat capacities and excess molar volumes for ethanol + n-decane and n-undecane systems. J. Chem. Thermodyn. 37, 935–940.

Peng, D.Y., Robinson, D.B., 1976. A New Two-Constant Equation of State. Ind. Eng. Chem. Fundam. 15, 59–64.

Peng, D.Y., Robinson, D.B., Song Wei, Y., Sadus, R.J., Valderrama, J.O., Spear, R.R., Robinson, R.L., Chao, K.C., Sadus, R.J., Al-Malah, K.I., 1994. Calculating critical transitions of fluid mixtures: Theory vs. experiment. Ind. Eng. Chem. Fundam. 40, 1376–1403.

Pereiro, A.B., Rodríguez, A., 2007. Mixing properties of binary mixtures presenting azeotropes at several temperatures. J. Chem. Thermodyn. 39, 1219–1230.

Pimentel-Rodas, A., Galicia-Luna, L.A., Castro-Arellano, J.J., 2017. Simultaneous Measurement of Dynamic Viscosity and Density of n-Alkanes at High Pressures. J. Chem. Eng. Data 62, 3946–3957.

Pin, M.M., Mascato, E., Mosteiro, L., Legido, L., 2003. Mixing Properties for the Ternary Mixture Methyl tert -Butyl Ether + 1-Butanol + Decane at 298 . 15 K † 758–762.

Pöhler, H., Kiran, E., 1997. Volumetric properties of carbon dioxide + ethanol at high pressures. J. Chem. Eng. Data 42, 384–388.

Poling, B.E., Prausnitz, J.M., O'Connel, J.P., 2001. The properties of gases & liquids. McGraw-Hill Educ. 1, 409.

Quevedo-Nolasco, R., Galicia-Luna, L.A., Elizalde-Solis, O., 2012. Compressed liquid densities for the (n-heptane+n-decane) and (n-octane+n-decane) systems from T=(313 to 363)K. J. Chem. Thermodyn. 44, 133–147.

Radzhabova, L.M., Stepanov, G. V., Abdulagatov, I.M., Shakhbanov, K.A., 2014. Experimental study of the isochoric heat capacity and liquid–gas coexistence-curve properties of sec-butanol in the near- and supercritical regions. Thermochim. Acta 575, 97–113.

Rahaman, M.A., Islam Aziz, M.S., Akhtar, S., 2011. Volumetric properties of some binary liquid systems: n-Heptane+Aromatic hydrocarbons between 303.15 and 323.15K. J. Mol. Liq. 162, 26–32.

Rajesh Kumar, B., Saravanan, S., 2016. Use of higher alcohol biofuels in diesel engines: A review. Renew. Sustain. Energy Rev. 60, 84–115.

Rao, M.V.P., Naidu, P.R., 1974. Excess Volumes of Binary Mixtures of Alcohols in Methylcyclohexane. Can. J. Chem. 52, 788–790.

Rasaiah, J., Stell, G., 1974. Three-body free-energy terms and effective potentials in polar fluids and ionic solutions. Chem. Phys. Lett. 25, 519--522.

Reamer, H.H., Selleck, F.T., Sage, B.H., Lacey, W.N., 1953. Phase Equilibria In Hydrocarbon Systems- Volumetric and Phase Behavior of Decane–Hydrogen Sulfide System. Ind. Eng. Chem. 45, 1810–1812.

Redlich, O., Kwong, J.N.S., 1948. An Equation of State. Fugacities of Geseous Solutions. Symp. Thermodyn. Mol. Struct. Solut. 233–244.

Regueira, T., Pantelide, G., Yan, W., Stenby, E.H., 2016. Density and phase equilibrium of the binary system methane + n-decane under high temperatures and pressures. Fluid Phase Equilib. 428, 48–61.

Roux, A.H., Roux-Desgranges, G., Grolier, J.-P.E., 1993. Excess molar heat capacities and enthalpies for 1-alkanol + N-alkane binary mixtures. New measurements and recommended

data. Fluid Phase Equilib. 89, 57–88.

Sadus, R.J., 1992. High Pressure Phase Behaviour of Multicomponent Fluid Mixtures. Elsevier, Amsterdam.

Safarov, J., Ahmadov, B., Mirzayev, S., Shahverdiyev, A., Hassel, E.P., 2015. Thermophysical properties of 1-butanol over a wide range of temperatures and pressures up to 200MPa. J. Mol. Liq. 209, 465–479.

Sage, B.H., Lavender, H.M., Lacey, W.N., 1940. Phase Equilibria in Hydrocarbon Systems: Methane-Decane System. Ind. Eng. Chem. 32, 743–747.

Salter, S.J., 1977. The influence of type and amount of alcohol on surfactant-oil-brine phase behavior and properties. In: Proceedings - SPE Annual Technical Conference and Exhibition. Society of Petroleum Engineers.

Salter, S.J., 1978. Selection Of Pseudo-Components In Surfactant-Oil-Brine-Alcohol Systems. In: SPE Symposium on Improved Methods of Oil Recovery. Society of Petroleum Engineers.

Sanmamed, Y.A., Dopazo-Paz, A., González-Salgado, D., Troncoso, J., Romaní, L., 2009. An accurate calibration method for high pressure vibrating tube densimeters in the density interval (700 to 1600)kg·m−3. J. Chem. Thermodyn. 41, 1060–1068.

Sastry, N.., 1997. Densities, excess volumes, speeds of sound and excess isentropic compressibilities for 2-butoxyethanol + n-hexane and + n-heptane mixtures at 303.15 K and 313.15 K. Fluid Phase Equilib. 128, 173–181.

Sastry, N. V, Valand, M.K., 1996. for 1-Propanol + and 1-Butanol + Heptane at 298.15 K and 308.15 K 9568, 1421–1425.

Sauer, S.G., Chapman, W.G., 2003. A parametric study of dipolar chain theory with applications to ketone mixtures. Ind. \& Eng. Chem. Res. 42, 5687--5696.

Sauermann, P., Holzapfel, K., Oprzynski, J., Kohler, F., Poot, W., de Loos, T.W., 1995. The pρ{variant}T properties of ethanol + hexane. Fluid Phase Equilib. 112, 249–272.

Schilling, G., Kleinrahm, R., Wagner, W., 2008. Measurement and correlation of the (p,ρ,T) relation of liquid n-heptane, n-nonane, 2,4-dichlorotoluene, and bromobenzene in the

temperature range from (233.15 to 473.15)K at pressures up to 30MPa for use as density reference liquids. J. Chem. Thermodyn. 40, 1095–1105.

Segade, L., Jime, J., Llano, D., Cabeza, Ä., Cabanas, M., Jime, E., Ciencias, F. De, Corun, U., 2003. Density , Surface Tension , and Refractive Index of Octane + 1-Alkanol Mixtures at T) 298 . 15 K 1251–1255.

Segovia, J.J., Fandiño, O., López, E.R., Lugo, L., Carmen Martín, M., Fernández, J., 2009. Automated densimetric system: Measurements and uncertainties for compressed fluids. J. Chem. Thermodyn. 41, 632–638.

Smith, J., Van Ness, H., Abbott, M., 2001. Introduction to Chemical Engineering Thermodynamics.

Soave, G., 1972. Equilibrium constants from a modified Redlich-Kwong equation of state. Chem. Eng. Sci. 27, 1197–1203.

Song Wei, Y., Sadus, R.J., 2000. Equations of State for the Calculation wei2000.pdf 46, 169–196.

Song, Y., Jian, W., Zhang, Y., Xing, W., Zhan, Y., Liu, S., Li, T.T., 2014. Density behavior of CO2 + decane mixtures by modified saft equation of state. Energy Procedia 61, 440–444.

Span, R., Lemmon, E.W., Jacobsen, R.T., Wagner, W., 1998. A reference quality equation of state for nitrogen. Int. J. Thermophys. 19, 1121–1132.

Spear, R.R., Robinson, R.L., Chao, K.C., 1969. Critical states of mixtures and equations of state. Ind. Eng. Chem. Fundam. 8, 2–8.

Starling, K.E., 1973. Fluid thermodynamic properties for light petroleum systems.

Stell, G., Rasaiah, J., Narang, H., 1974. Thermodynamic perturbation theory for simple polar fluids. II. Mol. Phys. 27, 1393--1414.

Stewart, J.W., 1956. Compression of solidified gases to 20,000 kg/cm2 at low temperature. J. Phys. Chem. Solids 1, 146--158.

Suhm, M.A., 2008. Hydrogen Bond Dynamics in Alcohol Clusters. pp. 1–57.

Sumara, J., Zarska, M., Dzida, M., Je, S., Góralski, P., 2013. High pressure physicochemical

properties of biodiesel components used for spray characteristics in diesel injection systems.

Taguchi, R., Machida, H., Sato, Y., Smith, R.L., 2009. High-Pressure Densities of 1-Alkyl-3-methylimidazolium Hexafluorophosphates and 1-Alkyl-3-methylimidazolium Tetrafluoroborates at Temperatures from (313 to 473) K and at Pressures up to 200 MPa 22–27.

Takagi, T., 1978. Ultrasonic velocity in binary mixtures under high pressures and their thermodynamic properties II: binary mixtures for benzene-toluene and benzene-o-xylene. Rev. Phys. Chem. Japan 48, 17–26.

Takagi, T., Teranishi, H., 1982. Ultrasonic speeds and thermodynamic properties of (benzene+ chlorobenzene) and (benzene+ bromobenzene) under high pressures. J. Chem. Thermodyn. 14, 577–584.

Takiguchi, Y., Uematsu, M., 1996. Densities for liquid ethanol in the temperature range from 310 K to 480 K at pressures up to 200 MPa. J. Chem. Thermodyn. 28, 7–16.

Tammann, G., 1895. The dependence of the volume of solutions on pressure. Z. Phys. Chem 17, 620–636.

Tanaka, R., Toyama, S., 1996. Excess molar heat capacities and excess molar volumes of (propan-2-ol , or butan-2-ol , or pentan-2-ol , or pentan-3-ol , or the temperature 298 . 15 K 1403–1410.

Teixeira, A.M., Arinelli, L. de O., de Medeiros, J.L., Araújo, O. de Q.F., 2018. Recovery of thermodynamic hydrate inhibitors methanol, ethanol and MEG with supersonic separators in offshore natural gas processing. J. Nat. Gas Sci. Eng. 52, 166–186.

Ter Minassian, L., Bouzar, K., Alba, C., 1988. Thermodynamic properties of liquid toluene. J. Phys. Chem. 92, 487--493.

Thomas, S., 2008. Enhanced Oil Recovery – An Overview 63, 9–19.

Ting, P.D., Joyce, P.C., Jog, P.K., Chapman, W.G., Thies, M.C., 2003. Phase equilibrium modeling of mixtures of long-chain and short-chain alkanes using Peng-Robinson and SAFT. Fluid Phase Equilib. 206, 267–286.

Torín-Ollarves, G.A., Segovia, J.J., Martín, M.C., Villamañán, M.A., 2012. Thermodynamic characterization of the mixture (1-butanol + iso-octane): Densities, viscosities, and isobaric heat capacities at high pressures. J. Chem. Thermodyn. 44, 75–83.

Toscani, S., Figuière, P., Szwarc, H., 1989. A magnetic-suspension apparatus to measure densities of liquids as a function of temperature at pressures up to 100 MPa Application to n-heptane. J. Chem. Thermodyn. 21, 1263–1277.

Toscani, S., Szwarc, H., 2004. Two empirical equations of state for liquids to improve p, V, T data representation and physical meaning. J. Chem. Eng. Data 49, 163–172.

Toscani, S., Szwarc, H., Chimie, L. De, Ura, D., Sud, U.P., 1993. An Empirical Equation of State for Liquids 591–597.

Treszczanowicz, A.J., Benson, G.C., 1977. Excess volumes for n-alkanols + n-alkanes I. Binary mixtures of methanol, ethanol, n-propanol, and n-butanol + n-heptane. J. Chem. Thermodyn. 9, 1189–1197.

Treszczanowicz, A.J., Benson, G.C., 1978. Excess volumes for n-alkanols + n-alkanes II. Binary mixtures of n-pentanol, n-hexanol, n-octanol, and n-decanol + n-heptane. J. Chem. Thermodyn. 10, 967–974.

Treszczanowicz, A.J., Kiyohara, O., Benson, G.C., 1981. Excess volumes for n-alkanols +n-alkanes IV. Binary mixtures of decan-1-ol +n-pentane, +n-hexane, +n-octane, +n-decane, and +n-hexadecane. J. Chem. Thermodyn. 13, 253–260.

Trindade, W.R. da S., dos Santos, R.G., 2017. Review on the characteristics of butanol, its production and use as fuel in internal combustion engines. Renew. Sustain. Energy Rev. 69, 642–651.

Troncoso, J., Bessières, D., Cerdeiriña, C.A., Carballo, E., Romaní, L., 2004. p ρ Tx Data for the Dimethyl Carbonate + Decane System. J. Chem. Eng. Data 49, 923–927.

Troncoso, J., Navia, P., Romaní, L., Bessieres, D., Lafitte, T., 2011. On the isobaric thermal expansivity of liquids On the isobaric thermal expansivity of liquids 094502.

Tumakaka, F., Gross, J., Sadowski, G., 2005. Thermodynamic modeling of complex systems using

PC-SAFT. Fluid Phase Equilib. 228–229, 89–98.

Tumlirz, O., 1900. L'equazione caratteristica del vapor d'acqua. Nuovo Cim. 11, 5--14.

Ulbig, P., Bubolz, M., Kornek, C., Schulz, S., 1997. Excess volumes of binary mixtures containing diisopropyl ether + 1-butanol or diisopropyl ether + diethyl ketone and ethanol + heptane at high pressures. J. Chem. Eng. Data 42, 449–452.

Valderrama, J.O., 2003. The state of the cubic equations of state. Ind. Eng. Chem. Res. 42, 1603–1618.

Valencia, J.L., González-Salgado, D., Troncoso, J., Peleteiro, J., Carballo, E., Romaní, L., 2009. Thermophysical characterization of liquids using precise density and isobaric heat capacity measurements as a function of pressure. J. Chem. Eng. Data 54, 904–915.

Vallés, C., Pérez, E., Cardoso, M., Domínguez, M., Mainar, A.M., 2004. Excess Enthalpy, Density, Viscosity, and Speed of Sound for the Mixture Tetrahydropyran + 1-Butanol at (283.15, 298.15, and 313.15) K. J. Chem. Eng. Data 49, 1460–1464.

Van der Waals, J.D., 1873. On the continuity of the gas and liquid state. Leiden Univ. Leiden, Netherlands 301.

Vargas, F.M., Gonzalez, D.L., Hirasaki, G.J., Chapman, W.G., 2009. Modeling asphaltene phase behavior in crude oil systems using the perturbed chain form of the statistical associating fluid theory (PC-SAFT) equation of state. Energy and Fuels 23, 1140–1146.

Vega-Maza, D., Carmen Martín, M., Martin Trusler, J.P., Segovia, J.J., 2013. Heat capacities and densities of the binary mixtures containing ethanol, cyclohexane or 1-hexene at high pressures. J. Chem. Thermodyn. 57, 550–557.

Vega, C., Paras, E., Monson, P., 1992. Solid--fluid equilibria for hard dumbbells via Monte Carlo simulation. J. Chem. Phys. 96, 9060--9072.

Vijande, J., Pin, M.M., Garcı, J., Valencia, L., Legido, L., 2006. J. Chem. Eng. Data 2006, 51, 1778-1782 (2).pdf 1778–1782.

Vimalchand, Pannalal Donohue, M.D., 1985. Thermodynamics of quadrupolar molecules: the perturbed-anisotropic-chain theory. Ind. \& Eng. Chem. Fundam. 24, 246--257.

von Solms, N., Jensen, L., Kofod, J.L., Michelsen, M.L., Kontogeorgis, G.M., 2007. Measurement and modelling of hydrogen bonding in 1-alkanol + n-alkane binary mixtures. Fluid Phase Equilib. 261, 272–280.

Wagner, D., Heintz, A., 1986. Excess volumes of binary 1-alkanol/nonane mixtures at temperatures between 293.15 and 333.15 K. J. Chem. Eng. Data 31, 483–487.

Wagner, W., Pruß, A., 2002. The IAPWS Formulation 1995 for the Thermodynamic Properties of Ordinary Water Substance for General and Scientific Use. J. Phys. Chem. Ref. Data 31, 387–535.

Walas, S.M., 2013. Phase equilibria in chemical engineering. Butterworth-Heinemann.

Walsh, J.M., Guedes, Henrique JR Gubbins, K.E., 1992. Physical theory for fluids of small associating molecules. J. Phys. Chem. 96, 10995--11004.

Watson, G., Zéberg-Mikkelsen, C.K., Baylaucq, A., Boned, C., 2006. High-pressure density measurements for the binary system ethanol + heptane. J. Chem. Eng. Data 51, 112–118.

Wertheim, M.S., 1984a. Fluids with highly directional attractive forces. II. Thermodynamic perturbation theory and integral equations. J. Stat. Phys. 35, 35–47.

Wertheim, M.S., 1984b. Fluids with highly directional attractive forces. I. Statistical thermodynamics. J. Stat. Phys. 35, 19–34.

Wertheim, M.S., 1986a. Fluids with highly directional attractive forces. IV. Equilibrium polymerization. J. Stat. Phys. 42, 477–492.

Wertheim, M.S., 1986b. Fluids with highly directional attractive forces. III. Multiple attraction sites. J. Stat. Phys. 42, 459–476.

Westwood, B.M., Kabadi, V.N., 2003. A novel pycnometer for density measurements of liquids at elevated temperatures. J. Chem. Thermodyn. 35, 1965–1974.

Wieczorek, S.A., 1984. Determination of the excess molar volumes of (butan-2-01 between use of a continuous dilution dilatometer.

Wise, M., Chapoy, A., Burgass, R., 2016. Solubility Measurement and Modeling of Methane in Methanol and Ethanol Aqueous Solutions. J. Chem. Eng. Data 61, 3200–3207.

Wolbach, J.P., Sandler, S.I., 1998. Behavior of Cross-associating Mixtures 5885, 2917–2928.

Wong, C.F., Hayduk, W., 1990. Molecular Diffusivities for Propene in 1-Butanol, Chlorobenzene, Ethylene Glycol, and n-Octane at Elevated Pressures. J. Chem. Eng. Data 35, 323–328.

Wu, Y., 2010. VCU Scholars Compass High-Pressure and High-Temperature Density Measurements of n- Decane , and Toluene.

Wu, Y., Bamgbade, B.A., Baled, H., Enick, R.M., Burgess, W.A., Tapriyal, D., Mchugh, M.A., 2013a. Liquid Densities of Xylene Isomers and 2 - Methylnaphthalene at Temperatures to 523 K and Pressures to 265 MPa : Experimental Determination and Equation of State Modeling.

Wu, Y., Bamgbade, B.A., Burgess, W.A., Tapriyal, D., Baled, H.O., Enick, R.M., Hugh, M.A.M., 2013b. E ff ect of Isomeric Structures of Branched Cyclic Hydrocarbons on Densities and Equation of State Predictions at Elevated Temperatures and Pressures.

Wu, Y., Xu, L., Zhang, H., Zeng, X., Chen, J., 2013c. Pressure-Volume-Temperature Property Determination for Fluids at Extreme Pressures. Postdoc J.

Xiong, Y., Kiran, E., 1995. Comparison of Sanchez--Lacombe and SAFT model in predicting solubility of polyethylene in high-pressure fluids. J. Appl. Polym. Sci. 55, 1805–1818.

Xu, K., Li, Y., Liu, W., 1998. Application of perturbation theory to chain and polar fluids: Pure alkanes, alkanols and water. Fluid Phase Equilib. 142, 55--66.

Yang, J., Meng, X., Wu, J., 2018. Liquid Density of n -Pentene, n -Hexene, and n -Heptene at Temperatures from 283.15 to 363.15 K and Pressures up to 100 MPa. J. Chem. Eng. Data acs.jced.8b00229.

Yang, Z., Wu, W., Dong, Z., Lin, M., Zhang, S., Zhang, J., 2019. Reducing the minimum miscibility pressure of CO2 and crude oil using alcohols. Colloids Surfaces A Physicochem. Eng. Asp. 568, 105–112.

Yin, J., Wu, J., Meng, X., Abdulagatov, I., 2011. Compressed liquid density measurements of dimethyl ether with a vibrating tube densimeter. J. Chem. Thermodyn. 43, 1371–1374.

Zamora-López, H.S., Galicia-Luna, L.A., Elizalde-Solis, O., Hernández-Rosales, I.P., Méndez-

Lango, E., 2012. Derived thermodynamic properties for the (ethanol + decane) and (carbon dioxide + ethanol + decane) systems at high pressures. J. Chem. Thermodyn. 55, 130–137.

Zarei, S., Feyzi, F., 2013. Boyle temperature from SAFT, PC-SAFT and SAFT-VR equations of state. J. Mol. Liq. 187, 114–128.

Zéberg-Mikkelsen, C.K., Lugo, L., Fernández, J., 2005a. Density measurements under pressure for the binary system (ethanol + methylcyclohexane). J. Chem. Thermodyn. 37, 1294–1304.

Zéberg-Mikkelsen, C.K., Lugo, L., García, J., Fernández, J., 2005b. Volumetric properties under pressure for the binary system ethanol+toluene. Fluid Phase Equilib. 235, 139–151.

Zhang, Y., Jian, W., Song, Y., Liu, W., Yang, M., Zhao, J., Liu, Y., Zhao, Y., 2015. (p, ρ, T) behavior of CO<inf>2</inf> + tetradecane systems: Experiments and thermodynamic modeling. J. Chem. Eng. Data 60, 1476–1486.

Zhurko, F. V., Manakov, A.Y., Kosyakov, V.I., 2010. Formation of gas hydrates in the systems methane–water–ROH (ROH=ethanol, n-propanol, i-propanol, i-butanol). Chem. Eng. Sci. 65, 900–905.

Zielkiewicz, J., 1993. Excess molar volumes of (heptane+ethanol+propan-1-ol) at the temperature 313.15 K. J. Chem. Thermodyn. 25, 1243–1248.

Živković, N. V., Šerbanović, S.S., Kijevčanin, M.L., Živković, E.M., 2013. Volumetric and Viscometric Behavior of Binary Systems 2-Butanol + PEG 200, + PEG 400, + Tetraethylene Glycol Dimethyl Ether, and + N -Methyl-2-pyrrolidone. J. Chem. Eng. Data 58, 3332–3341.

Zudkevitch, D., Kaufmann, T.G., n.d. the Benedict-Webb-Rubin Equation 12, 577–580.

Zúñiga-Moreno, A., Galicia-Luna, L.A., 2002. Densities of 1-Propanol and 2-Propanol via a Vibrating Tube Densimeter from 313 to 363 K and up to 25 MPa. J. Chem. Eng. Data 47, 155–160.

Zúñiga-Moreno, A., Galicia-Luna, L.A., Camacho-Camacho, L.E., 2005. Compressed Liquid Densities and Excess Volumes of CO 2 + Decane Mixtures from (313 to 363) K and Pressures up to 25 MPa. J. Chem. Eng. Data 50, 1030–1037.

Zúñiga-Moreno, A., Galicia-Luna, L.A., Camacho-Camacho, L.E., 2007a. Compressed liquid

densities of 1-butanol and 2-butanol at temperatures from 313 K to 363 K and pressures up to 25 MPa. J. Chem. Thermodyn. 39, 254–260.

Zúñiga-Moreno, A., Galicia-Luna, L.A., Sandler, S.I., 2007b. Measurements of compressed liquid densities for CO2 (1) + butan-1-ol (2) via a vibrating tube densimeter at temperatures from (313 to 363) K and pressures up to 25 MPa. J. Chem. Eng. Data 52, 1960–1969.

APPENDIX A

Excess Molar Volumes

Table A1: Excess Molar Volumes (V^E) of butan-1-ol (1) + n-octane (2) at various pressures and temperatures.

T/K	P/MPa	$V^E/m^3.kmol^{-1}$							
		x_1=0	*x_1=0.1269*	*x_1=0.3764*	*x_1=0.4968*	*x_1=0.6234*	*x_1=0.7440*	*x_1=0.8731*	*x_1=1*
313.15	0.1	0	2.3215E-04	4.0263E-04	3.9675E-04	2.9839E-04	1.9633E-04	8.7894E-05	0
313.15	1.14	0	2.2166E-04	3.8364E-04	3.7763E-04	2.8389E-04	1.8697E-04	8.3432E-05	0
313.15	2.14	0	2.1696E-04	3.7605E-04	3.7004E-04	2.7828E-04	1.8317E-04	8.1822E-05	0
313.15	3.15	0	2.1258E-04	3.6853E-04	3.6269E-04	2.7265E-04	1.7960E-04	8.0044E-05	0
313.15	4.16	0	2.0831E-04	3.6117E-04	3.5558E-04	2.6717E-04	1.7606E-04	7.8600E-05	0
313.15	5.17	0	2.0424E-04	3.5400E-04	3.4840E-04	2.6192E-04	1.7247E-04	7.7013E-05	0
313.15	6.18	0	2.0007E-04	3.4692E-04	3.4138E-04	2.5675E-04	1.6902E-04	7.5456E-05	0
313.15	7.19	0	1.9614E-04	3.4000E-04	3.3465E-04	2.5149E-04	1.6573E-04	7.3936E-05	0
313.15	8.2	0	1.9228E-04	3.3309E-04	3.2785E-04	2.4647E-04	1.6238E-04	7.2475E-05	0
313.15	9.23	0	1.8834E-04	3.2652E-04	3.2135E-04	2.4155E-04	1.5902E-04	7.1109E-05	0
313.15	10.23	0	1.8462E-04	3.2001E-04	3.1495E-04	2.3672E-04	1.5590E-04	6.9532E-05	0
313.15	11.24	0	1.8066E-04	3.1354E-04	3.0863E-04	2.3192E-04	1.5276E-04	6.8206E-05	0
313.15	12.25	0	1.7727E-04	3.0728E-04	3.0241E-04	2.2748E-04	1.4984E-04	6.6854E-05	0
313.15	13.26	0	1.7379E-04	3.0123E-04	2.9637E-04	2.2281E-04	1.4684E-04	6.5555E-05	0
313.15	14.27	0	1.7018E-04	2.9513E-04	2.9054E-04	2.1831E-04	1.4386E-04	6.4188E-05	0
313.15	15.27	0	1.6685E-04	2.8925E-04	2.8478E-04	2.1400E-04	1.4091E-04	6.2900E-05	0
313.15	16.28	0	1.6349E-04	2.8330E-04	2.7904E-04	2.0978E-04	1.3820E-04	6.1649E-05	0
313.15	17.29	0	1.6039E-04	2.7771E-04	2.7342E-04	2.0554E-04	1.3537E-04	6.0488E-05	0
313.15	18.3	0	1.5716E-04	2.7221E-04	2.6790E-04	2.0142E-04	1.3274E-04	5.9223E-05	0
313.15	19.3	0	1.5391E-04	2.6678E-04	2.6268E-04	1.9739E-04	1.3001E-04	5.8068E-05	0
313.15	20.31	0	1.5079E-04	2.6144E-04	2.5729E-04	1.9349E-04	1.2755E-04	5.6857E-05	0
323.15	0.1	0	2.6208E-04	4.5601E-04	4.4887E-04	3.3690E-04	2.2217E-04	9.9029E-05	0
323.15	1.15	0	2.4103E-04	4.1814E-04	4.1165E-04	3.0944E-04	2.0387E-04	9.0846E-05	0
323.15	2.15	0	2.3655E-04	4.1007E-04	4.0338E-04	3.0325E-04	1.9976E-04	8.9131E-05	0
323.15	3.17	0	2.3174E-04	4.0164E-04	3.9527E-04	2.9718E-04	1.9578E-04	8.7355E-05	0
323.15	4.18	0	2.2712E-04	3.9369E-04	3.8744E-04	2.9119E-04	1.9182E-04	8.5668E-05	0
323.15	5.19	0	2.2259E-04	3.8576E-04	3.7968E-04	2.8537E-04	1.8801E-04	8.3911E-05	0
323.15	6.2	0	2.1807E-04	3.7816E-04	3.7221E-04	2.7967E-04	1.8424E-04	8.2281E-05	0
323.15	7.22	0	2.1386E-04	3.7052E-04	3.6468E-04	2.7418E-04	1.8063E-04	8.0616E-05	0
323.15	8.23	0	2.0951E-04	3.6317E-04	3.5737E-04	2.6864E-04	1.7694E-04	7.8982E-05	0
323.15	9.24	0	2.0505E-04	3.5577E-04	3.5019E-04	2.6323E-04	1.7341E-04	7.7503E-05	0

323.15	10.25	0	2.0124E-04	3.4878E-04	3.4318E-04	2.5808E-04	1.7003E-04	7.5921E-05	0
323.15	11.25	0	1.9729E-04	3.4175E-04	3.3645E-04	2.5287E-04	1.6657E-04	7.4386E-05	0
323.15	12.27	0	1.9315E-04	3.3494E-04	3.2968E-04	2.4786E-04	1.6327E-04	7.2895E-05	0
323.15	13.27	0	1.8932E-04	3.2828E-04	3.2303E-04	2.4285E-04	1.6004E-04	7.1453E-05	0
323.15	14.26	0	1.8571E-04	3.2166E-04	3.1659E-04	2.3805E-04	1.5679E-04	7.0019E-05	0
323.15	15.29	0	1.8177E-04	3.1517E-04	3.1032E-04	2.3326E-04	1.5376E-04	6.8596E-05	0
323.15	16.3	0	1.7813E-04	3.0887E-04	3.0403E-04	2.2857E-04	1.5054E-04	6.7238E-05	0
323.15	17.3	0	1.7479E-04	3.0277E-04	2.9794E-04	2.2395E-04	1.4760E-04	6.5867E-05	0
323.15	18.3	0	1.7114E-04	2.9656E-04	2.9209E-04	2.1948E-04	1.4459E-04	6.4594E-05	0
323.15	19.3	0	1.6772E-04	2.9085E-04	2.8628E-04	2.1512E-04	1.4172E-04	6.3245E-05	0
323.15	20.29	0	1.6437E-04	2.8490E-04	2.8055E-04	2.1078E-04	1.3885E-04	6.2002E-05	0
333.15	0.1	0	3.0011E-04	5.1983E-04	5.1096E-04	3.8368E-04	2.5250E-04	1.1336E-04	0
333.15	1.13	0	2.6286E-04	4.5598E-04	4.4882E-04	3.3737E-04	2.2223E-04	9.9086E-05	0
333.15	2.13	0	2.5741E-04	4.4670E-04	4.3968E-04	3.3058E-04	2.1780E-04	9.7182E-05	0
333.15	3.14	0	2.5252E-04	4.3773E-04	4.3088E-04	3.2385E-04	2.1332E-04	9.5276E-05	0
333.15	4.15	0	2.4747E-04	4.2897E-04	4.2236E-04	3.1736E-04	2.0919E-04	9.3376E-05	0
333.15	5.16	0	2.4219E-04	4.2051E-04	4.1382E-04	3.1107E-04	2.0498E-04	9.1426E-05	0
333.15	6.17	0	2.3775E-04	4.1201E-04	4.0537E-04	3.0481E-04	2.0078E-04	8.9557E-05	0
333.15	7.18	0	2.3314E-04	4.0373E-04	3.9730E-04	2.9885E-04	1.9682E-04	8.7895E-05	0
333.15	8.19	0	2.2819E-04	3.9565E-04	3.8979E-04	2.9279E-04	1.9281E-04	8.6123E-05	0
333.15	9.2	0	2.2408E-04	3.8795E-04	3.8172E-04	2.8690E-04	1.8911E-04	8.4400E-05	0
333.15	10.21	0	2.1946E-04	3.8012E-04	3.7430E-04	2.8115E-04	1.8527E-04	8.2652E-05	0
333.15	11.22	0	2.1480E-04	3.7243E-04	3.6660E-04	2.7562E-04	1.8150E-04	8.1026E-05	0
333.15	12.23	0	2.1048E-04	3.6494E-04	3.5923E-04	2.7007E-04	1.7792E-04	7.9391E-05	0
333.15	13.24	0	2.0655E-04	3.5783E-04	3.5219E-04	2.6474E-04	1.7434E-04	7.7753E-05	0
333.15	14.25	0	2.0229E-04	3.5041E-04	3.4501E-04	2.5940E-04	1.7090E-04	7.6214E-05	0
333.15	15.26	0	1.9841E-04	3.4361E-04	3.3829E-04	2.5415E-04	1.6740E-04	7.4691E-05	0
333.15	16.27	0	1.9458E-04	3.3663E-04	3.3153E-04	2.4908E-04	1.6406E-04	7.3233E-05	0
333.15	17.27	0	1.9048E-04	3.3001E-04	3.2479E-04	2.4417E-04	1.6092E-04	7.1843E-05	0
333.15	18.28	0	1.8660E-04	3.2334E-04	3.1840E-04	2.3933E-04	1.5770E-04	7.0413E-05	0
333.15	19.28	0	1.8287E-04	3.1711E-04	3.1201E-04	2.3436E-04	1.5457E-04	6.8880E-05	0
333.15	20.28	0	1.7921E-04	3.1049E-04	3.0566E-04	2.2978E-04	1.5143E-04	6.7622E-05	0
343.15	0.1	0	3.3467E-04	5.8229E-04	5.7224E-04	4.3059E-04	2.8296E-04	1.2690E-04	0
343.15	1.14	0	2.8594E-04	4.9812E-04	4.8892E-04	3.6773E-04	2.4211E-04	1.0788E-04	0
343.15	2.14	0	2.8127E-04	4.8709E-04	4.7963E-04	3.6061E-04	2.3716E-04	1.0616E-04	0
343.15	3.14	0	2.7548E-04	4.7751E-04	4.7020E-04	3.5295E-04	2.3247E-04	1.0416E-04	0
343.15	4.16	0	2.6797E-04	4.6693E-04	4.6058E-04	3.4580E-04	2.2729E-04	1.0165E-04	0
343.15	5.17	0	2.6570E-04	4.5867E-04	4.5114E-04	3.3888E-04	2.2364E-04	1.0020E-04	0
343.15	6.18	0	2.5935E-04	4.4945E-04	4.4261E-04	3.3246E-04	2.1903E-04	9.7685E-05	0
343.15	7.19	0	2.5380E-04	4.4019E-04	4.3315E-04	3.2545E-04	2.1440E-04	9.5856E-05	0
343.15	8.2	0	2.4906E-04	4.3111E-04	4.2436E-04	3.1958E-04	2.0996E-04	9.3780E-05	0
343.15	9.21	0	2.4395E-04	4.2283E-04	4.1673E-04	3.1297E-04	2.0614E-04	9.1879E-05	0
343.15	10.22	0	2.3926E-04	4.1444E-04	4.0814E-04	3.0666E-04	2.0220E-04	9.0200E-05	0

343.15	11.23	0	2.3480E-04	4.0549E-04	3.9958E-04	3.0020E-04	1.9786E-04	8.8597E-05	0
343.15	12.24	0	2.2928E-04	3.9803E-04	3.9145E-04	2.9468E-04	1.9387E-04	8.6649E-05	0
343.15	13.25	0	2.2511E-04	3.9024E-04	3.8394E-04	2.8844E-04	1.8984E-04	8.4561E-05	0
343.15	14.26	0	2.2099E-04	3.8298E-04	3.7600E-04	2.8255E-04	1.8615E-04	8.2940E-05	0
343.15	15.27	0	2.1612E-04	3.7428E-04	3.6835E-04	2.7787E-04	1.8289E-04	8.1539E-05	0
343.15	16.27	0	2.1189E-04	3.6761E-04	3.6123E-04	2.7170E-04	1.7900E-04	7.9915E-05	0
343.15	17.28	0	2.0712E-04	3.5939E-04	3.5404E-04	2.6619E-04	1.7525E-04	7.8305E-05	0
343.15	18.28	0	2.0292E-04	3.5199E-04	3.4736E-04	2.6158E-04	1.7157E-04	7.6870E-05	0
343.15	19.29	0	2.0094E-04	3.4617E-04	3.4012E-04	2.5558E-04	1.6847E-04	7.5253E-05	0
343.15	20.29	0	1.9546E-04	3.3873E-04	3.3341E-04	2.5049E-04	1.6482E-04	7.3932E-05	0
353.15	0.1	0	3.7773E-04	6.5488E-04	6.4487E-04	4.8397E-04	3.1930E-04	1.4333E-04	0
353.15	1.14	0	3.0974E-04	5.4145E-04	5.3303E-04	4.0064E-04	2.6395E-04	1.1790E-04	0
353.15	2.14	0	3.0335E-04	5.3143E-04	5.2244E-04	3.9236E-04	2.5905E-04	1.1587E-04	0
353.15	3.14	0	2.9839E-04	5.2036E-04	5.1217E-04	3.8467E-04	2.5361E-04	1.1312E-04	0
353.15	4.16	0	2.9273E-04	5.1032E-04	5.0163E-04	3.7683E-04	2.4799E-04	1.1038E-04	0
353.15	5.16	0	2.8877E-04	4.9983E-04	4.9165E-04	3.6878E-04	2.4367E-04	1.0820E-04	0
353.15	6.18	0	2.8262E-04	4.8943E-04	4.8241E-04	3.6204E-04	2.3860E-04	1.0664E-04	0
353.15	7.19	0	2.7669E-04	4.7995E-04	4.7208E-04	3.5492E-04	2.3357E-04	1.0461E-04	0
353.15	8.2	0	2.7129E-04	4.6912E-04	4.6276E-04	3.4800E-04	2.2960E-04	1.0220E-04	0
353.15	9.21	0	2.6610E-04	4.6066E-04	4.5314E-04	3.4074E-04	2.2517E-04	9.9892E-05	0
353.15	10.22	0	2.6036E-04	4.5137E-04	4.4411E-04	3.3270E-04	2.2013E-04	9.8258E-05	0
353.15	11.23	0	2.5392E-04	4.4165E-04	4.3627E-04	3.2742E-04	2.1615E-04	9.6409E-05	0
353.15	12.24	0	2.5028E-04	4.3377E-04	4.2657E-04	3.2128E-04	2.1154E-04	9.4007E-05	0
353.15	13.25	0	2.4612E-04	4.2522E-04	4.1860E-04	3.1461E-04	2.0704E-04	9.2528E-05	0
353.15	14.26	0	2.4058E-04	4.1685E-04	4.1023E-04	3.0804E-04	2.0250E-04	9.0298E-05	0
353.15	15.25	0	2.3449E-04	4.0919E-04	4.0156E-04	3.0232E-04	1.9900E-04	8.8861E-05	0
353.15	16.27	0	2.3049E-04	3.9994E-04	3.9410E-04	2.9608E-04	1.9492E-04	8.6762E-05	0
353.15	17.27	0	2.2643E-04	3.9234E-04	3.8580E-04	2.9029E-04	1.9119E-04	8.5414E-05	0
353.15	18.29	0	2.2300E-04	3.8397E-04	3.7888E-04	2.8374E-04	1.8687E-04	8.3501E-05	0
353.15	19.29	0	2.1775E-04	3.7575E-04	3.7077E-04	2.7880E-04	1.8373E-04	8.2082E-05	0
353.15	20.29	0	2.1269E-04	3.6968E-04	3.6369E-04	2.7286E-04	1.7974E-04	7.9776E-05	0

Expanded combined uncertainties (k = 2) U_c are $U_c(T) = 0.02$ K, $U_c(P) = 0.032$ MPa, and $U_c(x_i) = 0.0002$, $U_c(V^E) = 1.82 \times 10^{-5}$ m^3. $kmol^{-1}$

Table A2: Excess Molar Volumes (V^E) of butan-1-ol (1) + n-decane (2) at various pressures and temperatures.

T/K	P/MPa	$V^E/m^3.kmol^{-1}$							
		x_1=0	*x_1=0.1269*	*x_1=0.3764*	*x_1=0.4968*	*x_1=0.6234*	*x_1=0.7440*	*x_1=0.8731*	*x_1=1*
313.15	0.1	0	6.5315E-03	6.2733E-03	5.9284E-03	5.4337E-03	4.6573E-03	3.8801E-03	0
313.15	1.14	0	2.8346E-04	5.1119E-04	5.1925E-04	4.2272E-04	2.6559E-04	1.5472E-04	0
313.15	2.14	0	2.7416E-04	4.9446E-04	5.0235E-04	4.0891E-04	2.5677E-04	1.4954E-04	0
313.15	3.15	0	2.6520E-04	4.7823E-04	4.8594E-04	3.9555E-04	2.4840E-04	1.4479E-04	0
313.15	4.16	0	2.5661E-04	4.6264E-04	4.6983E-04	3.8246E-04	2.4027E-04	1.3989E-04	0
313.15	5.17	0	2.4840E-04	4.4747E-04	4.5441E-04	3.6990E-04	2.3231E-04	1.3528E-04	0
313.15	6.18	0	2.4009E-04	4.3269E-04	4.3965E-04	3.5780E-04	2.2470E-04	1.3093E-04	0
313.15	7.19	0	2.3224E-04	4.1850E-04	4.2510E-04	3.4604E-04	2.1731E-04	1.2655E-04	0
313.15	8.2	0	2.2459E-04	4.0466E-04	4.1131E-04	3.3471E-04	2.1020E-04	1.2251E-04	0
313.15	9.23	0	2.1714E-04	3.9151E-04	3.9768E-04	3.2374E-04	2.0337E-04	1.1840E-04	0
313.15	10.23	0	2.0999E-04	3.7866E-04	3.8467E-04	3.1309E-04	1.9663E-04	1.1475E-04	0
313.15	11.24	0	2.0321E-04	3.6627E-04	3.7216E-04	3.0288E-04	1.9022E-04	1.1089E-04	0
313.15	12.25	0	1.9659E-04	3.5418E-04	3.5986E-04	2.9290E-04	1.8396E-04	1.0713E-04	0
313.15	13.26	0	1.9004E-04	3.4263E-04	3.4816E-04	2.8330E-04	1.7793E-04	1.0363E-04	0
313.15	14.27	0	1.8384E-04	3.3129E-04	3.3677E-04	2.7405E-04	1.7213E-04	1.0022E-04	0
313.15	15.27	0	1.7786E-04	3.2042E-04	3.2574E-04	2.6504E-04	1.6655E-04	9.7139E-05	0
313.15	16.28	0	1.7192E-04	3.1009E-04	3.1490E-04	2.5632E-04	1.6094E-04	9.3876E-05	0
313.15	17.29	0	1.6631E-04	2.9997E-04	3.0478E-04	2.4791E-04	1.5572E-04	9.0851E-05	0
313.15	18.3	0	1.6091E-04	2.9005E-04	2.9479E-04	2.3998E-04	1.5066E-04	8.7673E-05	0
313.15	19.3	0	1.5554E-04	2.8051E-04	2.8492E-04	2.3195E-04	1.4568E-04	8.5021E-05	0
313.15	20.31	0	1.5060E-04	2.7121E-04	2.7571E-04	2.2449E-04	1.4089E-04	8.2018E-05	0
323.15	0.1	0	6.8743E-03	6.6348E-03	6.2680E-03	5.7574E-03	4.9460E-03	4.1334E-03	0
323.15	1.15	0	3.4586E-04	6.2363E-04	6.3366E-04	5.1579E-04	3.2388E-04	1.8868E-04	0
323.15	2.15	0	3.3490E-04	6.0356E-04	6.1340E-04	4.9919E-04	3.1352E-04	1.8263E-04	0
323.15	3.17	0	3.2417E-04	5.8442E-04	5.9366E-04	4.8322E-04	3.0344E-04	1.7675E-04	0
323.15	4.18	0	3.1401E-04	5.6567E-04	5.7464E-04	4.6782E-04	2.9374E-04	1.7109E-04	0
323.15	5.19	0	3.0366E-04	5.4746E-04	5.5640E-04	4.5276E-04	2.8439E-04	1.6560E-04	0
323.15	6.2	0	2.9404E-04	5.3005E-04	5.3854E-04	4.3830E-04	2.7530E-04	1.6043E-04	0
323.15	7.22	0	2.8468E-04	5.1309E-04	5.2129E-04	4.2426E-04	2.6650E-04	1.5531E-04	0
323.15	8.23	0	2.7553E-04	4.9671E-04	5.0468E-04	4.1084E-04	2.5794E-04	1.5037E-04	0
323.15	9.24	0	2.6662E-04	4.8067E-04	4.8832E-04	3.9755E-04	2.4973E-04	1.4550E-04	0
323.15	10.25	0	2.5806E-04	4.6545E-04	4.7290E-04	3.8499E-04	2.4168E-04	1.4076E-04	0
323.15	11.25	0	2.4993E-04	4.5056E-04	4.5780E-04	3.7251E-04	2.3396E-04	1.3635E-04	0
323.15	12.27	0	2.4193E-04	4.3599E-04	4.4297E-04	3.6062E-04	2.2646E-04	1.3191E-04	0
323.15	13.27	0	2.3423E-04	4.2226E-04	4.2895E-04	3.4918E-04	2.1928E-04	1.2786E-04	0

323.15	14.26	0	2.2675E-04	4.0872E-04	4.1526E-04	3.3798E-04	2.1221E-04	1.2375E-04	0
323.15	15.29	0	2.1946E-04	3.9561E-04	4.0187E-04	3.2710E-04	2.0543E-04	1.1979E-04	0
323.15	16.3	0	2.1239E-04	3.8286E-04	3.8901E-04	3.1662E-04	1.9898E-04	1.1597E-04	0
323.15	17.3	0	2.0576E-04	3.7066E-04	3.7665E-04	3.0649E-04	1.9254E-04	1.1209E-04	0
323.15	18.3	0	1.9909E-04	3.5868E-04	3.6452E-04	2.9668E-04	1.8634E-04	1.0853E-04	0
323.15	19.3	0	1.9268E-04	3.4729E-04	3.5290E-04	2.8726E-04	1.8037E-04	1.0508E-04	0
323.15	20.29	0	1.8642E-04	3.3611E-04	3.4164E-04	2.7799E-04	1.7458E-04	1.0186E-04	0
333.15	0.1	0	7.1528E-03	6.9448E-03	6.5650E-03	6.0380E-03	5.1980E-03	4.3550E-03	0
333.15	1.13	0	4.3922E-04	7.9210E-04	8.0454E-04	6.5510E-04	4.1123E-04	2.3954E-04	0
333.15	2.13	0	4.2860E-04	7.7231E-04	7.8450E-04	6.3872E-04	4.0095E-04	2.3356E-04	0
333.15	3.14	0	4.1752E-04	7.5298E-04	7.6497E-04	6.2276E-04	3.9091E-04	2.2784E-04	0
333.15	4.15	0	4.0745E-04	7.3415E-04	7.4584E-04	6.0709E-04	3.8117E-04	2.2217E-04	0
333.15	5.16	0	3.9720E-04	7.1577E-04	7.2716E-04	5.9205E-04	3.7168E-04	2.1659E-04	0
333.15	6.17	0	3.8699E-04	6.9783E-04	7.0903E-04	5.7713E-04	3.6243E-04	2.1108E-04	0
333.15	7.18	0	3.7760E-04	6.8039E-04	6.9114E-04	5.6260E-04	3.5330E-04	2.0588E-04	0
333.15	8.19	0	3.6786E-04	6.6338E-04	6.7386E-04	5.4855E-04	3.4451E-04	2.0062E-04	0
333.15	9.2	0	3.5899E-04	6.4670E-04	6.5718E-04	5.3498E-04	3.3583E-04	1.9562E-04	0
333.15	10.21	0	3.4987E-04	6.3067E-04	6.4061E-04	5.2154E-04	3.2748E-04	1.9075E-04	0
333.15	11.22	0	3.4102E-04	6.1487E-04	6.2475E-04	5.0842E-04	3.1927E-04	1.8596E-04	0
333.15	12.23	0	3.3280E-04	5.9938E-04	6.0903E-04	4.9572E-04	3.1134E-04	1.8146E-04	0
333.15	13.24	0	3.2431E-04	5.8452E-04	5.9384E-04	4.8350E-04	3.0348E-04	1.7683E-04	0
333.15	14.25	0	3.1602E-04	5.6995E-04	5.7893E-04	4.7125E-04	2.9598E-04	1.7253E-04	0
333.15	15.26	0	3.0822E-04	5.5567E-04	5.6450E-04	4.5948E-04	2.8854E-04	1.6805E-04	0
333.15	16.27	0	3.0048E-04	5.4176E-04	5.5036E-04	4.4799E-04	2.8132E-04	1.6384E-04	0
333.15	17.27	0	2.9319E-04	5.2823E-04	5.3669E-04	4.3692E-04	2.7436E-04	1.5983E-04	0
333.15	18.28	0	2.8572E-04	5.1507E-04	5.2322E-04	4.2588E-04	2.6748E-04	1.5591E-04	0
333.15	19.28	0	2.7852E-04	5.0218E-04	5.1010E-04	4.1521E-04	2.6076E-04	1.5184E-04	0
333.15	20.28	0	2.7161E-04	4.8949E-04	4.9748E-04	4.0504E-04	2.5436E-04	1.4815E-04	0
343.15	0.1	0	7.3071E-03	7.1993E-03	6.8163E-03	6.3006E-03	5.4586E-03	4.6013E-03	0
343.15	1.14	0	5.7100E-04	1.0294E-03	1.0459E-03	8.5158E-04	5.3472E-04	3.1143E-04	0
343.15	2.14	0	5.6083E-04	1.0110E-03	1.0270E-03	8.3626E-04	5.2496E-04	3.0593E-04	0
343.15	3.14	0	5.5093E-04	9.9288E-04	1.0085E-03	8.2114E-04	5.1550E-04	3.0040E-04	0
343.15	4.16	0	5.4089E-04	9.7490E-04	9.9045E-04	8.0641E-04	5.0631E-04	2.9504E-04	0
343.15	5.17	0	5.3121E-04	9.5745E-04	9.7258E-04	7.9186E-04	4.9710E-04	2.8957E-04	0
343.15	6.18	0	5.2161E-04	9.4018E-04	9.5525E-04	7.7758E-04	4.8818E-04	2.8438E-04	0
343.15	7.19	0	5.1224E-04	9.2317E-04	9.3794E-04	7.6366E-04	4.7954E-04	2.7924E-04	0
343.15	8.2	0	5.0304E-04	9.0667E-04	9.2092E-04	7.4978E-04	4.7075E-04	2.7435E-04	0
343.15	9.21	0	4.9410E-04	8.9035E-04	9.0450E-04	7.3635E-04	4.6229E-04	2.6927E-04	0
343.15	10.22	0	4.8501E-04	8.7434E-04	8.8815E-04	7.2299E-04	4.5403E-04	2.6446E-04	0
343.15	11.23	0	4.7613E-04	8.5844E-04	8.7215E-04	7.1017E-04	4.4585E-04	2.5981E-04	0
343.15	12.24	0	4.6760E-04	8.4296E-04	8.5643E-04	6.9737E-04	4.3779E-04	2.5501E-04	0
343.15	13.25	0	4.5937E-04	8.2806E-04	8.4099E-04	6.8480E-04	4.2993E-04	2.5046E-04	0
343.15	14.26	0	4.5121E-04	8.1308E-04	8.2605E-04	6.7250E-04	4.2217E-04	2.4597E-04	0

343.15	15.27	0	4.4310E-04	7.9835E-04	8.1103E-04	6.6041E-04	4.1462E-04	2.4153E-04	0
343.15	16.27	0	4.3509E-04	7.8407E-04	7.9655E-04	6.4851E-04	4.0708E-04	2.3714E-04	0
343.15	17.28	0	4.2716E-04	7.6997E-04	7.8208E-04	6.3687E-04	3.9979E-04	2.3287E-04	0
343.15	18.28	0	4.1950E-04	7.5610E-04	7.6801E-04	6.2537E-04	3.9264E-04	2.2870E-04	0
343.15	19.29	0	4.1198E-04	7.4251E-04	7.5418E-04	6.1407E-04	3.8553E-04	2.2455E-04	0
343.15	20.29	0	4.0433E-04	7.2907E-04	7.4062E-04	6.0306E-04	3.7857E-04	2.2049E-04	0
353.15	0.1	0	7.5254E-04	1.4352E-03	1.4818E-03	1.2080E-03	7.4300E-04	4.1417E-04	0
353.15	1.14	0	7.5374E-04	1.3590E-03	1.3805E-03	1.1240E-03	7.0562E-04	4.1109E-04	0
353.15	2.14	0	7.4481E-04	1.3427E-03	1.3641E-03	1.1105E-03	6.9718E-04	4.0622E-04	0
353.15	3.14	0	7.3605E-04	1.3265E-03	1.3475E-03	1.0971E-03	6.8879E-04	4.0123E-04	0
353.15	4.16	0	7.2686E-04	1.3107E-03	1.3313E-03	1.0840E-03	6.8059E-04	3.9651E-04	0
353.15	5.16	0	7.1843E-04	1.2948E-03	1.3156E-03	1.0708E-03	6.7235E-04	3.9171E-04	0
353.15	6.18	0	7.0977E-04	1.2794E-03	1.2997E-03	1.0580E-03	6.6430E-04	3.8694E-04	0
353.15	7.19	0	7.0136E-04	1.2640E-03	1.2842E-03	1.0453E-03	6.5645E-04	3.8232E-04	0
353.15	8.2	0	6.9260E-04	1.2490E-03	1.2688E-03	1.0327E-03	6.4843E-04	3.7771E-04	0
353.15	9.21	0	6.8428E-04	1.2339E-03	1.2535E-03	1.0204E-03	6.4063E-04	3.7330E-04	0
353.15	10.22	0	6.7637E-04	1.2191E-03	1.2384E-03	1.0081E-03	6.3298E-04	3.6882E-04	0
353.15	11.23	0	6.6834E-04	1.2045E-03	1.2236E-03	9.9600E-04	6.2538E-04	3.6430E-04	0
353.15	12.24	0	6.6022E-04	1.1901E-03	1.2089E-03	9.8406E-04	6.1793E-04	3.5988E-04	0
353.15	13.25	0	6.5232E-04	1.1757E-03	1.1943E-03	9.7223E-04	6.1046E-04	3.5561E-04	0
353.15	14.26	0	6.4455E-04	1.1616E-03	1.1802E-03	9.6072E-04	6.0317E-04	3.5134E-04	0
353.15	15.25	0	6.3660E-04	1.1478E-03	1.1660E-03	9.4906E-04	5.9588E-04	3.4711E-04	0
353.15	16.27	0	6.2885E-04	1.1339E-03	1.1518E-03	9.3767E-04	5.8875E-04	3.4298E-04	0
353.15	17.27	0	6.2147E-04	1.1203E-03	1.1381E-03	9.2644E-04	5.8169E-04	3.3896E-04	0
353.15	18.29	0	6.1394E-04	1.1069E-03	1.1245E-03	9.1529E-04	5.7477E-04	3.3488E-04	0
353.15	19.29	0	6.0682E-04	1.0936E-03	1.1109E-03	9.0448E-04	5.6788E-04	3.3089E-04	0
353.15	20.29	0	5.9927E-04	1.0804E-03	1.0977E-03	8.9353E-04	5.6106E-04	3.2691E-04	0

Expanded combined uncertainties (k = 2) U_c are $U_c(T) = 0.02$ K, $U_c(P) = 0.032$ MPa, and $U_c(x_i) = 0.0002$, $U_c(V^E) = 1.89 \times 10^{-5}$ m^3. $kmol^{-1}$

Table A3: Excess Molar Volumes (V^E) of butan-2-ol (1) + n-octane (2) at various pressures and temperatures.

T/K	P/MPa	$V^E/m^3.kmol^{-1}$							
		x_1=0	*x_1=0.1262*	*x_1=0.3742*	*x_1=0.5002*	*x_1=0.6257*	*x_1=0.7501*	*x_1=0.8747*	*x_1=1*
313.15	0.1	0	4.7587E-04	7.3828E-04	6.8463E-04	5.6200E-04	3.9242E-04	2.2082E-04	0
313.15	1.14	0	4.2993E-04	6.9836E-04	6.4349E-04	5.0846E-04	3.3556E-04	1.7812E-04	0
313.15	2.14	0	4.1275E-04	6.7049E-04	6.1772E-04	4.8812E-04	3.2216E-04	1.7098E-04	0
313.15	3.15	0	3.9623E-04	6.4364E-04	5.9298E-04	4.6861E-04	3.0928E-04	1.6416E-04	0
313.15	4.16	0	3.8055E-04	6.1784E-04	5.6933E-04	4.4988E-04	2.9687E-04	1.5760E-04	0
313.15	5.17	0	3.6519E-04	5.9325E-04	5.4653E-04	4.3186E-04	2.8503E-04	1.5129E-04	0
313.15	6.18	0	3.5058E-04	5.6944E-04	5.2448E-04	4.1467E-04	2.7360E-04	1.4524E-04	0
313.15	7.19	0	3.3670E-04	5.4694E-04	5.0357E-04	3.9801E-04	2.6267E-04	1.3943E-04	0
313.15	8.2	0	3.2310E-04	5.2491E-04	4.8344E-04	3.8215E-04	2.5217E-04	1.3387E-04	0
313.15	9.23	0	3.1018E-04	5.0387E-04	4.6420E-04	3.6683E-04	2.4210E-04	1.2851E-04	0
313.15	10.23	0	2.9803E-04	4.8372E-04	4.4562E-04	3.5218E-04	2.3244E-04	1.2343E-04	0
313.15	11.24	0	2.8590E-04	4.6430E-04	4.2784E-04	3.3813E-04	2.2312E-04	1.1844E-04	0
313.15	12.25	0	2.7452E-04	4.4582E-04	4.1072E-04	3.2456E-04	2.1421E-04	1.1372E-04	0
313.15	13.26	0	2.6363E-04	4.2785E-04	3.9430E-04	3.1159E-04	2.0565E-04	1.0917E-04	0
313.15	14.27	0	2.5308E-04	4.1081E-04	3.7855E-04	2.9917E-04	1.9740E-04	1.0479E-04	0
313.15	15.27	0	2.4296E-04	3.9441E-04	3.6322E-04	2.8718E-04	1.8954E-04	1.0063E-04	0
313.15	16.28	0	2.3309E-04	3.7866E-04	3.4887E-04	2.7571E-04	1.8194E-04	9.6601E-05	0
313.15	17.29	0	2.2393E-04	3.6348E-04	3.3496E-04	2.6467E-04	1.7469E-04	9.2740E-05	0
313.15	18.3	0	2.1485E-04	3.4896E-04	3.2155E-04	2.5411E-04	1.6770E-04	8.9032E-05	0
313.15	19.3	0	2.0638E-04	3.3509E-04	3.0868E-04	2.4393E-04	1.6099E-04	8.5481E-05	0
313.15	20.31	0	1.9816E-04	3.2160E-04	2.9634E-04	2.3416E-04	1.5453E-04	8.2075E-05	0
323.15	0.1	0	5.8256E-04	8.8909E-04	8.3344E-04	6.7976E-04	4.7372E-04	2.7923E-04	0
323.15	1.15	0	5.1156E-04	8.3109E-04	7.6554E-04	6.0493E-04	3.9880E-04	2.1146E-04	0
323.15	2.15	0	4.9626E-04	8.0586E-04	7.4271E-04	5.8663E-04	3.8731E-04	2.0514E-04	0
323.15	3.17	0	4.8136E-04	7.8206E-04	7.2007E-04	5.6898E-04	3.7570E-04	1.9926E-04	0
323.15	4.18	0	4.6710E-04	7.5844E-04	6.9896E-04	5.5220E-04	3.6416E-04	1.9299E-04	0
323.15	5.19	0	4.5276E-04	7.3548E-04	6.7750E-04	5.3573E-04	3.5346E-04	1.8738E-04	0
323.15	6.2	0	4.3934E-04	7.1370E-04	6.5736E-04	5.1957E-04	3.4279E-04	1.8175E-04	0
323.15	7.22	0	4.2640E-04	6.9227E-04	6.3766E-04	5.0417E-04	3.3251E-04	1.7649E-04	0
323.15	8.23	0	4.1330E-04	6.7165E-04	6.1872E-04	4.8826E-04	3.2216E-04	1.7092E-04	0
323.15	9.24	0	4.0132E-04	6.5134E-04	6.0006E-04	4.7420E-04	3.1263E-04	1.6565E-04	0
323.15	10.25	0	3.8896E-04	6.3188E-04	5.8196E-04	4.6002E-04	3.0372E-04	1.6071E-04	0
323.15	11.25	0	3.7693E-04	6.1274E-04	5.6450E-04	4.4593E-04	2.9396E-04	1.5625E-04	0
323.15	12.27	0	3.6604E-04	5.9433E-04	5.4763E-04	4.3286E-04	2.8550E-04	1.5156E-04	0
323.15	13.27	0	3.5497E-04	5.7683E-04	5.3140E-04	4.2004E-04	2.7715E-04	1.4691E-04	0
323.15	14.26	0	3.4434E-04	5.5931E-04	5.1505E-04	4.0686E-04	2.6874E-04	1.4222E-04	0

323.15	15.29	0	3.3401E-04	5.4235E-04	5.0002E-04	3.9508E-04	2.6050E-04	1.3835E-04	0
323.15	16.3	0	3.2421E-04	5.2638E-04	4.8474E-04	3.8302E-04	2.5310E-04	1.3363E-04	0
323.15	17.3	0	3.1446E-04	5.1051E-04	4.7036E-04	3.7179E-04	2.4516E-04	1.3003E-04	0
323.15	18.3	0	3.0477E-04	4.9506E-04	4.5649E-04	3.6064E-04	2.3780E-04	1.2583E-04	0
323.15	19.3	0	2.9564E-04	4.8039E-04	4.4261E-04	3.4963E-04	2.3084E-04	1.2228E-04	0
323.15	20.29	0	2.8700E-04	4.6590E-04	4.2922E-04	3.3939E-04	2.2380E-04	1.1859E-04	0
333.15	0.1	0	6.7998E-04	1.0537E-03	9.8732E-04	8.0447E-04	5.6127E-04	3.4429E-04	0
333.15	1.13	0	6.0890E-04	9.8896E-04	9.1116E-04	7.2002E-04	4.7513E-04	2.5220E-04	0
333.15	2.13	0	5.9367E-04	9.6425E-04	8.8839E-04	7.0202E-04	4.6329E-04	2.4590E-04	0
333.15	3.14	0	5.7883E-04	9.4017E-04	8.6616E-04	6.8435E-04	4.5169E-04	2.3976E-04	0
333.15	4.15	0	5.6435E-04	9.1665E-04	8.4454E-04	6.6738E-04	4.4040E-04	2.3377E-04	0
333.15	5.16	0	5.5026E-04	8.9372E-04	8.2342E-04	6.5070E-04	4.2941E-04	2.2793E-04	0
333.15	6.17	0	5.3650E-04	8.7142E-04	8.0282E-04	6.3444E-04	4.1864E-04	2.2221E-04	0
333.15	7.18	0	5.2309E-04	8.4959E-04	7.8261E-04	6.1854E-04	4.0820E-04	2.1665E-04	0
333.15	8.19	0	5.1002E-04	8.2839E-04	7.6319E-04	6.0310E-04	3.9797E-04	2.1126E-04	0
333.15	9.2	0	4.9727E-04	8.0769E-04	7.4408E-04	5.8804E-04	3.8802E-04	2.0595E-04	0
333.15	10.21	0	4.8485E-04	7.8749E-04	7.2548E-04	5.7334E-04	3.7832E-04	2.0084E-04	0
333.15	11.22	0	4.7268E-04	7.6778E-04	7.0735E-04	5.5899E-04	3.6891E-04	1.9580E-04	0
333.15	12.23	0	4.6091E-04	7.4861E-04	6.8972E-04	5.4501E-04	3.5950E-04	1.9089E-04	0
333.15	13.24	0	4.4939E-04	7.2990E-04	6.7243E-04	5.3143E-04	3.5069E-04	1.8613E-04	0
333.15	14.25	0	4.3817E-04	7.1161E-04	6.5563E-04	5.1813E-04	3.4190E-04	1.8147E-04	0
333.15	15.26	0	4.2722E-04	6.9385E-04	6.3925E-04	5.0514E-04	3.3335E-04	1.7697E-04	0
333.15	16.27	0	4.1654E-04	6.7650E-04	6.2330E-04	4.9254E-04	3.2507E-04	1.7251E-04	0
333.15	17.27	0	4.0613E-04	6.5960E-04	6.0767E-04	4.8025E-04	3.1690E-04	1.6822E-04	0
333.15	18.28	0	3.9597E-04	6.4314E-04	5.9250E-04	4.6821E-04	3.0899E-04	1.6403E-04	0
333.15	19.28	0	3.8608E-04	6.2701E-04	5.7771E-04	4.5651E-04	3.0125E-04	1.5992E-04	0
333.15	20.28	0	3.7643E-04	6.1139E-04	5.6323E-04	4.4512E-04	2.9373E-04	1.5591E-04	0
343.15	0.1	0	7.9860E-04	1.2586E-03	1.1789E-03	9.5795E-04	6.8423E-04	3.7449E-04	0
343.15	1.14	0	7.2444E-04	1.1770E-03	1.0844E-03	8.5683E-04	5.6536E-04	3.0009E-04	0
343.15	2.14	0	7.1005E-04	1.1534E-03	1.0626E-03	8.3966E-04	5.5409E-04	2.9408E-04	0
343.15	3.14	0	6.9587E-04	1.1302E-03	1.0413E-03	8.2287E-04	5.4302E-04	2.8818E-04	0
343.15	4.16	0	6.8194E-04	1.1076E-03	1.0203E-03	8.0643E-04	5.3218E-04	2.8245E-04	0
343.15	5.17	0	6.6831E-04	1.0855E-03	1.0000E-03	7.9025E-04	5.2151E-04	2.7681E-04	0
343.15	6.18	0	6.5497E-04	1.0638E-03	9.8004E-04	7.7449E-04	5.1109E-04	2.7125E-04	0
343.15	7.19	0	6.4182E-04	1.0425E-03	9.6048E-04	7.5900E-04	5.0087E-04	2.6582E-04	0
343.15	8.2	0	6.2905E-04	1.0217E-03	9.4126E-04	7.4384E-04	4.9085E-04	2.6042E-04	0
343.15	9.21	0	6.1641E-04	1.0012E-03	9.2244E-04	7.2895E-04	4.8101E-04	2.5532E-04	0
343.15	10.22	0	6.0410E-04	9.8120E-04	9.0399E-04	7.1437E-04	4.7142E-04	2.5022E-04	0
343.15	11.23	0	5.9202E-04	9.6158E-04	8.8593E-04	7.0010E-04	4.6202E-04	2.4523E-04	0
343.15	12.24	0	5.8016E-04	9.4243E-04	8.6820E-04	6.8610E-04	4.5273E-04	2.4029E-04	0
343.15	13.25	0	5.6863E-04	9.2351E-04	8.5083E-04	6.7237E-04	4.4370E-04	2.3549E-04	0
343.15	14.26	0	5.5721E-04	9.0504E-04	8.3384E-04	6.5892E-04	4.3484E-04	2.3089E-04	0
343.15	15.27	0	5.4607E-04	8.8697E-04	8.1716E-04	6.4575E-04	4.2613E-04	2.2619E-04	0

343.15	16.27	0	5.3520E-04	8.6910E-04	8.0082E-04	6.3279E-04	4.1762E-04	2.2166E-04	0
343.15	17.28	0	5.2450E-04	8.5188E-04	7.8480E-04	6.2021E-04	4.0927E-04	2.1721E-04	0
343.15	18.28	0	5.1399E-04	8.3478E-04	7.6911E-04	6.0780E-04	4.0111E-04	2.1288E-04	0
343.15	19.29	0	5.0372E-04	8.1811E-04	7.5373E-04	5.9558E-04	3.9305E-04	2.0865E-04	0
343.15	20.29	0	4.9360E-04	8.0174E-04	7.3865E-04	5.8372E-04	3.8519E-04	2.0445E-04	0
353.15	0.1	0	9.5938E-04	1.5018E-03	1.3940E-03	1.1334E-03	7.7521E-04	4.6043E-04	0
353.15	1.14	0	8.6216E-04	1.4003E-03	1.2894E-03	1.0195E-03	6.7278E-04	3.5703E-04	0
353.15	2.14	0	8.4916E-04	1.3795E-03	1.2708E-03	1.0043E-03	6.6268E-04	3.5177E-04	0
353.15	3.14	0	8.3635E-04	1.3588E-03	1.2519E-03	9.8913E-04	6.5281E-04	3.4640E-04	0
353.15	4.16	0	8.2389E-04	1.3384E-03	1.2331E-03	9.7358E-04	6.4293E-04	3.4130E-04	0
353.15	5.16	0	8.1152E-04	1.3183E-03	1.2135E-03	9.5973E-04	6.3335E-04	3.3609E-04	0
353.15	6.18	0	7.9939E-04	1.2984E-03	1.1964E-03	9.4543E-04	6.2382E-04	3.3114E-04	0
353.15	7.19	0	7.8754E-04	1.2789E-03	1.1784E-03	9.3112E-04	6.1449E-04	3.2613E-04	0
353.15	8.2	0	7.7558E-04	1.2599E-03	1.1606E-03	9.1727E-04	6.0532E-04	3.2126E-04	0
353.15	9.21	0	7.6403E-04	1.2410E-03	1.1434E-03	9.0346E-04	5.9616E-04	3.1641E-04	0
353.15	10.22	0	7.5257E-04	1.2224E-03	1.1261E-03	8.8986E-04	5.8720E-04	3.1163E-04	0
353.15	11.23	0	7.4122E-04	1.2039E-03	1.1090E-03	8.7660E-04	5.7844E-04	3.0700E-04	0
353.15	12.24	0	7.3011E-04	1.1860E-03	1.0926E-03	8.6347E-04	5.6974E-04	3.0237E-04	0
353.15	13.25	0	7.1913E-04	1.1682E-03	1.0762E-03	8.5054E-04	5.6119E-04	2.9784E-04	0
353.15	14.26	0	7.0837E-04	1.1507E-03	1.0601E-03	8.3779E-04	5.5281E-04	2.9342E-04	0
353.15	15.25	0	6.9777E-04	1.1335E-03	1.0443E-03	8.2510E-04	5.4453E-04	2.8897E-04	0
353.15	16.27	0	6.8740E-04	1.1164E-03	1.0285E-03	8.1276E-04	5.3635E-04	2.8467E-04	0
353.15	17.27	0	6.7698E-04	1.0996E-03	1.0131E-03	8.0062E-04	5.2812E-04	2.8035E-04	0
353.15	18.29	0	6.6680E-04	1.0831E-03	9.9792E-04	7.8851E-04	5.2040E-04	2.7618E-04	0
353.15	19.29	0	6.5690E-04	1.0670E-03	9.8289E-04	7.7675E-04	5.1259E-04	2.7221E-04	0
353.15	20.29	0	6.4704E-04	1.0508E-03	9.6824E-04	7.6504E-04	5.0483E-04	2.6796E-04	0

The expanded combined uncertainties $U_c(k = 2)$ are $U_c(T)$= 0.02 K, $U_c(P)$ = 0.03 MPa, $U_c(x_i)$ = 0.0002, and $U_c(V^E)$ = 1.77 x 10^{-5} m^3. $kmol^{-1}$.

Table A4: Excess Molar Volumes (V^E) of butan-2-ol (1) + n-decane (2) at various pressures and temperatures.

T/K	P/MPa	$V^E/m^3.kmol^{-1}$							
		x_1=0	*x_1=0.1254*	*x_1=0.3754*	*x_1=0.5055*	*x_1=0.6240*	*x_1=0.7519*	*x_1=0.8740*	*x_1=1*
313.15	0.1	0	4.9992E-04	9.0875E-04	1.0099E-03	9.6422E-04	6.9449E-04	3.3492E-04	0
313.15	1.14	0	3.9824E-04	7.3985E-04	8.0696E-04	7.7100E-04	5.4452E-04	2.4773E-04	0
313.15	2.14	0	3.8315E-04	7.1199E-04	7.7645E-04	7.4185E-04	5.2395E-04	2.3833E-04	0
313.15	3.15	0	3.6783E-04	6.8436E-04	7.4642E-04	7.1335E-04	5.0387E-04	2.2907E-04	0
313.15	4.16	0	3.5390E-04	6.5844E-04	7.1819E-04	6.8624E-04	4.8471E-04	2.2053E-04	0
313.15	5.17	0	3.4144E-04	6.3423E-04	6.9150E-04	6.6072E-04	4.6665E-04	2.1231E-04	0
313.15	6.18	0	3.2847E-04	6.1006E-04	6.6527E-04	6.3555E-04	4.4889E-04	2.0419E-04	0
313.15	7.19	0	3.1613E-04	5.8699E-04	6.4012E-04	6.1163E-04	4.3202E-04	1.9649E-04	0
313.15	8.2	0	3.0205E-04	5.6331E-04	6.1465E-04	5.8745E-04	4.1497E-04	1.8875E-04	0
313.15	9.23	0	2.9216E-04	5.4306E-04	5.9227E-04	5.6586E-04	3.9975E-04	1.8181E-04	0
313.15	10.23	0	2.8083E-04	5.2222E-04	5.6969E-04	5.4441E-04	3.8447E-04	1.7491E-04	0
313.15	11.24	0	2.7020E-04	5.0250E-04	5.4811E-04	5.2378E-04	3.6990E-04	1.6828E-04	0
313.15	12.25	0	2.6072E-04	4.8414E-04	5.2788E-04	5.0425E-04	3.5622E-04	1.6201E-04	0
313.15	13.26	0	2.4993E-04	4.6501E-04	5.0732E-04	4.8469E-04	3.4240E-04	1.5592E-04	0
313.15	14.27	0	2.4092E-04	4.4772E-04	4.8832E-04	4.6643E-04	3.2956E-04	1.4982E-04	0
313.15	15.27	0	2.3093E-04	4.3016E-04	4.6928E-04	4.4853E-04	3.1684E-04	1.4412E-04	0
313.15	16.28	0	2.2170E-04	4.1353E-04	4.5117E-04	4.3124E-04	3.0469E-04	1.3856E-04	0
313.15	17.29	0	2.1505E-04	3.9909E-04	4.3515E-04	4.1569E-04	2.9358E-04	1.3362E-04	0
313.15	18.3	0	2.0597E-04	3.8333E-04	4.1808E-04	3.9959E-04	2.8219E-04	1.2834E-04	0
313.15	19.3	0	1.9850E-04	3.6906E-04	4.0248E-04	3.8457E-04	2.7160E-04	1.2357E-04	0
313.15	20.31	0	1.8996E-04	3.5441E-04	3.8668E-04	3.6970E-04	2.6115E-04	1.1879E-04	0
323.15	0.1	0	5.7419E-04	1.0776E-03	1.1906E-03	1.1155E-03	8.2039E-04	3.9947E-04	0
323.15	1.15	0	4.8324E-04	9.0463E-04	9.8983E-04	9.4982E-04	6.7983E-04	3.2439E-04	0
323.15	2.15	0	4.6901E-04	8.7827E-04	9.6094E-04	9.2243E-04	6.6030E-04	3.1533E-04	0
323.15	3.17	0	4.5712E-04	8.5300E-04	9.3251E-04	8.9434E-04	6.3918E-04	3.0342E-04	0
323.15	4.18	0	4.4256E-04	8.2741E-04	9.0484E-04	8.6798E-04	6.2038E-04	2.9471E-04	0
323.15	5.19	0	4.3091E-04	8.0423E-04	8.7915E-04	8.4334E-04	6.0264E-04	2.8611E-04	0
323.15	6.2	0	4.1748E-04	7.7900E-04	8.5129E-04	8.1584E-04	5.8170E-04	2.7387E-04	0
323.15	7.22	0	4.0438E-04	7.5704E-04	8.2805E-04	7.9441E-04	5.6786E-04	2.6978E-04	0
323.15	8.23	0	3.9423E-04	7.3650E-04	8.0542E-04	7.7269E-04	5.5271E-04	2.6307E-04	0
323.15	9.24	0	3.8162E-04	7.1393E-04	7.8094E-04	7.4921E-04	5.3564E-04	2.5461E-04	0
323.15	10.25	0	3.7160E-04	6.9417E-04	7.5908E-04	7.2828E-04	5.2079E-04	2.4778E-04	0
323.15	11.25	0	3.6094E-04	6.7360E-04	7.3648E-04	7.0619E-04	5.0444E-04	2.3909E-04	0
323.15	12.27	0	3.4970E-04	6.5342E-04	7.1442E-04	6.8512E-04	4.8931E-04	2.3163E-04	0

323.15	13.27	0	3.3981E-04	6.3451E-04	6.9365E-04	6.6518E-04	4.7493E-04	2.2466E-04	0
323.15	14.26	0	3.2774E-04	6.1026E-04	6.6555E-04	6.3608E-04	4.4937E-04	2.0448E-04	0
323.15	15.29	0	3.1941E-04	5.9821E-04	6.5448E-04	6.2797E-04	4.4896E-04	2.1355E-04	0
323.15	16.3	0	3.1132E-04	5.7970E-04	6.3311E-04	6.0622E-04	4.3128E-04	2.0148E-04	0
323.15	17.3	0	3.0266E-04	5.6351E-04	6.1550E-04	5.8954E-04	4.1992E-04	1.9691E-04	0
323.15	18.3	0	2.9272E-04	5.4701E-04	5.9802E-04	5.7340E-04	4.0901E-04	1.9300E-04	0
323.15	19.3	0	2.8362E-04	5.3068E-04	5.8025E-04	5.5628E-04	3.9689E-04	1.8715E-04	0
323.15	20.29	0	2.7505E-04	5.1464E-04	5.6261E-04	5.3937E-04	3.8437E-04	1.8058E-04	0
333.15	0.1	0	6.8968E-04	1.2498E-03	1.3917E-03	1.3349E-03	9.5380E-04	4.3589E-04	0
333.15	1.13	0	5.8324E-04	1.0861E-03	1.1852E-03	1.1327E-03	7.9997E-04	3.6391E-04	0
333.15	2.13	0	5.7060E-04	1.0622E-03	1.1585E-03	1.1068E-03	7.8181E-04	3.5568E-04	0
333.15	3.14	0	5.5780E-04	1.0376E-03	1.1317E-03	1.0813E-03	7.6381E-04	3.4736E-04	0
333.15	4.15	0	5.4361E-04	1.0127E-03	1.1049E-03	1.0560E-03	7.4593E-04	3.3924E-04	0
333.15	5.16	0	5.3218E-04	9.9019E-04	1.0803E-03	1.0322E-03	7.2903E-04	3.3162E-04	0
333.15	6.17	0	5.1944E-04	9.6714E-04	1.0551E-03	1.0082E-03	7.1216E-04	3.2392E-04	0
333.15	7.18	0	5.0684E-04	9.4436E-04	1.0303E-03	9.8476E-04	6.9557E-04	3.1641E-04	0
333.15	8.19	0	4.9624E-04	9.2352E-04	1.0072E-03	9.6264E-04	6.7985E-04	3.0918E-04	0
333.15	9.2	0	4.8548E-04	9.0270E-04	9.8463E-04	9.4068E-04	6.6433E-04	3.0231E-04	0
333.15	10.21	0	4.7249E-04	8.8055E-04	9.6102E-04	9.1835E-04	6.4866E-04	2.9503E-04	0
333.15	11.22	0	4.6289E-04	8.6123E-04	9.3962E-04	8.9775E-04	6.3416E-04	2.8835E-04	0
333.15	12.23	0	4.5113E-04	8.4067E-04	9.1713E-04	8.7651E-04	6.1922E-04	2.8160E-04	0
333.15	13.24	0	4.4244E-04	8.2254E-04	8.9707E-04	8.5719E-04	6.0534E-04	2.7539E-04	0
333.15	14.25	0	4.3178E-04	8.0329E-04	8.7619E-04	8.3730E-04	5.9128E-04	2.6899E-04	0
333.15	15.26	0	4.2266E-04	7.8513E-04	8.5642E-04	8.1822E-04	5.7794E-04	2.6280E-04	0
333.15	16.27	0	4.1229E-04	7.6678E-04	8.3635E-04	7.9927E-04	5.6452E-04	2.5678E-04	0
333.15	17.27	0	4.0261E-04	7.4934E-04	8.1736E-04	7.8088E-04	5.5150E-04	2.5088E-04	0
333.15	18.28	0	3.9387E-04	7.3217E-04	7.9864E-04	7.6303E-04	5.3897E-04	2.4511E-04	0
333.15	19.28	0	3.8461E-04	7.1544E-04	7.8020E-04	7.4548E-04	5.2650E-04	2.3942E-04	0
333.15	20.28	0	3.7408E-04	6.9777E-04	7.6133E-04	7.2757E-04	5.1395E-04	2.3367E-04	0
343.15	0.1	0	8.0904E-04	1.4967E-03	1.6325E-03	1.5595E-03	1.1159E-03	5.0716E-04	0
343.15	1.14	0	7.1264E-04	1.3260E-03	1.4463E-03	1.3821E-03	9.7620E-04	4.4399E-04	0
343.15	2.14	0	6.9969E-04	1.3019E-03	1.4202E-03	1.3571E-03	9.5856E-04	4.3597E-04	0
343.15	3.14	0	6.8726E-04	1.2788E-03	1.3948E-03	1.3329E-03	9.4141E-04	4.2814E-04	0
343.15	4.16	0	6.7355E-04	1.2548E-03	1.3689E-03	1.3083E-03	9.2407E-04	4.2027E-04	0
343.15	5.17	0	6.6161E-04	1.2322E-03	1.3443E-03	1.2848E-03	9.0746E-04	4.1271E-04	0
343.15	6.18	0	6.5071E-04	1.2110E-03	1.3207E-03	1.2619E-03	8.9143E-04	4.0544E-04	0
343.15	7.19	0	6.3934E-04	1.1894E-03	1.2971E-03	1.2395E-03	8.7543E-04	3.9820E-04	0
343.15	8.2	0	6.2779E-04	1.1678E-03	1.2738E-03	1.2172E-03	8.5965E-04	3.9101E-04	0
343.15	9.21	0	6.1645E-04	1.1469E-03	1.2508E-03	1.1953E-03	8.4425E-04	3.8405E-04	0
343.15	10.22	0	6.0511E-04	1.1259E-03	1.2282E-03	1.1736E-03	8.2895E-04	3.7703E-04	0
343.15	11.23	0	5.9342E-04	1.1054E-03	1.2057E-03	1.1521E-03	8.1385E-04	3.7013E-04	0
343.15	12.24	0	5.8233E-04	1.0849E-03	1.1837E-03	1.1312E-03	7.9903E-04	3.6340E-04	0
343.15	13.25	0	5.7202E-04	1.0656E-03	1.1626E-03	1.1110E-03	7.8476E-04	3.5692E-04	0

343.15	14.26	0	5.6273E-04	1.0472E-03	1.1421E-03	1.0914E-03	7.7089E-04	3.5065E-04	0
343.15	15.27	0	5.5200E-04	1.0277E-03	1.1213E-03	1.0716E-03	7.5687E-04	3.4424E-04	0
343.15	16.27	0	5.4217E-04	1.0093E-03	1.1011E-03	1.0521E-03	7.4322E-04	3.3803E-04	0
343.15	17.28	0	5.3334E-04	9.9194E-04	1.0819E-03	1.0337E-03	7.3016E-04	3.3211E-04	0
343.15	18.28	0	5.2322E-04	9.7345E-04	1.0621E-03	1.0148E-03	7.1682E-04	3.2603E-04	0
343.15	19.29	0	5.1301E-04	9.5551E-04	1.0426E-03	9.9614E-04	7.0371E-04	3.2006E-04	0
343.15	20.29	0	5.0505E-04	9.3923E-04	1.0244E-03	9.7887E-04	6.9139E-04	3.1447E-04	0
353.15	0.1	0	9.4741E-04	1.7909E-03	1.9555E-03	1.8768E-03	1.3355E-03	6.2450E-04	0
353.15	1.14	0	8.7024E-04	1.6205E-03	1.7681E-03	1.6897E-03	1.1934E-03	5.4274E-04	0
353.15	2.14	0	8.5893E-04	1.5986E-03	1.7438E-03	1.6665E-03	1.1771E-03	5.3527E-04	0
353.15	3.14	0	8.4701E-04	1.5765E-03	1.7197E-03	1.6433E-03	1.1606E-03	5.2784E-04	0
353.15	4.16	0	8.3617E-04	1.5551E-03	1.6960E-03	1.6206E-03	1.1448E-03	5.2060E-04	0
353.15	5.16	0	8.2422E-04	1.5331E-03	1.6722E-03	1.5979E-03	1.1285E-03	5.1329E-04	0
353.15	6.18	0	8.1283E-04	1.5118E-03	1.6487E-03	1.5754E-03	1.1127E-03	5.0609E-04	0
353.15	7.19	0	8.0153E-04	1.4908E-03	1.6259E-03	1.5534E-03	1.0973E-03	4.9901E-04	0
353.15	8.2	0	7.9047E-04	1.4697E-03	1.6030E-03	1.5318E-03	1.0819E-03	4.9204E-04	0
353.15	9.21	0	7.7746E-04	1.4476E-03	1.5794E-03	1.5095E-03	1.0662E-03	4.8484E-04	0
353.15	10.22	0	7.6794E-04	1.4289E-03	1.5584E-03	1.4890E-03	1.0518E-03	4.7838E-04	0
353.15	11.23	0	7.5683E-04	1.4085E-03	1.5364E-03	1.4680E-03	1.0369E-03	4.7160E-04	0
353.15	12.24	0	7.4664E-04	1.3890E-03	1.5148E-03	1.4475E-03	1.0225E-03	4.6500E-04	0
353.15	13.25	0	7.3630E-04	1.3695E-03	1.4936E-03	1.4274E-03	1.0081E-03	4.5851E-04	0
353.15	14.26	0	7.2417E-04	1.3491E-03	1.4719E-03	1.4067E-03	9.9350E-04	4.5182E-04	0
353.15	15.25	0	7.1611E-04	1.3318E-03	1.4524E-03	1.3879E-03	9.8031E-04	4.4585E-04	0
353.15	16.27	0	7.0493E-04	1.3124E-03	1.4316E-03	1.3680E-03	9.6618E-04	4.3948E-04	0
353.15	17.27	0	6.9494E-04	1.2936E-03	1.4114E-03	1.3486E-03	9.5252E-04	4.3328E-04	0
353.15	18.29	0	6.8410E-04	1.2751E-03	1.3910E-03	1.3294E-03	9.3893E-04	4.2709E-04	0
353.15	19.29	0	6.7618E-04	1.2581E-03	1.3725E-03	1.3114E-03	9.2629E-04	4.2131E-04	0
353.15	20.29	0	6.6796E-04	1.2412E-03	1.3537E-03	1.2935E-03	9.1366E-04	4.1559E-04	0

The expanded combined uncertainties $U_c(k = 2)$ are $U_c(T) = 0.02$ K, $U_c(P) = 0.03$ MPa, $U_c(x_i) = 0.0002$, and $U_c(V^E) = 1.74 \times 10^{-5}$ m^3. $kmol^{-1}$

Table A5: Excess Molar Volumes (V^E) of 2-methylpropan-1-ol (1) + n-octane (2) at various pressures and temperatures.

T/K	P/MPa	$V^E/m^3.kmol^{-1}$							
		x_1=0	*x_1=0.1267*	*x_1=0.3776*	*x_1=0.4996*	*x_1=0.6255*	*x_1=0.7499*	*x_1=0.8739*	*x_1=1*
313.15	0.1	0	3.2795E-04	6.8371E-04	7.6665E-04	7.2523E-04	6.1174E-04	4.1355E-04	0
313.15	1.14	0	2.2954E-04	4.7841E-04	5.3648E-04	5.0747E-04	4.2808E-04	2.8807E-04	0
313.15	2.14	0	2.2069E-04	4.5991E-04	5.1560E-04	4.8770E-04	4.1146E-04	2.7684E-04	0
313.15	3.15	0	2.1211E-04	4.4199E-04	4.9556E-04	4.6874E-04	3.9543E-04	2.6608E-04	0
313.15	4.16	0	2.0375E-04	4.2479E-04	4.7626E-04	4.5049E-04	3.8002E-04	2.5572E-04	0
313.15	5.17	0	1.9582E-04	4.0832E-04	4.5773E-04	4.3297E-04	3.6528E-04	2.4579E-04	0
313.15	6.18	0	1.8832E-04	3.9238E-04	4.3990E-04	4.1612E-04	3.5107E-04	2.3628E-04	0
313.15	7.19	0	1.8092E-04	3.7713E-04	4.2285E-04	3.9999E-04	3.3739E-04	2.2708E-04	0
313.15	8.2	0	1.7395E-04	3.6251E-04	4.0640E-04	3.8441E-04	3.2426E-04	2.1819E-04	0
313.15	9.23	0	1.6722E-04	3.4848E-04	3.9061E-04	3.6946E-04	3.1164E-04	2.0976E-04	0
313.15	10.23	0	1.6071E-04	3.3477E-04	3.7541E-04	3.5515E-04	2.9954E-04	2.0163E-04	0
313.15	11.24	0	1.5446E-04	3.2182E-04	3.6085E-04	3.4129E-04	2.8789E-04	1.9379E-04	0
313.15	12.25	0	1.4846E-04	3.0939E-04	3.4679E-04	3.2802E-04	2.7668E-04	1.8621E-04	0
313.15	13.26	0	1.4261E-04	2.9731E-04	3.3323E-04	3.1525E-04	2.6592E-04	1.7895E-04	0
313.15	14.27	0	1.3714E-04	2.8575E-04	3.2039E-04	3.0306E-04	2.5563E-04	1.7198E-04	0
313.15	15.27	0	1.3179E-04	2.7460E-04	3.0790E-04	2.9123E-04	2.4563E-04	1.6530E-04	0
313.15	16.28	0	1.2671E-04	2.6391E-04	2.9590E-04	2.7989E-04	2.3612E-04	1.5888E-04	0
313.15	17.29	0	1.2178E-04	2.5374E-04	2.8445E-04	2.6902E-04	2.2699E-04	1.5274E-04	0
313.15	18.3	0	1.1705E-04	2.4380E-04	2.7336E-04	2.5855E-04	2.1814E-04	1.4678E-04	0
313.15	19.3	0	1.1249E-04	2.3439E-04	2.6284E-04	2.4855E-04	2.0959E-04	1.4112E-04	0
313.15	20.31	0	1.0812E-04	2.2525E-04	2.5253E-04	2.3888E-04	2.0145E-04	1.3563E-04	0
323.15	0.1	0	3.6624E-04	7.6318E-04	8.5564E-04	8.0944E-04	6.8286E-04	4.5951E-04	0
323.15	1.15	0	2.8207E-04	5.8799E-04	6.5919E-04	6.2369E-04	5.2609E-04	3.5405E-04	0
323.15	2.15	0	2.7405E-04	5.7116E-04	6.4043E-04	6.0581E-04	5.1101E-04	3.4389E-04	0
323.15	3.17	0	2.6632E-04	5.5496E-04	6.2206E-04	5.8850E-04	4.9641E-04	3.3404E-04	0
323.15	4.18	0	2.5868E-04	5.3895E-04	6.0445E-04	5.7168E-04	4.8231E-04	3.2450E-04	0
323.15	5.19	0	2.5130E-04	5.2366E-04	5.8701E-04	5.5530E-04	4.6847E-04	3.1525E-04	0
323.15	6.2	0	2.4414E-04	5.0877E-04	5.7035E-04	5.3951E-04	4.5513E-04	3.0621E-04	0
323.15	7.22	0	2.3709E-04	4.9416E-04	5.5399E-04	5.2404E-04	4.4205E-04	2.9746E-04	0
323.15	8.23	0	2.3026E-04	4.8013E-04	5.3810E-04	5.0909E-04	4.2951E-04	2.8902E-04	0
323.15	9.24	0	2.2376E-04	4.6630E-04	5.2279E-04	4.9452E-04	4.1724E-04	2.8072E-04	0
323.15	10.25	0	2.1753E-04	4.5308E-04	5.0790E-04	4.8033E-04	4.0529E-04	2.7275E-04	0
323.15	11.25	0	2.1114E-04	4.4016E-04	4.9343E-04	4.6660E-04	3.9368E-04	2.6493E-04	0
323.15	12.27	0	2.0501E-04	4.2745E-04	4.7919E-04	4.5330E-04	3.8244E-04	2.5736E-04	0

323.15	13.27	0	1.9926E-04	4.1525E-04	4.6563E-04	4.4037E-04	3.7151E-04	2.4997E-04	0
323.15	14.26	0	1.9354E-04	4.0340E-04	4.5221E-04	4.2780E-04	3.6085E-04	2.4289E-04	0
323.15	15.29	0	1.8811E-04	3.9179E-04	4.3935E-04	4.1560E-04	3.5054E-04	2.3588E-04	0
323.15	16.3	0	1.8286E-04	3.8079E-04	4.2683E-04	4.0378E-04	3.4057E-04	2.2920E-04	0
323.15	17.3	0	1.7741E-04	3.6971E-04	4.1464E-04	3.9212E-04	3.3084E-04	2.2267E-04	0
323.15	18.3	0	1.7237E-04	3.5916E-04	4.0276E-04	3.8099E-04	3.2143E-04	2.1624E-04	0
323.15	19.3	0	1.6752E-04	3.4888E-04	3.9124E-04	3.7006E-04	3.1219E-04	2.1005E-04	0
323.15	20.29	0	1.6267E-04	3.3900E-04	3.8006E-04	3.5948E-04	3.0323E-04	2.0406E-04	0
333.15	0.1	0	4.2001E-04	8.7520E-04	9.8126E-04	9.2819E-04	7.8300E-04	5.2690E-04	0
333.15	1.13	0	3.5015E-04	7.2974E-04	8.1815E-04	7.7390E-04	6.5287E-04	4.3932E-04	0
333.15	2.13	0	3.4299E-04	7.1514E-04	8.0177E-04	7.5839E-04	6.3982E-04	4.3052E-04	0
333.15	3.14	0	3.3632E-04	7.0083E-04	7.8575E-04	7.4323E-04	6.2698E-04	4.2185E-04	0
333.15	4.15	0	3.2959E-04	6.8679E-04	7.7001E-04	7.2838E-04	6.1449E-04	4.1345E-04	0
333.15	5.16	0	3.2293E-04	6.7307E-04	7.5463E-04	7.1379E-04	6.0214E-04	4.0519E-04	0
333.15	6.17	0	3.1647E-04	6.5957E-04	7.3953E-04	6.9950E-04	5.9011E-04	3.9709E-04	0
333.15	7.18	0	3.1015E-04	6.4642E-04	7.2476E-04	6.8550E-04	5.7830E-04	3.8908E-04	0
333.15	8.19	0	3.0395E-04	6.3351E-04	7.1023E-04	6.7179E-04	5.6672E-04	3.8137E-04	0
333.15	9.2	0	2.9784E-04	6.2081E-04	6.9604E-04	6.5833E-04	5.5538E-04	3.7373E-04	0
333.15	10.21	0	2.9188E-04	6.0850E-04	6.8220E-04	6.4517E-04	5.4430E-04	3.6623E-04	0
333.15	11.22	0	2.8608E-04	5.9622E-04	6.6843E-04	6.3224E-04	5.3342E-04	3.5889E-04	0
333.15	12.23	0	2.8032E-04	5.8429E-04	6.5507E-04	6.1966E-04	5.2273E-04	3.5174E-04	0
333.15	13.24	0	2.7476E-04	5.7262E-04	6.4198E-04	6.0725E-04	5.1225E-04	3.4474E-04	0
333.15	14.25	0	2.6923E-04	5.6115E-04	6.2909E-04	5.9514E-04	5.0199E-04	3.3784E-04	0
333.15	15.26	0	2.6397E-04	5.4992E-04	6.1653E-04	5.8318E-04	4.9206E-04	3.3107E-04	0
333.15	16.27	0	2.5860E-04	5.3891E-04	6.0421E-04	5.7148E-04	4.8213E-04	3.2442E-04	0
333.15	17.27	0	2.5340E-04	5.2815E-04	5.9214E-04	5.6007E-04	4.7245E-04	3.1799E-04	0
333.15	18.28	0	2.4836E-04	5.1758E-04	5.8023E-04	5.4891E-04	4.6305E-04	3.1152E-04	0
333.15	19.28	0	2.4339E-04	5.0722E-04	5.6865E-04	5.3789E-04	4.5378E-04	3.0535E-04	0
333.15	20.28	0	2.3841E-04	4.9707E-04	5.5732E-04	5.2713E-04	4.4468E-04	2.9923E-04	0
343.15	0.1	0	5.0164E-04	1.0457E-03	1.1727E-03	1.1089E-03	9.3541E-04	6.2940E-04	0
343.15	1.14	0	4.3836E-04	9.1370E-04	1.0244E-03	9.6895E-04	8.1742E-04	5.5005E-04	0
343.15	2.14	0	4.3182E-04	9.0008E-04	1.0091E-03	9.5452E-04	8.0519E-04	5.4187E-04	0
343.15	3.14	0	4.2545E-04	8.8669E-04	9.9412E-04	9.4033E-04	7.9326E-04	5.3386E-04	0
343.15	4.16	0	4.1903E-04	8.7348E-04	9.7931E-04	9.2632E-04	7.8148E-04	5.2583E-04	0
343.15	5.17	0	4.1282E-04	8.6049E-04	9.6481E-04	9.1255E-04	7.6989E-04	5.1793E-04	0
343.15	6.18	0	4.0670E-04	8.4767E-04	9.5035E-04	8.9895E-04	7.5836E-04	5.1034E-04	0
343.15	7.19	0	4.0061E-04	8.3507E-04	9.3624E-04	8.8559E-04	7.4713E-04	5.0262E-04	0
343.15	8.2	0	3.9471E-04	8.2263E-04	9.2229E-04	8.7241E-04	7.3595E-04	4.9522E-04	0
343.15	9.21	0	3.8867E-04	8.1036E-04	9.0855E-04	8.5940E-04	7.2501E-04	4.8785E-04	0
343.15	10.22	0	3.8306E-04	7.9837E-04	8.9505E-04	8.4661E-04	7.1421E-04	4.8059E-04	0
343.15	11.23	0	3.7736E-04	7.8652E-04	8.8174E-04	8.3404E-04	7.0358E-04	4.7343E-04	0
343.15	12.24	0	3.7174E-04	7.7473E-04	8.6856E-04	8.2161E-04	6.9312E-04	4.6639E-04	0
343.15	13.25	0	3.6621E-04	7.6321E-04	8.5566E-04	8.0940E-04	6.8278E-04	4.5945E-04	0

343.15	14.26	0	3.6070E-04	7.5181E-04	8.4297E-04	7.9735E-04	6.7262E-04	4.5261E-04	0
343.15	15.27	0	3.5536E-04	7.4064E-04	8.3039E-04	7.8549E-04	6.6261E-04	4.4587E-04	0
343.15	16.27	0	3.5010E-04	7.2962E-04	8.1790E-04	7.7389E-04	6.5276E-04	4.3916E-04	0
343.15	17.28	0	3.4483E-04	7.1874E-04	8.0586E-04	7.6224E-04	6.4305E-04	4.3270E-04	0
343.15	18.28	0	3.3969E-04	7.0810E-04	7.9384E-04	7.5093E-04	6.3347E-04	4.2626E-04	0
343.15	19.29	0	3.3471E-04	6.9756E-04	7.8148E-04	7.3973E-04	6.2405E-04	4.1993E-04	0
343.15	20.29	0	3.2965E-04	6.8717E-04	7.7043E-04	7.2874E-04	6.1476E-04	4.1366E-04	0
353.15	0.1	0	6.1675E-04	1.2858E-03	1.4417E-03	1.3635E-03	1.1504E-03	7.7393E-04	0
353.15	1.14	0	5.5849E-04	1.1640E-03	1.3050E-03	1.2344E-03	1.0414E-03	7.0070E-04	0
353.15	2.14	0	5.5226E-04	1.1512E-03	1.2905E-03	1.2209E-03	1.0299E-03	6.9301E-04	0
353.15	3.14	0	5.4622E-04	1.1385E-03	1.2765E-03	1.2074E-03	1.0186E-03	6.8539E-04	0
353.15	4.16	0	5.4023E-04	1.1260E-03	1.2624E-03	1.1941E-03	1.0074E-03	6.7785E-04	0
353.15	5.16	0	5.3428E-04	1.1136E-03	1.2485E-03	1.1810E-03	9.9620E-04	6.7038E-04	0
353.15	6.18	0	5.2836E-04	1.1014E-03	1.2348E-03	1.1680E-03	9.8542E-04	6.6301E-04	0
353.15	7.19	0	5.2256E-04	1.0893E-03	1.2212E-03	1.1552E-03	9.7449E-04	6.5571E-04	0
353.15	8.2	0	5.1696E-04	1.0773E-03	1.2078E-03	1.1425E-03	9.6379E-04	6.4851E-04	0
353.15	9.21	0	5.1112E-04	1.0654E-03	1.1945E-03	1.1299E-03	9.5318E-04	6.4138E-04	0
353.15	10.22	0	5.0551E-04	1.0537E-03	1.1814E-03	1.1175E-03	9.4269E-04	6.3432E-04	0
353.15	11.23	0	4.9996E-04	1.0421E-03	1.1684E-03	1.1052E-03	9.3233E-04	6.2735E-04	0
353.15	12.24	0	4.9450E-04	1.0307E-03	1.1555E-03	1.0930E-03	9.2208E-04	6.2045E-04	0
353.15	13.25	0	4.8900E-04	1.0193E-03	1.1428E-03	1.0810E-03	9.1195E-04	6.1362E-04	0
353.15	14.26	0	4.8377E-04	1.0081E-03	1.1303E-03	1.0691E-03	9.0190E-04	6.0688E-04	0
353.15	15.25	0	4.7822E-04	9.9701E-04	1.1178E-03	1.0574E-03	8.9190E-04	6.0019E-04	0
353.15	16.27	0	4.7309E-04	9.8607E-04	1.1055E-03	1.0457E-03	8.8217E-04	5.9360E-04	0
353.15	17.27	0	4.6800E-04	9.7519E-04	1.0934E-03	1.0342E-03	8.7246E-04	5.8707E-04	0
353.15	18.29	0	4.6268E-04	9.6441E-04	1.0813E-03	1.0229E-03	8.6282E-04	5.8061E-04	0
353.15	19.29	0	4.5767E-04	9.5388E-04	1.0695E-03	1.0117E-03	8.5338E-04	5.7422E-04	0
353.15	20.29	0	4.5259E-04	9.4336E-04	1.0577E-03	1.0005E-03	8.4400E-04	5.6790E-04	0

The expanded combined uncertainties $U_c(k = 2)$ are $U_c(T) = 0.02$ K, $U_c(P) = 0.03$ MPa, $U_c(x_i) = 0.0002$, and $U_c(V^E) = 1.81 \times 10^{-5}$ m^3. $kmol^{-1}$

Table A6: Excess Molar Volumes (V^E) of 2-methylpropan-1-ol (1) + n-decane (2) at various pressures and temperatures.

T/K	P/MPa	$V^E/m^3.kmol^{-1}$							
		x_1=0	*x_1=0.1276*	*x_1=0.3749*	*x_1=0.5015*	*x_1=0.6249*	*x_1=0.7502*	*x_1=0.8750*	*x_1=1*
313.15	0.1	0	3.7096E-04	7.7336E-04	8.6719E-04	8.5267E-04	7.4076E-04	4.6560E-04	0
313.15	1.14	0	2.6739E-04	5.5721E-04	6.2469E-04	6.1418E-04	5.3344E-04	3.3543E-04	0
313.15	2.14	0	2.5782E-04	5.3728E-04	6.0236E-04	5.9223E-04	5.1433E-04	3.2338E-04	0
313.15	3.15	0	2.4860E-04	5.1804E-04	5.8081E-04	5.7100E-04	4.9594E-04	3.1208E-04	0
313.15	4.16	0	2.3968E-04	4.9948E-04	5.5998E-04	5.5057E-04	4.7818E-04	3.0068E-04	0
313.15	5.17	0	2.3128E-04	4.8161E-04	5.3994E-04	5.3092E-04	4.6113E-04	2.8998E-04	0
313.15	6.18	0	2.2269E-04	4.6435E-04	5.2063E-04	5.1177E-04	4.4450E-04	2.7951E-04	0
313.15	7.19	0	2.1489E-04	4.4793E-04	5.0201E-04	4.9354E-04	4.2865E-04	2.6960E-04	0
313.15	8.2	0	2.0720E-04	4.3173E-04	4.8401E-04	4.7585E-04	4.1331E-04	2.5990E-04	0
313.15	9.23	0	1.9978E-04	4.1629E-04	4.6666E-04	4.5886E-04	3.9851E-04	2.5060E-04	0
313.15	10.23	0	1.9265E-04	4.0133E-04	4.5001E-04	4.4240E-04	3.8424E-04	2.4162E-04	0
313.15	11.24	0	1.8576E-04	3.8705E-04	4.3382E-04	4.2656E-04	3.7049E-04	2.3300E-04	0
313.15	12.25	0	1.7911E-04	3.7310E-04	4.1840E-04	4.1133E-04	3.5718E-04	2.2465E-04	0
313.15	13.26	0	1.7274E-04	3.5989E-04	4.0329E-04	3.9660E-04	3.4438E-04	2.1657E-04	0
313.15	14.27	0	1.6653E-04	3.4693E-04	3.8898E-04	3.8252E-04	3.3214E-04	2.0891E-04	0
313.15	15.27	0	1.6057E-04	3.3451E-04	3.7499E-04	3.6872E-04	3.2025E-04	2.0162E-04	0
313.15	16.28	0	1.5508E-04	3.2258E-04	3.6173E-04	3.5565E-04	3.0874E-04	1.9419E-04	0
313.15	17.29	0	1.4930E-04	3.1104E-04	3.4870E-04	3.4274E-04	2.9772E-04	1.8724E-04	0
313.15	18.3	0	1.4379E-04	3.0003E-04	3.3608E-04	3.3054E-04	2.8705E-04	1.8057E-04	0
313.15	19.3	0	1.3885E-04	2.8938E-04	3.2418E-04	3.1866E-04	2.7678E-04	1.7403E-04	0
313.15	20.31	0	1.3384E-04	2.7875E-04	3.1265E-04	3.0735E-04	2.6689E-04	1.6785E-04	0
323.15	0.1	0	4.1925E-04	8.7411E-04	9.8008E-04	9.6354E-04	8.3698E-04	5.2630E-04	0
323.15	1.15	0	3.2913E-04	6.8602E-04	7.6908E-04	7.5611E-04	6.5671E-04	4.1296E-04	0
323.15	2.15	0	3.2043E-04	6.6787E-04	7.4862E-04	7.3604E-04	6.3927E-04	4.0197E-04	0
323.15	3.17	0	3.1194E-04	6.4996E-04	7.2878E-04	7.1653E-04	6.2234E-04	3.9133E-04	0
323.15	4.18	0	3.0365E-04	6.3277E-04	7.0939E-04	6.9745E-04	6.0571E-04	3.8090E-04	0
323.15	5.19	0	2.9542E-04	6.1583E-04	6.9049E-04	6.7896E-04	5.8963E-04	3.7073E-04	0
323.15	6.2	0	2.8773E-04	5.9955E-04	6.7210E-04	6.6095E-04	5.7394E-04	3.6093E-04	0
323.15	7.22	0	2.7999E-04	5.8369E-04	6.5428E-04	6.4335E-04	5.5869E-04	3.5130E-04	0
323.15	8.23	0	2.7262E-04	5.6815E-04	6.3690E-04	6.2619E-04	5.4390E-04	3.4199E-04	0
323.15	9.24	0	2.6538E-04	5.5313E-04	6.2009E-04	6.0951E-04	5.2951E-04	3.3294E-04	0
323.15	10.25	0	2.5826E-04	5.3832E-04	6.0355E-04	5.9339E-04	5.1528E-04	3.2405E-04	0
323.15	11.25	0	2.5138E-04	5.2395E-04	5.8753E-04	5.7759E-04	5.0170E-04	3.1547E-04	0
323.15	12.27	0	2.4482E-04	5.1012E-04	5.7196E-04	5.6229E-04	4.8832E-04	3.0709E-04	0

323.15	13.27	0	2.3832E-04	4.9665E-04	5.5663E-04	5.4733E-04	4.7538E-04	2.9895E-04	0
323.15	14.26	0	2.3182E-04	4.8344E-04	5.4184E-04	5.3279E-04	4.6276E-04	2.9099E-04	0
323.15	15.29	0	2.2579E-04	4.7053E-04	5.2756E-04	5.1868E-04	4.5046E-04	2.8328E-04	0
323.15	16.3	0	2.1989E-04	4.5800E-04	5.1360E-04	5.0482E-04	4.3840E-04	2.7575E-04	0
323.15	17.3	0	2.1394E-04	4.4578E-04	4.9978E-04	4.9135E-04	4.2677E-04	2.6844E-04	0
323.15	18.3	0	2.0830E-04	4.3401E-04	4.8657E-04	4.7843E-04	4.1550E-04	2.6125E-04	0
323.15	19.3	0	2.0277E-04	4.2248E-04	4.7358E-04	4.6561E-04	4.0444E-04	2.5432E-04	0
323.15	20.29	0	1.9739E-04	4.1125E-04	4.6105E-04	4.5326E-04	3.9372E-04	2.4755E-04	0
333.15	0.1	0	4.8167E-04	1.0039E-03	1.1255E-03	1.1067E-03	9.6110E-04	6.0445E-04	0
333.15	1.13	0	4.0944E-04	8.5350E-04	9.5689E-04	9.4078E-04	8.1707E-04	5.1380E-04	0
333.15	2.13	0	4.0209E-04	8.3825E-04	9.3983E-04	9.2401E-04	8.0249E-04	5.0459E-04	0
333.15	3.14	0	3.9502E-04	8.2324E-04	9.2303E-04	9.0743E-04	7.8812E-04	4.9562E-04	0
333.15	4.15	0	3.8801E-04	8.0852E-04	9.0645E-04	8.9112E-04	7.7405E-04	4.8672E-04	0
333.15	5.16	0	3.8108E-04	7.9408E-04	8.9036E-04	8.7528E-04	7.6018E-04	4.7802E-04	0
333.15	6.17	0	3.7419E-04	7.7981E-04	8.7434E-04	8.5968E-04	7.4657E-04	4.6947E-04	0
333.15	7.18	0	3.6748E-04	7.6598E-04	8.5864E-04	8.4427E-04	7.3323E-04	4.6111E-04	0
333.15	8.19	0	3.6083E-04	7.5217E-04	8.4332E-04	8.2930E-04	7.2010E-04	4.5283E-04	0
333.15	9.2	0	3.5446E-04	7.3873E-04	8.2834E-04	8.1427E-04	7.0722E-04	4.4473E-04	0
333.15	10.21	0	3.4821E-04	7.2563E-04	8.1346E-04	7.9972E-04	6.9459E-04	4.3677E-04	0
333.15	11.22	0	3.4181E-04	7.1255E-04	7.9887E-04	7.8551E-04	6.8217E-04	4.2896E-04	0
333.15	12.23	0	3.3579E-04	6.9984E-04	7.8466E-04	7.7142E-04	6.6999E-04	4.2130E-04	0
333.15	13.24	0	3.2996E-04	6.8740E-04	7.7055E-04	7.5765E-04	6.5801E-04	4.1377E-04	0
333.15	14.25	0	3.2401E-04	6.7493E-04	7.5674E-04	7.4407E-04	6.4623E-04	4.0636E-04	0
333.15	15.26	0	3.1805E-04	6.6291E-04	7.4314E-04	7.3076E-04	6.3463E-04	3.9908E-04	0
333.15	16.27	0	3.1243E-04	6.5113E-04	7.3002E-04	7.1771E-04	6.2327E-04	3.9198E-04	0
333.15	17.27	0	3.0695E-04	6.3950E-04	7.1695E-04	7.0485E-04	6.1219E-04	3.8504E-04	0
333.15	18.28	0	3.0140E-04	6.2799E-04	7.0409E-04	6.9225E-04	6.0121E-04	3.7803E-04	0
333.15	19.28	0	2.9596E-04	6.1675E-04	6.9148E-04	6.7990E-04	5.9046E-04	3.7131E-04	0
333.15	20.28	0	2.9067E-04	6.0584E-04	6.7924E-04	6.6776E-04	5.7989E-04	3.6467E-04	0
343.15	0.1	0	5.8376E-04	1.2169E-03	1.3647E-03	1.3416E-03	1.1652E-03	7.3259E-04	0
343.15	1.14	0	5.1410E-04	1.0712E-03	1.2010E-03	1.1808E-03	1.0255E-03	6.4483E-04	0
343.15	2.14	0	5.0768E-04	1.0585E-03	1.1868E-03	1.1668E-03	1.0133E-03	6.3715E-04	0
343.15	3.14	0	5.0161E-04	1.0459E-03	1.1726E-03	1.1528E-03	1.0013E-03	6.2965E-04	0
343.15	4.16	0	4.9583E-04	1.0334E-03	1.1586E-03	1.1392E-03	9.8929E-04	6.2210E-04	0
343.15	5.17	0	4.8981E-04	1.0212E-03	1.1450E-03	1.1258E-03	9.7759E-04	6.1473E-04	0
343.15	6.18	0	4.8409E-04	1.0091E-03	1.1313E-03	1.1123E-03	9.6609E-04	6.0741E-04	0
343.15	7.19	0	4.7825E-04	9.9718E-04	1.1178E-03	1.0991E-03	9.5456E-04	6.0029E-04	0
343.15	8.2	0	4.7275E-04	9.8518E-04	1.1046E-03	1.0859E-03	9.4311E-04	5.9306E-04	0
343.15	9.21	0	4.6694E-04	9.7345E-04	1.0914E-03	1.0731E-03	9.3195E-04	5.8601E-04	0
343.15	10.22	0	4.6150E-04	9.6203E-04	1.0784E-03	1.0602E-03	9.2087E-04	5.7911E-04	0
343.15	11.23	0	4.5620E-04	9.5051E-04	1.0657E-03	1.0477E-03	9.0997E-04	5.7219E-04	0
343.15	12.24	0	4.5057E-04	9.3919E-04	1.0531E-03	1.0352E-03	8.9918E-04	5.6537E-04	0
343.15	13.25	0	4.4539E-04	9.2801E-04	1.0405E-03	1.0231E-03	8.8840E-04	5.5869E-04	0

343.15	14.26	0	4.4000E-04	9.1688E-04	1.0281E-03	1.0107E-03	8.7791E-04	5.5199E-04	0
343.15	15.27	0	4.3470E-04	9.0606E-04	1.0160E-03	9.9881E-04	8.6742E-04	5.4547E-04	0
343.15	16.27	0	4.2954E-04	8.9531E-04	1.0039E-03	9.8694E-04	8.5707E-04	5.3897E-04	0
343.15	17.28	0	4.2435E-04	8.8469E-04	9.9178E-04	9.7526E-04	8.4701E-04	5.3260E-04	0
343.15	18.28	0	4.1944E-04	8.7416E-04	9.8013E-04	9.6361E-04	8.3693E-04	5.2623E-04	0
343.15	19.29	0	4.1441E-04	8.6379E-04	9.6845E-04	9.5216E-04	8.2696E-04	5.2006E-04	0
343.15	20.29	0	4.0941E-04	8.5347E-04	9.5699E-04	9.4076E-04	8.1711E-04	5.1384E-04	0
353.15	0.1	0	6.9800E-04	1.4765E-03	1.6631E-03	1.6348E-03	1.4200E-03	8.9223E-04	0
353.15	1.14	0	6.5686E-04	1.3693E-03	1.5350E-03	1.5093E-03	1.3108E-03	8.2423E-04	0
353.15	2.14	0	6.5088E-04	1.3569E-03	1.5215E-03	1.4959E-03	1.2991E-03	8.1692E-04	0
353.15	3.14	0	6.4551E-04	1.3449E-03	1.5079E-03	1.4827E-03	1.2874E-03	8.0968E-04	0
353.15	4.16	0	6.3937E-04	1.3332E-03	1.4946E-03	1.4695E-03	1.2763E-03	8.0250E-04	0
353.15	5.16	0	6.3407E-04	1.3213E-03	1.4814E-03	1.4566E-03	1.2647E-03	7.9547E-04	0
353.15	6.18	0	6.2852E-04	1.3095E-03	1.4682E-03	1.4435E-03	1.2538E-03	7.8824E-04	0
353.15	7.19	0	6.2251E-04	1.2981E-03	1.4552E-03	1.4308E-03	1.2426E-03	7.8127E-04	0
353.15	8.2	0	6.1699E-04	1.2866E-03	1.4425E-03	1.4182E-03	1.2316E-03	7.7442E-04	0
353.15	9.21	0	6.1155E-04	1.2750E-03	1.4295E-03	1.4054E-03	1.2207E-03	7.6756E-04	0
353.15	10.22	0	6.0625E-04	1.2639E-03	1.4168E-03	1.3930E-03	1.2098E-03	7.6076E-04	0
353.15	11.23	0	6.0094E-04	1.2525E-03	1.4042E-03	1.3808E-03	1.1992E-03	7.5392E-04	0
353.15	12.24	0	5.9557E-04	1.2414E-03	1.3918E-03	1.3684E-03	1.1885E-03	7.4723E-04	0
353.15	13.25	0	5.9020E-04	1.2305E-03	1.3796E-03	1.3564E-03	1.1780E-03	7.4070E-04	0
353.15	14.26	0	5.8513E-04	1.2195E-03	1.3672E-03	1.3443E-03	1.1675E-03	7.3406E-04	0
353.15	15.25	0	5.8015E-04	1.2086E-03	1.3553E-03	1.3323E-03	1.1571E-03	7.2754E-04	0
353.15	16.27	0	5.7471E-04	1.1979E-03	1.3432E-03	1.3206E-03	1.1469E-03	7.2118E-04	0
353.15	17.27	0	5.6974E-04	1.1875E-03	1.3313E-03	1.3088E-03	1.1367E-03	7.1489E-04	0
353.15	18.29	0	5.6452E-04	1.1767E-03	1.3193E-03	1.2971E-03	1.1266E-03	7.0842E-04	0
353.15	19.29	0	5.5967E-04	1.1663E-03	1.3077E-03	1.2858E-03	1.1167E-03	7.0217E-04	0
353.15	20.29	0	5.5455E-04	1.1560E-03	1.2963E-03	1.2743E-03	1.1068E-03	6.9594E-04	0

The expanded combined uncertainties $U_c(k = 2)$ are $U_c(T) = 0.02$ K, $U_c(P) = 0.03$ MPa, $U_c(x_i) = 0.0002$, and $U_c(V^E) = 1.88 \times 10^{-5}$ m^3. $kmol^{-1}$

APPENDIX B

Thermal Expansivity

Table B1: Thermal Expansivity (α_p) of butan-1-ol (1) + n-octane (2) at various pressures and temperatures.

T/K	P/MPa	α_p/K^{-1}							
		x_1=0	*x_1=0.1259*	*x_1=0.3750*	*x_1=0.5002*	*x_1=0.6258*	*x_1=0.7503*	*x_1=0.8750*	*x_1=1*
313.15	0.1	9.6446E-03	1.0029E-02	1.0781E-02	1.1126E-02	1.1263E-02	1.1819E-02	1.2342E-02	1.3501E-02
313.15	1.14	9.5702E-03	9.9521E-03	1.0702E-02	1.1047E-02	1.1186E-02	1.1743E-02	1.2269E-02	1.3431E-02
313.15	2.14	9.4889E-03	9.8685E-03	1.0615E-02	1.0960E-02	1.1102E-02	1.1660E-02	1.2189E-02	1.3355E-02
313.15	3.15	9.4090E-03	9.7862E-03	1.0529E-02	1.0875E-02	1.1019E-02	1.1578E-02	1.2110E-02	1.3279E-02
313.15	4.16	9.3304E-03	9.7054E-03	1.0445E-02	1.0790E-02	1.0938E-02	1.1497E-02	1.2032E-02	1.3204E-02
313.15	5.17	9.2531E-03	9.6258E-03	1.0362E-02	1.0708E-02	1.0857E-02	1.1418E-02	1.1955E-02	1.3130E-02
313.15	6.18	9.1771E-03	9.5476E-03	1.0281E-02	1.0626E-02	1.0778E-02	1.1339E-02	1.1879E-02	1.3057E-02
313.15	7.19	9.1023E-03	9.4706E-03	1.0200E-02	1.0546E-02	1.0700E-02	1.1261E-02	1.1804E-02	1.2984E-02
313.15	8.2	9.0288E-03	9.3949E-03	1.0121E-02	1.0466E-02	1.0623E-02	1.1185E-02	1.1729E-02	1.2913E-02
313.15	9.23	8.9564E-03	9.3203E-03	1.0043E-02	1.0388E-02	1.0547E-02	1.1110E-02	1.1656E-02	1.2842E-02
313.15	10.23	8.8851E-03	9.2469E-03	9.9668E-03	1.0311E-02	1.0472E-02	1.1035E-02	1.1584E-02	1.2772E-02
313.15	11.24	8.8150E-03	9.1747E-03	9.8913E-03	1.0236E-02	1.0398E-02	1.0962E-02	1.1513E-02	1.2702E-02
313.15	12.25	8.7460E-03	9.1036E-03	9.8170E-03	1.0161E-02	1.0326E-02	1.0889E-02	1.1442E-02	1.2634E-02
313.15	13.26	8.6781E-03	9.0336E-03	9.7438E-03	1.0088E-02	1.0254E-02	1.0818E-02	1.1372E-02	1.2566E-02
313.15	14.27	8.6112E-03	8.9646E-03	9.6716E-03	1.0015E-02	1.0183E-02	1.0747E-02	1.1304E-02	1.2499E-02
313.15	15.27	8.5453E-03	8.8967E-03	9.6006E-03	9.9436E-03	1.0113E-02	1.0678E-02	1.1236E-02	1.2432E-02
313.15	16.28	8.4804E-03	8.8298E-03	9.5305E-03	9.8731E-03	1.0045E-02	1.0609E-02	1.1168E-02	1.2367E-02
313.15	17.29	8.4165E-03	8.7640E-03	9.4615E-03	9.8037E-03	9.9768E-03	1.0541E-02	1.1102E-02	1.2302E-02
313.15	18.3	8.3536E-03	8.6990E-03	9.3935E-03	9.7352E-03	9.9098E-03	1.0474E-02	1.1036E-02	1.2237E-02
313.15	19.3	8.2916E-03	8.6351E-03	9.3264E-03	9.6677E-03	9.8437E-03	1.0408E-02	1.0972E-02	1.2174E-02
313.15	20.31	8.2305E-03	8.5721E-03	9.2603E-03	9.6011E-03	9.7785E-03	1.0342E-02	1.0907E-02	1.2111E-02
323.15	0.1	9.4225E-03	9.7984E-03	1.0533E-02	1.0870E-02	1.1000E-02	1.1541E-02	1.2047E-02	1.3175E-02
323.15	1.15	9.3490E-03	9.7228E-03	1.0455E-02	1.0791E-02	1.0924E-02	1.1466E-02	1.1975E-02	1.3106E-02
323.15	2.15	9.2686E-03	9.6401E-03	1.0369E-02	1.0705E-02	1.0841E-02	1.1384E-02	1.1896E-02	1.3030E-02
323.15	3.17	9.1896E-03	9.5588E-03	1.0284E-02	1.0621E-02	1.0760E-02	1.1303E-02	1.1819E-02	1.2956E-02
323.15	4.18	9.1119E-03	9.4789E-03	1.0201E-02	1.0538E-02	1.0679E-02	1.1223E-02	1.1742E-02	1.2882E-02
323.15	5.19	9.0356E-03	9.4003E-03	1.0119E-02	1.0456E-02	1.0600E-02	1.1145E-02	1.1666E-02	1.2809E-02
323.15	6.2	8.9605E-03	9.3230E-03	1.0039E-02	1.0375E-02	1.0522E-02	1.1067E-02	1.1591E-02	1.2737E-02
323.15	7.22	8.8866E-03	9.2470E-03	9.9596E-03	1.0296E-02	1.0444E-02	1.0991E-02	1.1517E-02	1.2666E-02
323.15	8.23	8.8140E-03	9.1722E-03	9.8816E-03	1.0218E-02	1.0369E-02	1.0915E-02	1.1444E-02	1.2595E-02

323.15	9.24	8.7425E-03	9.0986E-03	9.8048E-03	1.0141E-02	1.0294E-02	1.0841E-02	1.1372E-02	1.2526E-02
323.15	10.25	8.6722E-03	9.0262E-03	9.7292E-03	1.0065E-02	1.0220E-02	1.0768E-02	1.1301E-02	1.2457E-02
323.15	11.25	8.6030E-03	8.9549E-03	9.6547E-03	9.9903E-03	1.0147E-02	1.0695E-02	1.1230E-02	1.2389E-02
323.15	12.27	8.5349E-03	8.8847E-03	9.5814E-03	9.9167E-03	1.0076E-02	1.0624E-02	1.1161E-02	1.2321E-02
323.15	13.27	8.4679E-03	8.8157E-03	9.5092E-03	9.8442E-03	1.0005E-02	1.0554E-02	1.1092E-02	1.2254E-02
323.15	14.26	8.4019E-03	8.7476E-03	9.4381E-03	9.7727E-03	9.9352E-03	1.0484E-02	1.1025E-02	1.2188E-02
323.15	15.29	8.3369E-03	8.6807E-03	9.3680E-03	9.7023E-03	9.8665E-03	1.0416E-02	1.0958E-02	1.2123E-02
323.15	16.3	8.2730E-03	8.6147E-03	9.2989E-03	9.6328E-03	9.7987E-03	1.0348E-02	1.0892E-02	1.2058E-02
323.15	17.3	8.2100E-03	8.5498E-03	9.2309E-03	9.5644E-03	9.7319E-03	1.0281E-02	1.0826E-02	1.1995E-02
323.15	18.3	8.1479E-03	8.4858E-03	9.1638E-03	9.4969E-03	9.6659E-03	1.0215E-02	1.0762E-02	1.1931E-02
323.15	19.3	8.0868E-03	8.4227E-03	9.0978E-03	9.4304E-03	9.6009E-03	1.0150E-02	1.0698E-02	1.1869E-02
323.15	20.29	8.0266E-03	8.3606E-03	9.0326E-03	9.3648E-03	9.5367E-03	1.0086E-02	1.0635E-02	1.1807E-02
333.15	0.1	9.2161E-03	9.5848E-03	1.0304E-02	1.0632E-02	1.0758E-02	1.1284E-02	1.1777E-02	1.2876E-02
333.15	1.13	9.1433E-03	9.5099E-03	1.0226E-02	1.0555E-02	1.0683E-02	1.1210E-02	1.1706E-02	1.2808E-02
333.15	2.13	9.0638E-03	9.4281E-03	1.0141E-02	1.0470E-02	1.0601E-02	1.1129E-02	1.1628E-02	1.2734E-02
333.15	3.14	8.9856E-03	9.3477E-03	1.0058E-02	1.0386E-02	1.0520E-02	1.1049E-02	1.1551E-02	1.2660E-02
333.15	4.15	8.9087E-03	9.2686E-03	9.9755E-03	1.0304E-02	1.0440E-02	1.0971E-02	1.1475E-02	1.2587E-02
333.15	5.16	8.8332E-03	9.1908E-03	9.8946E-03	1.0223E-02	1.0362E-02	1.0893E-02	1.1400E-02	1.2516E-02
333.15	6.17	8.7589E-03	9.1144E-03	9.8149E-03	1.0143E-02	1.0284E-02	1.0817E-02	1.1326E-02	1.2444E-02
333.15	7.18	8.6859E-03	9.0392E-03	9.7365E-03	1.0065E-02	1.0208E-02	1.0741E-02	1.1253E-02	1.2374E-02
333.15	8.19	8.6140E-03	8.9652E-03	9.6594E-03	9.9876E-03	1.0133E-02	1.0667E-02	1.1181E-02	1.2305E-02
333.15	9.2	8.5434E-03	8.8924E-03	9.5835E-03	9.9116E-03	1.0059E-02	1.0593E-02	1.1110E-02	1.2236E-02
333.15	10.21	8.4739E-03	8.8208E-03	9.5088E-03	9.8366E-03	9.9866E-03	1.0521E-02	1.1040E-02	1.2168E-02
333.15	11.22	8.4055E-03	8.7504E-03	9.4352E-03	9.7629E-03	9.9148E-03	1.0450E-02	1.0970E-02	1.2101E-02
333.15	12.23	8.3382E-03	8.6810E-03	9.3628E-03	9.6902E-03	9.8440E-03	1.0379E-02	1.0902E-02	1.2034E-02
333.15	13.24	8.2720E-03	8.6128E-03	9.2914E-03	9.6186E-03	9.7743E-03	1.0310E-02	1.0834E-02	1.1968E-02
333.15	14.25	8.2068E-03	8.5456E-03	9.2212E-03	9.5480E-03	9.7055E-03	1.0241E-02	1.0768E-02	1.1903E-02
333.15	15.26	8.1427E-03	8.4795E-03	9.1520E-03	9.4784E-03	9.6376E-03	1.0173E-02	1.0702E-02	1.1839E-02
333.15	16.27	8.0795E-03	8.4144E-03	9.0838E-03	9.4099E-03	9.5708E-03	1.0107E-02	1.0636E-02	1.1775E-02
333.15	17.27	8.0173E-03	8.3502E-03	9.0166E-03	9.3424E-03	9.5048E-03	1.0041E-02	1.0572E-02	1.1712E-02
333.15	18.28	7.9561E-03	8.2871E-03	8.9504E-03	9.2758E-03	9.4397E-03	9.9756E-03	1.0508E-02	1.1650E-02
333.15	19.28	7.8958E-03	8.2248E-03	8.8852E-03	9.2101E-03	9.3756E-03	9.9114E-03	1.0446E-02	1.1588E-02
333.15	20.28	7.8364E-03	8.1636E-03	8.8210E-03	9.1454E-03	9.3123E-03	9.8480E-03	1.0383E-02	1.1527E-02
343.15	0.1	9.0240E-03	9.3862E-03	1.0092E-02	1.0413E-02	1.0533E-02	1.1048E-02	1.1528E-02	1.2602E-02
343.15	1.14	8.9518E-03	9.3120E-03	1.0015E-02	1.0336E-02	1.0459E-02	1.0974E-02	1.1457E-02	1.2535E-02
343.15	2.14	8.8729E-03	9.2309E-03	9.9304E-03	1.0251E-02	1.0378E-02	1.0894E-02	1.1380E-02	1.2462E-02
343.15	3.14	8.7954E-03	9.1511E-03	9.8475E-03	1.0169E-02	1.0298E-02	1.0815E-02	1.1304E-02	1.2389E-02
343.15	4.16	8.7193E-03	9.0728E-03	9.7660E-03	1.0087E-02	1.0219E-02	1.0737E-02	1.1229E-02	1.2317E-02
343.15	5.17	8.6445E-03	8.9957E-03	9.6858E-03	1.0007E-02	1.0141E-02	1.0660E-02	1.1155E-02	1.2246E-02
343.15	6.18	8.5709E-03	8.9200E-03	9.6069E-03	9.9282E-03	1.0065E-02	1.0585E-02	1.1082E-02	1.2176E-02
343.15	7.19	8.4986E-03	8.8455E-03	9.5293E-03	9.8505E-03	9.9894E-03	1.0510E-02	1.1010E-02	1.2106E-02
343.15	8.2	8.4274E-03	8.7723E-03	9.4530E-03	9.7741E-03	9.9152E-03	1.0437E-02	1.0939E-02	1.2037E-02
343.15	9.21	8.3575E-03	8.7002E-03	9.3778E-03	9.6988E-03	9.8421E-03	1.0364E-02	1.0868E-02	1.1969E-02

343.15	10.22	8.2887E-03	8.6294E-03	9.3039E-03	9.6247E-03	9.7700E-03	1.0292E-02	1.0799E-02	1.1902E-02
343.15	11.23	8.2211E-03	8.5597E-03	9.2310E-03	9.5517E-03	9.6990E-03	1.0222E-02	1.0730E-02	1.1836E-02
343.15	12.24	8.1545E-03	8.4911E-03	9.1594E-03	9.4797E-03	9.6290E-03	1.0152E-02	1.0663E-02	1.1770E-02
343.15	13.25	8.0890E-03	8.4236E-03	9.0888E-03	9.4089E-03	9.5601E-03	1.0083E-02	1.0596E-02	1.1705E-02
343.15	14.26	8.0246E-03	8.3571E-03	9.0193E-03	9.3391E-03	9.4921E-03	1.0016E-02	1.0530E-02	1.1641E-02
343.15	15.27	7.9611E-03	8.2917E-03	8.9509E-03	9.2704E-03	9.4250E-03	9.9488E-03	1.0465E-02	1.1577E-02
343.15	16.27	7.8987E-03	8.2273E-03	8.8835E-03	9.2026E-03	9.3590E-03	9.8829E-03	1.0400E-02	1.1515E-02
343.15	17.28	7.8372E-03	8.1639E-03	8.8171E-03	9.1359E-03	9.2938E-03	9.8178E-03	1.0337E-02	1.1452E-02
343.15	18.28	7.7767E-03	8.1015E-03	8.7517E-03	9.0701E-03	9.2295E-03	9.7535E-03	1.0274E-02	1.1391E-02
343.15	19.29	7.7171E-03	8.0400E-03	8.6872E-03	9.0052E-03	9.1661E-03	9.6901E-03	1.0212E-02	1.1330E-02
343.15	20.29	7.6584E-03	7.9795E-03	8.6237E-03	8.9412E-03	9.1036E-03	9.6275E-03	1.0151E-02	1.1270E-02
353.15	0.1	8.8447E-03	9.2012E-03	9.8945E-03	1.0209E-02	1.0325E-02	1.0829E-02	1.1298E-02	1.2351E-02
353.15	1.14	8.7730E-03	9.1275E-03	9.8180E-03	1.0132E-02	1.0252E-02	1.0756E-02	1.1228E-02	1.2285E-02
353.15	2.14	8.6948E-03	9.0470E-03	9.7343E-03	1.0049E-02	1.0171E-02	1.0677E-02	1.1152E-02	1.2212E-02
353.15	3.14	8.6179E-03	8.9679E-03	9.6520E-03	9.9668E-03	1.0092E-02	1.0598E-02	1.1076E-02	1.2140E-02
353.15	4.16	8.5424E-03	8.8901E-03	9.5711E-03	9.8860E-03	1.0013E-02	1.0521E-02	1.1002E-02	1.2068E-02
353.15	5.16	8.4681E-03	8.8137E-03	9.4916E-03	9.8065E-03	9.9365E-03	1.0445E-02	1.0928E-02	1.1998E-02
353.15	6.18	8.3952E-03	8.7386E-03	9.4134E-03	9.7283E-03	9.8607E-03	1.0370E-02	1.0856E-02	1.1928E-02
353.15	7.19	8.3235E-03	8.6648E-03	9.3364E-03	9.6513E-03	9.7860E-03	1.0296E-02	1.0785E-02	1.1859E-02
353.15	8.2	8.2530E-03	8.5922E-03	9.2607E-03	9.5755E-03	9.7125E-03	1.0223E-02	1.0714E-02	1.1791E-02
353.15	9.21	8.1837E-03	8.5208E-03	9.1862E-03	9.5009E-03	9.6401E-03	1.0151E-02	1.0644E-02	1.1724E-02
353.15	10.22	8.1156E-03	8.4506E-03	9.1129E-03	9.4274E-03	9.5687E-03	1.0080E-02	1.0576E-02	1.1658E-02
353.15	11.23	8.0485E-03	8.3815E-03	9.0408E-03	9.3551E-03	9.4984E-03	1.0010E-02	1.0508E-02	1.1592E-02
353.15	12.24	7.9826E-03	8.3135E-03	8.9698E-03	9.2839E-03	9.4291E-03	9.9415E-03	1.0441E-02	1.1527E-02
353.15	13.25	7.9178E-03	8.2467E-03	8.8999E-03	9.2137E-03	9.3608E-03	9.8735E-03	1.0375E-02	1.1463E-02
353.15	14.26	7.8540E-03	8.1809E-03	8.8311E-03	9.1446E-03	9.2935E-03	9.8064E-03	1.0309E-02	1.1399E-02
353.15	15.25	7.7912E-03	8.1161E-03	8.7633E-03	9.0765E-03	9.2271E-03	9.7403E-03	1.0245E-02	1.1336E-02
353.15	16.27	7.7294E-03	8.0524E-03	8.6966E-03	9.0095E-03	9.1617E-03	9.6750E-03	1.0181E-02	1.1274E-02
353.15	17.27	7.6686E-03	7.9897E-03	8.6309E-03	8.9434E-03	9.0972E-03	9.6106E-03	1.0118E-02	1.1213E-02
353.15	18.29	7.6087E-03	7.9279E-03	8.5661E-03	8.8783E-03	9.0337E-03	9.5470E-03	1.0056E-02	1.1152E-02
353.15	19.29	7.5498E-03	7.8671E-03	8.5024E-03	8.8141E-03	8.9709E-03	9.4843E-03	9.9950E-03	1.1092E-02
353.15	20.29	7.4917E-03	7.8072E-03	8.4395E-03	8.7508E-03	8.9091E-03	9.4224E-03	9.9344E-03	1.1032E-02

Expanded combined uncertainties ($k = 2$) U_c are $U_c(T) = 0.02\ K$. $U_c(P) = 0.032\ MPa$. $U_c(x_i) = 0.0002$. $U_{c,r} = (\alpha_p) = 0.038$.

Table B2: Thermal Expansivity (α_p) of butan-1-ol (1) + n-decane (2) at various pressures and temperatures.

T/K	P/MPa	α_p/K^{-1}							
		x_1=0	*x_1=0.1269*	*x_1=0.3764*	*x_1=0.4968*	*x_1=0.6234*	*x_1=0.7440*	*x_1=0.8731*	*x_1=1*
313.15	0.1	8.9818E-03	1.2155E-02	1.5841E-02	1.6890E-02	1.6621E-02	1.5340E-02	1.4604E-02	1.3501E-02
313.15	1.14	8.9203E-03	1.2076E-02	1.5748E-02	1.6794E-02	1.6528E-02	1.5255E-02	1.4525E-02	1.3431E-02
313.15	2.14	8.8530E-03	1.1990E-02	1.5646E-02	1.6689E-02	1.6426E-02	1.5162E-02	1.4439E-02	1.3355E-02
313.15	3.15	8.7867E-03	1.1906E-02	1.5545E-02	1.6585E-02	1.6326E-02	1.5070E-02	1.4354E-02	1.3279E-02
313.15	4.16	8.7214E-03	1.1822E-02	1.5445E-02	1.6482E-02	1.6226E-02	1.4979E-02	1.4269E-02	1.3204E-02
313.15	5.17	8.6570E-03	1.1739E-02	1.5347E-02	1.6381E-02	1.6128E-02	1.4889E-02	1.4186E-02	1.3130E-02
313.15	6.18	8.5936E-03	1.1658E-02	1.5250E-02	1.6281E-02	1.6031E-02	1.4801E-02	1.4103E-02	1.3057E-02
313.15	7.19	8.5311E-03	1.1578E-02	1.5154E-02	1.6182E-02	1.5935E-02	1.4713E-02	1.4022E-02	1.2984E-02
313.15	8.2	8.4695E-03	1.1499E-02	1.5059E-02	1.6084E-02	1.5841E-02	1.4626E-02	1.3941E-02	1.2913E-02
313.15	9.23	8.4088E-03	1.1421E-02	1.4966E-02	1.5987E-02	1.5747E-02	1.4541E-02	1.3862E-02	1.2842E-02
313.15	10.23	8.3490E-03	1.1344E-02	1.4873E-02	1.5892E-02	1.5655E-02	1.4456E-02	1.3783E-02	1.2772E-02
313.15	11.24	8.2900E-03	1.1268E-02	1.4782E-02	1.5798E-02	1.5563E-02	1.4373E-02	1.3705E-02	1.2702E-02
313.15	12.25	8.2318E-03	1.1193E-02	1.4692E-02	1.5704E-02	1.5473E-02	1.4290E-02	1.3628E-02	1.2634E-02
313.15	13.26	8.1745E-03	1.1119E-02	1.4603E-02	1.5612E-02	1.5384E-02	1.4208E-02	1.3552E-02	1.2566E-02
313.15	14.27	8.1179E-03	1.1046E-02	1.4515E-02	1.5521E-02	1.5295E-02	1.4127E-02	1.3477E-02	1.2499E-02
313.15	15.27	8.0621E-03	1.0974E-02	1.4428E-02	1.5431E-02	1.5208E-02	1.4047E-02	1.3402E-02	1.2432E-02
313.15	16.28	8.0071E-03	1.0903E-02	1.4342E-02	1.5342E-02	1.5122E-02	1.3968E-02	1.3329E-02	1.2367E-02
313.15	17.29	7.9528E-03	1.0833E-02	1.4258E-02	1.5254E-02	1.5037E-02	1.3890E-02	1.3256E-02	1.2302E-02
313.15	18.3	7.8993E-03	1.0763E-02	1.4174E-02	1.5167E-02	1.4952E-02	1.3813E-02	1.3184E-02	1.2237E-02
313.15	19.3	7.8465E-03	1.0695E-02	1.4091E-02	1.5081E-02	1.4869E-02	1.3737E-02	1.3113E-02	1.2174E-02
313.15	20.31	7.7943E-03	1.0627E-02	1.4009E-02	1.4996E-02	1.4786E-02	1.3661E-02	1.3042E-02	1.2111E-02
323.15	0.1	8.7616E-03	1.1870E-02	1.5480E-02	1.6506E-02	1.6240E-02	1.4983E-02	1.4259E-02	1.3175E-02
323.15	1.15	8.7011E-03	1.1792E-02	1.5388E-02	1.6411E-02	1.6149E-02	1.4899E-02	1.4181E-02	1.3106E-02
323.15	2.15	8.6347E-03	1.1707E-02	1.5287E-02	1.6307E-02	1.6048E-02	1.4807E-02	1.4096E-02	1.3030E-02
323.15	3.17	8.5694E-03	1.1624E-02	1.5187E-02	1.6205E-02	1.5949E-02	1.4717E-02	1.4012E-02	1.2956E-02
323.15	4.18	8.5051E-03	1.1541E-02	1.5089E-02	1.6103E-02	1.5851E-02	1.4627E-02	1.3929E-02	1.2882E-02
323.15	5.19	8.4417E-03	1.1460E-02	1.4992E-02	1.6003E-02	1.5754E-02	1.4538E-02	1.3847E-02	1.2809E-02
323.15	6.2	8.3793E-03	1.1379E-02	1.4896E-02	1.5904E-02	1.5658E-02	1.4451E-02	1.3766E-02	1.2737E-02
323.15	7.22	8.3177E-03	1.1300E-02	1.4801E-02	1.5807E-02	1.5564E-02	1.4365E-02	1.3685E-02	1.2666E-02
323.15	8.23	8.2571E-03	1.1222E-02	1.4708E-02	1.5710E-02	1.5470E-02	1.4279E-02	1.3606E-02	1.2595E-02
323.15	9.24	8.1974E-03	1.1146E-02	1.4616E-02	1.5615E-02	1.5378E-02	1.4195E-02	1.3528E-02	1.2526E-02
323.15	10.25	8.1385E-03	1.1070E-02	1.4525E-02	1.5521E-02	1.5287E-02	1.4111E-02	1.3450E-02	1.2457E-02
323.15	11.25	8.0804E-03	1.0995E-02	1.4435E-02	1.5428E-02	1.5197E-02	1.4029E-02	1.3373E-02	1.2389E-02
323.15	12.27	8.0232E-03	1.0921E-02	1.4346E-02	1.5336E-02	1.5108E-02	1.3948E-02	1.3298E-02	1.2321E-02
323.15	13.27	7.9667E-03	1.0848E-02	1.4258E-02	1.5245E-02	1.5020E-02	1.3867E-02	1.3223E-02	1.2254E-02

323.15	14.26	7.9111E-03	1.0776E-02	1.4172E-02	1.5155E-02	1.4933E-02	1.3787E-02	1.3149E-02	1.2188E-02
323.15	15.29	7.8562E-03	1.0705E-02	1.4086E-02	1.5067E-02	1.4847E-02	1.3709E-02	1.3075E-02	1.2123E-02
323.15	16.3	7.8021E-03	1.0635E-02	1.4001E-02	1.4979E-02	1.4762E-02	1.3631E-02	1.3003E-02	1.2058E-02
323.15	17.3	7.7488E-03	1.0566E-02	1.3918E-02	1.4892E-02	1.4678E-02	1.3554E-02	1.2931E-02	1.1995E-02
323.15	18.3	7.6961E-03	1.0498E-02	1.3835E-02	1.4807E-02	1.4595E-02	1.3478E-02	1.2860E-02	1.1931E-02
323.15	19.3	7.6442E-03	1.0431E-02	1.3754E-02	1.4722E-02	1.4513E-02	1.3403E-02	1.2790E-02	1.1869E-02
323.15	20.29	7.5929E-03	1.0364E-02	1.3673E-02	1.4638E-02	1.4431E-02	1.3328E-02	1.2721E-02	1.1807E-02
333.15	0.1	8.5568E-03	1.1607E-02	1.5153E-02	1.6160E-02	1.5897E-02	1.4659E-02	1.3945E-02	1.2876E-02
333.15	1.13	8.4970E-03	1.1530E-02	1.5062E-02	1.6066E-02	1.5806E-02	1.4576E-02	1.3868E-02	1.2808E-02
333.15	2.13	8.4315E-03	1.1447E-02	1.4962E-02	1.5963E-02	1.5706E-02	1.4485E-02	1.3784E-02	1.2734E-02
333.15	3.14	8.3671E-03	1.1364E-02	1.4863E-02	1.5862E-02	1.5608E-02	1.4395E-02	1.3701E-02	1.2660E-02
333.15	4.15	8.3036E-03	1.1282E-02	1.4766E-02	1.5761E-02	1.5511E-02	1.4307E-02	1.3619E-02	1.2587E-02
333.15	5.16	8.2411E-03	1.1202E-02	1.4670E-02	1.5662E-02	1.5415E-02	1.4219E-02	1.3538E-02	1.2516E-02
333.15	6.17	8.1795E-03	1.1123E-02	1.4575E-02	1.5565E-02	1.5321E-02	1.4133E-02	1.3457E-02	1.2444E-02
333.15	7.18	8.1189E-03	1.1045E-02	1.4481E-02	1.5468E-02	1.5227E-02	1.4047E-02	1.3378E-02	1.2374E-02
333.15	8.19	8.0591E-03	1.0968E-02	1.4389E-02	1.5373E-02	1.5135E-02	1.3963E-02	1.3300E-02	1.2305E-02
333.15	9.2	8.0002E-03	1.0892E-02	1.4298E-02	1.5278E-02	1.5044E-02	1.3880E-02	1.3222E-02	1.2236E-02
333.15	10.21	7.9422E-03	1.0817E-02	1.4208E-02	1.5185E-02	1.4954E-02	1.3797E-02	1.3146E-02	1.2168E-02
333.15	11.22	7.8850E-03	1.0743E-02	1.4119E-02	1.5093E-02	1.4865E-02	1.3716E-02	1.3070E-02	1.2101E-02
333.15	12.23	7.8286E-03	1.0670E-02	1.4031E-02	1.5002E-02	1.4777E-02	1.3636E-02	1.2995E-02	1.2034E-02
333.15	13.24	7.7730E-03	1.0598E-02	1.3944E-02	1.4912E-02	1.4690E-02	1.3556E-02	1.2922E-02	1.1968E-02
333.15	14.25	7.7182E-03	1.0527E-02	1.3859E-02	1.4824E-02	1.4604E-02	1.3477E-02	1.2848E-02	1.1903E-02
333.15	15.26	7.6642E-03	1.0457E-02	1.3774E-02	1.4736E-02	1.4519E-02	1.3400E-02	1.2776E-02	1.1839E-02
333.15	16.27	7.6109E-03	1.0388E-02	1.3691E-02	1.4649E-02	1.4435E-02	1.3323E-02	1.2705E-02	1.1775E-02
333.15	17.27	7.5583E-03	1.0320E-02	1.3608E-02	1.4564E-02	1.4352E-02	1.3247E-02	1.2634E-02	1.1712E-02
333.15	18.28	7.5065E-03	1.0253E-02	1.3527E-02	1.4479E-02	1.4270E-02	1.3172E-02	1.2564E-02	1.1650E-02
333.15	19.28	7.4554E-03	1.0186E-02	1.3446E-02	1.4396E-02	1.4189E-02	1.3098E-02	1.2495E-02	1.1588E-02
333.15	20.28	7.4049E-03	1.0121E-02	1.3366E-02	1.4313E-02	1.4108E-02	1.3024E-02	1.2427E-02	1.1527E-02
343.15	0.1	8.3656E-03	1.1365E-02	1.4856E-02	1.5848E-02	1.5586E-02	1.4364E-02	1.3658E-02	1.2602E-02
343.15	1.14	8.3066E-03	1.1289E-02	1.4766E-02	1.5755E-02	1.5496E-02	1.4282E-02	1.3583E-02	1.2535E-02
343.15	2.14	8.2419E-03	1.1206E-02	1.4667E-02	1.5653E-02	1.5398E-02	1.4192E-02	1.3499E-02	1.2462E-02
343.15	3.14	8.1782E-03	1.1124E-02	1.4569E-02	1.5552E-02	1.5300E-02	1.4103E-02	1.3417E-02	1.2389E-02
343.15	4.16	8.1156E-03	1.1044E-02	1.4472E-02	1.5452E-02	1.5204E-02	1.4015E-02	1.3336E-02	1.2317E-02
343.15	5.17	8.0538E-03	1.0964E-02	1.4377E-02	1.5354E-02	1.5109E-02	1.3929E-02	1.3255E-02	1.2246E-02
343.15	6.18	7.9930E-03	1.0886E-02	1.4283E-02	1.5257E-02	1.5015E-02	1.3843E-02	1.3176E-02	1.2176E-02
343.15	7.19	7.9332E-03	1.0808E-02	1.4190E-02	1.5161E-02	1.4922E-02	1.3758E-02	1.3097E-02	1.2106E-02
343.15	8.2	7.8742E-03	1.0732E-02	1.4099E-02	1.5066E-02	1.4831E-02	1.3675E-02	1.3020E-02	1.2037E-02
343.15	9.21	7.8160E-03	1.0657E-02	1.4008E-02	1.4973E-02	1.4740E-02	1.3592E-02	1.2943E-02	1.1969E-02
343.15	10.22	7.7588E-03	1.0583E-02	1.3919E-02	1.4881E-02	1.4651E-02	1.3511E-02	1.2868E-02	1.1902E-02
343.15	11.23	7.7023E-03	1.0510E-02	1.3831E-02	1.4789E-02	1.4563E-02	1.3430E-02	1.2793E-02	1.1836E-02
343.15	12.24	7.6467E-03	1.0438E-02	1.3744E-02	1.4699E-02	1.4476E-02	1.3350E-02	1.2719E-02	1.1770E-02
343.15	13.25	7.5919E-03	1.0367E-02	1.3658E-02	1.4610E-02	1.4389E-02	1.3272E-02	1.2646E-02	1.1705E-02
343.15	14.26	7.5378E-03	1.0297E-02	1.3573E-02	1.4522E-02	1.4304E-02	1.3194E-02	1.2573E-02	1.1641E-02

343.15	15.27	7.4845E-03	1.0228E-02	1.3490E-02	1.4436E-02	1.4220E-02	1.3117E-02	1.2502E-02	1.1577E-02
343.15	16.27	7.4320E-03	1.0159E-02	1.3407E-02	1.4350E-02	1.4137E-02	1.3041E-02	1.2431E-02	1.1515E-02
343.15	17.28	7.3802E-03	1.0092E-02	1.3325E-02	1.4265E-02	1.4055E-02	1.2966E-02	1.2361E-02	1.1452E-02
343.15	18.28	7.3291E-03	1.0026E-02	1.3244E-02	1.4181E-02	1.3974E-02	1.2892E-02	1.2292E-02	1.1391E-02
343.15	19.29	7.2787E-03	9.9600E-03	1.3165E-02	1.4098E-02	1.3893E-02	1.2818E-02	1.2224E-02	1.1330E-02
343.15	20.29	7.2290E-03	9.8952E-03	1.3086E-02	1.4016E-02	1.3814E-02	1.2746E-02	1.2156E-02	1.1270E-02
353.15	0.1	8.1870E-03	1.1142E-02	1.4587E-02	1.5566E-02	1.5305E-02	1.4095E-02	1.3397E-02	1.2351E-02
353.15	1.14	8.1285E-03	1.1066E-02	1.4497E-02	1.5473E-02	1.5216E-02	1.4014E-02	1.3321E-02	1.2285E-02
353.15	2.14	8.0646E-03	1.0984E-02	1.4398E-02	1.5372E-02	1.5118E-02	1.3925E-02	1.3239E-02	1.2212E-02
353.15	3.14	8.0016E-03	1.0903E-02	1.4301E-02	1.5271E-02	1.5021E-02	1.3836E-02	1.3157E-02	1.2140E-02
353.15	4.16	7.9396E-03	1.0823E-02	1.4205E-02	1.5172E-02	1.4925E-02	1.3749E-02	1.3076E-02	1.2068E-02
353.15	5.16	7.8786E-03	1.0744E-02	1.4111E-02	1.5075E-02	1.4831E-02	1.3663E-02	1.2997E-02	1.1998E-02
353.15	6.18	7.8185E-03	1.0666E-02	1.4017E-02	1.4978E-02	1.4738E-02	1.3578E-02	1.2918E-02	1.1928E-02
353.15	7.19	7.7593E-03	1.0590E-02	1.3925E-02	1.4883E-02	1.4645E-02	1.3494E-02	1.2840E-02	1.1859E-02
353.15	8.2	7.7010E-03	1.0514E-02	1.3834E-02	1.4789E-02	1.4554E-02	1.3411E-02	1.2763E-02	1.1791E-02
353.15	9.21	7.6436E-03	1.0440E-02	1.3744E-02	1.4696E-02	1.4465E-02	1.3329E-02	1.2687E-02	1.1724E-02
353.15	10.22	7.5870E-03	1.0366E-02	1.3656E-02	1.4604E-02	1.4376E-02	1.3248E-02	1.2612E-02	1.1658E-02
353.15	11.23	7.5313E-03	1.0294E-02	1.3568E-02	1.4513E-02	1.4288E-02	1.3169E-02	1.2538E-02	1.1592E-02
353.15	12.24	7.4763E-03	1.0223E-02	1.3482E-02	1.4424E-02	1.4202E-02	1.3090E-02	1.2465E-02	1.1527E-02
353.15	13.25	7.4222E-03	1.0152E-02	1.3397E-02	1.4336E-02	1.4116E-02	1.3011E-02	1.2392E-02	1.1463E-02
353.15	14.26	7.3688E-03	1.0083E-02	1.3312E-02	1.4248E-02	1.4032E-02	1.2934E-02	1.2321E-02	1.1399E-02
353.15	15.25	7.3162E-03	1.0014E-02	1.3229E-02	1.4162E-02	1.3948E-02	1.2858E-02	1.2250E-02	1.1336E-02
353.15	16.27	7.2644E-03	9.9469E-03	1.3147E-02	1.4077E-02	1.3866E-02	1.2783E-02	1.2180E-02	1.1274E-02
353.15	17.27	7.2133E-03	9.8803E-03	1.3066E-02	1.3993E-02	1.3784E-02	1.2708E-02	1.2111E-02	1.1213E-02
353.15	18.29	7.1628E-03	9.8145E-03	1.2986E-02	1.3909E-02	1.3703E-02	1.2635E-02	1.2042E-02	1.1152E-02
353.15	19.29	7.1131E-03	9.7497E-03	1.2907E-02	1.3827E-02	1.3624E-02	1.2562E-02	1.1975E-02	1.1092E-02
353.15	20.29	7.0641E-03	9.6856E-03	1.2829E-02	1.3746E-02	1.3545E-02	1.2490E-02	1.1908E-02	1.1032E-02

Expanded combined uncertainties ($k = 2$) U_c are $U_c(T) = 0.02\ K.\ U_c(P) = 0.032\ MPa.\ U_c(x_i) = 0.0002.\ U_{c,r} = (\alpha_p) = 0.038.$

Table B3: Thermal Expansivity (α_p) of butan-2-ol (1) + n-octane (2) at various pressures and temperatures.

T/K	P/MPa	α_p/K^{-1}							
		x_1=0	*x_1=0.1262*	*x_1=0.3742*	*x_1=0.5002*	*x_1=0.6257*	*x_1=0.7501*	*x_1=0.8747*	*x_1=1*
313.15	0.1	9.6446E-03	1.1190E-02	1.3584E-02	1.4134E-02	1.4413E-02	1.4395E-02	1.4824E-02	1.4715E-02
313.15	1.14	9.5702E-03	1.1111E-02	1.3497E-02	1.4045E-02	1.4323E-02	1.4304E-02	1.4731E-02	1.4622E-02
313.15	2.14	9.4889E-03	1.1025E-02	1.3401E-02	1.3947E-02	1.4224E-02	1.4205E-02	1.4628E-02	1.4520E-02
313.15	3.15	9.4090E-03	1.0940E-02	1.3307E-02	1.3851E-02	1.4127E-02	1.4107E-02	1.4527E-02	1.4419E-02
313.15	4.16	9.3304E-03	1.0856E-02	1.3214E-02	1.3757E-02	1.4031E-02	1.4011E-02	1.4427E-02	1.4320E-02
313.15	5.17	9.2531E-03	1.0774E-02	1.3123E-02	1.3663E-02	1.3936E-02	1.3916E-02	1.4329E-02	1.4222E-02
313.15	6.18	9.1771E-03	1.0693E-02	1.3032E-02	1.3571E-02	1.3842E-02	1.3822E-02	1.4232E-02	1.4125E-02
313.15	7.19	9.1023E-03	1.0613E-02	1.2943E-02	1.3480E-02	1.3750E-02	1.3729E-02	1.4136E-02	1.4030E-02
313.15	8.2	9.0288E-03	1.0535E-02	1.2856E-02	1.3391E-02	1.3659E-02	1.3638E-02	1.4041E-02	1.3936E-02
313.15	9.23	8.9564E-03	1.0457E-02	1.2769E-02	1.3302E-02	1.3569E-02	1.3548E-02	1.3948E-02	1.3843E-02
313.15	10.23	8.8851E-03	1.0381E-02	1.2683E-02	1.3215E-02	1.3480E-02	1.3459E-02	1.3856E-02	1.3751E-02
313.15	11.24	8.8150E-03	1.0306E-02	1.2599E-02	1.3129E-02	1.3393E-02	1.3371E-02	1.3765E-02	1.3661E-02
313.15	12.25	8.7460E-03	1.0231E-02	1.2516E-02	1.3044E-02	1.3306E-02	1.3284E-02	1.3675E-02	1.3572E-02
313.15	13.26	8.6781E-03	1.0158E-02	1.2434E-02	1.2960E-02	1.3221E-02	1.3199E-02	1.3587E-02	1.3484E-02
313.15	14.27	8.6112E-03	1.0086E-02	1.2353E-02	1.2877E-02	1.3137E-02	1.3114E-02	1.3500E-02	1.3397E-02
313.15	15.27	8.5453E-03	1.0015E-02	1.2273E-02	1.2795E-02	1.3053E-02	1.3031E-02	1.3413E-02	1.3311E-02
313.15	16.28	8.4804E-03	9.9451E-03	1.2194E-02	1.2714E-02	1.2971E-02	1.2948E-02	1.3328E-02	1.3226E-02
313.15	17.29	8.4165E-03	9.8760E-03	1.2116E-02	1.2634E-02	1.2890E-02	1.2867E-02	1.3244E-02	1.3142E-02
313.15	18.3	8.3536E-03	9.8078E-03	1.2039E-02	1.2556E-02	1.2810E-02	1.2787E-02	1.3161E-02	1.3060E-02
313.15	19.3	8.2916E-03	9.7406E-03	1.1963E-02	1.2478E-02	1.2731E-02	1.2708E-02	1.3079E-02	1.2978E-02
313.15	20.31	8.2305E-03	9.6743E-03	1.1888E-02	1.2401E-02	1.2653E-02	1.2629E-02	1.2998E-02	1.2898E-02
323.15	0.1	9.4225E-03	1.0942E-02	1.3293E-02	1.3831E-02	1.4103E-02	1.4081E-02	1.4498E-02	1.4386E-02
323.15	1.15	9.3490E-03	1.0864E-02	1.3207E-02	1.3743E-02	1.4014E-02	1.3992E-02	1.4405E-02	1.4294E-02
323.15	2.15	9.2686E-03	1.0778E-02	1.3112E-02	1.3647E-02	1.3916E-02	1.3893E-02	1.4304E-02	1.4193E-02
323.15	3.17	9.1896E-03	1.0694E-02	1.3019E-02	1.3552E-02	1.3819E-02	1.3797E-02	1.4204E-02	1.4093E-02
323.15	4.18	9.1119E-03	1.0612E-02	1.2927E-02	1.3458E-02	1.3724E-02	1.3701E-02	1.4105E-02	1.3995E-02
323.15	5.19	9.0356E-03	1.0530E-02	1.2836E-02	1.3365E-02	1.3630E-02	1.3607E-02	1.4008E-02	1.3898E-02
323.15	6.2	8.9605E-03	1.0450E-02	1.2747E-02	1.3274E-02	1.3538E-02	1.3514E-02	1.3912E-02	1.3803E-02
323.15	7.22	8.8866E-03	1.0371E-02	1.2659E-02	1.3184E-02	1.3446E-02	1.3423E-02	1.3817E-02	1.3709E-02
323.15	8.23	8.8140E-03	1.0293E-02	1.2572E-02	1.3095E-02	1.3356E-02	1.3332E-02	1.3724E-02	1.3616E-02
323.15	9.24	8.7425E-03	1.0217E-02	1.2486E-02	1.3008E-02	1.3267E-02	1.3243E-02	1.3631E-02	1.3524E-02
323.15	10.25	8.6722E-03	1.0141E-02	1.2401E-02	1.2922E-02	1.3179E-02	1.3155E-02	1.3540E-02	1.3434E-02
323.15	11.25	8.6030E-03	1.0067E-02	1.2318E-02	1.2836E-02	1.3093E-02	1.3068E-02	1.3451E-02	1.3344E-02
323.15	12.27	8.5349E-03	9.9937E-03	1.2235E-02	1.2752E-02	1.3007E-02	1.2983E-02	1.3362E-02	1.3256E-02

323.15	13.27	8.4679E-03	9.9214E-03	1.2154E-02	1.2669E-02	1.2923E-02	1.2898E-02	1.3275E-02	1.3169E-02
323.15	14.26	8.4019E-03	9.8502E-03	1.2074E-02	1.2587E-02	1.2840E-02	1.2815E-02	1.3189E-02	1.3084E-02
323.15	15.29	8.3369E-03	9.7800E-03	1.1995E-02	1.2506E-02	1.2757E-02	1.2732E-02	1.3103E-02	1.2999E-02
323.15	16.3	8.2730E-03	9.7109E-03	1.1917E-02	1.2426E-02	1.2676E-02	1.2651E-02	1.3019E-02	1.2915E-02
323.15	17.3	8.2100E-03	9.6426E-03	1.1840E-02	1.2347E-02	1.2596E-02	1.2571E-02	1.2936E-02	1.2833E-02
323.15	18.3	8.1479E-03	9.5754E-03	1.1764E-02	1.2269E-02	1.2517E-02	1.2491E-02	1.2854E-02	1.2751E-02
323.15	19.3	8.0868E-03	9.5090E-03	1.1689E-02	1.2193E-02	1.2439E-02	1.2413E-02	1.2774E-02	1.2671E-02
323.15	20.29	8.0266E-03	9.4436E-03	1.1614E-02	1.2117E-02	1.2362E-02	1.2336E-02	1.2694E-02	1.2592E-02
333.15	0.1	9.2161E-03	1.0712E-02	1.3027E-02	1.3556E-02	1.3820E-02	1.3796E-02	1.4201E-02	1.4086E-02
333.15	1.13	9.1433E-03	1.0635E-02	1.2941E-02	1.3468E-02	1.3732E-02	1.3707E-02	1.4109E-02	1.3995E-02
333.15	2.13	9.0638E-03	1.0551E-02	1.2847E-02	1.3372E-02	1.3635E-02	1.3610E-02	1.4009E-02	1.3895E-02
333.15	3.14	8.9856E-03	1.0467E-02	1.2755E-02	1.3278E-02	1.3539E-02	1.3514E-02	1.3910E-02	1.3796E-02
333.15	4.15	8.9087E-03	1.0385E-02	1.2664E-02	1.3185E-02	1.3444E-02	1.3419E-02	1.3812E-02	1.3699E-02
333.15	5.16	8.8332E-03	1.0305E-02	1.2574E-02	1.3093E-02	1.3351E-02	1.3326E-02	1.3715E-02	1.3603E-02
333.15	6.17	8.7589E-03	1.0225E-02	1.2485E-02	1.3003E-02	1.3259E-02	1.3233E-02	1.3620E-02	1.3509E-02
333.15	7.18	8.6859E-03	1.0147E-02	1.2397E-02	1.2913E-02	1.3169E-02	1.3143E-02	1.3526E-02	1.3416E-02
333.15	8.19	8.6140E-03	1.0070E-02	1.2311E-02	1.2825E-02	1.3079E-02	1.3053E-02	1.3434E-02	1.3324E-02
333.15	9.2	8.5434E-03	9.9942E-03	1.2226E-02	1.2739E-02	1.2991E-02	1.2965E-02	1.3342E-02	1.3233E-02
333.15	10.21	8.4739E-03	9.9195E-03	1.2142E-02	1.2653E-02	1.2904E-02	1.2878E-02	1.3252E-02	1.3143E-02
333.15	11.22	8.4055E-03	9.8458E-03	1.2060E-02	1.2568E-02	1.2818E-02	1.2792E-02	1.3164E-02	1.3055E-02
333.15	12.23	8.3382E-03	9.7733E-03	1.1978E-02	1.2485E-02	1.2734E-02	1.2707E-02	1.3076E-02	1.2968E-02
333.15	13.24	8.2720E-03	9.7018E-03	1.1897E-02	1.2403E-02	1.2650E-02	1.2623E-02	1.2989E-02	1.2882E-02
333.15	14.25	8.2068E-03	9.6314E-03	1.1818E-02	1.2321E-02	1.2568E-02	1.2540E-02	1.2904E-02	1.2797E-02
333.15	15.26	8.1427E-03	9.5620E-03	1.1740E-02	1.2241E-02	1.2486E-02	1.2459E-02	1.2820E-02	1.2713E-02
333.15	16.27	8.0795E-03	9.4935E-03	1.1662E-02	1.2162E-02	1.2406E-02	1.2378E-02	1.2737E-02	1.2631E-02
333.15	17.27	8.0173E-03	9.4261E-03	1.1586E-02	1.2084E-02	1.2326E-02	1.2299E-02	1.2655E-02	1.2549E-02
333.15	18.28	7.9561E-03	9.3596E-03	1.1511E-02	1.2007E-02	1.2248E-02	1.2221E-02	1.2574E-02	1.2469E-02
333.15	19.28	7.8958E-03	9.2940E-03	1.1436E-02	1.1931E-02	1.2171E-02	1.2143E-02	1.2494E-02	1.2389E-02
333.15	20.28	7.8364E-03	9.2294E-03	1.1363E-02	1.1855E-02	1.2094E-02	1.2067E-02	1.2415E-02	1.2311E-02
343.15	0.1	9.0240E-03	1.0500E-02	1.2784E-02	1.3304E-02	1.3563E-02	1.3535E-02	1.3931E-02	1.3814E-02
343.15	1.14	8.9518E-03	1.0424E-02	1.2698E-02	1.3217E-02	1.3475E-02	1.3447E-02	1.3840E-02	1.3723E-02
343.15	2.14	8.8729E-03	1.0340E-02	1.2605E-02	1.3122E-02	1.3378E-02	1.3350E-02	1.3740E-02	1.3624E-02
343.15	3.14	8.7954E-03	1.0257E-02	1.2513E-02	1.3028E-02	1.3283E-02	1.3255E-02	1.3641E-02	1.3526E-02
343.15	4.16	8.7193E-03	1.0176E-02	1.2422E-02	1.2935E-02	1.3189E-02	1.3161E-02	1.3544E-02	1.3429E-02
343.15	5.17	8.6445E-03	1.0096E-02	1.2333E-02	1.2844E-02	1.3096E-02	1.3068E-02	1.3448E-02	1.3334E-02
343.15	6.18	8.5709E-03	1.0017E-02	1.2245E-02	1.2754E-02	1.3005E-02	1.2977E-02	1.3354E-02	1.3240E-02
343.15	7.19	8.4986E-03	9.9392E-03	1.2158E-02	1.2665E-02	1.2915E-02	1.2886E-02	1.3261E-02	1.3148E-02
343.15	8.2	8.4274E-03	9.8628E-03	1.2072E-02	1.2578E-02	1.2826E-02	1.2798E-02	1.3169E-02	1.3056E-02
343.15	9.21	8.3575E-03	9.7875E-03	1.1988E-02	1.2492E-02	1.2738E-02	1.2710E-02	1.3078E-02	1.2966E-02
343.15	10.22	8.2887E-03	9.7135E-03	1.1904E-02	1.2406E-02	1.2652E-02	1.2623E-02	1.2989E-02	1.2878E-02
343.15	11.23	8.2211E-03	9.6405E-03	1.1822E-02	1.2322E-02	1.2567E-02	1.2538E-02	1.2901E-02	1.2790E-02
343.15	12.24	8.1545E-03	9.5686E-03	1.1741E-02	1.2240E-02	1.2483E-02	1.2454E-02	1.2814E-02	1.2704E-02
343.15	13.25	8.0890E-03	9.4978E-03	1.1661E-02	1.2158E-02	1.2400E-02	1.2371E-02	1.2728E-02	1.2619E-02

343.15	14.26	8.0246E-03	9.4280E-03	1.1582E-02	1.2077E-02	1.2318E-02	1.2289E-02	1.2643E-02	1.2535E-02
343.15	15.27	7.9611E-03	9.3592E-03	1.1504E-02	1.1998E-02	1.2237E-02	1.2208E-02	1.2560E-02	1.2452E-02
343.15	16.27	7.8987E-03	9.2914E-03	1.1428E-02	1.1919E-02	1.2157E-02	1.2128E-02	1.2477E-02	1.2370E-02
343.15	17.28	7.8372E-03	9.2247E-03	1.1352E-02	1.1842E-02	1.2079E-02	1.2049E-02	1.2396E-02	1.2289E-02
343.15	18.28	7.7767E-03	9.1588E-03	1.1277E-02	1.1765E-02	1.2001E-02	1.1971E-02	1.2316E-02	1.2209E-02
343.15	19.29	7.7171E-03	9.0939E-03	1.1203E-02	1.1690E-02	1.1924E-02	1.1895E-02	1.2237E-02	1.2131E-02
343.15	20.29	7.6584E-03	9.0299E-03	1.1131E-02	1.1615E-02	1.1848E-02	1.1819E-02	1.2158E-02	1.2053E-02
353.15	0.1	8.8447E-03	1.0304E-02	1.2561E-02	1.3074E-02	1.3328E-02	1.3298E-02	1.3685E-02	1.3564E-02
353.15	1.14	8.7730E-03	1.0227E-02	1.2476E-02	1.2987E-02	1.3240E-02	1.3210E-02	1.3594E-02	1.3474E-02
353.15	2.14	8.6948E-03	1.0144E-02	1.2383E-02	1.2892E-02	1.3143E-02	1.3113E-02	1.3495E-02	1.3375E-02
353.15	3.14	8.6179E-03	1.0062E-02	1.2291E-02	1.2799E-02	1.3048E-02	1.3018E-02	1.3396E-02	1.3278E-02
353.15	4.16	8.5424E-03	9.9809E-03	1.2201E-02	1.2707E-02	1.2955E-02	1.2925E-02	1.3300E-02	1.3182E-02
353.15	5.16	8.4681E-03	9.9013E-03	1.2111E-02	1.2616E-02	1.2863E-02	1.2832E-02	1.3204E-02	1.3087E-02
353.15	6.18	8.3952E-03	9.8230E-03	1.2024E-02	1.2526E-02	1.2772E-02	1.2741E-02	1.3110E-02	1.2994E-02
353.15	7.19	8.3235E-03	9.7459E-03	1.1937E-02	1.2438E-02	1.2682E-02	1.2652E-02	1.3018E-02	1.2902E-02
353.15	8.2	8.2530E-03	9.6701E-03	1.1852E-02	1.2351E-02	1.2594E-02	1.2563E-02	1.2926E-02	1.2812E-02
353.15	9.21	8.1837E-03	9.5954E-03	1.1768E-02	1.2265E-02	1.2507E-02	1.2476E-02	1.2836E-02	1.2722E-02
353.15	10.22	8.1156E-03	9.5218E-03	1.1685E-02	1.2180E-02	1.2421E-02	1.2390E-02	1.2747E-02	1.2634E-02
353.15	11.23	8.0485E-03	9.4494E-03	1.1603E-02	1.2096E-02	1.2336E-02	1.2305E-02	1.2660E-02	1.2547E-02
353.15	12.24	7.9826E-03	9.3780E-03	1.1523E-02	1.2014E-02	1.2252E-02	1.2221E-02	1.2573E-02	1.2461E-02
353.15	13.25	7.9178E-03	9.3078E-03	1.1443E-02	1.1933E-02	1.2170E-02	1.2139E-02	1.2488E-02	1.2377E-02
353.15	14.26	7.8540E-03	9.2385E-03	1.1365E-02	1.1853E-02	1.2088E-02	1.2057E-02	1.2404E-02	1.2293E-02
353.15	15.25	7.7912E-03	9.1703E-03	1.1287E-02	1.1773E-02	1.2008E-02	1.1977E-02	1.2321E-02	1.2211E-02
353.15	16.27	7.7294E-03	9.1031E-03	1.1211E-02	1.1695E-02	1.1929E-02	1.1898E-02	1.2239E-02	1.2130E-02
353.15	17.27	7.6686E-03	9.0369E-03	1.1136E-02	1.1618E-02	1.1850E-02	1.1819E-02	1.2158E-02	1.2050E-02
353.15	18.29	7.6087E-03	8.9716E-03	1.1062E-02	1.1542E-02	1.1773E-02	1.1742E-02	1.2079E-02	1.1971E-02
353.15	19.29	7.5498E-03	8.9073E-03	1.0988E-02	1.1467E-02	1.1697E-02	1.1666E-02	1.2000E-02	1.1892E-02
353.15	20.29	7.4917E-03	8.8439E-03	1.0916E-02	1.1393E-02	1.1622E-02	1.1591E-02	1.1922E-02	1.1815E-02

Expanded combined uncertainties (k = 2) U_c are $U_c(T) = 0.02\ K$. $U_c(P) = 0.032\ MPa$. $U_c(x_i) = 0.0002$. $U_{c,r} = (\alpha_p) = 0.035$.

Table B4: Thermal Expansivity (α_p) of butan-2-ol (1) + n-decane (2) at various pressures and temperatures.

T/K	P/MPa	α_p/K^{-1}							
		$x_1=0$	$x_1=0.1254$	$x_1=0.3754$	$x_1=0.5055$	$x_1=0.6240$	$x_1=0.7519$	$x_1=0.8740$	$x_1=1$
313.15	0.1	8.9818E-03	1.0963E-02	1.3600E-02	1.4853E-02	1.5534E-02	1.5511E-02	1.4859E-02	1.4715E-02
313.15	1.14	8.9203E-03	1.0893E-02	1.3521E-02	1.4769E-02	1.5449E-02	1.5423E-02	1.4770E-02	1.4622E-02
313.15	2.14	8.8530E-03	1.0816E-02	1.3434E-02	1.4678E-02	1.5355E-02	1.5327E-02	1.4673E-02	1.4520E-02
313.15	3.15	8.7867E-03	1.0741E-02	1.3349E-02	1.4588E-02	1.5263E-02	1.5231E-02	1.4578E-02	1.4419E-02
313.15	4.16	8.7214E-03	1.0666E-02	1.3264E-02	1.4498E-02	1.5172E-02	1.5137E-02	1.4483E-02	1.4320E-02
313.15	5.17	8.6570E-03	1.0593E-02	1.3180E-02	1.4410E-02	1.5081E-02	1.5045E-02	1.4390E-02	1.4222E-02
313.15	6.18	8.5936E-03	1.0521E-02	1.3098E-02	1.4323E-02	1.4992E-02	1.4953E-02	1.4298E-02	1.4125E-02
313.15	7.19	8.5311E-03	1.0449E-02	1.3017E-02	1.4237E-02	1.4904E-02	1.4862E-02	1.4207E-02	1.4030E-02
313.15	8.2	8.4695E-03	1.0379E-02	1.2936E-02	1.4152E-02	1.4817E-02	1.4773E-02	1.4117E-02	1.3936E-02
313.15	9.23	8.4088E-03	1.0309E-02	1.2857E-02	1.4068E-02	1.4730E-02	1.4684E-02	1.4028E-02	1.3843E-02
313.15	10.23	8.3490E-03	1.0241E-02	1.2778E-02	1.3986E-02	1.4645E-02	1.4597E-02	1.3941E-02	1.3751E-02
313.15	11.24	8.2900E-03	1.0173E-02	1.2701E-02	1.3904E-02	1.4561E-02	1.4510E-02	1.3854E-02	1.3661E-02
313.15	12.25	8.2318E-03	1.0106E-02	1.2624E-02	1.3823E-02	1.4478E-02	1.4425E-02	1.3769E-02	1.3572E-02
313.15	13.26	8.1745E-03	1.0040E-02	1.2549E-02	1.3742E-02	1.4396E-02	1.4341E-02	1.3684E-02	1.3484E-02
313.15	14.27	8.1179E-03	9.9750E-03	1.2474E-02	1.3663E-02	1.4314E-02	1.4257E-02	1.3601E-02	1.3397E-02
313.15	15.27	8.0621E-03	9.9108E-03	1.2400E-02	1.3585E-02	1.4234E-02	1.4175E-02	1.3519E-02	1.3311E-02
313.15	16.28	8.0071E-03	9.8474E-03	1.2327E-02	1.3508E-02	1.4154E-02	1.4094E-02	1.3437E-02	1.3226E-02
313.15	17.29	7.9528E-03	9.7847E-03	1.2255E-02	1.3431E-02	1.4076E-02	1.4013E-02	1.3357E-02	1.3142E-02
313.15	18.3	7.8993E-03	9.7229E-03	1.2183E-02	1.3356E-02	1.3998E-02	1.3933E-02	1.3278E-02	1.3060E-02
313.15	19.3	7.8465E-03	9.6619E-03	1.2113E-02	1.3281E-02	1.3921E-02	1.3855E-02	1.3199E-02	1.2978E-02
313.15	20.31	7.7943E-03	9.6016E-03	1.2043E-02	1.3207E-02	1.3845E-02	1.3777E-02	1.3122E-02	1.2898E-02
323.15	0.1	8.7616E-03	1.0705E-02	1.3294E-02	1.4525E-02	1.5195E-02	1.5171E-02	1.4529E-02	1.4386E-02
323.15	1.15	8.7011E-03	1.0636E-02	1.3216E-02	1.4443E-02	1.5111E-02	1.5084E-02	1.4442E-02	1.4294E-02
323.15	2.15	8.6347E-03	1.0560E-02	1.3130E-02	1.4352E-02	1.5018E-02	1.4989E-02	1.4346E-02	1.4193E-02
323.15	3.17	8.5694E-03	1.0486E-02	1.3046E-02	1.4263E-02	1.4927E-02	1.4895E-02	1.4251E-02	1.4093E-02
323.15	4.18	8.5051E-03	1.0412E-02	1.2962E-02	1.4175E-02	1.4836E-02	1.4802E-02	1.4158E-02	1.3995E-02
323.15	5.19	8.4417E-03	1.0340E-02	1.2880E-02	1.4088E-02	1.4747E-02	1.4710E-02	1.4065E-02	1.3898E-02
323.15	6.2	8.3793E-03	1.0268E-02	1.2798E-02	1.4002E-02	1.4659E-02	1.4619E-02	1.3974E-02	1.3803E-02
323.15	7.22	8.3177E-03	1.0198E-02	1.2718E-02	1.3917E-02	1.4572E-02	1.4530E-02	1.3884E-02	1.3709E-02
323.15	8.23	8.2571E-03	1.0128E-02	1.2638E-02	1.3833E-02	1.4485E-02	1.4441E-02	1.3796E-02	1.3616E-02
323.15	9.24	8.1974E-03	1.0060E-02	1.2560E-02	1.3750E-02	1.4400E-02	1.4354E-02	1.3708E-02	1.3524E-02
323.15	10.25	8.1385E-03	9.9923E-03	1.2482E-02	1.3668E-02	1.4316E-02	1.4267E-02	1.3622E-02	1.3434E-02
323.15	11.25	8.0804E-03	9.9256E-03	1.2406E-02	1.3587E-02	1.4233E-02	1.4182E-02	1.3536E-02	1.3344E-02
323.15	12.27	8.0232E-03	9.8598E-03	1.2330E-02	1.3507E-02	1.4151E-02	1.4098E-02	1.3452E-02	1.3256E-02
323.15	13.27	7.9667E-03	9.7948E-03	1.2256E-02	1.3428E-02	1.4069E-02	1.4014E-02	1.3369E-02	1.3169E-02

323.15	14.26	7.9111E-03	9.7307E-03	1.2182E-02	1.3349E-02	1.3989E-02	1.3932E-02	1.3286E-02	1.3084E-02
323.15	15.29	7.8562E-03	9.6674E-03	1.2109E-02	1.3272E-02	1.3910E-02	1.3851E-02	1.3205E-02	1.2999E-02
323.15	16.3	7.8021E-03	9.6050E-03	1.2037E-02	1.3196E-02	1.3831E-02	1.3770E-02	1.3125E-02	1.2915E-02
323.15	17.3	7.7488E-03	9.5433E-03	1.1966E-02	1.3120E-02	1.3753E-02	1.3691E-02	1.3045E-02	1.2833E-02
323.15	18.3	7.6961E-03	9.4824E-03	1.1895E-02	1.3046E-02	1.3677E-02	1.3612E-02	1.2967E-02	1.2751E-02
323.15	19.3	7.6442E-03	9.4223E-03	1.1826E-02	1.2972E-02	1.3601E-02	1.3534E-02	1.2890E-02	1.2671E-02
323.15	20.29	7.5929E-03	9.3630E-03	1.1757E-02	1.2899E-02	1.3526E-02	1.3458E-02	1.2813E-02	1.2592E-02
333.15	0.1	8.5568E-03	1.0466E-02	1.3015E-02	1.4227E-02	1.4888E-02	1.4864E-02	1.4230E-02	1.4086E-02
333.15	1.13	8.4970E-03	1.0398E-02	1.2937E-02	1.4145E-02	1.4805E-02	1.4777E-02	1.4143E-02	1.3995E-02
333.15	2.13	8.4315E-03	1.0323E-02	1.2852E-02	1.4056E-02	1.4713E-02	1.4683E-02	1.4048E-02	1.3895E-02
333.15	3.14	8.3671E-03	1.0250E-02	1.2769E-02	1.3967E-02	1.4622E-02	1.4589E-02	1.3954E-02	1.3796E-02
333.15	4.15	8.3036E-03	1.0177E-02	1.2686E-02	1.3880E-02	1.4532E-02	1.4497E-02	1.3861E-02	1.3699E-02
333.15	5.16	8.2411E-03	1.0106E-02	1.2604E-02	1.3794E-02	1.4444E-02	1.4406E-02	1.3770E-02	1.3603E-02
333.15	6.17	8.1795E-03	1.0035E-02	1.2524E-02	1.3708E-02	1.4356E-02	1.4316E-02	1.3680E-02	1.3509E-02
333.15	7.18	8.1189E-03	9.9654E-03	1.2444E-02	1.3624E-02	1.4270E-02	1.4228E-02	1.3591E-02	1.3416E-02
333.15	8.19	8.0591E-03	9.8968E-03	1.2365E-02	1.3541E-02	1.4184E-02	1.4140E-02	1.3503E-02	1.3324E-02
333.15	9.2	8.0002E-03	9.8291E-03	1.2288E-02	1.3459E-02	1.4100E-02	1.4053E-02	1.3416E-02	1.3233E-02
333.15	10.21	7.9422E-03	9.7624E-03	1.2211E-02	1.3378E-02	1.4017E-02	1.3968E-02	1.3330E-02	1.3143E-02
333.15	11.22	7.8850E-03	9.6965E-03	1.2135E-02	1.3297E-02	1.3934E-02	1.3883E-02	1.3246E-02	1.3055E-02
333.15	12.23	7.8286E-03	9.6315E-03	1.2061E-02	1.3218E-02	1.3853E-02	1.3800E-02	1.3162E-02	1.2968E-02
333.15	13.24	7.7730E-03	9.5674E-03	1.1987E-02	1.3140E-02	1.3772E-02	1.3717E-02	1.3080E-02	1.2882E-02
333.15	14.25	7.7182E-03	9.5042E-03	1.1914E-02	1.3063E-02	1.3693E-02	1.3636E-02	1.2999E-02	1.2797E-02
333.15	15.26	7.6642E-03	9.4417E-03	1.1842E-02	1.2986E-02	1.3614E-02	1.3555E-02	1.2918E-02	1.2713E-02
333.15	16.27	7.6109E-03	9.3801E-03	1.1771E-02	1.2910E-02	1.3536E-02	1.3475E-02	1.2839E-02	1.2631E-02
333.15	17.27	7.5583E-03	9.3193E-03	1.1700E-02	1.2836E-02	1.3459E-02	1.3397E-02	1.2760E-02	1.2549E-02
333.15	18.28	7.5065E-03	9.2593E-03	1.1631E-02	1.2762E-02	1.3383E-02	1.3319E-02	1.2683E-02	1.2469E-02
333.15	19.28	7.4554E-03	9.2000E-03	1.1562E-02	1.2689E-02	1.3308E-02	1.3242E-02	1.2606E-02	1.2389E-02
333.15	20.28	7.4049E-03	9.1415E-03	1.1494E-02	1.2617E-02	1.3234E-02	1.3166E-02	1.2531E-02	1.2311E-02
343.15	0.1	8.3656E-03	1.0245E-02	1.2759E-02	1.3956E-02	1.4610E-02	1.4584E-02	1.3957E-02	1.3814E-02
343.15	1.14	8.3066E-03	1.0178E-02	1.2682E-02	1.3875E-02	1.4527E-02	1.4499E-02	1.3871E-02	1.3723E-02
343.15	2.14	8.2419E-03	1.0104E-02	1.2598E-02	1.3786E-02	1.4435E-02	1.4405E-02	1.3776E-02	1.3624E-02
343.15	3.14	8.1782E-03	1.0031E-02	1.2515E-02	1.3698E-02	1.4345E-02	1.4312E-02	1.3683E-02	1.3526E-02
343.15	4.16	8.1156E-03	9.9591E-03	1.2432E-02	1.3611E-02	1.4256E-02	1.4220E-02	1.3591E-02	1.3429E-02
343.15	5.17	8.0538E-03	9.8883E-03	1.2351E-02	1.3525E-02	1.4168E-02	1.4130E-02	1.3500E-02	1.3334E-02
343.15	6.18	7.9930E-03	9.8185E-03	1.2271E-02	1.3441E-02	1.4081E-02	1.4041E-02	1.3411E-02	1.3240E-02
343.15	7.19	7.9332E-03	9.7496E-03	1.2192E-02	1.3357E-02	1.3995E-02	1.3952E-02	1.3322E-02	1.3148E-02
343.15	8.2	7.8742E-03	9.6818E-03	1.2115E-02	1.3275E-02	1.3910E-02	1.3865E-02	1.3235E-02	1.3056E-02
343.15	9.21	7.8160E-03	9.6149E-03	1.2038E-02	1.3193E-02	1.3826E-02	1.3779E-02	1.3149E-02	1.2966E-02
343.15	10.22	7.7588E-03	9.5488E-03	1.1962E-02	1.3112E-02	1.3744E-02	1.3694E-02	1.3064E-02	1.2878E-02
343.15	11.23	7.7023E-03	9.4837E-03	1.1887E-02	1.3033E-02	1.3662E-02	1.3610E-02	1.2980E-02	1.2790E-02
343.15	12.24	7.6467E-03	9.4195E-03	1.1812E-02	1.2954E-02	1.3581E-02	1.3527E-02	1.2897E-02	1.2704E-02
343.15	13.25	7.5919E-03	9.3561E-03	1.1739E-02	1.2877E-02	1.3501E-02	1.3446E-02	1.2816E-02	1.2619E-02
343.15	14.26	7.5378E-03	9.2936E-03	1.1667E-02	1.2800E-02	1.3422E-02	1.3365E-02	1.2735E-02	1.2535E-02

343.15	15.27	7.4845E-03	9.2319E-03	1.1596E-02	1.2724E-02	1.3344E-02	1.3285E-02	1.2655E-02	1.2452E-02
343.15	16.27	7.4320E-03	9.1711E-03	1.1525E-02	1.2649E-02	1.3267E-02	1.3206E-02	1.2577E-02	1.2370E-02
343.15	17.28	7.3802E-03	9.1110E-03	1.1455E-02	1.2575E-02	1.3191E-02	1.3128E-02	1.2499E-02	1.2289E-02
343.15	18.28	7.3291E-03	9.0517E-03	1.1387E-02	1.2502E-02	1.3115E-02	1.3051E-02	1.2422E-02	1.2209E-02
343.15	19.29	7.2787E-03	8.9932E-03	1.1319E-02	1.2429E-02	1.3041E-02	1.2974E-02	1.2346E-02	1.2131E-02
343.15	20.29	7.2290E-03	8.9354E-03	1.1251E-02	1.2358E-02	1.2967E-02	1.2899E-02	1.2271E-02	1.2053E-02
353.15	0.1	8.1870E-03	1.0040E-02	1.2524E-02	1.3709E-02	1.4357E-02	1.4331E-02	1.3708E-02	1.3564E-02
353.15	1.14	8.1285E-03	9.9732E-03	1.2448E-02	1.3628E-02	1.4274E-02	1.4246E-02	1.3622E-02	1.3474E-02
353.15	2.14	8.0646E-03	9.8999E-03	1.2364E-02	1.3539E-02	1.4183E-02	1.4152E-02	1.3528E-02	1.3375E-02
353.15	3.14	8.0016E-03	9.8277E-03	1.2281E-02	1.3452E-02	1.4093E-02	1.4059E-02	1.3435E-02	1.3278E-02
353.15	4.16	7.9396E-03	9.7565E-03	1.2200E-02	1.3366E-02	1.4004E-02	1.3968E-02	1.3344E-02	1.3182E-02
353.15	5.16	7.8786E-03	9.6863E-03	1.2119E-02	1.3280E-02	1.3917E-02	1.3878E-02	1.3254E-02	1.3087E-02
353.15	6.18	7.8185E-03	9.6172E-03	1.2040E-02	1.3196E-02	1.3830E-02	1.3789E-02	1.3165E-02	1.2994E-02
353.15	7.19	7.7593E-03	9.5490E-03	1.1961E-02	1.3113E-02	1.3745E-02	1.3701E-02	1.3077E-02	1.2902E-02
353.15	8.2	7.7010E-03	9.4818E-03	1.1884E-02	1.3031E-02	1.3660E-02	1.3615E-02	1.2990E-02	1.2812E-02
353.15	9.21	7.6436E-03	9.4155E-03	1.1807E-02	1.2950E-02	1.3577E-02	1.3529E-02	1.2905E-02	1.2722E-02
353.15	10.22	7.5870E-03	9.3501E-03	1.1732E-02	1.2870E-02	1.3494E-02	1.3445E-02	1.2820E-02	1.2634E-02
353.15	11.23	7.5313E-03	9.2857E-03	1.1657E-02	1.2790E-02	1.3413E-02	1.3361E-02	1.2737E-02	1.2547E-02
353.15	12.24	7.4763E-03	9.2221E-03	1.1584E-02	1.2712E-02	1.3332E-02	1.3279E-02	1.2655E-02	1.2461E-02
353.15	13.25	7.4222E-03	9.1594E-03	1.1511E-02	1.2635E-02	1.3253E-02	1.3197E-02	1.2573E-02	1.2377E-02
353.15	14.26	7.3688E-03	9.0975E-03	1.1439E-02	1.2559E-02	1.3174E-02	1.3117E-02	1.2493E-02	1.2293E-02
353.15	15.25	7.3162E-03	9.0365E-03	1.1369E-02	1.2484E-02	1.3097E-02	1.3037E-02	1.2414E-02	1.2211E-02
353.15	16.27	7.2644E-03	8.9763E-03	1.1299E-02	1.2409E-02	1.3020E-02	1.2959E-02	1.2336E-02	1.2130E-02
353.15	17.27	7.2133E-03	8.9169E-03	1.1229E-02	1.2336E-02	1.2944E-02	1.2881E-02	1.2259E-02	1.2050E-02
353.15	18.29	7.1628E-03	8.8582E-03	1.1161E-02	1.2263E-02	1.2869E-02	1.2805E-02	1.2182E-02	1.1971E-02
353.15	19.29	7.1131E-03	8.8003E-03	1.1094E-02	1.2191E-02	1.2795E-02	1.2729E-02	1.2107E-02	1.1892E-02
353.15	20.29	7.0641E-03	8.7432E-03	1.1027E-02	1.2120E-02	1.2722E-02	1.2654E-02	1.2033E-02	1.1815E-02

Expanded combined uncertainties (k = 2) U_c are $U_c(T) = 0.02\ K.\ U_c(P) = 0.032\ MPa.\ U_c(x_i) = 0.0002.\ U_{c,r} = (\alpha_p) = 0.035.$

Table B5: Thermal Expansivity (α_p) of 2-methlpropan-1-ol (1) + n-octane (2) at various pressures and temperatures.

T/K	P/MPa	α_p/K^{-1}							
		$x_1=0$	$x_1=0.1267$	$x_1=0.3776$	$x_1=0.4996$	$x_1=0.6255$	$x_1=0.7499$	$x_1=0.8739$	$x_1=1$
313.15	0.1	9.6446E-03	1.1759E-02	1.3876E-02	1.4385E-02	1.4571E-02	1.4609E-02	1.4874E-02	1.1991E-02
313.15	1.14	9.5702E-03	1.1666E-02	1.3777E-02	1.4284E-02	1.4469E-02	1.4506E-02	1.4769E-02	1.1919E-02
313.15	2.14	9.4889E-03	1.1566E-02	1.3669E-02	1.4174E-02	1.4357E-02	1.4393E-02	1.4653E-02	1.1839E-02
313.15	3.15	9.4090E-03	1.1467E-02	1.3562E-02	1.4065E-02	1.4247E-02	1.4282E-02	1.4540E-02	1.1761E-02
313.15	4.16	9.3304E-03	1.1369E-02	1.3457E-02	1.3958E-02	1.4139E-02	1.4172E-02	1.4428E-02	1.1683E-02
313.15	5.17	9.2531E-03	1.1273E-02	1.3354E-02	1.3853E-02	1.4032E-02	1.4065E-02	1.4318E-02	1.1607E-02
313.15	6.18	9.1771E-03	1.1179E-02	1.3252E-02	1.3749E-02	1.3927E-02	1.3959E-02	1.4210E-02	1.1531E-02
313.15	7.19	9.1023E-03	1.1086E-02	1.3152E-02	1.3647E-02	1.3824E-02	1.3854E-02	1.4103E-02	1.1457E-02
313.15	8.2	9.0288E-03	1.0995E-02	1.3054E-02	1.3546E-02	1.3722E-02	1.3751E-02	1.3998E-02	1.1383E-02
313.15	9.23	8.9564E-03	1.0906E-02	1.2956E-02	1.3447E-02	1.3621E-02	1.3650E-02	1.3894E-02	1.1310E-02
313.15	10.23	8.8851E-03	1.0818E-02	1.2861E-02	1.3349E-02	1.3522E-02	1.3550E-02	1.3792E-02	1.1239E-02
313.15	11.24	8.8150E-03	1.0731E-02	1.2766E-02	1.3253E-02	1.3424E-02	1.3451E-02	1.3692E-02	1.1168E-02
313.15	12.25	8.7460E-03	1.0645E-02	1.2673E-02	1.3158E-02	1.3328E-02	1.3354E-02	1.3593E-02	1.1098E-02
313.15	13.26	8.6781E-03	1.0561E-02	1.2582E-02	1.3064E-02	1.3233E-02	1.3259E-02	1.3495E-02	1.1029E-02
313.15	14.27	8.6112E-03	1.0479E-02	1.2492E-02	1.2972E-02	1.3140E-02	1.3164E-02	1.3399E-02	1.0961E-02
313.15	15.27	8.5453E-03	1.0397E-02	1.2403E-02	1.2881E-02	1.3047E-02	1.3071E-02	1.3304E-02	1.0893E-02
313.15	16.28	8.4804E-03	1.0317E-02	1.2315E-02	1.2791E-02	1.2957E-02	1.2980E-02	1.3210E-02	1.0827E-02
313.15	17.29	8.4165E-03	1.0238E-02	1.2228E-02	1.2703E-02	1.2867E-02	1.2889E-02	1.3118E-02	1.0761E-02
313.15	18.3	8.3536E-03	1.0160E-02	1.2143E-02	1.2615E-02	1.2778E-02	1.2800E-02	1.3027E-02	1.0696E-02
313.15	19.3	8.2916E-03	1.0084E-02	1.2059E-02	1.2529E-02	1.2691E-02	1.2712E-02	1.2937E-02	1.0632E-02
313.15	20.31	8.2305E-03	1.0008E-02	1.1976E-02	1.2444E-02	1.2605E-02	1.2625E-02	1.2849E-02	1.0568E-02
323.15	0.1	9.4225E-03	1.1500E-02	1.3580E-02	1.4079E-02	1.4259E-02	1.4293E-02	1.4548E-02	1.1711E-02
323.15	1.15	9.3490E-03	1.1409E-02	1.3482E-02	1.3979E-02	1.4158E-02	1.4191E-02	1.4444E-02	1.1639E-02
323.15	2.15	9.2686E-03	1.1309E-02	1.3375E-02	1.3870E-02	1.4047E-02	1.4079E-02	1.4330E-02	1.1560E-02
323.15	3.17	9.1896E-03	1.1211E-02	1.3269E-02	1.3762E-02	1.3938E-02	1.3969E-02	1.4217E-02	1.1483E-02
323.15	4.18	9.1119E-03	1.1114E-02	1.3165E-02	1.3656E-02	1.3831E-02	1.3861E-02	1.4107E-02	1.1406E-02
323.15	5.19	9.0356E-03	1.1020E-02	1.3063E-02	1.3552E-02	1.3725E-02	1.3754E-02	1.3998E-02	1.1331E-02
323.15	6.2	8.9605E-03	1.0926E-02	1.2963E-02	1.3449E-02	1.3621E-02	1.3649E-02	1.3891E-02	1.1256E-02
323.15	7.22	8.8866E-03	1.0835E-02	1.2863E-02	1.3348E-02	1.3519E-02	1.3546E-02	1.3786E-02	1.1183E-02
323.15	8.23	8.8140E-03	1.0745E-02	1.2766E-02	1.3248E-02	1.3418E-02	1.3444E-02	1.3682E-02	1.1110E-02
323.15	9.24	8.7425E-03	1.0656E-02	1.2670E-02	1.3150E-02	1.3318E-02	1.3344E-02	1.3579E-02	1.1039E-02
323.15	10.25	8.6722E-03	1.0569E-02	1.2575E-02	1.3053E-02	1.3220E-02	1.3245E-02	1.3479E-02	1.0968E-02
323.15	11.25	8.6030E-03	1.0483E-02	1.2482E-02	1.2958E-02	1.3124E-02	1.3147E-02	1.3379E-02	1.0898E-02
323.15	12.27	8.5349E-03	1.0399E-02	1.2390E-02	1.2864E-02	1.3029E-02	1.3051E-02	1.3281E-02	1.0829E-02
323.15	13.27	8.4679E-03	1.0316E-02	1.2299E-02	1.2771E-02	1.2935E-02	1.2957E-02	1.3185E-02	1.0761E-02

323.15	14.26	8.4019E-03	1.0234E-02	1.2210E-02	1.2680E-02	1.2842E-02	1.2864E-02	1.3090E-02	1.0694E-02
323.15	15.29	8.3369E-03	1.0154E-02	1.2122E-02	1.2590E-02	1.2751E-02	1.2772E-02	1.2996E-02	1.0628E-02
323.15	16.3	8.2730E-03	1.0074E-02	1.2035E-02	1.2501E-02	1.2661E-02	1.2681E-02	1.2904E-02	1.0562E-02
323.15	17.3	8.2100E-03	9.9965E-03	1.1950E-02	1.2414E-02	1.2573E-02	1.2592E-02	1.2813E-02	1.0497E-02
323.15	18.3	8.1479E-03	9.9198E-03	1.1865E-02	1.2327E-02	1.2485E-02	1.2504E-02	1.2723E-02	1.0433E-02
323.15	19.3	8.0868E-03	9.8442E-03	1.1782E-02	1.2242E-02	1.2399E-02	1.2417E-02	1.2634E-02	1.0370E-02
323.15	20.29	8.0266E-03	9.7697E-03	1.1700E-02	1.2158E-02	1.2314E-02	1.2331E-02	1.2547E-02	1.0308E-02
333.15	0.1	9.2161E-03	1.1262E-02	1.3310E-02	1.3801E-02	1.3975E-02	1.4005E-02	1.4252E-02	1.1452E-02
333.15	1.13	9.1433E-03	1.1171E-02	1.3213E-02	1.3701E-02	1.3875E-02	1.3904E-02	1.4148E-02	1.1381E-02
333.15	2.13	9.0638E-03	1.1072E-02	1.3107E-02	1.3593E-02	1.3765E-02	1.3793E-02	1.4035E-02	1.1304E-02
333.15	3.14	8.9856E-03	1.0975E-02	1.3002E-02	1.3486E-02	1.3657E-02	1.3684E-02	1.3924E-02	1.1227E-02
333.15	4.15	8.9087E-03	1.0879E-02	1.2899E-02	1.3381E-02	1.3550E-02	1.3576E-02	1.3814E-02	1.1151E-02
333.15	5.16	8.8332E-03	1.0785E-02	1.2797E-02	1.3277E-02	1.3445E-02	1.3471E-02	1.3707E-02	1.1077E-02
333.15	6.17	8.7589E-03	1.0693E-02	1.2697E-02	1.3175E-02	1.3342E-02	1.3367E-02	1.3600E-02	1.1003E-02
333.15	7.18	8.6859E-03	1.0602E-02	1.2599E-02	1.3075E-02	1.3240E-02	1.3264E-02	1.3496E-02	1.0931E-02
333.15	8.19	8.6140E-03	1.0513E-02	1.2502E-02	1.2976E-02	1.3140E-02	1.3163E-02	1.3393E-02	1.0859E-02
333.15	9.2	8.5434E-03	1.0425E-02	1.2407E-02	1.2878E-02	1.3042E-02	1.3064E-02	1.3292E-02	1.0788E-02
333.15	10.21	8.4739E-03	1.0339E-02	1.2313E-02	1.2782E-02	1.2945E-02	1.2966E-02	1.3192E-02	1.0718E-02
333.15	11.22	8.4055E-03	1.0254E-02	1.2220E-02	1.2688E-02	1.2849E-02	1.2869E-02	1.3094E-02	1.0649E-02
333.15	12.23	8.3382E-03	1.0171E-02	1.2129E-02	1.2595E-02	1.2755E-02	1.2774E-02	1.2997E-02	1.0581E-02
333.15	13.24	8.2720E-03	1.0088E-02	1.2039E-02	1.2503E-02	1.2662E-02	1.2681E-02	1.2901E-02	1.0514E-02
333.15	14.25	8.2068E-03	1.0008E-02	1.1951E-02	1.2412E-02	1.2570E-02	1.2588E-02	1.2807E-02	1.0448E-02
333.15	15.26	8.1427E-03	9.9281E-03	1.1864E-02	1.2323E-02	1.2480E-02	1.2497E-02	1.2714E-02	1.0382E-02
333.15	16.27	8.0795E-03	9.8498E-03	1.1778E-02	1.2235E-02	1.2391E-02	1.2408E-02	1.2623E-02	1.0318E-02
333.15	17.27	8.0173E-03	9.7727E-03	1.1693E-02	1.2149E-02	1.2303E-02	1.2319E-02	1.2533E-02	1.0254E-02
333.15	18.28	7.9561E-03	9.6968E-03	1.1610E-02	1.2063E-02	1.2217E-02	1.2232E-02	1.2444E-02	1.0191E-02
333.15	19.28	7.8958E-03	9.6221E-03	1.1527E-02	1.1979E-02	1.2131E-02	1.2146E-02	1.2357E-02	1.0128E-02
333.15	20.28	7.8364E-03	9.5485E-03	1.1446E-02	1.1896E-02	1.2047E-02	1.2062E-02	1.2270E-02	1.0067E-02
343.15	0.1	9.0240E-03	1.1042E-02	1.3064E-02	1.3546E-02	1.3717E-02	1.3743E-02	1.3982E-02	1.1214E-02
343.15	1.14	8.9518E-03	1.0952E-02	1.2967E-02	1.3448E-02	1.3617E-02	1.3642E-02	1.3879E-02	1.1144E-02
343.15	2.14	8.8729E-03	1.0854E-02	1.2861E-02	1.3340E-02	1.3507E-02	1.3532E-02	1.3767E-02	1.1067E-02
343.15	3.14	8.7954E-03	1.0757E-02	1.2757E-02	1.3233E-02	1.3400E-02	1.3424E-02	1.3656E-02	1.0991E-02
343.15	4.16	8.7193E-03	1.0662E-02	1.2654E-02	1.3129E-02	1.3294E-02	1.3317E-02	1.3548E-02	1.0916E-02
343.15	5.17	8.6445E-03	1.0569E-02	1.2553E-02	1.3026E-02	1.3190E-02	1.3212E-02	1.3441E-02	1.0842E-02
343.15	6.18	8.5709E-03	1.0477E-02	1.2454E-02	1.2924E-02	1.3087E-02	1.3108E-02	1.3335E-02	1.0769E-02
343.15	7.19	8.4986E-03	1.0387E-02	1.2356E-02	1.2824E-02	1.2986E-02	1.3006E-02	1.3231E-02	1.0697E-02
343.15	8.2	8.4274E-03	1.0299E-02	1.2260E-02	1.2726E-02	1.2886E-02	1.2906E-02	1.3129E-02	1.0627E-02
343.15	9.21	8.3575E-03	1.0212E-02	1.2165E-02	1.2629E-02	1.2788E-02	1.2808E-02	1.3029E-02	1.0557E-02
343.15	10.22	8.2887E-03	1.0126E-02	1.2072E-02	1.2534E-02	1.2692E-02	1.2710E-02	1.2930E-02	1.0487E-02
343.15	11.23	8.2211E-03	1.0042E-02	1.1980E-02	1.2440E-02	1.2597E-02	1.2615E-02	1.2832E-02	1.0419E-02
343.15	12.24	8.1545E-03	9.9590E-03	1.1890E-02	1.2348E-02	1.2503E-02	1.2520E-02	1.2736E-02	1.0352E-02
343.15	13.25	8.0890E-03	9.8776E-03	1.1801E-02	1.2256E-02	1.2411E-02	1.2427E-02	1.2641E-02	1.0286E-02
343.15	14.26	8.0246E-03	9.7975E-03	1.1713E-02	1.2167E-02	1.2320E-02	1.2336E-02	1.2548E-02	1.0220E-02

343.15	15.27	7.9611E-03	9.7187E-03	1.1626E-02	1.2078E-02	1.2231E-02	1.2246E-02	1.2456E-02	1.0155E-02
343.15	16.27	7.8987E-03	9.6411E-03	1.1541E-02	1.1991E-02	1.2142E-02	1.2157E-02	1.2365E-02	1.0091E-02
343.15	17.28	7.8372E-03	9.5648E-03	1.1457E-02	1.1905E-02	1.2055E-02	1.2069E-02	1.2276E-02	1.0028E-02
343.15	18.28	7.7767E-03	9.4896E-03	1.1374E-02	1.1820E-02	1.1969E-02	1.1983E-02	1.2188E-02	9.9659E-03
343.15	19.29	7.7171E-03	9.4157E-03	1.1293E-02	1.1737E-02	1.1885E-02	1.1898E-02	1.2101E-02	9.9043E-03
343.15	20.29	7.6584E-03	9.3429E-03	1.1212E-02	1.1654E-02	1.1801E-02	1.1814E-02	1.2016E-02	9.8435E-03
353.15	0.1	8.8447E-03	1.0839E-02	1.2838E-02	1.3315E-02	1.3481E-02	1.3504E-02	1.3736E-02	1.0993E-02
353.15	1.14	8.7730E-03	1.0749E-02	1.2742E-02	1.3216E-02	1.3381E-02	1.3404E-02	1.3634E-02	1.0924E-02
353.15	2.14	8.6948E-03	1.0651E-02	1.2636E-02	1.3108E-02	1.3272E-02	1.3294E-02	1.3522E-02	1.0847E-02
353.15	3.14	8.6179E-03	1.0555E-02	1.2532E-02	1.3002E-02	1.3165E-02	1.3186E-02	1.3412E-02	1.0772E-02
353.15	4.16	8.5424E-03	1.0461E-02	1.2430E-02	1.2898E-02	1.3059E-02	1.3079E-02	1.3304E-02	1.0698E-02
353.15	5.16	8.4681E-03	1.0368E-02	1.2330E-02	1.2796E-02	1.2955E-02	1.2975E-02	1.3197E-02	1.0625E-02
353.15	6.18	8.3952E-03	1.0277E-02	1.2231E-02	1.2695E-02	1.2853E-02	1.2872E-02	1.3092E-02	1.0553E-02
353.15	7.19	8.3235E-03	1.0187E-02	1.2133E-02	1.2595E-02	1.2753E-02	1.2771E-02	1.2989E-02	1.0481E-02
353.15	8.2	8.2530E-03	1.0099E-02	1.2038E-02	1.2497E-02	1.2654E-02	1.2671E-02	1.2888E-02	1.0411E-02
353.15	9.21	8.1837E-03	1.0013E-02	1.1943E-02	1.2401E-02	1.2556E-02	1.2573E-02	1.2787E-02	1.0342E-02
353.15	10.22	8.1156E-03	9.9280E-03	1.1851E-02	1.2306E-02	1.2460E-02	1.2476E-02	1.2689E-02	1.0273E-02
353.15	11.23	8.0485E-03	9.8445E-03	1.1759E-02	1.2213E-02	1.2366E-02	1.2381E-02	1.2592E-02	1.0206E-02
353.15	12.24	7.9826E-03	9.7623E-03	1.1669E-02	1.2120E-02	1.2272E-02	1.2287E-02	1.2496E-02	1.0139E-02
353.15	13.25	7.9178E-03	9.6815E-03	1.1581E-02	1.2030E-02	1.2181E-02	1.2195E-02	1.2402E-02	1.0073E-02
353.15	14.26	7.8540E-03	9.6020E-03	1.1493E-02	1.1940E-02	1.2090E-02	1.2104E-02	1.2310E-02	1.0009E-02
353.15	15.25	7.7912E-03	9.5239E-03	1.1407E-02	1.1852E-02	1.2001E-02	1.2014E-02	1.2218E-02	9.9444E-03
353.15	16.27	7.7294E-03	9.4470E-03	1.1323E-02	1.1766E-02	1.1914E-02	1.1926E-02	1.2128E-02	9.8812E-03
353.15	17.27	7.6686E-03	9.3713E-03	1.1239E-02	1.1680E-02	1.1827E-02	1.1839E-02	1.2040E-02	9.8187E-03
353.15	18.29	7.6087E-03	9.2968E-03	1.1157E-02	1.1596E-02	1.1742E-02	1.1753E-02	1.1952E-02	9.7570E-03
353.15	19.29	7.5498E-03	9.2235E-03	1.1076E-02	1.1513E-02	1.1658E-02	1.1668E-02	1.1866E-02	9.6961E-03
353.15	20.29	7.4917E-03	9.1513E-03	1.0996E-02	1.1431E-02	1.1575E-02	1.1585E-02	1.1782E-02	9.6359E-03

Expanded combined uncertainties (k = 2) U_c are $U_c(T) = 0.02\ K.\ U_c(P) = 0.032\ MPa.\ U_c(x_i) = 0.0002.\ U_{c,r} = (\alpha_p) = 0.041.$

Table B6: Thermal Expansivity (α_p) of 2-methlpropan-1-ol (1) + n-decane (2) at various pressures and temperatures.

T/K	P/MPa	α_p/K^{-1}							
		x_1=0	*x_1=0.1276*	*x_1=0.3749*	*x_1=0.5015*	*x_1=0.6249*	*x_1=0.7502*	*x_1=0.8750*	*x_1=1*
313.15	0.1	8.9818E-03	1.0944E-02	1.3721E-02	1.4708E-02	1.5690E-02	1.4947E-02	1.4926E-02	1.1991E-02
313.15	1.14	8.9203E-03	1.0864E-02	1.3628E-02	1.4612E-02	1.5589E-02	1.4851E-02	1.4827E-02	1.1919E-02
313.15	2.14	8.8530E-03	1.0777E-02	1.3527E-02	1.4508E-02	1.5479E-02	1.4745E-02	1.4718E-02	1.1839E-02
313.15	3.15	8.7867E-03	1.0691E-02	1.3427E-02	1.4404E-02	1.5370E-02	1.4641E-02	1.4612E-02	1.1761E-02
313.15	4.16	8.7214E-03	1.0607E-02	1.3328E-02	1.4302E-02	1.5262E-02	1.4538E-02	1.4506E-02	1.1683E-02
313.15	5.17	8.6570E-03	1.0523E-02	1.3231E-02	1.4202E-02	1.5156E-02	1.4437E-02	1.4403E-02	1.1607E-02
313.15	6.18	8.5936E-03	1.0442E-02	1.3136E-02	1.4103E-02	1.5051E-02	1.4337E-02	1.4300E-02	1.1531E-02
313.15	7.19	8.5311E-03	1.0361E-02	1.3042E-02	1.4005E-02	1.4948E-02	1.4238E-02	1.4200E-02	1.1457E-02
313.15	8.2	8.4695E-03	1.0282E-02	1.2949E-02	1.3909E-02	1.4846E-02	1.4141E-02	1.4100E-02	1.1383E-02
313.15	9.23	8.4088E-03	1.0204E-02	1.2857E-02	1.3814E-02	1.4746E-02	1.4045E-02	1.4002E-02	1.1310E-02
313.15	10.23	8.3490E-03	1.0127E-02	1.2767E-02	1.3720E-02	1.4647E-02	1.3950E-02	1.3906E-02	1.1239E-02
313.15	11.24	8.2900E-03	1.0051E-02	1.2678E-02	1.3628E-02	1.4549E-02	1.3857E-02	1.3810E-02	1.1168E-02
313.15	12.25	8.2318E-03	9.9763E-03	1.2590E-02	1.3537E-02	1.4453E-02	1.3765E-02	1.3716E-02	1.1098E-02
313.15	13.26	8.1745E-03	9.9027E-03	1.2503E-02	1.3447E-02	1.4358E-02	1.3674E-02	1.3623E-02	1.1029E-02
313.15	14.27	8.1179E-03	9.8302E-03	1.2418E-02	1.3358E-02	1.4264E-02	1.3584E-02	1.3532E-02	1.0961E-02
313.15	15.27	8.0621E-03	9.7588E-03	1.2334E-02	1.3270E-02	1.4171E-02	1.3495E-02	1.3442E-02	1.0893E-02
313.15	16.28	8.0071E-03	9.6884E-03	1.2251E-02	1.3184E-02	1.4079E-02	1.3408E-02	1.3353E-02	1.0827E-02
313.15	17.29	7.9528E-03	9.6190E-03	1.2169E-02	1.3099E-02	1.3989E-02	1.3322E-02	1.3265E-02	1.0761E-02
313.15	18.3	7.8993E-03	9.5506E-03	1.2088E-02	1.3014E-02	1.3900E-02	1.3236E-02	1.3178E-02	1.0696E-02
313.15	19.3	7.8465E-03	9.4832E-03	1.2008E-02	1.2931E-02	1.3812E-02	1.3152E-02	1.3092E-02	1.0632E-02
313.15	20.31	7.7943E-03	9.4167E-03	1.1929E-02	1.2849E-02	1.3725E-02	1.3069E-02	1.3008E-02	1.0568E-02
323.15	0.1	8.7616E-03	1.0687E-02	1.3414E-02	1.4385E-02	1.5350E-02	1.4621E-02	1.4596E-02	1.1711E-02
323.15	1.15	8.7011E-03	1.0608E-02	1.3323E-02	1.4291E-02	1.5250E-02	1.4526E-02	1.4498E-02	1.1639E-02
323.15	2.15	8.6347E-03	1.0522E-02	1.3222E-02	1.4187E-02	1.5140E-02	1.4421E-02	1.4391E-02	1.1560E-02
323.15	3.17	8.5694E-03	1.0438E-02	1.3124E-02	1.4085E-02	1.5032E-02	1.4318E-02	1.4285E-02	1.1483E-02
323.15	4.18	8.5051E-03	1.0354E-02	1.3026E-02	1.3984E-02	1.4926E-02	1.4216E-02	1.4181E-02	1.1406E-02
323.15	5.19	8.4417E-03	1.0272E-02	1.2930E-02	1.3885E-02	1.4821E-02	1.4116E-02	1.4079E-02	1.1331E-02
323.15	6.2	8.3793E-03	1.0192E-02	1.2836E-02	1.3787E-02	1.4718E-02	1.4017E-02	1.3978E-02	1.1256E-02
323.15	7.22	8.3177E-03	1.0112E-02	1.2743E-02	1.3690E-02	1.4616E-02	1.3919E-02	1.3878E-02	1.1183E-02
323.15	8.23	8.2571E-03	1.0034E-02	1.2651E-02	1.3595E-02	1.4515E-02	1.3823E-02	1.3780E-02	1.1110E-02
323.15	9.24	8.1974E-03	9.9570E-03	1.2561E-02	1.3501E-02	1.4416E-02	1.3728E-02	1.3683E-02	1.1039E-02
323.15	10.25	8.1385E-03	9.8811E-03	1.2471E-02	1.3409E-02	1.4318E-02	1.3635E-02	1.3588E-02	1.0968E-02
323.15	11.25	8.0804E-03	9.8065E-03	1.2384E-02	1.3318E-02	1.4221E-02	1.3542E-02	1.3493E-02	1.0898E-02
323.15	12.27	8.0232E-03	9.7329E-03	1.2297E-02	1.3227E-02	1.4126E-02	1.3451E-02	1.3400E-02	1.0829E-02

323.15	13.27	7.9667E-03	9.6604E-03	1.2211E-02	1.3139E-02	1.4032E-02	1.3361E-02	1.3309E-02	1.0761E-02
323.15	14.26	7.9111E-03	9.5890E-03	1.2127E-02	1.3051E-02	1.3939E-02	1.3273E-02	1.3219E-02	1.0694E-02
323.15	15.29	7.8562E-03	9.5187E-03	1.2044E-02	1.2964E-02	1.3847E-02	1.3185E-02	1.3129E-02	1.0628E-02
323.15	16.3	7.8021E-03	9.4494E-03	1.1962E-02	1.2879E-02	1.3757E-02	1.3099E-02	1.3042E-02	1.0562E-02
323.15	17.3	7.7488E-03	9.3810E-03	1.1881E-02	1.2795E-02	1.3668E-02	1.3014E-02	1.2955E-02	1.0497E-02
323.15	18.3	7.6961E-03	9.3137E-03	1.1801E-02	1.2712E-02	1.3580E-02	1.2930E-02	1.2869E-02	1.0433E-02
323.15	19.3	7.6442E-03	9.2473E-03	1.1723E-02	1.2629E-02	1.3493E-02	1.2847E-02	1.2785E-02	1.0370E-02
323.15	20.29	7.5929E-03	9.1819E-03	1.1645E-02	1.2548E-02	1.3407E-02	1.2765E-02	1.2701E-02	1.0308E-02
333.15	0.1	8.5568E-03	1.0450E-02	1.3134E-02	1.4092E-02	1.5042E-02	1.4325E-02	1.4296E-02	1.1452E-02
333.15	1.13	8.4970E-03	1.0372E-02	1.3043E-02	1.3998E-02	1.4943E-02	1.4230E-02	1.4199E-02	1.1381E-02
333.15	2.13	8.4315E-03	1.0287E-02	1.2944E-02	1.3895E-02	1.4834E-02	1.4126E-02	1.4093E-02	1.1304E-02
333.15	3.14	8.3671E-03	1.0203E-02	1.2846E-02	1.3794E-02	1.4727E-02	1.4024E-02	1.3988E-02	1.1227E-02
333.15	4.15	8.3036E-03	1.0121E-02	1.2750E-02	1.3694E-02	1.4621E-02	1.3923E-02	1.3885E-02	1.1151E-02
333.15	5.16	8.2411E-03	1.0040E-02	1.2655E-02	1.3596E-02	1.4517E-02	1.3823E-02	1.3784E-02	1.1077E-02
333.15	6.17	8.1795E-03	9.9601E-03	1.2561E-02	1.3499E-02	1.4415E-02	1.3725E-02	1.3683E-02	1.1003E-02
333.15	7.18	8.1189E-03	9.8817E-03	1.2469E-02	1.3403E-02	1.4313E-02	1.3629E-02	1.3585E-02	1.0931E-02
333.15	8.19	8.0591E-03	9.8045E-03	1.2378E-02	1.3309E-02	1.4214E-02	1.3533E-02	1.3488E-02	1.0859E-02
333.15	9.2	8.0002E-03	9.7284E-03	1.2289E-02	1.3216E-02	1.4115E-02	1.3439E-02	1.3392E-02	1.0788E-02
333.15	10.21	7.9422E-03	9.6536E-03	1.2200E-02	1.3124E-02	1.4018E-02	1.3347E-02	1.3297E-02	1.0718E-02
333.15	11.22	7.8850E-03	9.5798E-03	1.2113E-02	1.3034E-02	1.3922E-02	1.3255E-02	1.3204E-02	1.0649E-02
333.15	12.23	7.8286E-03	9.5072E-03	1.2028E-02	1.2945E-02	1.3828E-02	1.3165E-02	1.3112E-02	1.0581E-02
333.15	13.24	7.7730E-03	9.4357E-03	1.1943E-02	1.2857E-02	1.3735E-02	1.3076E-02	1.3021E-02	1.0514E-02
333.15	14.25	7.7182E-03	9.3653E-03	1.1860E-02	1.2770E-02	1.3643E-02	1.2989E-02	1.2932E-02	1.0448E-02
333.15	15.26	7.6642E-03	9.2959E-03	1.1778E-02	1.2684E-02	1.3552E-02	1.2902E-02	1.2844E-02	1.0382E-02
333.15	16.27	7.6109E-03	9.2275E-03	1.1697E-02	1.2600E-02	1.3463E-02	1.2816E-02	1.2757E-02	1.0318E-02
333.15	17.27	7.5583E-03	9.1601E-03	1.1617E-02	1.2516E-02	1.3375E-02	1.2732E-02	1.2671E-02	1.0254E-02
333.15	18.28	7.5065E-03	9.0937E-03	1.1538E-02	1.2434E-02	1.3288E-02	1.2649E-02	1.2586E-02	1.0191E-02
333.15	19.28	7.4554E-03	9.0283E-03	1.1460E-02	1.2353E-02	1.3201E-02	1.2567E-02	1.2503E-02	1.0128E-02
333.15	20.28	7.4049E-03	8.9637E-03	1.1383E-02	1.2273E-02	1.3117E-02	1.2486E-02	1.2420E-02	1.0067E-02
343.15	0.1	8.3656E-03	1.0230E-02	1.2877E-02	1.3825E-02	1.4762E-02	1.4055E-02	1.4023E-02	1.1214E-02
343.15	1.14	8.3066E-03	1.0153E-02	1.2787E-02	1.3731E-02	1.4664E-02	1.3961E-02	1.3927E-02	1.1144E-02
343.15	2.14	8.2419E-03	1.0069E-02	1.2689E-02	1.3629E-02	1.4556E-02	1.3858E-02	1.3821E-02	1.1067E-02
343.15	3.14	8.1782E-03	9.9859E-03	1.2592E-02	1.3529E-02	1.4449E-02	1.3756E-02	1.3718E-02	1.0991E-02
343.15	4.16	8.1156E-03	9.9044E-03	1.2496E-02	1.3429E-02	1.4344E-02	1.3656E-02	1.3615E-02	1.0916E-02
343.15	5.17	8.0538E-03	9.8242E-03	1.2402E-02	1.3332E-02	1.4241E-02	1.3557E-02	1.3514E-02	1.0842E-02
343.15	6.18	7.9930E-03	9.7453E-03	1.2309E-02	1.3235E-02	1.4139E-02	1.3459E-02	1.3415E-02	1.0769E-02
343.15	7.19	7.9332E-03	9.6677E-03	1.2218E-02	1.3140E-02	1.4038E-02	1.3363E-02	1.3317E-02	1.0697E-02
343.15	8.2	7.8742E-03	9.5913E-03	1.2128E-02	1.3047E-02	1.3939E-02	1.3269E-02	1.3220E-02	1.0627E-02
343.15	9.21	7.8160E-03	9.5161E-03	1.2039E-02	1.2954E-02	1.3841E-02	1.3175E-02	1.3125E-02	1.0557E-02
343.15	10.22	7.7588E-03	9.4421E-03	1.1951E-02	1.2863E-02	1.3745E-02	1.3084E-02	1.3031E-02	1.0487E-02
343.15	11.23	7.7023E-03	9.3692E-03	1.1865E-02	1.2774E-02	1.3650E-02	1.2993E-02	1.2939E-02	1.0419E-02
343.15	12.24	7.6467E-03	9.2975E-03	1.1780E-02	1.2685E-02	1.3556E-02	1.2903E-02	1.2848E-02	1.0352E-02
343.15	13.25	7.5919E-03	9.2268E-03	1.1696E-02	1.2598E-02	1.3464E-02	1.2815E-02	1.2758E-02	1.0286E-02

343.15	14.26	7.5378E-03	9.1572E-03	1.1614E-02	1.2512E-02	1.3373E-02	1.2728E-02	1.2669E-02	1.0220E-02
343.15	15.27	7.4845E-03	9.0886E-03	1.1532E-02	1.2427E-02	1.3283E-02	1.2642E-02	1.2582E-02	1.0155E-02
343.15	16.27	7.4320E-03	9.0211E-03	1.1452E-02	1.2343E-02	1.3194E-02	1.2557E-02	1.2496E-02	1.0091E-02
343.15	17.28	7.3802E-03	8.9545E-03	1.1373E-02	1.2261E-02	1.3107E-02	1.2474E-02	1.2411E-02	1.0028E-02
343.15	18.28	7.3291E-03	8.8890E-03	1.1295E-02	1.2179E-02	1.3020E-02	1.2391E-02	1.2327E-02	9.9659E-03
343.15	19.29	7.2787E-03	8.8243E-03	1.1218E-02	1.2099E-02	1.2935E-02	1.2310E-02	1.2244E-02	9.9043E-03
343.15	20.29	7.2290E-03	8.7606E-03	1.1142E-02	1.2019E-02	1.2851E-02	1.2230E-02	1.2163E-02	9.8435E-03
353.15	0.1	8.1870E-03	1.0026E-02	1.2642E-02	1.3581E-02	1.4509E-02	1.3809E-02	1.3775E-02	1.0993E-02
353.15	1.14	8.1285E-03	9.9496E-03	1.2553E-02	1.3488E-02	1.4411E-02	1.3716E-02	1.3679E-02	1.0924E-02
353.15	2.14	8.0646E-03	9.8661E-03	1.2455E-02	1.3386E-02	1.4303E-02	1.3613E-02	1.3574E-02	1.0847E-02
353.15	3.14	8.0016E-03	9.7840E-03	1.2358E-02	1.3286E-02	1.4197E-02	1.3511E-02	1.3470E-02	1.0772E-02
353.15	4.16	7.9396E-03	9.7032E-03	1.2263E-02	1.3187E-02	1.4092E-02	1.3412E-02	1.3368E-02	1.0698E-02
353.15	5.16	7.8786E-03	9.6238E-03	1.2169E-02	1.3090E-02	1.3989E-02	1.3313E-02	1.3268E-02	1.0625E-02
353.15	6.18	7.8185E-03	9.5456E-03	1.2077E-02	1.2994E-02	1.3888E-02	1.3216E-02	1.3169E-02	1.0553E-02
353.15	7.19	7.7593E-03	9.4687E-03	1.1986E-02	1.2900E-02	1.3788E-02	1.3121E-02	1.3072E-02	1.0481E-02
353.15	8.2	7.7010E-03	9.3930E-03	1.1897E-02	1.2807E-02	1.3689E-02	1.3027E-02	1.2976E-02	1.0411E-02
353.15	9.21	7.6436E-03	9.3186E-03	1.1809E-02	1.2715E-02	1.3592E-02	1.2934E-02	1.2881E-02	1.0342E-02
353.15	10.22	7.5870E-03	9.2453E-03	1.1722E-02	1.2624E-02	1.3496E-02	1.2842E-02	1.2788E-02	1.0273E-02
353.15	11.23	7.5313E-03	9.1731E-03	1.1636E-02	1.2535E-02	1.3401E-02	1.2752E-02	1.2696E-02	1.0206E-02
353.15	12.24	7.4763E-03	9.1021E-03	1.1552E-02	1.2447E-02	1.3308E-02	1.2663E-02	1.2606E-02	1.0139E-02
353.15	13.25	7.4222E-03	9.0322E-03	1.1469E-02	1.2361E-02	1.3216E-02	1.2576E-02	1.2516E-02	1.0073E-02
353.15	14.26	7.3688E-03	8.9633E-03	1.1387E-02	1.2275E-02	1.3126E-02	1.2489E-02	1.2428E-02	1.0009E-02
353.15	15.25	7.3162E-03	8.8955E-03	1.1306E-02	1.2191E-02	1.3036E-02	1.2404E-02	1.2342E-02	9.9444E-03
353.15	16.27	7.2644E-03	8.8286E-03	1.1226E-02	1.2108E-02	1.2948E-02	1.2320E-02	1.2256E-02	9.8812E-03
353.15	17.27	7.2133E-03	8.7628E-03	1.1148E-02	1.2026E-02	1.2861E-02	1.2236E-02	1.2172E-02	9.8187E-03
353.15	18.29	7.1628E-03	8.6980E-03	1.1070E-02	1.1945E-02	1.2775E-02	1.2155E-02	1.2088E-02	9.7570E-03
353.15	19.29	7.1131E-03	8.6341E-03	1.0994E-02	1.1865E-02	1.2690E-02	1.2074E-02	1.2006E-02	9.6961E-03
353.15	20.29	7.0641E-03	8.5711E-03	1.0919E-02	1.1786E-02	1.2607E-02	1.1994E-02	1.1925E-02	9.6359E-03

Expanded combined uncertainties (k = 2) U_c are $U_c(T) = 0.02\ K$. $U_c(P) = 0.032\ MPa$. $U_c(x_i) = 0.0002$. $U_{c,r} = (\alpha_p) = 0.041$.

APPENDIX C

Isothermal Compressibility

Table C1: Isothermal Compressibility (κ_T) of butan-1-ol (1) + n-octane (2) at various pressures and temperatures.

T/K	P/MPa	κ_T /MPa^{-1}							
		x_1=0	*x_1=0.1259*	*x_1=0.3750*	*x_1=0.5002*	*x_1=0.6258*	*x_1=0.7503*	*x_1=0.8750*	*x_1=1*
313.15	0.1	1.4077E-03	1.4074E-03	1.3682E-03	1.3301E-03	1.2719E-03	1.2041E-03	1.1225E-03	1.0348E-03
313.15	1.14	1.3878E-03	1.3878E-03	1.3498E-03	1.3128E-03	1.2560E-03	1.1899E-03	1.1104E-03	1.0251E-03
313.15	2.14	1.3662E-03	1.3665E-03	1.3297E-03	1.2939E-03	1.2388E-03	1.1745E-03	1.0972E-03	1.0145E-03
313.15	3.15	1.3451E-03	1.3456E-03	1.3101E-03	1.2754E-03	1.2219E-03	1.1594E-03	1.0842E-03	1.0040E-03
313.15	4.16	1.3245E-03	1.3252E-03	1.2909E-03	1.2573E-03	1.2053E-03	1.1446E-03	1.0714E-03	9.9369E-04
313.15	5.17	1.3043E-03	1.3053E-03	1.2721E-03	1.2396E-03	1.1890E-03	1.1301E-03	1.0589E-03	9.8354E-04
313.15	6.18	1.2847E-03	1.2858E-03	1.2538E-03	1.2223E-03	1.1731E-03	1.1159E-03	1.0465E-03	9.7355E-04
313.15	7.19	1.2654E-03	1.2668E-03	1.2358E-03	1.2053E-03	1.1575E-03	1.1019E-03	1.0344E-03	9.6371E-04
313.15	8.2	1.2466E-03	1.2482E-03	1.2182E-03	1.1887E-03	1.1423E-03	1.0882E-03	1.0225E-03	9.5402E-04
313.15	9.23	1.2282E-03	1.2300E-03	1.2010E-03	1.1725E-03	1.1273E-03	1.0747E-03	1.0108E-03	9.4447E-04
313.15	10.23	1.2102E-03	1.2122E-03	1.1842E-03	1.1565E-03	1.1126E-03	1.0615E-03	9.9934E-04	9.3507E-04
313.15	11.24	1.1926E-03	1.1948E-03	1.1677E-03	1.1409E-03	1.0982E-03	1.0485E-03	9.8804E-04	9.2581E-04
313.15	12.25	1.1754E-03	1.1777E-03	1.1515E-03	1.1256E-03	1.0841E-03	1.0358E-03	9.7693E-04	9.1669E-04
313.15	13.26	1.1586E-03	1.1610E-03	1.1357E-03	1.1106E-03	1.0702E-03	1.0233E-03	9.6601E-04	9.0770E-04
313.15	14.27	1.1421E-03	1.1447E-03	1.1202E-03	1.0959E-03	1.0566E-03	1.0110E-03	9.5527E-04	8.9884E-04
313.15	15.27	1.1260E-03	1.1287E-03	1.1050E-03	1.0815E-03	1.0433E-03	9.9892E-04	9.4471E-04	8.9011E-04
313.15	16.28	1.1102E-03	1.1130E-03	1.0902E-03	1.0674E-03	1.0302E-03	9.8708E-04	9.3432E-04	8.8151E-04
313.15	17.29	1.0947E-03	1.0977E-03	1.0756E-03	1.0535E-03	1.0174E-03	9.7544E-04	9.2411E-04	8.7303E-04
313.15	18.3	1.0796E-03	1.0827E-03	1.0613E-03	1.0400E-03	1.0048E-03	9.6401E-04	9.1406E-04	8.6468E-04
313.15	19.3	1.0648E-03	1.0680E-03	1.0473E-03	1.0266E-03	9.9241E-04	9.5278E-04	9.0417E-04	8.5644E-04
313.15	20.31	1.0502E-03	1.0535E-03	1.0336E-03	1.0136E-03	9.8027E-04	9.4175E-04	8.9445E-04	8.4832E-04
323.15	0.1	1.5131E-03	1.5108E-03	1.4646E-03	1.4209E-03	1.3556E-03	1.2791E-03	1.1877E-03	1.0875E-03
323.15	1.15	1.4916E-03	1.4896E-03	1.4448E-03	1.4023E-03	1.3386E-03	1.2640E-03	1.1749E-03	1.0773E-03
323.15	2.15	1.4683E-03	1.4665E-03	1.4231E-03	1.3820E-03	1.3201E-03	1.2475E-03	1.1608E-03	1.0660E-03
323.15	3.17	1.4454E-03	1.4440E-03	1.4020E-03	1.3621E-03	1.3020E-03	1.2314E-03	1.1469E-03	1.0550E-03
323.15	4.18	1.4232E-03	1.4220E-03	1.3813E-03	1.3427E-03	1.2842E-03	1.2156E-03	1.1334E-03	1.0441E-03
323.15	5.19	1.4014E-03	1.4005E-03	1.3611E-03	1.3237E-03	1.2668E-03	1.2001E-03	1.1200E-03	1.0334E-03
323.15	6.2	1.3801E-03	1.3795E-03	1.3414E-03	1.3051E-03	1.2498E-03	1.1849E-03	1.1069E-03	1.0228E-03
323.15	7.22	1.3593E-03	1.3589E-03	1.3220E-03	1.2868E-03	1.2331E-03	1.1699E-03	1.0941E-03	1.0125E-03
323.15	8.23	1.3390E-03	1.3388E-03	1.3031E-03	1.2690E-03	1.2167E-03	1.1553E-03	1.0814E-03	1.0022E-03
323.15	9.24	1.3191E-03	1.3192E-03	1.2846E-03	1.2515E-03	1.2006E-03	1.1409E-03	1.0690E-03	9.9215E-04

323.15	10.25	1.2997E-03	1.2999E-03	1.2665E-03	1.2344E-03	1.1849E-03	1.1268E-03	1.0568E-03	9.8223E-04
323.15	11.25	1.2807E-03	1.2811E-03	1.2487E-03	1.2177E-03	1.1695E-03	1.1130E-03	1.0447E-03	9.7245E-04
323.15	12.27	1.2621E-03	1.2628E-03	1.2314E-03	1.2012E-03	1.1544E-03	1.0994E-03	1.0329E-03	9.6282E-04
323.15	13.27	1.2439E-03	1.2448E-03	1.2144E-03	1.1851E-03	1.1395E-03	1.0860E-03	1.0213E-03	9.5334E-04
323.15	14.26	1.2261E-03	1.2271E-03	1.1977E-03	1.1694E-03	1.1250E-03	1.0729E-03	1.0099E-03	9.4399E-04
323.15	15.29	1.2087E-03	1.2099E-03	1.1814E-03	1.1539E-03	1.1107E-03	1.0601E-03	9.9870E-04	9.3478E-04
323.15	16.3	1.1916E-03	1.1930E-03	1.1654E-03	1.1388E-03	1.0967E-03	1.0475E-03	9.8767E-04	9.2571E-04
323.15	17.3	1.1749E-03	1.1765E-03	1.1497E-03	1.1239E-03	1.0830E-03	1.0350E-03	9.7682E-04	9.1676E-04
323.15	18.3	1.1586E-03	1.1603E-03	1.1344E-03	1.1094E-03	1.0695E-03	1.0229E-03	9.6615E-04	9.0795E-04
323.15	19.3	1.1426E-03	1.1444E-03	1.1194E-03	1.0951E-03	1.0563E-03	1.0109E-03	9.5565E-04	8.9926E-04
323.15	20.29	1.1269E-03	1.1289E-03	1.1046E-03	1.0811E-03	1.0433E-03	9.9912E-04	9.4532E-04	8.9070E-04
333.15	0.1	1.6220E-03	1.6178E-03	1.5653E-03	1.5162E-03	1.4438E-03	1.3588E-03	1.2577E-03	1.1452E-03
333.15	1.13	1.5988E-03	1.5949E-03	1.5439E-03	1.4961E-03	1.4256E-03	1.3427E-03	1.2440E-03	1.1344E-03
333.15	2.13	1.5736E-03	1.5701E-03	1.5207E-03	1.4743E-03	1.4058E-03	1.3251E-03	1.2290E-03	1.1225E-03
333.15	3.14	1.5490E-03	1.5458E-03	1.4980E-03	1.4530E-03	1.3863E-03	1.3079E-03	1.2143E-03	1.1108E-03
333.15	4.15	1.5249E-03	1.5221E-03	1.4758E-03	1.4322E-03	1.3673E-03	1.2910E-03	1.1998E-03	1.0993E-03
333.15	5.16	1.5014E-03	1.4989E-03	1.4540E-03	1.4118E-03	1.3487E-03	1.2744E-03	1.1856E-03	1.0879E-03
333.15	6.17	1.4785E-03	1.4763E-03	1.4328E-03	1.3918E-03	1.3304E-03	1.2581E-03	1.1717E-03	1.0768E-03
333.15	7.18	1.4561E-03	1.4542E-03	1.4120E-03	1.3722E-03	1.3125E-03	1.2422E-03	1.1580E-03	1.0658E-03
333.15	8.19	1.4342E-03	1.4325E-03	1.3917E-03	1.3531E-03	1.2950E-03	1.2266E-03	1.1445E-03	1.0549E-03
333.15	9.2	1.4128E-03	1.4114E-03	1.3718E-03	1.3344E-03	1.2778E-03	1.2112E-03	1.1313E-03	1.0443E-03
333.15	10.21	1.3918E-03	1.3907E-03	1.3523E-03	1.3160E-03	1.2610E-03	1.1962E-03	1.1183E-03	1.0338E-03
333.15	11.22	1.3713E-03	1.3704E-03	1.3333E-03	1.2980E-03	1.2445E-03	1.1814E-03	1.1055E-03	1.0234E-03
333.15	12.23	1.3513E-03	1.3507E-03	1.3146E-03	1.2804E-03	1.2283E-03	1.1669E-03	1.0930E-03	1.0133E-03
333.15	13.24	1.3317E-03	1.3313E-03	1.2963E-03	1.2632E-03	1.2124E-03	1.1526E-03	1.0806E-03	1.0032E-03
333.15	14.25	1.3125E-03	1.3123E-03	1.2784E-03	1.2463E-03	1.1969E-03	1.1387E-03	1.0685E-03	9.9333E-04
333.15	15.26	1.2938E-03	1.2938E-03	1.2609E-03	1.2297E-03	1.1816E-03	1.1249E-03	1.0566E-03	9.8360E-04
333.15	16.27	1.2754E-03	1.2756E-03	1.2438E-03	1.2135E-03	1.1666E-03	1.1115E-03	1.0448E-03	9.7400E-04
333.15	17.27	1.2575E-03	1.2578E-03	1.2270E-03	1.1976E-03	1.1519E-03	1.0982E-03	1.0333E-03	9.6454E-04
333.15	18.28	1.2399E-03	1.2404E-03	1.2105E-03	1.1820E-03	1.1375E-03	1.0852E-03	1.0219E-03	9.5523E-04
333.15	19.28	1.2226E-03	1.2234E-03	1.1943E-03	1.1667E-03	1.1234E-03	1.0725E-03	1.0108E-03	9.4604E-04
333.15	20.28	1.2058E-03	1.2067E-03	1.1785E-03	1.1517E-03	1.1095E-03	1.0599E-03	9.9980E-04	9.3699E-04
343.15	0.1	1.7341E-03	1.7283E-03	1.6700E-03	1.6156E-03	1.5362E-03	1.4429E-03	1.3322E-03	1.2075E-03
343.15	1.14	1.7091E-03	1.7037E-03	1.6471E-03	1.5941E-03	1.5167E-03	1.4256E-03	1.3175E-03	1.1960E-03
343.15	2.14	1.6819E-03	1.6770E-03	1.6221E-03	1.5708E-03	1.4954E-03	1.4069E-03	1.3016E-03	1.1834E-03
343.15	3.14	1.6555E-03	1.6509E-03	1.5977E-03	1.5479E-03	1.4746E-03	1.3885E-03	1.2859E-03	1.1710E-03
343.15	4.16	1.6296E-03	1.6254E-03	1.5739E-03	1.5255E-03	1.4543E-03	1.3704E-03	1.2705E-03	1.1588E-03
343.15	5.17	1.6043E-03	1.6005E-03	1.5505E-03	1.5037E-03	1.4343E-03	1.3527E-03	1.2554E-03	1.1468E-03
343.15	6.18	1.5797E-03	1.5762E-03	1.5277E-03	1.4823E-03	1.4148E-03	1.3354E-03	1.2405E-03	1.1349E-03
343.15	7.19	1.5555E-03	1.5524E-03	1.5054E-03	1.4613E-03	1.3956E-03	1.3184E-03	1.2259E-03	1.1233E-03
343.15	8.2	1.5320E-03	1.5291E-03	1.4836E-03	1.4408E-03	1.3769E-03	1.3017E-03	1.2116E-03	1.1118E-03
343.15	9.21	1.5090E-03	1.5064E-03	1.4623E-03	1.4207E-03	1.3585E-03	1.2853E-03	1.1975E-03	1.1005E-03
343.15	10.22	1.4864E-03	1.4842E-03	1.4414E-03	1.4011E-03	1.3405E-03	1.2692E-03	1.1837E-03	1.0894E-03

343.15	11.23	1.4644E-03	1.4625E-03	1.4210E-03	1.3818E-03	1.3228E-03	1.2534E-03	1.1701E-03	1.0784E-03
343.15	12.24	1.4429E-03	1.4412E-03	1.4009E-03	1.3630E-03	1.3055E-03	1.2380E-03	1.1567E-03	1.0676E-03
343.15	13.25	1.4219E-03	1.4204E-03	1.3814E-03	1.3445E-03	1.2886E-03	1.2228E-03	1.1436E-03	1.0570E-03
343.15	14.26	1.4013E-03	1.4001E-03	1.3622E-03	1.3264E-03	1.2719E-03	1.2079E-03	1.1307E-03	1.0465E-03
343.15	15.27	1.3811E-03	1.3801E-03	1.3434E-03	1.3086E-03	1.2556E-03	1.1932E-03	1.1180E-03	1.0362E-03
343.15	16.27	1.3614E-03	1.3607E-03	1.3250E-03	1.2913E-03	1.2396E-03	1.1788E-03	1.1055E-03	1.0261E-03
343.15	17.28	1.3421E-03	1.3416E-03	1.3070E-03	1.2742E-03	1.2239E-03	1.1647E-03	1.0932E-03	1.0160E-03
343.15	18.28	1.3232E-03	1.3229E-03	1.2894E-03	1.2575E-03	1.2085E-03	1.1509E-03	1.0811E-03	1.0062E-03
343.15	19.29	1.3047E-03	1.3046E-03	1.2721E-03	1.2412E-03	1.1934E-03	1.1372E-03	1.0693E-03	9.9645E-04
343.15	20.29	1.2866E-03	1.2867E-03	1.2551E-03	1.2251E-03	1.1786E-03	1.1239E-03	1.0576E-03	9.8687E-04
353.15	0.1	1.8491E-03	1.8421E-03	1.7785E-03	1.7190E-03	1.6325E-03	1.5311E-03	1.4108E-03	1.2741E-03
353.15	1.14	1.8223E-03	1.8157E-03	1.7539E-03	1.6960E-03	1.6116E-03	1.5127E-03	1.3952E-03	1.2619E-03
353.15	2.14	1.7932E-03	1.7870E-03	1.7271E-03	1.6710E-03	1.5889E-03	1.4926E-03	1.3781E-03	1.2485E-03
353.15	3.14	1.7647E-03	1.7590E-03	1.7010E-03	1.6465E-03	1.5666E-03	1.4730E-03	1.3614E-03	1.2353E-03
353.15	4.16	1.7370E-03	1.7317E-03	1.6754E-03	1.6225E-03	1.5449E-03	1.4537E-03	1.3450E-03	1.2224E-03
353.15	5.16	1.7099E-03	1.7050E-03	1.6504E-03	1.5991E-03	1.5235E-03	1.4348E-03	1.3289E-03	1.2096E-03
353.15	6.18	1.6834E-03	1.6789E-03	1.6260E-03	1.5762E-03	1.5026E-03	1.4163E-03	1.3131E-03	1.1971E-03
353.15	7.19	1.6575E-03	1.6534E-03	1.6021E-03	1.5538E-03	1.4822E-03	1.3981E-03	1.2976E-03	1.1847E-03
353.15	8.2	1.6323E-03	1.6285E-03	1.5787E-03	1.5318E-03	1.4621E-03	1.3803E-03	1.2823E-03	1.1725E-03
353.15	9.21	1.6076E-03	1.6041E-03	1.5559E-03	1.5104E-03	1.4425E-03	1.3628E-03	1.2673E-03	1.1605E-03
353.15	10.22	1.5834E-03	1.5803E-03	1.5335E-03	1.4893E-03	1.4233E-03	1.3457E-03	1.2526E-03	1.1487E-03
353.15	11.23	1.5598E-03	1.5570E-03	1.5116E-03	1.4687E-03	1.4044E-03	1.3289E-03	1.2381E-03	1.1371E-03
353.15	12.24	1.5368E-03	1.5342E-03	1.4902E-03	1.4486E-03	1.3859E-03	1.3124E-03	1.2239E-03	1.1257E-03
353.15	13.25	1.5142E-03	1.5119E-03	1.4693E-03	1.4288E-03	1.3678E-03	1.2962E-03	1.2099E-03	1.1144E-03
353.15	14.26	1.4921E-03	1.4901E-03	1.4487E-03	1.4095E-03	1.3500E-03	1.2803E-03	1.1962E-03	1.1033E-03
353.15	15.25	1.4706E-03	1.4688E-03	1.4287E-03	1.3905E-03	1.3326E-03	1.2646E-03	1.1826E-03	1.0924E-03
353.15	16.27	1.4494E-03	1.4480E-03	1.4090E-03	1.3719E-03	1.3155E-03	1.2493E-03	1.1694E-03	1.0816E-03
353.15	17.27	1.4288E-03	1.4275E-03	1.3897E-03	1.3537E-03	1.2988E-03	1.2343E-03	1.1563E-03	1.0710E-03
353.15	18.29	1.4085E-03	1.4075E-03	1.3708E-03	1.3359E-03	1.2823E-03	1.2195E-03	1.1435E-03	1.0605E-03
353.15	19.29	1.3887E-03	1.3880E-03	1.3523E-03	1.3184E-03	1.2662E-03	1.2050E-03	1.1308E-03	1.0502E-03
353.15	20.29	1.3694E-03	1.3688E-03	1.3342E-03	1.3012E-03	1.2504E-03	1.1907E-03	1.1184E-03	1.0401E-03

Expanded combined uncertainties (k = 2) U_c are $U_c(T)$ = 0.02 K, $U_c(P)$ = 0.032 MPa, and $U_c(x_i)$ = 0.0002, $U_{c,r}(\kappa_T)$ = 0.044 .

Table C2: Isothermal Compressibility (κ_T) of butan-1-ol (1) + n-decane (2) at various pressures and temperatures.

T/K	P/MPa	κ_T /MPa^{-1}							
		x_1=0	*x_1=0.1269*	*x_1=0.3764*	*x_1=0.4968*	*x_1=0.6234*	*x_1=0.7440*	*x_1=0.8731*	*x_1=1*
313.15	0.1	1.2121E-03	1.2369E-03	1.2501E-03	1.2411E-03	1.2099E-03	1.1610E-03	1.1091E-03	1.0348E-03
313.15	1.14	1.1969E-03	1.2223E-03	1.2368E-03	1.2285E-03	1.1977E-03	1.1494E-03	1.0982E-03	1.0251E-03
313.15	2.14	1.1803E-03	1.2064E-03	1.2223E-03	1.2146E-03	1.1844E-03	1.1367E-03	1.0864E-03	1.0145E-03
313.15	3.15	1.1641E-03	1.1908E-03	1.2081E-03	1.2009E-03	1.1713E-03	1.1243E-03	1.0747E-03	1.0040E-03
313.15	4.16	1.1482E-03	1.1755E-03	1.1941E-03	1.1875E-03	1.1585E-03	1.1120E-03	1.0633E-03	9.9369E-04
313.15	5.17	1.1326E-03	1.1606E-03	1.1803E-03	1.1743E-03	1.1458E-03	1.0999E-03	1.0520E-03	9.8354E-04
313.15	6.18	1.1173E-03	1.1459E-03	1.1668E-03	1.1614E-03	1.1334E-03	1.0880E-03	1.0409E-03	9.7355E-04
313.15	7.19	1.1023E-03	1.1314E-03	1.1535E-03	1.1486E-03	1.1211E-03	1.0763E-03	1.0300E-03	9.6371E-04
313.15	8.2	1.0877E-03	1.1173E-03	1.1405E-03	1.1361E-03	1.1091E-03	1.0648E-03	1.0192E-03	9.5402E-04
313.15	9.23	1.0733E-03	1.1034E-03	1.1276E-03	1.1237E-03	1.0972E-03	1.0535E-03	1.0086E-03	9.4447E-04
313.15	10.23	1.0592E-03	1.0897E-03	1.1150E-03	1.1116E-03	1.0856E-03	1.0424E-03	9.9821E-04	9.3507E-04
313.15	11.24	1.0454E-03	1.0764E-03	1.1026E-03	1.0997E-03	1.0741E-03	1.0314E-03	9.8794E-04	9.2581E-04
313.15	12.25	1.0318E-03	1.0632E-03	1.0904E-03	1.0879E-03	1.0628E-03	1.0206E-03	9.7784E-04	9.1669E-04
313.15	13.26	1.0185E-03	1.0503E-03	1.0784E-03	1.0764E-03	1.0517E-03	1.0100E-03	9.6789E-04	9.0770E-04
313.15	14.27	1.0055E-03	1.0377E-03	1.0666E-03	1.0650E-03	1.0407E-03	9.9958E-04	9.5810E-04	8.9884E-04
313.15	15.27	9.9272E-04	1.0252E-03	1.0550E-03	1.0538E-03	1.0299E-03	9.8929E-04	9.4845E-04	8.9011E-04
313.15	16.28	9.8019E-04	1.0130E-03	1.0436E-03	1.0428E-03	1.0193E-03	9.7916E-04	9.3894E-04	8.8151E-04
313.15	17.29	9.6788E-04	1.0010E-03	1.0323E-03	1.0319E-03	1.0089E-03	9.6918E-04	9.2958E-04	8.7303E-04
313.15	18.3	9.5581E-04	9.8926E-04	1.0213E-03	1.0212E-03	9.9862E-04	9.5936E-04	9.2036E-04	8.6468E-04
313.15	19.3	9.4397E-04	9.7769E-04	1.0104E-03	1.0107E-03	9.8849E-04	9.4968E-04	9.1128E-04	8.5644E-04
313.15	20.31	9.3234E-04	9.6631E-04	9.9969E-04	1.0004E-03	9.7852E-04	9.4015E-04	9.0233E-04	8.4832E-04
323.15	0.1	1.2910E-03	1.3123E-03	1.3192E-03	1.3074E-03	1.2739E-03	1.2226E-03	1.1672E-03	1.0875E-03
323.15	1.15	1.2747E-03	1.2967E-03	1.3051E-03	1.2940E-03	1.2610E-03	1.2104E-03	1.1558E-03	1.0773E-03
323.15	2.15	1.2570E-03	1.2798E-03	1.2897E-03	1.2793E-03	1.2469E-03	1.1969E-03	1.1433E-03	1.0660E-03
323.15	3.17	1.2396E-03	1.2632E-03	1.2746E-03	1.2648E-03	1.2331E-03	1.1837E-03	1.1309E-03	1.0550E-03
323.15	4.18	1.2225E-03	1.2469E-03	1.2598E-03	1.2506E-03	1.2194E-03	1.1707E-03	1.1188E-03	1.0441E-03
323.15	5.19	1.2058E-03	1.2309E-03	1.2452E-03	1.2367E-03	1.2060E-03	1.1579E-03	1.1069E-03	1.0334E-03
323.15	6.2	1.1895E-03	1.2152E-03	1.2308E-03	1.2229E-03	1.1929E-03	1.1454E-03	1.0951E-03	1.0228E-03
323.15	7.22	1.1735E-03	1.1998E-03	1.2167E-03	1.2094E-03	1.1799E-03	1.1330E-03	1.0836E-03	1.0125E-03
323.15	8.23	1.1578E-03	1.1847E-03	1.2029E-03	1.1961E-03	1.1672E-03	1.1208E-03	1.0722E-03	1.0022E-03
323.15	9.24	1.1424E-03	1.1699E-03	1.1893E-03	1.1831E-03	1.1546E-03	1.1089E-03	1.0610E-03	9.9215E-04
323.15	10.25	1.1273E-03	1.1554E-03	1.1759E-03	1.1702E-03	1.1423E-03	1.0971E-03	1.0500E-03	9.8223E-04
323.15	11.25	1.1125E-03	1.1411E-03	1.1627E-03	1.1576E-03	1.1301E-03	1.0855E-03	1.0392E-03	9.7245E-04
323.15	12.27	1.0980E-03	1.1271E-03	1.1498E-03	1.1452E-03	1.1182E-03	1.0741E-03	1.0285E-03	9.6282E-04
323.15	13.27	1.0838E-03	1.1134E-03	1.1371E-03	1.1329E-03	1.1064E-03	1.0628E-03	1.0180E-03	9.5334E-04
323.15	14.26	1.0699E-03	1.0999E-03	1.1246E-03	1.1209E-03	1.0949E-03	1.0518E-03	1.0076E-03	9.4399E-04
323.15	15.29	1.0562E-03	1.0867E-03	1.1123E-03	1.1090E-03	1.0835E-03	1.0409E-03	9.9741E-04	9.3478E-04

323.15	16.3	1.0428E-03	1.0736E-03	1.1002E-03	1.0974E-03	1.0723E-03	1.0302E-03	9.8737E-04	9.2571E-04
323.15	17.3	1.0297E-03	1.0609E-03	1.0883E-03	1.0859E-03	1.0612E-03	1.0196E-03	9.7747E-04	9.1676E-04
323.15	18.3	1.0168E-03	1.0483E-03	1.0765E-03	1.0746E-03	1.0503E-03	1.0093E-03	9.6773E-04	9.0795E-04
323.15	19.3	1.0041E-03	1.0360E-03	1.0650E-03	1.0635E-03	1.0396E-03	9.9903E-04	9.5814E-04	8.9926E-04
323.15	20.29	9.9167E-04	1.0239E-03	1.0537E-03	1.0526E-03	1.0291E-03	9.8895E-04	9.4868E-04	8.9070E-04
333.15	0.1	1.3728E-03	1.3927E-03	1.3953E-03	1.3811E-03	1.3450E-03	1.2906E-03	1.2312E-03	1.1452E-03
333.15	1.13	1.3554E-03	1.3761E-03	1.3803E-03	1.3668E-03	1.3313E-03	1.2775E-03	1.2190E-03	1.1344E-03
333.15	2.13	1.3364E-03	1.3580E-03	1.3639E-03	1.3512E-03	1.3163E-03	1.2632E-03	1.2057E-03	1.1225E-03
333.15	3.14	1.3177E-03	1.3403E-03	1.3478E-03	1.3358E-03	1.3016E-03	1.2492E-03	1.1927E-03	1.1108E-03
333.15	4.15	1.2995E-03	1.3229E-03	1.3320E-03	1.3207E-03	1.2872E-03	1.2354E-03	1.1798E-03	1.0993E-03
333.15	5.16	1.2817E-03	1.3058E-03	1.3165E-03	1.3059E-03	1.2730E-03	1.2219E-03	1.1672E-03	1.0879E-03
333.15	6.17	1.2642E-03	1.2891E-03	1.3012E-03	1.2913E-03	1.2590E-03	1.2085E-03	1.1547E-03	1.0768E-03
333.15	7.18	1.2471E-03	1.2727E-03	1.2862E-03	1.2770E-03	1.2452E-03	1.1954E-03	1.1425E-03	1.0658E-03
333.15	8.19	1.2303E-03	1.2566E-03	1.2715E-03	1.2628E-03	1.2317E-03	1.1825E-03	1.1304E-03	1.0549E-03
333.15	9.2	1.2139E-03	1.2408E-03	1.2570E-03	1.2490E-03	1.2184E-03	1.1698E-03	1.1185E-03	1.0443E-03
333.15	10.21	1.1978E-03	1.2253E-03	1.2428E-03	1.2353E-03	1.2053E-03	1.1573E-03	1.1069E-03	1.0338E-03
333.15	11.22	1.1820E-03	1.2101E-03	1.2288E-03	1.2219E-03	1.1924E-03	1.1450E-03	1.0954E-03	1.0234E-03
333.15	12.23	1.1665E-03	1.1951E-03	1.2151E-03	1.2087E-03	1.1797E-03	1.1329E-03	1.0840E-03	1.0133E-03
333.15	13.24	1.1514E-03	1.1805E-03	1.2015E-03	1.1957E-03	1.1672E-03	1.1210E-03	1.0729E-03	1.0032E-03
333.15	14.25	1.1365E-03	1.1661E-03	1.1883E-03	1.1829E-03	1.1549E-03	1.1092E-03	1.0619E-03	9.9333E-04
333.15	15.26	1.1219E-03	1.1520E-03	1.1752E-03	1.1704E-03	1.1429E-03	1.0977E-03	1.0511E-03	9.8360E-04
333.15	16.27	1.1076E-03	1.1381E-03	1.1623E-03	1.1580E-03	1.1310E-03	1.0863E-03	1.0405E-03	9.7400E-04
333.15	17.27	1.0935E-03	1.1245E-03	1.1497E-03	1.1458E-03	1.1193E-03	1.0752E-03	1.0300E-03	9.6454E-04
333.15	18.28	1.0798E-03	1.1111E-03	1.1372E-03	1.1338E-03	1.1077E-03	1.0642E-03	1.0197E-03	9.5523E-04
333.15	19.28	1.0663E-03	1.0980E-03	1.1250E-03	1.1220E-03	1.0964E-03	1.0533E-03	1.0095E-03	9.4604E-04
333.15	20.28	1.0530E-03	1.0851E-03	1.1129E-03	1.1104E-03	1.0852E-03	1.0426E-03	9.9951E-04	9.3699E-04
343.15	0.1	1.4572E-03	1.4777E-03	1.4778E-03	1.4617E-03	1.4228E-03	1.3644E-03	1.3005E-03	1.2075E-03
343.15	1.14	1.4386E-03	1.4600E-03	1.4618E-03	1.4464E-03	1.4082E-03	1.3505E-03	1.2876E-03	1.1960E-03
343.15	2.14	1.4183E-03	1.4407E-03	1.4444E-03	1.4298E-03	1.3923E-03	1.3353E-03	1.2734E-03	1.1834E-03
343.15	3.14	1.3984E-03	1.4217E-03	1.4272E-03	1.4134E-03	1.3766E-03	1.3204E-03	1.2595E-03	1.1710E-03
343.15	4.16	1.3790E-03	1.4032E-03	1.4104E-03	1.3974E-03	1.3612E-03	1.3057E-03	1.2459E-03	1.1588E-03
343.15	5.17	1.3600E-03	1.3850E-03	1.3938E-03	1.3816E-03	1.3461E-03	1.2913E-03	1.2324E-03	1.1468E-03
343.15	6.18	1.3413E-03	1.3671E-03	1.3776E-03	1.3660E-03	1.3312E-03	1.2771E-03	1.2192E-03	1.1349E-03
343.15	7.19	1.3230E-03	1.3496E-03	1.3616E-03	1.3507E-03	1.3165E-03	1.2631E-03	1.2062E-03	1.1233E-03
343.15	8.2	1.3052E-03	1.3324E-03	1.3459E-03	1.3357E-03	1.3021E-03	1.2494E-03	1.1934E-03	1.1118E-03
343.15	9.21	1.2876E-03	1.3156E-03	1.3305E-03	1.3210E-03	1.2880E-03	1.2359E-03	1.1808E-03	1.1005E-03
343.15	10.22	1.2704E-03	1.2991E-03	1.3153E-03	1.3064E-03	1.2740E-03	1.2226E-03	1.1684E-03	1.0894E-03
343.15	11.23	1.2536E-03	1.2828E-03	1.3004E-03	1.2922E-03	1.2603E-03	1.2095E-03	1.1562E-03	1.0784E-03
343.15	12.24	1.2371E-03	1.2669E-03	1.2858E-03	1.2781E-03	1.2469E-03	1.1967E-03	1.1442E-03	1.0676E-03
343.15	13.25	1.2209E-03	1.2513E-03	1.2714E-03	1.2643E-03	1.2336E-03	1.1840E-03	1.1323E-03	1.0570E-03
343.15	14.26	1.2051E-03	1.2360E-03	1.2572E-03	1.2507E-03	1.2205E-03	1.1716E-03	1.1207E-03	1.0465E-03
343.15	15.27	1.1895E-03	1.2209E-03	1.2433E-03	1.2373E-03	1.2077E-03	1.1593E-03	1.1092E-03	1.0362E-03
343.15	16.27	1.1743E-03	1.2062E-03	1.2296E-03	1.2241E-03	1.1950E-03	1.1472E-03	1.0979E-03	1.0261E-03

343.15	17.28	1.1593E-03	1.1916E-03	1.2162E-03	1.2112E-03	1.1826E-03	1.1354E-03	1.0868E-03	1.0160E-03
343.15	18.28	1.1446E-03	1.1774E-03	1.2029E-03	1.1984E-03	1.1703E-03	1.1237E-03	1.0759E-03	1.0062E-03
343.15	19.29	1.1302E-03	1.1634E-03	1.1899E-03	1.1859E-03	1.1583E-03	1.1122E-03	1.0651E-03	9.9645E-04
343.15	20.29	1.1161E-03	1.1497E-03	1.1771E-03	1.1735E-03	1.1464E-03	1.1008E-03	1.0545E-03	9.8687E-04
353.15	0.1	1.5441E-03	1.5671E-03	1.5665E-03	1.5488E-03	1.5069E-03	1.4437E-03	1.3748E-03	1.2741E-03
353.15	1.14	1.5242E-03	1.5482E-03	1.5495E-03	1.5326E-03	1.4913E-03	1.4289E-03	1.3610E-03	1.2619E-03
353.15	2.14	1.5026E-03	1.5276E-03	1.5308E-03	1.5148E-03	1.4743E-03	1.4127E-03	1.3460E-03	1.2485E-03
353.15	3.14	1.4814E-03	1.5074E-03	1.5125E-03	1.4973E-03	1.4576E-03	1.3968E-03	1.3312E-03	1.2353E-03
353.15	4.16	1.4607E-03	1.4875E-03	1.4945E-03	1.4802E-03	1.4412E-03	1.3812E-03	1.3167E-03	1.2224E-03
353.15	5.16	1.4404E-03	1.4681E-03	1.4769E-03	1.4633E-03	1.4250E-03	1.3658E-03	1.3024E-03	1.2096E-03
353.15	6.18	1.4206E-03	1.4491E-03	1.4595E-03	1.4468E-03	1.4092E-03	1.3507E-03	1.2883E-03	1.1971E-03
353.15	7.19	1.4011E-03	1.4304E-03	1.4425E-03	1.4305E-03	1.3936E-03	1.3359E-03	1.2745E-03	1.1847E-03
353.15	8.2	1.3821E-03	1.4121E-03	1.4258E-03	1.4144E-03	1.3782E-03	1.3213E-03	1.2609E-03	1.1725E-03
353.15	9.21	1.3634E-03	1.3941E-03	1.4093E-03	1.3987E-03	1.3631E-03	1.3069E-03	1.2475E-03	1.1605E-03
353.15	10.22	1.3451E-03	1.3765E-03	1.3932E-03	1.3832E-03	1.3483E-03	1.2928E-03	1.2343E-03	1.1487E-03
353.15	11.23	1.3272E-03	1.3592E-03	1.3773E-03	1.3680E-03	1.3337E-03	1.2788E-03	1.2213E-03	1.1371E-03
353.15	12.24	1.3096E-03	1.3422E-03	1.3617E-03	1.3530E-03	1.3193E-03	1.2652E-03	1.2086E-03	1.1257E-03
353.15	13.25	1.2924E-03	1.3256E-03	1.3463E-03	1.3383E-03	1.3052E-03	1.2517E-03	1.1960E-03	1.1144E-03
353.15	14.26	1.2755E-03	1.3093E-03	1.3312E-03	1.3238E-03	1.2913E-03	1.2384E-03	1.1836E-03	1.1033E-03
353.15	15.25	1.2590E-03	1.2932E-03	1.3164E-03	1.3095E-03	1.2776E-03	1.2254E-03	1.1714E-03	1.0924E-03
353.15	16.27	1.2427E-03	1.2775E-03	1.3018E-03	1.2955E-03	1.2641E-03	1.2126E-03	1.1594E-03	1.0816E-03
353.15	17.27	1.2268E-03	1.2620E-03	1.2874E-03	1.2817E-03	1.2509E-03	1.1999E-03	1.1476E-03	1.0710E-03
353.15	18.29	1.2112E-03	1.2469E-03	1.2733E-03	1.2681E-03	1.2378E-03	1.1875E-03	1.1360E-03	1.0605E-03
353.15	19.29	1.1959E-03	1.2320E-03	1.2595E-03	1.2548E-03	1.2250E-03	1.1753E-03	1.1245E-03	1.0502E-03
353.15	20.29	1.1809E-03	1.2173E-03	1.2458E-03	1.2416E-03	1.2123E-03	1.1632E-03	1.1133E-03	1.0401E-03

Expanded combined uncertainties (k = 2) U_c are $U_c(T) = 0.02$ K, $U_c(P) = 0.032$ MPa, and $U_c(x_i) = 0.0002$, $U_{c,r}(\kappa_T) = 0.044$.

Table C3: Isothermal Compressibility (κ_T) of butan-2-ol (1) + n-octane (2) at various pressures and temperatures.

T/K	P/MPa	κ_T /MPa^{-1}							
		$x_1=0$	$x_1=0.1262$	$x_1=0.3742$	$x_1=0.5002$	$x_1=0.6257$	$x_1=0.7501$	$x_1=0.8747$	$x_1=1$
313.15	0.1	1.4077E-03	1.4518E-03	1.4561E-03	1.4232E-03	1.3691E-03	1.2982E-03	1.2178E-03	1.1159E-03
313.15	1.14	1.3878E-03	1.4333E-03	1.4393E-03	1.4072E-03	1.3537E-03	1.2834E-03	1.2038E-03	1.1029E-03
313.15	2.14	1.3662E-03	1.4132E-03	1.4211E-03	1.3897E-03	1.3369E-03	1.2673E-03	1.1885E-03	1.0887E-03
313.15	3.15	1.3451E-03	1.3935E-03	1.4031E-03	1.3725E-03	1.3203E-03	1.2515E-03	1.1735E-03	1.0748E-03
313.15	4.16	1.3245E-03	1.3742E-03	1.3856E-03	1.3557E-03	1.3041E-03	1.2359E-03	1.1587E-03	1.0612E-03
313.15	5.17	1.3043E-03	1.3553E-03	1.3683E-03	1.3391E-03	1.2882E-03	1.2207E-03	1.1443E-03	1.0478E-03
313.15	6.18	1.2847E-03	1.3368E-03	1.3514E-03	1.3229E-03	1.2726E-03	1.2058E-03	1.1301E-03	1.0347E-03
313.15	7.19	1.2654E-03	1.3186E-03	1.3348E-03	1.3070E-03	1.2573E-03	1.1911E-03	1.1162E-03	1.0218E-03
313.15	8.2	1.2466E-03	1.3008E-03	1.3185E-03	1.2913E-03	1.2422E-03	1.1767E-03	1.1026E-03	1.0092E-03
313.15	9.23	1.2282E-03	1.2834E-03	1.3025E-03	1.2759E-03	1.2275E-03	1.1625E-03	1.0892E-03	9.9678E-04
313.15	10.23	1.2102E-03	1.2664E-03	1.2868E-03	1.2608E-03	1.2129E-03	1.1486E-03	1.0760E-03	9.8461E-04
313.15	11.24	1.1926E-03	1.2497E-03	1.2713E-03	1.2460E-03	1.1987E-03	1.1350E-03	1.0631E-03	9.7265E-04
313.15	12.25	1.1754E-03	1.2333E-03	1.2562E-03	1.2314E-03	1.1847E-03	1.1216E-03	1.0504E-03	9.6092E-04
313.15	13.26	1.1586E-03	1.2172E-03	1.2413E-03	1.2171E-03	1.1709E-03	1.1084E-03	1.0379E-03	9.4940E-04
313.15	14.27	1.1421E-03	1.2014E-03	1.2267E-03	1.2031E-03	1.1574E-03	1.0955E-03	1.0257E-03	9.3808E-04
313.15	15.27	1.1260E-03	1.1860E-03	1.2123E-03	1.1892E-03	1.1441E-03	1.0828E-03	1.0136E-03	9.2696E-04
313.15	16.28	1.1102E-03	1.1708E-03	1.1982E-03	1.1756E-03	1.1310E-03	1.0703E-03	1.0018E-03	9.1605E-04
313.15	17.29	1.0947E-03	1.1560E-03	1.1843E-03	1.1623E-03	1.1182E-03	1.0580E-03	9.9021E-04	9.0532E-04
313.15	18.3	1.0796E-03	1.1414E-03	1.1707E-03	1.1492E-03	1.1055E-03	1.0460E-03	9.7880E-04	8.9478E-04
313.15	19.3	1.0648E-03	1.1271E-03	1.1573E-03	1.1363E-03	1.0931E-03	1.0341E-03	9.6758E-04	8.8443E-04
313.15	20.31	1.0502E-03	1.1130E-03	1.1441E-03	1.1236E-03	1.0809E-03	1.0225E-03	9.5656E-04	8.7425E-04
323.15	0.1	1.5131E-03	1.5515E-03	1.5482E-03	1.5126E-03	1.4563E-03	1.3836E-03	1.3007E-03	1.1958E-03
323.15	1.15	1.4916E-03	1.5316E-03	1.5303E-03	1.4955E-03	1.4398E-03	1.3677E-03	1.2856E-03	1.1818E-03
323.15	2.15	1.4683E-03	1.5100E-03	1.5108E-03	1.4767E-03	1.4218E-03	1.3504E-03	1.2692E-03	1.1665E-03
323.15	3.17	1.4454E-03	1.4887E-03	1.4916E-03	1.4584E-03	1.4041E-03	1.3335E-03	1.2531E-03	1.1516E-03
323.15	4.18	1.4232E-03	1.4680E-03	1.4728E-03	1.4404E-03	1.3868E-03	1.3168E-03	1.2372E-03	1.1369E-03
323.15	5.19	1.4014E-03	1.4477E-03	1.4543E-03	1.4227E-03	1.3698E-03	1.3005E-03	1.2217E-03	1.1225E-03
323.15	6.2	1.3801E-03	1.4278E-03	1.4362E-03	1.4053E-03	1.3530E-03	1.2845E-03	1.2065E-03	1.1083E-03
323.15	7.22	1.3593E-03	1.4083E-03	1.4184E-03	1.3883E-03	1.3366E-03	1.2688E-03	1.1916E-03	1.0944E-03
323.15	8.23	1.3390E-03	1.3892E-03	1.4010E-03	1.3715E-03	1.3205E-03	1.2533E-03	1.1769E-03	1.0808E-03
323.15	9.24	1.3191E-03	1.3704E-03	1.3839E-03	1.3551E-03	1.3047E-03	1.2382E-03	1.1625E-03	1.0675E-03
323.15	10.25	1.2997E-03	1.3521E-03	1.3671E-03	1.3389E-03	1.2892E-03	1.2233E-03	1.1484E-03	1.0544E-03
323.15	11.25	1.2807E-03	1.3341E-03	1.3506E-03	1.3231E-03	1.2739E-03	1.2086E-03	1.1345E-03	1.0415E-03
323.15	12.27	1.2621E-03	1.3165E-03	1.3343E-03	1.3075E-03	1.2589E-03	1.1943E-03	1.1209E-03	1.0289E-03
323.15	13.27	1.2439E-03	1.2993E-03	1.3184E-03	1.2922E-03	1.2442E-03	1.1802E-03	1.1075E-03	1.0165E-03
323.15	14.26	1.2261E-03	1.2823E-03	1.3028E-03	1.2772E-03	1.2298E-03	1.1663E-03	1.0943E-03	1.0043E-03
323.15	15.29	1.2087E-03	1.2657E-03	1.2874E-03	1.2624E-03	1.2155E-03	1.1527E-03	1.0814E-03	9.9230E-04

323.15	16.3	1.1916E-03	1.2495E-03	1.2724E-03	1.2479E-03	1.2016E-03	1.1393E-03	1.0688E-03	9.8055E-04
323.15	17.3	1.1749E-03	1.2335E-03	1.2575E-03	1.2336E-03	1.1878E-03	1.1262E-03	1.0563E-03	9.6901E-04
323.15	18.3	1.1586E-03	1.2178E-03	1.2430E-03	1.2196E-03	1.1744E-03	1.1133E-03	1.0441E-03	9.5767E-04
323.15	19.3	1.1426E-03	1.2025E-03	1.2287E-03	1.2058E-03	1.1611E-03	1.1006E-03	1.0320E-03	9.4652E-04
323.15	20.29	1.1269E-03	1.1874E-03	1.2146E-03	1.1923E-03	1.1481E-03	1.0881E-03	1.0202E-03	9.3558E-04
333.15	0.1	1.6220E-03	1.6555E-03	1.6460E-03	1.6079E-03	1.5496E-03	1.4752E-03	1.3901E-03	1.2823E-03
333.15	1.13	1.5988E-03	1.6341E-03	1.6268E-03	1.5895E-03	1.5319E-03	1.4581E-03	1.3739E-03	1.2672E-03
333.15	2.13	1.5736E-03	1.6108E-03	1.6059E-03	1.5695E-03	1.5126E-03	1.4396E-03	1.3563E-03	1.2507E-03
333.15	3.14	1.5490E-03	1.5880E-03	1.5854E-03	1.5498E-03	1.4937E-03	1.4214E-03	1.3389E-03	1.2345E-03
333.15	4.15	1.5249E-03	1.5657E-03	1.5652E-03	1.5305E-03	1.4751E-03	1.4035E-03	1.3219E-03	1.2187E-03
333.15	5.16	1.5014E-03	1.5439E-03	1.5455E-03	1.5116E-03	1.4569E-03	1.3860E-03	1.3052E-03	1.2032E-03
333.15	6.17	1.4785E-03	1.5225E-03	1.5261E-03	1.4930E-03	1.4390E-03	1.3688E-03	1.2888E-03	1.1879E-03
333.15	7.18	1.4561E-03	1.5016E-03	1.5070E-03	1.4748E-03	1.4214E-03	1.3519E-03	1.2728E-03	1.1729E-03
333.15	8.19	1.4342E-03	1.4811E-03	1.4884E-03	1.4569E-03	1.4042E-03	1.3353E-03	1.2570E-03	1.1583E-03
333.15	9.2	1.4128E-03	1.4610E-03	1.4701E-03	1.4393E-03	1.3872E-03	1.3191E-03	1.2415E-03	1.1439E-03
333.15	10.21	1.3918E-03	1.4413E-03	1.4521E-03	1.4220E-03	1.3706E-03	1.3031E-03	1.2263E-03	1.1297E-03
333.15	11.22	1.3713E-03	1.4220E-03	1.4344E-03	1.4051E-03	1.3543E-03	1.2874E-03	1.2114E-03	1.1159E-03
333.15	12.23	1.3513E-03	1.4031E-03	1.4171E-03	1.3884E-03	1.3382E-03	1.2720E-03	1.1968E-03	1.1022E-03
333.15	13.24	1.3317E-03	1.3846E-03	1.4001E-03	1.3721E-03	1.3225E-03	1.2569E-03	1.1824E-03	1.0889E-03
333.15	14.25	1.3125E-03	1.3665E-03	1.3834E-03	1.3560E-03	1.3070E-03	1.2421E-03	1.1683E-03	1.0757E-03
333.15	15.26	1.2938E-03	1.3487E-03	1.3670E-03	1.3402E-03	1.2918E-03	1.2275E-03	1.1544E-03	1.0628E-03
333.15	16.27	1.2754E-03	1.3312E-03	1.3508E-03	1.3247E-03	1.2769E-03	1.2132E-03	1.1408E-03	1.0502E-03
333.15	17.27	1.2575E-03	1.3141E-03	1.3350E-03	1.3095E-03	1.2622E-03	1.1991E-03	1.1274E-03	1.0377E-03
333.15	18.28	1.2399E-03	1.2973E-03	1.3194E-03	1.2945E-03	1.2478E-03	1.1852E-03	1.1143E-03	1.0255E-03
333.15	19.28	1.2226E-03	1.2809E-03	1.3042E-03	1.2798E-03	1.2336E-03	1.1716E-03	1.1014E-03	1.0135E-03
333.15	20.28	1.2058E-03	1.2647E-03	1.2891E-03	1.2653E-03	1.2196E-03	1.1583E-03	1.0887E-03	1.0017E-03
343.15	0.1	1.7341E-03	1.7634E-03	1.7491E-03	1.7088E-03	1.6487E-03	1.5725E-03	1.4858E-03	1.3750E-03
343.15	1.14	1.7091E-03	1.7405E-03	1.7285E-03	1.6891E-03	1.6297E-03	1.5543E-03	1.4683E-03	1.3586E-03
343.15	2.14	1.6819E-03	1.7155E-03	1.7061E-03	1.6676E-03	1.6091E-03	1.5343E-03	1.4493E-03	1.3408E-03
343.15	3.14	1.6555E-03	1.6911E-03	1.6841E-03	1.6466E-03	1.5888E-03	1.5148E-03	1.4306E-03	1.3234E-03
343.15	4.16	1.6296E-03	1.6672E-03	1.6626E-03	1.6259E-03	1.5688E-03	1.4956E-03	1.4123E-03	1.3063E-03
343.15	5.17	1.6043E-03	1.6437E-03	1.6414E-03	1.6057E-03	1.5493E-03	1.4768E-03	1.3944E-03	1.2895E-03
343.15	6.18	1.5797E-03	1.6208E-03	1.6207E-03	1.5858E-03	1.5301E-03	1.4583E-03	1.3767E-03	1.2731E-03
343.15	7.19	1.5555E-03	1.5984E-03	1.6003E-03	1.5663E-03	1.5113E-03	1.4402E-03	1.3595E-03	1.2569E-03
343.15	8.2	1.5320E-03	1.5764E-03	1.5804E-03	1.5471E-03	1.4928E-03	1.4225E-03	1.3425E-03	1.2411E-03
343.15	9.21	1.5090E-03	1.5549E-03	1.5608E-03	1.5283E-03	1.4747E-03	1.4050E-03	1.3259E-03	1.2256E-03
343.15	10.22	1.4864E-03	1.5338E-03	1.5416E-03	1.5098E-03	1.4569E-03	1.3879E-03	1.3095E-03	1.2103E-03
343.15	11.23	1.4644E-03	1.5131E-03	1.5227E-03	1.4917E-03	1.4394E-03	1.3711E-03	1.2935E-03	1.1954E-03
343.15	12.24	1.4429E-03	1.4929E-03	1.5041E-03	1.4739E-03	1.4223E-03	1.3546E-03	1.2778E-03	1.1807E-03
343.15	13.25	1.4219E-03	1.4731E-03	1.4860E-03	1.4564E-03	1.4054E-03	1.3384E-03	1.2623E-03	1.1663E-03
343.15	14.26	1.4013E-03	1.4536E-03	1.4681E-03	1.4392E-03	1.3888E-03	1.3224E-03	1.2472E-03	1.1521E-03
343.15	15.27	1.3811E-03	1.4346E-03	1.4506E-03	1.4224E-03	1.3726E-03	1.3068E-03	1.2323E-03	1.1382E-03
343.15	16.27	1.3614E-03	1.4159E-03	1.4333E-03	1.4058E-03	1.3566E-03	1.2915E-03	1.2176E-03	1.1246E-03

343.15	17.28	1.3421E-03	1.3976E-03	1.4164E-03	1.3895E-03	1.3409E-03	1.2764E-03	1.2033E-03	1.1112E-03
343.15	18.28	1.3232E-03	1.3796E-03	1.3998E-03	1.3735E-03	1.3254E-03	1.2615E-03	1.1891E-03	1.0980E-03
343.15	19.29	1.3047E-03	1.3620E-03	1.3835E-03	1.3578E-03	1.3103E-03	1.2470E-03	1.1753E-03	1.0851E-03
343.15	20.29	1.2866E-03	1.3447E-03	1.3674E-03	1.3423E-03	1.2954E-03	1.2327E-03	1.1616E-03	1.0724E-03
353.15	0.1	1.8491E-03	1.8752E-03	1.8573E-03	1.8150E-03	1.7533E-03	1.6755E-03	1.5873E-03	1.4735E-03
353.15	1.14	1.8223E-03	1.8506E-03	1.8353E-03	1.7939E-03	1.7330E-03	1.6558E-03	1.5685E-03	1.4558E-03
353.15	2.14	1.7932E-03	1.8239E-03	1.8113E-03	1.7709E-03	1.7108E-03	1.6344E-03	1.5480E-03	1.4366E-03
353.15	3.14	1.7647E-03	1.7977E-03	1.7877E-03	1.7484E-03	1.6890E-03	1.6135E-03	1.5279E-03	1.4178E-03
353.15	4.16	1.7370E-03	1.7721E-03	1.7647E-03	1.7263E-03	1.6677E-03	1.5929E-03	1.5082E-03	1.3994E-03
353.15	5.16	1.7099E-03	1.7470E-03	1.7421E-03	1.7046E-03	1.6468E-03	1.5727E-03	1.4889E-03	1.3813E-03
353.15	6.18	1.6834E-03	1.7225E-03	1.7199E-03	1.6833E-03	1.6262E-03	1.5529E-03	1.4700E-03	1.3635E-03
353.15	7.19	1.6575E-03	1.6985E-03	1.6981E-03	1.6624E-03	1.6061E-03	1.5335E-03	1.4514E-03	1.3461E-03
353.15	8.2	1.6323E-03	1.6750E-03	1.6768E-03	1.6419E-03	1.5863E-03	1.5144E-03	1.4331E-03	1.3290E-03
353.15	9.21	1.6076E-03	1.6519E-03	1.6558E-03	1.6218E-03	1.5669E-03	1.4957E-03	1.4152E-03	1.3123E-03
353.15	10.22	1.5834E-03	1.6294E-03	1.6352E-03	1.6021E-03	1.5478E-03	1.4773E-03	1.3977E-03	1.2959E-03
353.15	11.23	1.5598E-03	1.6073E-03	1.6151E-03	1.5827E-03	1.5291E-03	1.4593E-03	1.3805E-03	1.2797E-03
353.15	12.24	1.5368E-03	1.5856E-03	1.5953E-03	1.5637E-03	1.5108E-03	1.4416E-03	1.3635E-03	1.2639E-03
353.15	13.25	1.5142E-03	1.5644E-03	1.5758E-03	1.5450E-03	1.4927E-03	1.4242E-03	1.3469E-03	1.2484E-03
353.15	14.26	1.4921E-03	1.5436E-03	1.5568E-03	1.5266E-03	1.4750E-03	1.4072E-03	1.3306E-03	1.2331E-03
353.15	15.25	1.4706E-03	1.5233E-03	1.5380E-03	1.5086E-03	1.4576E-03	1.3904E-03	1.3146E-03	1.2182E-03
353.15	16.27	1.4494E-03	1.5033E-03	1.5196E-03	1.4909E-03	1.4405E-03	1.3740E-03	1.2989E-03	1.2035E-03
353.15	17.27	1.4288E-03	1.4837E-03	1.5016E-03	1.4735E-03	1.4237E-03	1.3578E-03	1.2835E-03	1.1890E-03
353.15	18.29	1.4085E-03	1.4645E-03	1.4838E-03	1.4564E-03	1.4072E-03	1.3419E-03	1.2683E-03	1.1749E-03
353.15	19.29	1.3887E-03	1.4457E-03	1.4664E-03	1.4396E-03	1.3910E-03	1.3263E-03	1.2534E-03	1.1609E-03
353.15	20.29	1.3694E-03	1.4272E-03	1.4493E-03	1.4231E-03	1.3751E-03	1.3110E-03	1.2388E-03	1.1473E-03

Expanded combined uncertainties (k = 2) U_c are $U_c(T) = 0.02$ K, $U_c(P) = 0.032$ MPa, and $U_c(x_i) = 0.0002$, $U_{c,r}(\kappa_T) = 0.038$.

Table C4: Isothermal Compressibility (κ_T) of butan-2-ol (1) + n-decane (2) at various pressures and temperatures.

T/K	P/MPa	κ_T /MPa^{-1}							
		x_1=0	*x_1=0.1254*	*x_1=0.3754*	*x_1=0.5055*	*x_1=0.6240*	*x_1=0.7519*	*x_1=0.8740*	*x_1=1*
313.15	0.1	1.2121E-03	1.2556E-03	1.3007E-03	1.3126E-03	1.3081E-03	1.2661E-03	1.1967E-03	1.1159E-03
313.15	1.14	1.1969E-03	1.2411E-03	1.2871E-03	1.2994E-03	1.2953E-03	1.2532E-03	1.1837E-03	1.1029E-03
313.15	2.14	1.1803E-03	1.2252E-03	1.2723E-03	1.2851E-03	1.2813E-03	1.2392E-03	1.1696E-03	1.0887E-03
313.15	3.15	1.1641E-03	1.2096E-03	1.2577E-03	1.2709E-03	1.2676E-03	1.2253E-03	1.1557E-03	1.0748E-03
313.15	4.16	1.1482E-03	1.1944E-03	1.2434E-03	1.2570E-03	1.2540E-03	1.2117E-03	1.1421E-03	1.0612E-03
313.15	5.17	1.1326E-03	1.1794E-03	1.2293E-03	1.2433E-03	1.2407E-03	1.1984E-03	1.1287E-03	1.0478E-03
313.15	6.18	1.1173E-03	1.1647E-03	1.2155E-03	1.2299E-03	1.2275E-03	1.1852E-03	1.1156E-03	1.0347E-03
313.15	7.19	1.1023E-03	1.1502E-03	1.2018E-03	1.2167E-03	1.2146E-03	1.1723E-03	1.1026E-03	1.0218E-03
313.15	8.2	1.0877E-03	1.1361E-03	1.1885E-03	1.2036E-03	1.2019E-03	1.1595E-03	1.0899E-03	1.0092E-03
313.15	9.23	1.0733E-03	1.1222E-03	1.1753E-03	1.1908E-03	1.1894E-03	1.1470E-03	1.0774E-03	9.9678E-04
313.15	10.23	1.0592E-03	1.1085E-03	1.1623E-03	1.1782E-03	1.1771E-03	1.1347E-03	1.0652E-03	9.8461E-04
313.15	11.24	1.0454E-03	1.0951E-03	1.1496E-03	1.1658E-03	1.1650E-03	1.1226E-03	1.0531E-03	9.7265E-04
313.15	12.25	1.0318E-03	1.0820E-03	1.1371E-03	1.1536E-03	1.1530E-03	1.1107E-03	1.0413E-03	9.6092E-04
313.15	13.26	1.0185E-03	1.0690E-03	1.1248E-03	1.1416E-03	1.1413E-03	1.0989E-03	1.0296E-03	9.4940E-04
313.15	14.27	1.0055E-03	1.0563E-03	1.1127E-03	1.1297E-03	1.1297E-03	1.0874E-03	1.0181E-03	9.3808E-04
313.15	15.27	9.9272E-04	1.0439E-03	1.1007E-03	1.1181E-03	1.1183E-03	1.0760E-03	1.0069E-03	9.2696E-04
313.15	16.28	9.8019E-04	1.0316E-03	1.0890E-03	1.1066E-03	1.1070E-03	1.0648E-03	9.9579E-04	9.1605E-04
313.15	17.29	9.6788E-04	1.0196E-03	1.0775E-03	1.0953E-03	1.0960E-03	1.0538E-03	9.8488E-04	9.0532E-04
313.15	18.3	9.5581E-04	1.0078E-03	1.0661E-03	1.0842E-03	1.0851E-03	1.0429E-03	9.7416E-04	8.9478E-04
313.15	19.3	9.4397E-04	9.9616E-04	1.0549E-03	1.0733E-03	1.0744E-03	1.0323E-03	9.6361E-04	8.8443E-04
313.15	20.31	9.3234E-04	9.8475E-04	1.0439E-03	1.0625E-03	1.0638E-03	1.0217E-03	9.5324E-04	8.7425E-04
323.15	0.1	1.2910E-03	1.3324E-03	1.3749E-03	1.3857E-03	1.3809E-03	1.3405E-03	1.2732E-03	1.1958E-03
323.15	1.15	1.2747E-03	1.3169E-03	1.3604E-03	1.3718E-03	1.3673E-03	1.3268E-03	1.2594E-03	1.1818E-03
323.15	2.15	1.2570E-03	1.2999E-03	1.3446E-03	1.3565E-03	1.3524E-03	1.3118E-03	1.2443E-03	1.1665E-03
323.15	3.17	1.2396E-03	1.2833E-03	1.3291E-03	1.3415E-03	1.3377E-03	1.2971E-03	1.2294E-03	1.1516E-03
323.15	4.18	1.2225E-03	1.2670E-03	1.3139E-03	1.3267E-03	1.3233E-03	1.2826E-03	1.2148E-03	1.1369E-03
323.15	5.19	1.2058E-03	1.2510E-03	1.2989E-03	1.3122E-03	1.3092E-03	1.2683E-03	1.2005E-03	1.1225E-03
323.15	6.2	1.1895E-03	1.2353E-03	1.2842E-03	1.2979E-03	1.2952E-03	1.2543E-03	1.1864E-03	1.1083E-03
323.15	7.22	1.1735E-03	1.2199E-03	1.2697E-03	1.2838E-03	1.2815E-03	1.2406E-03	1.1726E-03	1.0944E-03
323.15	8.23	1.1578E-03	1.2048E-03	1.2555E-03	1.2700E-03	1.2680E-03	1.2270E-03	1.1590E-03	1.0808E-03
323.15	9.24	1.1424E-03	1.1900E-03	1.2415E-03	1.2564E-03	1.2547E-03	1.2137E-03	1.1456E-03	1.0675E-03
323.15	10.25	1.1273E-03	1.1755E-03	1.2278E-03	1.2430E-03	1.2417E-03	1.2006E-03	1.1325E-03	1.0544E-03
323.15	11.25	1.1125E-03	1.1612E-03	1.2142E-03	1.2299E-03	1.2288E-03	1.1877E-03	1.1196E-03	1.0415E-03
323.15	12.27	1.0980E-03	1.1471E-03	1.2009E-03	1.2169E-03	1.2161E-03	1.1750E-03	1.1069E-03	1.0289E-03
323.15	13.27	1.0838E-03	1.1334E-03	1.1879E-03	1.2041E-03	1.2036E-03	1.1625E-03	1.0945E-03	1.0165E-03
323.15	14.26	1.0699E-03	1.1198E-03	1.1750E-03	1.1916E-03	1.1914E-03	1.1502E-03	1.0822E-03	1.0043E-03
323.15	15.29	1.0562E-03	1.1065E-03	1.1623E-03	1.1792E-03	1.1793E-03	1.1381E-03	1.0702E-03	9.9230E-04

323.15	16.3	1.0428E-03	1.0935E-03	1.1499E-03	1.1671E-03	1.1674E-03	1.1262E-03	1.0583E-03	9.8055E-04
323.15	17.3	1.0297E-03	1.0807E-03	1.1376E-03	1.1551E-03	1.1556E-03	1.1145E-03	1.0467E-03	9.6901E-04
323.15	18.3	1.0168E-03	1.0681E-03	1.1256E-03	1.1433E-03	1.1441E-03	1.1029E-03	1.0352E-03	9.5767E-04
323.15	19.3	1.0041E-03	1.0557E-03	1.1137E-03	1.1317E-03	1.1327E-03	1.0916E-03	1.0240E-03	9.4652E-04
323.15	20.29	9.9167E-04	1.0435E-03	1.1020E-03	1.1202E-03	1.1215E-03	1.0804E-03	1.0129E-03	9.3558E-04
333.15	0.1	1.3728E-03	1.4131E-03	1.4543E-03	1.4647E-03	1.4597E-03	1.4212E-03	1.3560E-03	1.2823E-03
333.15	1.13	1.3554E-03	1.3966E-03	1.4389E-03	1.4498E-03	1.4452E-03	1.4066E-03	1.3412E-03	1.2672E-03
333.15	2.13	1.3364E-03	1.3785E-03	1.4221E-03	1.4336E-03	1.4294E-03	1.3906E-03	1.3250E-03	1.2507E-03
333.15	3.14	1.3177E-03	1.3608E-03	1.4056E-03	1.4176E-03	1.4138E-03	1.3749E-03	1.3091E-03	1.2345E-03
333.15	4.15	1.2995E-03	1.3434E-03	1.3894E-03	1.4019E-03	1.3985E-03	1.3594E-03	1.2934E-03	1.2187E-03
333.15	5.16	1.2817E-03	1.3263E-03	1.3734E-03	1.3864E-03	1.3834E-03	1.3442E-03	1.2781E-03	1.2032E-03
333.15	6.17	1.2642E-03	1.3096E-03	1.3578E-03	1.3713E-03	1.3686E-03	1.3293E-03	1.2630E-03	1.1879E-03
333.15	7.18	1.2471E-03	1.2932E-03	1.3424E-03	1.3563E-03	1.3540E-03	1.3146E-03	1.2482E-03	1.1729E-03
333.15	8.19	1.2303E-03	1.2771E-03	1.3272E-03	1.3416E-03	1.3396E-03	1.3001E-03	1.2336E-03	1.1583E-03
333.15	9.2	1.2139E-03	1.2613E-03	1.3124E-03	1.3271E-03	1.3255E-03	1.2859E-03	1.2193E-03	1.1439E-03
333.15	10.21	1.1978E-03	1.2458E-03	1.2977E-03	1.3129E-03	1.3116E-03	1.2719E-03	1.2052E-03	1.1297E-03
333.15	11.22	1.1820E-03	1.2305E-03	1.2834E-03	1.2989E-03	1.2979E-03	1.2581E-03	1.1914E-03	1.1159E-03
333.15	12.23	1.1665E-03	1.2156E-03	1.2692E-03	1.2851E-03	1.2844E-03	1.2446E-03	1.1779E-03	1.1022E-03
333.15	13.24	1.1514E-03	1.2009E-03	1.2553E-03	1.2716E-03	1.2712E-03	1.2313E-03	1.1645E-03	1.0889E-03
333.15	14.25	1.1365E-03	1.1865E-03	1.2416E-03	1.2582E-03	1.2581E-03	1.2182E-03	1.1514E-03	1.0757E-03
333.15	15.26	1.1219E-03	1.1723E-03	1.2282E-03	1.2451E-03	1.2452E-03	1.2053E-03	1.1385E-03	1.0628E-03
333.15	16.27	1.1076E-03	1.1584E-03	1.2149E-03	1.2322E-03	1.2326E-03	1.1926E-03	1.1258E-03	1.0502E-03
333.15	17.27	1.0935E-03	1.1448E-03	1.2019E-03	1.2195E-03	1.2201E-03	1.1801E-03	1.1134E-03	1.0377E-03
333.15	18.28	1.0798E-03	1.1314E-03	1.1891E-03	1.2069E-03	1.2078E-03	1.1678E-03	1.1011E-03	1.0255E-03
333.15	19.28	1.0663E-03	1.1182E-03	1.1765E-03	1.1946E-03	1.1957E-03	1.1557E-03	1.0890E-03	1.0135E-03
333.15	20.28	1.0530E-03	1.1052E-03	1.1640E-03	1.1824E-03	1.1838E-03	1.1438E-03	1.0772E-03	1.0017E-03
343.15	0.1	1.4572E-03	1.4976E-03	1.5387E-03	1.5492E-03	1.5443E-03	1.5079E-03	1.4447E-03	1.3750E-03
343.15	1.14	1.4386E-03	1.4799E-03	1.5223E-03	1.5333E-03	1.5288E-03	1.4923E-03	1.4288E-03	1.3586E-03
343.15	2.14	1.4183E-03	1.4607E-03	1.5044E-03	1.5160E-03	1.5120E-03	1.4751E-03	1.4114E-03	1.3408E-03
343.15	3.14	1.3984E-03	1.4418E-03	1.4868E-03	1.4990E-03	1.4954E-03	1.4583E-03	1.3943E-03	1.3234E-03
343.15	4.16	1.3790E-03	1.4232E-03	1.4695E-03	1.4823E-03	1.4790E-03	1.4418E-03	1.3775E-03	1.3063E-03
343.15	5.17	1.3600E-03	1.4050E-03	1.4525E-03	1.4658E-03	1.4630E-03	1.4256E-03	1.3610E-03	1.2895E-03
343.15	6.18	1.3413E-03	1.3872E-03	1.4359E-03	1.4496E-03	1.4472E-03	1.4096E-03	1.3449E-03	1.2731E-03
343.15	7.19	1.3230E-03	1.3697E-03	1.4195E-03	1.4337E-03	1.4316E-03	1.3939E-03	1.3290E-03	1.2569E-03
343.15	8.2	1.3052E-03	1.3526E-03	1.4034E-03	1.4181E-03	1.4163E-03	1.3785E-03	1.3134E-03	1.2411E-03
343.15	9.21	1.2876E-03	1.3357E-03	1.3875E-03	1.4027E-03	1.4013E-03	1.3633E-03	1.2981E-03	1.2256E-03
343.15	10.22	1.2704E-03	1.3192E-03	1.3720E-03	1.3875E-03	1.3865E-03	1.3484E-03	1.2830E-03	1.2103E-03
343.15	11.23	1.2536E-03	1.3030E-03	1.3566E-03	1.3726E-03	1.3719E-03	1.3337E-03	1.2682E-03	1.1954E-03
343.15	12.24	1.2371E-03	1.2870E-03	1.3416E-03	1.3580E-03	1.3576E-03	1.3192E-03	1.2536E-03	1.1807E-03
343.15	13.25	1.2209E-03	1.2714E-03	1.3268E-03	1.3436E-03	1.3435E-03	1.3050E-03	1.2393E-03	1.1663E-03
343.15	14.26	1.2051E-03	1.2561E-03	1.3122E-03	1.3294E-03	1.3296E-03	1.2910E-03	1.2253E-03	1.1521E-03
343.15	15.27	1.1895E-03	1.2410E-03	1.2979E-03	1.3154E-03	1.3159E-03	1.2773E-03	1.2115E-03	1.1382E-03
343.15	16.27	1.1743E-03	1.2262E-03	1.2838E-03	1.3017E-03	1.3024E-03	1.2637E-03	1.1979E-03	1.1246E-03

343.15	17.28	1.1593E-03	1.2117E-03	1.2700E-03	1.2881E-03	1.2892E-03	1.2504E-03	1.1846E-03	1.1112E-03
343.15	18.28	1.1446E-03	1.1974E-03	1.2563E-03	1.2748E-03	1.2761E-03	1.2373E-03	1.1714E-03	1.0980E-03
343.15	19.29	1.1302E-03	1.1834E-03	1.2429E-03	1.2617E-03	1.2632E-03	1.2244E-03	1.1585E-03	1.0851E-03
343.15	20.29	1.1161E-03	1.1696E-03	1.2297E-03	1.2488E-03	1.2506E-03	1.2117E-03	1.1458E-03	1.0724E-03
353.15	0.1	1.5441E-03	1.5856E-03	1.6277E-03	1.6389E-03	1.6344E-03	1.6002E-03	1.5389E-03	1.4735E-03
353.15	1.14	1.5242E-03	1.5667E-03	1.6102E-03	1.6220E-03	1.6179E-03	1.5835E-03	1.5218E-03	1.4558E-03
353.15	2.14	1.5026E-03	1.5462E-03	1.5912E-03	1.6035E-03	1.5999E-03	1.5652E-03	1.5031E-03	1.4366E-03
353.15	3.14	1.4814E-03	1.5260E-03	1.5724E-03	1.5854E-03	1.5822E-03	1.5472E-03	1.4848E-03	1.4178E-03
353.15	4.16	1.4607E-03	1.5063E-03	1.5540E-03	1.5676E-03	1.5648E-03	1.5295E-03	1.4668E-03	1.3994E-03
353.15	5.16	1.4404E-03	1.4869E-03	1.5360E-03	1.5500E-03	1.5477E-03	1.5122E-03	1.4492E-03	1.3813E-03
353.15	6.18	1.4206E-03	1.4679E-03	1.5182E-03	1.5328E-03	1.5308E-03	1.4951E-03	1.4318E-03	1.3635E-03
353.15	7.19	1.4011E-03	1.4493E-03	1.5007E-03	1.5158E-03	1.5143E-03	1.4783E-03	1.4148E-03	1.3461E-03
353.15	8.2	1.3821E-03	1.4310E-03	1.4836E-03	1.4992E-03	1.4980E-03	1.4618E-03	1.3981E-03	1.3290E-03
353.15	9.21	1.3634E-03	1.4131E-03	1.4667E-03	1.4828E-03	1.4819E-03	1.4456E-03	1.3816E-03	1.3123E-03
353.15	10.22	1.3451E-03	1.3955E-03	1.4502E-03	1.4667E-03	1.4662E-03	1.4297E-03	1.3655E-03	1.2959E-03
353.15	11.23	1.3272E-03	1.3783E-03	1.4339E-03	1.4508E-03	1.4506E-03	1.4140E-03	1.3496E-03	1.2797E-03
353.15	12.24	1.3096E-03	1.3613E-03	1.4178E-03	1.4352E-03	1.4354E-03	1.3986E-03	1.3340E-03	1.2639E-03
353.15	13.25	1.2924E-03	1.3447E-03	1.4021E-03	1.4198E-03	1.4203E-03	1.3834E-03	1.3187E-03	1.2484E-03
353.15	14.26	1.2755E-03	1.3284E-03	1.3866E-03	1.4047E-03	1.4055E-03	1.3685E-03	1.3037E-03	1.2331E-03
353.15	15.25	1.2590E-03	1.3123E-03	1.3714E-03	1.3899E-03	1.3910E-03	1.3538E-03	1.2889E-03	1.2182E-03
353.15	16.27	1.2427E-03	1.2966E-03	1.3564E-03	1.3753E-03	1.3766E-03	1.3393E-03	1.2743E-03	1.2035E-03
353.15	17.27	1.2268E-03	1.2811E-03	1.3417E-03	1.3609E-03	1.3625E-03	1.3251E-03	1.2600E-03	1.1890E-03
353.15	18.29	1.2112E-03	1.2659E-03	1.3272E-03	1.3467E-03	1.3486E-03	1.3111E-03	1.2460E-03	1.1749E-03
353.15	19.29	1.1959E-03	1.2510E-03	1.3129E-03	1.3327E-03	1.3349E-03	1.2973E-03	1.2321E-03	1.1609E-03
353.15	20.29	1.1809E-03	1.2364E-03	1.2989E-03	1.3190E-03	1.3214E-03	1.2838E-03	1.2185E-03	1.1473E-03

Expanded combined uncertainties (k = 2) U_c are $U_c(T)$ = 0.02 K, $U_c(P)$ = 0.032 MPa, and $U_c(x_i)$ = 0.0002, $U_{c,r}(\kappa_T)$ = 0.038 .

Table C5: Isothermal Compressibility (κ_T) of 2-methylpropan-1-ol (1) + n-octane (2) at various pressures and temperatures.

T/K	P/MPa	κ_T /MPa^{-1}							
		$x_1=0$	$x_1=0.1267$	$x_1=0.3776$	$x_1=0.4996$	$x_1=0.6255$	$x_1=0.7499$	$x_1=0.8739$	$x_1=1$
313.15	0.1	1.4077E-03	1.4794E-03	1.4799E-03	1.4458E-03	1.3915E-03	1.3189E-03	1.2335E-03	1.1408E-03
313.15	1.14	1.3878E-03	1.4582E-03	1.4608E-03	1.4274E-03	1.3738E-03	1.3019E-03	1.2175E-03	1.1282E-03
313.15	2.14	1.3662E-03	1.4351E-03	1.4401E-03	1.4074E-03	1.3545E-03	1.2834E-03	1.2000E-03	1.1144E-03
313.15	3.15	1.3451E-03	1.4126E-03	1.4198E-03	1.3879E-03	1.3356E-03	1.2652E-03	1.1829E-03	1.1009E-03
313.15	4.16	1.3245E-03	1.3907E-03	1.3999E-03	1.3687E-03	1.3171E-03	1.2475E-03	1.1662E-03	1.0876E-03
313.15	5.17	1.3043E-03	1.3692E-03	1.3804E-03	1.3500E-03	1.2990E-03	1.2301E-03	1.1498E-03	1.0746E-03
313.15	6.18	1.2847E-03	1.3483E-03	1.3613E-03	1.3316E-03	1.2813E-03	1.2131E-03	1.1337E-03	1.0618E-03
313.15	7.19	1.2654E-03	1.3278E-03	1.3426E-03	1.3136E-03	1.2639E-03	1.1965E-03	1.1180E-03	1.0492E-03
313.15	8.2	1.2466E-03	1.3078E-03	1.3243E-03	1.2960E-03	1.2469E-03	1.1801E-03	1.1027E-03	1.0369E-03
313.15	9.23	1.2282E-03	1.2882E-03	1.3064E-03	1.2787E-03	1.2302E-03	1.1642E-03	1.0876E-03	1.0247E-03
313.15	10.23	1.2102E-03	1.2691E-03	1.2889E-03	1.2618E-03	1.2139E-03	1.1485E-03	1.0728E-03	1.0128E-03
313.15	11.24	1.1926E-03	1.2504E-03	1.2716E-03	1.2452E-03	1.1978E-03	1.1332E-03	1.0584E-03	1.0011E-03
313.15	12.25	1.1754E-03	1.2321E-03	1.2548E-03	1.2289E-03	1.1821E-03	1.1181E-03	1.0442E-03	9.8957E-04
313.15	13.26	1.1586E-03	1.2142E-03	1.2383E-03	1.2130E-03	1.1667E-03	1.1034E-03	1.0303E-03	9.7825E-04
313.15	14.27	1.1421E-03	1.1967E-03	1.2220E-03	1.1973E-03	1.1516E-03	1.0889E-03	1.0167E-03	9.6713E-04
313.15	15.27	1.1260E-03	1.1796E-03	1.2062E-03	1.1820E-03	1.1368E-03	1.0748E-03	1.0034E-03	9.5619E-04
313.15	16.28	1.1102E-03	1.1628E-03	1.1906E-03	1.1669E-03	1.1223E-03	1.0609E-03	9.9029E-04	9.4544E-04
313.15	17.29	1.0947E-03	1.1464E-03	1.1753E-03	1.1522E-03	1.1081E-03	1.0472E-03	9.7747E-04	9.3488E-04
313.15	18.3	1.0796E-03	1.1303E-03	1.1603E-03	1.1377E-03	1.0941E-03	1.0339E-03	9.6489E-04	9.2448E-04
313.15	19.3	1.0648E-03	1.1146E-03	1.1456E-03	1.1235E-03	1.0804E-03	1.0208E-03	9.5256E-04	9.1426E-04
313.15	20.31	1.0502E-03	1.0992E-03	1.1312E-03	1.1095E-03	1.0669E-03	1.0079E-03	9.4046E-04	9.0421E-04
323.15	0.1	1.5131E-03	1.5909E-03	1.5830E-03	1.5463E-03	1.4902E-03	1.4159E-03	1.3275E-03	1.2124E-03
323.15	1.15	1.4916E-03	1.5679E-03	1.5625E-03	1.5265E-03	1.4711E-03	1.3975E-03	1.3101E-03	1.1990E-03
323.15	2.15	1.4683E-03	1.5430E-03	1.5401E-03	1.5050E-03	1.4503E-03	1.3775E-03	1.2912E-03	1.1842E-03
323.15	3.17	1.4454E-03	1.5187E-03	1.5182E-03	1.4840E-03	1.4299E-03	1.3579E-03	1.2727E-03	1.1698E-03
323.15	4.18	1.4232E-03	1.4949E-03	1.4968E-03	1.4634E-03	1.4100E-03	1.3387E-03	1.2546E-03	1.1556E-03
323.15	5.19	1.4014E-03	1.4717E-03	1.4758E-03	1.4432E-03	1.3905E-03	1.3200E-03	1.2368E-03	1.1417E-03
323.15	6.2	1.3801E-03	1.4490E-03	1.4553E-03	1.4234E-03	1.3714E-03	1.3016E-03	1.2195E-03	1.1280E-03
323.15	7.22	1.3593E-03	1.4269E-03	1.4352E-03	1.4041E-03	1.3527E-03	1.2836E-03	1.2025E-03	1.1145E-03
323.15	8.23	1.3390E-03	1.4052E-03	1.4155E-03	1.3851E-03	1.3343E-03	1.2660E-03	1.1858E-03	1.1013E-03
323.15	9.24	1.3191E-03	1.3841E-03	1.3962E-03	1.3665E-03	1.3164E-03	1.2488E-03	1.1695E-03	1.0884E-03
323.15	10.25	1.2997E-03	1.3634E-03	1.3773E-03	1.3483E-03	1.2988E-03	1.2319E-03	1.1536E-03	1.0757E-03
323.15	11.25	1.2807E-03	1.3432E-03	1.3588E-03	1.3304E-03	1.2815E-03	1.2153E-03	1.1379E-03	1.0631E-03
323.15	12.27	1.2621E-03	1.3234E-03	1.3407E-03	1.3129E-03	1.2646E-03	1.1991E-03	1.1226E-03	1.0508E-03
323.15	13.27	1.2439E-03	1.3041E-03	1.3229E-03	1.2958E-03	1.2480E-03	1.1832E-03	1.1076E-03	1.0388E-03
323.15	14.26	1.2261E-03	1.2852E-03	1.3055E-03	1.2790E-03	1.2318E-03	1.1676E-03	1.0929E-03	1.0269E-03
323.15	15.29	1.2087E-03	1.2667E-03	1.2884E-03	1.2625E-03	1.2158E-03	1.1523E-03	1.0785E-03	1.0152E-03

323.15	16.3	1.1916E-03	1.2485E-03	1.2717E-03	1.2463E-03	1.2002E-03	1.1373E-03	1.0643E-03	1.0038E-03
323.15	17.3	1.1749E-03	1.2308E-03	1.2553E-03	1.2304E-03	1.1849E-03	1.1226E-03	1.0505E-03	9.9247E-04
323.15	18.3	1.1586E-03	1.2135E-03	1.2392E-03	1.2149E-03	1.1698E-03	1.1082E-03	1.0369E-03	9.8138E-04
323.15	19.3	1.1426E-03	1.1965E-03	1.2234E-03	1.1996E-03	1.1551E-03	1.0941E-03	1.0235E-03	9.7048E-04
323.15	20.29	1.1269E-03	1.1799E-03	1.2079E-03	1.1846E-03	1.1406E-03	1.0802E-03	1.0105E-03	9.5976E-04
333.15	0.1	1.6220E-03	1.7077E-03	1.6926E-03	1.6536E-03	1.5958E-03	1.5199E-03	1.4288E-03	1.2886E-03
333.15	1.13	1.5988E-03	1.6829E-03	1.6704E-03	1.6323E-03	1.5752E-03	1.5000E-03	1.4100E-03	1.2742E-03
333.15	2.13	1.5736E-03	1.6559E-03	1.6464E-03	1.6091E-03	1.5528E-03	1.4784E-03	1.3895E-03	1.2584E-03
333.15	3.14	1.5490E-03	1.6296E-03	1.6228E-03	1.5865E-03	1.5308E-03	1.4572E-03	1.3694E-03	1.2430E-03
333.15	4.15	1.5249E-03	1.6040E-03	1.5997E-03	1.5643E-03	1.5093E-03	1.4365E-03	1.3498E-03	1.2278E-03
333.15	5.16	1.5014E-03	1.5789E-03	1.5772E-03	1.5425E-03	1.4883E-03	1.4163E-03	1.3306E-03	1.2129E-03
333.15	6.17	1.4785E-03	1.5544E-03	1.5551E-03	1.5213E-03	1.4677E-03	1.3964E-03	1.3118E-03	1.1983E-03
333.15	7.18	1.4561E-03	1.5305E-03	1.5334E-03	1.5004E-03	1.4475E-03	1.3770E-03	1.2934E-03	1.1839E-03
333.15	8.19	1.4342E-03	1.5071E-03	1.5122E-03	1.4800E-03	1.4278E-03	1.3580E-03	1.2754E-03	1.1698E-03
333.15	9.2	1.4128E-03	1.4843E-03	1.4915E-03	1.4600E-03	1.4084E-03	1.3394E-03	1.2577E-03	1.1560E-03
333.15	10.21	1.3918E-03	1.4619E-03	1.4712E-03	1.4404E-03	1.3894E-03	1.3211E-03	1.2405E-03	1.1424E-03
333.15	11.22	1.3713E-03	1.4401E-03	1.4513E-03	1.4212E-03	1.3709E-03	1.3032E-03	1.2236E-03	1.1290E-03
333.15	12.23	1.3513E-03	1.4188E-03	1.4318E-03	1.4024E-03	1.3526E-03	1.2857E-03	1.2070E-03	1.1159E-03
333.15	13.24	1.3317E-03	1.3979E-03	1.4127E-03	1.3840E-03	1.3348E-03	1.2686E-03	1.1907E-03	1.1030E-03
333.15	14.25	1.3125E-03	1.3775E-03	1.3939E-03	1.3659E-03	1.3173E-03	1.2517E-03	1.1748E-03	1.0903E-03
333.15	15.26	1.2938E-03	1.3576E-03	1.3756E-03	1.3481E-03	1.3002E-03	1.2353E-03	1.1592E-03	1.0779E-03
333.15	16.27	1.2754E-03	1.3380E-03	1.3576E-03	1.3308E-03	1.2833E-03	1.2191E-03	1.1439E-03	1.0656E-03
333.15	17.27	1.2575E-03	1.3189E-03	1.3399E-03	1.3137E-03	1.2668E-03	1.2033E-03	1.1290E-03	1.0536E-03
333.15	18.28	1.2399E-03	1.3002E-03	1.3226E-03	1.2970E-03	1.2507E-03	1.1877E-03	1.1143E-03	1.0417E-03
333.15	19.28	1.2226E-03	1.2819E-03	1.3057E-03	1.2806E-03	1.2348E-03	1.1725E-03	1.0999E-03	1.0301E-03
333.15	20.28	1.2058E-03	1.2640E-03	1.2890E-03	1.2645E-03	1.2192E-03	1.1575E-03	1.0857E-03	1.0187E-03
343.15	0.1	1.7341E-03	1.8295E-03	1.8082E-03	1.7673E-03	1.7080E-03	1.6306E-03	1.5371E-03	1.3689E-03
343.15	1.14	1.7091E-03	1.8027E-03	1.7844E-03	1.7443E-03	1.6857E-03	1.6091E-03	1.5167E-03	1.3535E-03
343.15	2.14	1.6819E-03	1.7736E-03	1.7585E-03	1.7194E-03	1.6616E-03	1.5858E-03	1.4945E-03	1.3367E-03
343.15	3.14	1.6555E-03	1.7452E-03	1.7331E-03	1.6950E-03	1.6379E-03	1.5629E-03	1.4728E-03	1.3202E-03
343.15	4.16	1.6296E-03	1.7175E-03	1.7083E-03	1.6711E-03	1.6147E-03	1.5405E-03	1.4515E-03	1.3040E-03
343.15	5.17	1.6043E-03	1.6905E-03	1.6840E-03	1.6477E-03	1.5921E-03	1.5186E-03	1.4307E-03	1.2880E-03
343.15	6.18	1.5797E-03	1.6641E-03	1.6602E-03	1.6248E-03	1.5699E-03	1.4972E-03	1.4104E-03	1.2724E-03
343.15	7.19	1.5555E-03	1.6383E-03	1.6370E-03	1.6024E-03	1.5481E-03	1.4762E-03	1.3904E-03	1.2571E-03
343.15	8.2	1.5320E-03	1.6131E-03	1.6142E-03	1.5804E-03	1.5268E-03	1.4557E-03	1.3709E-03	1.2420E-03
343.15	9.21	1.5090E-03	1.5885E-03	1.5919E-03	1.5589E-03	1.5060E-03	1.4356E-03	1.3518E-03	1.2272E-03
343.15	10.22	1.4864E-03	1.5644E-03	1.5701E-03	1.5378E-03	1.4856E-03	1.4159E-03	1.3332E-03	1.2127E-03
343.15	11.23	1.4644E-03	1.5409E-03	1.5487E-03	1.5172E-03	1.4656E-03	1.3966E-03	1.3149E-03	1.1984E-03
343.15	12.24	1.4429E-03	1.5180E-03	1.5277E-03	1.4970E-03	1.4460E-03	1.3777E-03	1.2969E-03	1.1844E-03
343.15	13.25	1.4219E-03	1.4955E-03	1.5072E-03	1.4771E-03	1.4268E-03	1.3592E-03	1.2794E-03	1.1707E-03
343.15	14.26	1.4013E-03	1.4735E-03	1.4870E-03	1.4577E-03	1.4079E-03	1.3411E-03	1.2621E-03	1.1571E-03
343.15	15.27	1.3811E-03	1.4520E-03	1.4673E-03	1.4387E-03	1.3895E-03	1.3233E-03	1.2453E-03	1.1438E-03
343.15	16.27	1.3614E-03	1.4310E-03	1.4480E-03	1.4200E-03	1.3714E-03	1.3059E-03	1.2288E-03	1.1308E-03

343.15	17.28	1.3421E-03	1.4104E-03	1.4290E-03	1.4017E-03	1.3536E-03	1.2888E-03	1.2126E-03	1.1179E-03
343.15	18.28	1.3232E-03	1.3903E-03	1.4105E-03	1.3837E-03	1.3362E-03	1.2720E-03	1.1967E-03	1.1053E-03
343.15	19.29	1.3047E-03	1.3706E-03	1.3923E-03	1.3661E-03	1.3192E-03	1.2556E-03	1.1811E-03	1.0929E-03
343.15	20.29	1.2866E-03	1.3513E-03	1.3744E-03	1.3488E-03	1.3024E-03	1.2395E-03	1.1658E-03	1.0807E-03
353.15	0.1	1.8491E-03	1.9560E-03	1.9298E-03	1.8871E-03	1.8264E-03	1.7477E-03	1.6520E-03	1.4532E-03
353.15	1.14	1.8223E-03	1.9271E-03	1.9041E-03	1.8624E-03	1.8025E-03	1.7245E-03	1.6299E-03	1.4368E-03
353.15	2.14	1.7932E-03	1.8958E-03	1.8762E-03	1.8356E-03	1.7764E-03	1.6993E-03	1.6058E-03	1.4188E-03
353.15	3.14	1.7647E-03	1.8652E-03	1.8489E-03	1.8093E-03	1.7509E-03	1.6746E-03	1.5823E-03	1.4011E-03
353.15	4.16	1.7370E-03	1.8354E-03	1.8223E-03	1.7836E-03	1.7259E-03	1.6504E-03	1.5593E-03	1.3838E-03
353.15	5.16	1.7099E-03	1.8063E-03	1.7962E-03	1.7584E-03	1.7015E-03	1.6268E-03	1.5368E-03	1.3668E-03
353.15	6.18	1.6834E-03	1.7779E-03	1.7706E-03	1.7338E-03	1.6776E-03	1.6037E-03	1.5148E-03	1.3501E-03
353.15	7.19	1.6575E-03	1.7501E-03	1.7456E-03	1.7097E-03	1.6542E-03	1.5810E-03	1.4932E-03	1.3338E-03
353.15	8.2	1.6323E-03	1.7230E-03	1.7211E-03	1.6861E-03	1.6313E-03	1.5589E-03	1.4722E-03	1.3177E-03
353.15	9.21	1.6076E-03	1.6966E-03	1.6972E-03	1.6630E-03	1.6089E-03	1.5372E-03	1.4515E-03	1.3019E-03
353.15	10.22	1.5834E-03	1.6707E-03	1.6737E-03	1.6403E-03	1.5869E-03	1.5160E-03	1.4313E-03	1.2864E-03
353.15	11.23	1.5598E-03	1.6454E-03	1.6507E-03	1.6181E-03	1.5654E-03	1.4952E-03	1.4115E-03	1.2712E-03
353.15	12.24	1.5368E-03	1.6207E-03	1.6282E-03	1.5964E-03	1.5443E-03	1.4748E-03	1.3921E-03	1.2562E-03
353.15	13.25	1.5142E-03	1.5966E-03	1.6062E-03	1.5751E-03	1.5236E-03	1.4548E-03	1.3731E-03	1.2415E-03
353.15	14.26	1.4921E-03	1.5730E-03	1.5846E-03	1.5542E-03	1.5033E-03	1.4353E-03	1.3545E-03	1.2271E-03
353.15	15.25	1.4706E-03	1.5499E-03	1.5634E-03	1.5338E-03	1.4835E-03	1.4161E-03	1.3363E-03	1.2129E-03
353.15	16.27	1.4494E-03	1.5273E-03	1.5427E-03	1.5137E-03	1.4640E-03	1.3973E-03	1.3185E-03	1.1989E-03
353.15	17.27	1.4288E-03	1.5052E-03	1.5223E-03	1.4941E-03	1.4450E-03	1.3789E-03	1.3010E-03	1.1852E-03
353.15	18.29	1.4085E-03	1.4836E-03	1.5024E-03	1.4748E-03	1.4263E-03	1.3609E-03	1.2838E-03	1.1718E-03
353.15	19.29	1.3887E-03	1.4624E-03	1.4829E-03	1.4559E-03	1.4079E-03	1.3432E-03	1.2670E-03	1.1585E-03
353.15	20.29	1.3694E-03	1.4417E-03	1.4637E-03	1.4373E-03	1.3899E-03	1.3258E-03	1.2505E-03	1.1455E-03

Expanded combined uncertainties (k = 2) U_c are $U_c(T) = 0.02$ K, $U_c(P) = 0.032$ MPa, and $U_c(x_i) = 0.0002$, $U_{c,r}(\kappa_T) = 0.044$.

Table C6: Isothermal Compressibility (κ_T) of 2-methylpropan-1-ol (1) + n-decane (2) at various pressures and temperatures.

T/K	P/MPa	κ_T /MPa^{-1}							
		$x_1=0$	$x_1=0.1276$	$x_1=0.3749$	$x_1=0.5015$	$x_1=0.6249$	$x_1=0.7502$	$x_1=0.8750$	$x_1=1$
313.15	0.1	1.2121E-03	1.2765E-03	1.3268E-03	1.3415E-03	1.3365E-03	1.2890E-03	1.2105E-03	1.1408E-03
313.15	1.14	1.1969E-03	1.2594E-03	1.3105E-03	1.3257E-03	1.3209E-03	1.2738E-03	1.1958E-03	1.1282E-03
313.15	2.14	1.1803E-03	1.2408E-03	1.2928E-03	1.3085E-03	1.3039E-03	1.2574E-03	1.1798E-03	1.1144E-03
313.15	3.15	1.1641E-03	1.2227E-03	1.2754E-03	1.2916E-03	1.2873E-03	1.2412E-03	1.1641E-03	1.1009E-03
313.15	4.16	1.1482E-03	1.2049E-03	1.2583E-03	1.2751E-03	1.2710E-03	1.2253E-03	1.1487E-03	1.0876E-03
313.15	5.17	1.1326E-03	1.1875E-03	1.2416E-03	1.2588E-03	1.2549E-03	1.2098E-03	1.1337E-03	1.0746E-03
313.15	6.18	1.1173E-03	1.1705E-03	1.2253E-03	1.2429E-03	1.2392E-03	1.1945E-03	1.1189E-03	1.0618E-03
313.15	7.19	1.1023E-03	1.1538E-03	1.2092E-03	1.2273E-03	1.2238E-03	1.1795E-03	1.1044E-03	1.0492E-03
313.15	8.2	1.0877E-03	1.1375E-03	1.1935E-03	1.2119E-03	1.2087E-03	1.1648E-03	1.0902E-03	1.0369E-03
313.15	9.23	1.0733E-03	1.1216E-03	1.1781E-03	1.1969E-03	1.1938E-03	1.1504E-03	1.0762E-03	1.0247E-03
313.15	10.23	1.0592E-03	1.1060E-03	1.1629E-03	1.1821E-03	1.1792E-03	1.1362E-03	1.0626E-03	1.0128E-03
313.15	11.24	1.0454E-03	1.0907E-03	1.1481E-03	1.1676E-03	1.1649E-03	1.1223E-03	1.0491E-03	1.0011E-03
313.15	12.25	1.0318E-03	1.0757E-03	1.1335E-03	1.1534E-03	1.1508E-03	1.1087E-03	1.0360E-03	9.8957E-04
313.15	13.26	1.0185E-03	1.0610E-03	1.1193E-03	1.1394E-03	1.1370E-03	1.0953E-03	1.0231E-03	9.7825E-04
313.15	14.27	1.0055E-03	1.0467E-03	1.1053E-03	1.1257E-03	1.1235E-03	1.0822E-03	1.0104E-03	9.6713E-04
313.15	15.27	9.9272E-04	1.0326E-03	1.0915E-03	1.1122E-03	1.1101E-03	1.0692E-03	9.9797E-04	9.5619E-04
313.15	16.28	9.8019E-04	1.0188E-03	1.0780E-03	1.0990E-03	1.0971E-03	1.0565E-03	9.8576E-04	9.4544E-04
313.15	17.29	9.6788E-04	1.0053E-03	1.0648E-03	1.0860E-03	1.0842E-03	1.0441E-03	9.7377E-04	9.3488E-04
313.15	18.3	9.5581E-04	9.9200E-04	1.0518E-03	1.0732E-03	1.0716E-03	1.0318E-03	9.6200E-04	9.2448E-04
313.15	19.3	9.4397E-04	9.7901E-04	1.0390E-03	1.0606E-03	1.0592E-03	1.0198E-03	9.5045E-04	9.1426E-04
313.15	20.31	9.3234E-04	9.6627E-04	1.0265E-03	1.0483E-03	1.0470E-03	1.0080E-03	9.3910E-04	9.0421E-04
323.15	0.1	1.2910E-03	1.3654E-03	1.4140E-03	1.4279E-03	1.4227E-03	1.3753E-03	1.2965E-03	1.2124E-03
323.15	1.15	1.2747E-03	1.3471E-03	1.3966E-03	1.4110E-03	1.4060E-03	1.3591E-03	1.2807E-03	1.1990E-03
323.15	2.15	1.2570E-03	1.3271E-03	1.3775E-03	1.3925E-03	1.3878E-03	1.3414E-03	1.2635E-03	1.1842E-03
323.15	3.17	1.2396E-03	1.3075E-03	1.3589E-03	1.3744E-03	1.3700E-03	1.3240E-03	1.2465E-03	1.1698E-03
323.15	4.18	1.2225E-03	1.2884E-03	1.3406E-03	1.3567E-03	1.3525E-03	1.3070E-03	1.2300E-03	1.1556E-03
323.15	5.19	1.2058E-03	1.2697E-03	1.3227E-03	1.3393E-03	1.3353E-03	1.2903E-03	1.2137E-03	1.1417E-03
323.15	6.2	1.1895E-03	1.2514E-03	1.3052E-03	1.3222E-03	1.3185E-03	1.2739E-03	1.1978E-03	1.1280E-03
323.15	7.22	1.1735E-03	1.2335E-03	1.2880E-03	1.3055E-03	1.3020E-03	1.2578E-03	1.1822E-03	1.1145E-03
323.15	8.23	1.1578E-03	1.2160E-03	1.2711E-03	1.2891E-03	1.2858E-03	1.2421E-03	1.1669E-03	1.1013E-03
323.15	9.24	1.1424E-03	1.1989E-03	1.2546E-03	1.2730E-03	1.2699E-03	1.2266E-03	1.1519E-03	1.0884E-03
323.15	10.25	1.1273E-03	1.1821E-03	1.2384E-03	1.2572E-03	1.2543E-03	1.2114E-03	1.1372E-03	1.0757E-03
323.15	11.25	1.1125E-03	1.1656E-03	1.2225E-03	1.2417E-03	1.2389E-03	1.1965E-03	1.1227E-03	1.0631E-03
323.15	12.27	1.0980E-03	1.1495E-03	1.2069E-03	1.2264E-03	1.2239E-03	1.1819E-03	1.1086E-03	1.0508E-03
323.15	13.27	1.0838E-03	1.1338E-03	1.1916E-03	1.2115E-03	1.2091E-03	1.1675E-03	1.0947E-03	1.0388E-03
323.15	14.26	1.0699E-03	1.1183E-03	1.1766E-03	1.1968E-03	1.1946E-03	1.1534E-03	1.0811E-03	1.0269E-03

323.15	15.29	1.0562E-03	1.1032E-03	1.1619E-03	1.1824E-03	1.1804E-03	1.1396E-03	1.0677E-03	1.0152E-03
323.15	16.3	1.0428E-03	1.0884E-03	1.1475E-03	1.1682E-03	1.1664E-03	1.1260E-03	1.0545E-03	1.0038E-03
323.15	17.3	1.0297E-03	1.0739E-03	1.1333E-03	1.1543E-03	1.1527E-03	1.1126E-03	1.0416E-03	9.9247E-04
323.15	18.3	1.0168E-03	1.0597E-03	1.1194E-03	1.1407E-03	1.1392E-03	1.0995E-03	1.0290E-03	9.8138E-04
323.15	19.3	1.0041E-03	1.0457E-03	1.1057E-03	1.1273E-03	1.1259E-03	1.0866E-03	1.0166E-03	9.7048E-04
323.15	20.29	9.9167E-04	1.0320E-03	1.0923E-03	1.1141E-03	1.1129E-03	1.0739E-03	1.0043E-03	9.5976E-04
333.15	0.1	1.3728E-03	1.4589E-03	1.5074E-03	1.5209E-03	1.5162E-03	1.4684E-03	1.3895E-03	1.2886E-03
333.15	1.13	1.3554E-03	1.4391E-03	1.4887E-03	1.5027E-03	1.4983E-03	1.4510E-03	1.3725E-03	1.2742E-03
333.15	2.13	1.3364E-03	1.4177E-03	1.4683E-03	1.4829E-03	1.4788E-03	1.4319E-03	1.3539E-03	1.2584E-03
333.15	3.14	1.3177E-03	1.3966E-03	1.4482E-03	1.4635E-03	1.4596E-03	1.4133E-03	1.3356E-03	1.2430E-03
333.15	4.15	1.2995E-03	1.3761E-03	1.4287E-03	1.4445E-03	1.4409E-03	1.3950E-03	1.3177E-03	1.2278E-03
333.15	5.16	1.2817E-03	1.3560E-03	1.4095E-03	1.4259E-03	1.4224E-03	1.3770E-03	1.3002E-03	1.2129E-03
333.15	6.17	1.2642E-03	1.3364E-03	1.3906E-03	1.4076E-03	1.4044E-03	1.3594E-03	1.2831E-03	1.1983E-03
333.15	7.18	1.2471E-03	1.3171E-03	1.3722E-03	1.3897E-03	1.3867E-03	1.3422E-03	1.2662E-03	1.1839E-03
333.15	8.19	1.2303E-03	1.2983E-03	1.3541E-03	1.3721E-03	1.3693E-03	1.3252E-03	1.2498E-03	1.1698E-03
333.15	9.2	1.2139E-03	1.2799E-03	1.3364E-03	1.3548E-03	1.3523E-03	1.3086E-03	1.2336E-03	1.1560E-03
333.15	10.21	1.1978E-03	1.2619E-03	1.3191E-03	1.3379E-03	1.3355E-03	1.2923E-03	1.2177E-03	1.1424E-03
333.15	11.22	1.1820E-03	1.2443E-03	1.3020E-03	1.3213E-03	1.3191E-03	1.2763E-03	1.2022E-03	1.1290E-03
333.15	12.23	1.1665E-03	1.2270E-03	1.2853E-03	1.3050E-03	1.3030E-03	1.2606E-03	1.1869E-03	1.1159E-03
333.15	13.24	1.1514E-03	1.2101E-03	1.2689E-03	1.2890E-03	1.2872E-03	1.2452E-03	1.1719E-03	1.1030E-03
333.15	14.25	1.1365E-03	1.1935E-03	1.2529E-03	1.2732E-03	1.2716E-03	1.2300E-03	1.1572E-03	1.0903E-03
333.15	15.26	1.1219E-03	1.1773E-03	1.2371E-03	1.2578E-03	1.2564E-03	1.2152E-03	1.1428E-03	1.0779E-03
333.15	16.27	1.1076E-03	1.1614E-03	1.2216E-03	1.2427E-03	1.2414E-03	1.2006E-03	1.1287E-03	1.0656E-03
333.15	17.27	1.0935E-03	1.1458E-03	1.2065E-03	1.2278E-03	1.2267E-03	1.1863E-03	1.1148E-03	1.0536E-03
333.15	18.28	1.0798E-03	1.1305E-03	1.1916E-03	1.2132E-03	1.2122E-03	1.1722E-03	1.1012E-03	1.0417E-03
333.15	19.28	1.0663E-03	1.1156E-03	1.1769E-03	1.1988E-03	1.1980E-03	1.1584E-03	1.0878E-03	1.0301E-03
333.15	20.28	1.0530E-03	1.1009E-03	1.1626E-03	1.1848E-03	1.1841E-03	1.1448E-03	1.0747E-03	1.0187E-03
343.15	0.1	1.4572E-03	1.5566E-03	1.6066E-03	1.6201E-03	1.6165E-03	1.5679E-03	1.4891E-03	1.3689E-03
343.15	1.14	1.4386E-03	1.5354E-03	1.5865E-03	1.6006E-03	1.5973E-03	1.5492E-03	1.4707E-03	1.3535E-03
343.15	2.14	1.4183E-03	1.5123E-03	1.5646E-03	1.5794E-03	1.5763E-03	1.5287E-03	1.4506E-03	1.3367E-03
343.15	3.14	1.3984E-03	1.4897E-03	1.5431E-03	1.5586E-03	1.5558E-03	1.5086E-03	1.4309E-03	1.3202E-03
343.15	4.16	1.3790E-03	1.4677E-03	1.5221E-03	1.5382E-03	1.5356E-03	1.4889E-03	1.4116E-03	1.3040E-03
343.15	5.17	1.3600E-03	1.4461E-03	1.5015E-03	1.5182E-03	1.5159E-03	1.4696E-03	1.3927E-03	1.2880E-03
343.15	6.18	1.3413E-03	1.4251E-03	1.4813E-03	1.4986E-03	1.4965E-03	1.4507E-03	1.3742E-03	1.2724E-03
343.15	7.19	1.3230E-03	1.4044E-03	1.4616E-03	1.4794E-03	1.4775E-03	1.4322E-03	1.3561E-03	1.2571E-03
343.15	8.2	1.3052E-03	1.3843E-03	1.4422E-03	1.4605E-03	1.4588E-03	1.4140E-03	1.3383E-03	1.2420E-03
343.15	9.21	1.2876E-03	1.3645E-03	1.4232E-03	1.4420E-03	1.4405E-03	1.3961E-03	1.3209E-03	1.2272E-03
343.15	10.22	1.2704E-03	1.3452E-03	1.4046E-03	1.4239E-03	1.4226E-03	1.3786E-03	1.3038E-03	1.2127E-03
343.15	11.23	1.2536E-03	1.3263E-03	1.3863E-03	1.4061E-03	1.4050E-03	1.3614E-03	1.2870E-03	1.1984E-03
343.15	12.24	1.2371E-03	1.3078E-03	1.3684E-03	1.3886E-03	1.3877E-03	1.3445E-03	1.2706E-03	1.1844E-03
343.15	13.25	1.2209E-03	1.2896E-03	1.3509E-03	1.3715E-03	1.3707E-03	1.3280E-03	1.2544E-03	1.1707E-03
343.15	14.26	1.2051E-03	1.2719E-03	1.3337E-03	1.3546E-03	1.3541E-03	1.3117E-03	1.2386E-03	1.1571E-03
343.15	15.27	1.1895E-03	1.2545E-03	1.3168E-03	1.3381E-03	1.3377E-03	1.2958E-03	1.2231E-03	1.1438E-03

343.15	16.27	1.1743E-03	1.2374E-03	1.3002E-03	1.3219E-03	1.3216E-03	1.2801E-03	1.2079E-03	1.1308E-03
343.15	17.28	1.1593E-03	1.2207E-03	1.2840E-03	1.3060E-03	1.3059E-03	1.2647E-03	1.1929E-03	1.1179E-03
343.15	18.28	1.1446E-03	1.2044E-03	1.2680E-03	1.2903E-03	1.2904E-03	1.2496E-03	1.1782E-03	1.1053E-03
343.15	19.29	1.1302E-03	1.1884E-03	1.2523E-03	1.2750E-03	1.2752E-03	1.2348E-03	1.1638E-03	1.0929E-03
343.15	20.29	1.1161E-03	1.1727E-03	1.2370E-03	1.2599E-03	1.2602E-03	1.2202E-03	1.1497E-03	1.0807E-03
353.15	0.1	1.5441E-03	1.6582E-03	1.7114E-03	1.7253E-03	1.7234E-03	1.6735E-03	1.5949E-03	1.4532E-03
353.15	1.14	1.5242E-03	1.6354E-03	1.6898E-03	1.7044E-03	1.7027E-03	1.6533E-03	1.5750E-03	1.4368E-03
353.15	2.14	1.5026E-03	1.6107E-03	1.6663E-03	1.6816E-03	1.6802E-03	1.6313E-03	1.5534E-03	1.4188E-03
353.15	3.14	1.4814E-03	1.5866E-03	1.6432E-03	1.6593E-03	1.6581E-03	1.6097E-03	1.5321E-03	1.4011E-03
353.15	4.16	1.4607E-03	1.5629E-03	1.6207E-03	1.6374E-03	1.6365E-03	1.5885E-03	1.5113E-03	1.3838E-03
353.15	5.16	1.4404E-03	1.5398E-03	1.5986E-03	1.6160E-03	1.6153E-03	1.5678E-03	1.4910E-03	1.3668E-03
353.15	6.18	1.4206E-03	1.5172E-03	1.5770E-03	1.5950E-03	1.5945E-03	1.5475E-03	1.4710E-03	1.3501E-03
353.15	7.19	1.4011E-03	1.4951E-03	1.5558E-03	1.5744E-03	1.5741E-03	1.5275E-03	1.4514E-03	1.3338E-03
353.15	8.2	1.3821E-03	1.4735E-03	1.5350E-03	1.5541E-03	1.5541E-03	1.5080E-03	1.4323E-03	1.3177E-03
353.15	9.21	1.3634E-03	1.4524E-03	1.5147E-03	1.5343E-03	1.5344E-03	1.4888E-03	1.4135E-03	1.3019E-03
353.15	10.22	1.3451E-03	1.4317E-03	1.4947E-03	1.5149E-03	1.5152E-03	1.4700E-03	1.3951E-03	1.2864E-03
353.15	11.23	1.3272E-03	1.4114E-03	1.4752E-03	1.4958E-03	1.4963E-03	1.4515E-03	1.3770E-03	1.2712E-03
353.15	12.24	1.3096E-03	1.3916E-03	1.4560E-03	1.4771E-03	1.4777E-03	1.4334E-03	1.3593E-03	1.2562E-03
353.15	13.25	1.2924E-03	1.3722E-03	1.4372E-03	1.4587E-03	1.4595E-03	1.4156E-03	1.3419E-03	1.2415E-03
353.15	14.26	1.2755E-03	1.3532E-03	1.4187E-03	1.4407E-03	1.4417E-03	1.3982E-03	1.3249E-03	1.2271E-03
353.15	15.25	1.2590E-03	1.3346E-03	1.4007E-03	1.4230E-03	1.4241E-03	1.3811E-03	1.3081E-03	1.2129E-03
353.15	16.27	1.2427E-03	1.3164E-03	1.3829E-03	1.4056E-03	1.4069E-03	1.3643E-03	1.2917E-03	1.1989E-03
353.15	17.27	1.2268E-03	1.2985E-03	1.3655E-03	1.3886E-03	1.3900E-03	1.3478E-03	1.2756E-03	1.1852E-03
353.15	18.29	1.2112E-03	1.2810E-03	1.3484E-03	1.3718E-03	1.3734E-03	1.3316E-03	1.2599E-03	1.1718E-03
353.15	19.29	1.1959E-03	1.2639E-03	1.3317E-03	1.3554E-03	1.3571E-03	1.3156E-03	1.2444E-03	1.1585E-03
353.15	20.29	1.1809E-03	1.2471E-03	1.3152E-03	1.3393E-03	1.3411E-03	1.3000E-03	1.2291E-03	1.1455E-03

Expanded combined uncertainties (k = 2) U_c are $U_c(T)$ = 0.02 K, $U_c(P)$ = 0.032 MPa, and $U_c(x_i)$ = 0.0002, $U_{c,r}(\kappa_T)$ = 0.044 .

APPENDIX D

Calibration Data

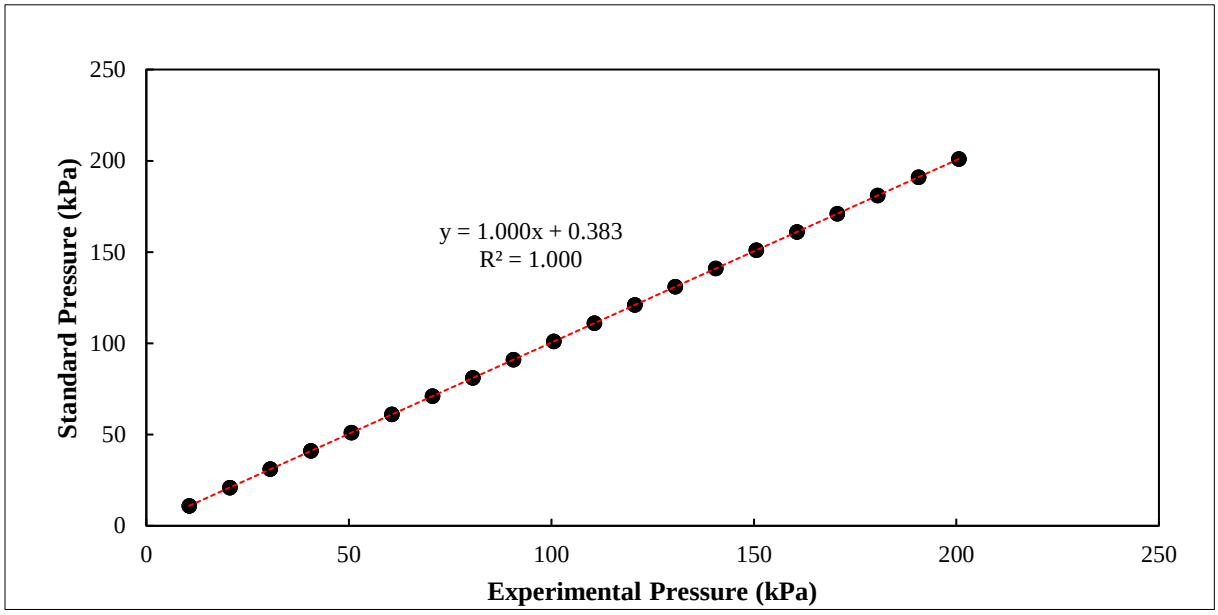

Figure D1: Calibration plot for pressure.

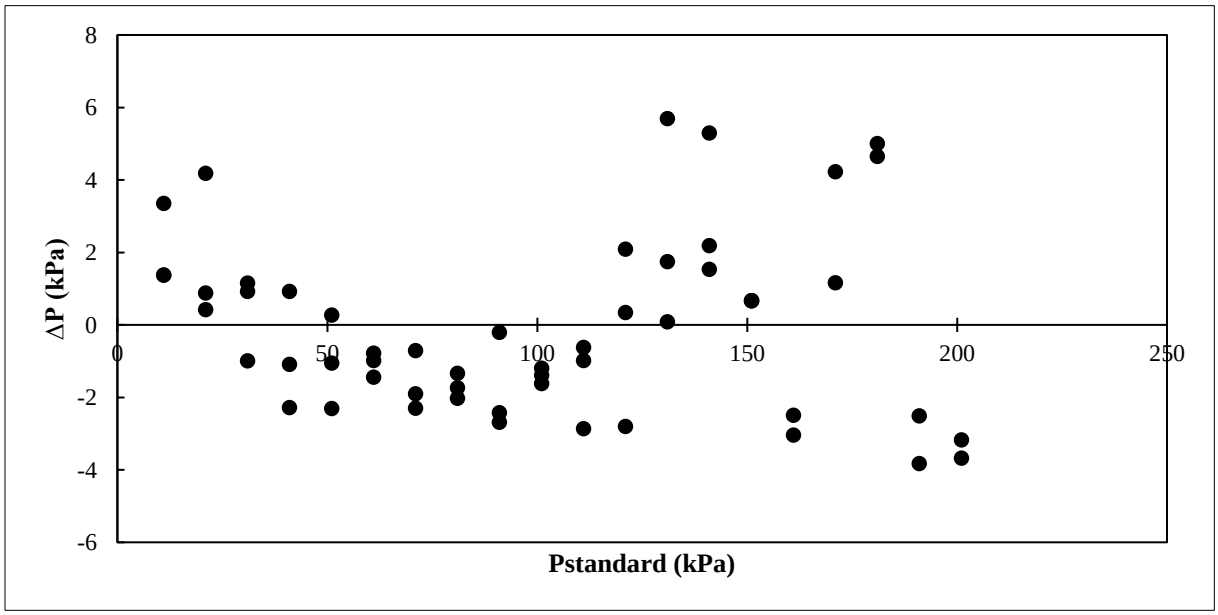

Figure D2: Deviation between the corrected and standard pressures.

APPENDIX E

Uncertainty

Composition Uncertainty:

The uncertainty in composition was calculated using the method outlined below for all six binary systems. The binary systems butan-1-ol (1) + n-octane (2) is used as an example.

Uncertainty from mass balance = 0.0001 g

Molar mass (MM) of component 1 (butan-1-ol) = 74.122 g/mol

Molar mass of component 2 (n-octane) = 114.23 g/mol

Mass (m) of component 1 = 21.024 g

Mass of component 2 = 19.377 g

$$\text{Number of moles (n)of component 1} = \frac{m_1}{MM_1} = \frac{21.024}{74.122} = 0.28364\ mol$$

Similarly, the number of moles of component 2 is 0.16963 mol.

$$\text{Composition (x) of component 1} = \frac{n_1}{n_1 + n_2} = \frac{0.28364}{0.28364 + 0.16963} = 0.62576$$

Composition of component 2 in solution = 1 – x_1 = 1 – 0.62576 = 0.37424

The maximum uncertainty from the preparation of the calibration curve can be calculated by using the uncertainty from the mass balance.

$$m_1 + uncertainty\ from\ mass\ balance = 21.024 + 0.0001 = 21.0241\ g$$

$$n_1 = \frac{m_1}{MM_1} = \frac{21.0241}{74.122} = 0.28364\ mol$$

$$m_1 - uncertainty\ from\ mass\ balance = 21.024 - 0.0001 = 21.0239\ g$$

$$n_1 = \frac{m_1}{MM_1} = \frac{21.0239}{74.122} = 0.28364\ mol$$

Similar calculations were conducted for component 2.

Thereafter the composition was calculated.

$$x_1 = \frac{n_1}{n_1 + n_2} = \frac{0.28364}{0.28364 + 0.16963} = 0.62576$$

Finally, the difference between the actual and manipulated compositions was computed as follows:

$$\sigma = |0.6257622 - 0.6257623| = |9.46774\ x\ 10^{-8}| = 9.46774\ x\ 10^{-8}$$

Similarly, the difference was calculated to be $9.46774\ x\ 10^{-8}$.

Furthermore, the following cases were also considered, and similar calculations were carried out.

1. $m_1 +$ unceratinty from mass balance and $m_2 -$ unceratinty from mass balance.
2. $m_1 +$ unceratinty from mass balance and $m_1 +$ unceratinty from mass balance.

The maximum sigma (σ_{max}) from preparation of the calibration curve was taken as the highest of the four values ($2.3225\ x\ 10^{-6}$).

The maximum uncertainty from the preparation of the calibration curve can be computed as follows:

$$u_c = \frac{\sigma_{max}}{\sqrt{3}} = \frac{2.3225\ x\ 10^{-6}}{\sqrt{3}} = 1.3409\ x\ 10^{-6}$$

The uncertainty from the purity of the chemical species were also accounted for as outlined below.

Uncertainty from purity = 0.01 g

$$m_1\ x\ (1 - uncertainty\ from\ purity) = 21.024\ x\ (1 - 0.01) = 20.8138\ g$$

Similarly, we get 19.1832 g for component 2.

Thereafter, the number of moles of components 1 and 2 were calculated and similar calculations, as previously outlined, were conducted to obtain the maximum sigma in the composition of component 1 due to the chemical purity. This value was computed to be 0.001.

The uncertainty in x_1, from the chemical purity, was then computed using the formula outlined previously and are as follows:

1. Uncertainty due to chemical purity

$$u_c = 1.0\ x\ 10^{-4}$$

Hence, the uncertainty in the composition was calculated as follows:

$$u_{c_1} = \sqrt{{u_{c_{calib}}}^2 + {u_{c_{purity}}}^2} = \sqrt{1.3409\ x\ 10^{-6} + 1.3546\ x\ 10^{-4}} = 0.0001$$

A coverage factor k = of 2 was utilised for 95% confidence interval. Therefore,

$$u_c\ x\ 2 = 0.0002$$

Pressure Uncertainty:

Transducer Range: 0 – 25 MPs.

Therefore,

$$\sigma = 0.05\ x\ transducer\ range = 0.05\ x\ 25 = 12.5\ kPa$$

$$u_{transducer} = \frac{\sigma}{\sqrt{3}} = \frac{12.5}{\sqrt{3}} = 7.2169\ kPa$$

The maximum deviation between experimental and standard pressure is 5.6955 kPa.

Hence,

$$u_{calibration} = \frac{\sigma}{\sqrt{3}} = \frac{5.6955}{\sqrt{3}} = 3.2883\ kPa$$

$u_{stability} = 6.5$ (resolution and stability of display)

$u_{type\ B} = 12$ (historical measurements in similar systems from literature)

The combined uncertainty was calculated as,

$$u_{c_p} = \sqrt{u_{calib}(P)^2 + u_{supp}(P)^2 + u_{stab}(P)^2 + +u_{type\ B}(P)^2} =$$

$$\sqrt{7.2169 + 3.2883 + 42.3 + 144} = 15.8\ kPa$$

Using a coverage factor of 2 gives a maximum combined uncertainty of,

$$U_c = u_{c_p}\ x\ 2 = 32kPa = 0.032\ MPa$$